UNCLASSIFIED

AD 400 151

Reproduced
by the

ARMED SERVICES TECHNICAL INFORMATION AGENCY
ARLINGTON HALL STATION
ARLINGTON 12, VIRGINIA



UNCLASSIFIED

NOTICE: When government or other drawings, specifications or other data are used for any purpose other than in connection with a definitely related government procurement operation, the U. S. Government thereby incurs no responsibility, nor any obligation whatsoever; and the fact that the Government may have formulated, furnished, or in any way supplied the said drawings, specifications, or other data is not to be regarded by implication or otherwise as in any manner licensing the holder or any other person or corporation, or conveying any rights or permission to manufacture, use or sell any patented invention that may in any way be related thereto.

400 151

63-3-1

DEPARTMENT OF THE ARMY
CORPS OF ENGINEERS

CATALOGED BY ASTIA
AS AD No. 400151

T- 1488 a--q

BAUM, F.A. et al

PHYSICS OF AN EXPLOSION

Pages 954

ASTIA
APR 5 1963

U S Army
Engineer Research And
Development Laboratories

FORT BELVOIR, VIRGINIA

PHYSICS OF AN EXPLOSION

T-1488 (a-q)

by

F. A. Baum, K. P. Stanyukovich and B. I. Shekhter

Source

Russian Book: FIZMATGIZ, MOSCOW (1959)

Translated for

U.S. Army Engineer
Research and Development Laboratories
Information Resources Branch
Technical Information Section

by

Research Information Service
122 East 55th Street
New York 22, New York

CONTENTS

		Page
Preface		1
CHAPTER 1.	General Characteristics of Explosives	4
CHAPTER 2.	Sensitivity of Explosives to External Influences	22
CHAPTER 3.	Thermochemistry of Explosives	115
CHAPTER 4.	Reactions of Explosive Breakdown	156
CHAPTER 5.	Elements of Gas Dynamics	208
CHAPTER 6.	Elementary Theory of Shock Waves	262
CHAPTER 7.	Theory of Detonation Waves	298
CHAPTER 8.	Excitation and Propagation of Detonations	339
CHAPTER 9.	Initial Parameters of a Shock Wave at an Interface	375
CHAPTER 10.	Combustion of Explosives	413
CHAPTER 11.	Brisance of Explosives	496
CHAPTER 12.	Cumulation	546
CHAPTER 13.	Explosion in Air	657
CHAPTER 14.	Explosions in Dense Media	790
CHAPTER 15.	Sympathetic Detonation	896
SUPPLEMENT.	Toward the Theory of Cumulation of Gases	937
INDEX		

Explosives which are capable of achieving a considerable amount of work after extremely short periods of time are effectively one of the most powerful sources of energy at the present time.

In munitions, explosives are employed for different kinds of fire-arms, for ammunition and blasting media, for missiles and destructive purposes. Under the conditions of modern warfare, explosives play an extremely important role and are used in colossal quantities. Explosives are also widely used for domestic purposes in constructional and mining work; for breaking through canals, for blasting holes and drilling wells, for clearing ground, etc. Explosive methods for hydraulic work are now successfully used for the solution of problems connected with the grandiose construction plans of Communism. Therefore, consideration of the physical problems of explosion and the phenomena accompanying it are of great interest.

In this book an attempt is made to fill the important gap in the literature concerning the physics of an explosion and the processes occurring in the environment under the action of an explosion.

The only detailed books on the theory of explosions at the present day are still the textbooks by K.K. SNITKO on "Teoriya vzryvchatykh veshchestv" (Theory of explosives) (Part I, 1934, and Part II, 1936) and also by N.A. SOKOLOV "Kurs teorii VV" (Course on the theory of explosives). During the period of more than twenty years since these books were published, the study of explosions has developed rapidly due to the work of a number of Russian and foreign scientists. Many assumptions made in

/

SNITKO's and SOKOLOV's books are now out of date. A number of important problems which have only been widely studied or solved in recent years are either not discussed at all in these books or are quite inadequately treated in them.

Today, the physics of an explosion, making extensive use of the methods of gas dynamics, theoretical and experimental physics, physical chemistry, etc., is capable of describing analytically a number of complicated phenomena which were formerly only treated qualitatively at the very best. This has led to it being converted into a quite orderly and rigid science embracing a wide circle of extremely important and complicated theoretical and applied problems. In this connection, it became necessary to make a critical generalization of the numerous investigations on the physics of an explosion which are occasionally disconnected and contradictory.

The content and distribution of the material in the present book gives fundamentally a contemporary presentation on the physics of an explosion. Because the book should not only define the level of present-day knowledge attained on a number of problems but should also give their further development in perspective, the authors thought it necessary to explain briefly, with respect to objectives or preliminary investigations, some problems which in their opinion can become of real value in modern science and technology. It can be assumed that in such a form the present book will be useful not only to scientific workers but also to student-physicists and engineers specializing in this interesting branch of science.

The authors, having considered in detail the physical phenomena

occurring during an explosion, do not deal at all herein with the problems of atomic explosion, as they believe that its specific peculiarities should be described in detail in a special monograph. However, some of the laws governing the propagation of impact waves in various media can also be used in the analysis of the effect of an atomic explosion. Considerable attention is paid in this book to the applied problems of gas dynamics of unsteady flows, without which it is impossible to study the problems arising in the physics of an explosion.

The authors would like to draw the attention of the readers to the fact that this is the first attempt in producing a contemporary monograph on the physics of an explosion and consequently may contain a number of errors which we hope the readers will report to us.

Chapters I, II, IV, V, VI, VII, VIII, X were written by F.A. BAUM; Chapters XIII and XIV by K.P. STANYUKOVICH; Chapters III, IX and XV by B.I. SHEKHTER. Chapters XI and XII were written jointly by BAUM and STANYUKOVICH, § 46 by SHEKHTER, § 86 by STANYUKOVICH and BAUM, § 98 and § 87 by BAUM and SHEKHTER and the Appendix was written by STANYUKOVICH.

The authors wish to express their gratitude to M.A. SADOVSKIY, A.S. KOMPANEYTS and G.I. POKROVSKIY for their valuable comments when they examined the manuscript.

Chapter I

General Characteristics of Explosives

§ 1. The phenomenon of an explosion.

An explosion in the wide sense of the word is a process of rapid physical and chemical transformation of a system into mechanical work, accompanied by a change of its potential energy. The work accomplished during an explosion is due to the rapid expansion of gases or vapours independently of whether they already exist or are formed at the time of the explosion.

The most essential sign of an explosion is the rapid jump in pressure in the medium surrounding the place of the explosion. This is the direct reason for the wide-spread effect of an explosion.

Explosions can be produced by various physical or chemical phenomena.

The following examples can be given of explosions due to physical causes:

1. The "explosion" of a steam boiler or bomb containing compressed gas. In the first case the phenomenon is produced by the rapid change of superheated water into a vapour state and in the second case by the increase in pressure of the gas in the bomb. In both cases the explosion arises as a result of overcoming the resistance of the walls of the container, and its destructive effect depends on the pressure of the steam or gas in the container.

2. Explosions caused by powerful spark discharges, for example, lightning or the passage of a high voltage electric current through thin

metallic threads.

In the case of powerful discharges, the difference in potential levels off in a time interval of the order $10^{-6} - 10^{-7}$ sec, thanks to which a colossal energy density is attained in the discharge zone and extremely high temperatures (of the order of tens of thousands of degrees) arise, which in their turn leads to a large increase in pressure of the air at the point of discharge and the spread of an intense disturbance through the surrounding medium.

The explosions of wires under the action of electric energy are caused by the sudden change of the metal into a vapour state; the temperature in this case reaches magnitudes of the order of 20,000°.

Explosions based on such physical phenomena have an extremely limited application and are chiefly the subjects of specialised scientific researches.

We will only consider explosions produced by the processes of chemical transformations of explosives.

Explosives are comparatively unstable systems in the thermodynamical sense, which under the influence of external actions are capable of extremely rapid exothermic transformations, accompanied by the formation of very heated gases or vapours.

The gaseous explosion products due to the exceptionally high rate of the chemical reaction practically occupy the volume of the explosive itself at the first instant and, as a rule, they are in a greatly compressed state, because the pressure at the place of the explosion increases sharply.

From what has been said it follows that the ability of chemical systems to explosive transformations is determined by the three following

factors: the exothermicity of the process, the high rate of its propagation and the presence of gaseous (vapour) reaction products. These properties can be exhibited in explosives to varying degrees; it is only their totality which gives the character of an explosion to the phenomenon.

Let us consider the meaning of each of these factors.

Exothermicity of a reaction. The evolution of heat is the first necessary condition without which the occurrence of an explosive process is generally impossible. If the reaction were not accompanied by heat evolution, then its spontaneous development and, consequently, the self-propagation of the explosion would be excluded. It is evident that substances requiring a constant supply of external energy for their decomposition cannot possess explosive properties.

On account of the thermal energy of the reaction, heating of the gaseous products leads to temperatures of several thousand degrees and to their subsequent expansion. The higher the heat of reaction and the rate of its propagation, then the greater is the destructive power of the explosion.

The heat of reaction is a criterion of the efficiency of the explosive and is its most important characteristic.

For modern explosives which find the widest application in practice, the heat of the explosive transformation fluctuates within the limits of 900 to 1800 kcal/kg.

High rate of the process. The most characteristic feature of an explosion, which distinguishes it sharply from normal chemical reactions, is the high rate of the process. The change to the final explosion products occurs within hundred-thousandths or even millionths of a second.

The high rate of energy evolution defines the advantage of explosives over ordinary fuels. Nevertheless as regard the total energy content referred to an equal quantity by weight, even the most energy-rich explosives do not exceed normal fuel systems, but on explosion they attain an incomparably higher volume concentration or energy density.

This can be seen, for example, from the data given in Table 1.

Table 1.

The heats of explosion and calorific values of some explosives and fuel mixtures.

Explosive or fuel	Heat of explosion or calorific value referred to 1 kg explosive or fuel mixture, kcal
Pyroxylin (13.3% N)	1040
Nitroglycerine	1485
Mixture of benzene and oxygen	2330
Mixture of carbon and oxygen	2130
Mixture of hydrogen and oxygen	3230

The combustion of ordinary fuels proceeds comparatively slowly which leads to a considerable expansion of the reaction products during the process and to an essential dispersal of the energy evolved by means of heat conductivity and radiation. For these reasons only a relatively low energy density by volume in the combustion products is attained in a given case.

Explosive processes, on the other hand, proceed so quickly that it can be considered that all the energy is practically evolved into the space occupied by the explosive itself, which leads to the high energy

concentrations which are not attained under the conditions of the normal course of chemical reactions.

Particularly high energy densities are attained during the explosion of the condensed (solid or liquid) explosives which are strictly the only ones used in practice. This is explained by the fact that these explosives possess a significantly smaller specific volume than the gaseous fuel mixtures (see Table 2).

Table 2.

Volume density of energy of some explosives and fuel mixtures

Name of explosive or fuel mixture	Volume density of energy, referred to 1 l. explosive or fuel mixture, kcal/l
Pyroxylin (13.3% N)	1350
Nitroglycerine	2380
Mixture of carbon and oxygen	4,1
Mixture of benzene vapours and oxygen. .	4,4
Mixture of hydrogen and oxygen	1,7

The numbers given for fuels (carbon, benzene) are calculated on the assumption that the combustion of these substances is completely achieved in the initial volume occupied by the corresponding mixture.

From the given data it is evident that the energy density by volume attainable during the explosion of standard explosives exceeds the energy density for normal fuels by a factor of hundreds or even thousands. This is responsible for the greater power of the explosion and the destructive ability.

It must be noted that an unsatisfactory method of estimating the power

of an explosion is accepted by a number of authors as a graphic indication of the value of the rate of the process under explosive conditions. For a quantitative estimate of the power of an explosion the following relationship is used

$$B = \frac{MQI}{\tau} = \frac{MQID}{l}. \tag{1.1}$$

where B is the power of the explosion, M is the weight of the explosive charge, τ is the time (in sec) of propagation of the explosion through the explosive charge, Q is the heat of explosion in kcal/kg, I is the mechanical equivalent of heat, D is the linear rate of propagation of the explosion and l is the length of the charge.

According to this formula, for a given finite value of Q, the power of the explosion B should increase without bound as the time τ decreases, so that as $\tau \to 0, B \to \infty$.

Formula (1.1) is unsatisfactory because in it the criterion of the power of the explosion i.e. the work capable of producing products of explosion in unit time, is mistakenly taken to be a magnitude proportional to the rate D of the propagation of the explosion through the charge, or the rate of evolution of energy during the explosive decomposition reaction.

We note that the power referred to unit volume of explosion products under the conditions of their free discharge into space should be proportional to ρq^3 where ρ is the density of the explosion products and q is the rate of their discharge into space.

The rapid course of the processes of explosive transformation can be judged on the basis of data concerning the linear rate of propagation of

the explosion through the explosive charge. The maximum rate D of the propagation of the explosion for the modern explosives used in practice fluctuates between the limits 2000 to 9000 m/sec.

Gas formation. The high pressures arising during the explosion and the destructive effect caused by them could not be achieved if the chemical reaction were not accompanied by the formation of a sufficiently large quantity of gaseous products. These products, found at the moment of explosion in an extremely compressed state, are the physical agents which on expansion cause the extremely rapid change of the potential energy of the explosive into mechanical work or the kinetic energy of moving gases.

The volume of gaseous explosion products (calculated under normal physical conditions) of some explosives is given in Table 3.

Table 3.

The volume of explosion products.

Name of explosive	Volume of gaseous explosion products in l.	
	for 1 kg explosive	for 1 l. explosive
Pyroxylin (13.3 N)	765	995
Picric acid	715	1145
Trotyl	740	1180
Nitroglycerine	690	1105

Thus, for 1 l. of normal explosives about 1000 l. of gaseous products are formed, which are under very high pressure at the moment of explosion.

The maximum pressure during the explosion of condensed explosives attains hundreds of thousands atmospheres. Evidently, such pressures

cannot be realised under the conditions of flow of normal chemical reactions.

During the explosion of gaseous systems an increase in volume does not usually occur and in some cases the explosive transformation is even accompanied by a decrease in volume.

An example of such a reaction is the explosion of detonating gas

$$2H_2 + O_2 \rightarrow 2H_2O + 2 \cdot 57{,}8 \text{ kcal.}$$

as a result of which a decrease in volume by one third occurs. However, this decrease in volume is compensated by the exothermicity and high rate of the process, due to which the pressure during explosion does, nevertheless, reach a magnitude of the order of 10 atm.

The value of the gas formation factor can be established by a series of reactions during which gaseous products are not formed. The simplest reaction of this type is the well-known thermite reaction

$$2Al + Fe_2O_3 = Al_2O_3 + 2Fe + 198 \text{ kcal.}$$

which occurs, as a rule, without explosion in spite of the fact that the thermal effect of the reaction is sufficient for the heating of the end products (Fe, Al_2O_3) to 3000°, at which they are in a liquid state. Under the ignition conditions of large quantities of a thermite mixture phenomena sometimes occur which are reminiscent in their character of a normal explosion. Analysis of such explosions leads to the conclusion that they are mainly due to secondary phenomena connected with the heating and expansion of the surrounding air and also the air included in the porous mass of the thermite mixture. Moreover an extremely rapid combustion of the pulverized powder-forming aluminium can also partially occur due to

the oxygen in the air. In this case one of the reaction products - Al_2O_3 - will be found partially in the vapour state.

In contrast to thermite and other similar mixtures we also have a number of substances which possess all the characteristic properties of explosives, in spite of the fact that during their decomposition they form products which are found in a solid state under normal conditions.

A typical example of such substances is silver acetylide which readily explodes according to the following scheme:

$$Ag_2C_2 \rightarrow 2Ag + 2C + 87 \text{ kcal.}$$

It is evident that silver should behave as a monoatomic gas under the temperature conditions of the reaction.

Thus, on the basis of the qualitative laws established by us, it can be concluded that only the simultaneous combination of the three basis factors - exothermicity, high process rate and gas formation - can guarantee that the phenomenon possesses the joint properties giving it the character of a normal explosion.

§ 2. Classification of explosive processes.

Depending on the conditions of initiation of the chemical reaction, the character of the explosive and some other factors, the processes of explosive transformation can be propagated at a varying rate and can possess essential qualitative differences.

As regards the character and rate of their propagation, all the explosive processes known to us are divided into the following basic types: combustion, explosion and detonation.

The processes of combustion proceed comparatively slowly and at a changeable rate - usually ranging from fractions of a centimetre to several metres per second. The combustion rate varies essentially with the external pressure and increases noticeably with increase of the latter.

In the open air this process proceeds relatively sluggishly and is not accompanied by any significant sound effect.

In a confined space the process proceeds much more energetically and is characterised by a more or less rapid increase in pressure and by the ability of the gaseous combustion products to produce the energy needed to propel a projectile similar to that which occurs during the firing of a gun. Combustion is the characteristic form of the explosive transformation of powders.

In comparison with combustion, explosion is a qualitatively different form of propagation of the process.

The distinguishing qualities of an explosion are: a rapid jump in pressure at the site of explosion and a changing rate of propagation of the process measurable in thousands of metres per second and depending comparatively little on external conditions. The action of an explosion is characterised by sharp impact of gases on the surrounding medium causing crushing and severe deformation of objects at comparatively small distances from the place of explosion.

Detonation is an explosion propagated at a constant rate which is the maximum possible for the given explosive and the given conditions and which exceeds the speed of sound in the given substance. Detonation does not differ from an explosion in the character and nature of the phenomena but it represents its stationary form.

Best Available Copy

The detonation rate under given conditions for each explosive is completely determined by a constant which is one of its most important characteristics. Under the detonation conditions the maximum destructive effect of an explosion is attained.

The processes of explosion and detonation differ essentially from the processes of combustion with respect to the character of their propagation: combustion transmits to the mass of the explosive by means of thermal conductivity, diffusion and radiation, whilst explosion and detonation are propagated by means of the compression of the substance by a shock wave.

More detailed characteristics of the various forms of explosive transformation will be given in the following chapters.

§ 3. Classification of explosives.

Today an enormous number of explosives are known which differ widely both with respect to composition and to their physico-chemical and explosive properties. Because of this, it is necessary to classify them systematically for convenience of investigation.

All explosives can be divided into two basic groups: explosive chemical compounds and explosive mixtures.

Explosive chemical compounds are relatively unstable chemical systems capable of rapid exothermic transformations under the action of external influences, as a result of which there occurs complete rupture or the intramolecular bonds and the subsequent recombination of the free atoms (or ions) into thermodynamically stable products.

The majority of explosives of this group are oxygen-containing organic compounds capable of partial or complete intramolecular combustion.

There are, however, quite a number of explosive endothermic compounds not containing oxygen which under explosion conditions decompose into their basic elements. An example of this type of compound is lead azide which decomposes on explosion into free nitrogen and lead with an evolution of energy equal to the heat of formation of this azide from the elements.

Such compounds, as a rule, possess quite an unstable molecular structure and high sensitivity to external actions, which greatly limits and frequently excludes the possibility of their practical use.

As an example of such particularly unstable compounds we can quote the halogen and sulphur compounds of nitrogen, such as: NCl_3, NHI_2, N_2S_4, which readily explode as a result of negligible mechanical influences.

The instability of explosive compounds, according to VAN'T HOFF, is due to their containing molecules possessing special so-called explosophoric atom groupings which include:

C ≡ C group, present in acetylene derivatives,

N - X group, in halogen compounds of nitrogen,

N = N group, in azides, diazo compounds, tetrazoles,

N = C group, in salts of fulminic acid or fulminates,

N = O group, in nitrates and nitro compounds,

O - O group, in peroxides and ozonides,

O - Cl group, in chlorates and perchlorates.

Explosive mixtures are systems containing at least two components unconnected with one another chemically. Usually one of the components of

the mixture is a substance which is relatively oxygen-rich, and the second component, on the other hand, is a combustible substance which either contains no oxygen whatsoever or contains it in a quantity insufficient for complete intramolecular oxidation.

Explosive mixtures are either gaseous, liquid, solid or heterogeneous systems.

Gaseous mixtures have no practical application in explosive technology due to the low energy density obtained during their explosion. Gaseous mixtures are, however, of great scientific interest. Their investigation has led to vital results in the study of the propagation processes of an explosion and also in the mechanism and kinetics of explosive reactions.

Gaseous mixtures which are dangerous as regards explosions are frequently encountered under different practical conditions. Thus, in coal-mines fire-damp which is a mixture of methane and air is often formed.

The combustible components of liquid explosives are usually substances which burn with a large thermal effect, such as benzene, toluene, mono-nitro compounds. As oxidizers fuming nitric acid and tetranitromethane are frequently used.

Such liquid mixtures are quite powerful explosives but in practice they are rarely used because of their high sensitivity and unsuitability for application.

Solid explosive mixtures are very numerous and find a wide application both in the civil and military spheres. Depending on the chemical nature of the oxidizing agent in their composition, these mixtures can be divided into appropriate sub-groups the most important of which are the ammonium-

Best Available Copy

nitrate explosives or ammonites. The basic component of these substances is ammonium nitrate NH_4NO_3 the content of which varies from 40 to 95% in the different compositions. As combustible component, use is made of the various nitro-aromatic explosive compounds (Trotyl, dinitrobenzene, etc.) which contain insufficient oxygen to form the products of complete combustion.

In the simplest ammonites the combustible components are such substances as coal, sawdust and various resins. Examples of ammonites are asphaltite (95% NH_4NO_3, 5% asphalt) and Amatol (80% NH_4NO_3, 20% Trotyl). Ammonites are used extensively for civilian applications and are convenient substitutes for basic explosives in war-time.

Dynamites, smokeless powders and explosive alloys occupy the chief place among explosive systems. The basic explosive component of dynamites is nitroglycerine. To the dynamite group belong:

a) nitrogelatin of composition: 93% nitroglycerine and 7% colloxylin;

b) gelatin-dynamites: 62-63% nitroglycerine, 27-25% potassium nitrate, 2-3% colloxylin and 8% absorber;

c) powder-forming dynamites or grisoutine compositions: 29-30% nitroglycerine, 0.8-1.0% collodion cotton, 69.5 - 68.5% ammonium nitrate, up to 0.8% soda or chalk.

The smokeless powders are systems which have cellulose nitrates as the basic explosive component. Some types of smokeless powders contain, moreover, nitroglycerine or other explosives as well.

Explosive substances and explosive systems can be divided into four groups with respect to the basic fields of their application:

1) initiating explosives,

2) high explosives,

3) missile explosives or powders,

4) pyrotechnical compositions.

Initiating explosives. These are employed as initiators of explosive processes to stimulate detonation of the basic explosives, for example, to stimulate detonation in shells, mines, aerial bombs, blasting media, etc.

The distinguishing properties of initiating explosives are:

a) the ability to explode in the form of detonation under the influence of insignificant external thermal or mechanical actions;

b) their explosive transformation is characterized by the fact that the period of increase in its rate up to a maximum is very small, incomparably less than in explosives of other types. In some initiating substances as, for example, in lead azide, the period of acceleration of the process is practically absent, i.e. the process immediately changes into the detonating form independently of the dimensions of the charge.

Thanks to this it requires only an extremely small charge of initiator to stimulate explosion of high explosives.

Initiating explosives are used pre-eminently in the form of capsule-detonators (c-d). Some initiating explosives are used in compositions destined for equipping capsule-igniters (c-i).

The most important representatives of this group of explosives are:

1. The salts of heavy metals of fulminic acid or the so-called fulminates. Of these mercury fulminate $Hg(ONC)_2$ is the most important.

2. Salts of hydrazoic acid or azides. The most widely used is lead azide, PbN_6.

The initiating explosives also include some organic azides, for example, cyanurictriazide, $C_3N_3(N_3)_3$.

3. Salts of heavy metals of styphnic acid. Their most important representatives are lead styphnate or trinitroresorcinate $C_6H(NO_2)_3O_2Pb.H_2O$.

4. Carbides of heavy metals or acetylides, for example, silver acetylide Ag_2C_2.

5. Initiating mixtures employed as detonating or igniting compositions (the latter consist mainly of mercury fulminate, potassium chlorate and antimony trisulphide) are used in c-i and c-d.

The initiating explosives of practical interest also include tetrazene $C_2H_8ON_{10}$, which is a derivative of an unsaturated nitrogen-hydrogen compound N_4H_4, and some nitro-aromatic diazo-compounds, for example, diazodinitrophenol.

Because of their ability to detonate directly under the influence of external actions, initiating explosives are sometimes called primary explosives.

<u>High explosives</u> are employed as explosive charges for various munition and blasting purposes. In contrast to initiating explosives, they possess considerably greater stability. Their detonation is produced under the influence of relatively large external actions, usually with the help of initiating explosives. Because of this, in contrast to the initiating explosives, they are sometimes called secondary explosives. Their basic form of explosive transformation is also detonation, but during the stimulation of an explosion the period of rate increase of the process up to a maximum is considerably longer for high explosives than for initiating

explosives.

The most important representatives of explosive compounds of this group are:

1. Nitrates or esters of nitric acid. The most important of them are nitroglycerine (glyceryltrinitrate) $C_3H_5(ONO_2)_3$, PETN (pentaerythritol tetranitrate) $C(CH_2ONO_2)_4$, cellulose nitrates e.g. $C_{24}H_{29}O_9(ONO_2)_{11}$.

2. Nitro-compounds. Of the huge number of these compounds, the most widely used are nitro-compounds of the aromatic series, mainly trinitro-derivatives. Among them are:

Trotyl (trinitrotoluene) $C_6H_2(NO_2)_3CH_3$,

picric acid (trinitrophenol) $C_6H_2(NO_2)_3OH$,

Tetryl (trinitrophenylmethylnitramine) $C_6H_2(NO_2)_3N \begin{cases} CH_3 \\ NO_2 \end{cases}$

Of the non-aromatic nitro-compounds, note must be made of:

Hexogen (trimethylenetrinitramine) $C_3H_6O_6N_6$,

nitroguanidine $HN = C \begin{cases} NH_2 \\ NHNO_2 \end{cases}$

tetranitromethane $C(NO_2)_4$.

The most important representatives of the explosive mixtures belonging to this group are ammonites, dynamites and also some alloys, for example the alloys of Trotyl with Hexogen, etc.

Missile explosives or powders.

Powders are mainly used for missile purposes. Their basic form of explosive transformation is rapid combustion.

They are divided into two groups:

a) powders of mechanical mixtures and

b) powders of nitrocellulose or smokeless powders.

An example of the first sub-group is smoky powder, consisting of 75% potassium nitrate, 15% wood charcoal and 10% sulphur.

Nitrocellulose powders, depending on the nature of the solvent, can be used for gelatinisation of their basic component, nitrocellulose, and are divided into several groups:

a) powders in a volatile solvent or pyroxylin powders containing up to 98% of pyroxylin, hydroxy-ether solvent, diphenylamine and moisture;

b) powders in a low-volatility solvent or ballistites, in which nitroglycerine, nitrodiglycol and such like substances serve as solvent of pyroxylin. Ballistites are prepared from the so-called soluble pyroxylin and contain up to 40% nitroglycerine, in which this form of pyroxylin is dissolved, and up to 15% of other additives.

c) Powders in a mixed solvent or cordites are prepared from the so-called insoluble pyroxylin; they contain up to 60% nitroglycerine and as an additional solvent up to 1.5% acetone and some other additives.

d) Powders in a non-volatile solvent, in which such explosives as Trotyl, dinitrotoluene etc. are used to prevent pyroxylin gelatinising.

As regards the categories of explosives, reference should also be made to pyrotechnic compositions, which under known conditions are capable of detonation and possess a comparatively high sensitivity to external actions. Pyrotechnic compositions, as a rule, are mechanical mixtures of inorganic oxidizers with organic and metallic fuels and cementing additives. The basic form of the explosive transformation of these mixtures is combustion.

Chapter II

SENSITIVITY OF EXPLOSIVES TO EXTERNAL INFLUENCES

§ 4. Initial or initiating impulse.

Explosives, depending on the composition, possess greater or smaller ability to withstand external influences without undergoing explosion i.e. spontaneously developing chemical transformation.

The smaller the influence necessary to stimulate explosive transformation in a substance, then the greater is its sensitivity.

A characteristic corresponding to this sensitivity of explosives to external influences is the magnitude of the initial or initiating impulse which is required to excite explosion in them under given conditions.

Various forms of energy can be used as the initial impulse: mechanical, thermal and electrical energy, the energy of radiation and also the energy of another initiating explosive.

The quantity of energy necessary to stimulate explosion even for one and the same explosive in a given state is not a strictly constant magnitude and can fluctuate appreciably depending on the form of the initial impulse and the character of the transmission of the influence to the explosive.

Thus, for example, under the conditions of rapid heating of the explosive achieved at high temperatures, initiation of the explosion can be attained at considerably less expenditure of energy than under the

conditions of slow heating achieved at lower temperatures.

During the slow compression of some explosives possessing relatively low sensitivity, an explosion cannot be produced even in the case when the quantity of work done during the compression is large and extremely high pressures are attained, whilst under conditions of sudden shock the initiation of an explosion in corresponding explosives can be produced for considerably less expenditure of energy. According to BRIDGMAN's data, Trotyl under conditions of static compression does not explode even at pressures of the order of 50,000 atm. or higher.

Moreover, the form and magnitude of the initial impulse affects essentially the character and development of the explosive processes. Thus, for example, under the action of a heat pulse combustion of an explosive is obtained under certain conditions only, whilst under the influence of an impact and particularly that of the explosion of an initiating explosive its detonation is pre-eminently attained.

In order to produce initiation of an explosion, it is primarily necessary that the initial impulse be applied to the explosive charge under conditions under which sufficiently high concentrations of energy will be attained even if only in a localised zone of the system. Particularly high concentrations of energy naturally arise during the stimulation of an explosion by means of initiating explosives, which have been extremely widely used in explosives technology because they possess this property.

There is no rigid equivalence between the various forms of initial impulse with respect to the results of their action on one and the same

explosive. Thus, for example, lead azide is more sensitive to mechanical influences than to a thermal impulse, whilst the picture is the reverse for lead styphnate.

A chlorine-hydrogen mixture ($Cl_2 + H_2$) is passive to a heat pulse, but easily explodes under the action of light rays, which excite an intensive photo-chemical chain reaction in the gas.

The selectivity of explosives towards their response to an external impulse is determined by the combined manifestation of those of their chemical and physical properties which can influence essentially the conditions of consumption of energy by the substances and the stimulation in them of a chemical reaction by some initiating impulse.

§ 5. Sensitivity of explosives to heat pulses.

A measure of the sensitivity of an explosive to a heat pulse is usually given by the explosion temperature established for quite definite experimental conditions.

The explosion temperature is the temperature to which a given quantity of explosive should be heated to obtain its ignition, during which the chemical transformation of the substance is accompanied by a greater or lesser sound effect.

To secure explosion it is necessary to increase the heat supply specified by the course of the chemical reaction so that it exceeds the heat losses due to conductivity and radiation of heat.

Explosion occurs at the moment when the rate of the process reaches some critical value corresponding to explosive conditions.

Thus, on heating an explosive the explosion temperature is always preceded by a period of acceleration of the chemical reaction. The interval of time between the commencement of heating and the moment of explosion of the explosive is called the induction period or the ignition time lag.

For explosive substances the connection between the ignition time lag and the explosion temperature is expressed by the law which was first obtained by N.N. SEMENOV:

$$\tau = Ce^{\frac{E}{RT}}, \qquad (5.1)$$

where τ is the ignition time lag in sec, E is the activation energy of the explosive appropriate for an explosive reaction in cal/mole, R is the gas constant equal to 1.986 cal/mol deg.; C is a constant dependent on the composition of the explosive; T is the explosion or ignition temperature in degrees Kelvin.

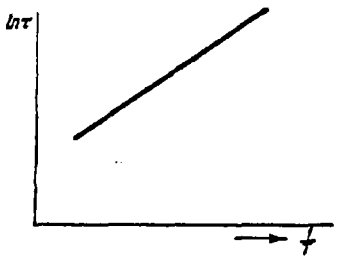


Fig.1. Variation of ignition time lag with temperature.

From this expression it is evident that on decrease of the activation energy E and on increase of the ignition temperature T, the ignition time lag τ decreases rapidly. The variation (5.1) can be conveniently presented in the logarithmic form

$$\ln \tau = \ln C + \frac{E}{RT}.$$

From this expression it follows that between $\ln \tau$ and $\frac{1}{T}$ there exists a linear dependency (Fig. 1), which has been confirmed experimentally for the majority of the explosives investigated.

The slope of the straight line on this graph equals $\frac{E}{R}$. Thus, on the basis of experimental data concerning explosion temperatures it is possible to determine E which is an important characteristic for explosives.

The explosion temperature of an explosive is not a strictly constant magnitude, but varies essentially with the experimental conditions: the quantity of tested explosive, its degree of pulverisation, the methods of testing and other factors determining the conditions of heat supply and auto-acceleration of the reaction. Because of this, in order to obtain comparable results the tests must be carried out under strictly defined, standard conditions.

In determining explosion temperatures of condensed explosives, the following two methods are most widely used:

1) A given quantity of explosive at a certain initial temperature is heated at constant rate. In this way the temperature is determined at which ignition occurs. The explosion temperature thus obtained depends mainly on the initial temperature of the explosive and becomes higher as the rate of heating increases. This method is in wide-spread use for practical tests on explosives.

2) The second method consists of establishing the relationship between the change in ignition time lag and the temperature; experimental results are usually expressed in the form of a graph (Fig. 2). This method which permits the response of an explosive to a heat pulse to be

characterized more precisely and completely is used pre-eminently in research and much more rarely for routine tests on explosives.

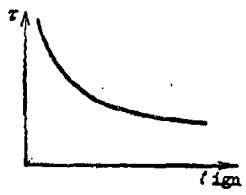


Fig. 2. Variation of ignition delay with temperature.

For every explosive, under corresponding experimental conditions, there exists a temperature below which ignition generally does not occur however long the explosive is heated. This is explained as follows.

The process of thermal decomposition of an explosive can be divided into three periods: the induction period connected with the formation of the initial centres of reaction, the period of auto-acceleration of the reaction and the period of its extinguishment.

At sufficiently high heating temperatures the induction period is small; as a result of auto-acceleration of the reaction its rate can attain a critical value v_{cr}, corresponding to the commencement of ignition in the presence of a sufficient quantity of as yet undecomposed material.

If, however, the heating temperature of the explosive is below a certain limit and the reaction rate increases too slowly as a result, then the initial explosive is depleted sooner than the critical value of the reaction rate v_{cr} is attained. In this case because of the unfavourable relationship between the external heat supply and the heat losses, auto-acceleration of the reaction can indeed not occur. From this it can be concluded that the explosion temperature up to a known limit should

depend on the quantity of explosive undergoing heating, that is, it should decrease somewhat on increase in the quantity of explosive.

According to PATRY's investigations for 1 g. mercury fulminate the explosion temperature equals 128°; for 10 g. it is 115°C; the ignition time lag exceeded 7 hours.

The minimum explosion temperatures for some explosives are given in Table 4 (weight of explosive = 0.05 g.).

Table 4.

Explosion temperatures of some explosives

Name of explosive	Explosion temperature, t°C	Ignition time lag, τ sec
Trinitrotoluene	275	423
Trinitrophenol	275	143
Trinitroxylene	300	240
Trinitroresorcinol	245	31
Trinitrophloroglucine	200	18
Trinitrophenylnitramine	87	85
Tetryl	180	40
Trinitrophenolethylnitramine	160	25

The minimum explosion temperatures of explosives are of interest mainly from the point of view of problems connected with safety techniques. At the same time, however, it must be remembered that on increasing the mass of the heated explosive the minimum explosion temperature can be considerably lower than in laboratory experiments due to the changed conditions of heat supply.

Of the physical properties of explosives the most essential quantity for processes of thermal initiation is their volatility.

The conditions of ignition and the explosion temperature depend to a large extent on the ratio of the rate of the chemical reaction to the rate of the vaporization (sublimation) of the explosive. The value of this factor for explosive processes was first established by BELYAEV.

If the quantity of explosive is small and it possesses high volatility, then the substance can be completely consumed in the heating process by means of sublimation or vaporization sooner than the necessary conditions for the vigorous auto-acceleration of the reaction are attained.

Thus, for trinitroaniline and trinitrophenylenediamine each taken in a quantity of 0·05 g, it was not possible to detect ignition even at temperatures exceeding 600°C. On increasing the quantity to 0·1 g, ignition was attained under the following conditions: for trinitroaniline at τ = 2·8 sec, t = 500°C; for trinitrophenylenediamine at τ = 11·2 sec, t = 520°C.

On decreasing the temperature below 500°C for trinitrophenylenediamine, ignition could not be attained because of the decrease in the reaction rate and the value prevailing for the volatility factor at these temperatures.

It is evident that at higher pressures the volatility of the explosive will decrease noticeably and at sufficiently high pressures will be almost completely eliminated.

In some cases during the practical application of explosives, the initiation of the explosion is achieved by extremely brief heat pulses (for example, during the transmission of an explosion from a capsule-igniter to a capsule-detonator), during which the ignition time lag does not exceed thousandths or even ten-thousandths of a second.

The conditions of ignition and the explosion temperature depend to a large extent on the ratio of the rate of the chemical reaction to the rate of the vaporization (sublimation) of the explosive. The value of this factor for explosive processes was first established by BELYAEV.

If the quantity of explosive is small and it possesses high volatility, then the substance can be completely consumed in the heating process by means of sublimation or vaporization sooner than the necessary conditions for the vigorous auto-acceleration of the reaction are attained.

Thus, for trinitroaniline and trinitrophenylenediamine each taken in a quantity of 0·05 g, it was not possible to detect ignition even at temperatures exceeding 600°C. On increasing the quantity to 0·1 g, ignition was attained under the following conditions: for trinitroaniline at τ = 2·8 sec, t = 500°C; for trinitrophenylenediamine at τ = 11·2 sec, t = 520°C.

On decreasing the temperature below 500°C for trinitrophenylenediamine, ignition could not be attained because of the decrease in the reaction rate and the value prevailing for the volatility factor at these temperatures.

It is evident that at higher pressures the volatility of the explosive will decrease noticeably and at sufficiently high pressures will be almost completely eliminated.

In some cases during the practical application of explosives, the initiation of the explosion is achieved by extremely brief heat pulses (for example, during the transmission of an explosion from a capsule-igniter to a capsule-detonator), during which the ignition time lag does not exceed thousandths or even ten-thousandths of a second.

570°C which is of the same order of magnitude as the temperature given above for this explosive.

Nevertheless it must be noted that, generally speaking, extreme care must be taken in using such methods of extrapolation for the following reasons:

a) the possibility cannot be excluded that a change can occur in the very character of the chemical decomposition of the explosive on transfer from lower temperatures to higher temperatures;

b) under standard conditions of testing explosives for sensitivity to a heat surge we identify the ignition temperature of the explosive with the temperature of its heat source which for very small ignition delays ($\tau < 10^4$ sec) cannot be considered correct (the actual temperature to which the explosive is heated will, of course, be noticeably lower).

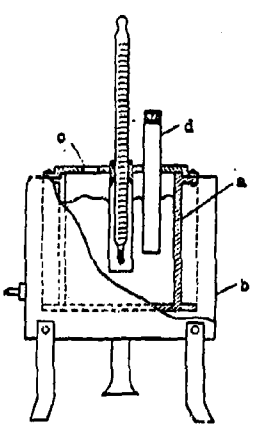


Fig. 3. Apparatus for determining explosion temperature.

To determine the explosion temperatures of explosives, devices of various construction are employed. Most frequently, tests are carried out with the apparatus presented schematically in Fig.3.

It consists of a metallic cylindrical bath, a, filled with Wood's alloy. Heating is achieved by means of an electric current with the help of a nichrome coil. The temperature of the bath is regulated by means of rheostats. To decrease heat

transfer and for convenience of working, the bath is surrounded by a brass jacket, b, leaving an air clearance between the bath and the jacket.

The top of the bath is covered by an iron lid, c, with orifices; through the central orifice passes a thermometer embedded in the alloy and protected from the effects of the explosion by a metal case; the other orifices are used for the passage into the bath of special cartridge cases containing explosive, d. The charge is normally 0.05 g.

The determinations are carried out according to one of the following methods.

1. A cartridge charged with explosive and plugged with a stopper, is introduced into the bath previously heated to 100°. Immediately after the insertion of the cartridge the bath temperature is increased uniformly at the rate of 20° per minute and the temperature is noted at which ignition occurs.

2. The bath is heated to a definite temperature close to the expected explosion temperature; the charged cartridge is embedded in the alloy to a determined depth and the time elapsing until ignition occurs is recorded. By means of a series of experiments it is possible to establish within an accuracy of 5° the least temperature below which ignition does not occur when the test is continued for a definite period of time (5 min. or 5 sec).

This temperature is also taken to be nominally the explosion temperature of the explosive.

3. In some cases the test on the explosive is carried out in sealed glass ampoules which makes it possible to change the explosive during the period of test. A special glass apparatus (illustrated in Fig. 4) was

proposed by KOSTEVITCH for this purpose.

Explosion temperature data for the most important explosives are given in Table 5 (delay time 5 min).

To determine the explosion temperatures of explosives for very small ignition delays, BOWDEN and YOFFE employed the method of rapid adiabatic compression of air over the explosive. In this case the minimum degree of compression of the gas was determined at which explosion occurred for a given quantity of explosive.

From the results of these experiments the corresponding temperatures were calculated using the well-known relationship

$$T_1 = T_0\left(\frac{v_0}{v_1}\right)^{\gamma-1},$$

where v_0 is the initial volume of gas, v_1 is the final volume of

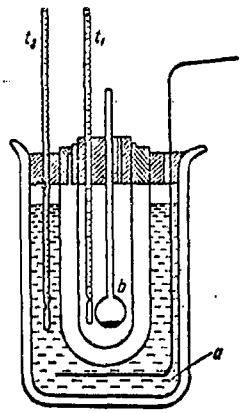


Fig.4. KOSTEVITCH's apparatus for explosion temperature determination;
t_1, t_2 - thermometers,
a - bath,
b - ampoule loaded with explosive.

Table 5

The explosion temperature of some explosives

Name of explosive	Explosion temperature, °C	Name of explosive	Explosion temperature, °C
Mercury fulminate	175—180	Tetryl	190—200
Lead azide	315—330	Hexogen	225—235
Silver azide	310—320	PETN	210—220
Lead styphnate	270—280	Xylyl	315—330
Pyroxylin	185—195	Amatol	220
Nitroglycerine	200—205	Smokeless gunpowder	180—200
Trotyl	300—310	Smoky gunpowder	290—310
Picric acid	295—310		

gas under the conditions of its compression, γ is the adiabatic index, T_0 and T_1 are the initial and final temperatures in °K. The data obtained are given in Table 6.

Table 6.

Explosive	Ignition delay, microsec	Explosion temperature, °C
Nitroglycerine	150	450—480
PETN	—	460—500
Lead azide	10	570—600
Tetrazene.	5	400—450

§ 6. Impact sensitivity of explosives.

Tests on the impact sensitivity of explosives are carried out by means of drop-hammer machines.

The basis of the test is to determine the energy of the impact necessary to obtain either explosions alone or failures alone or a definite proportion of the two.

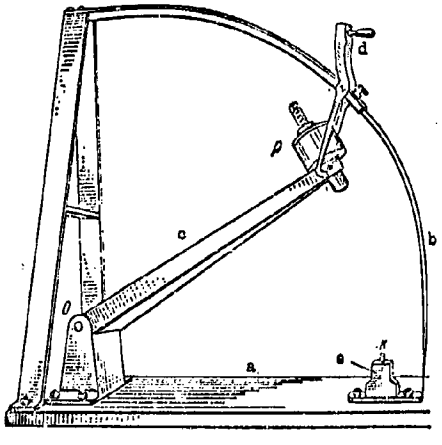


Fig. 5. Arc drop-hammer machine.

In testing initiating explosives possessing particularly high impact sensitivity, an arc drop-hammer machine is usually used (Fig. 5).

It consists of an iron base, a, with a steel anvil, a graduated measuring arc, b and a load, p, attached to the end of the rotating

arm, c. The load is maintained at a certain height by a hinged supporting arm, d, which can travel along the arc and is attached to it by a clamp. On the anvil there is a guide block, e, for a steel striking pin, k, with a flat.

A definite quantity of explosive (usually 0.02 g) is compressed under pressure (500 or 1000 kg/cm^2) into the brass cap of a capsule of a pistol cartridge and covered with foil (Fig. 6). The capsule is installed by means of a special centreing bracket at the centre of the anvil under the flat of the striking pin.

The sensitivity of the initiating explosives to impact is taken to be characterised by the upper and lower limits of sensitivity i.e. the minimum drop height H of the load at which 100% explosions are obtained for a definite number of tests (usually not less than ten) and the maximum drop height of the load at which 100% failures are obtained for the same number of tests.

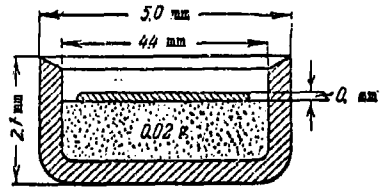


Fig. 6. Capsule.

The upper limit of sensitivity H_{100} defines the condition of "no-failure" of the capsule and the lower limit H_0 the condition for handling it without danger.

Whilst testing initiating substances or products from them, the upper and lower limits are sometimes supplemented by the construction of a complete curve of sensitivity, the general character of which is shown in Fig. 7.

In testing the less sensitive high explosives a vertical impact

machine is usually used (Fig. 8). It consists of two vertical and strictly parallel guides, a, between which a load, b, can move freely. The weight of the load is chosen according to the sensitivity of the explosives being investigated. The load is fitted with a small head, c, which is fixed between the grips of a release clamp, d. The latter slides along a special guide and together with the load can be fixed at any required height. Below, on the fixed base, there is a massive steel anvil, e, on which are placed the devices containing the explosive to be investigated.

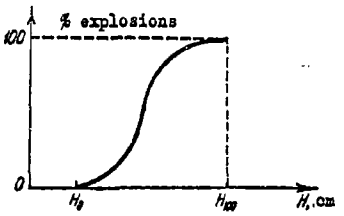


Fig. 7. Curve of impact sensitivity of initiating explosives.

Today, plunger devices are widely used (Fig. 9). The plunger device consists of an anvil and face, for which standard steel roller bearings are used (d = 10 mm, h = 10 mm), guide sleeve and a base. In working with this device the quantity of explosive used is 0.05 g.

To obtain the required results on impact sensitivity in testing explosives it is necessary, above all, to maintain identical experimental conditions. Special attention should be given to the quality of the plunger devices; the clearances between the face, the anvil and the sleeve should be completely determined.

The drop height of the load in tests should not exceed the limit at which residual deformation arises in the elements of the system; other-

wise the experimental conditions become indeterminate.

The sensitivity of high explosives to impact is most frequently characterised by one of the following methods:

1. The determination of the percentage of explosions obtained on dropping the weight from a definite height. The standard test conditions are: the weight of the load P = 10 kg and its drop height H = 25 cm (or P = 2 kg and H = 50 cm). The results of the determinations for some explosives are given in Table 7.

2. The determination of the critical energy of impact $(K_{50} = PH)$, corresponding to 50% probability of explosion.

Many investigators (SOKOLOV, URBANSKIY, WELLER, TAYLOR, etc.) adhere to the opinion that in estimating the impact sensitivity of an explosive it is necessary to subtract from the total impact

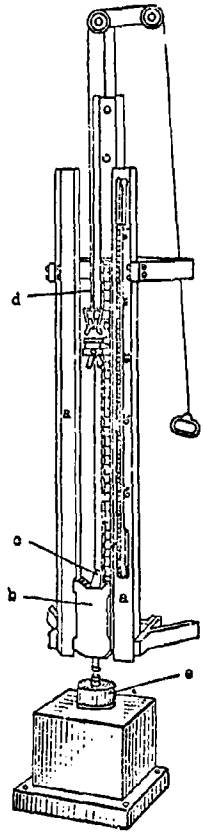


Fig. 8. Vertical drop-hammer machine.

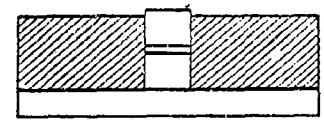


Fig. 9. Plunger device

energy that part which is consumed by the rebound of the load and in this

Table 7.

Impact sensitivity of high explosives

The tests were carried out with samples of high-purity explosives (P = 10 kg, H = 26 cm).

Name of explosive	Number of explosions in 100 tests	Name of explosive	Number of explosions in 100 tests
Trotyl	4—8	Styphnic acid	64
Trinitrophenol	18	Hexogen	75—80
Trinitroxylyl	22	PETN	100
Trinitrocresol	34	Amatol 80/20* . . .	16—18
Tetryl	45—55		

connection recommend as a characteristic of the sensitivity of an explosive the magnitude

$$K_{50} = P(H - H_0) = PH(1 - \alpha), \qquad (6.1)$$

where H_0 is the rebound height of the load and $\alpha = \frac{H_0}{H}$.

Rebound of the load occurs due to the elasticity of the material of the weight, the plunger devices, the anvil, etc.

In determining the impact sensitivity of an explosive it is not possible to guarantee the strict maintenance of identical experimental conditions, since in repeated tests explosions and failures are distributed

* 80/20 signifies that the composition of amatol is 80% ammonium nitrate and 20% trotyl.

statistically according to the law of errors. The experimental errors decrease appreciably with increase in the number of impacts.

Research has shown that if a sufficiently large number of tests is carried out at each height, then the sensitivity curve constructed directly on the basis of experimental data coincides almost completely with the distribution curve calculated on the basis of probability laws.

Accepting the magnitude K_{50}, according to formula (6.1), as the criterion for the sensitivity of an explosive, some investigators (MURAOUR, TAYLOR, YUILL, etc.) assumed that this part of the energy during impact is completely, or almost completely, consumed in the explosive contained in the plunger device. However it is not difficult to prove that the magnitude K_{50} does not represent the proportion of energy which is responsible for the excitation of an explosion.

The total energy balance on dropping the load into an uncharged device can be represented in the following way to a sufficient approximation:

$$K = K_1 + K_2,$$

where $K = PH$ is the energy acquired by the load at the moment of impact, K_1 is the irreversible loss of energy in the impact machine system, K_2 is the energy of elastic deformation of the plunger devices and the metallic elements of the machine.

The energy of the elastic deformation of metal K_2 is consumed in the rebound of the load, i.e.

$$K_2 = PH_0.$$

On testing the explosive in a standard case the height of the load

rebound can be quite large.

According to our experiments, when a load of 10 kg is dropped from various heights onto an uncharged plunger device the magnitude H_0 changes as shown in Table 8.

Table 8.

Drop height and load rebound

H, cm	H_0, cm	$a = \frac{H_0}{H}$
15	7.0	0.47
20	9.5	0.47
25	12.0	0.48
30	14.5	0.48
35	18.0	0.51
40	21.0	0.52
45	24.0	0.53
50	26.8	0.54
60	32.0	0.53

From these data it is evident that the ratio H_0/H for a given construction of machine and plunger device has an average value 0.5 and on increase in the drop height of the load it increases somewhat. However at sufficiently large values of H the magnitude H_0 begins to decrease appreciably which is connected with the additional irreversible energy consumption in the plastic deformation of the metal.

Thus it is possible to conclude that in the absence of an explosive the energy losses in the system amount on an average to about 50% of the total impact energy.

When the load drops on a device charged with explosive, the total

energy balance will be

$$K = K_1' + K_2' + K_3',$$

where K_1' is the irreversible energy loss in the impact machine system; K_2' is the energy of elastic deformation; K_3' is the energy absorbed by the explosive.

Experiment shows that for devices charged with explosives the load rebound height H_0' differs only insignificantly from H_0 the rebound height in the absence of explosive. Thus, for standard test conditions (P = 10 kg and H = 25 cm), $(H_0 - H_0')$ amounts in all to only 1.5 - 2.0 cm.

This fact implies that a negligible part only of the impact kinetic energy is absorbed by the explosive itself. The predominant portion of the energy, just as in the absence of explosive, is used up in the load rebound and the irreversible losses in the impact machine system. Under standard test conditions the thickness of the explosive layer in the compressed state is of the order of 0.1 mm, because K_1' should be only insignificantly less than K_1 .

Thus, it must be concluded that $K_{50} = P(H - H_0')$ does not represent the portion of the energy which is dissipated in the explosive itself and should be of the same order as K_1

Because of this, K_{50} as a quantitative measure of sensitivity is an extremely nominal magnitude and can only serve as a characteristic for comparing explosives under given test conditions. On changing the construction and the characteristics of the impact machine and plunger devices the relationship between K_1' and K_2' and consequently the

magnitude K_{50} will essentially change, which is the fundamental reason for the absence of proper agreement between the data on the sensitivity of explosives derived by various authors.

The energy K_3 absorbed on impact in the explosive itself cannot be determined exactly and therefore cannot be used directly as a criterion of the sensitivity of the explosive.

The critical conditions under which it is possible to initiate an explosion will depend not only on the total quantity of energy absorbed by the substance during impact but also on the maximum stresses, arising in the explosive, under the influence of which movement of the particles, plastic deformation, flow of explosive through the clearances and other phenomena leading to its heating occur. On increasing these stresses the temperature of the foci of heating will increase and the probability of explosion, as a rule, increases even in the case when the energy of absorption of the explosive does not increase.

The stresses arising in an explosive upon impact in a drop-hammer machine can easily be determined from data on the energy of elastic deformation K_2'.

In the calculations it is possible to neglect the elastic deformation of the main impact machine and load, because the compression in them will be considerably less than in the cylinders since the stresses in them are spread over an incomparably larger area

According to the theory of elasticity it is sufficiently accurate to take

$$K_2' = \frac{v_{max}^2 ls}{2E_{red}}, \qquad (6.2)$$

where σ_{max} is the maximum stress arising in the metal of the cylinders, l is the height of the cylinders, s is their cross-sectional area, E_{red} is the reduced modulus of elasticity of the rollers-explosive system.

The magnitude E_{red} is only a little less than the modulus of compression of the metal of the rollers, since the thickness of the explosive layer (0.1 mm), taking part in the elastic deformation, amounts to only 1/200 of the total height of the rollers (l = 20 mm).

The energy of elastic deformation of the metal is consumed in the load rebound i.e.

$$\frac{\sigma_{max}^2 ls}{2E_{red}} = PH_0', \quad \sigma_{max} = a\sqrt{E_{red}PH_0'}, \tag{6.3}$$

where $a = \sqrt{\frac{2}{ls}}$.

The expression (6.3) can serve as an estimate of the maximum stresses arising on impact in an explosive, since σ_{max} in the metal of the cylinders and in the explosive should be equal.

On using the usual plunger devices and standard test conditions (P = 10 kg, H = 25 cm) for high explosives, σ_{max} attains 15,000 kg/cm^2. σ_{max} is a magnitude which determines to a known extent the state of the explosive (the degree of its deformation and the compression of the air enclosed in it) which should be taken into account in estimating the possible regions of local heating of the explosive and the probability of explosion occurring in it.

The expression (6.3) shows that the experimental results on the impact sensitivity of an explosive should to some extent depend on the

load rebound height and the elastic properties of the cylinder metal. Experimental investigations confirm this:

1) It is known, for example, that the use of copper cylinders requires a somewhat greater impact energy to obtain explosion than the use of steel cylinders. The modulus of elasticity of copper, $E = 10^6$ kg/cm^2 and for steel, $E = 2 \times 10^6$ kg/cm^2. Therefore for copper cylinders at a given load drop height, the rebound height is somewhat less than for steel cylinders.

2) In the presence of a rubber layer between the plunger device and the base of the impact machine, the load rebound height increases noticeably, and to obtain a given percentage of explosions it is necessary to consume correspondingly larger amounts of impact energy, which at first glance would appear to contradict the supposition expressed above concerning the possible effect of the magnitude σ_{max} on the probability of an explosion occurring on impact. This contradiction, however, is only apparent, since the rubber layer is responsible for a considerable decrease in E because of the relatively small value for the modulus of elasticity of rubber.

3) Numerous investigations show that on increasing the weight of the dropping load somewhat more energy is required to initiate explosion than is necessary in the case of impact with a lighter load from the same height, which is evident from the data of WELLER and WENTSELBERG given in Table 9.

Table 9.

The variation of the critical impact energy K_{50} ($\frac{kgm}{cm^2}$) with the weight of the load (kg)

Explosive	Weight of load				
	0.75	1	2	5	10
PETN	7.32	6.90	7.55	7.04	8.06
Tetryl	6.64	6.93	7.10	7.42	7.49
Trotyl	9.31	9.52	9.70	9.69	10.32
Xylyl	5.16	5.15	5.77	6.93	7.07
Trinitromesitylene	5.77	5.89	5.97	7.21	7.29

The reason for the decrease in the critical impact energy on using a lighter load is explained, in the opinion of some investigators, by the fact that due to the higher impact velocity there arises a higher surface pressure for a somewhat smaller total compression of the explosive.

A clearer physical explanation of this phenomenon can be given starting from the following considerations.

According to SHERBONE the magnitude of the elastic deformation occurring in the system under the influence of an impact is determined mainly by the kinetic energy of the impact, whilst the extent of the viscous deformations depends basically on the impulse acquired by the system.

If the impact kinetic energy remains constant, then the character of the change in impulse depending on the velocity of the dropping load is determined by the ratio $I \approx \frac{C}{v}$,

since $\frac{mv^2}{2} = C = \text{const}$ and $I = mv$.

From this it follows that with increase in the drop velocity of the

load, the impulse, and consequently the extent of the viscous deformations, decreases somewhat, and the elastic deformations in the metal increase correspondingly, causing some increase in the load rebound. The latter circumstance should in its turn lead to a corresponding increase in σ_{max}, as follows from expression (6.3).

§ 7. The sensitivity of explosives to puncturing and friction.

Sensitivity to puncturing is defined only for initiating compounds or mixtures intended for use in puncturing capsule-igniters and capsule-detonators.

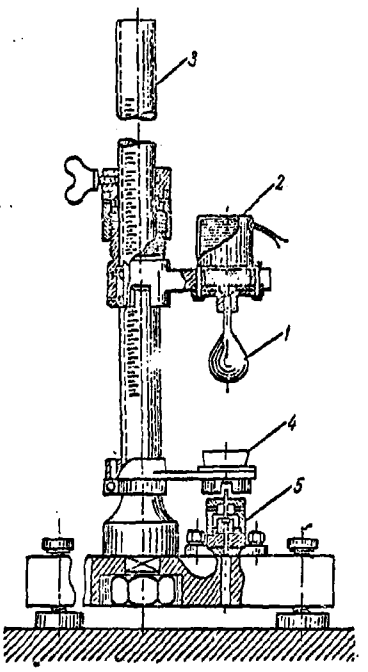


Fig. 10. RDULTOVSKIY's electric impact machine. 1 - load; 2 - electromagnet; 3 - stand; 4 - sleeve; 5 - mounting with capsule and pin.

To test the sensitivity of an explosive to puncturing RDULTOVSKIY's electric impact machine is usually used; its construction is illustrated in Fig. 10.

The pear-shaped load 1 is maintained at a given height by means of an electromagnet 2. The explosive to be tested is pressed under a definite pressure into a cartridge case, the top is covered with tinfoil and in this form it is placed in a special mounting covered by a lid 5. Through the opening in the lid exactly in the middle of the capsule is passed a

steel pin of standard dimensions. The jettisoning of the load onto the pin is caused by disconnecting the circuit of the electro-magnet. In this case the sensitivity is said to be characterized by the upper and lower limits.

Friction as a form of initial impulse is rarely used in practice, only in the special abrasive compositions which find extremely limited application today. The sensitivity of an explosive to friction is mainly of interest from the point of view of safety techniques in the production and application of explosives.

Existing methods for the determination of sensitivity to friction are not distinguished by great accuracy and cannot form the basis for the rigid quantitative characterization of explosives with respect to their sensitivity to this impulse.

The following methods of testing for sensitivity to friction are well-known:

1. Test on a friction pendulum (Fig. 11). The pendulum 1 with the help of the arc 2 can be fixed at a given height. As the pendulum falls the removable shoe of its corresponding weight passes over a face with a groove 3 filled with explosive; in so doing the convex surface of the shoe strongly grinds against the explosive. In the tests the minimum drop height of the pendulum

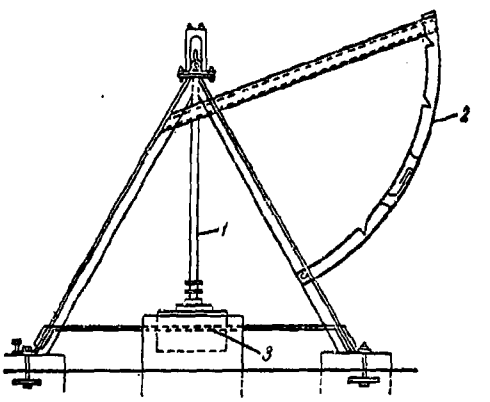


Fig.11. Friction pendulum.

and the number of oscillations to the commencement of ignition are determined.

In this method it is difficult to regulate exactly the clearance between the surface of the shoe and the groove which has an effect on the magnitude of the frictional force; for the method used the friction is essentially combined with the impact.

2. The testing of explosives for sliding friction is carried out in an apparatus illustrated schematically in Fig. 12.

In this apparatus the explosive undergoes friction between two plates 1, 2. The lower friction surface, on which is placed the explosive, is immovable. The upper friction plate rotates at a given speed. With the help of the load 3 it is possible to regulate the frictional force.

In this method of testing, the sensitivity of an explosive to friction is usually characterized by the force of compression of the explosive between the plates at which, for a given rotational speed, explosion occurs. In this case the time from the commencement of the test to the moment of explosion is determined.

3. BOWDEN and GURTON in investigating the sensitivity of solid explosives to friction used the apparatus shown in Fig. 13. In this apparatus the thin layer of explosive (about 25 mg) is pressed by means of a loading screw onto the steel plate 2. The sliding plate is caused to move by the impact of the load 3, which is a pendulum falling at a given speed; in this case the explosive undergoes a rapid movement. The results of some tests according to this method are given in Table 10.

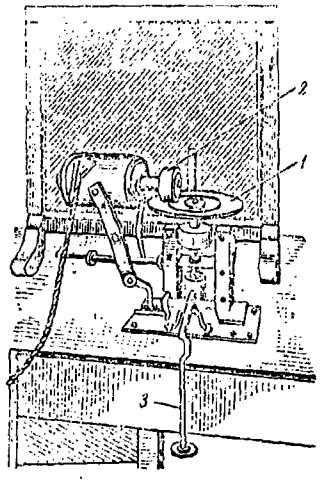


Fig.12. Apparatus for the determination of the sensitivity of an initiating explosive to friction.

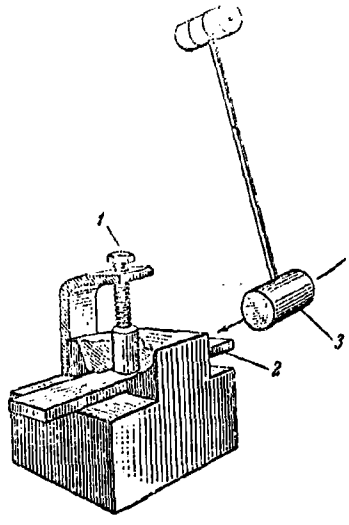


Fig.13. Apparatus for the determination of the sensitivity of solid explosives to friction.

Table 10.

The sensitivity of explosives to friction according to BOWDEN and GURTON.

Explosive	Load, kg	Drop height, km	Frequency of explosions, %
PETN	1600	70	0
Hexogen	1600	70	0
Lead azide	1600	70	100
" "	64	70	10
" "	64	60	0
Lead styphnate	64	60	80
" "	64	45	60
" "	64	40	0
Mercury fulminate	64	5.0	10
" "	64	2.5	0

From the table it is evident that PETN and Hexogen possess a negligible sensitivity to friction in comparison with initiating explosives.

Table 11.

The effect of additives on the sensitivity of explosives to friction.

Name of additive	Melting point of additive, °C	Frequency of the explosions, %	
		Lead azide (H = 60 cm)	Lead styphnate (H = 40 cm)
No additive	—	0	0
Silver bromide	434	0	3
Silver iodide	550	100	83
Bismuthite	685	100	100
Lead glance	1114	100	100

In the presence of an extremely small quantity of crushed glass, these explosives under the same conditions gave 100% explosions. The sensitivity of the corresponding initiating explosives to friction in the presence of high-melting additives (with melting point $> 500^{\circ}C$) also increase essentially, as is evident from Table 11.

BOWDEN and his co-workers showed that there was a noticeable effect on the sensitivity of explosives to friction, all other conditions being the same, due to the thermal conductivity of the sliding body (slider) with respect to the explosive.

A highly-polished glass disc is covered with a thin film of nitroglycerine and is rotated at a constant speed. The load on the slider is

gradually increased until explosion occurs. The experimental results are presented in Fig. 14.

The minimum friction force in grams is given on the ordinate axis on the left; on the right is given the minimum load necessary for explosion to occur. The abscissa axis gives the thermal conductivity. The different curves correspond to different rates of rotation of the disc.

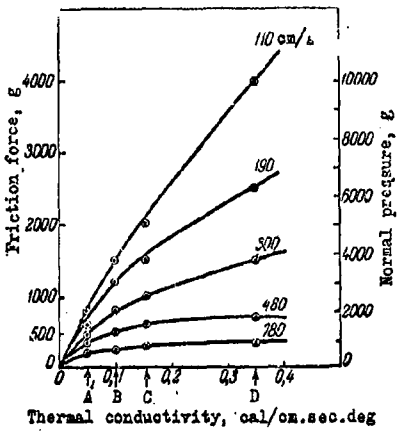


Fig.14. The variation of the friction force necessary for the initiation of explosion in nitroglycerine versus the thermal conductivity of the sliding body with respect to the explosive.

For constantan, the coefficient of thermal conductivity $k = 0.05$ (A), for steel $k = 0.1$ (B), for nickel $k = 0.16$ (C) and for tungsten $k = 0.35$ (D).

From the diagram it is evident that if the sliding contact is a bad heat conductor (for example, constantan), then explosions occur much more readily than in the case of a good heat conductor (for example, tungsten).

§ 8. The sensitivity of explosives to vibration during firing.

During firing from artillery guns the possibility is not excluded of the premature action of the ammunition which in some way or other is connected with the stresses arising in the explosive charges at the moment of firing due to the forces of inertia.

The maximum stresses λ_{max} arising in an explosive charge can readily be estimated from the following assumptions:

a) the possibility of linear movement of the explosive charge during firing is excluded due to its close proximity to the base of the shell.

b) the density and structure of the explosive throughout its mass are completely uniform, as a result of which the stresses at any point of a given cross-section should be the same.

The maximum force acting on the base of the shell equals

$$F = \pi R^2 P_{max},$$

where R is the semi-bore diameter of the shell, P_{max} is the maximum pressure of the powder gases.

The maximum acceleration acquired by the shell is, correspondingly:

$$a = \frac{\pi R^2 P_{max}}{Q} g,$$

where Q is the weight of the shell, g is the acceleration of the force of gravity.

The explosive charge, on acquiring this acceleration at any cross-section x, will develop at this section the inertia force:

$$F_{in} = \pi R^2 P_{max} \frac{\omega_x}{Q},$$

where ω_x is the weight of the part of the explosive charge corresponding to the section x.

The maximum inertia force is attained in the bottom layer, i.e. when ω_x equals half the weight of the explosive charge ω. The force per unit area of cross-section of the explosive charge, or the maximum stress, therefore equals

$$\lambda_{max} = P_{max} \frac{\omega}{Q} \frac{K^2}{r^2}, \qquad (8.1)$$

where r is the radius of the explosive charge at the cross-section under greatest stress.

The expression for λ_{max} can also be represented in the following form:

$$\lambda_{max} = \rho_0 \frac{HSP_{max}}{Q}, \qquad (8.2)$$

where H is the length of the charge, S is the cross-sectional area of the shell, ρ is the density of the explosive.

It is not difficult to note that formula (8.2) can easily be changed to the form (8.1).

It is accepted that to secure safe conditions during firing it is necessary that λ_{max} does not exceed some limiting value λ_{cr}, dependent on the sensitivity of the given explosive, at which the possibility of its ignition or explosion is completely excluded. The results of determinations of λ_{cr} carried out under given experimental conditions for certain explosives are given in Table 12.

Table 12.

The critical stresses for certain explosives.

Name of explosive	λ_{cr}, kg/cm^2
Trotyl	1800
Trotyl-Hexogen alloy (50/50) . .	1400
Tetryl	850
PETN with 5% phlegmatizator. . .	750
Amatol (80/20)	1400

It follows, however, that it must be stressed that λ_{cr} cannot be considered as some constant criterion for a given explosive, since in real ammunition ignition of the explosive can occur at essentially different values of λ depending on the physical properties of the charge and other test conditions (construction of the object, the presence of spaces, sharp edges in the body, defects in the equipment, etc).

As has already been said in § 4, even under conditions where extremely high stresses (of the order of 10^4 kg/cm^2 and higher) are achieved, the ignition of the explosive does not occur, if the possibility is eliminated of the displacement and rapid flow of the explosive, leading to the development of regions of intense local heating.

The structure of the explosive charge has a large effect on the explosion hazard during firing. Some defects in the charge are especially harmful, such as external blisters, air bubbles, cracks and macro-crystalline impurities, which under certain conditions can be centres of dangerous heating.

Whilst using pressed explosive charges it is necessary that the pressure of the compression exceeds the stresses which can arise in the explosive at the moment of firing. If this does not apply, the possibility is not excluded of the appearance of intensive displacements of the explosive particles and other forms of deformation of the charge, which is especially dangerous in the presence of spaces or sharp edges in the given section of the chamber of the shell.

Insufficient density of the explosive charge can in certain cases lead to a disturbance of the "no-failure" action of the shell (mine) due to strong consolidation of the charge at the moment of firing and the

formation in this connection of a space between the explosive charge and the fuse.

Safe conditions during firing depend not only on the combined effect of the factors given above, but also on the character of the acceleration of the shell, i.e. on the interval of time during which the pressure in the bore attains a value P_{max}. The smaller this interval of time, the more dynamic is the load experienced by the explosive charge and the less will be its deformation for a given stress.

The results of the relevant investigations give no reason to doubt the fact that the mechanism of excitation of explosion during firing is directly connected with the thermal ignition of the explosive and the conditions of its initiation approximate to the conditions during impact and friction.

§ 9. The sensitivity of explosives to the action of initiating substances.

As initiators of explosive processes, initiating substances are used mainly to produce detonation of high explosives.

The sensitivity of explosives to detonation during the action of an initiator or, as is usually said in this case, their susceptibility to detonation, is usually characterized by the magnitude of the limiting initiating charge.

The limiting initiating charge is called the minimum charge of the initiating explosive responsible for the detonation of a definite quantity of the high explosive being investigated. It is usual to judge the

excitation of detonation by the character of the rupture of a lead disc by means of the explosive. The higher the limiting initiating charge, then the less is the susceptibility to detonation of the high explosive under consideration.

The stimulating (initiating) ability of various initiating substances with respect to the same high explosive is not identical. The higher the rate of detonation of the initiating substance and the less the period of acceleration of the explosion i.e. the period of increase in the rate of the process up to a maximum, then the greater is its initiating ability. Lead azide and mercury fulminate possess almost the same rate of detonation; however, the section in which the detonation process occurs is considerably shorter for lead azide than for mercury fulminate. Because of this the initiating ability of lead azide is considerably greater than that of mercury fulminate, especially under the conditions of action of small-sized capsule-detonators. For a relatively large-sized initiator, the initiating abilities of lead azide and mercury fulminate are approximately the same.

The magnitude of the limiting initiating charge is determined not only by the properties of the explosive initiator and the susceptibility to detonation of the high explosive being tested, but also by a number of other factors connected with the choice of casing, the conditions of installation of the initiator, etc.; these are considered in detail in special courses on the means of initiation. From this, however, it is clear that to obtain comparable results tests of explosives for susceptibility to detonation should be carried out under strictly standardized conditions.

The test method is as follows. 0.5 or 1.0 g of the explosive to be investigated is compressed under a pressure of about 1000 kg/cm^2 into a normal capsule cartridge, then the appropriate weight (see below) of initiating substance is passed into the cartridge, the small cup is secured and the capsule charge is pressed under a pressure of 500 kg/cm^2. The capsule having been charged in this way is exploded in a special container over a 5 mm lead plate, as is shown in Fig. 15.

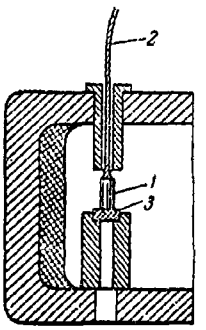


Fig. 15. Container for exploding the capsule.

The initiation of the explosion of the capsule 1 is carried out by means of a fuse 2. The detonation is considered complete if the orifice in the lead plate 3 is greater or equal to the diameter of the capsule. Some data on limiting initiating charges are given in Table 13.

The initiating ability of an initiator depends to a marked extent on the surface to be initiated. With increase in the latter, the initiating ability of the initiator increases to a known limit. The optimum conditions of initiation are attained when $\frac{d}{D} = 1$, where d is the diameter of the initiator and D is the diameter of the initiatable charge.

Table 13.

Limiting initiating charges, g.

Initiating charge	Tested explosive		
	Tetryl	Picric acid	Trotyl
Mercury fulminate. . .	0,29	0,30	0,36
.Lead azide	0.025	0,025	0,09

SUKHOV's data on limiting initiating charges referred to unit initiatable surface are given for some explosives in Table 14.

Table 14.

Tested explosive, g/cm^2	PETN	Tetryl	Trotyl
Limiting initiating charge, g/cm^2	0.70	0.82	0.90

§ 10. Initiation of explosion during impact and friction.

The initiation process of an explosion under the action of impact (or other forms of mechanical impulse) is an extremely complicated phenomenon which has not yet been investigated completely in all its details.

According to BERTHELOT, the action of an external impulse,

independently of the form of the applied energy, reduces in the end to a rapid thermal change and to a rise in temperature even if only in a narrowly localised region of the explosive system.

The direct reason responsible for the beginning of explosive decomposition of the molecules is the increase in temperature in the explosive above its self-ignition point.

If, however, it were assumed, as some investigators did assume, that the heat absorbed during impact is propagated uniformly because of the small size of the volume occupied by the whole weight of explosive, then the heating temperature would clearly be insufficient for the [illegible] of an explosive reaction. On the assumption that the entire impact energy (corresponding to 50% probability of explosion) is entirely co[illegible] only by heating the explosive, TAYLOR and YUILL on the basis of their experiments with mercury fulminate estimated that the temperature increase of the explosive does not exceed 20° which is clearly insufficient for the ignition of this explosive. Similar estimates, carried out for picric acid, show that for this mechanism the rise in temperature reaches 330°C. It is evident that under impact conditions, the duration of the impact being measured only in ten-thousandths of a second, self-ignition of the picric acid at this temperature cannot be guaranteed.

The temperatures calculated in this way are clearly over-estimated, since the energy actually absorbed by the explosive, as has already been explained earlier, is considerably less than the so-called critical impact energy.

Thus we see that on the basis of only a single overall thermal effect of impact it is not possible to explain the process creating explosion.

TAYLOR and YUILL expressed views against the thermal mechanism of initiating an explosion, in supposing that during impact direct activation of the molecules without an intermediate thermal stage can occur.

These investigators' ideas concerning the mechanism of explosion initiation during impact for the case of solid crystalline explosives were developed in the tribochemical hypothesis proposed by them. The mechanism of the process, according to this hypothesis, as as follows.

Under the influence of impact on the surface and edges of the [illegible] separate crystals there arise normal and tangential stresses, as a result of which extremely strong friction arises between the mutually displaced surfaces of the particles and on the friction surfaces [illegible] molecules are formed in a considerably greater quantity than would follow from Maxwell's distribution law.

Thus, according to this hypothesis, the main reason for explosion initiation under the action of impact is the tribochemical reaction arising on the friction surfaces of explosive crystals.

It must also be said that the phenomena arising in an explosive under the action of an impact are not of course limited to friction alone but bear a considerably more complicated character (crushing of crystals, plastic flow of the substance, compression of air bubbles, etc).

Above, it has already been noted that one of the parameters defining the state of the explosion at the moment of impact is the stress arising in it, σ_{max}. However, in reality the stress is not distributed uniformly through the explosive and because its physical structure is disordered (internal cavities, irregular shape, disordered arrangement of the crystals, etc), there can arise in separate localised sections "peaks"

of increased stresses, which will under given conditions be the foci of regions of maximum local heating. It is evident that these foci or "hot spots" should at the same time be the most likely centres of explosion initiation.

In this case, initiation of explosion will be attained only when the temperature of the "hot spot" is sufficient for the ignition of the explosive with an ignition time lag not exceeding the duration of the impact. The hypothesis concerning the possibility of explosion occurring during impact due to the direct influence of regions of localised heating was first expressed by CHARITON, whilst BELYAEV was the first to prove experimentally the ability of an explosive to be initiated thermally under the influence of extremely brief ($\tau = 10^{-4}$ sec) heating of local regions.

To obtain this kind of local heating in small volumes of the order of a few cubic microns BELYAEV used thin platinum wires ($\delta = 2—5\ \mu$), passing through the explosive, which were heated by the current of a condenser discharge. This method seemed suitable in that with its help it is possible to obtain extremely high energy concentrations for a negligible total consumption of energy. The heating period of the micro-volumes of explosive in this case was not more than $10^{-3} - 10^{-4}$ sec.

BELYAEV's experiments showed that at atmospheric pressure a highly-sensitive explosive such as nitrogen trichloride, detonates only during the localised heating of a small volume to temperatures of the order of several thousands of degrees, but for nitroglycerine detonation does not occur even under the experimental conditions under which a unique "explosion" of the wire occurs accompanied by an increase in its

temperature to 20,000°.

However, under these test conditions the temperatures of the regions of local heating of given explosives in reality exceeded only slightly their temperatures of vaporization since the energy supplied would have been absorbed by the vaporization process.

In this connection additional investigations were carried out under a pressure of one hundred atmospheres. The increase in pressure leads to an increase in the boiling point and consequently should lead simultaneously to an increase in the maximum temperature of the regions of localised heating and thus cause the development of a chemical reaction in the explosive.

The results of these experiments are as follows:

1. Under a pressure of 100 atm. nitrogen trichloride detonates during a considerably shorter (about 10-15 times) heat pulse than at atmospheric pressure. The minimum energy necessary for exciting its detonation, under given test conditions, amounted to 9.6×10^{-7} cal. This energy can produce heating of the wire by at most about 170°.

2. Nitroglycerine under atmospheric pressure which does not deflagrate even under very powerful heat pulses attaining 10^{-3} cal energy deflagrated under the pressure of 100 atm with an impulse of the order of 10^{-3} cal, but its explosion was not achieved consistently. Approximate calculation shows that for the critical impact conditions under which nitroglycerine explodes, a pressure of over 10,000 atm. develops in the layer in which the regions of localised heating arise.

3. In volatile explosives localised heating itself cannot produce an explosion on its own. It is necessary to combine the localised heating

with a relatively high pressure, which condition is fulfilled during a sufficiently strong impact of the explosive.

The possibility of the thermal initiation of "hot spots" during impact was directly proved by tudying the sensitivity of liquid explosives, and plastic and molten solid explosives by BOWDEN, YOFFE and their co-workers.

They showed that the impact sensitivity of explosives increases noticeably when there are small bubbles of air or another gas present in them. Thus, for example, the impact energy for nitroglycerine, containing air bubbles of radius 5×10^{-3} cm, necessary to obtain 100% explosions equals 400 gcm; in the absence of bubbles in the nitroglycerine an impact energy of the order of $10^5 - 10^6$ gcm was necessary to secure regular explosions. The initiation of the explosive in the first case occurs due to the adiabatic compression of the gas present in the bubble. The temperature increases rapidly. In the second case, explosion is evidently produced by the viscous heating of the liquid during the rapid discharge from the clearance between the impacting surfaces. It was seen that the quantity of gas capable of sensitizing the explosive (increasing its sensitivity) is very small, of the order of 3×10^{-10} g and that the quantity of heat evolved during compression of the air in one bubble amounts to only 10^{-7} cal. The minimum degree of compression of the gas necessary to excite explosion amounted to $p_2/p_1 \approx 20$.

With increase in the initial pressure of the gaseous occlusions, the sensitivity of the nitroglycerine decreases correspondingly because of the decrease in the degree of compression of the gas. The experiments were carried out in a closed vessel where p_1 could change from 1 to

100 atm.

In experiments on the initiation of explosion of liquid and solid explosives by friction it was established by the cited authors that the conditions of explosion are determined by the regions of local heating arising in the explosive during sliding of the bodies. The maximum temperature of heating is limited by the melting point of the corresponding body.

Experiments carried out with metals and melts of different melting points showed that large loads and sliding rates cannot of themselves produce an explosion of nitroglycerine provided that the local temperature does not attain 480 - 500°C.

BRIDGMAN also drew similar conclusions concerning the role of thermal effects for the initiation of an explosion under the influence of powerful mechanical deformations of the explosive. Two types of tests were carried out by him with different explosives. In the first test, the explosive underwent a hydrostatic pressure of 50,000 kg/cm^2, imposed so that it produced a powerful deformation of the tested object under the combined action of high pressure and shear (of the order of 60 radians).

In the second test, the explosive was subjected to a pressure of 100,000 kg/cm^2, but at a comparatively small shearing deformation. On the basis of his experiments BRIDGMAN drew the general conclusion that shearing by itself, unless it is accompanied by high temperature, cannot produce detonation.

For the majority of secondary explosives friction between the crystals or between the crystals and the metal surface itself cannot be the reason for the initiation of explosion, since rapid decomposition of the explosive

occurs at temperatures exceeding its melting point. During this time the maximum increase in temperature under these conditions cannot exceed the melting point of this explosive.

BOWDEN and his co-workers, however, showed that in the friction process sufficiently intense foci of heating can be formed, necessary for securing the explosion of these explosives when sufficiently high-melting additives have been introduced into their composition.

In contrast to secondary explosives, initiating explosives even in the pure state are exploded more or less readily under conditions of friction, since their explosion on heating always occurs in the solid state.

These authors by means of photo-recording have established for the majority of explosives both during impact and during friction that an explosion begins as a relatively slow combustion, the velocity of which increases to several hundred m/sec and then changes quickly to detonation with a velocity of the order of 2000 m/sec.

In initiating explosives of the PbN_6 type explosion always arises as a detonating type.

BOWDEN and YOFFE arrive at the general conclusion that the initiation of the majority of liquid, plastic and solid explosives by impact and friction is always connected with regions of localised heating occurring in the explosive as "hot spots" of finite dimensions ($r_0 = 10^{-3} - 10^{-5}$ cm), which fulfil the role of the initial centres of thermal ignition. The "hot spots" can form as a consequence of one of the following causes:

a) the adiabatic compression of small quantities of gases or vapours included in cavities present in the explosive or arising in it at the

moment.

b) the friction of the solid parts - pre-eminently in the presence of high-boiling additives and

c) the viscous heating during rapid discharge of the explosive (at sufficiently high impact energies).

It is impossible, of course, to agree with some investigators (GARNER and others) in whose opinion detonation of explosives can arise as a result of the activation of separate isolated molecules. During the decomposition of these activated molecules, the energy of the reaction is quickly dissipated by heat conductivity, thanks to which the necessary conditions are not created for the acceleration of the process.

In research carried out with TRILLA and OKE, MURAOUR showed that the impact of high-velocity electrons or α -particles does not produce an explosion even of such highly-sensitive explosives as nitrogen iodide, silver acetylide or lead azide; at the same time there occurs in them the decomposition of separate isolated molecules, or even of a group of mixed molecules, expressed, for example, in the blackening of lead azide or silver acetylide.

RIDEAL and ROBINSON estimated the temperature and time necessary for the decomposition of the "hot spots" for various explosives, determined experimentally the period of time from the moment of impact to that of explosion and showed after this time the "hot spots" succeed in reacting completely.

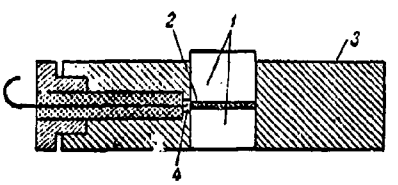


Fig.16 Plunger device for the determination of the interval of time from impact to explosion.

The test was carried out on the following explosives: nitrogen iodide, PETN, hexogen and Tetryl. The load of explosive 2 is placed in a plunger device (Fig. 16) between two roller bearings 1. The sleeve 3 of the device was provided with two transverse ducts 4 for the discharge of the gaseous products of explosion. A third duct was drilled perpendicular to one of these two ducts nearer to the lower layer of explosive.

During the passage of ionised explosion products through this duct, electric circuits were closed which made it possible to fix the moment of explosion. The moment of impact in its turn was determined by an electric circuit closed through the contact of the load with the upper roller. The corresponding time intervals were determined by means of an oscillograph. The least time recorded by the apparatus amounted to 20 micro sec. The mean results of the determinations are given below (Table 15).

Table 15.

The mean interval from the moment of impact to explosion

(P = 4 kg, H = 59 cm)

Name of explosive	microsec	Name of explosive	microsec
Nitrogen iodide . .	20	Hexogen (50 mg) . .	260
PETN (50 mg) . . .	230	Hexogen (25 mg) . .	340
PETN (25 mg) . . .	240	Tetryl (50 mg) . .	350
PETN (10 mg) . . .	230	Tetryl (35 mg) . .	320

On decrease in the impact energy, the time necessary for explosion increases somewhat. Thus, for P = 4 kg and H = 34 cm it was shown that for PETN (25 mg) τ = 390 micro sec, for Hexogen (25 mg) τ =

450 micro sec. The addition of quartz (18%) to PETN decreases the time necessary for explosion to 80 micro sec.

In the absence of explosive from the plunger device at P = 4 kg and H = 59 cm the duration of impact (the interval of time from the moment of impact to the moment of load rebound) was shown to equal 460 micro sec. Using this method, the authors also determined the rate of the radial outflow of the explosive during impact which was equal to 15 m/sec for Hexogen at P = 1.5 kg and H = 75 cm.

Under somewhat different test conditions carried out by BOWDEN and GURTON the duration of impact did not exceed 300 micro sec and the delay time for PETN and Hexogen fluctuated between the limits of 60 and 150 micro sec.

These authors' data concerning delay times seem to us to be more exact, since in them the moment when the explosion begins was determined directly by the displacement given on the photo-recorder, whilst in RIDEAL and ROBERTSON's experiments the delay time includes the additional time necessary for the propagation of the flame through the weight of explosive until it reaches the electrodes.

RIDEAL and ROBERTSON carried out a theoretical calculation of the critical temperature at which the substance at a "hot spot" succeeds in reacting completely during a given interval of time τ. For this, they estimated the heat losses outside the "hot spot", and the reaction heats and kinetic characteristics of the corresponding explosives were taken to be such that they were established during their slow thermal decomposition.

Let a be the radius of the "hot spot", ρ the density of the explosive, c its heat capacity, θ the increase in temperature at any

point at a distance r (outside the "hot spot") attainable in the interval of time τ due to heat conductivity.

It is assumed that the focus of heating at the initial moment has the same temperature at all points, which exceeds the temperature of the surrounding medium by θ_0. Then the heat given out by the "hot spot" to the surrounding medium after time τ equals

$$Q_1 = \int_0^\infty 4\pi r^2 \theta \rho c \, dr, \tag{10.1}$$

where θ is defined by Fourier's basic law of heat transfer which for the given case (spherical symmetry) is written in the following form:

$$\frac{\partial \theta}{\partial \tau} = \frac{k}{\rho c}\left[\frac{\partial^2 \theta}{\partial r^2} - \frac{2}{r}\frac{\partial \theta}{\partial r}\right]$$

(k is the coefficient of thermal conductivity).

The boundary conditions here are

$$\theta = 0 \quad \text{at} \quad \tau = 0 \quad \text{for} \quad r > a,$$
$$\theta = \theta_0 \quad \text{at} \quad \tau = 0 \quad \text{for} \quad r < a,$$

which permits the equation to be solved and the temperature at any point to be estimated in an explicit manner. If the temperature of the "hot spot" is nearly the same as the reaction temperature and the time τ is very small, then the heat evolved by the "hot spot" after this time as a result of the reaction equals

$$Q_2 = \frac{4}{3}\pi a^3 \rho q t A e^{-\frac{E}{RT}}, \tag{10.2}$$

where q is the reaction heat referred to unit mass, $Ae^{-E/RT}$ is the quantity of substance reacted per sec per unit volume (the rate of the

chemical reaction).

The critical temperature of the "hot spot" can be determined from the condition of thermal equilibrium, i.e. that

$$Q_1 = Q_2.$$

The coefficient of thermal conductivity, heat capacity and density for all the explosives in the calculations were taken to be, respectively, 2.4×10^{-4}, 0.3 and 1.3 in CGS units. The time τ was assumed to be as follows:

for "hot spots" with radius 10^{-3} cm $\tau = 10^{-4}$ sec
" " " " " 10^{-4} cm $\tau = 10^{-6}$ sec,
" " " " " 10^{-5} cm $\tau = 10^{-8}$ sec,
" " " " " 10^{-6} cm $\tau = 10^{-10}$ sec.

In Table 16 the critical temperatures are given of the "hot spots" calculated for these conditions.

Table 16.

The critical temperatures t_{cr} °C of "hot spots" for some explosives.

Name of explosive	$a = 10^{-3}$ cm	$a = 10^{-4}$ cm	$a = 10^{-5}$ cm	$a = 10^{-6}$ cm
PETN	350	440	560	730
Hexogen	385	485	620	820
Cyclotetramethylene-tetranitramine . . .	405	500	625	805
Ethylenedinitramine. .	400	590	930	1775
Tetryl	425	570	815	1250
Ethylenediaminedinitrate	600	835	1255	2225
Ammonium nitrate	590	825	1230	2180

In the opinion of the cited authors, the estimated critical temperatures agree satisfactorily with the impact sensitivity of these explosives.

The period of decomposition of the explosive at the "hot spots" was determined by the authors from the following kinetic relationships:

$$\left.\begin{aligned} mc\,dT &= (m-x)\,qAe^{\frac{E}{RT}}\,d\tau - b(T-T_0)\,d\tau, \\ dx &= (m-x)\,Ae^{-\frac{E}{RT}}\,d\tau, \end{aligned}\right\} \qquad (10.3)$$

where $m = \frac{4}{3}\pi a^3\rho$ is the mass of the "hot spot", x is the quantity of explosive decomposed after time τ at the "hot spot".

The heat given to the surrounding medium is determined from the second term on the right-hand side of the first equation. The time τ can be calculated by the method of numerical integration, if the initial conditions are known.

The results of the calculation give values of t_{cr} equal to 440°C and 485°C for PETN and Hexogen respectively at $a = 10^{-4}$ cm and reaction time $\tau = 10^{-6}$ sec. From this it is clear that the explosive at the "hot spots" can react completely after intervals of time which are considerably shorter than the impact time.

BOWDEN and YOFFE established by various methods that the minimum temperatures necessary to excite the explosion of nitro-glycerine, Hexogen and PETN, both under conditions of friction and impact and for the rapid adiabatic compression of air, are of the order 430 - 500°C; this agrees well with the calculated values of t_{cr} given above. One of the possible

reasons for the occurrence of "hot spots" under impact is the heating during viscous flow of the explosive. This flow can take place due to the formation in the impact zone of small volumes of liquid explosive flowing through the spaces between the solid particles.

For the quantitative estimate of the temperatures in such processes, we consider the flow of a liquid through a capillary of constant cross-section. Neglecting the heat losses due to thermal conductivity and liquid compression, the increase in temperature θ can be determined approximately, as according to POISEUILLE's law for laminar flow with constant viscosity it equals

$$\theta = \frac{8l\eta v}{Ja^2 \rho c}, \tag{10.4}$$

where l is the length of the capillary, a is its radius, v is the average rate of flow, J is the mechanical equivalent of heat, η is the viscosity, ρ is the density of the explosive and c is its heat capacity.

Taking $l = 0.1$ cm, $\eta = 0.3$ CGS units, $v = 10^3$ cm/sec (according to experiment), $a = 10^{-4}$ cm, $\rho = 1.3$ g/cm^3 and $c = 0.3$ cal/g deg, we obtain $\theta = 1470^\circ$C.

To obtain for the conditions given above a flow rate equal to 10^3 cm/sec, σ_{max} should be of the order of 10,000 kg/cm^2 which is frequently the case under the explosion conditions of high explosives at impact.

The case considered of the capillary flow of an explosive, as has already been shown, is not of course the solitary reason for the occurrence of an explosion on impact. Even for one and the same explosive the conditions and the probability of the formation of "hot spots" can be

essentially different depending on the possible character of the deformation of the explosive on impact. Thus, for example, it is possible to consider that on testing an explosive in standard devices with no clearances between the sleeve and the rollers, a decisive role in the formation of "hot spots" will be played by the processes of internal local deformations (micro displacements, adiabatic compression of the gas bubbles, capillary flow etc.), passing under the action of the appropriate pressures into a closed volume of the same explosive. On the other hand, if as a result of impact the explosive charge is capable of deformation and if under the influence of the pressures arising during impact it penetrates into some of the spaces, then the processes of plastic and viscous flow of the explosive and the effects of friction of the particles will have a definite significance together with the air spaces in the initiation of explosion.

From what has been described it is possible to conclude that independently of the character of the deformation of the explosive and the conditions of formation of active centres, the initiation of an explosion for all forms of mechanical impulse occurs as a result of the local processes of thermal ignition of the explosive.

An understanding of the mechanism of explosion initiation is of essential importance in the correct solution of many practical problems connected with accident prevention whilst using explosives.

§ 11. The dependence of the sensitivity of explosives on various factors.

The sensitivity of the same explosive can change greatly, depending

on the action of various physical factors. The basic factors of a physical kind, showing an effect on the sensitivity of explosives to external actions, are:

1) temperature, 2) heat capacity and thermal conductivity of the substance, 3) volatility, 4) state of aggregation, 5) structure, 6) density of the substance, 7) magnitude of the crystals.

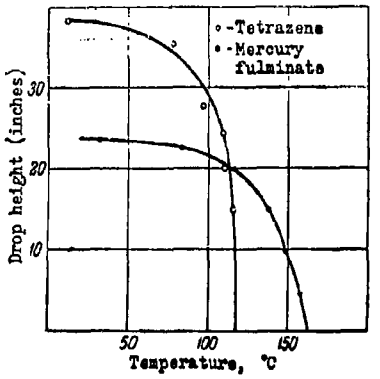


Fig.17. The variation of the impact sensitivity of tetrazene and mercury fulminate with initial temperature.

The effect of the enumerated factors is shown on the sensitivity to a varying degree depending on the character of the initiating impulse applied to excite explosion. We will consider the effect of each of these factors separately.

On increasing the temperature the sensitivity of explosives increases sharply and at temperatures approaching explosion temperatures they explode from even a weak impulse. The variation of the impact sensitivity with temperature is represented in Fig. 17 for mercury fulminate and tetrazene from the data by TAYLOR and YUILL.

For a considerable decrease in the temperature, the sensitivity of an explosive decreases. Thus, on cooling mercury fulminate to the temperature of liquid air, it often gives failure on ignition. The effect of a severe cooling on the sensitivity of explosives is illustrated by the data of Table 17.

Table 17.

The effect of initial temperature on the limiting initiating charge.

Name of explosive	Least quantity of mercury fulminate necessary to excite explosion, g	
	t=20° C	t = 110° C
Nitrogelatin	0.25	1.0
Pyroxylin	0.25	2.0 } failures
Picric acid	0.25	2.0 }

Heat capacity and thermal conductivity have an effect mainly on the sensitivity of explosives to a heat pulse. On increasing the heat capacity it is necessary to expend a greater quantity of heat in order to heat the substance to temperatures at which its ignition is achieved. A similar effect is shown by thermal conductivity; the smaller the latter becomes, the higher are the local temperatures which can be attained during heating of the substance; high thermal conductivity responsible for the rapid dispersal of heat through the body, on the other hand, impedes the formation or development of foci of ignition.

A noticeable effect of the quoted factors was established during the investigation of the processes of ignition and combustion of some mixtures containing metallic alloys (Fe - Si, Si - Al).

In tests on impact sensitivity, heat capacity and thermal conductivity show less effect, because in this case the decisive factor in initiation is

the formation of the local processes connected with the occurrence of "hot spots". The time necessary for the formation of these foci and the development of reactions in them is so small ($\sim 10^{-5}$ sec) that thermal conductivity cannot show any noticeable effect on the general character of the phenomenon.

A large effect on the conditions and development of the processes of thermal initiation of explosives is shown by their volatility. BELYAEV established that the conditions of ignition of volatile substances are determined to a considerable extent by the relationship between the rate of the chemical reaction and the rate of their vaporization.

If the explosion temperature of an explosive is higher than its boiling point, then, as BELYAEV showed, ignition of the substance can occur only in the vapours (either in a mixture of vapour and air or with the products of the thermal decomposition of the explosive).

If the explosion temperature is lower than the boiling point of the explosive, as, for example, for Hexogen ($t_{boil} = 340^{\circ}C$, $t_{ign} = 230^{\circ}C$), then the decisive role in the process of spontaneous ignition will evidently be played by the reactions occurring in the condensed phase and in the intermediate decomposition products.

In BELYAEV's opinion, the character of the explosion is defined by the relationship between the boiling point and the explosion temperature. If the boiling point is higher than the explosion temperature, then the explosion should have a detonating character; for the reverse relationship of these temperatures the explosion should occur as a more or less rapid combustion. This point of view, however, is contradicted by many experimental data.

Noticing the fallibility of BELYAEV's criterion, ANDREEV quite correctly points out the following circumstances which are guides in the determination and estimate of the character of the explosion.

During thermal initiation of the explosion, ignition of the explosive first occurs, followed by a more or less brief period of its violent combustion. If the combustion is unstable, then the explosion can be completed in the detonating form, as occurs in nitro-glycerine. A criterion of the instability of the process is the excess of gas supply (due to the reaction) over gas exhaust. In this case a rapid auto-acceleration occurs of the combustion which under favourable conditions (sufficient weight etc) changes in the end to detonation.

During a study of ignition processes ANDREEV found that for some explosives (Trotyl, picric acid, xylol) during rapid heating explosion does not occur but there is a flameless decomposition if the temperature of heating is higher than a certain limit. In ANDREEV's opinion, this phenomenon is explained by the hypothesis that on rapid heating of the substance until the boiling point is attained the concentration of decomposition products of the condensed phases, which play an essential role in the processes of spontaneous ignition, is small. The vapours of the explosive which possess a considerably higher temperature of spontaneous ignition than the boiling point decompose without an explosion; however, if the heating temperature exceeds the temperature of spontaneous ignition of the vapours, then explosion occurs. A known confirmation of this explanation is the fact that, for example, Tetryl does not have an upper limit. The boiling point of Tetryl (310°C) is considerably higher than its explosion temperature (195°C) because its spontaneous ignition occurs

before it vaporizes.

Volatility which plays an essential role in the processes of thermal initiation of an explosion can, however, have practically no effect on the impact sensitivity of explosives and less so on their tendency to detonation under the influence of an initiator, because the heatings and initiation of explosion in these cases are achieved under conditions of very high pressures at which vaporization is completely or almost entirely suppressed.

The dependence of the sensitivity of explosives on the state of aggregation has quite a general character; during the change of the substance from the solid state to the liquid state, its sensitivity, as a rule, increases which explains the higher temperature and the greater content of internal energy in the substance in the liquid state, the excess corresponding to the latent heat of fusion. Under the conditions of thermal initiation, the quoted variation is determined by the fact that in the liquid state the substance possesses a greater vapour pressure and therefore ignites more readily.

Thus, for example, it has been established that in the liquid state nitro-glycerine is noticeably more sensitive than solid frozen nitro-glycerine, provided this does not contain spaces in the form of liquid nitro-glycerine drops.

However, in some cases the possibility is not excluded of increasing the sensitivity on transfer of the substance from the liquid state to the solid due to the formation of crystalline modifications of lower stability. An example of such a transfer is the labile form of solid nitro-glycerine characterized by increased sensitivity to external influences.

As regards the effects of structure, density and the magnitude of the crystals, it must be shown first of all that these factors have an effect mainly and most markedly on the susceptibility of explosives to detonation and to a lesser degree show an influence on their impact sensitivity.

This is explained by the fact that the limiting initiating charge, which is a measure of the susceptibility of explosives to detonation, should as an initiator of explosion not only cause the detonating process but also its subsequent propagation through the charge. This indicates mainly that within the limits of the charge under test a normal rate of detonation should be attained.

The readiness with which an explosive reaction is stimulated depends mainly on the structure of the substance whilst the conditions of transfer of the stimulating process to normal detonation and its subsequent steady propagation through the charge depend essentially on the physical properties of the explosive charge by means of which this process is propagated.

In determining impact sensitivity on an impact machine the mechanical impulse is transmitted to an extremely thin layer of explosive, the isolated localised volumes of which serve as centres for the excitation of an intense chemical reaction, which, generally speaking, could lead either to the development of normal detonation or to the extinguishment of the explosion.

However, the layer of explosive in the given case is so small that the physical properties which influence essentially the character of the propagation of the process through the charge cannot be of great significance under the conditions being considered.

In Fig. 18 two possible types of development of the process are illustrated for the effect of an initiating impulse.

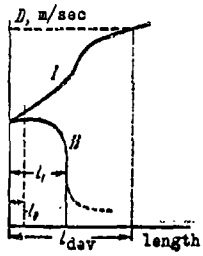


Fig. 18. Change in explosion rate in the charge of initiating explosive.

Curve I gives the development of normal detonation; Curve II the extinguished explosion. The length l_0 is the thickness of the layer of explosive in the plunger device, the length l_1 is the portion after which the explosion dies away sharply.

From the diagram it is evident that, within the limits of the charge in the device, the rate of the process cannot attain one of its limiting values.

The statement made concerning the preferential influence of the physical factors given above on the tendency of explosives to detonation is confirmed experimentally.

Data on the influence of the physical structure are especially significant in this respect. We will demonstrate this by the following examples.

a) An explosive in a gelatineous state has a very much worse susceptibility to detonation than the same explosive in a non-gelatineous state, which is easily established by a comparison of pyroxylin and pyroxylin powders.

Pyroxylin powders, as is well-known, differ from pure pyroxylin in their structure and content of "additives" (residual solvent, stabilizer,

moisture). Pyroxylin powders, as a rule, possess a very high impact sensitivity, yielding little in this respect to pure pyroxylin, which to a considerable extent could be referred to the effect of the "additives" mentioned above.

Thus, the pyroxylin powder for rifles under standard test conditions gives 80% explosions, i.e. it is more sensitive than Hexogen, in spite of the fact that it contains about 3.5% inert additives.

At the same time pyroxylin powder, in contrast to pyroxylin itself, possesses an extremely low susceptibility to detonation. It does not detonate in capsule-detonator No. 8. We note that pure pyroxylin in the compressed state detonates readily in a capsule with 0.3 g of mercury fulminate.

b) In the compressed state explosives possess a considerably greater tendency to detonation than in the molten state, even for the same density (Trotyl, picric acid, etc.).

c) Molten mixtures of some nitro-compounds, for example, a molten eutectic comprising 95% Trotyl and 5% xylyl, possess considerably greater susceptibility to detonation than either of these explosives separately.

With respect to its impact sensitivity this melt does not differ noticeably from Trotyl.

The molten eutectic of Trotyl and xylyl differs from molten Trotyl in possessing a considerably finer crystalline structure. This leads to a considerable increase in the initiation zone of the number of active centres, the reaction rate and the evolution of energy during the development of a normal detonating process.

LEYTMAN succeeded under special cooling conditions in obtaining the

same eutectic melt with a considerably coarser crystalline structure, which did not possess ary advantage over molten Trotyl with regard to susceptibility to detonation.

LEYTMAN's investigations also showed that many explosives (Trotyl, xylyl, Hexogen, etc.), obtained in the finely divided state by precipitating them from solution, possess a greatly increased susceptibility to detonation in comparison to the same explosives with a normal quantity of crystals.

The effect of the degree of dispersion of the crystals of explosives on the susceptibility to detonation is characterized by the following data in Table 18, according to LEYTMAN.

The information encountered in the literature concerning the effect of crystal size on the impact sensitivity of explosives is extremely contradictory. Analysis of the data available shows all the same that crystal size influences mainly initiating explosives which possess high sensitivity to mechanical actions.

It was noted that coarse crystals of some azides sometimes explode on lightly touching, fracture of the crystal, etc., which, in the opinion of some investigators, is explained, strictly, not by the dimensions of the crystals but by the alterations in the crystal structure due to the conditions of crystallisation.

In the places where such alterations occur, the energy of the crystal lattice can be considerably greater than normal.

Whilst testing a large number of aromatic nitrocompounds, LEYTMAN did not succeed in a single case in detecting a noticeable change in their impact sensitivity on transfer from normal crystals to finely divided

Table 18

The effect of the degree of dispersion of crystals on the tendency to detonation.

Name of explosive	Minimum charge of lead azide, g	
	for particles passing through a sieve with 2500 holes/cm^2	for ... obtained by precipitation from a solution in water
Trinitroxylene	0.34	0.08
Trinitrobenzene	0.19	0.06
Trinitrotoluene	0.10	0.04

particles, the dimensions of which varied within the limits of 1 to 4 μ.

It is accepted that with increase in the density of an explosive, its sensitivity decreases. This factor actually shows a marked effect on the susceptibility of the explosive to detonation and has an especially marked influence in this respect on the behaviour of ammonites, chloratites and certain other explosives. On increase in the density of the latter above a known limit their susceptibility to detonation decreases sharply.

The effect of the density of explosives on the susceptibility to detonation can be illustrated by the following data (Table 19).

At the same time it was established that the density of charges shows essentially less effect on their impact sensitivity than on their susceptibility to detonation.

Table 19.

The effect of density of a cheddite charge on the susceptibility to detonation.

Density, g/cm^3	0,66	0,88	1,20	1,30	1,39	1,46
Minimum initiating charge of mercury fulminate, g	0.3	0,3	0,75	1,5	2,0	3,0

Some initiating explosives (mercury fulminate, diazodinitrophenol, trinitrotriazidobenzene, etc.) on increase in density above a certain limit under practical conditions of application (capsule-detonators) lose the ability to detonate under the influence of a heat pulse; the decomposition of these substances under pressing acquires the character of a more or less rapid combustion. This phenomenon known by the name "dead pressing" was quite thoroughly investigated by AVANESOV and FEOKTISTOVA and also by ANDREEV. During thermal initiation of explosion of the majority of explosives, detonation is always preceded by a period of violent combustion. The change from combustion to a detonating form of explosion is achieved under definite critical conditions in the sense of pressure and auto-acceleration of the reaction.

It was established by the above mentioned investigators that the phenomenon of "dead pressing" does not characterize any special state of the substance in which it loses its detonating ability, but it means that

Table 19.

The effect of density of a cheddite charge on the susceptibility to detonation.

Density, g/cm^3	0,66	0,88	1,20	1,30	1,39	1,46
Minimum initiating charge of mercury fulminate, g	0,3	0,3	0,75	1,5	2,0	3,0

Some initiating explosives (mercury fulminate, diazodinitrophenol, trinitrotriazidobenzene, etc.) on increase in density above a certain limit under practical conditions of application (capsule-detonators) lose the ability to detonate under the influence of a heat pulse; the decomposition of these substances under pressing acquires the character of a more or less rapid combustion. This phenomenon known by the name "dead pressing" was quite thoroughly investigated by AVANESOV and FEOKTISTOVA and also by ANDREEV. During thermal initiation of explosion of the majority of explosives, detonation is always preceded by a period of violent combustion. The change from combustion to a detonating form of explosion is achieved under definite critical conditions in the sense of pressure and auto-acceleration of the reaction.

It was established by the above mentioned investigators that the phenomenon of "dead pressing" does not characterize any special state of the substance in which it loses its detonating ability, but it means that

the acceleration of combustion proceeds slowly because the change from combustion to detonation cannot be achieved within the limits of a small charge.

The slowing-up of the acceleration process of combustion in its turn is determined by the decrease in the porosity of the charge at increased densities. According to the data of AVANESOV and FEOKTISTOVA in any "pressed" charge it is possible to produce a change from combustion to detonation, if the strength of the case and the degree of hermetic sealing of the charge are increased correspondingly.

The sensitivity of explosives can change sharply on the introduction of inert additives into the charge. The influence of the latter is felt mainly on the sensitivity of explosives to mechanical actions. Different kinds of additives do not show the same effect on the sensitivity of explosives; in some cases the sensitivity increases and in others decreases.

Additives capable of increasing the sensitivity of explosives are called sensitizers and additives which decrease the sensitivity of explosives are called phlegmatizers.

Good sensitizers, as a rule, are substances which possess great hardness, sharp edges and high melting-point, as, for example, powdered glass, sand, particles of certain metals, etc. They provide concentrations of impact energy on the sharp edges, they are foci of intense friction and they lead to the formation in the charge of numerous centres of local heating capable of causing explosion in it. RIDEAL and ROBERTSON's experiments showed that in the presence of sensitizers the period of time τ from the moment of impact to explosion is sharply curtailed; thus

for pure PETN τ = 240 micro sec; but in the presence of 18% quartz it is only 80 micro sec.

COPP and UBBELOHDE on the basis of their experiments with various high explosives note that if the hardness of the added substances is more than 4 on the Mohs scale, then the sensitivity of explosives increases with increase in the percentage concentration of the additives.

BOWDEN and GURTON, on the other hand, consider that the melting point of the additive particles, not their hardness, gives the decisive effect on the sensitivity of explosives to mechanical actions. The results of the corresponding tests carried out by these authors for PETN are given in Table 20.

Table 20

The effect of additives on the sensitivity of PETN to impact and friction.

Additive	Hardness by Mohs scale	Melting point °C	Frequency of explosions, %	
			during friction	during impact
Pure PETN	1,8	141	0	2
Silver nitrate	2—3	212	0	2
Potassium acetate	1—1,5	324	0	0
Potassium dichromate	2—3	398	0	0
Silver bromide	2—3	434	50	6
Lead chloride	2—3	501	60	27
Borax	3—4	560	100	30
Bismuthite (Bi_2O_3)	2—2,5	685	100	42
Glass	7	800	100	100
Rock salt	2—2,5	804	50	0
Copper glance	2,5—2,7	1100	100	50
Calcite	3	1339	100	43

Analogous results were obtained for Hexogen.

On the basis of analysis of the experimental data, the authors arrived at the following conclusions.

1. Sensitizing properties only occur in additives (independently of their hardness) the melting points of which are higher than the critical temperature necessary to excite explosion of the given explosive at the "hot spots".

For such sensitizers with respect to PETN and Hexogen, only additives with melting points higher than 430-450°C are used.

2. Hard particles of additives increase the sensitivity of explosives to a greater degree than soft particles under conditions such that their melting point is higher than the corresponding critical value for the given explosive.

From Table 20 it is evident that of all the substances tested, glass possessing the greatest hardness was also the best sensitizer under the test conditions of PETN for impact sensitivity.

The best phlegmatizing properties are possessed by such substances as, for example, paraffin, wax, vaseline, camphor, etc. By covering the crystal surfaces by a soft elastic film they permit a more uniform distribution of stresses in the charge and a decrease in the friction between the separate particles which leads to an essential restriction of the surface reactions and of the probability of "hot spots" occurring.

The character of the influence of inert additives on the sensitivity depends to a considerable extent on the relationship between the physical-mechanical properties (particularly, the hardness) of the explosive itself and these additives. Thus FROLOV and BAUM's experiments showed that talc,

Table 21

The effect of talc on the impact sensitivity of Trotyl and Hexogen.

Talc content, % %	% explosions	
	Trotyl	Hexogen
1	4	84
2.5	8	80
5.0	8	36
10.0	24	12
20.0	52	8
40.0	68	8
50.0	74	4

which is a phlegmatizer with respect to Hexogen, is at the same time quite an active sensitizer with respect to Trotyl (Table 21).

We note that talc occupies a central place on the hardness scale between Trotyl and Hexogen.

HOLEVO shows that the effect of inert additions is determined not only by their physical properties but depends essentially on the conditions of deformation of the charge on impact. He confirms this by the following experiments. The impact sensitivity of explosives is determined both in normal devices and in HOLEVO's device illustrated in Fig. 19. In devices of this construction, the charge on impact can be squeezed more or less easily into

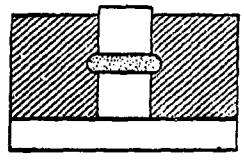


Fig. 19. HOLEVO's plunger device.

the groove whilst in normal devices it can only flow partially into the clearance between the cylinders and the sleeve.

Test results showed that in certain cases whilst using standard devices the addition of paraffin leads to a noticeable increase in the sensitivity of explosives, whilst aluminium powder and aluminium oxide possessing extremely high hardness or silica behave like phlegmatizers. Thus, for example, a mixture of Hexogen and aluminium powder, in a 1:1 proportion, for an impact energy of 3 kgm gives some failures in standard devices, whilst in HOLEVO's devices under the same conditions it gives 100% explosions, i.e. it is even more sensitive than pure Hexogen. Upon the addition of 10% paraffin to this mixture for the same impact energy in standard devices, 80% explosions were obtained and in HOLEVO's devices 40% explosions.

HOLEVO notices that in the presence of paraffin the sensitivity increases only when the charge without paraffin deforms slightly and does not extrude into the clearance of a standard device; in the presence of paraffin this form of deformation does not increase noticeably.

The sensitizing actions of hard additives, in HOLEVO's opinion, clearly only appear when conditions are favourable for the rapid flow (extrusion) of the charge in the device. In this case in the charge, as a rule, more favourable conditions are caused for the creation of local volumes of high temperature.

In conclusion it must be noted that, of course, it is not possible to consider the process of extrusion of the explosive into the clearance or the groove as the only reason for the occurrence of an explosion on impact, which by the way is confirmed by the results of HOLEVO's own

experiments. Thus, in testing a number of high explosives, including such highly sensitive ones as nitro-glycerine, Tetryl and Hexogen, in devices with a groove it was not possible to obtain explosions. In normal devices these explosives secured a high percentage of explosions for considerably lower energy of impact.

The reasons for the different sensitivity of explosive compounds have not yet been investigated sufficiently fully. It is sometimes attempted to explain these differences by the effect of thermo-chemical factors; thus, it is supposed that with decrease in the heat of formation of an explosive its sensitivity should increase.

This law does actually hold within known limits. The majority of highly sensitive initiating explosives are endothermic compounds, whilst less sensitive high explosives in a majority of cases are exothermic compounds.

However, numerous examples of deviation from the given rule can be quoted even for explosives which are close to one another in their chemical nature. Thus, for example, the more endothermic azides of lead and mercury are less sensitive to impact than the azides of silver and strontium.

A marked lack of correspondence between heat of formation and sensitivity also occurs in many nitro-compounds of the aromatic series, which is evident, for example, from Table 22. Trinitrophloroglucinol which according to its heat of formation should be an extremely stable compound is characterized by particularly high impact sensitivity, in comparison to the remaining explosives in this table.

Table 22.

Impact sensitivity of some high explosives.

(P = 10 kg and H = 25 cm)

Name of explosive	Heat of formation kcal/mole	% explosions
a-trinitrotoluol	13.0	8
trinitroaniline	19,5	0
trinitrophenol	49,6	18
trinitroresorcinol	117.3	64
trinitrophloroglucinol . . .	159,6	100

Thus, it must be concluded that the heat of formation itself cannot in any way be a criterion for the comparative estimate of the sensitivity of explosive compounds.

BERTHELOT supposed that on increase in the heat of explosive decomposition or the potential energy of the system the sensitivity of explosives increases. In practice a number of cases do actually occur where this rule is confirmed (Table 23).

Table 23

The variation of impact sensitivity with heat of explosion.

Name of explosive	Heat of explosion kcal/kg	Impact sensitivity K_{50} kg.m/cm^2
Nitroglycerine	1485	0.16
PETN	1403	0.80
Hexogen	1390	1.30
Tetryl	1095	1.60
Picric acid	1030	2.0
Trotyl	1010	3,5

However, on detailed consideration of the question it appears that the given rule does not hold within wider limits. Thus, the heat of explosion of Hexogen is more than three times that of mercury fulminate but the latter is of very considerably greater sensitivity. We find similar contradictions in comparing a whole series of other explosives.

The majority of the most widely used explosive compounds (Trotyl, picric acid, Hexogen and others) are in general thermodynamically unstable and possess relatively high stability under normal conditions, which can be explained to a certain extent by the kinetic conditions of their decomposition at high temperatures. The most fundamental kinetic characteristic of a substance is its energy of activation E.

We will turn our attention to high values of E and unusually large values of the magnitude Z for a number of explosives which decompose according to the monomolecular law,

$$\frac{dx}{dt} = k(a - x),$$

where $k = Ze^{-\frac{E}{RT}}$ is the rate constant of the chemical reaction (Table 24).

Table 24.

Kinetic constants of certain explosives.

Explosive	E kcal/mole	log Z
Nitroglycerine (125–150° C)	45 000	23.5
Pyroxylin (155–175°) . . .	56 000	24.0
Tetryl (liquid)	60 000	27.5
Picric acid	58 000	22.5
Trotyl	53 000	19.0

SEMENOV shows that high values of E make explosives stable at low temperatures whilst unusually large values of the pre-exponential factor Z makes their violent decomposition possible at higher temperatures.

The activation energy of an explosive is usually determined from the conditions of their thermal decomposition or on the basis of the data concerning the variation between the explosion temperature and the ignition time lag. Starting from this, some investigators consider that the sensitivity of explosives to a heat pulse should be determined above all by their activation energies. However, analysis of the data available, presented in Table 25, does not confirm this hypothesis. The activation energy was determined on the basis of data concerning explosion temperatures. Weight of explosive is 0.1 g.

Table 25.

Activation energies and explosion temperatures of some explosives (according to BAUM).

Explosive	E, cal/mole	Sensitivity to heat pulse	
		t_{ign}, °C	τ, sec
Lead azide	26 000	330	16
Silver azide	23 400	210	21
Barium azide	18 500	257	18
Strontium azide	11 500	230	9
Trotyl	27 800	340	13
Trinitroaniline	28 000	460	12
Trinitrophenol	26 000	340	13
Trinitrophloroglucinol	27 000	200	17
Tetryl	23 100	190	22
Trinitrophenylnitramine	41 000	95	24

The series of explosives given in the table is characterized by quite similar values of E but they differ essentially with respect to explosion temperatures. Trinitrophenylnitramine possesses the highest value of activation energy whilst it is one of the most sensitive solid explosives towards a heat pulse.

The absence of a regular law between explosion temperature and activation energy of explosives is explained above all by the fact that the latter is not a constant magnitude but changes essentially for one and the same explosive depending on the temperature and character of the chemical reaction.

Thus, according to ANDREEV's investigations, for calcium azide E changes within the limits of 20,000 cal/mole at 70°C and 34,000 cal/mole at 135°C. He showed that the reaction products of CaN_6 at lower temperatures consist of calcium hydrazide and at higher temperatures of the nitride; under explosion conditions decomposition occurs with the separation of free metal.

At temperatures up to 100°C trinitrotriazidobenzene is decomposed according to the equation

$$C_6(N_3)_3(NO_2)_3 \longrightarrow C_6(NO)_6 + 3N_2,$$

i.e. the reaction leads to the formation of hexanitrobenzene, which is itself an explosive compound; at higher temperatures complete decomposition of the benzene nucleus can occur.

The energy characteristics considered by us so far - heats of formation and explosion, activation energy - are magnitudes characterizing the overall properties of the molecules of the explosive

compounds. They do not characterize directly the energy level of the separate intermolecular bonds or the atomic complexes which can have a decisive effect on the strength of the whole elementary structure.

The different bonds occurring in molecules are not of equal value either with respect to their own strength or with respect to their effect on the stability of the molecular structure as a whole.

Thus, for example, in Tetryl the least stable bond is that which connects the carbon atom in the nucleus with the complex $-N\begin{matrix}CH_3\\NO_2\end{matrix}$.

However the separation of this complex during the time of reaction does not produce destruction of the basic benzene nucleus, just as the separation of the NO_2 group in pyroxylin still does not mean the destruction of the basic carbon chain of the molecule.

All the same, the structure of the molecule can be radically destroyed as soon as the bond between the basic carbon atoms in some part of the benzene nucleus or the carbon skeleton of the molecule is broken. This scission will occur at the place of the weakest bond.

Therefore, in estimating the sensitivity of explosives it is necessary to consider the peculiarities of their molecular structure and the bonds upon which the stability of the molecule as a whole depends.

The question of the connection between the sensitivity of explosives and their structure is dealt with in only a few research works, in particular, the work carried out by BAUM and BAGAL in 1945-1947.

The nature of this connection has been very clearly established for inorganic azides.

The results of X-ray and electron examinations showed that many

inorganic azides possess an ionic crystal lattice, because the chemical bond between the nitrogen and the corresponding metals in them, as a rule, is heteropolar.

Because of this it is possible to consider that the stability of the elementary structure and consequently the stability of these azides should to a considerable extent depend on the energy U of the crystal lattice, determined by the force of electrostatic attraction between the corresponding ions (N_3^- and M^+). The greater the energy of the crystal lattice, then the more stable is the given azide and the smaller its sensitivity should be under the conditions of detonating decomposition. The results of our experiments on the determination of impact sensitivity confirm this hypothesis (Table 26).

Table 26.

Impact sensitivity of certain azides.

Azide	Purity of the product, %	Test conditions		Upper limit of sensitivity	
		weight of load, kg	diameter of face, mm	drop height, mm	% explosions
PbN_6	99,4	1.52	1.55	225	100
CdN_6	99,7	1.52	1.55	195	100
CaN_6	99.2	1.52	1.40	119	100
BaN_6	99.5	1.52	1.35	65	100
NgN_3	99.8	1.52	1.50	235	100
CuN_3	99,4	1.52	1,40	125	100
AgN_3	98.5	1.52	1,35	80	100

The azides given here possess a more or less clearly expressed heteropolar structure. Estimates made using BORN's cycle showed that in a number of azides of divalent metals, compared with PbN_6, the lattice energy for CdN_6 is 57 kcal less, for CaN_6 it is 138 kcal less and for BaN_6 it is 150 kcal less; for a number of azides of monovalent metals, compared with HgN_3, the lattice energy for CuN_3 is 24 kcal less, and for AgN_3 it is 66 kcal less. As would be expected, the sensitivity of the corresponding azides increases in the same order.

Gold azide $Au(N_3)_3$ is of great theoretical interest. The formation of the ion Au^{+++} requires the separation of two electrons from the stable closed shell d^{10}, which is connected with great expenditure of energy and makes the ionic structure of gold azide unfavourable from the energy point of view. This circumstance leads to the formation of an extremely unstable covalent bond Au-N, which corresponds to the probable structure

$$-\underset{|}{Au}-N=\overset{+}{N}=\overset{-}{N}.$$

Because of this, gold azide should be a barely-stable and very sensitive explosive. Thus, its explosion temperature equals 75°C for a delay time of 2 sec; it explodes under very insignificant mechanical actions, CuN_6 behaves similarly.

BOWDEN in his researches reached agreement with the hypotheses developed by us concerning the sensitivity of azides.

§ 12. The thermal decomposition of explosives.

It was established earlier that the mechanism of explosion initiation under the influence of a heat pulse, impact and friction is connected with

the processes of thermal decomposition of explosives. These processes also play an extremely important role in phenomena connected with the chemical stability of explosives.

The decomposition processes of explosives obey the general laws of chemical kinetics and according to them their flow rate depends very greatly on temperature.

In certain cases, using the laws of chemical kinetics, it is possible to calculate more or less accurately the time during which, for a given temperature and reaction rate constant, a definite portion of the explosive decomposes.

The basic law of chemical kinetics is the law of mass action, according to which the reaction rate at a given moment is proportional to the product of the concentrations of the reactants at that moment of time.

For monomolecular reactions when only one form of molecule undergoes transformation and the stoichiometric coefficient in the reaction equation equals unity, i.e. for reactions of the type AB → A + B, the law of mass action gives

$$v = \frac{dx}{dt} = k(a - x), \tag{12.1}$$

where v is the rate of the chemical reaction; a is the initial concentration of the substance; x is the quantity of the substance decomposed at a given moment of time t and k is the reaction rate constant showing what part of the substance reacts per unit time.

Integrating equation (12.1), we obtain

$$\int_0^x \frac{dx}{a - x} = \int_0^t k\,dt,$$

whence

$$\ln \frac{a-x}{a} = -kt \quad \text{or} \quad a-x = ae^{-kt}. \tag{12.2}$$

Graphically, this variation is expressed in the form of a curve (Fig. 20).

From (12.2) and the diagram it follows that the concentration and, consequently, the reaction rate decreases continuously with time.

The characteristic of thermal stability of the substance is usually taken to be the time τ during which a definite portion of the substance reacts. It is evident that

$$\tau = \frac{1}{k} \ln \frac{100}{100-x}, \tag{12.3}$$

where x is expressed as a percentage.

SAPOZHNIKOV, ROBERTSON and other investigators established that this law, in particular, is obtained with stable cellulose nitrates in the first

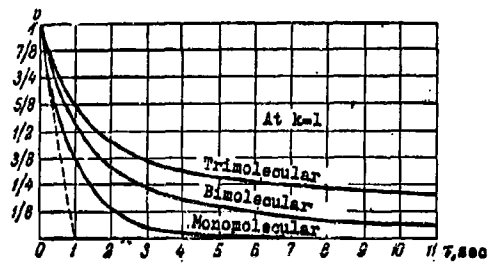


Fig. 20. The variation of reaction rate with time.

period of their heating in a stream of carbon dioxide carrying the products of decomposition. The magnitude of the constant depends on the concen-

tration of nitrogen in the cellulose nitrate. The variation of the reaction rate constant (in relative units) with the concentration of nitrogen in the cellulose nitrates according to KLIMENKO is shown in Fig. 21. From the diagram it follows that the larger the concentration of nitrogen in the cellulose nitrate, then the higher is its decomposition rate at the given temperature.

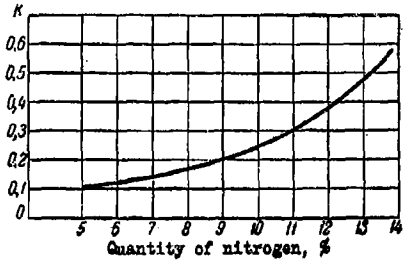


Fig. 21. The variation of the reaction rate constant with the nitrogen concentration in cellulose nitrates.

The thermal decomposition of some explosives under given conditions possesses an auto-catalytic character which is more or less clearly expressed. Auto-catalytic decomposition at high temperatures is characteristic of cellulose nitrates. Thermal decomposition of liquid Trotyl (at temperatures of the order of 300°C and above) and some other explosives (for example, Tetryl, ammonium nitrate) is also accompanied by auto-catalytic phenomena.

The role of autocatalysts, accelerating the processes of explosive decomposition, is assumed mainly by the intermediate reaction products, in particular, some radicals and oxides of nitrogen recovered during the course of the reaction. Thus, during the thermal decomposition of cellulose nitrates, about 40% of all the oxides of nitrogen produced separate in the form of NO_2. It oxidizes the cellulose nitrate and is reduced to NO. If the decomposition occurs in the presence of the oxygen in the air, then NO is again oxidized to NO_2, etc.

The role of positive catalysts of the reaction can also be fulfilled by certain additions to the explosive, for example, traces of free acids, fine particles of metals (Pt, Ni, Ag, Fe, etc.) and oxides of metals (Fe_2O_3, Al_2O_3, MnO_2, etc.) and, in some cases, traces of moisture.

It is characteristic of auto-catalytic reactions that the increase in rate is progressive as the decomposition products accumulate up to a definite limit (maximum) after which the rate begins to decrease, which is connected with a considerable decrease in the concentration of the initial substances. A very small rate is characteristic of the initial stage of the auto-catalytic reactions. In this stage (induction period) an accumulation of the active intermediate product occurs.

The kinetic equations for auto-catalytic reactions are in general quite complicated. For an auto-catalytic homogeneous reaction of the first order the kinetic equation has the form

$$\frac{dx}{dt} = kx(a - x),$$

where x is the concentration of the catalysing product.

Integration of this equation gives

$$\ln \frac{ax}{a - x} = kat, \tag{12.4}$$

which corresponds to a curve with a maximum at

$$x = \frac{a}{2}.$$

It is not always possible to describe the character of the thermal decomposition of explosives by a kinetic equation of one type. In particular, according to ANDREEV's investigations, confirmed by BAUM's

data, the thermal decomposition of the azides of calcium and barium during the auto-acceleration of the reaction corresponds to the so-called topochemical type of development of reaction zones from the initial centres of chemical reactions formed in the induction period. The final stage of decomposition of these substances strictly obeys the monomolecular law.

When the initial number of nuclei is constant, the rate of the topochemical reaction

$$\frac{dx}{dt} = kx^{\frac{2}{3}} \quad \text{or} \quad x = \left(\frac{k}{3}\right)^3 \tau^3, \tag{12.5}$$

i.e. the concentration of the decomposing substance should be proportional to the cube of the time τ.

The expression (12.5) requires a linear relationship between log x (or log p, where p is the pressure of the decomposition products) and log τ. The results obtained by BAUM for the period of auto-acceleration of the decomposition reaction of BaN_6 (Fig. 22) show that this condition holds only up to a known limit. Later there occurs a clearly expressed increase in the growth of log p compared with log τ. This is easily explained if it is supposed that new initial centres of reaction form and develop, which seems more likely than that the number of initial centres remain unchanged over the whole course of the

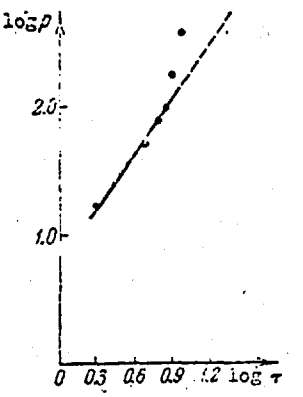


Fig. 22. Decomposition of barium azide at 155°C.

Best Available Copy

reaction.

The period of auto-acceleration of the thermal decomposition of some explosives, according to SEMENOV, proceeds according to a chain mechanism thanks to the regeneration during the reaction of active intermediate products of decomposition. It was shown that the processes of ignition and combustion of many gaseous systems do indeed proceed according to this mechanism (see Chapter X).

In the opinion of some investigators, the development of chain reactions can also occur during the thermal decomposition of condensed explosives. Thus, according to APIN, the pre-explosion rate increase of the thermal decomposition of lead azide proceeds according to a chain mechanism. The rate of the process is expressed by the relation

$$v = A e^{\varphi},$$

whilst

$$\varphi = C_2 e^{-\frac{E}{RT}},$$

where T is the temperature and E is the activation energy.

GRAY and YOFFE on the basis of the results of their experiments came to the conclusion that the thermal decomposition of methylnitrate and ethylnitrate, preceding their ignition and explosion, occurs according to a thermal-chain mechanism and proceeds in the vapour phase. In the given case the acceleration of the reaction is partially connected with self-heating, due to the formation of rapidly branching chains during the course of the reaction (see Chapter X).

According to PHILLIPS, the first stage in the decomposition of alkylnitrates is connected with the formation of a free radical and of nitrogen peroxide and is assumed to occur according to the following

mechanism:

$$RCH_2ONO_2 \rightleftarrows RCH_2O + NO_2,$$
$$RCH_2O + RCH_2ONO_2 \longrightarrow RCH_2OH + RCHONO_2,$$
$$RCHONO_2 \longrightarrow RCHO + NO_2.$$

Later oxidizing-reducing reactions follow between these products with the formation of such gases as NO, CO, etc.

Temperature has an exceptionally large influence on the rate of chemical reactions. Because change in temperature has a comparatively small effect on concentration, then in the chemical kinetic equation $v = kC_1C_2 \ldots$ (where $C_1, C_2, \ldots$ are the corresponding concentrations) the effect of temperature on reaction rate practically reduces to its effect on the rate constant k.

For an approximate estimate of the effect of temperature on reaction rate in a comparatively small temperature range, it is possible to use the temperature rate coefficient k_{t+10}/k_t, giving the magnitude of the rate constant on increasing the temperature by 10°.

Experimental data show that on increasing the temperature by 10° the reaction rate for typical explosives increases 2-4 times. This means that on increasing the temperature by 100° the rates of the chemical reactions increase by $2^{10} - 4^{10}$ times. The data given above cease to be true for temperatures approaching the explosion temperature.

According to ROBERTSON, the decomposition rate of nitroglycerine (on heating it in a stream of carbon dioxide) changes with increase in temperature as given in Table 27 (the average value of the temperature coefficient is 4.0).

Table 27.

The decomposition of nitroglycerine at various temperatures.

Temperature, °C	Quantity of nitrogen evolved in mg (after 15 min)	Temperature coefficient of reaction rate (by 10° steps)
90	0.010	—
100	0.044	4.4
110	0.20	4.5
120	0.74	3.7
130	2.72	3.7
135	4.87	3.6

For the same temperatures the decomposition rate of various explosives is different. Thus, the decomposition rate of nitroglycerine is approximately 10 times higher than that of pyroxylin, but the decomposition rate of Trotyl in its turn is many times less than the decomposition rate of pyroxylin .

A series of data characterising the thermal stability of some explosives is given in Tables 28-30.

The variation of reaction rate with temperature is determined from ARRHENIUS's equation

$$k = Ze^{-\frac{E}{RT}}. \qquad (12.6)$$

According to ARRHENIUS, by no means all the molecules can take part in the reaction, but only the active molecules with energy exceeding some magnitude E characteristic for the given reaction. The magnitude E is known as the energy of activation. The factor $e^{-E/RT}$ characterizes the relative number of active molecules.

For bimolecular reactions the magnitude Z is proportional to the number of collisions per second. For monomolecular reactions Z is a constant proportional to the probability of decomposition of the molecules. It must be noted that the factor Z is a constant magnitude only to a first approximation. In fact the magnitude Z does vary slightly with temperature.

The estimation of the values E and Z are carried out analytically or graphically based on the investigations of reaction rates at various temperatures.



Fig. 23. The variation of the reaction rate constant with temperature.

The graphical connection between ln k and the reciprocal of the temperature is expressed by a straight line (Fig. 23). The tangent of the angle between this line and the abscissa axis is determined by the magnitude $\frac{E}{R}$, and the intercept on the ordinate axis gives ln Z. By this means the values E and Z may be determined for many reactions of the thermal decomposition of explosives following a monomolecular law.

For the determination of the activation energy E, as has already been stated, data are frequently used concerning the ignition time lags, starting from the relationship

$$\ln \tau = \ln c + \frac{E}{RT}.$$

Using this method BAUM found that the decomposition process of azides at temperatures corresponding to explosion conditions is characterized by

two extremely different stages of development which have a definite temperature boundary. For each of these stages, as can be seen from Fig. 24, the variation between $\ln \tau$ and $\frac{1}{T}$ has a linear character. If we start from the lower straight lines which determine the decomposition process at higher temperatures, then for the activation energy E of the corresponding azides we obtain the following values:

Formula of azide	PbN_6	AgN_3	BaN_6	SrN_6
E, cal/mole	26 000	23 400	18 500	10 500
Temperature range, °C .	330—350	230—250	310—320	270

If we start from the upper straight lines corresponding to lower temperatures, then we find that the activation energy of PbN_6 equals 51,000 cal/mole and that of SrN_6 equals 33,500 cal/mole. According to

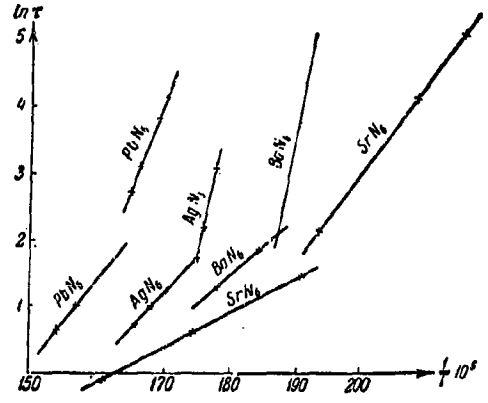


Fig. 24. The variation of the ignition time lag with temperature for some azides.

APIN's data, the activation energy of lead azide equals 50,000 - 55,000 cal./mole which agrees with the results given above.

The variation of activation energy with temperature occurs not only for azides but also for other explosives, which is, of course, explained by the change in character of the course of the decomposition reaction with temperature. Thus, it has been established by SAPOZHNIKOV that the composition of the decomposition products of pyroxylin changes with change in the temperature of the reaction. The change in the kinetic constants for nitroglycerine and pyroxylin is given in Table 28 from the data of ROGINSKI and other authors.

Table 28.

The kinetic constants of nitroglycerine and pyroxylin.

Substance	Temperature range, °C	Energy of activation E, cal/mole	log z
Nitroglycerine	90—125	42 600	18.0
"	125—150	45 000	23.5
"	150—190	48 000	—
Pyroxylin (13% nitrogen)	90—135	44 000	21.0
Ditto	140—155	48 000	—
"	155—175	56 000	24.0

The values of E and log Z for some explosives, obtained whilst investigating the kinetics of slow thermal decomposition, are given in Table 29.

In recent years ROBERTSON investigated the thermal decomposition of a number of high explosives at temperatures close to the explosion

Table 29.

Kinetic constants for some explosives

Name of explosive	E, cal/mole	log Z
Trotyl	53 000	19,0
Picric acid	58 000	22.5
Mercury fulminate	25 400	11.0

temperatures and established the nature of the decomposition and kinetic constants for them (Table 30).

Table 30.

Decomposition rate constants for some explosives

Name of explosive	Temperature range, °C	Reaction rate constant k, sec^{-1}
PETN	193—222	$10^{19.4}e^{-47000/RT}$
Ethylenediamine	230—357	$10^{13.1}e^{-40500/RT}$
Ammonium nitrate	243—361	$10^{13.8}e^{-40500/RT}$
Ethylenedinitramine	184—254	$10^{12.8}e^{-30600/RT}$
Tetryl		$10^{15.4}e^{-38400/RT}$

Knowing the reaction rate constant, it is possible to calculate the time during which a definite portion of the substance decomposes at a given temperature. As an example we will consider the decomposition period of 1% nitroglycerine at a temperature of 90°C. Using the data of Table 28,

we find that

$$k = 10^{18} e^{-\frac{42000}{303 \cdot 1{,}986}} = 2.38 \cdot 10^{-8} \text{ sec}^{-1},$$
$$\tau_{1\%} = \frac{0.01}{k} = \frac{0.01}{2{,}38 \cdot 10^{-8}} \approx 4.2 \cdot 10^{5} \text{ sec} \approx 5 \text{ days}.$$

COPP and UBBELOHDE used this method for estimating the temperature of short-lived localised foci of explosion ("hot spots"), arising under conditions of impact and friction, extrapolating the calculation beyond the temperature limits at which the kinetic characteristics (E and Z) of the corresponding explosives had been determined.

Some results of the calculations for PETN showing the portion α of decomposed explosive for various intervals of time and various temperatures are given in Table 31.

Table 31.

The thermal decomposition of PETN

Temperature, °C	Portion of decomposed PETN (α)		
	$\tau = 10^{-3}$ sec	$\tau = 5 \cdot 10^{-4}$ sec	$\tau = 10^{-5}$ sec
227	0.0003	0.0001	0
327	0.47	0.27	0.006
427	~1.0	~1.0	0.82
477	~1,0	~1.0	~1.0

Because the centres of heating continue to exist for 10^{-4} to 10^{-5} sec, then in order to complete the reaction in them temperatures of the order 430 - 480°C are necessary, which agrees well with the values found experimentally by BOWDEN and GURTON. We note, however, that such extra-

///

polations, especially for very high temperatures, are not sufficiently reliable.

In kinetic calculations it can also be taken into account that for a number of explosives thermal decomposition is only one of the component elements of the complicated process of decompo. tion. Thus, under the conditions of storage of powders and cellulose nitrates, the process of hydrolytic decomposition must be considered to no less an extent than the process of purely thermal decomposition.

Bibliography.

1. N.A. Sokolov, Teoriya vzryvchatykh veshchestv (Theory of explosives), Oborongiz (1938).
2. K.K. Andreev, Termicheskoye razlozheniye i goreniye vzryvchatykh veshchestv (Thermal decomposition and combustion of explosives), Gosenergoizdat (1957).
3. N.N. Semenov, Chemical Kinetics and Chain Reactions, Oxford University Press, (1935).
4. A.F. Belyaev, Sbornik statey po teorii vzryvchatykh veshchestv (Symposium on the theory of explosives) Oborongiz (1940).
5. M. Patry, Goreniye i detonatsiya vzryvchatykh veshchestv (Combustion and detonation of explosives), Oborongiz (1938).
6. F.A. Baum, Trubochnyye porokha (Smoky powders), Oborongiz (1940).
7. P.W. Bridgman, The Physics of High Pressures, New York, Macmillan Co. (1931), London, Bell & Sons (1931).
8. E.K. Rideal and A.J.B. Robertson, Proc. Roy. Soc. A 195, 135 (1948).
9. A.F. Belyaev, Dokl. Akad. Nauk 24, No. 3, (1939).
10. K.K. Andreev, Dokl. Akad. Nauk 44, No. 1, (1944).
11. J.B. Chariton and S.B. Ratner, Dokl. Akad. Nauk 41, 293 (1943).
12. F.P. Bowden and A.D. Yoffe, The Initiation and Growth of Explosion in Liquids and Solids. Cambridge University Press (1952).
13. K.K. Andreev, Dokl. Akad. Nauk 51, 29 (1946).
14. A.J.B. Robertson, Trans. Faraday Soc., 44, 977 (1948).
15. A.F. Belyaev and A.E. Belyaeva, Dokl. Akad. Nauk 56, 491 (1947).

16. W.E. Garner and J. Maggs, Proc. Roy. Soc. A 172, 229 (1939).

17. G.K. Klimenko, Metody issytaniya porokhov (Methods of testing powders), Oborongiz (1941).

Thermochemistry of explosives

§ 13. General data.

In appraising explosives as sources of energy it is first necessary to know the quantity of energy evolved by unit mass in the process of transformation, the volume and composition of the transformation products and their temperature. The hydrodynamic theory of detonation and the combustion theory, too, cannot be developed without a knowledge of these characteristics.

Explosion processes are chemical processes.

From elementary thermodynamics it follows that the change in internal energy of the system

$$\Delta E = q - A, \tag{13.1}$$

where q is the heat evolved or absorbed by the system, A is the work done by the system.

It is proved in hydrodynamics that

$$A = \int_{v_1}^{v_2} p\,dv. \tag{13.2}$$

Thus it is possible to establish the connection between the thermal effect of the reaction and the change in internal energy or heat content from basic principles. The thermal effect is the name usually given to the quantity of heat evolved or absorbed during a reaction. This quantity of heat usually refers to 1 g mol or 1 kg of the substance.

In chemistry it is usually accepted that the thermal effects of exothermic reactions are positive and of endothermic are negative. On the other hand, in using a sign system in thermodynamics, positive values are assumed for the absorbed heat q and negative values for evolved heat. To reconcile the two sign systems it is appropriate to denote the thermal effects by another letter, for example Q. It is obvious that $Q = -q$.

For processes occurring at constant volume, $A = 0$ and

$$Q_v = -\Delta E. \tag{13.3}$$

Here Q_v is the thermal effect at constant volume.

If the process occurs at constant pressure, then

$$Q_p = -(\Delta E + p\,\Delta v) = -\Delta i, \tag{13.4}$$

where Q_p is the thermal effect at constant pressure.

Thus, the thermal effect at constant volume equals the decrease in internal energy of the system and the thermal effect at constant pressure equals the decrease in heat content of the system.

The difference between the thermal effects at constant volume and constant pressure follows from expressions (13.3) and (13.4) and equals

$$Q_v - Q_p = p\,\Delta v. \tag{13.5}$$

In the theory of explosives the following thermal effects must be considered: the heat of formation, the heat of combustion of the substances and the heat of explosion.

The heat of formation is the thermal effect obtained during the formation of one gram-mole of a given compound from free elements under standard conditions. Standard conditions are taken to be a temperature

of 25°C and pressure of 1 atm* of all the substances taking part in the reaction and the states of aggregation in which they are normally found under these conditions.

The heat of combustion of a substance is the quantity of heat evolved during the combustion of the substance in an oxygen atmosphere.

The heat of explosion is the quantity of heat which is evolved during the explosion of one gram-mole of explosive; for the purposes of comparison of various explosives with one another, this magnitude usually refers to 1 kg of explosive.

Equation (13.5) establishes in a general form the connection between the thermal effects at constant volume and at constant pressure. If the reacting substances are ideal gases and if the temperature up to and after the reaction remain the same (its intermediate changes have no significance), then equation (13.5) can be written in the following way:

$$Q_v = Q_p + p(v_2 - v_1) = Q_p + pv(n_2 - n_1) = \\ = Q_p + \Delta nRT = Q_p + 1.987\,\Delta nT \text{ cal},$$

where v is the volume of one gram-molecule and n_2 and n_1 are the number of moles at the end and the beginning of the process; $n_2 - n_1 = \Delta n$. If the thermal effect refers to the temperature 25°C (298°K) and is estimated in large calories, then $RT = 0.592$ and

$$Q_v = Q_p + 0.592\,\Delta n \text{ kcal}.$$

This important practical relationship remains true when solid or liquid substances take part in the reaction. In this case it is possible to neglect the change in volume due to the change in the number of moles

* 1 atm = 760 mm Hg.

of these substances in comparison with the change in volume of the gaseous components of the system, i.e. Δn is the change in the number of moles of the gaseous components of the reaction.

Thus, for the combustion reaction of the substance in oxygen

$$C_aH_bO_cN_d+\left(a+\frac{b}{4}-\frac{c}{2}\right)O_2=aCO_2+\frac{b}{2}H_2O+\frac{d}{2}N_2+Q.$$

If the substance $C_aH_bO_cN_d$ is a solid and the water formed after the reaction is liquid, then

$$\Delta n=a+\frac{d}{2}-\left(a+\frac{b}{4}-\frac{c}{2}\right)=\frac{d}{2}+\frac{c}{2}-\frac{b}{4}$$

and

$$Q_v=Q_p+0.592\left(\frac{d}{2}+\frac{c}{2}-\frac{b}{4}\right)\ \text{kcal}.$$

The thermal effect depends on the temperature at which the reaction takes place. The variation of the thermal effect with temperature can be estimated using the arguments given above.

We will consider, as an example, the monomolecular decomposition reaction occurring at constant volume according to the equation

$$MN=M+N.$$

For two different initial temperatures T_1 and T_2 the thermal effects of the reaction equal $Q_v^{T_1}$ and $Q_v^{T_2}$. According to (13.3) $Q_v=-\Delta E$, where $\Delta E=E_M+E_N-E_{MN}$.

Differentiating (13.3) with respect to T for $v=\text{const}$ and taking into account that $\left(\frac{\partial q}{\partial T}\right)_v=\left(\frac{\partial E}{\partial T}\right)_v=c_v$, where c_v is the heat capacity at constant volume, we obtain:

$$\frac{dQ_v}{dT}=-\left(\frac{\partial\Delta E}{\partial T}\right)_v=-(c_{vM}+c_{vN}-c_{vMN})=\Delta c_v.$$

Integrating the equation obtained, we find that

$$Q_v^{T_2} = Q_v^{T_1} - \int_{T_1}^{T_2} \Delta c_v \, dT. \tag{13.6}$$

If the process occurs at $p = \text{const}$, then, according to (13.4) E must be replaced by i and the heat capacity at constant volume is replaced by the heat capacity at constant pressure (c_p), then

$$Q_p^{T_2} = Q_p^{T_1} - \int_{T_1}^{T_2} \Delta c_p \, dT. \tag{13.7}$$

These formulae can be generalised for any reactions if Δc is taken to mean the algebraic sum of the heat capacities which is determined by giving a minus sign to the heat capacity of the substances taking part in the reaction and a positive sign to the products of the reaction. If the average values of the heat capacities in the temperature interval $T_2 - T_1$ are used, then the formulae take the form

$$Q_v^{T_2} = Q_v^{T_1} - \Delta \bar{c}_v (T_2 - T_1)$$

and

$$Q_p^{T_2} = Q_p^{T_1} - \Delta \bar{c}_p (T_2 - T_1).$$

It is usually understood that $Q_v^{T_1}$ and $Q_p^{T_1}$ denote the thermal effects at the standard temperature 25°C.

§ 14. The calculation of thermal effects.

The basis of thermochemistry is Hess's law: the thermal effect of a reaction does not depend on its course but only on the initial and final

states. This law was stated and proved experimentally by W.N. Hess in 1840. The law follows directly from elementary principles of thermodynamics.

The application of Hess's law requires that the reactions take place under identical conditions (at $v = \text{const}$ or $p = \text{const}$).

Hess's law on the independence of the thermal effect from the path of the reaction permits the thermal effects of some reactions to be calculated from the thermal effects of other reactions which are more accessible by direct measurements or from data given in thermodynamic tables.

For example, it is required to determine the heat of formation of an explosive $C_aH_bO_cN_d$ knowing its heat of combustion in oxygen

$$C_aH_bO_cN_d + \left(a + \frac{b}{4} - \frac{c}{2}\right)O_2 = aCO_2 + \frac{b}{2}H_2O + \frac{d}{2}N_2.$$

In order to calculate the heat of formation we consider three states of our system: the elements, the explosive and oxygen, and the combustion products. We will denote the thermal effects on transfer from one state to another by Q_{12}, Q_{23} and Q_{13} :

$$Q_{13}\left[\begin{array}{l} aC,\ \frac{b}{2}H_2,\left(a+\frac{b}{4}\right)O_2,\ \frac{d}{2}N_2 \\ C_aH_bO_cN_d + \left(a + \frac{b}{4} - \frac{c}{2}\right)O_2 \\ aCO_2,\ \frac{b}{2}H_2O,\ \frac{d}{2}N_2 \end{array}\right. \begin{array}{l} \longleftarrow \\ Q_{12} \\ \longleftarrow \\ \longleftarrow \\ Q_{23}. \end{array}$$

According to Hess's law

$$Q_{13} = Q_{12} + Q_{23}.$$

Q_{13}, the heat of formation of the combustion products from the elements, is determined from thermochemical tables as the sum of the heats of

formation of $(aCO_2+\frac{b}{2}H_2O)$. Q_{28} , if needed, is taken from the tables or calculated according to the methods considered below. Q_{12} , the heat of formation, is estimated thus:

$$Q_{12}=Q_{18}-Q_{28}.$$

The heat of explosive transformation is calculated from the known heat of formation and the reaction of explosive transformation as the difference between the heat of formation of the explosion products from the elements and the heat of formation of the explosive.

For the calculation it is necessary to use consistent quantities, i.e. Q_v or Q_p , converting them where necessary according to the expression

$$Q_v=Q_p+\Delta nRT$$

In thermodynamic tables the magnitudes of $\Delta i=-Q_p$ are usually given. For the heat of explosion the final result is converted to Q_v . This is explained by the fact that under practical conditions the transformation is accompanied by a sharp increase in pressure and relatively small change in volume, since the free expansion of the products formed during explosion and combustion is prevented by the casings (gun barrel, manometric bomb, calorimetric bomb). In the case of detonation the formation of explosion products proceeds at such a rate that in practice the explosion products are formed in a volume almost the same as the volume of the explosive charge, even in the case when the charge is not installed in a casing.

The heat of explosive transformation, which is one of the basic characteristics of an explosive, can be determined directly by experimental

means (calorimetric measurements, the accuracy of which today is within 0.1%).

In addition, the heat of explosion can also be calculated theoretically if the composition of the explosion products is known, which, strictly speaking, is defined not only by the properties of the explosive but also by the characteristics of the charge and the given conditions. This problem will be considered in detail in the next chapter.

Calculation must be used when it is impossible to determine the heat of explosion experimentally or when it is required to make a preliminary theoretical estimate of an explosive or explosive system which has not yet been synthesised.

The basic difficulty in the calculations is the absence of reliable data on the heats of formation of explosives. However, this difficulty can also be avoided, since modern thermochemistry gives the means of calculating these data if the molecular structure of the substance is known.

Comparison of the heats of formation or heats of dissociation of various compounds reveals that it is possible to attribute a definite energy to every bond, which remains more or less constant for any compound. The sum of these bond energies is approximately equal to the energy of formations of molecules of compounds made from free atoms.

In Table 32 the average values of the bond energies are given, obtained by YA.K. SYRKIN as a result of comparing the experimental thermodynamic data for a large number and variety of compounds.

Table 32.

The energy of a covalent bond

Bond	Energy, kcal	Bond	Energy, kcal
H—H	106,2	$C\overset{O}{\underset{OC}{<}}$ (esters)	327
C—H	85,56	C—N	53,5
C—C	62,77	C=N	84
C=C	101,16	N—N	27
C≡C (acetylene)	128,15	N=N	80
O—H	110	N≡N	170
O—O	35	N—H (NH_3)	83,3
O=O	117	N—O	61
C—O(alcohols and ethers)	75	N=O	108
C=O(aldehydes)	150	$^{+}N\overset{O}{\underset{O^{-}}{<}}$	$169 < E < 186$
C=O(ketones)	156	C—O—NO_2 (nitrates)	~312
C=O (CH_2O)	144	C—NO_2 (nitro-compounds)	~240
$C\overset{O}{\underset{OH}{<}}$ (HCOOH)	348	N—NO_2	~231
$C\overset{O}{\underset{OH}{<}}$ (other acids)	360		

All these values refer to standard temperature and apply only to covalent bonds which usually exist in organic compounds. With their help, it is easy to determine not only the heats of formation of organic compounds from free atoms but also the heat of formation from elements to the standard state (from solid graphite, gaseous H_2, N_2, O_2 etc.), the heat of combustion and the heat of the chemical reactions. The heats of formation are calculated for the gaseous state.

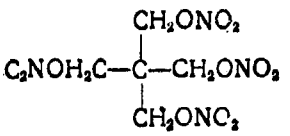
It should be mentioned, however, that the additivity of the bond energies does not always hold. This is stipulated by the structure of the substance. Because of this the heats of formation obtained by summing the bond energies sometimes differ from those established experimentally.

Thus, for example, the energy of formation of a branched hydrocarbon is somewhat high[illegible]an that of the correspond.ng normal hydrocarbon.

The isomeric effect, i.e. the increase in energy with branching, holds not only for hydrocarbons but also for compounds of other classes (alcohols, ethers, ketones, etc . Thus, the heat content Δi during transfer from normal pentane to tetramethylmethane decreases by approximately 5 kcal, since the heat of formation of tetramethylmethane is 5 kcal/mole greater than that of normal pentane.

We will evaluate, as an example, the heat of formation of PETN and Hexogen, using the data given in Table 32.

1. Pentaerythritol tetranitrate (PETN)



The heat of formation of this explosive from the atoms equals

$$Q_{form} = 4 \times 62.77 + 8 \times 85.56 + 4 \times 312 = 2183.6 \quad \text{kcal/mole.}$$

To determine the heats of formation from the elements it is necessary to determine the heat of sublimation of 5 carbon atoms (-125 kcal/g atom), the heat of dissociation of two nitrogen molecules, six oxygen molecules and four hydrogen molecules. Using the data of Table 32, we find that:

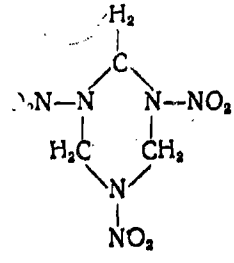
for 5C	heat of sublimation equals	$5 \times 125 = 625$ kcal,
for $4H_2$	heat of dissociation equals	$4 \times 102.6 = 410.4$ kcal,
for $2H_2$	" " " "	$2 \times 170 = 340$ kcal.
for $6O_2$	" " " "	$6 \times 117 = 702$ kcal.
		$\sum q = 2077.4$ kcal.

The heat of formation of PETN from the elements equals:

$$Q_v = Q_{form} - \sum q = 2183.6 - 2077.4 = 106.2 \quad \text{kcal/mole.}$$

If, however, analogously to tetramethylmethane it is taken into account that the correction for the isomeric effect equals 5 kcal, then finally we obtain Q_v = 111 kcal/mole. According to experimental data the heat of formation of PETN equals 122.4 kcal/mole.

2. Hexogen



The heat of formation from the atoms equals

$$Q_{form} = 6 \times 85.56 + 6 \times 53.5 + 3 \times 231 = 1527.4 \quad \text{kcal/mole,}$$
$$\sum q = 3 \times 125 + 3 \times 170 + 3 \times 117 + 3 \times 102.6 = 1543.8 \quad \text{kcal.}$$

The heat of formation from the elements

$$Q_v = Q_{form} - \sum q = 1527.5 - 1543.8 = -16.4 \quad \text{kcal/mole}$$

The experimental value of the heat of formation of Hexogen equals

$$Q_v = -20.9 \quad \text{kcal/mole.}$$

The divergence between the calculated and experimental data is somewhat changed if the heats of vaporization and condensation of these

explosives are taken into account.

More accurate values for the heats of formation can be calculated from the estimated heat of combustion. The latter is calculated (at constant pressure) by KHARASCH's method, developed by KASATKIN, PLANOVSKIY and KUL'BAKH.

By considering any organic compound such as a hydrocarbon, in which some of the hydrogen atoms are replaced by other atoms and groups of atoms, and by considering the heat of combustion as a function of the number of electrons moving during combustion from the carbon and hydrogen atoms to the oxygen atoms, KHARASCH derived the relationship

$$Q_{comb} = 26.05(4A + B - p) + \sum k_i \Delta_i \qquad (14.1)$$

for liquid organic compounds, where 26.05 kcal/mole electron is the heat of scission of the bonds C-C and C-H and of the subsequent formation of CO_2 and H_2O; $4A + B$ is the number of removable electrons for normal paraffins (A and B are the numbers of carbon and hydrogen atoms in the molecule); p is the number of migrated electrons in a molecule of the substance (the migrated electrons are the electrons of the hydrogen and carbon atoms linked with the oxygen); k_i is the number of the same substituents in the molecule and Δ_i is the corresponding correction factor for the given substituent, taking into account the change in the electron structure in normal paraffins due to the polarization of the bonds caused by the introduction of the substituent.

The sign of Δ_i is determined by the direction of the migration of electrons on introducing the substituent. It is negative for the transfer of electrons from the carbon atoms (corresponding to a decrease

in energy of the molecule) and positive for movement in the reverse direction.

Equation (14.1) holds on the assumption that the action of the substituent newly introduced into the molecule does not vary with the presence of other substituents, i.e. if the mutual effect of the atoms in the molecule is neglected. This assumption, however, does not lead to a large error in the estimate of the heat of combustion, since the importance of the term $\Sigma k_i A_i$ is comparatively small.

The values of the heat correction factors are given in Table 33.

Table 33

Heat correction factors

Type of grouping, substituents and bonds	A_i, kcal
Ketone group in aliphatic (aromatic) compounds $Al-CO-Al$; primary aromatic amines $Ar-NH_2$; secondary aliphatic alcohols; nitramine group $N-NO_2$	6.5
Bond between aromatic radicals; ethylene bond in the closed cycle; chlorine in aromatic compounds	— 6.5
Bond between aromatic radicals and hydroxyl group $Ar-OH$; tertiary aliphatic alcohols	3.5
Bond between aromatic and aliphatic radicals $Ar-Al$; bond between aromatic amine and aromatic (aliphatic) radical $Ar-N-Ar$	— 3.5
Secondary aliphatic amines $Al-NH-Al$; tertiary aromatic amines $(Ar)_3N$; aliphatic and aromatic ethers $Al-O-Al$	19.5
Primary aliphatic amines $Al-NH_2$; primary aliphatic alcohols, secondary aromatic amines $(Ar)_2NH$	13
Aliphatic esters	16.5
Nitrogroup in aliphatic and aromatic compounds $Al-NO_2$	— 13
Tertiary aliphatic amines $(Al)_3N$	26

As an example, we will calculate the heat of combustion of Trotyl $C_6H_5(NO_2)_3CH_3$: $A = 7$, $B = 5$, $p = 0$, correction factors: $\Delta_1 = -3{,}5$ (bond $Ar - Al$) and $\Delta_2 = -13$ ($ArNO_2$).

$$Q_{comb} = 26.05(4 \times 7 + 5) + (-3{,}5 - 3 \times 13) = 817.5 \quad \text{kcal/mole},$$

which approximates to the experimental data (817.1 kcal/mole).

For all thermochemical calculations it is important to know the thermal effects of as large a number of elementary reactions as possible. The heats of such reactions are given in thermochemical tables. In these tables, data is given on the thermal effects at constant pressure referred to standard temperature. All the substances taking part in the reaction are assumed to be in the states in which they usually exist under standard conditions.

For some substances the heats of formation are also given in a physical state in which they cannot exist under standard conditions. Thus, for example, the heats of formation of water are given for the liquid and gaseous states, whilst water at a temperature of 25°C is a liquid with vapour pressure 23.8mm Hg. Therefore, the given heat of formation of gaseous water implies only that so much heat would be evolved in the gaseous state under given conditions.

More complete thermochemical tables of the heats of formation can be found in hand-books of physico-chemical constants.

The tables presented here (Tables 34 and 35) give only the heats of formation of the more important compounds and explosives.

Numerical values of the heats of explosion of the various explosives are often taken to be completely definite and unchangeable characteristics

Table 34

Heats of formation (Q_p) for standard states.

Substance	Heat of formation kcal/mole	State of aggregation
H_2	0	Gas
H	— 51.8	»
O_2	0	»
O_3	33.93	»
O	— 58.5	»
C (graphite)	0	Solid
N_2	0	Gas
N	— 85.0	»
S rhombic	0	Solid
H_2O	57.801	Gas
H_2O	68.318	Liquid
H_2O_2	44.87	Gas
HCN	— 32.9	»
NH_3	11.04	»
N_2O	— 19.65	»
NO	— 21.60	»
NO_2	— 7.96	»
N_2O_4	— 3.1	»
HNO_3	41.5	Liquid
KNO_3	118.1	Solid
$NaNO_3$	111.7	»
NH_4NO_3	87.4	»
$KClO_3$	93.2	»
$NaClO_3$	83.6	»
$KClO_4$	104.5	»
$NaClO_4$	93.0	»
NH_4ClO_4	70.2	»
Al_2O_3	393.3	»
Fe_3O_4	265.7	»
Fe_2O_3	198.5	»
Sb_2S_3	38.2	»
MgO	145.8	»
CO	26.393	Gas
CO_2	94.03	»
CH_4 methane	17.87	»
C_2H_6 ethane	20.19	»
C_3H_8 propane	24.75	»
C_4H_{10} butane	29.7	»
C_5H_{12} pentane	34.7	»
C_6H_{14} hexane	40.0	»
C_7H_{16} heptane	45.4	»
C_8H_{18} octane	52.7	»
C_2H_4 ethylene	— 12.56	»
C_2H_2 acetylene	— 57.15	»
C_6H_6 benzene	— 11.12	Solid
C_7H_8 toluene	— 1.93	»
CH_3O methyl alcohol	57.03	»
C_2H_5OH ethyl alcohol	66.35	»

Table 35

Heats of formation of the more important explosives (Q_v)

Name of explosive	Chemical formula	Molecular weight	Q_v, kcal/mole
Hydrazoic acid	HN_3	43	— 64.4
Lead azide	PbN_6	291.3	— 107.0
Mercury fulminate	$Hg(ONC)_2$	284.6	— 65.4
Lead trinitroresorcinate	$C_6H(NO_2)_3O_2Pb \cdot H_2O$	468.[illegible]	199.8
Cyanuric tri azide	C_3N_{12}	[illegible]	— 222.0
Trinitrotriazidobenzene	$C_6(NO_2)_3(N_3)_3$	336	— 272
Guanidine nitrate	$HNC(NH_2)_2HNO_3$	122	87.5
Nitroguanidine	$HNC<^{NH \cdot NO_2}_{NH_2}$	104	18.96
Hexogen	$C_3H_6O_6N_6$	222	— 20.9
Glycol dinitrate	$C_2H_4(ONO_2)_2$	152	54.8
Glycerine trinitrate	$C_3H_5(ONO_2)_3$	227	83.71
Erythritol tetranitrate	$C_4H_6(ONO_2)_4$	302	114
Pentaerythritol tetranitrate (PETN)	$C_5H_8(ONO_2)_4$	316	123.1
Mannitol hexanitrate	$C_6H_8(ONO_2)_6$	452	106.1
m - Dinitrobenzene	$C_6H_4(NO_2)_2$	168	5.7
1,3,5-Trinitrobenzene	$C_6H_3(NO_2)_3$	213	2.3
2,4,6-Trinitrochloro-benzene	$C_6H_2(NO_2)_3Cl$	247.5	— 11.1
2,4-Dinitrotoluene	$C_6H_3(NO_2)_2CH_3$	182	15.3
2,4,6-Trinitrotoluene (Trotyl)	$C_6H_2(NO_2)_3CH_3$	227	13.5
2,4,6-Trinitro-m-xylene	$C_6H(NO_2)_3(CH_3)_2$	241	19.2
Dinitrophenol	$C_6H_3(NO_2)_2OH$	184	53.3
Trinitrophenol	$C_6H(NO_2)_3OH$	229	50.6
Trinitrocresol	$C_6H(NO_2)_3(OH)CH_3$	243	52.7
Trinitroresorcinol (styphnic acid)	$C_6H(NO_2)_3(OH)_2$	245	102.1
Trinitroanisole	$C_6H_2(NO_2)_3OCH_3$	243	35.5
Trinitrophenylmethyl-nitramine (Tetryl)	$C_6H_2(NO_2)_3N<^{CH_3}_{NO_2}$	278	— 9.9
Tetranitroaniline	$C_6H(NO_2)_4NH_2$		— 21.5
1,5-Dinitronaphthalene	$C_{10}H_6(NO_2)_2$	218	— 7.1
1,8-Dinitronaphthalene	to like	"	— 8.4
1,3,8-Trinitronaphthalene	$C_{10}H_5(NO_2)_3$	263	6.9
Hexanitrodiphenylamine	$[C_6H_2(NO_2)_3]NH$	439	— 12.3
Nitrate of trinitrophenyl-glycol ether	$C_6H_2(NO_2)_3OC_2H_4ONO_2$	318	61.4
Ammonium picrate	$C_6H_2(NO_2)_3ONH_4$	246	90
Potassium picrate	$C_6H_2(NO_2)_3OK$	267	113
Tetranitromethane	$C(NO_2)_4$	196	— 11.9
Nitrates of cellulose	14,15% N		532 kcal/kg
	13,48% N		571 "
	12,35% N		641 "
	11,97% N		664 "
	11,12% N		669 "

Table 36

Heats of explosive transformation of explosives

Name of explosive	Q_v, kcal/kg (water in vapour state)	Density of charge g/cm³
Glycoldinitrite	1580	1.5
Glycerinetranitrite	1485	1.6
Erythritol tetranitrate	1414	—
Pentaerythritol tetranitrate	1400	1.54
Hexogen	1390	—
Mannitol hexanitrate	1365	1.56
Tetryl	1090	1.56
Trinitrophenol	1030	1.45
Trotyl	1010	1.52
Dinitrobenzene	870	1.45
Mercury fulminate	414	—
Lead azide	367	—
Ammonium nitrate	344	—
Smoky powder	665	1.20
Oxyliquits (absorbers: peat, wood, meal, coal, moss)	1600—2000	~1.0
Ammonium picrate	865	—
Nitrogelatin	1500	1.45
Pyroxylin (13.3% N)	1040	1.30

Table 37

Heats of explosive transformation of ammonites

Mixture composition	Quantitative composition, %	Q_v, kcal/kg (water, steam)
Ammonium nitrate	100	344
Ammonium nitrate + coal	93.0 + 7.0	365
Ammonium nitrate + dinitrobenzene	83.0 + 17.0	980
Ammonium nitrate + dinitrotoluene	85.0 + 15.0	970
Ammonium nitrate + dinitronaphthalene	87.5 + 12.5	945
Ammonium nitrate + trotyl	79.0 + 21.0	1010
Ammonium nitrate + trinitroxylene	82.0 + 18.0	990

of each explosive. This is completely untrue since the relationship between the reaction products of an explosive transformation depends only to a certain extent on the characteristics of the explosive charge but mainly on the cooling conditions. Because of this the thermal effect of the reaction also changes.

Therefore the heat of explosion of a given explosive is not a constant magnitude and varies within certain limits. The calculated values of the heats of explosive transformation for a number of explosives are given in Table 36, compiled from various sources. Table 37 presents the heats of explosive transformation calculated by K.K. SNITKO for a number of ammonium-nitrate type explosives. The compositions given are calculated for the complete combustion of the components.

From the data in the tables it follows that in the most widely used explosives the heat of explosive transformation varies from 1000 to 1500 kcal/kg.

§ 15. The experimental determination of thermal effects.

The experimental determination of thermal effects (heats of combustion and explosive transformation) is carried out by means of a calorimetric apparatus, which consists basically of a calorimetric bomb. The calorimetric bomb (Fig. 25) of the normal calorimetric apparatus consists of a container made of nickel chrome steel (stainless and acid proof) with a capacity of about 300 cm^3. A massive lid is fitted to the container covering the bomb. Lead packing is used for the necessary hermetic sealing.

Normal bombs are used at comparatively low pressures (100-200 atm.); to carry out experiments at pressures of 3-4 thousand atmospheres, bombs of special construction are used.

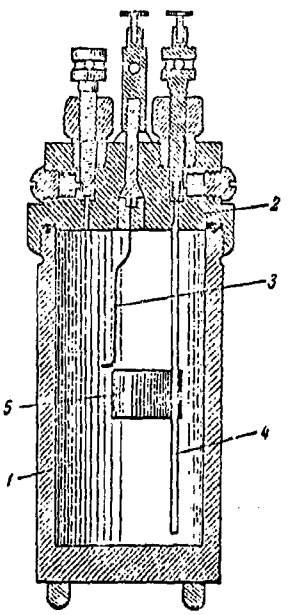


Fig. 25. Calorimetric bomb; 1 - container; 2 - lid; 3,4 - contact; 5 - crucible.

The second part of the calorimetric apparatus is the calorimeter itself, which consists of a small nickel-plated brass calorimetric tank and a copper protective calorimetric dish.

In the small tank there is a given quantity of water, which is carefully stirred by a propellor mixer, which guarantees an even temperature. The temperature of the water in the small tank is measured by means of an accurate Beckmann thermometer. The small tank is installed in the protective isothermal or adiabatic jacket and covered on the top with the lid.

The protecting vessel is a double-walled cylinder with a double bottom. The walls of the vessel (external and internal) are polished which decreases the absorption by the vessel of radiation energy. Moreover, the space between the walls is filled with water. Because of the fact that the mass of water is significant and the walls are polished, the temperature of the vessel is practically unchanged during the experiment. A general view of a

calorimetric apparatus with an isothermal jacket is given in Fig. 26.

To determine the quantity of heat evolved during combustion or explosive transformation, a few grams of carefully dried substance are taken. This weighed portion is put in a platinum or quartz crucible, fitted inside the bomb. To determine the heat of combustion, oxygen is introduced

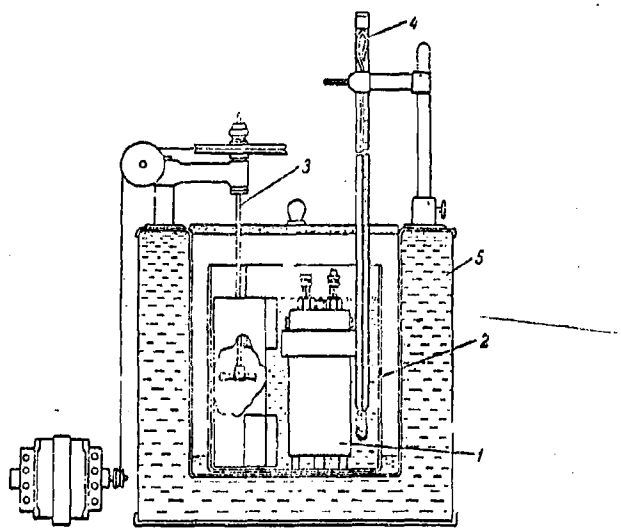


Fig. 26. Calorimetric apparatus: 1 - calorimetric bomb, 2 - small calorimetric tank, 3 - mixer, 4 - thermometer, 5 - isothermal calorimetric jacket.

into the bomb at a pressure of 25 atm, and to determine the heat of explosive transformation nitrogen is introduced or a vacuum is created at a few millimetres of mercury. Ignition of the substance is caused by an iron wire carrying an electric current.

The heat evolved in the bomb during combustion or explosion is given to the water, the change in temperature of which is measured on the

thermometer. The quantity of heat evolved in the bomb is consumed in heating the water and the calorimeter, i.e.

$$Q = c(T_f - T_i) = (W + W_0)(T_f - T_i), \qquad (15.1)$$

where W is the thermal capacity of the given water and W_0 is the thermal capacity of the apparatus ("water value" or water equivalent): T_f is the final and T_0 the initial temperature of the calorimeter; W is determined directly by weighing the water; W_0 is a constant for the given apparatus.

The water equivalent of the calorimeter is usually determined by burning in the bomb a standard chemically pure substance, the heat of combustion of which is known; then only the value W_0 is unknown in the expression (15.1) and this is readily determined from the experimental data. By this method of determining the water equivalent the effects of various factors are automatically considered: the work of the mixer, the effect of heat loss from the protruding parts of the apparatus, errors due to the change of the heat capacity of water with temperature.

As standard substances use is usually made of chemically pure benzoic or salicylic acid, naphthalene, camphor and others.

Apart from W and W_0 it is also necessary to know the temperature difference $(T_f - T_i)$ in order to determine Q. T_i is taken directly from experiment. As regards T_f, due to the heat radiation into the surrounding medium the maximum value on the thermometer is less than the maximum possible value of T_f (in the case when radiation is absent) by some magnitude ΔT. ΔT, known as the radiation factor, is cal-

culated from experimental data.

It should be mentioned that although by the method described it is possible to determine the heat of combustion in oxygen of all combustible substances, it is possible to determine the heat of explosive transformation in a nitrogen atmosphere or vacuum only for explosives which are readily ignitible by means of an incandescent wire. This refers to such explosives as pyroxylin, gunpowder, nitroglycerine, etc. The heat of explosion of nitroaromatic explosives is determined by calculation or experimentally in special calorimetric apparatuses with bombs of capacity up to 30 litres. The initiation of explosive transformation is achieved in this case by means of an electrodetonator.

§ 16. The final temperature of an explosion.

The final temperature of an explosion means the maximum temperature to which the reaction products of the explosive become heated.

Up to the present, the direct experimental determination of the final temperature of an explosion has been very difficult. The difficulties of measurement are due to the facts that the interval of time during which the maximum temperature is attained is extremely small and that when the maximum is attained the temperature of the explosion products begins to fall rapidly.

The usual methods of measuring comparatively low temperatures in which the measuring appliance is placed in contact with the hot body cannot be used for measuring high temperatures. At temperatures above 2000°K only optical methods are suitable in practice.

The impossibility of measuring the final temperature of an explosion by the contact method is also due to the considerable [illegible] effect of the explosion. To determine the temperatures of an explosion optical pyrometry is used, since the explosion is always accompanied by a flash of light.

This type of experiment has been carried out repeatedly by numerous investigators (MURAOUR, PATRY, WOOD). However these experiments did not give positive results. The negative result of these experiments is explained as being due to the luminescence which is in fact produced by secondary phenomena.

Thus, MURAOUR and his co-workers established that a considerable quantity of the light during an explosion is due to the luminescence of the surrounding atmosphere caused by the passage of a shock wave through it. In this case both the continuous and the line spectrum of the substances entering into the composition of the surrounding atmosphere are produced.

In 1945 ALENTSEV, BELYAEV, SOBOLEV and STEPANOV developed a more complete method for the spectroscopic determination of the luminescence temperature of the explosion of explosives. Below, the method used by these authors and the results obtained by them are described briefly.

To eliminate the luminescence produced by a shock wave in the atmosphere and to obtain approximately the conditions assumed during the calculations (see below), explosion is produced in an aqueous film. It seems that the luminescence is centred inside the test-tube in which the explosive was located before explosion. Moreover, the surface brightness of the luminescence was quite uniform. A continuous spectrum was obtained.

All this allowed the authors to suppose that under the test conditions luminescence of the incandescent products of explosion was obtained in the initial space of the charge and a photograph permitted the maximum temperature to be judged, since as this decreases the brightness decreases rapidly.

To determine the temperature a method was chosen in which the relative distribution of energy in the spectrum is measured at various wave lengths.

For explosives it has been established that during explosion they emit a continuous spectrum, i.e. the explosion products are heat emitters.

The distribution of energy in a spectrum of a gray body of constant absorptive power a is determined from the relationship

$$I(\lambda, T)\,d\lambda = a\lambda^{-5}C_1 e^{-\frac{C_2}{\lambda T}}\,d\lambda, \qquad (16.1)$$

where $I(\lambda, T)$ is the spectral light intensity, λ is the wave length, C_1 and C_2 are constants: $C_1 = 2\pi c^2 h = 3.74 \times 10^5$ cm^2 erg/sec, $C_2 = \frac{hc}{k} = 1.432$ cm. deg (c is the velocity of light, h is Planck's constant and k is Boltzmann's constant), T is the temperature.

Taking logarithms, we obtain

$$\ln I + 5\ln\lambda + \text{const} = -\frac{C_2}{\lambda T}. \qquad (16.2)$$

Denoting the left-hand side of (16.2) by $f(\lambda, T)$, we obtain:

$$f(\lambda, T) = -\frac{C_2}{\lambda T}, \qquad (16.3)$$

i.e. for a gray body there exists a linear relationship between $f(\lambda, T)$

and $\frac{1}{\lambda}$. In the co-ordinates $\left(\frac{1}{\lambda}, f(\lambda, T)\right)$ the relationship (16.3) will be represented by a straight line with the tangent of the angle of slope defining the temperature of the investigated source of light:

$$\tan \varphi = -\frac{C_2}{T}.$$

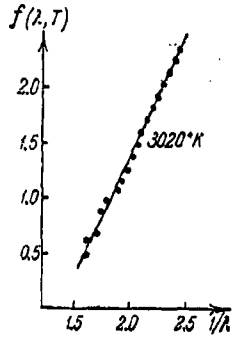


Fig. 27. Determination of the final temperature of an explosion for glycoldinitrate.

Experiment confirms that the connection between $f(\lambda, T)$ and $\frac{1}{\lambda}$ for the luminescence of an explosion is indeed linear. For the construction of the graph of $f(\lambda, T)$ versus $\frac{1}{\lambda}$, the spectrograms obtained were examined with a microphotometer. Values of intensity were obtained by means of a calibrated filament lamp with a tungsten filament at a filament temperature of 2526°K through a graded clearing agent. The exposure time was 10^{-3} sec.

The results of the treatment of one of the photographs are given in Fig. 27 for glycoldinitrate.

It was established first of all that the form of the light density curves for the plates used for an exposure of 10^{-3} sec or less does not depend on the exposure.

The temperature determined in this way is the colour temperature. For bodies the emission of which is not selective (black or gray bodies), this coincides with the actual temperature of the body. For the majority of metals and their oxides which display some selectivity of emission, the colour temperature is somewhat higher than the actual temperature and

temperature of the luminescence with increase in the density of the explosive powders. The extremely high temperatures obtained at small charge densities should be regarded as due to the luminescence of the bubbles of air compressed by the explosion to very high pressures.

PATERSON exploded charges of alternate layers of table salt and a very dense plastic explosive in water. It was shown that the explosive with almost completely expelled air emits only a little light during detonation but from the layer of salt intense light is emitted during the passage of the shock wave (luminescence of compressed air bubbles).

HEMING showed that during the explosion of charges of explosive powders the luminescence changes depending on the nature of the gas filling the spaces between the granules.

The data of Table 38 show that the final temperature of explosion of liquid explosives, for which the test conditions exclude the luminescence temperature of the surrounding medium and the bubbles of gas, is considerably lower than the calculated value. The latter is determined on the assumption that the course of the explosion process is adiabetic.

For the calculation it is assumed that all the energy of the explosion is thermal energy, whilst the theoretical considerations developed by LANDAU and STANYUKOVITCH show that for condensed explosives part of the pressure should not depend on the temperature but should be determined by the elastic resisting forces. From this it follows that the greater the initial density of the explosive charge, then the greater should be the portion of the energy of the explosion converted into energy of elastic deformation. Consequently, the higher the charge density of the given explosive, then the lower should be the temperature of the detonation

differs from it by some tens of degrees.

The average values of the temperature, each obtained from several photographs, are given in Table 38.

Table 38

The final temperature of explosion of some liquid explosives

Explosive	Density g/cm^3	T, °K (exp.)	T, °K (calc.)
Methylnitrate	1,21	3050	4560
Glycerine trinitrate	1,60	3150	4520
Glycoldinitrate	1,50	3160	4700

The authors reckon that the temperatures are determined within an accuracy of $\pm$ 100°. Accuracy of the method used in determining the final temperature of the explosion would be necessary in a more detailed investigation to establish the degree of correspondence between the radiation of explosion products and the radiation of an absolutely black body.

Attempts to use this method to determine the temperature of an explosion of explosive powders were unsuccessful. Thus, for PETN for a charge density of 0.9 g/cm^3 the temperature was equal to 6650°K, i.e. considerably greater than the calculated value. Increasing the charge density to 1.1 g/cm^3 decreased the temperature to 5750°K. For still greater densities (1.60 g/cm^3) the brightness of the flash decreased so that the spectrograms obtained on specially sensitive plates were unsuitable for treatment. These experiments undoubtedly show the rapid decrease in

products behind the front of the detonation wave, other conditions remaining the same. Also in calculating the final temperature of the explosion, only the variation of the thermal capacity with temperature is taken into account, and not its variation with pressure, since the latter has been only slightly investigated. It is possible that for the pressures and densities which are characteristic for detonation it is more correct to consider, as did ALENTSEV, SOBOLEV and BELYAEV, that the thermal capacity of the detonation products equals the thermal capacity of the solid body or of the liquid.

Assuming that the detonation products behave similarly to a solid body, we will estimate the final temperature of explosion of glycoldinitrate, the heat of explosion of which equals $Q_v = 1580$ kcal/kg = 240 kcal/mole.

For solid bodies the thermal capacity at constant volume c_v tends to a definite limit at high temperatures

$$c_v = 3nR = 5.96\,n \ \frac{\text{cal}}{\text{mole deg.}}$$

where n is the number of atoms in the molecule.

Using this rule, we find the heat capacity of the explosion products of glycoldinitrate $C_2H_4N_2O_8$ which forms, during the explosion, products consisting of 14 gram-atoms per gram-molecule of explosive.

The thermal capacity of the explosion products equals

$$c_v = 5.96 \times 14 = 83.44 \ \frac{\text{cal}}{\text{deg.}}$$

The temperature of the explosion products is determined from the following relationship:

$$T = \frac{Q_v}{c_v} + T_0 = \frac{240 \times 1000}{83.44} + 298 = 3180^\circ \text{ K},$$

where T_0 is the initial temperature of the explosive. From the experiment $T = 3160°$ K is obtained, i.e. the calculated temperature is very close to that determined experimentally.

It is not yet possible to make more penetrating deductions, based on the correspondence obtained between the experimental and calculated data, since the experimental material accumulated on this problem is still insufficient. However, there is no doubt that the method developed by ALENTSEV, SOBOLEV and others of determining experimentally the final temperature of explosion of liquid explosives definitely merits attention. The problem of determining the final temperature of explosion of explosive powders remains open.

In spite of the known achievements in the field of determining experimentally the final temperature of an explosion, due to the complexity of the method, it is usual to calculate it from the thermal capacity of the explosion products or from their internal energy.

The basis of the calculation is the supposition that an explosion is an adiabatic process, occurring at constant volume, and that the energy of chemical transformation evolved in the explosion process is consumed only by heating the products of the transformation. It is also assumed that the thermal capacity of the explosion products depends only on the temperature but does not vary with the pressure (density) of the explosion products. For the processes of rapid combustion (for example, powders in munitions), the consumption of heat by heating of the barrel and by the work of expanding the combustion products is known to occur. This too is not taken into account in the calculation, as this would involve a much more complicated calculation.

To calculate the temperature of the explosion products it is necessary to know the laws of change in the thermal capacity of these products with temperature or the change in the internal energies of the explosion products. Today the theory of this process has been developed satisfactorily.

Below, a short summary is given for practical calculations.

The contemporary theory of heat capacities is based on the quantum theory and on the analysis of molecular and atomic spectra. Analysis of these spectra gives the necessary data for determining the thermodynamic functions of the various substances and their thermal capacities. We recall that the thermal capacity

$$c = \frac{dq}{dT} \qquad (dq = dE + dA) \tag{16.4}$$

is the name given to the quantity of heat necessary to heat unit quantity of the substance (one mole) by 1° (molar thermal capacity). The heat capacity and the magnitude of q depends on the conditions of the process.

The heat capacity at constant volume (c_v) differs from the heat capacity at constant pressure (c_p). If the process occurs at $v = \text{const}$, then $dA = 0$ and

$$c_v = \frac{dq}{dT} = \left(\frac{\partial E}{\partial T}\right)_v.$$

If the process occurs at $p = \text{const}$, then $dA = p\,dv$ and

$$c_p = \frac{dq}{dT} = \left(\frac{\partial E}{\partial T}\right)_p + p\left(\frac{\partial v}{\partial T}\right)_p.$$

For the difference in heat capacities we obtain

$$c_p - c_v = \left(\frac{\partial E}{\partial T}\right)_p + p\left(\frac{\partial v}{\partial T}\right)_p - \left(\frac{\partial E}{\partial T}\right)_v. \tag{16.5}$$

For ideal gases

$$\left(\frac{\partial E}{\partial T}\right)_p = \left(\frac{\partial E}{\partial T}\right)_v \quad \text{and} \quad p\left(\frac{\partial v}{\partial T}\right)_p = p\,\frac{\partial}{\partial T}\left(\frac{R}{p}\,T\right)_p = R,$$

i.e.

$$c_p - c_v = R.$$

For real gases the difference somewhat exceeds R. This, however, cannot be taken into account in practical calculations.

For liquid and solid bodies formula (16.5) is usually replaced by empirical formulae. The quantity of heat necessary for heating a body from temperature T_1 to temperature T_2, corresponding to the equation (16.4), is determined from the expression

$$q = \int_{T_1}^{T_2} c\,dT.$$

If an average value is taken for the heat capacity over a small temperature range, we obtain:

$$q = \bar{c}(T_2 - T_1),$$

where c is the average heat capacity over the interval $T_2 - T_1$.

The correct relationship between the real and the average heat capacity for c_p and c_v is:

$$\int_{T_1}^{T_2} c\,dT = \bar{c}(T_2 - T_1).$$

According to quantum theory, the heat capacity of gases consists of three terms corresponding to the translational, rotational and vibrational degrees of freedom:

$$c_v = c_{\text{trans.}} + c_{\text{rot.}} + c_{\text{vib.}} \qquad (16.6)$$

The kinetic theory of gases gives the energy of translation of one mole of monatomic gas by the following relationship:

$$E_{\text{trans}} = \frac{3}{2} RT,$$

whence

$$c_v = c_{\text{trans.}} = \frac{dE_{\text{trans.}}}{dT} = \frac{3}{2} R.$$

For polyatomic molecules, kinetic theory gives:

$$c_v = \frac{m}{2} R, \quad c_p = \frac{m+2}{2} R, \quad k = \frac{c_p}{c_v} = \frac{m+2}{m},$$

where m is the number of degrees of freedom equal respectively to 3, 5 and 6 for mon-, di- and tri-atomic molecules. Only monatomic gases conform strictly to kinetic theory up to very high temperatures.

The rotational degrees of freedom arise at very low temperatures, whilst for every degree of freedom the energy must equal $\frac{1}{2}RT$, which gives for diatomic or polyatomic linear molecules

$$c_{\text{rot.}} = R \quad \text{(two degrees of freedom of rotation);}$$

for other polyatomic molecules

$$c_{\text{rot.}} = \frac{3}{2} R \quad \text{(three degrees of freedom of rotation).}$$

The stimulation of vibrational degrees of freedom depends on the temperature and conforms to the conditions of quantum theory. The thermal capacity obtained due to vibrational movement is defined for gases according to the DEBYE-EINSTEIN formula

$$c_{\text{vib.}} = \sum_m C_E\left(\frac{\theta}{T}\right), \tag{16.7}$$

where

$$C_E = \frac{3R\left(\frac{\theta}{T}\right)^2 e^{\frac{\theta}{T}}}{\left(e^{\frac{\theta}{T}} - 1\right)^2};$$

$\theta = \frac{h}{k}\omega = 4.788 \times 10^{-11}\ \omega$ is the so-called characteristic temperature, ω is the frequency of the vibrations, m is the number of degrees of freedom.

In this formula the parameter ω (the frequency of the natural vibrations) is determined depending on the properties of the substance. Usually the value of the characteristic temperature θ for various bodies is given in tables.

In calculating the final temperature of an explosion for solid explosion products it is possible to take the heat capacity $c_v = 3Rn$. The heat capacity of solid bodies tends to this limiting value with increase in temperature (Fig. 28).

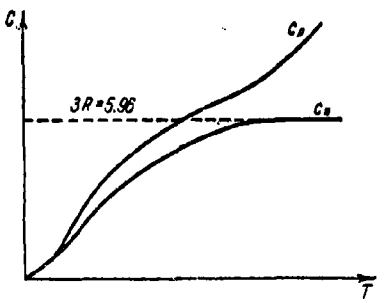


Fig. 28. The variation of the heat capacity of a solid body with temperature.

The number m for gases is found from the following considerations. Each of the n atoms of the molecule in the free state possesses three translational degrees of freedom. These $3n$ degrees of freedom are maintained in the molecule. Three of them must be for

translational motion and 2 (linear molecules) or 3 (non-linear molecules) for rotational motion.

The number of vibrational deg es of freedom

$$m = 3n - 5 \quad \text{(linear molecules) and}$$

$$m = 3n - 6 \quad \text{(non-linear molecules).}$$

Finally, for gases we have

$$c_v = \frac{5}{2} R + \sum_{1}^{3n-5} C_E\left(\frac{\theta}{T}\right) \quad \text{for linear molecules and}$$

$$c_v = 3R + \sum_{1}^{3n-6} C_E\left(\frac{\theta}{T}\right) \quad \text{for non-linear polyatomic molecules.}$$

For symmetrically constructed molecules two (or more) frequencies ω can coincide. The vibrations corresponding to them are known as doubly, three times, etc., degenerate. In the sum of the expressions for C_E they occur with the factors 2, 3, etc. The magnitudes $C_E(\theta/T)$ are calculated from the corresponding data presented in hand-books of physico-chemical quantities.

The magnitudes $\theta = \frac{h}{k}\omega$ for gases encountered in explosion products and derived by optical means are given in Table 39. The degrees of degeneracy of the corresponding frequencies are given in brackets.

The data of Table 39 are used to calculate heat capacity. For example, the heat capacity of NH_3 (non-linear molecule) varies with the temperature according to the following law. Of the six frequencies one is doubly and another three times degenerate. Thus,

$$c_v = 3R + C_E\left(\frac{1300}{T}\right) + 2C_E\left(\frac{2330}{T}\right) + 3C_E\left(\frac{4470}{T}\right).$$

Table 39

Characteristic temperatures of some gases

Diatomic gases	θ	Monatomic gases	θ_1	θ_2	θ_3
H_2	6130	CO_2	954 (2)	1920	3360
Cl_2	801	N_2O	842 (2)	1840	3190
O_2	2224	H_2O	2280	5150	5360
N_2	3350	SO_2	750	1650	1950
HCl	2938	NH_3	1360	2330 (2)	4470 (3)
NO	2705	CH_4	1870 (3)	2180 (3)	2170 (2)
CO	3085				4320

The heat capacity of CO is expressed by the relationship

$$c_v = \frac{5}{2}R + C_E\left(\frac{3085}{T}\right).$$

At $T = 3085°$ K $\theta/T = 1$. This corresponds in the tables of the functions $C_E(\theta/T)$ to a value of $C_E = 1.828 \approx 1.83$ and $C_v = \frac{5}{2}R$ + 1.83 = 6.80 cal/mole degree.

At very high temperatures, apart from the terms just calculated, it is necessary to take into account the energy of electronic excitation. Today, tables have been set up containing the heat capacities of various gases taking into account all the calculated factors. For practical calculations it is convenient to express the results by an analytical relationship. Usually it is given in the form of a power series

$(C = a_0 + a_1T + a_2T^2 + \ldots)$ with accurately estimated coefficients.

In practice, estimates of the final temperatures of an explosion frequently make use of KAST's binomial formulae for the mean molecular heat capacities in the temperature range from 0° to t°C.

For diatomic gases $\bar{c}_v = 4.8 + 4.5 \times 10^{-4} t$.

For steam $\bar{c}_v = 4.0 + 21.5 \times 10^{-4} t$.

For carbon dioxide $\bar{c}_v = 9.8 + 5.8 \times 10^{-4} t$.

For tetratomic gases $\bar{c}_v = 10.0 + 4.5 \times 10^{-4} t$.

For pentatomic gases $\bar{c}_v = 12.0 + 4.5 \times 10^{-4} t$.

A comparison of the results of the determination of the mean heat capacities according to KAST's formulae and according to internal energies shows that decreased values of the heat capacities are obtained according to KAST's formulae and consequently increased values for the final temperature of explosion.

The final temperature of an explosion can also be estimated if the internal energy of the explosion products is known.

If the process occurs at constant volume, then on the assumption that all the heat of reaction is consumed in heating the explosion products it is possible to write:

$$Q_v^0 = \sum_1^n n_i \Delta E_{i,}$$

where Q_v^0 is the heat of explosion referred to 0°C; n_i is the number of gram-moles of the i-th product of the explosion; ΔE_i is the change in internal energy of the i-th product of the explosion in the temperature range 0° — t °C.

The values of ΔE_i for some gases and Al_2O_3 are given in Table 40.

Let us determine as an example the final temperature of the explosion of PETN, for which the approximate reaction of explosive transformation can be written as:

$$C_5H_8O_{12}N_4 = 3CO_2 + 2CO + 4H_2O + 2N_2.$$

Table 40.

Internal energies of explosion products (kcal/mole).

t, °C	CO	CO_2	H_2	$H_2O_{(g)}$	$H_2O_{(l)}$	O_2	N_2	NO	CH_4	NH_3	Al_2O_3
100	0.50	0.73	0.49	0.61	10.84	0,51	0,50	0,51	0,71	0.68	2.0
500	2.61	4.36	2.50	3.28	13.51	2.75	2,57	2,69	4.78	4.08	12.1
1000	5.58	9.87	5.13	7.24	17.47	5,93	5,50	5,76	12.48	9.81	27.5
1200	6.85	12.23	6.25	9.06	19.23	7.26	6.75	7,06	16,10	12,47	34.3
1400	8.15	14.64	7,41	10.85	20,08	8.62	8.03	8.38	19,94	15.28	41.5
1600	9,46	17.11	8.61	12.78	23,01	10,00	9,33	9,72	23,94	18,22	49.1
1800	10.80	19.62	9.84	14,77	25,00	11,41	10.65	11,08	28.06	21.25	57.0
2000	12.14	22.14	11.11	16.81	27.04	12.84	11,99	12,44	32,30	24,37	65.3
2200	13.50	24.70	12.40	18.89	23.12	14.28	13,33	13,82	36,62	27.55	99,8
2400	14.87	27.27	13.72	21.03	31.26	15,76	14,69	15,21	41,01	30,80	108,4
2600	16,25	29,86	15.06	23.19	33.42	17.25	16.06	16,60	45.45	34,09	117.0
2800	17.63	32.47	16,42	25.38	35.61	18.77	17,43	18,00	49,95	37,43	125,6
3000	19.01	35.09	17.79	27.57	37.80	20.28	18,81	19,40	54.49	40,80	134.2
3200	20.41	37.74	19,19	29.79	40.02	21.84	20.20	20.81	59.03	44,77	142,8
3400	21.80	40.39	20,60	32,06	42.29	23.39	21.59	22,22	63.63	47,60	151.4
3600	23,29	43.05	22,01	34,33	44.61	24,97	22.99	23.65	68,23	51.03	160,0
3800	24,61	45.72	23,45	36,61	46,84	26.56	24,38	25,07	72.86	54.49	168,6
4000	26,01	48,40	24,88	38,90	49.13	28,15	25.79	26.50	77.51	57.97	177,2
4200	27.43	51.10	26.34	41.19	51.42	29,76	27,20	27.94	82,17	61.45	
4400	28,84	53,80	27,80	43.49	53.72	31.88	28,61	29.39	86.87	64,95	
4600	30.26	56,51	29,27	45.81	56.04	33,00	30.03	30,84	91.58	68.46	
4800	31,68	59.24	30.75	48.14	58.37	34,63	31.45	32.30	96.29	71.98	
5000	33.10	61.97	32.22	50.48	60,71	36,26	32.87	33,76	100,91	75.51	

The heat of explosion $Q_{v(l)}$ = 489 kcal/mole.

Let the temperature of explosion $t°$ = 4000°C. Then

$$\sum n_i \Delta E_{t_i} = 496.90 \text{ kcal,}$$

which is greater than $Q_{v(l)}$ by 7.9 kcal.

Now let the final temperature of explosion t = 3800°C, which gives $\Sigma n_i \Delta E_{ti}$ = 471.26 kcal, which is less than the heat of explosion by 13.74. Supposing that in a small temperature range (200°) the internal energy changes linearly with temperature, we find that on changing the temperature by one degree the internal energy of the explosion products is

changed by

$$\frac{496.90 - 471.26}{200} = 0.1282 \text{ kcal/degree.}$$

The final temperature of explosion equals

$$t = 4000 - \frac{7.9}{0.1282} = 3939^\circ \text{C} \approx 4210^\circ \text{K.}$$

Sometimes it is necessary to change the final temperature of explosion in various mixed explosives.

The final temperature of an explosion is determined by the expression

$$t = \frac{Q_v}{\sum \bar{c}_v} = \frac{Q_1 - Q_2}{\sum \bar{c}_v},$$

where Q_1 is the heat of formation of the explosion products, Q_2 is the heat of formation of the components of the explosive mixture.

Analysing the given formula, it can be established that the final temperature of explosion increases with increase in the heat of formation of the explosion products and with decrease in the heat of formation of the explosive components for a decrease or comparatively small increase in the heat capacity of the explosion products. The final temperature of an explosion can also be increased by the introduction of easily oxidized substances which give a greater quantity of heat during the consumption of a similar (or less) amount of oxygen during their own oxidation, than during the oxidation of carbon or hydrogen. Of the additions to explosive compositions which are useful for increasing the final temperature of the explosion, mention can be made of aluminium and magnesium in a finely divided state.

The effectiveness of the introduction into ammonites of aluminium and magnesium to increase their final temperature of explosion is confirmed by

the following data for the heats of combustion:

Reaction	Thermal effect of the reaction
$2Al + 1.5\,O_2 = Al_2O_3$,	393.3 kcal or 3,85 kcal/g,
$3Mg + 1.5\,O_2 = 3MgO$,	437.4 kcal or 3.61 kcal/g,
$1,5C + 1.5\,O_2 = 1,5CO_2$,	141.5 kcal or 2.24 kcal/g,
$3H_2 + 1.5\,O_2 = 3H_2O$.	173.4 kcal or 3.21 kcal/g.

The ratio of the thermal effect of the reaction to the heat capacity of its products is highest for Al_2O_3 and MgO which bears witness to the increase in the final temperature of explosion on the introduction of these metals into the composition of the explosive system.

The introduction of aluminium and magnesium unconditionally increases the power and efficiency of the explosive (brisance). However, it was shown experimentally that the introduction of these substances into high explosives, in spite of the increase in the total heat of explosive transformation, decreases the rate of detonation. This circumstance permits the assumption that the oxidation reaction of aluminium and magnesium is secondary with respect to the process of the detonating transformation of the explosive. The latter statement means that the introduction of these additives should not increase directly the temperature in the front of the detonation wave.

The formation of the oxides Al_2O_3 and MgO can proceed as a result of the inter-reaction of these metals with the products of the explosive transformation of the explosive and probably also on account of their oxidation by the oxygen in the air. In any case the reaction is favourable from the energy viewpoint which is demonstrated by the increased brisance

of an explosive, especially of ammonites, containing aluminium and magnesium.

In many cases it is necessary to lower the final temperature of explosion or combustion, which is especially important for powders. We also encounter such a necessity when carrying out blasting in shafts which are dangerous as regards gas and dust. For the explosives used in such shafts the final temperature of the products of their explosive transformation should not exceed definite values.

Decrease in the final temperature of explosion is achieved by using exactly opposite measures to those used for increasing this temperature, i.e. by decreasing the heat of formation of the explosion products, increasing their heat capacity and increasing the heat of formation of the explosive itself. In practice this is attained by upsetting the oxygen balance, and by introducing special additives which increase the overall heat capacity of the explosion products. For this purpose, an increase of the ratio of the number of H atoms to the number of C atoms in the elementary composition of the explosive is recommended, since the heat capacity of CO and CO_2 calculated for 1 g at high temperatures is considerably less than the heat capacity of 1 g of steam.

In safety explosives, the additives used to decrease the final temperature of the explosion are chlorides, sulphates, bicarbonates etc; in powders they are hydrocarbons, resins, nitro compounds of the aromatic series, etc.

BIBLIOGRAPHY

1. A.I. Brodskiy, Fizicheskaya chimiya (Physical Chemistry). Goskhimizdat (1948).
2. K.K. Snitko, Izv. Artilleriyskoy akademii 30, 118 (1940).
3. L. Pauling, "The Nature of the Chemical Bond", Oxford Univ. Press, (1940).
4. Ya. K. Syrkin and M.E. Dyatkina, Khimicheskaya svyaz' i stroyeniye molekul (The chemical bond and structure of molecules), Gozkhimizdat (1947).

   See also "Structure of Molecules", Butterworths (1950) by the same authors.
5. I.A. Kablukov, Gozkhimtekhizdat (1934).
6. S. Paterson, Nature 167, 479 (1951).

Chapter IV

REACTIONS OF EXPLOSIVE BREAKDOWN

§ 17. General data. T.No. 1488d

To estimate the possible destructive effect of an explosion, it is necessary to know the specific volume of the products of the explosive transformation, the detonation pressure and the heat of explosion, as has already been mentioned. These characteristics in their turn are determined by the composition of the explosion products, i.e. by the reactions of the explosive transformation of the substance.

The composition of the explosion products is also important in order to judge the safety of various explosives in use for underground work, so that the explosion products are harmless to the human body.

The reactions of explosive transformations can be established theoretically and from the data on the composition of the cooled products of the explosion. The accurate determination of the composition of explosion products and of the heat of explosion is an extremely complex problem. This is explained by the following reasons.

1. The composition of the cooled explosion products determined from the result of chemical analysis depends essentially on the external conditions (surrounding medium, cooling time) and can differ from the initial composition of the explosion products which corresponds to the maximum temperature and pressure of the explosion.

A very great influence on the final composition of the explosion products is exerted by their cooling time, during which so-called

secondary reactions occur between the explosion products. The course of these reactions is determined by the laws of chemical equilibrium.

2. The character of explosive reactions changes noticeably depending on the means of initiating the explosion (heating, impact, initiation by a detonator, etc.), the density of the explosive charge, the temperature and external pressure at which the reaction occurs.

According to MURAOUR's data, during ignition under a very high pressure a number of secondary explosives lose their brisance and ability to undergo a normal detonation, which is attested by a change in the character and rate of the reaction. RYABININ also shows that at a pressure of 45,000 kg/cm^2 and a temperature of 235°C the breakdown rate of barium azide is 58 times less than its breakdown rate at atmospheric pressure and the same temperature.

The factors given and especially the method of exciting reaction predetermines to a considerable extent the character of the process which can occur as detonation, rapid combustion or slow decomposition. It is evident that in all these cases the composition of the breakdown products can be different.

For example, ammonium nitrate can decompose according to the following basic equations depending on the conditions of initiation of the reaction:

1) $NH_4NO_3 \rightleftarrows NH_3 + HNO_3$ - 41.3 kcal (on careful heating to a temperature somewhat higher than the melting-point).

2) $NH_4NO_3 = N_2O + 2H_2O$ + 10.2 kcal (on heating to 260-285°C);

3) $NH_4NO_3 = N_2 + 0.5O_2 + 2H_2O$ + 30.7 kcal (explosion, excited by a capsule-detonator);

4) $NH_4NO_3 = 0.75N_2 + 0.5NO_2 + 2H_2O$ + 29.5 kcal (on rapid

heating to 400-500°C).

The processes of slow decomposition of organic explosives is usually accompanied by the formation of a copious quantity of oxides of nitrogen and a number of liquid and solid organic compounds.

During rapid combustion of explosives and powders under relatively high pressures quite a profound decomposition of the molecules of the substance occurs and the breakdown products consist mainly of such simple substances as CO_2, CO, H_2O, H_2 and N_2.

Under the conditions of detonation the quantitative and qualitative composition of the transformation products differs noticeably from the composition of the combustion products of the same explosive. This is explained by the fact that during detonation higher pressures arise under the influence of which, according to the LE CHATELIER principle, a disturbance occurs in the balance between the reaction products so that the volume of the system decreases, i.e. so that processes of association of the molecules and partial formation of free carbon ($2CO \rightleftarrows CO_2 + C$) tend to develop. With increase in the charge density (which is equivalent to an increase in the detonation pressure) these processes are of course more strongly developed, since the detonation products become richer in CO_2 and C with a corresponding decrease in the quantity of CO. This is well confirmed by the experimental data given in Table 41.

§ 18. Theoretical calculation of the composition of the products of an explosive transformation

The character of the explosion products is determined above all by the stoichiometric composition of the explosive.

Table 41

The composition of detonation products for varying initial charge densities.

Composition of explosion products per 1 kg explosive (in moles)	Tetryl		Picric acid	
	ρ_0=1.56 g/cm^3	ρ_0=0.9 g/cm^3	ρ_0=1.45 g/cm^3	ρ_0=1.0 g/cm^3
CO_2	5.59	3.02	7.88	4.49
CO	10.85	18.83	10.18	17.60
C	5.80	0.30	6.80	0.80
H_2O	5.91	3.03	4.60	4.02
H_2	1.84	3.64	1.08	1.70
N_2	7.82	7.73	5.81	5.02
NH_3	—	0.30	0.30	0.10
HCN	0.60	1.20	0.33	0.66
C_2N_2	0.58	0.20	0.40	1.20
CH_4	0.27	0.48	0.12	0.16
C_mH_m	0.03	0.02	0.01	0.04
Specific volume of gases, l/kg	750	860	690	780

The majority of explosives are organic compounds with molecules containing pre-eminently such elements as C, H, O and N. Because of this the most characteristic products of an explosive transformation are CO_2, H_2O, CO, H_2, N_2, NO, O_2 and C. Apart from these products, during an explosion CH_4, C_2N_2 and other products can be formed in insignificant quantities.

At the moment of explosion a number of reactions between these substances can occur which, depending on the elementary composition of the explosive, can determine the final composition of the explosion products.

The following reactions have a decisive significance in the composition of explosion products:

$$2C + O_2 \longrightarrow 2CO + 2 \times 26.4 \text{ kcal},$$
$$N_2 + 3H_2 \rightleftarrows 2NH_3 + 2 \times 11.0 \text{ kcal},$$
$$2CO \rightleftarrows CO_2 + C + 41.2 \text{ kcal},$$
$$2H_2 + O_2 \rightleftarrows 2H_2O + 2 \times 57.8 \text{ kcal},$$
$$CO + H_2O \rightleftarrows CO_2 + H_2 + 10.4 \text{ kcal},$$
$$2NO \rightleftarrows N_2 + O_2 + 2 \times 21.6 \text{ kcal}.$$

The NO formation reaction is endothermic and acquires noticeable development only at very high temperatures, so that in the majority of cases it is of secondary importance only.

The following reactions have a slight influence on the composition of explosion products:

$$CO + H_2 \rightleftarrows H_2O + C + 31.4 \text{ kcal},$$
$$N_2 + 3H_2 \rightleftarrows 2NH_3 + 2 \cdot 11.0 \text{ kcal},$$
$$C_2N_2 \rightleftarrows 2C + N_2 + 68.5 \text{ kcal},$$
$$2HCN \rightleftarrows 2C + N_2 + H_2 + 2 \cdot 30.7 \text{ kcal}.$$

During cooling of the explosion products secondary reactions can develop connected mainly with the formation of methane:

$$C + 2H_2 \rightleftarrows CH_4 + 17.9 \text{ kcal},$$
$$CO + 3H_2 \rightleftarrows CH_4 + H_2O + 49.3 \text{ kcal},$$
$$2CO + 2H_2 \rightleftarrows CH_4 + CO_2 + 59.1 \text{ kcal}.$$

At the moment of explosion methane is formed only in negligible quantities which is confirmed by the results of special experiments. The explosions of explosive charges in these experiments were carried out under conditions where "freezing" of the initial composition of the explosion products is attained by rapidly cooling them by means of external

work. For this purpose charges installed in tough thick-walled lead or steel appliances or in special lead bombs were exploded in an evacuated bomb. Under these conditions among the explosion products of picric acid there was detected not less than 0.2% CH_4, whilst according to the data of SARRO and VIEILLE the quantity of methane in slowly cooled explosion products amounts to about 5%.

The composition of the explosion products can be calculated theoretically, starting from the general laws of chemical thermodynamics. Here the following assumptions are made.

1. At the temperatures and excessively high pressures occurring during explosion, the reactions proceed so quickly that in spite of the extremely short duration of the phenomenon, a chemical equilibrium is established between the explosion products.

The results of calculations on detonation velocities for gaseous mixtures assuming an equilibrium state between the reacting components indirectly confirm the validity of this assumption. From Table 42 it is evident that the detonation velocities of gaseous mixtures calculated in this way for all cases are in considerably better agreement with experimental data than those calculations based on a quantitative reaction.

2. Explosion is an adiabatic process during which the external energy is expended only by the heating-up of the products.

Moreover, it is supposed that the explosive process occurring in a detonation form is isochoric i.e. it is completed within the volume of the explosive charge itself.

3. It is also often assumed that the equation of state of ideal gases and the thermodynamic consequences arising from it are also

Table 42

Calculated and experimental values for the detonation velocities of gaseous mixtures, m/sec.

Composition of gaseous mixture	Calculated values		Experimental values
	based on a quantitative reaction	based on equilibrium conditions	
$2H_2 + O_2$	3278	2806	2819
$2H_2 + O_2 + N_2$	2712	2378	2407
$2H_2 + O_2 + 3N_2$	2194	2053	2055
$2H_2 + O_2 + 5N_2$	1927	1850	1822
$2H_2 + O_2 + O_2$	2630	2302	2314
$2H_2 + O_2 + 3O_2$	2092	1925	1922
$2H_2 + O_2 + 5O_2$	1825	1735	1710
$2H_2 + O_2 + 2H_2$	3650	3354	3273
$2H_2 + O_2 + 4H_2$	3769	3627	3527

applicable to the conditions of an explosion which is characterized by high pressures.

In theoretical calculations the principal difficulty is not in the actual application of the equations of state corresponding to explosive conditions; it is due to the rather awkward equations obtained which can only be solved numerically.

Applied to the processes of rapid combustion which are characterized by comparatively low pressures, the equations of state of ideal gases (or the approximate van der Waals equation) leads to completely satisfactory results.

The course of the chemical reactions and the conditions of equilibrium. As is known, all spontaneously occurring processes tend to increase the entropy $(\Delta S > 0)$ or decrease the free energy $(\Delta F < 0)$. The

magnitude ΔF or the maximum work A serve as a measure of the chemical affinity and define the course of the chemical reactions.

For the general case of the reaction

$$\nu_1 L_1 + \nu_2 L_2 + \ldots \rightleftarrows \nu_1' M_1 + \nu_2' M_2 + \ldots, \tag{18.1}$$

where ν_i is the number of gram-molecules of type L_i, etc.

The maximum work is defined by the expression

$$A = -\Delta F = RT(\ln K_c - \Delta \ln c), \tag{18.2}$$

where K_c is the equilibrium constant which according to the law of mass action equals

$$K_c = \frac{C_{M_1}^{\nu_1'} C_{M_2}^{\nu_2'} \ldots}{C_{L_1}^{\nu_1} C_{L_2}^{\nu_2} \ldots},$$

$$\Delta \ln c = \nu_1' \ln c_{M_1} + \nu_2' \ln c_{M_2} + \ldots - \nu_1 \ln c_{L_1} - \nu_2 \ln c_{L_2} - \ldots$$

The equation (18.2) is the equation of the chemical isotherm.

$c_{L_1}, c_{L_2}, \ldots, c_{M_1}, c_{M_2}$ are the initial concentrations of the reactants;

$C_{L_1}, C_{L_2}, \ldots, C_{M_1}, C_{M_2}$ are the equilibrium concentrations of the reactants,

whilst $C_i = \frac{n_i}{v}$, where n_i is the number of moles of the given component, v is the total volume of the system;

$$\Delta = \nu_1' + \nu_2' + \ldots - \nu_1 - \nu_2 - \ldots$$

Thus

$$\Delta \ln c = \ln \frac{c_{M_1}^{\nu_1'} c_{M_2}^{\nu_2'} \ldots}{c_{L_1}^{\nu_1} c_{L_2}^{\nu_2} \ldots}.$$

Replacing the concentrations by the partial pressures p_i with the help of the equation of state of ideal gases, where

$$p_i = \frac{n_i}{v} RT = C_i RT,$$

we obtain

$$A = -\Delta F = RT(\ln K_p - \Delta \ln p_0), \tag{18.3}$$

where p_0 is the pressure at which the gases take part in the reaction and p are the equilibrium pressures.

The values K_p and K_c do not coincide; in the general case

$$K_p = K_c (RT)^{\Delta\nu}. \tag{18.4}$$

In a number of cases it is more expedient to express the concentrations in the form of mole fractions

$$N_i = \frac{n_i}{n},$$

where n is the total number of moles in a gaseous mixture.

Since $p_i = N_i p$ where p is the total pressure of the gaseous mixture

$$K_N = K_p p^{\Delta\nu} = K_c \left(\frac{RT}{p}\right)^{\Delta\nu}. \tag{18.5}$$

At $\Delta\nu = 0$ (for example, for the reaction $2NO \rightleftarrows N_2 + O_2$)

$$K_N = K_p = K_c.$$

Equation (18.2) shows that A can be taken to have any values depending on such arbitrary parameters as the initial and final concentrations or the partial pressures. Therefore, for a comparative estimate of the forces of chemical affinity the concept of normal chemical affinity is used. The magnitude of the normal chemical affinity is usually its

value at unit concentrations and partial pressures of all the reacting components, whilst it refers to standard temperature.

The equilibrium constants vary with change in temperature. The dependence of K_c and K_p on temperature is given by the isochoric and isobaric equations respectively:

$$\frac{d \ln K_c}{dT} = -\frac{\Delta E}{RT^2} = -\frac{Q_v}{RT^2}, \tag{18.6}$$

$$\frac{d \ln K_p}{dT} = -\frac{\Delta I}{RT^2} = -\frac{Q_p}{RT^2}, \tag{18.7}$$

where ΔE and ΔI are the changes in internal energy and enthalpy of the system, Q_v and Q_p are the thermal effects of the reaction at constant volume and pressure.

The relationships (18.2), (18.6), (18.7) and the deductions derived from them are fulfilled strictly only for those systems the gaseous components of which satisfy the laws of ideal gases.

For non-ideal systems in which the equation of state $pv = nRT$ is not applicable, the derived relationships are not completely true. In particular, K_p ceases to be a function of temperature alone and varies also with pressure. This fact must be borne in mind when considering reactions which occur during detonation.

The application of the laws of equilibrium to the compressed products of detonation is largely possible if the basis of the estimate of the derived thermodynamic functions is taken to be the equation of state corresponding to the pressure of the explosion. The expression for the thermodynamic potential in the general form is

$$\Phi = \Phi^0 + RT \ln p + \int_1^p \left[v - \frac{RT}{p} \right] dp. \tag{18.8}$$

For ideal gases the integral on the right equals zero and formula (18.8) leads directly to the relationship (18.2).

For non-ideal gases this integral represents the correction for the deviation from the ideal state and can be calculated from the given equation of state $p = f(\rho, T)$.

However, the solution of the problem is simplified considerably, if in the thermodynamic relationships describing the equilibrium of ideal gases, the partial pressures are replaced by the so-called activities.

The activity is defined by two conditions: 1) the thermodynamic equations for maximum work and the equilibrium of ideal gases hold also for non-ideal gases, if the pressures are replaced by activities, 2) the activity coincides with the pressure if the latter is so small that the gas becomes ideal.

From this definition it follows that in the gaseous mixture for each of its components

$$\Phi_i = \Phi_i^0 + RT \ln f_i. \tag{18.9}$$

Consequently, in a system not satisfying the laws of ideal gases the constant will not be given by $\ln K_p = \Delta \ln p_i$ but will be given by $\ln K_f = \Delta \ln f_i$; the real equilibrium constant depending on temperature alone will be not K_p but

$$K_f = \frac{f_{M_1}^{\nu_1} f_{M_2}^{\nu_2} \cdots}{f_{L_1}^{\nu_1} f_{L_2}^{\nu_2} \cdots}. \tag{18.10}$$

The equation (18.9) can be used directly for equilibrium calculations only in the case when

simply. Taking into account that $\left(\frac{\partial \Phi}{\partial p}\right)_T = v$ (molar volume) and differentiating the expression (18.9) we obtain

$$\left(\frac{\partial \Phi}{\partial p}\right)_T = RT\left(\frac{\partial \ln f}{\partial p}\right)_T = v$$

or

$$d \ln f = \frac{v}{RT} dp. \tag{18.11}$$

Integration of the right-hand side of the expression (18.11) can be carried out if the equation of state is given. For the detonation products it is possible, for example, to use the equation of state proposed by LANDAU and STANYUKOVICH

$$p = A\rho^{\lambda+1} + B(\rho)\rho T. \tag{18.12}$$

For practical calculations it is convenient to introduce the <u>activity coefficient</u> γ expressing the deviation of the gases from the ideal state. In this case

$$f = \gamma p. \tag{18.13}$$

We note that this expression does not depend on any approximations and represents simply the definition of the activity coefficient.

Corresponding to the definition of partial pressure the relationships are obtained for partial activity

$$f_i = \gamma_i p_i, \tag{18.14}$$

where γ_i is the activity coefficient of the given component in the mixture; $p_i = N_i p$ is its partial pressure equal to the molar fraction

multiplied by the total pressure p of the mixture.

Now it is possible to represent the equilibrium constant K_f of formula (18.10) in the form

$$\ln K_f = \Delta \ln f = \Delta \ln p_i + \Delta \ln \gamma_i$$

or

$$K_f = K_p \frac{\gamma_{M_1}^{\nu_1'} \gamma_{M_2}^{\nu_2'} \cdots}{\gamma_{L_1}^{\nu_1''} \gamma_{L_2}^{\nu_2''} \cdots}. \tag{18.15}$$

The problem of changing from K_p to K_f reduces to finding the activity coefficients γ_i since according to the definition K_f coincides formally with K_p estimated by the usual method for ideal gases.

The magnitudes γ can be considered within a satisfactory degree of accuracy to be identical for all gases and vapours at the same reduced pressure $\pi = p/p_c$ and temperature $\tau = \frac{T}{T_c}$ where p_c and T_c are the critical pressure and temperature.

It was shown above that the variations of K_c and K_p with temperature are given by equations (18.6) and (18.7).

Integration of equation (18.7) gives

$$\ln K_p = -\int \frac{Q_p}{RT^2} dT + \text{const}, \tag{18.16}$$

where $Q_p = Q_p(T)$.

According to KIRCHOFF's equation

$$Q_p = Q_0 - \int_0^T \Delta c_p \, dT. \tag{18.17}$$

According to NERNST the constant of integration $\text{const} = \Delta j$, where Δj is the difference between the chemical constants of the reacting gases. They can be determined from the vapour equation for the cooled reaction products according to the following relationship

$$j = \frac{S_0 - c_0}{4{,}575}, \tag{18.18}$$

where S_0 is the entropy at $T = 0$ and $c_0 = c_p$ for the low temperatures at which vibrational frequencies are not invoked, but rotational frequencies do occur.

Introducing expression (18.17) into formula (17.16) and integrating, we obtain

$$\log K_p = \frac{Q_0}{4{,}575} + \int_0^T \frac{dT}{4{,}575\,T^2} \int_0^T \Delta c_p \Delta T + \Delta j. \tag{18.19}$$

For the solution of equation (18.19) Δj is usually established experimentally and the heat capacity is expressed by equations of the type $c = a + bT + cT^2 + \ldots$ which leads to approximate formulae which are not sufficiently accurate especially at high temperatures.

Spectroscopy and theoretical physics make it possible, however, to estimate thermodynamic functions including equilibrium constants to an accuracy far exceeding the average accuracy of the usual methods used in chemical thermodynamics.

Such calculations can be carried out today for various reactions up to extremely high temperatures. They are based on modern methods of quantum statistics, and recently have found increasingly wide application in theoretical calculations connected with the determination of the state of

combustion and detonation products and also of shock-wave parameters taking into account the processes of dissociation and ionisation of air (see Chapter VI). The calculated values of the equilibrium constants of some reactions are given in Table 43 (LEWIS and VON ELBE's data).

Reaction equations of explosive breakdown. During the study of explosive reactions for convenience all explosives are divided into three groups depending on the proportions of oxygen and combustible elements in a molecule of the explosive compound (or in explosive compositions):

1) explosives with positive oxygen balance, i.e. with a quantity of oxygen sufficient for complete oxidation of the combustible elements;

2) explosives with negative oxygen balance but with a quantity of oxygen sufficient for complete vaporization;

3) explosives with a quantity of oxygen insufficient for complete vaporization, i.e. with an essentially negative oxygen balance.

First group of explosives. The condition characterizing organic explosives of the general formula $C_aH_bO_cN_d$ belonging to the first group is

$$2a + \frac{b}{2} \leqslant c. \tag{18.20}$$

A typical representative of this group is nitroglycerine. Here we refer to explosive mixtures computed for complete combustion.

For a mixture of organic explosives of the type

$$C_aH_bO_cN_d + xC_{a_1}H_{b_1}O_{c_1}N_{d_1}, \tag{18.21}$$

where the first substance has insufficient oxygen and the second has excess oxygen, the value of x is easily determined from the condition

Table 43

Equilibrium constants (derived values of log K_p) for various reactions.

Temperature	Reaction										
	$2H \rightleftarrows H_2$	$2O \rightleftarrows O_2$	$2N \rightleftarrows N_2$	$CO+\frac{1}{2}O_2 \rightleftarrows CO_2$	$H_2+\frac{1}{2}O_2 \rightleftarrows H_2O$	$OH+\frac{1}{2}H_2 \rightleftarrows H_2O$	$CO+H_2O \rightleftarrows CO_2+H_2$	$C+\frac{1}{2}O_2 \rightleftarrows CO$	$O_2+O \rightleftarrows O_3$	$NO+\frac{1}{2}O_2 \rightleftarrows NO_2$	$\frac{1}{2}N_2+\frac{1}{2}O_2 \rightleftarrows NO$
300	— 70,23	— 80.2	— 118.1	— 44,72	— 39,77	— 43,3	— 4,947	— 24,08	— 11.83	— 6,42	— 15,04
400	— 51.35	— 58.6	— 86,9	— 32.43	— 29,26	— 31,7	— 3.167	— 19,23	— 7.16	— 3.94	— 11.13
600	— 32.41	— 36,9	— 55.8	— 20,07	— 18,64	— 20.0	— 1.433	— 14.41	— 2.48	— 1.44	— 7,19
800	— 22,88	— 26,1	— 40.2	— 13.89	— 13,28	— 14.07	— 0.610	— 11,98	— 0.13	— 0,18	— 5,231
1000	— 17.13	— 19,48	— 30,9	— 10,20	— 10.05	— 10.53	— 0,147	— 10,52	+ 1.29	+ 0.57	— 4,052
1200	— 13,28	— 15.10	— 24.6	— 7,755	— 7,90	— 8,17	+ 0,145	— 9,530	+ 2,24	+ 1.08	— 3.267
1400	— 10.51	— 11.97	— 20.1	— 5,999	— 6.34	— 6.47	+ 0,341	— 8,817	+ 2.92	+ 1.43	— 2,706
1600	— 8.429	— 9,61	— 16.8	— 4.715	— 5,20	— 6,47	+ 0.485	— 8.277	+ 3.42	+ 1.69	— 2,285
1800	— 6,803	— 7,772	— 14.0	— 3,690	— 4.27	— 4,19	+ 0,580	— 7,80	+ 3.82	+ 1,89	— 1.99
2000	— 5.496	— 6.298	— 12.0	— 2,862	— 3.52	— 3,40	+ 0,658	— 7,504	+ 4,15	+ 2.07	— 1.695
2200	— 4.424	— 5.091	— 10.3	— 2.193	— 2,91	— 2.74	+ 0,717	— 7,221	+ 4,41	+ 2,18	— 1,579
2400	— 3.529	— 4.078	— 8,83	— 1.648	— 2,41	— 2,19	+ 0,762	— 0,960	+ 4,63	+ 2,29	— 1.300
2600	— 2,769	— 3.226	— 7.60	— 1.206	— 2,00	— 1.74	+ 0,794	— 6.777	+ 4.81	+ 2,39	— 1.150
2300	— 2,115	— 2.495	— 6.56	— 0,811	— 1,63	— 1,34	+ 0,819	— 6.595	+ 4.97	+ 2.48	— 1.019
3000	— 1.548	— 1,858	— 5.65	— 0,470	— 1,31	— 0,999	+ 0.840	— 6,440	+ 5,11	+ 2.56	— 0.907
3200	— 1.051	— 1,290	— 4.85	—	—	—	—	—	+ 5.23	—	— 0,807
3500	— 0.409	— 0.577	— 3,83	—	—	—	—	—	+ 5.39	—	— 0.680
4000	+ 0.449	+ 0,379	— 2.46	—	—	—	—	—	+ 5.60	—	— 0,513
5000	+ 1.654	+ 1,715	— 0.524	—	—	—	—	—	+ 5,86	—	— 0.279

$$2a + \frac{b}{2} - c = x\left(c_1 - 2a - \frac{b_1}{2}\right). \qquad (13.22)$$

For the most frequently used mixtures of organic [illegible] ammonium nitrate

$$C_aH_bO_cN_d + xNH_4NO_3$$

the value of x for which completeness of combustion of the mixture is secured is determined by the expression

$$x = 2a + \frac{b}{2} - c.$$

The results of experimental investigations showed that the course of the reactions of explosive breakdown of this group corresponds approximately with the principle of the maximum evolution of heat, i.e. the cooled explosion products consist basically of the products of complete combustion.

According to this the equation for the explosive breakdown of nitroglycerine can be written in the following form:

$$C_3H_5(ONO_2)_3 \rightarrow 3CO_2 + 2{,}5H_2O + 0{,}25O_2 + 1.5N_2 + Q.$$

However, at the moment of explosion, in spite of the extremely high pressure, due to the high temperature, partial dissociation of the products of complete oxidation (CO_2, H_2O) and the formation of some endothermic compounds (NO, C_2N_2 etc.) can occur.

For ammonites, the final temperature of explosion does not usually exceed 3000°K and these processes are not noticeably developed. For explosives with a final temperature of explosion of more than 4000°K (for example, for nitroglycerine, nitrogelatin, etc.) these processes acquire a considerable influence.

For example, for nitrogelatin consisting of 92% nitroglycerine and 8% colloxylin, under conditions of explosion for which "freezing" of the explosion products took

corresponding to the following reaction equation:

$$C_{14,1}H_{22,8}O_{39,3}N_{12,8} = 13.09CO_2 + 0.98CO + 11.13H_2O + 0.21H_2 + 0,03CH_4 + 0.70NO + 0.15O_2 + 6,05N_2.$$

From this reaction, by the way, it is evident that H_2O undergoes dissociation to a considerably less extent than CO_2.

In the general case during the theoretical calculation of the composition of explosion products the possibility should be considered of the following reactions occurring

$$2CO_2 \rightleftarrows 2CO + O_2,$$
$$2H_2O \rightleftarrows 2H_2 + O_2,$$
$$N_2 + O_2 \rightleftarrows 2NO.$$

Then the reaction of explosive breakdown in the general form can be expressed by the equation

$$C_aH_bO_cN_d = xCO_2 + yCO + zO_2 + uH_2O + wH_2 + fNO + mN_2.$$

To determine the unknown quantities we set up the following equations:

$$x + y = a,$$
$$2x + y + 2z + u + f = c,$$
$$u + w = \frac{b}{2},$$
$$f + 2m = d.$$

Moreover, for the equilibrium constants of the given reactions it is

possible to write:

$$K_p^{CO_2} = \frac{p^2 \frac{y^2}{n^2} p \frac{z}{n}}{p^2 \frac{x^2}{n^2}} = \frac{p}{n} \frac{y^2 z}{x^2},$$

$$K_p^{H_2O} = \frac{p}{n} \frac{w^2}{u^2} z,$$

$$K_p^{NO} = \frac{f^2}{mz},$$

where p is the total pressure of the system; n is the sum of all the gaseous molecules.

The number n in the given case is determined by the relationship

$$n = x + y + u + w + z + f + m = \left(a + \frac{b}{2} + d\right) + (z - m).$$

For more exact calculations the values of K_p should be replaced by values of K_f .

The pressure p starting from the given equation of state can be expressed as a function of the volume v (or density ρ) and temperature, $p = f(\rho, T)$. The pressure is given by the conditions of explosion. Because it is assumed that the explosion takes place in the volume of the charge itself, then $\rho = \rho_0$, where ρ_0 is the initial density of the charge. If we start from the equation of ideal gases, then

$$\frac{p}{n} = \frac{RT}{v_0} = \rho_0 RT.$$

Thus, to solve the problem we have a system of seven equations from which it is possible to determine uniquely all the unknowns knowing the temperature T and the corresponding values of K_p or K_f . If T

is unknown, then taking values of T the problem is solved by the method of successive approximation.

The solution of this system is rather complicated and requires much time even in the case starting from fundamental relationships for an ideal gas.

However, studying the equilibrium conditions of corresponding reactions, we reach the conclusion that the formation of nitric oxide NO and the dissociation of H_2O under explosion conditions can be neglected in the majority of cases, which does not reflect in any way essentially on the final results during the determination of the thermal effect and specific volume of the gaseous products of explosion. In this case the solution of the problem is considerably simplified.

The formation reaction of nitric oxide NO occurs at very high temperatures and does not depend on pressure since it proceeds without change of volume

$$NO \rightleftarrows \frac{1}{2}N_2 + \frac{1}{2}O_2 + 21.4 \text{ kcal.}$$

Let a and b be the initial concentrations of nitrogen and oxygen, x is the concentration of NO in the equilibrium mixture. Then the equilibrium constants are expressed by the relationship

$$K_p = K_c = \frac{\sqrt{x}}{\sqrt{\left(a-\frac{x}{2}\right)\left(b-\frac{x}{2}\right)}}.$$

For air $a = 0.792$ and $b = 0.208$.

The variation of the equilibrium constants with temperature is shown in Fig. 29. The data referring to temperatures above 3800°K were obtained

by extrapolation.

Calculations show that for corresponding temperatures and relationships between nitrogen and oxygen in the explosion products the quantity of nitric oxide formed is not large and does not exceed 1-3% of the total volume of gases at 4000°K.

The equilibrium of the formation and dissociation reactions of water vapour was investigated in detail for different temperatures including very high temperatures. Let the reaction

$$2H_2 + O_2 \rightleftarrows 2H_2O$$

occur at constant pressure and temperature. Let us express the equilibrium constant of this reaction by the degree of dissociation. If there was

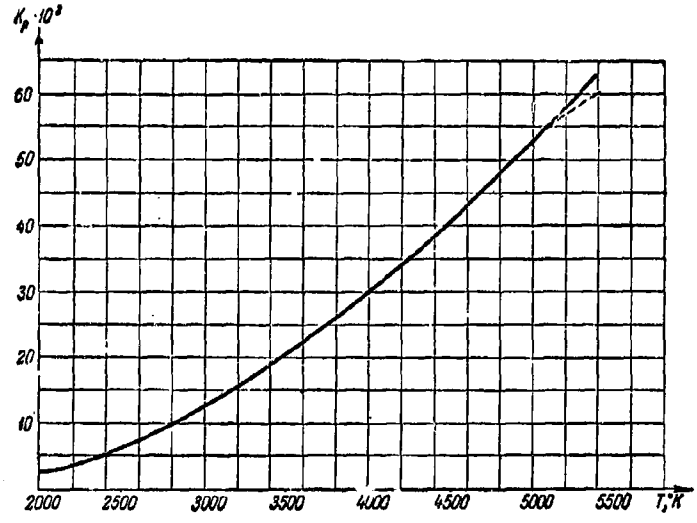


Fig. 29. The variation of K_p with temperature for the reaction $N_2 + O_2 \rightleftarrows 2NO$.

initially one mole of water vapour and its degree of dissociation is α at the given temperature, then in the equilibrium mixture $n_{H_2O} = (1-\alpha)$ moles, $n_{H_2} = \alpha$ moles and $n_{O_2} = \frac{\alpha}{2}$ moles.

The total number of moles in the equilibrium mixture amounts to

$$n = (1-\alpha) + \alpha + \frac{\alpha}{2} = 1 + \frac{\alpha}{2}.$$

then

$$K_p^{H_2O} = \frac{p_{H_2}^2 p_{O_2}}{p_{H_2O}^2} = \frac{\left(\frac{\alpha}{1+\frac{\alpha}{2}}\right)^2 p^2 \frac{\alpha p}{2\left(1+\frac{\alpha}{2}\right)}}{\frac{(1-\alpha)^2}{\left(1+\frac{\alpha}{2}\right)^2} p^2} = \frac{\alpha^3 p}{(1-\alpha)^2(2+\alpha)}. \tag{18.23}$$

Using expression (18.23), it is possible to calculate α for any p and T, if $K_p^{H_2O}$ is known.

The variation of K_p with temperature is determined by means of (18.16). In using the exact quantum formulae for heat capacity, it has the form

$$\log K_p^{H_2O} = -\frac{113943}{4.5757} + \frac{6.24}{1.987}\log T - \frac{3688 \times 10^{-5}}{2 \times 4.575} T - \frac{0.474 \times 10^{-8}}{6 \times 4.575} T^2 + 4.04. \tag{18.24}$$

For the rapid determination of $K_p^{H_2O}$ it is convenient to use Fig. 30, based on fundamental data due to LEWIS and VON ELBE, supplemented by other authors.

Calculations show that even at a temperature of 4000°K and pressure of 10,000 atm. the degree of dissociation of H_2O amounts in all to only 4.00% and consequently there is a good reason for neglecting it in

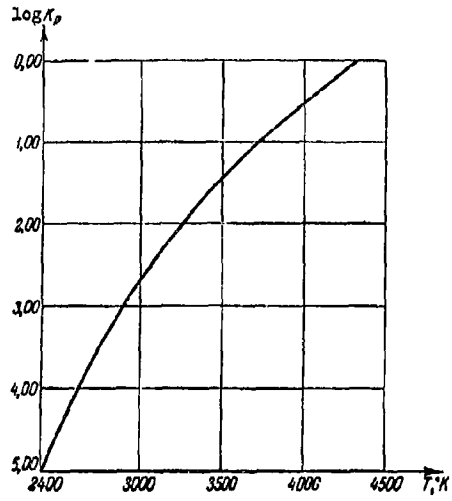


Fig. 30. Variation of K_p with temperature for the reaction $2H_2 + O_2 \rightleftarrows 2H_2O$

calculations of explosive reactions. The variations of the degree of dissociation of water (in percentages) with temperature and pressure are given in Table 44.

The equilibrium of the formation and dissociation reactions of carbon dioxide

$$2CO + O_2 \rightleftarrows 2CO_2$$

has also been studied thoroughly at various temperatures and pressures. The equilibrium constant expressed by α has the form

$$K_p^{CO_2} = \frac{p\alpha^3}{(2+\alpha)(1-\alpha)^2}. \qquad (18.25)$$

Table 44

Degree of dissociation of water (in percentages) at different temperatures and pressures.

T, °K	p (atm)									
	1	10	100	1000	5000	10 000	15 000	20 000	30 000	100 000
2000	0.560	0.0260	0.121	0.0560	0.0328	0.0259	0.0226	0.0203	0.0180	0.0125
2400	2,90	1.340	0.626	0,290	0.169	0.134	0,117	0.106	0.093	0.063
2800	9,60	4.440	2,070	0.960	0.562	0.445	0,389	0.353	0,309	0,207
3200	23,80	11.000	5.130	2.380	1.390	1.100	0,962	0,873	0.764	0,513
3600	47,30	21.400	10.020	4.730	2.760	2.190	1.915	1.740	1,520	1.002
4000	86.60	40.500	18.700	8,660	5.070	4,010	3.500	3.190	2.780	1.870
4400	100,00	69.500	32,300	15.000	8,780	6.950	6,080	5,520	4.810	3.230
4800	100.00	100.00	50,000	23,200	13.510	10.730	9,380	8,530	7,450	5.000
5200	100.00	100.00	65.900	30,600	17.900	14.100	12.400	11.200	9,800	6.590

The variation of K_p with temperature is shown in Fig. 31.

The data referring to temperatures above 3800°K were obtained by extrapolation.

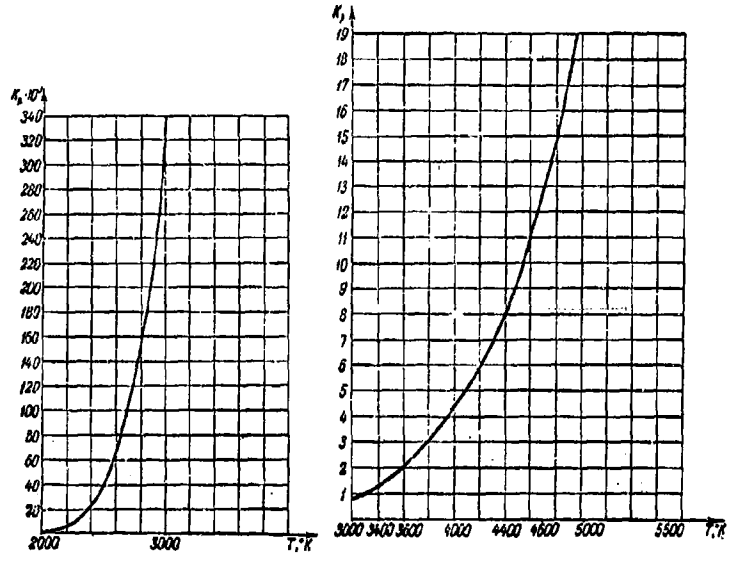


Fig. 31. Variation of K_p with temperature for the reaction $2CO + O_2 \rightleftarrows 2CO_2$.

Calculations show that at temperatures of the order of 4000° the dissociation of carbon dioxide becomes noticeable even at very high pressures (Table 45); for exact calculations it should be taken into account.

Thus, neglecting the formation of nitric oxide and the dissociation of water vapour for the reasons described, to determine the composition of the explosion products, the system of equations

$$\left.\begin{aligned} x + y &= a, \\ 2x + y + 2z &= c - \frac{b}{2}, \\ K_p^{CO_2} &= \frac{y^2 z}{x^2}\frac{\bar{p}_n}{n}, \end{aligned}\right\}$$

can be written, whilst $n = N + z$, where $N = a + \frac{b}{2} + \frac{d}{2}$;

$\bar{p}_n = f(\rho_0, T)$ is determined from the given equation of state.

Table 45

Degree of dissociation of CO_2 (in percentages)

for different temperatures and pressures.

p (atm)	T°K		
	2000	3000	4000
1 000	0,0353	6,136	27,260
10 000	0,0164	2,856	12,680
30 000	0,0113	1,975	8,760
50 000	0,0096	1,665	7,400
100 000	0,0076	1,330	5,910

The equation of state $p(v - \alpha) = RT$ can be used for application to combustion processes, in this case $p = \frac{RT}{v - \alpha}$, where α is the co-volume. For explosive processes occurring in a detonating form, the corresponding equations of state have such a complicated form that in their turn they lead to rather cumbersome expressions for the equilibrium constants.

Moreover, it must be noted that the equation of state due to LANDAU and STANYUKOVICH and others (for example, JONES) in the majority of cases leads to somewhat excessive values of the detonation velocity.

To avoid these complications it is expedient to proceed in the following way. The quantity p_u, which in the given case is the average pressure of the explosion products, on "instantaneous" detonation can be expressed quite simply in terms of the detonation velocity (see Chapter VII)

$$p_u = \frac{1}{8}\rho_0 D^2$$

The detonation velocity can be determined experimentally easily and with great accuracy and is known for the majority of explosives.

In this case the expression for the constant takes the following form:

$$K_p = \frac{1}{8}\frac{y^2 z \rho_0 D^2}{9.81 \cdot 10^5 x^2 (N+z)}. \tag{18.26}$$

The solution of this system reduces to the solution of equations of the third degree.

As an example we will calculate the composition of the explosion products of a stoichiometric mixture of heptane and tetranitromethane

$$x C(NO_2)_4 + C_7H_{16}.$$

Using expression (18.22), we find that $x = 3.50$ which corresponds to the following proportion of components: tetranitromethane 87.8% and heptane 12.2%.

Let us now depict the reaction of explosive breakdown in the following form (for 1 kg of mixture):

$$C_{13,13}H_{20,20}O_{36,80}N_{17,00} = xCO_2 + yCO + zO_2 + uH_2O + wN_2 + Q_v.$$

From experiments it is known that for this mixture the detonation

velocity D = 7380 m/sec and the density ω_0 = 1.40 g/cm^3.

Consequently,

$$\bar{p}_n = \frac{1.40 \cdot 7.38^2 \cdot 10^8}{9.81 \cdot 8 \cdot 10^4} = 97400 \text{ kg/cm}^3;$$
$$N = a + \frac{b}{2} + \frac{d}{2} = 32.18;$$
$$n = 32.18 + z.$$

A temperature T = 4200°K is assumed for which $K_p^{CO_2} = 6$. To determine the unknowns we set up the following equations:

$$x + y = 13.13,$$
$$u = \frac{b}{2} = 11.18,$$
$$2x + y + u + 2z = 36.36,$$
$$w = \frac{d}{2} = 8.95,$$
$$\frac{y^2 z \times 97400}{x^2 (32.18 + z)} = 6.$$

Solving the system with respect to x, we obtain

$$x^3 + a_1' y^2 + a_2' y - a_3' = 0,$$

where

$$a_1 = \frac{c'' + 2a - Mc'' - 2NM}{1 - M}; \quad a_2' = \frac{2ac'' + a^2}{1 - M}; \quad a_3' = \frac{a^2 c''}{1 - M};$$
$$c'' = c - a - u; \quad M = \frac{K_p^{CO_2}}{\bar{p}_n}.$$

To solve this equation we introduce a new variable by supposing that

$$x' = x + \frac{a_1}{3},$$

then our equation can be reduced to the form

$$x'^3 - 1.3x' + 10.0 = 0.$$

Applying CARDAN's formula to find the roots of the equation, we obtain

$$x' = -2.18 \text{ and, consequently, } x = 10.02;\ y = 3.11;\ z = 1.55.$$

Thus, at T = 4200°K we will have a reaction equation:

$$C_{13,13}H_{20,20}O_{36,36}N_{17,80} = 10.02\,CO_2 + 3.11\,CO + 11.10H_2O + 1.55\,O_2 + 8.95N_2 + Q_v.$$

We will check the validity of the selected temperature. The heat of formation of the explosion products equals 1765.4 kcal/kg. The heat of formation of the mixture equals 22.4 kcal/kg. The heat of explosion equals 1743 kcal/kg. For this heat of explosion, an estimate of the final temperature of explosion gives T = 4750°K.

The temperature obtained differs essentially from the selected temperature so that it is necessary to repeat the calculation. Now we will assume T = 4500°K at which $K_p^{CO_2}$ = 9.60. For the solution of this problem we will have the following system:

$$\begin{aligned} x + y &= 13.13, \\ u &= \frac{b}{2} = 11.10, \\ 2x + y + u + 2z &= 36.36, \\ w &= \frac{d}{2} = 8.95, \\ 9.6 &= \frac{y^2 z \cdot 97400}{x^2 (32.18 + z)}, \end{aligned}$$

which leads to the equation

$$x'^3 - 2x' + 120 = 0.$$

Solving this equation, we determine

$$x = x' + \frac{a_1}{3} = -4.80 + \frac{38.38}{3} \approx 8.00,$$
$$y = 5.13, \quad z = 2.06.$$

For this composition of explosion products Q_v = 1528 kcal/kg; T = 4550°K which is close to the selected temperature.

Thus the reaction equation of explosive breakdown of the mixture can be taken to be

$$C_{13,13}H_{20,20}O_{36,36}N_{17,90} = 8.00\,CO_2 + 5.13\,CO + 11.11\,H_2O + 2.06\,O_2 + 8.95\,N_2 + 1528 \text{ kcal/kg}.$$

Second group of explosives. It is not possible to draw an exact line between the second and third group of explosives. One and the same explosive depending on the conditions can detonate either with the formation only of gaseous products or with the partial separation of free carbon. On increase of the charge density (which is equivalent to an increase in the detonation pressure), other conditions remaining the same, the probability of the formation of free carbon increases.

The form of explosive decomposition also exerts a strong influence on the character of the explosion products. Thus nitrocellulose powders under normal conditions of application belong to the second group; during detonation they separate out a certain quantity of free carbon, i.e. they behave under these conditions similarly to explosives of the third group.

As the oxygen content in a molecule of explosive (or molecules of

mixture) decreases, then the reaction

$$2CO \rightleftarrows CO_2 + C,$$

acquires a greater significance and the probability of carbon separation increases.

However, there exist a number of explosives with proportions of oxygen and combustible elements in the molecule such that they definitely belong to the second group under any conditions. Typical representatives of such explosives are PETN and Hexogen in which only gaseous products are always formed during their explosive decomposition.

For explosives of the type $C_aH_bO_cN_d$ the characteristic criterion which shows that they belong to the second group is

$$a + \frac{b}{2} \geqslant c > a. \tag{18.27}$$

This criterion is not satisfied, for example, by the majority of the nitro-derivatives of the aromatic series, including Trotyl, xylyl etc. Picric acid and Tetryl, for which this condition is fulfilled, detonate at large densities with separation of a noticeable quantity of free carbon.

On the basis of analysis of experimental data, MALLARD and LE CHATELIER proposed an approximate rule for the determination of the composition of explosion products applicable to explosives with a negative oxygen balance. Here they started with the following hypothesis. At the moment of explosion only products of direct oxidation are formed, namely, the oxygen first oxidizes the carbon to CO and its remaining portion is divided equally between H_2 and CO as a result of which CO_2 and H_2O are partially formed. According to this law the approximate equation of

explosive transformation of PETN will be

$$C(CH_2ONO_2)_4 \longrightarrow 5CO + 4H_2 + 3{,}5O + 2N_2 \longrightarrow$$
$$3{,}5CO_2 + 1{,}5CO + 3{,}5H_2O + 0{,}5H_2 + 2N_2$$

which on the whole reflects quite closely the actual composition of the explosive products of PETN. However, for a number of other explosives the application of this rule leads to a considerable discrepancy between the results of theoretical calculation and the composition of explosion products established experimentally. The discrepancy is explained above all by the fact that the principle itself of equal distribution of oxygen between CO and H_2, accepted by these scientists, is not substantiated and is based on the rule of greatest evolution of heat, according to which both the reactions

$$2CO + O_2 \longrightarrow 2CO_2 + 2 \times 68.1 \text{ kcal},$$
$$2H_2 + O_2 \longrightarrow 2H_2O + 2 \times 68.3 \text{ kcal}$$

(for liquid water) are, for example, equally probable.

It is evident, however, that for the same pressures and temperatures dissociation of CO_2 is developed to a considerably greater degree than dissociation of H_2O, so that the reaction of H_2O formation will prevail over the reaction of CO_2 formation.

On the basis of these arguments and the analysis of results of rigid calculations on the equilibrium states between explosion products, BRINKLEY and WILSON developed a rule for the approximate determination of an explosion reaction by considering it possible to neglect completely the dissociation of water vapour.

For explosives satisfying the condition $a + \frac{b}{2} \geqslant c > a$, the

approximate equation of explosive decomposition has the form

$$C_aH_bO_cN_d \longrightarrow \frac{b}{2}H_2O + \left(c - a - \frac{b}{2}\right)CO_2 + \left(2a - c + \frac{b}{2}\right)CO + \frac{d}{2}N_2.$$

Applied to Hexogen and PETN this rule gives

$$C_3H_6O_6N_6 \longrightarrow 3H_2O + 3CO + 3N_2,$$
$$C(CH_2ONO_2)_4 \longrightarrow 3CO_2 + 2CO + 4H_2O + 2N_2.$$

For a comparative estimate of the approximate method data are given in Table 46 of the composition of the explosion products of PETN obtained experimentally under conditions of extremely rapid cooling and also based on the theoretical calculation of equilibrium states.

Table 46

The composition of the explosion products of PETN in moles per gram-molecule of explosive.

Detonation products	Approximate composition	Composition derived from equilibrium data	Composition derived from experimental data
CO_2	3 (3.5)	3.1	2.9
CO	2 (1.5)	1.9	2.1
H_2O	4 (3.5)	3.5	3.5
H_2	— (0.5)	0.5	0.5
N_2	2 (2.0)	2	1.8
NO	— —	—	0.4

From Table 46 it is evident that the approximate equation in the given case is in satisfactory agreement with the experimental results and theoretical calculation (in brackets the data are given which were obtained

according to MALLARD and LE CHATELIER's method).

The basic explosion products of explosives of the second group are CO_2, H_2O, CO, H_2 and N_2. Moreover, for explosives close to the first group, insignificant quantities of O_2 and NO can be found in the explosion products. Neglecting these, the reaction of explosive transformation can be expressed by the equation

$$C_aH_bO_cN_d = x\,CO_2 + y\,CO + z\,H_2 + u\,H_2O + \frac{d}{2}\,N_2.$$

The relationship between CO, CO_2, H_2O and H_2 can evidently be determined from the water gas equilibrium:

$$CO + H_2O \rightleftarrows CO_2 + H_2.$$

To find the unknowns the following equations can be set up:

$$\begin{aligned} x + y &= a, \\ 2x + y + u &= c, \\ z + u &= \frac{b}{2}, \\ K_p = K_c &= \frac{yu}{xz}. \end{aligned}$$

The equilibrium reaction of water gas proceeds without change in volume, therefore $K_p = K_c = K_w$.

Given the final temperature of explosion T_1, we find K_w from the graph (Fig. 32). This graph is based on specific data for K_w up to $T = 3800^\circ K$ and extrapolated for higher temperatures. The solution of the system reduces to the solution of a quadratic equation.

Having determined the values of x, y, z and u, the decomposition equation of the given explosive is set up and the corresponding temperature T_2 is calculated from the composition of the explosion products. If

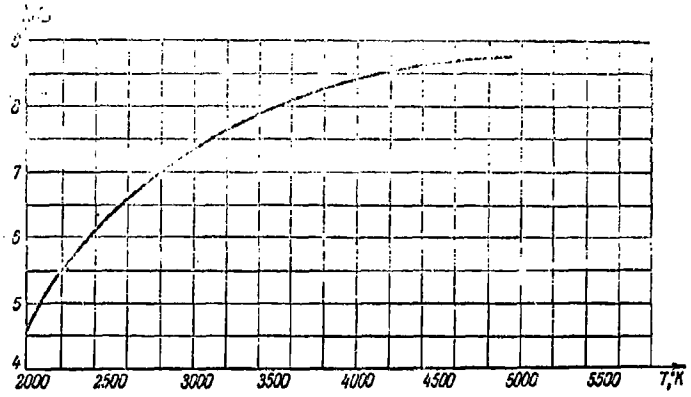


Fig. 32. The variation of K_{10} with temperature for the reaction

$$CO + H_2O \rightleftarrows CO_2 + H_2$$

the difference $T_2 - T_1$ is not large, then the composition of products obtained is taken to be the desired composition. If this difference is large, then a new temperature is taken, usually $\frac{T_2 + T_1}{2}$ and the calculation is repeated.

For the initial choice of the temperature T_1 it is convenient to determine this starting from the approximate reaction equation of the given explosive. We will explain the method of calculation by means of a concrete example. We will determine the composition of the explosion products of Hexogen.

The approximate equation for the explosive reaction of this explosive is

$$C_3H_6O_6N_6 \longrightarrow 3H_2O + 3CO + 3N_2 + Q_v.$$

Determining the final temperature of explosion from this, we find that $T \approx 3700°$ K.

We take a temperature $T_1 = 3800°$ K , for which

$$K_{\alpha} = 8.30.$$

Now we write the equation for the explosive decomposition of Hexogen in the form

$$C_3H_6O_6N_6 \longrightarrow x\,CO_2 + y\,CO + u\,H_2O + z\,H_2 + 3N_2 + Q_v.$$

To find the unknowns, we have

$$\begin{aligned} x + y &= 3, \\ 2x + y + u &= 6, \\ u + z &= 3, \\ \frac{yu}{xz} &= 8.3. \end{aligned}$$

Solving this system with respect to x , we find that

$$\frac{(3-x)^2}{x^2} = 10.3$$

or

$$9.3x^2 + 6x - 9 = 0,$$

whence $x = 0.76$; $y = 2.24$; $u = 2.24$; $z = 0.76$.

Thus, for $T = 3800°$ K the composition of the explosion products will be

$$C_3H_6O_6N_6 \longrightarrow 0{,}76\,CO_2 + 2{,}24\,CO + 2{,}24\,H_2O + 0{,}76\,H_2 + 3N_2.$$

Let us verify the validity of the selected temperature

Heat of formation of explosion products	$Q_{1,3} = 260.4$ kcal
Heat of formation of Hexogen	$Q_{1,2} = -20.9$ kcal
Heat of explosion	$Q_v = 281.3$ kcal/mole.

Determining the temperature of explosion, we obtain

$$T_2 = 3750^\circ\ \text{K},$$

which is close to the given temperature. Thus, the reaction described can be taken as the equation of explosive decomposition of Hexogen. Starting from this reaction, we also determine

$$Q_v = \frac{281.7 \cdot 10^3}{222} = 1270 \text{ kcal/kg and } V_0 = \frac{22.41 \cdot 9 \cdot 1000}{222} = 910 \text{ l/kg}.$$

Third group of explosives. This includes organic explosives with essentially negative oxygen balance, the explosion products of which can contain free carbon. The decisive criterion for an explosive to belong to the third group is

$$a + \frac{b}{2} > c. \tag{18.28}$$

As has already been stated, it is not possible to draw an exact line between the second and third groups.

The criterion (18.28) should be accepted only in the case when the explosives satisfying it can detonate under appropriate test conditions with the formation of free carbon. These conditions, as will be shown below, can be determined by theoretical calculation.

Under any conditions, the third group includes only those explosives, where the oxygen in a molecule does not suffice even to oxidize this carbon into CO $(a > c)$. A typical representative of these explosives is Trotyl.

Explosion products of the third group, as investigators have shown, consist mainly of CO, H_2O, C, N_2 and insignificant quantities of CO_2 and H_2. If the latter are neglected, then the approximate reaction equation

for this group, according to BRINKLEY and WILSON, in a general form will be:

$$C_aH_bO_cN_d \longrightarrow \frac{b}{2}H_2O + \left(c - \frac{b}{2}\right)CO + \left(a - c + \frac{b}{2}\right)c + \frac{d}{2}N_2. \quad (18,29)$$

(18.29)

In the opinion of these investigators, equation (18.29) characterizes sufficiently accurately the composition of the detonation products for high-density explosives and in the majority of cases gives very close agreement with theoretical data.

Corresponding to the expression (18.29) the reactions of explosive decomposition of picric acid and Trotyl should be written in the following way:

$$C_6H_2(NO_2)_3OH \longrightarrow 1.5H_2O + 5.5CO + 0.5C + 1.5N_2,$$
$$C_6H_2(NO_2)_3CH_3 \longrightarrow 2.5H_2O + 3.5CO + 3.5C + 1.5N_2.$$

It is interesting to compare these data with the results of specific calculations carried out by BRINKLEY and WILSON.

In calculating the equilibrium state for the explosion products of Trotyl, they started from the following possible reactions:

$$H_2O + CO \rightleftarrows CO_2 + H_2, \qquad 2NO + 2H_2 \rightleftarrows 2H_2O + N_2,$$
$$2CO \rightleftarrows CO_2 + C, \qquad 3H_2 + CO \rightleftarrows CH_4 + H_2O,$$
$$2H_2 + O_2 \rightleftarrows 2H_2O, \qquad 3H_2 + N_2 \rightleftarrows 2NH_3.$$

Comparative data for Trotyl are given in Table 47 (in moles per 1 kg explosive).

As we see, the agreement is satisfactory on the whole. From the table it also follows that in calculations of the composition of explosion products for this group the formation reactions of NH_3, CH_4, NO and O_2 could be neglected unconditionally. In this approximation the reactions determining the composition of the explosion products are

$$CO + H_2O \rightleftarrows CO_2 + H_2,$$
$$2CO \rightleftarrows CO_2 + C,$$

The latter reaction, the so-called gas generation reaction, is heterogeneous.

Table 47

The composition of explosion products of Trotyl in moles.

Detonation products	According to the approximate equation (18.29)	According to equilibrium data
H_2	0	0
CO_2	0	1.92
CO	15.77	11.64
H_2O	11.12	10.96
N_2	6.67	6.60
O_2	0	0
NO	0	0.04
CH_4	0	0
NH_3	0	0.04
C	15.77	17.32

With increase in temperature, the equilibrium of this reaction is displaced to the left. The high pressures characteristic of detonation processes permit the formation of solid carbon. Which of these factors predominates can be established in each concrete case from calculation.

The variation of the equilibrium constants of gas generation with

temperature is determined from the formula

$$\log K_p = -\frac{8947.7}{T} + 2.4673 \log T - 0.0010824T + 0{,}116 \cdot 10^{-6} T^2 + 2.772. \qquad (18.30)$$

To determine K_p it is convenient to use Table 48, based on the relationship (18.30).

Table 48

The values of K_p for the reaction $2CO \rightleftarrows CO_2 + C + 41{,}2$ kcal.

T° K	K_p	T° K	K_p
1000	1.815	3000	1462200
1500	1906	3500	3944500
2000	5496	4000	3871600
2500	39455	4500	18836000

We will write the equation of explosive decomposition for explosives of the third group in the general form:

$$C_a H_b O_c N_d \longrightarrow x\,CO_2 + y\,CO + u\,H_2O + z\,H_2 + \nu C + \frac{d}{2} N_2.$$

To determine the unknowns, we set up the following equations:

$$x + y + \nu = a,$$
$$z + u = \frac{b}{2},$$
$$2x + y + u = c,$$
$$K_w = \frac{yu}{xz},$$
$$K_p^{CO} = \frac{py^2}{nx}.$$

It is evident that in the given case

$$n = a + \frac{b}{2} + \frac{d}{2} - \nu.$$

The magnitude of is determined in just the same way as for the first group.

After appropriate substitutions the last equation takes the form

$$K_p = \frac{\rho_0 D^2 y^2}{8 \cdot 10^4 n x}. \tag{18.31}$$

Our system can be reduced to an equation of the third degree of general form

$$Ax^3 + Bx^2 + Cx + D = 0.$$

The next step in the calculation is identical to that for the first and second groups.

For explosives not satisfying the condition $a \geqslant c$ it is not possible to predetermine earlier whether free carbon will separate out on detonation or not.

To obtain an answer to this question, we proceed in the following way. First of all, the calculation is carried out as for the second group assuming complete vaporization. Having obtained values for x, y, z and u, the temperature of explosion is then calculated and its corresponding value for K_p^{CO} found.

The value of K_p found is compared with

$$K'_p = \frac{\rho_0 D^2 y^2}{8 \cdot 10^4 n x}$$

for the given conditions of density of the explosive charge. If $K'_p > K_p$, then it is easily seen that solid carbon is separated out (for K'_p to

become equal to K_p, the value of y should decrease and the value of x increase which is connected with the disturbance of the equilibrium towards the side of separation of free carbon). If $K'_p < K_p$, then for the given conditions solid carbon should not be separated and the composition of the explosion products found can be considered to be the real composition. The average detonation pressure $\bar{p}$, as will be shown in Chapter VII, equals

$$\bar{p} = \rho_0 (\varkappa - 1) Q_v \cdot 10^{-4} \text{ kg/cm}^2,$$

where $\varkappa \approx 3$ is the isentropic coefficient and Q_v is the heat of explosion of unit mass of explosive.

Then the limiting density $\rho_{0\,lim}$ of the explosive, at which the reaction begins to occur with separation of solid carbon, can be established from the equality condition $K_p = K'_p$; whence

$$p_{lim} = (\varkappa - 1)\rho_0 Q_v \cdot 10^{-4} = \frac{K_p n x}{y^2},$$

where Q_v is the heat of explosion referred to unit mass of explosive. From this

$$\rho_{0\,lim} = \frac{K_p n x}{y^2 (\varkappa - 1) Q_v} 10^4 \text{ kg sec}^2/\text{m}^4. \qquad (18.32)$$

In conclusion we will consider two concrete examples.

Example 1. It is required to calculate the composition of the explosion products of Trotyl at

$$\rho_0 = 1.50 \text{ g/cm}^3 \quad (D = 6500 \text{ m/sec}).$$

Starting from the approximate reaction equation, we are given a

temperature of explosion $T = 3000°$, at which $K_w = 7.4$ and $K_p = 1.46 \times 10^6$.

To find the unknowns, we set up the equations

$$\begin{aligned} x + y + \nu &= 7, \\ 2x + y + u &= 6, \\ z + u &= 2.5, \\ \frac{yu}{zx} &= 7.4, \end{aligned}$$

$$\frac{\rho_0 D^2 y^2}{8Nx} = \frac{80750\, y^2}{(11-\nu)\, x} = 1.46 \times 10^6; \quad \frac{y^2}{x} = 183.8.$$

Solving this system of equations, we find:

$$y = 5.4; \quad x = 0.16; \quad u = 0.38; \quad z = 2.12$$

and

$$\nu = 1.44.$$

Let us prove the validity of the selected temperature.

Heat of formation of explosion products . .	$Q_{1,3} = 179.6$ kcal
Heat of formation of one mole of Trotyl	$Q_{1,2} = +13$ kcal
Heat of explosion.	$Q_p = 166.6$ kcal/mole.

Determining the temperature of explosion, we obtain $t_1 = 2150°$ C or $T_1 = 2423°$ K, which diverges considerably from the selected temperature. We repeat the calculation, taking $T = 2700°$ K.

At this temperature, $K_w = 7.0$ and $K_p = 6.3 \times 10^5$.

Solving the system of equations, we find that:

$$y = 4.70; \quad x = 0.52; \quad u = 0.78; \quad z = 1.72$$

and

$$\nu = 1.78.$$

For this composition of explosion products

$$Q_{1,3} = 193.86 \text{ kcal}; \quad Q_v = 180.86 \text{ kcal/mole},$$

whence for the temperature of explosion we obtain

$$T_2 = 2673^\circ \text{ K}.$$

This temperature is very close to the selected temperature. Thus, the temperature of explosion can be taken to equal 2700°K and the reaction equation of explosive decomposition of Trotyl at $\rho_0 = 1.50$ g/cm^3 will have the following form:

$$C_6H_2(NO_2)_2CH_3 = \\ = 0.52\,CO_2 + 4.70\,CO + 0.78\,H_2O + 1.72\,H_2 + 1.78\,C + 1.5\,N_2.$$

Example 2. It is required to determine the limiting density of picric acid, at which (or above which) detonation will be accompanied by the separation of free carbon.

At first we will carry through the calculation for the composition of the explosion products on the assumption of complete vaporization

$$C_6H_2(NO_2)_3OH \longrightarrow x\,CO_2 + y\,CO + u\,H_2O + z\,H_2 + 1{,}5N_2.$$

We will take a temperature of explosion $T = 2900^\circ$ K at which $K_w = 7.20$. To find the unknowns we write down the following equations:

$$\begin{aligned} x + y &= 6, \\ 2x + y + u &= 7, \\ z + y &= 1.5, \\ \frac{yu}{zx} &= 7.20, \end{aligned}$$

The solution of the problem reduces to the solution of a quadratic equation

$$6.2x^2 + 10.6x - 6 = 0.$$

From this we determine

$$x = 0.45, \quad y = 5.55, \quad u = 0,55$$

and

$$z = 0,95.$$

Let us verify the validity of the selected temperature.

Heat of formation of explosion products . .	$Q_{1,3} = 221.76$ kcal
Heat of formation of picric acid .	$Q_{1,2} = +46.8$ kcal
Heat of explosion.	$Q_v = 174.96$ kcal.

From this $t = 2648°$ C or $T = 2921°$ K.

This temperature is close to the selected temperature. Thus the reaction equation of explosive decomposition of picric acid will have the form

$$C_6H_2(NO_2)_3OH = 0.45\,CO_2 + 5.55\,CO + 0.95\,H_2 + 0.55\,H_2O + 1.5\,N_2.$$

At $T = 2900°$ the equilibrium constant of gas generation K_p = 5.63 x 10^5.

Taking $\varkappa = 3$, according to formula (18.32) we determine the limiting density of picric acid at which (or above which) its detonation will be accompanied with separation of free carbon:

$$\rho_{0\,lim} = \frac{K_p\,\varkappa n \cdot 10^4}{y^2(\varkappa - 1)Q} = \frac{5.63 \times 10^5 \times 0.45 \times 9 \times 10^4}{5.5^2 \times 2 \times 800 \times 427 \times 9.81} = 112 \text{ kg sec}^2/\text{m}^4$$

or

$$\rho_{0\,lim} = 1,10 \text{ g/cm}^3.$$

§ 19. Method for the experimental investigation of explosion products

An investigation of explosion products really means the determination of their composition and volume. For this purpose a given quantity of explosive is exploded in a special bomb. Then the explosion products cooled down to room temperature undergo chemical analysis.

Whilst investigating the combustion products of powders, burning is usually carried out in a calorimetric bomb which makes it possible to combine this investigation with the determination of the heat of explosive decomposition.

Explosion of high explosives is most frequently accomplished in the bomb shown in Fig. 33 or in special calorimetric bombs. The internal volume of the bomb for explosions is 20 l; the thickness of the walls is 12 cm; the bomb is designed for the explosion of up to 200 g of high explosive. In it up to 1 kg of powder can be burned. The bomb is covered with a massive lid. To guarantee hermetic sealing between the lid and the bomb, an annular lead strip is fitted.

The explosive charge is installed in the bomb on a wire support. Explosion is carried out by means of an electrodetonator with non-insulated leads in order to eliminate the effect of a combustible insulation on the composition of the explosion products.

Directly before the explosion the air is evacuated from the bomb until the vacuum is of the order of a few mm of mercury. For this purpose the bomb possesses a valve which also serves as the exit for the gases after explosion.

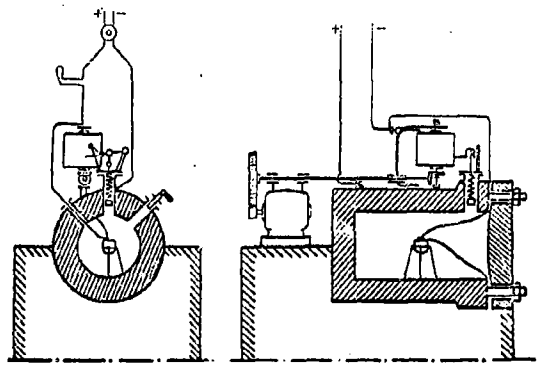


Fig. 33. Bomb for explosions.

The explosion products are cooled and the gases are passed into a gasometer to determine their volume. The volume of the gases can be determined to satisfactory accuracy by means of a mercury manometer which communicates with the interval volume of the bomb.

The volume of gases referred to a temperature 0°C and a pressure 760 mm Hg is calculated according to the formula

$$v_0 = \frac{v\,(p - w) \times 273M}{760\,Ta}, \tag{19.1}$$

where v_0 is the volume of dry gases referred to standard conditions (in litres), v is the internal volume of the bomb, p is the pressure of the cooled gases (in mm Hg), w is the pressure of saturated water vapour at room temperature, T is the temperature of the cooled gases (room temperature), a is the weight of the explosive to be exploded,

M is the weight of explosive to which the volume v_0 refers.

The quantitative composition of the gaseous explosion products is determined by the usual methods of gas analysis. For this purpose a sample of gas is taken from the bomb. The analysis is based on the successive quantitative absorption of the separate gases by different absorbents.

The following are used as absorbents:

for CO_2, an aqueous solution of caustic potash,

for O_2, an alkaline solution of pyrogallol $[1,2,3C_6H_3(OH)_3]$,

for CO, an ammoniacal solution of cuprous chloride (Cu_2Cl_2),

for NO, a saturated solution of ferrous sulphate ($FeSO_4$),

for NH_3, a dilute sulphuric or hydrochloric acid,

for N_2, H_2 and CH_4, sufficiently good absorbents are not available.

The determination of H_2 and CH_4 is usually carried out in the following way. After absorption of the enumerated gases, the remaining portion of the gas is mixed with a measured quantity of oxygen and is burned in an explosive pipette by means of an electric spark. After this the total increase in volume Δv is determined, which occurs as the result of the reactions:

$$2H_2 + O_2 \longrightarrow 2H_2O. \qquad (a)$$

$$CH_4 + 2O_2 \longrightarrow CO_2 + 2H_2O. \qquad (b)$$

The quantity of H_2 and CH_4 is estimated on the basis of the following arguments. From reaction (a) it is evident that during the burning of two moles of H_2 the volume of gas is decreased by three moles; if there were originally x volumes of H_2 in the mixture, then the decrease in

volume due to their combustion should be

$$\Delta v_1 = \frac{3}{2} x.$$

From reaction (b) it follows that during the burning of one mole of CH_4 the volume is decreased by two moles; if there were y volumes of CH_4 in the mixture, then the decrease in volume due to their combustion will be

$$\Delta v_2 = 2y.$$

The total decrease in volume after burning will be

$$\Delta v = \Delta v_1 + \Delta v_2 = \frac{3}{2} x + 2y, \tag{19.2}$$

where Δv is determined by direct measurement; y equals the volume of CO_2 formed.

Thus, the only unknown is x.

The quantity of N_2 is determined either as the difference between the volume of mixture taken for analysis and the sum of the volumes of all of its determined constituent components, or directly by measurement of the remainder after burning and absorption of the CO_2 and O_2.

The exact quantity of H_2O formed can be determined only by conducting the test in a bomb with two valves, an inlet and an outlet. For this purpose the gases are passed from the bomb to the gasometer through previously weighed tubes filled with calcium chloride. After this a stream of carefully dried air is passed through the inlet valve into the bomb. The quantity of water formed during the explosion is determined by the increase in weight of the absorption tubes.

If there is a solid residue in the explosion products, then it can be

collected and analysed by the usual methods of analytical chemistry.

In the cases where there is no solid residue in the explosion products, the quantity of water is found by the difference between the weight of the exploded explosive and the total weight of all the dry gases.

Calculation, according to the results of gas analysis, of the number of moles of separate components is achieved by means of the formula

$$n_i = \frac{C_i v_a}{100 v_0}, \qquad (19.3)$$

where C_i is the percentage volume of the given gas, v_a is the volume of all the dry gas (in litres), v_0 is the molar volume equal to 22.41 l at 0°C.

The number of moles of H_2O is determined from the formula

$$f = \frac{sM}{18a},$$

where s is the quantity of H_2O found (in grams), a is the weight of exploded explosive.

On the basis of the analytical data the reaction equation of explosive decomposition is readily determined. We will explain this by means of the following example.

On exploding 50 g of a cellulose nitrate containing 13.1% nitrogen in a bomb, 33.76 l of dry gases were obtained (p = 760 mm Hg and t = 0°C). They contain:

CO_2 — 21,7%; CO — 48,75%; CH_4 — 0,59%; H_2 — 13,26% and N_2 — 15,70%.

The molecular composition of the cellulose nitrate is $C_{24}H_{29.5}O_{9.5}(ONO_2)_{10.5}$

and

$$M = 1120.5 \text{ g.}$$

The volume of gaseous explosion products of a mole of cellulose nitrate

$$v_o = \frac{33.76 \times 1120.5}{50} = 756.5 \text{ l.}$$

Number of moles of

$$CO_2 = \frac{756.5 \times 21.7}{100 \times 22.41} = 7.33;$$

their weight equals $7.33 \times 44 = 322.5$ g.

The number of moles of

$$CO = \frac{756.5 \times 48.75}{100 \times 22.41} = 16.46;$$

their weight equals $16.46 \times 28 = 461.0$ g.

The number of moles of

$$CH_4 = \frac{756.5 \times 0.59}{100 \times 22.41} = 0.20;$$

their weight equals $0.2 \times 16 = 3.2$ g.

The number of moles of

$$H_2 = \frac{756.5 \times 13.26}{100 \times 22.41} = 4.48;$$

their weight equals $4.48 \times 2 = 9.0$ g.

The number of moles of

$$N_2 = \frac{756.5 \times 15.70}{100 \times 22.41} = 5.30;$$

their weight equals $5.3 \times 28 = 148$ g.

The total weight of gases equals 944.2 g.

There are solid substances in th[illegible]losion products of cellulose nitrate, therefore the difference between the weight of a mole of cellulose nitrate and the weight of gaseous products could be taken as the quantity of water formed during the explosion; its weight will equal 1120.5 - 944.2 = 176.3 g or 9.8 moles.

As a result of these calculations, the reaction equation of explosive transformation of cellulose nitrate will have the form

$$C_{24}H_{29,5}O_{9,5}(ONO_2)_{10,5} =$$
$$= 7,33\,CO_2 + 16,46\,CO + 0,2\,CH_4 + 4,48\,H_2 + 5,3\,N_2 + 9,8H_2O.$$

Bibliography.

1. Ya.M. Paushkin, Khimicheskiy sostav i svoystva reaktivnykh topliv (Chemical composition and properties of jet fuels), Izv. Akad. Nauk, U.S.S.R. (1958). English translation shortly to be published by Pergamon Press.
2. R.N. Wimpress, Internal Ballistics of Solid-Fuel Rockets. McGraw-Hill (1950).
3. R.H. Cole, Underwater Explosions. Princeton Univ. Press (1948).
4. B. Lewis and G. von Elbe, Combustion, Flames and Explosions of Gases. Cambridge University Press (1938).
5. J. Corner, Theory of the Interior Ballistics of Guns. John Wiley & Sons (1950). New York.
6. E.V. Vritske, A.F. Kapustinskiy et al., Termicheskie konstanty vzryvchatykh veshchestv, (Thermal constants of explosives), Izd. Akad. Nauk, U.S.S.R. (1949).

Chapter V

ELEMENTS OF GAS DYNAMICS

T-No. 1488e.

§ 20. Equations of gas dynamics.

The basic equations of gas dynamics are derived from the laws of conservation of mass, of momentum and of energy.

In all the following arguments whilst considering the motion of a gas (fluid) we assume that the moving medium fills the space, i.e. any small volume of it contains an extremely large number of molecules.

When speaking of an infinitesimally small volume of the medium we assume that it is nevertheless quite large in comparison with the length of the mean free path of the molecules in this medium. Therefore, when considering the transfer of some particle of the medium, we should remember that in this case it is a question of the motion of some fixed volume containing a large number of molecules but which is extremely small in comparison with the volume occupied by the whole medium.

Also, in determining the parameters of motion of the medium, we will neglect completely the processes of dissipation of energy which can arise in the medium due to internal friction (viscosity) and the heat exchange between the separate elements of the medium under the action of thermal conductivity. Such motion is known as the motion of an ideal fluid.

The absence of heat exchange between separate elements of the fluid (and also between the fluid and the external medium) signifies that the motion occurs adiabatically.

The motion of the medium (gas, fluid) can be studied by two methods - the LAGRANGE method and the EULER method.

The first method reduces to the determination of the parameters of state (density, pressure, temperature or entropy) and of motion (velocity and co-ordinates) of every fixed particle of the medium at any given moment of time.

The second method, on the other hand, reduces to the determination for every given point in the space of the variation of cited parameters with time; in other words, all the parameters of the medium are considered as functions of the co-ordinates and time, i.e. as functions of the four arguments x, y, z and t, the so-called Euler variables.

Below, we will give the result of the basic equations of gas dynamics in Euler's form, which are more convenient for the study and solution of the problems connected with the gas-dynamics of an explosion.

We will consider first the law of conservation of mass. At a time t_0 let us consider an infinitely small volume of liquid $\delta\tau_0$ which at time t changes into the volume $\delta\tau$. Since during the motion of a fluid, the quantity of a substance should remain unchanged, then

$$\rho_0 \delta\tau_0 = \rho\,\delta\tau = \text{const.} \tag{20.1}$$

where ρ_0 and ρ are the densities of the fluid at times t_0 and t respectively.

Taking the total derivative of (20.1) with respect to time we obtain

$$\frac{d(\rho\delta\tau)}{dt} = 0 \quad \text{or} \quad \frac{d\rho}{dt} + \rho\frac{d(\delta\tau)}{\delta\tau\, dt} = 0.$$

The magnitude $\frac{1}{\delta\tau}\frac{d(\delta\tau)}{dt}$ expresses the rate of the corresponding

volumetric expansion of the fluid in the neighbourhood of the given point and equals the divergence of the velocity at this point; consequently, we will have

$$\frac{d\rho}{dt} + \rho \operatorname{div} v = 0.$$

From vector analysis it is known that

$$\operatorname{div} v = \frac{\partial u}{\partial x} + \frac{\partial v}{\partial y} + \frac{\partial w}{\partial z}.$$

Consequently, in Cartesian co-ordinates, we have

$$\frac{1}{\rho}\frac{d\rho}{dt} + \frac{\partial u}{\partial x} + \frac{\partial v}{\partial y} + \frac{\partial w}{\partial z} = 0. \tag{20.2}$$

This expression is the equation of continuity in Euler's variables.

We will turn now to the result of the equation characterizing the law of conservation of momentum. For this purpose, we will isolate some volume in the medium, assuming that the medium is not acted upon by external forces. Let p be the pressure in the medium, then the total force acting on the whole surface f of the isolated volume due to the medium surrounding it equals

$$-\oint p\, df.$$

Transforming this integral into a volume integral according to the Ostrogradskiy-Gauss method, we have

$$-\oint p\, df = -\int \operatorname{grad} p\, dv.$$

From this it is evident that in each element of volume dv a force $\operatorname{grad} p\, dv$ acts, whilst a force $\operatorname{grad} p$ acts on unit volume of the

medium.

We can equate this force to the product of the mass ρ of unit volume of the medium and the acceleration $\frac{dv}{dt}$, i.e.

$$\frac{dv}{dt}+\frac{1}{\rho}\operatorname{grad} p=0. \tag{20.3}$$

The derivative $\frac{dv}{dt}$ is the acceleration of a given particle of the medium moving in space and not the acceleration at a given stationary point in space. To determine the acceleration of a particle at a given fixed point in space we express the derivative $\frac{dv}{dt}$ according to the formula of vector analysis

$$\frac{dv}{dt}=\frac{\partial v}{\partial t}+(v\nabla)v. \tag{20.4}$$

The first term of the right-hand side of this equation defines the acceleration at a given point in space for constant x, y and z, and the second term is the acceleration due to the change in velocity (for a given moment in time) on transfer from the given point in space to a point separated from it by a distance dr, traversed by the particle in time dt.

Using (20.3) we can now represent equation (20.4) in the following form:

$$\frac{\partial v}{\partial t}+(v\nabla)v+\frac{1}{\rho}\operatorname{grad} p=0. \tag{20.5}$$

Equation (20.5) is the required equation for the motion of the fluid, also known as the Euler equation.

We will now derive the equation characterizing the law of conservation of energy. It has already been stated earlier that we will consider only adiabatic motion of the medium. For adiabatic motion the entropy of each particle of the fluid remains constant.

Denoting the entropy relative to unit mass of the medium by S, we can express the condition of adiabatic motion of the medium in the form

$$\frac{dS}{dt} = 0. \tag{20.6}$$

Here, as has already been mentioned, the complete derivative of entropy with respect to time signifies the change in entropy of the given particle moving in space.

Because

$$\frac{dS}{dt} = \frac{\partial S}{\partial t} + \sum_{i=1}^{3} \frac{\partial S}{\partial x_i} \frac{\partial x_i}{\partial t} = \frac{\partial S}{\partial t} + v \operatorname{grad} S,$$

where x_i are the co-ordinates of a particle at a given point in space ($i = 1,2,3$), then the condition of adiabatic motion in Euler form can be written in the form

$$\frac{\partial S}{\partial t} + v \operatorname{grad} S = 0. \tag{20.7}$$

If at some initial moment the entropy for all the particles of the medium were identical, then due to the adiabatic process they remain constant during the further motion of the medium. In this case the condition of adiabatic motion takes the form

$$S = S_0 = \text{const.} \tag{20.8}$$

This motion is known as isentropic.

Combining the basic equations derived by us with the equation of state of the form

$$p = p(\rho;\ T)$$

or the equation of state

$$p = p(\rho;\ S), \tag{20.9}$$

we obtain the closed system of equations

$$\left.\begin{aligned} &\frac{\partial \rho}{\partial t} + \operatorname{div} \rho \boldsymbol{v} = 0, \\ &\frac{\partial \boldsymbol{v}}{\partial t} + (\boldsymbol{v}\nabla)\boldsymbol{v} + \frac{1}{\rho}\operatorname{grad} p = 0, \\ &\frac{\partial S}{\partial t} + \boldsymbol{v} \operatorname{grad} S = 0, \\ &p = p(\rho;\ S), \end{aligned}\right\} \tag{20.10}$$

determining for given initial and boundary conditions the parameters $v,\ p,\ \rho$ and S (or T) characterizing the motion and state of the fluid (gas) as functions of r and t.

We will now transform the equations of gas dynamics from the vector form to the co-ordinate form in which they are more convenient for solution and study.

In the orthogonal system of co-ordinates the basic equations of gas dynamics take the form:

$$\left.\begin{aligned}
&\frac{\partial \rho}{\partial t}+u\frac{\partial \rho}{\partial x}+v\frac{\partial \rho}{\partial y}+w\frac{\partial \rho}{\partial z}+\rho\left(\frac{\partial u}{\partial x}+\frac{\partial v}{\partial y}+\frac{\partial w}{\partial z}\right)=0,\\
&\frac{\partial u}{\partial t}+u\frac{\partial u}{\partial x}+v\frac{\partial u}{\partial y}+w\frac{\partial u}{\partial z}+\frac{1}{\rho}\frac{\partial p}{\partial x}=0,\\
&\frac{\partial v}{\partial t}+u\frac{\partial v}{\partial x}+v\frac{\partial v}{\partial y}+w\frac{\partial v}{\partial z}+\frac{1}{\rho}\frac{\partial p}{\partial y}=0,\\
&\frac{\partial w}{\partial t}+u\frac{\partial w}{\partial x}+v\frac{\partial w}{\partial y}+w\frac{\partial w}{\partial z}+\frac{1}{\rho}\frac{\partial p}{\partial z}=0,\\
&\frac{\partial S}{\partial t}+u\frac{\partial S}{\partial x}+v\frac{\partial S}{\partial y}+w\frac{\partial S}{\partial z}=0,\\
&p=p(\rho;\ S),
\end{aligned}\right\} \qquad (20.11)$$

where u, v and w signify the projections of the velocity v on the x, y and z axes.

In the cases when the parameters determining the motion and state of the medium depend on the time, i.e. when in a given region of space these parameters change with time, the motion of the medium is said to be unsteady. On the other hand, in the cases when the parameters of the moving medium at every given point in space remain unchanged with time, the motion is said to be steady. It is evident that all the partial derivatives with respect to time in our equations become zero and the system of equations (20.11) are considerably simplified.

Whilst studying later the phenomena connected with the detonation of explosives and the effect of an explosion, we will be concerned mainly with the unsteady motion of a gas.

In many cases of motion of the media their density can be considered to be unchangeable, i.e. constant throughout the whole volume of the fluid during the whole time of motion. It is said that this motion is that of an incompressible fluid. In this case the general equations of gas dynamics are greatly simplified. In fact, if $\rho = \text{const}$, then $S = S_0 =$

const. and all the partial derivatives of the density become zero. We arrive at a system of four equations with four unknowns (u, v, w and p), of which three equations, the Euler equations of motion, remain unchanged and the equation of continuity takes the form

$$\frac{\partial u}{\partial x}+\frac{\partial v}{\partial y}+\frac{\partial w}{\partial z}=\operatorname{div} v=0. \tag{20.12}$$

As will be shown below (Chapter XIV), whilst solving a number of problems connected with the effect of an explosion in dense media (water, earth, rock etc.) already at relatively small distances from the source of the explosion, the compressibility of the surrounding media can be practically neglected and the differential equations for an incompressible fluid used.

We will now introduce the concept of the so-called streamlines. These are the lines, the tangents of which indicate the direction of the velocity vector at the point of contact at a given moment in time; they are determined by the system of differential equations

$$\frac{dx}{u}=\frac{dy}{v}=\frac{dz}{w}.$$

For steady motion of the fluid the streamlines remain unchanged with respect to time and coincide with the trajectories of particles of the fluid. For unsteady motion this coincidence does of course not occur; the tangents to the streamlines give the direction of the velocity of various particles of the medium at successive points in space at a definite moment in time, whilst the tangents to the trajectories give the direction of the velocity of definite particles at successive moments in time.

§ 21. Bernoulli's equation.

The equations of gas dynamics, as has already been said, are appreciably simplified in the case of the steady flow of a fluid (gas).

Now because $\frac{\partial v}{\partial t}=0$, the equation (20.5) reduces to the equality

$$(v\nabla)v+\frac{1}{\rho}\operatorname{grad}p=0. \tag{21.1}$$

We transform this equation, using the well-known thermodynamic relationship

$$di=T\,dS+\frac{dp}{\rho}, \tag{21.2}$$

where i is the heat content of the medium.

In the case of adiabatic motion for every particle (along every streamline) $dS=0$ and

$$di=\frac{1}{\rho}\,dp. \tag{21.3}$$

It is also known from vector analysis that

$$(v\nabla)v=\frac{1}{2}\operatorname{grad}q^2-[v\operatorname{rot}v], \tag{21.4}$$

where $q=\sqrt{u^2+v^2+w^2}$ is the absolute value of the flow velocity.

Taking into account equalities (21.3) and (21.4) we can now rewrite equation (21.1) in the form

$$\operatorname{grad}\left(\frac{q^2}{2}+i\right)=[v\operatorname{rot}v]. \tag{21.5}$$

The vector $[v\operatorname{rot}v]$ is perpendicular to the velocity v; therefore its projection on the direction perpendicular to the streamline equals zero at every point of it. From this it follows that

$$\frac{q^2}{2}+i=\text{const.} \tag{21.6}$$

Equation (21.6) is known as Bernoulli's equation.

We note that the value of the constant differs generally speaking for different streamlines. In the case of isentropic flow the values of the constant are identical for all the streamlines and Bernoulli's equation takes the form

$$\frac{q^2}{2}+i=i_0=\text{const.}$$

where i_0 is the heat content of the medium in the state of flow.

§ 22. One-dimensional isentropic motion of a gas.

The theory of one-dimensional unsteady motion of a compressible medium is mainly of importance for the explanation of the physical laws of unsteady motion in general, and in particular it permits the solution of a number of concrete problems connected with the definition of the parameters of motion and the state of the detonation products.

In the case of one-dimensional motion the basic equations of gas dynamics can be represented in the form

$$\left.\begin{aligned}\frac{\partial \ln\rho}{\partial t}+u\frac{\partial \ln\rho}{\partial x}+\frac{\partial u}{\partial x}=0,\\ \frac{\partial u}{\partial t}+u\frac{\partial u}{\partial x}+\frac{1}{\rho}\frac{\partial p}{\partial x}=0.\end{aligned}\right\} \tag{22.1}$$

For isentropic processes

$$p=A\rho^n. \tag{22.2}$$

From (22.2) it follows that because

$$\left(\frac{\partial p}{\partial \rho}\right)_s=c^2,$$

where c is the velocity of sound, then

$$\frac{dp}{\rho} = c^2 d\ln\rho = di \tag{22.3}$$

and

$$c = (An)^{\frac{1}{2}} \rho^{\frac{n-1}{2}}.$$

From this we find that

$$d\ln\rho = \frac{2}{n-1} d\ln c. \tag{22.4}$$

Substituting from (22.4) the value of $d\ln\rho$ in the first equation of the system (22.1) and multiplying it term-by-term by c we arrive at the expression

$$\frac{\partial c}{\partial t} + u\frac{\partial c}{\partial x} + \frac{n-1}{2} c\frac{\partial u}{\partial x} = 0. \tag{22.5}$$

Analogously, using (22.3) and (22.4), the second equation of system (22.1) can be written in the form

$$\frac{\partial u}{\partial t} + u\frac{\partial u}{\partial x} + \frac{2}{n-1} c\frac{\partial c}{\partial x} = 0. \tag{22.6}$$

Having multiplied (22.5) by $\frac{2}{n-1}$ and adding or subtracting it from the derived equation (22.6), we obtain

$$\frac{\partial}{\partial t}\left(u \pm \frac{2}{n-1} c\right) + (u \pm c)\frac{\partial\left(u \pm \frac{2}{n-1} c\right)}{\partial x} = 0. \tag{22.7}$$

Taking into account that

$$\frac{2}{n-1} c = \int c d\ln\rho,$$

it is possible to represent our system of equations also in the form of

the relationship

$$\frac{\partial}{\partial t}\left(u \pm \int c\,d\ln\rho\right) + (u \pm c)\frac{\partial}{\partial x}\left(u \pm \int c\,d\ln\rho\right) = 0. \tag{22.8}$$

From equations (22.8) and (22.7) it is evident that the given state of the medium defined by the magnitudes $u + \int c\,d\ln\rho$ or $u + \frac{2}{n-1}c$ is propagated at a velocity $u + c$ in the positive direction of the x-axis with the motion of the medium and the state defined by the magnitudes $u - \int c\,d\ln\rho$ or $u - \frac{2}{n-1}c$ is propagated at a velocity $u - c$ against the motion of the medium. In these circumstances the propagation of a disturbance at a velocity up to the speed of sound will occur both in a positive and in a negative direction along the x-axis; at a gas velocity above the speed of sound disturbances will depend on the course and their propagation will occur only in a positive direction along the x-axis (here we will assume that the origin of the co-ordinates moves together with the source of the disturbance). Waves of one direction encountering waves of another direction will interact with them and, consequently, the propagation of waves in opposing directions will not be independent.

Equations in the form (22.7) are especially suitable for investigation. In the case when the index of isentropy $n = 3$ which, as will be shown below (see § 41), holds for the greatly compressed detonation products of condensed explosives, the system of equations (22.7) takes the very simple form

$$\frac{\partial(u \pm c)}{\partial t} + (u \pm c)\frac{\partial(u \pm c)}{\partial x} = 0 \tag{22.9}$$

and if we denote $u+c=\alpha$, $u-c=\beta$, then

$$\frac{\partial\alpha}{\partial t}+\alpha\frac{\partial\alpha}{\partial x}=0;\quad \frac{\partial\beta}{\partial t}+\beta\frac{\partial\beta}{\partial x}=0. \tag{22.10}$$

The solution of system (22.9) is

$$\left.\begin{aligned} x&=(u+c)t+F_1(u+c),\\ x&=(u-c)t+F_2(u-c),\end{aligned}\right\} \tag{22.11}$$

where $F_1(u+c)$ and $F_2(u-c)$ are two arbitrary functions of $u+c$ and $u-c$ respectively.

The solution of (22.11) which is the general solution of the differential equations in the case $n=3$ can be written conveniently in the form

$$x=\alpha t+F_1(\alpha);\quad x=\beta t+F_2(\beta). \tag{22.12}$$

Analysing equation (22.9) and its solution (22.12), it is possible to conclude that the given states defined by the magnitudes $u+c=\alpha$ and $u-c=\beta$ are propagated in the medium for $n=3$ independently of one another. This is also shown by the fact that the magnitudes α and β are defined in equations (22.9) for given initial and boundary conditions quite independently.

Special solutions. We have established above that waves exist in two opposing directions, which in the general case $(n\neq 3)$ interact with one another. At $p=A\rho^n$ they are described by the relationships

$$\frac{\partial}{\partial t}\left(u\pm\frac{2}{n-1}c\right)+(u\pm c)\frac{\partial}{\partial x}\left(u\pm\frac{2}{n-1}c\right)=0. \tag{22.13}$$

In the case when

$$u+\frac{2}{n-1}c=\text{const}, \tag{22.14a}$$

$$u-\frac{2}{n-1}c=\text{const}, \tag{22.14b}$$

equations (22.13) are satisfied identically.

Having determined from (22.14a) that

$$\frac{\partial c}{\partial x}=-\frac{n-1}{2}\frac{\partial u}{\partial x},$$

it is possible to reduce equation (22.6) to the form

$$\frac{\partial u}{\partial t}+(u-c)\frac{\partial u}{\partial x}=0. \tag{22.15}$$

Analogously, having determined from (22.14b) that

$$\frac{\partial c}{\partial t}=+\frac{n-1}{2}\frac{\partial u}{\partial t},$$

equation (22.6) can take the form

$$\frac{\partial u}{\partial t}+(u+c)\frac{\partial u}{\partial x}=0. \tag{22.16}$$

The solution of the system of equations (22.15) and (22.16) is

$$x=(u\pm c)t+F(u), \tag{22.17}$$

where $F(u)$ is an arbitrary function.

It must be remembered that u and c are connected directly by the relationships (22.14a) and (22.14b). In the general case when the isentropic equation has the form $p=p(\rho)$, these relationships reduce to

$$u\pm\int c\,d\ln\rho=\text{const}.$$

The solutions given above for the system

$$\left.\begin{aligned} x &= (u+c)\,t + F_1(u), \quad u - \frac{2}{n-1}\,c = \text{const}, \\ x &= (u-c)\,t + F_2(u), \quad u + \frac{2}{n-1}\,c = \text{const} \end{aligned}\right\} \tag{22.18}$$

are known as special solutions and describe the particular case of wave propagation in only one direction. These waves are known as simple waves. We will study these waves in more detail using the method of characteristics.

§ 23. Characteristics of the equations of gas dynamics.

In a stationary medium small disturbances are propagated in all directions at the velocity of sound. In the most general case, when the medium moves and the velocity of the motion depends on x, y, z and t, the velocity of propagation of small disturbances will be composed of the local velocity of the motion of the medium and the local velocity of sound at every point in space. In this case the velocity of the disturbance will be defined by the three different equations

$$\left.\begin{aligned} \frac{dx}{dt} &= u \pm a_1 c, \\ \frac{dy}{dt} &= v \pm a_2 c, \\ \frac{dz}{dt} &= w \pm a_3 c, \end{aligned}\right\} \tag{23.1}$$

where $\frac{dx}{dt}, \frac{dy}{dt}, \frac{dz}{dt}$ are the projections of the velocity D of propagation of the front of the disturbance on the corresponding coordinate axes and a_1, a_2, a_3 are the direction cosines normal to the surface of the front.

The solution of the system of equations (23.1) for given initial conditions of motion defines some hyper-surface

$$f(x, y, z, t) = 0, \tag{23.2}$$

which is the surface of the front of the disturbance. These surfaces are called characteristic surfaces or characteristics.

Disturbances can be propagated in the form of compression waves or rarefaction waves. Compression waves describe the motion of the medium when during motion of any element of the medium the pressure in it increases. On the other hand, when the pressure decreases during the motion of any element of the medium, we are concerned with rarefaction waves.

In the case of one-dimensional unsteady motion of a gas the equation (2.23) takes the form $f(x, t) = 0$ and the characteristics will be represented by lines in the plane x, t, the slope of which $\frac{dx}{dt}$ at any point equals the local velocity of propagation of sound relative to a fixed system of co-ordinates.

Depending on whether the disturbances are propagated in the positive or negative direction of x we will have two families of characteristics which we will call C_+ and C_- characteristics for which

$$\left(\frac{dx}{dt}\right)_+ = u + c, \quad \left(\frac{dx}{dt}\right)_- = u - c.$$

For simple waves, it is seen from (22.13) that these characteristics correspond to the relationships:

$$u + \frac{2}{n-1} c = \text{const},$$
$$u - \frac{2}{n-1} c = \text{const}.$$

They are called Riemann's invariants and are the characteristics of the basic system of equations (22.13) in the u, c plane; in this system u and c are taken to be independent variables and x and t are dependent variables. These characteristics are represented as parallel lines in the u, c plane.

Apart from the characteristics considered by us, there is also a family of characteristics expressing the properties of entropic disturbances. For adiabatic flow S=const for any particle, therefore they are transferred together with the substance, i.e. the velocity of their propagation

$$\left(\frac{dx}{dt}\right)_s = u.$$

In the case of $n=3$ $\frac{dx}{dt}=\text{const}$, and the fronts of the disturbances will be propagated according to the laws

$$\left.\begin{aligned} x &= \alpha t + x_1, \\ x &= \beta t + x_2, \end{aligned}\right\} \tag{23.3}$$

where x_1 and x_2 are constants and $u+c=\alpha=\text{const}$; $u-c=\beta=\text{const}$, i.e. these characteristics in the x, t plane will be represented by straight lines.

Differentiating equations (22.17) for a simple wave, we will have

$$dx = (u \pm c)\, dt + [t \pm c'(u) + F'(u)]\, du.$$

At the same time along the characteristics C_+ and C_- we have

$$dx = (u \pm c)\, dt.$$

Comparing both equations we come to the conclusion that along the characteristics

$$[t \pm tc'(u) + F'(u)]\, du = 0.$$

The expression in square brackets cannot be identically equal to zero,

therefore $du = 0$ and $u = \text{const.}$.

Thus, we reach the conclusion that along each characteristic of the corresponding family C_+ or C_- the velocity remains constant and consequently the other parameters too.

This indicates that any state in the medium will move at a constant velocity, $\bar{u} + \bar{c}$ or $\bar{u} - \bar{c}$, inherent to this state.

From this property of simple waves it follows directly that the C_+ characteristics (for waves propagating to the right) or the C_- characteristics (for waves propagating to the left) are represented respectively by families of straight lines in the x, t planes.

For the purpose of a more graphic explanation of the properties of simple waves, we will consider the following two cases.

A tube closed at one end (on the right), contains gas which is confined by means of a piston on the left.

During the movement of the piston a simple rarefaction wave arises.

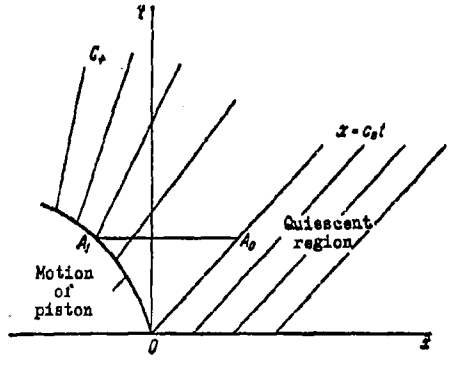


Fig. 34. Family of characteristics for the simple rarefaction wave arising during the outward motion of a piston from a tube.

In Fig. 34 a family of C_+ characteristics is represented for this wave as divergent straight lines formed on the curve $x = x(t)$ describing the motion of the piston. To the right of the characteristic $x = c_0 t$ there spreads a region of quiescent gas in which all the characteristics are parallel to one another.

The divergence of the characteristics in this wave is explained as follows. As a result of the initial acceleration of the piston in the initial elementary portion of its path, the first rarefaction wave arises which will move relative to the piston from left to right with a velocity $u+c_0$, since the front of the disturbance moves through the quiescent gas with the velocity of sound c_0 and the disturbed gas moves after the piston. The next wave of the disturbance which runs from the piston during its further acceleration cannot therefore reach the front of the first elementary disturbance, and so on. Because of this, the slope of the C_+ characteristics to the ordinate axis will decrease in proportion to the acceleration of the piston, i.e. these lines will diverge.

The section A_1A_0 on this figure corresponding to some definite moment in time represents the region of gas embraced by the rarefaction wave up to the given moment in time; it is evident that as time increases, the region of disturbance will expand.

In Fig. 35 a similar sketch is given for the simple compression wave formed during the acceleration of the motion of a piston into a tube. During every elementary acceleration separate compression waves leave the piston, the velocity of propagation of which is defined by the slope of the C_+ -characteristics to the ordinate axis. The slope of these lines to the ordinate increases gradually. This is explained by the fact that every following elementary wave will be propagated through a gas which has been compressed to a greater extent by the preceding wave, so that the amplitude of the wave will increase continually. The convergent cluster of characteristics in Fig. 35, which should finally intersect, points to a tendency to form a shock wave. However the intersection of the

characteristics from the physical viewpoint is absurd; since the velocity along any characteristic remains constant, as has already been explained, we will have a many-valued function $u(x, t)$. at the point of intersection. This point can be interpreted as the place where the shock wave originates.

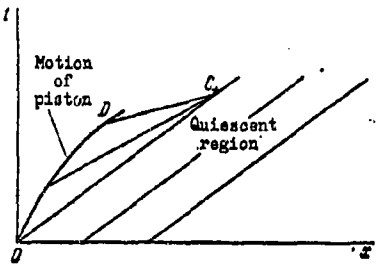


Fig. 35. Family of characteristics for a simple compression wave arising during forward motion of a piston into a tube.

We will consider below the problem of the conditions under which shock waves occur (§ 28).

Earlier we have proved that in a simple wave throughout the whole region of movement during the whole time the Riemann invariants remain constant; they are denoted (for isentropic motion) by

$$I_+ = u + \frac{2}{n-1} c = \text{const}; \quad I_- = u - \frac{2}{n-1} c = \text{const}.$$

The Riemann invariants themselves are characteristics in the u, c plane. Along each of the C_+ and C_- characteristics the values of I_+ or I_-, respectively, remains constant. Small disturbances of the I_+ magnitude are propagated only along the C_+ characteristics, and the disturbances of I_- along the C_- characteristics. In the waves running to the right I_- is constant over the whole range of motion and in the waves running to the left I_+ is constant. From what has been described the property mentioned above for simple waves follows as a particular case, that is, the linearity of one of the families of C characteristics. This is easily proved. Let the wave be propagated to the right. In this

case along each of the C_+ characteristics the magnitude of I_+ remains constant. Moreover, the magnitude of I_- is also constant on the characteristics and for simple waves it is constant over the whole range of motion of the gas. But from the constancy of the two magnitudes I_+ and I_- on any C_+ characteristic it follows that $u = \text{const}$ and $c = \text{const}$ on this characteristic which leads directly to the conclusion regarding the linearity of these characteristics.

It is also easily proved that if the region I of any type of flow is bounded by a region II of stationary flow ($\rho = \text{const}$, $p = \text{const}$, $u = \text{const}$), then region I is a simple wave. In fact in region II I_+ and I_- are constant and the C_+ and C_- characteristics are linear. The boundary between the two regions is one of the C_+ characteristics illustrated in Fig. 36 as a thicker line, i.e. the C_+ lines do not go from one region into another. The C_- characteristics do go from one region to another and take from region II to region I the constant magnitude I_- which remains constant over the whole region of this flow representing a simple wave.

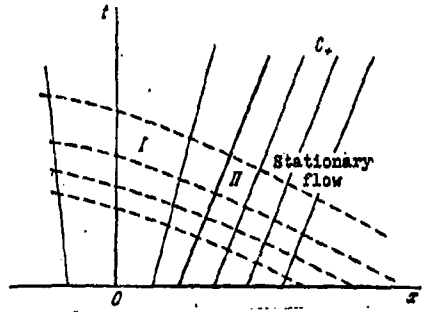


Fig. 36. Motion of wave (I) bordering onto a region of stationary flow (II)

It follows from what has been said that the simple wave always borders on the region of quiescent stationary flow, but the velocity of propagation of this wave front can be represented as the velocity of the displacement of the boundary between the two regions which represents some

slight discontinuity.

Indeed, because the motion on both sides from this boundary is described by different equations, then this boundary represents the discontinuity of some derived magnitudes, which (the derivatives) coincide with some characteristic.

In the case when $F(u)=0$ in equation (22.7) we will have

$$\left.\begin{aligned} \frac{x}{t}&=u+c, \quad u-\frac{2}{n-1}c=\alpha, \\ \frac{x}{t}&=u-c, \quad u+\frac{2}{n-1}c=\beta. \end{aligned}\right\} \tag{23.4}$$

In the given case the motion of the medium will be a similarity flow (automodel') as u and c are functions of only one independent variable $z=\frac{x}{t}$. Here we are dealing with a particular case of the class of similarity flows. In the general case $z=\frac{x}{t^{a_1}}$. In the problem considered $a_1=1$.

In similarity flow the distribution of all parameters depends only on x and t in the form of their ratio $\frac{x}{t}$ possessing the dimension of velocity, i.e. these distributions at different moments in time will be similar to one another. If lengths are measured in units increasing in proportion to t, then the picture of the motion will not generally change. This is the most characteristic property of a similarity flow.

The simplest example of this motion is the motion of a gas in a cylindrical tube closed at one end by a piston which immediately begins to move out of the tube at a constant velocity. In this case all the characteristics on the x, t plane will originate from one point. These waves are therefore given the name centered. In Fig. 37 the

centering of a rarefaction wave is shown, the characteristics of which are represented by a cluster of divergent straight lines.

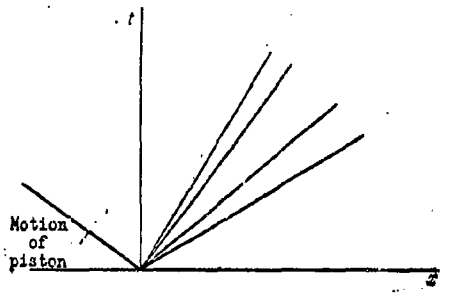


Fig. 37. Centering of a rarefaction wave.

In the case of isentropic one-dimensional motions and also of isentropic motions with an axial (cylindrical) and central (spherical) symmetry all the parameters of the medium depend on one space co-ordinate r and it is not difficult to prove that the equations of gas dynamics take the form

$$\left.\begin{aligned} &\frac{\partial u}{\partial t}+u\frac{\partial u}{\partial r}+\frac{1}{\rho}\frac{\partial p}{\partial r}=0,\\ &\frac{\partial \rho}{\partial t}+u\frac{\partial \rho}{\partial r}+\rho\frac{\partial u}{\partial r}+N\frac{\rho u}{r}=0,\\ &p=A\rho^{n}, \end{aligned}\right\} \tag{23.5}$$

where $N=0$ for one-dimensional motion, $N=1$ for motion with a cylindrical symmetry and $N=2$ for motion with a spherical symmetry.

For motions with axial or central symmetry the characteristics in r, t co-ordinates will not be straight lines.

In fact, applying to system (23.5) the transformations carried out in § 22 we obtain the equations

$$\frac{\partial}{\partial t}\left(u\pm\frac{2}{n-1}c\right)+(u\pm c)\frac{\partial\left(u\pm\frac{2}{n-1}c\right)}{\partial r}\pm\frac{Nuc}{r}=0. \tag{23.6}$$

Thus, the characteristics are determined as before by the equations

$$\frac{dr}{dt} = u \pm c,$$

but they are no longer lines on which the values of $u \pm \frac{2}{n-1} c$ are maintained constant, i.e. they are not straight lines on either the $(x; t)$ plane or the $(u; c)$ plane. Only at large distances from the centre or from the axis of symmetry does the magnitude $\frac{Nuc}{r}$ become quite small and the characteristics will approach the characteristics for one-dimensional motion.

§ 24. Steady isentropic flow.

For a steady one-dimensional flow, Bernoulli's equation holds

$$i + \frac{u^2}{2} = i_0 = \text{const}, \tag{24.1}$$

whence

$$u = \sqrt{2(i_0 - i)}.$$

During the discharge of a gas into a vacuum when $p \to 0$ and $i \to 0$ we have

$$u_{max} = \sqrt{2i_0}. \tag{24.2}$$

But for isentropic processes according to (21.3)

$$di = \frac{dp}{\rho} = c^2 d \ln \rho = \frac{2}{n-1} c\, dc,$$

whence

$$i = \frac{c^2}{n-1}. \tag{24.3}$$

Taking into account (24.2) we find that

$$u_{max} = \sqrt{\frac{2}{n-1}}\, c_0, \tag{24.4}$$

where c_0 is the velocity of sound in the quiescent medium.

To determine the critical velocity of discharge of the gas u_{cr} we will consider a stream moving in a nozzle which first contracts uniformly and then expands (Laval nozzle). We will consider the motion of the gas to be uniform across the cross-section of the nozzle and the velocity to be in a direction along the axis of the cross-section.

The linear dimensions of the vessel will be considered to be very large in comparison with the diameter of the tube. Therefore the velocity of the gas in the vessel can be taken to be zero and all the parameters of state of the gas to be constant.

The consumption of gas per second across the cross-section of the nozzle equals $g = \rho us$ where s is the area of the cross-section of the nozzle; this magnitude should evidently remain constant along the whole nozzle, i.e.

$$g = \rho us = \text{const.} \tag{24.5}$$

The maximum density of the stream $j = \rho u$ will be attained at the narrowest cross-section. From this it follows that

$$dj = u\,d\rho + \rho\,du = 0. \tag{24.6}$$

On the other hand, it follows from Bernoulli's equation that

$$\frac{dp}{\rho} = di = -u\,du. \tag{24.7}$$

Having determined ρ, from this and substituting its value in (24.6) we find that

$$u^2 = \frac{dp}{d\rho} = c^2,$$

whence

$$u_{cr} = \pm c_{cr},$$

which points to the attainment at the minimum nozzle cross-section of the sonic discharge regime. This section is known as the critical section and the value $u_{cr} = c_{cr}$ is also known as the critical value.

For $p = A\rho^n$ Bernoulli's equation can be represented in the form

$$\frac{u^2}{2} + \frac{c^2}{n-1} = I_0 = \text{const}, \tag{24.8}$$

and for the critical section it takes the form

$$\frac{c_{cr}^2}{2} + \frac{c_{cr}^2}{n-1} = \frac{c_0^2}{n-1},$$

whence it follows that

$$u_{cr} = c_{cr} = \sqrt{\frac{2}{n+1}}\, c_0 = \text{const}. \tag{24.9}$$

From the relationships (24.8) and (24.9) it is possible to obtain the expression

$$u^2 - c_{cr}^2 = \frac{2}{n+1}(u^2 - c^2), \tag{24.10}$$

which will also hold for three-dimensional flows of gas, if u is replaced by the complete velocity v.

§ 25. Unilateral outflow of a formerly quiescent gas.

Some portion of a tube is filled with gas confined at both sides by baffle plates. Outside this portion there is a vacuum. We will denote the distance between the baffle plates by l. We will take the origin

of the co-ordinates to be at the right-hand baffle (Fig. 38). The area of the tube cross-section is constant and is assumed to equal unity.

At time $t = 0$ we remove the baffle at $x = 0$. Then an unsteady outflow of gas begins into the vacuum, and simultaneously a rarefaction wave arises directed towards the left, i.e. we are concerned here with a simple rarefaction wave. The boundaries of the wave at any time are: on the right, the front of the gases flowing into the vacuum which is displaced to the right; on the left, the front of the rarefaction wave. It is evident that the wave will be described by a particular solution of the gas-dynamics equations, [illegible] wave is a wave in one direction propagating through undisturbed gas.

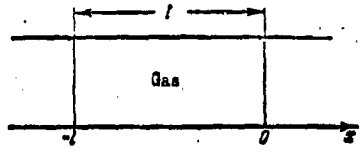


Fig. 38. Derivation of the rules for the unilateral outflow of gas into a vacuum.

Here it must be noted that the front of the gas flowing to the right into the vacuum cannot be considered as a wave, since here the gas particles which themselves move do not lead to a motion of any medium. The distribution of velocity and gas density on both sides of the removed baffle plate are described by one and the same equations.

To solve the problem set we should use the equations

$$x = (u - c)t + F(u), \tag{25.1}$$

$$u = -\frac{2}{n-1}c + \text{const}. \tag{25.2}$$

For determining the unknown $F(u)$ and the const we use the following boundary conditions. For a quiescent gas $u = 0$ and $c = c_n$. Consequently

$$0 = -\frac{2}{n-1} c_0 + \text{const},$$

whence

$$\text{const} = \frac{2}{n-1} c_0$$

and the second equation takes the final form

$$u = \frac{2}{n-1} (c_0 - c). \tag{25.3}$$

The limiting velocity during outflow into a vacuum will evidently be determined by the relationship

$$u_{max} = \frac{2}{n-1} c_0, \tag{25.4}$$

i.e.

$$\frac{u_{max\,(unsteady)}}{u_{max\,(steady)}} \sqrt{\frac{2}{n-1}}, \tag{25.5}$$

which follows directly from a comparison of expressions (25.4) and (24.4). At $n < 3$ this ratio will always be greater than unity. Thus, for example, for air $(n = \frac{7}{5})$ the velocity of the unsteady outflow is approximately 2.2 times greater than the velocity of a steady motion.

This is explained by the fact that for an unsteady flow one part of the gas can have an energy considerably greater, and another part considerably less, than the average energy of the gas, whilst in the case of steady flow the energy of all particles taking part in the motion is the same. In the process of motion in unsteady flows, as will be shown below, a continuous redistribution of energy occurs throughout the mass of the moving stream.

We will now prove that $F(u)$ in (25.1) should be identically equal to zero, since the motion of the gas initially at $t = 0$ was determined

at the section $x=0$.

In fact, for $F(u)=0$ equation (25.1) takes the form

$$x=(u-c)t, \tag{25.6}$$

whence at $t=0, x=0, u-c=\frac{0}{0}$, i.e. u and c are indeterminate, which corresponds exactly to the conditions of our problem. Indeed, at the initial moment when the baffle plate is taken away, u and c do not have definite values, since the velocity u increases in steps from zero to its limiting value $u_{max}=\frac{2}{n-1}c_n$, and the density, pressure and velocity of sound decrease in steps to zero from their initial values.

Thus the solution finally takes the form

$$\left.\begin{aligned} u-c&=\frac{x}{t};\\ u&=\frac{2}{n-1}(c_n-c). \end{aligned}\right\} . \tag{25.7}$$

The gas motion being considered is a similarity flow because all the parameters characterizing it are functions of $\frac{x}{t}$.

We will now define the law of motion of the rarefaction wave front. This front over the whole region of the wave at any moment in time is bounded by undisturbed gas; therefore on the front $u=0$ and $c=c_n$, consequently, for it equation (25.7) gives

$$\frac{x}{t}=-c_n, \tag{25.8}$$

i.e. the rarefaction wave front actually moves from right to left relative to the stationary observer at the velocity of sound. The relationship $x=-c_nt$ is the characteristic of our equations.

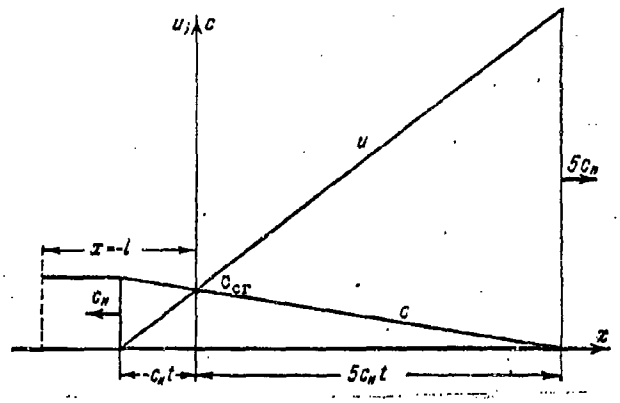


Fig. 39. Distribution of u and c during unilateral outflow of gas.

Having determined u and c from (25.7) we find that

$$\left.\begin{aligned} c &= \frac{2}{n+1}c_n - \frac{n-1}{n+1}\frac{x}{t} = \frac{2}{n+1}c_n\left(1 - \frac{n-1}{2}\frac{x}{c_n t}\right), \\ u &= \frac{2}{n+1}c_n\left(1 + \frac{x}{c_n t}\right). \end{aligned}\right\} \tag{25.9}$$

Equations (25.9) give the distribution of u and c over the whole range of the disturbance with respect to time. It is evident from these equations that at any time the distribution of u and c is characterised by straight lines. From equations (25.9) it follows that at the section $x = 0$

$$u = c = \frac{2}{n+1}c_n = c_{cr}, \tag{25.10}$$

i.e. the critical discharge regime is established. It is evident that the state, at which $u = c$, is not transferred through the gas, since the velocity of the transfer of this state $\frac{dx}{dt} = u - c = 0$.

On the rarefaction wave front $u=0$, $c=c_н$. On the front of the out-flowing gases $u=u_{max}=\frac{2}{n-1}c_н$, $c=0$. At $n=1.4$ (diatomic gas) equations (25.9) give

$$\left.\begin{aligned} c &= \frac{5}{6}c_н\left(1-\frac{x}{c_н t}\right), \\ u &= \frac{5}{6}c_н\left(1+\frac{x}{c_н t}\right). \end{aligned}\right\} \qquad (25.11)$$

The graphs of distribution of u and c (Fig. 39) correspond to this case. The left and right arrows indicate, respectively, the direction of motion of the wave front and the front of the moving particles of gas.

§ 26. The general solution for one-dimensional isentropic motions of gas.

We have considered above two classes of gas motion: 1) $p=$ const and $u=$ const which corresponds to stationary flow and 2) when over the whole region covered by the disturbance one of the Riemann invariants (I_+ or I_-) is constant, which is a characteristic property of simple waves. Here we will consider the general case of a motion when neither I_+ or I_- is constant in the region of the disturbance; only one cross-section in the region of disturbance on the x, t plane corresponds to the pair or values I_+ , I_- .

To derive the general solutions of one-dimensional isentropic motion we use the equations

$$\left.\begin{aligned} &\frac{\partial u}{\partial t}+u\frac{\partial u}{\partial x}+\frac{\partial I}{\partial x}=0, \\ &\frac{\partial I}{\partial t}+u\frac{\partial I}{\partial x}+c^2\frac{\partial u}{\partial x}=0. \end{aligned}\right\} \qquad (26.1)$$

The independent variables here are x and t. We will now change to new independent variables u and l, considering x and t as dependent variables. For this purpose we establish the partial derivatives of the system of differential equations in the Jacobian form (functional determinants).

The Jacobian $\frac{\partial (y_1, y_2)}{\partial (x_1, x_2)}$ is the determinant

$$\begin{vmatrix} \frac{\partial y_1}{\partial x_1} & \frac{\partial y_1}{\partial x_2} \\ \frac{\partial y_2}{\partial x_1} & \frac{\partial y_2}{\partial x_2} \end{vmatrix} = \frac{\partial (y_1, y_2)}{\partial (x_1, x_2)} = \frac{\partial y_1}{\partial x_1} \frac{\partial y_2}{\partial x_2} - \frac{\partial y_1}{\partial x_2} \frac{\partial y_2}{\partial x_1}.$$

As a result the system (26.1) takes the form

$$\frac{\partial (u, x)}{\partial (t, x)} + u \frac{\partial (t, u)}{\partial (t, x)} + \frac{\partial (t, l)}{\partial (t, x)} = 0,$$
$$\frac{\partial (l, x)}{\partial (t, x)} + u \frac{\partial (t, l)}{\partial (t, x)} + c^2 \frac{\partial (t, u)}{\partial (t, x)} = 0.$$

To change to the independent variables (u, l) we now multiply these equations by $\frac{\partial (t, x)}{\partial (u, l)}$ assuming that this Jacobian does not become zero anywhere within the range of the desired solutions. It is known that during the multiplication or division of Jacobians described symbolically it is possible to consider them as ordinary fractions. As a result of the transformation we obtain

$$\left.\begin{aligned} \frac{\partial (u, x)}{\partial (u, l)} + u \frac{\partial (t, u)}{\partial (u, l)} + \frac{\partial (t, l)}{\partial (u, l)} = 0, \\ \frac{\partial (l, x)}{\partial (u, l)} + u \frac{\partial (t, l)}{\partial (u, l)} + c^2 \frac{\partial (t, u)}{\partial (u, l)} = 0. \end{aligned}\right\} \quad (26.2)$$

Multiplying out the Jacobians, we will have

$$\left.\begin{aligned} \frac{\partial x}{\partial t} - u\frac{\partial t}{\partial t} + \frac{\partial t}{\partial u} = 0, \\ \frac{\partial x}{\partial u} - u\frac{\partial t}{\partial u} + c^2\frac{\partial t}{\partial t} = 0. \end{aligned}\right\} \tag{26.3}$$

To transform this system into a system of linear differential equations we will carry out the so-called Legendre transformation, introducing a new function $\psi = \psi(u, t)$ by means of the relationship

$$x = ut - \frac{\partial \psi}{\partial u}. \tag{26.4}$$

Then the equations take the form

$$\frac{\partial t}{\partial u} = \frac{\partial^2 \psi}{\partial u\, \partial t}; \quad t + c^2\frac{\partial t}{\partial t} = \frac{\partial^2 \psi}{\partial u^2}. \tag{26.5}$$

The first equation gives

$$t = \frac{\partial \psi}{\partial t}. \tag{26.6}$$

Using (26.6), we convert the second equation to the form

$$\frac{\partial \psi}{\partial t} + c^2\frac{\partial^2 \psi}{\partial t^2} = \frac{\partial^2 \psi}{\partial u^2}. \tag{26.7}$$

Thus as a result of the given transformations we have derived a single linear (with respect to ψ) differential equation from a system of non-linear equations.

Equation (26.4) now correspondingly takes the form

$$x = u\frac{\partial \psi}{\partial t} - \frac{\partial \psi}{\partial u}. \tag{26.8}$$

Integrating equation (26.7) for appropriate initial and boundary conditions we determine ψ; then according to formulae (26.6) and (26.8) we

determine t and x respectively and therefore the remaining parameters of the motion under consideration.

For an ideal gas $c^2=(\gamma-1)t$ and the basic equation (26.7) takes the form

$$(\gamma-1)t\frac{\partial^2\psi}{\partial t^2}+\frac{\partial\psi}{\partial t}=\frac{\partial^2\psi}{\partial u^2}. \tag{26.9}$$

This equation can be integrated in the general form for the condition

$$\frac{3-\gamma}{\gamma-1}=2N,\quad \gamma=\frac{3+2N}{1+2N},\quad N=0,\ 1,\ 2,\ 3,\ \ldots.$$

This condition is satisfied, in particular, by a diatomic gas ($\gamma=\frac{7}{5}$, $N=2$) and the compressed detonation products of condensed explosives ($\gamma=3$, $N=0$). Using N instead of γ we rewrite (26.9) in the form

$$\frac{2}{2N+1}t\frac{\partial^2\psi}{\partial t^2}-\frac{\partial^2\psi}{\partial u^2}+\frac{\partial\psi}{\partial t}=0. \tag{26.10}$$

We will denote the function satisfying this solution for a given value of N by ψ_N. Then for the function ψ_0 (at $N=0$) we will have

$$2t\frac{\partial^2\psi_0}{\partial t^2}-\frac{\partial^2\psi_0}{\partial u^2}+\frac{\partial\psi_0}{\partial t}=0. \tag{26.11}$$

We now introduce a new variable $w=\sqrt{2t}$. For this

$$\frac{\partial w}{\partial t}=\frac{1}{w},\quad \frac{\partial\psi_0}{\partial t}=\frac{\partial\psi_0}{\partial w}\frac{\partial w}{\partial t}=\frac{\partial\psi_0}{w\,\partial w},$$
$$\frac{\partial^2\psi_0}{\partial t^2}=\frac{\partial}{\partial w}\left[\frac{1}{w}\frac{\partial\psi_0}{\partial w}\right]\frac{\partial w}{\partial t}=\frac{1}{w^2}\left[\frac{\partial^2\psi_0}{\partial w^2}-\frac{\partial\psi_0}{w\,\partial w}\right],$$

and equation (26.11) takes the form

$$\frac{\partial^2\psi_0}{\partial w^2}-\frac{\partial^2\psi_0}{\partial u^2}=0. \tag{26.12}$$

This is the well-known wave equation, the general solution of which is

$$\psi_0 = f_1(w+u) + f_2(w-u), \tag{26.13}$$

where f_1 and f_2 are arbitrary functions.

Converting again from w to l we will have

$$\psi_0 = f_1(\sqrt{2l}+u) + f_2(\sqrt{2l}-u). \tag{26.14}$$

It is possible to show that if the function ψ_N is known, then the function ψ_{N+1} is obtained by simple differentiation. Indeed, differentiating equation (26.10) with respect to l we obtain

$$\frac{2}{2N+1} l \frac{\partial^2}{\partial l^2}\left(\frac{\partial \psi_N}{\partial l}\right) + \frac{2N+3}{2N+1}\frac{\partial}{\partial l}\left(\frac{\partial \psi_N}{\partial l}\right) - \frac{\partial^2}{\partial u^2}\left(\frac{\partial \psi_N}{\partial l}\right) = 0. \tag{26.15}$$

We now introduce instead of u the variable

$$u^* = u\sqrt{\frac{2N+3}{2N+1}};$$

in this case (26.10) gives the equation

$$\frac{2}{2N+3} l \frac{\partial^2}{\partial l^2}\left(\frac{\partial \psi_N}{\partial l}\right) + \frac{\partial}{\partial l}\left(\frac{\partial \psi_N}{\partial l}\right) - \left(\frac{\partial^2}{\partial u^{*2}}\right)\left(\frac{\partial \psi_N}{\partial l}\right) = 0,$$

coinciding with equation (26.15) for the function $\psi_{N+1}(l, u)$ (by replacing N by $N+1$)

$$\frac{2}{2(N+1)+1} l \frac{\partial^2}{\partial l^2}(\psi_{N+1}) + \frac{\partial}{\partial l}(\psi_{N+1}) - \frac{\partial^2}{\partial u^2}(\psi_{N+1}) = 0.$$

From this it follows that

$$\psi_{N+1}(l, u) = \frac{\partial \psi_N}{\partial l}(l, u^*). \tag{26.16}$$

Having differentiated N times the function ψ_0, we obtain a general solution of equation (26.11)

$$\psi = \frac{\partial^N}{\partial l^N}\left\{f_1(\sqrt{2(2N+1)}\, l + u) + f_2(\sqrt{2(2N+1)}\, l - u)\right\}. \tag{26.17}$$

The functions f_1 and f_2 in the definition of ψ should be written in the general form. We recall that $N=0$ for ψ_0. Transforming from l to c we find that

$$\sqrt{2(2N+1)\,l}=(2N+1)\,c=\frac{2}{\gamma-1}c$$

and equation (26.17) takes the form

$$\psi=\frac{\partial^N}{\partial c^N}\left\{f_1\left(\frac{2}{\gamma-1}c+u\right)+f_2\left(\frac{2}{\gamma-1}c-u\right)\right\}.$$

The expressions standing as arguments in the arbitrary functions, as we already know, are Riemann invariants which are constant on the characteristics.

As would be expected, the general solution of the two equations (26.3) in partial derivatives of the first order depends on the two arbitrary functions.

In the case $N=0,\ \gamma=3$ and

$$\psi_0=f_1(\sqrt{2l}+u)+f_2(\sqrt{2l}-u).$$

For this

$$t=\frac{\partial\psi}{\partial l}=\frac{f_1'(\sqrt{2l}+u)+f_2'(\sqrt{2l}-u)}{\sqrt{2l}}=\frac{f_1'(c+u)+f_2'(c-u)}{c} \tag{26.18}$$

and according to (26.8)

$$\begin{aligned}x&=ut-f_1'(c+u)+f_2'(c-u)=\\&=\frac{u}{c}[f_1'(c+u)+f_2'(c-u)]-f_1(c+u)+f_2(c-u).\end{aligned} \tag{26.19}$$

We write the relationship (26.18) in the form

$$ct=f_1'(c+u)+f_2'(c-u). \tag{26.20}$$

Substituting successively f_1' and f_2' from (26.20) in (26.19), we

obtain

$$\left.\begin{aligned} x &= (u+c)\,t - 2f_1'(u+c) = (u+c)\,t + F_1(u+c), \\ x &= (u-c)\,t + 2f_2'(c-u) = (u-c)\,t - F_2(u-c), \end{aligned}\right\} \tag{26.21}$$

i.e. we arrive at the general solutions, already known to us, for the case $\gamma = 3$.

To find the general solution of the gas-dynamic equations, we transformed from the independent variables x and t to the independent variables u and t, by dividing the system (26.1) by the Jacobian

$$\Delta = \frac{\partial(u, t)}{\partial(t, x)},$$

assuming that $\Delta \neq 0$. For simple waves this method of solution does not apply, since for them u and t (or u and c) are definite functions which are mutually dependent on one another and therefore the given Jacobian becomes identically zero.

In § 23 it was established that the simple wave is always bounded either by a quiescent region or by a region of stationary flow. Therefore the motion described by the general solution (26.17) cannot border directly onto these regions and is separated from them by the intermediate region of the simple wave. The boundary between the simple wave and the wave described by the general solution is always a characteristic by necessity since it is simultaneously the boundary between the regions of two different analytical solutions.

To solve the various concrete problems the necessity arises for determining the value of ψ on this limiting characteristic.

The conditions for combining a simple wave with the wave described by the general solution can be fulfilled by substituting the expressions

(26.6) and (26.8) for x and t in the equation for the simple wave

$$x=(u\pm c)\,t+f(u).$$

In this case we obtain

$$\frac{\partial\psi}{\partial u}\pm c\frac{\partial\psi}{\partial t}+f(u)=0. \tag{26.22}$$

Since for a simple wave and consequently on the limiting characteristic

then $$du=\pm c\,d\ln\rho=\pm\frac{dt}{c};\quad c=\pm\frac{dt}{du},$$

whence $$\frac{\partial\psi}{\partial u}+f(u)=0,$$

$$\psi=-\int f(u)\,du. \tag{26.23}$$

which also determines the required boundary value for ψ. In the particular case when $f(u)=0$ (centered waves) $\psi=\text{const}$. Since the function ψ itself is given correct to a constant, then without decreasing the generality it is possible to assume $\psi=0$ on the boundary characteristic.

The region characterized by the general solution can also be joined on the left and on the right with regions characterized by general solutions or, on the one side, with a region described by a particular solution and on the other side by a region described by a general solution. There can also be the case when there are regions of particular solutions on both sides of the region of general solution. The simple wave should always be joined on one side either to a quiescent region or to a region of fixed motion. On the other side there can be either a region of a complex wave or of a stationary wave.

The region of disturbance described by the general solutions can also

be bounded on the one side by a wall which leads to reflection and frequently to a complicated interreaction of the various waves.

The region of the general solution in a number of cases can be bounded on one or both sides by regions of disturbance possessing different entropy, i.e. separated from them by the so-called particular or contact discontinuity.

The general solutions obtained, if the initial or boundary conditions are known, make it possible to solve a number of important concrete problems connected with the determination of the motion during reflection of the rarefaction wave from the wall, during bilateral outflow of gas from the tube, the interaction of the rarefaction wave with shock waves, etc.

§ 27. Reflection of a centered rarefaction wave from a wall.

In § 25 we considered the motion of a rarefaction wave arising during the sudden removal of the right-hand baffle plate from the pipe. The solutions found by us for this case hold only up to time $t = t_1$, i.e. until the rarefaction wave reaches the left wall at a distance l from the origin of the co-ordinates. It is evident that

$$t_1 = \frac{l}{c_*}. \tag{27.1}$$

After this, reflection occurs of the wave which will be propagated through the already disturbed gas and therefore will be described by general solutions of the basic gas-dynamic equations.

In Fig. 40 the characteristics for the reflection process of a wave

are illustrated.

In regions 1 and 1' the gas is stationary; in region 3, it moves from left to right at a constant velocity; 2 is the region of the incident rarefaction wave with straight-line C_- characteristics. Region 5 is that of a reflected wave with straight-line C_+ characteristics. Region 4 is a region of interaction or mutual penetration of two rarefaction waves in which the straight-line characteristics become distorted. For this region a solution of the gas-dynamic equations ought also to be found. This solution is completely determined by the boundary conditions. The first condition is that on the wall (ab) at $x=-l$ and any $t \geqslant t_1 = \frac{l}{c_*}$ the velocity of the gas is identically equal to zero. Substituting these conditions in relationship (26.4)

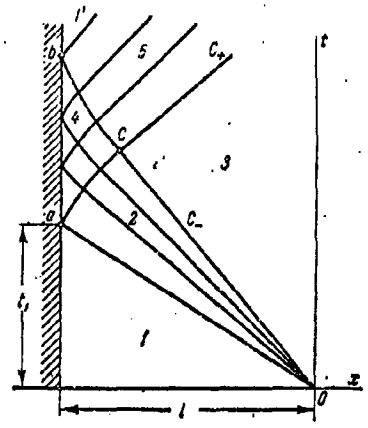


Fig. 40. Reflection of a centered rarefaction wave from the wall.

$$x = ut - \frac{\partial \psi}{\partial u},$$

we will have

$$\frac{\partial \psi}{\partial u} = +l. \tag{27.2}$$

The second condition is easily found by considering the boundary joining the reflected wave to the incident simple wave. This boundary is the section ac of the C_+ characteristics arising at the wall at time t_1.

Therefore on it we should have

$$u+\frac{2}{n-1}c=\text{const}.$$

On the wall (at point a) $u=0$ and $\text{const}=\frac{2}{n-1}c_{\text{н}}$. On this boundary, as was proved above, we should have $\psi=0$. Thus, the second condition gives

$$u=\frac{2}{n-1}(c_{\text{н}}-c),\quad \psi=0. \tag{27.3}$$

Starting from these two boundary conditions the arbitrary functions F_1 and F_2 can be easily determined.

Expressing c in terms of i, we obtain for the characteristic at the join

$$u=\sqrt{2(2N+1)}\,[\sqrt{i_{\text{н}}}-\sqrt{i}].$$

In this case the arbitrary functions will depend on the arguments:

$$F_1=F_1[\sqrt{2(2N+1)\,i_{\text{н}}}];\quad F_2=F_2[\sqrt{2(2N+1)}\,(2\sqrt{i}-\sqrt{i_{\text{н}}})].$$

It is possible to prove that $F_2=0$ and the function always satisfying these conditions is

$$\psi=\frac{i}{2N!}\frac{\partial^{N-1}}{\partial\theta^{N-1}}\frac{[(\sqrt{\theta}+u)^2-\theta_{\text{н}}]^2}{\sqrt{\theta}}, \tag{27.4}$$

where

$$\theta=Ri=\left(\frac{2}{n-1}c\right)^2,\quad R=2(2N+1).$$

Detailed consideration of this problem can be found in STANYUKOVICH's book "Neustanovivshiyesya dvizheniya sploshnoy sredy" (Unsteady motion of a uniform medium).

We will now introduce some important results of calculations, obtained from the exact solutions derived above.

The total impulse acting on the wall is determined from the relationship

$$I = \xi \sqrt{2 M_{\text{н}} E_{\text{н}}}, \tag{27.5}$$

where $M_{\text{н}}$ and $E_{\text{н}}$ are the total mass and energy of gas in the state of rest,

$$\xi = \sqrt{2N+3}\, \frac{(2N+1)!}{2^{2N+1} N! (N+1)!}.$$

The value of ξ for various values of n and N are given below:

n	3	5/8	7/8	1
N	0	1	2	∞
ξ	0.865	0.839	0.825	0.796

We can see that the value of ξ depends little on the value of n.

The determination of the parameters in the reflected wave at $n=3$ presents a problem of great interest to us.

Taking into account that in the case under consideration $F_2 = 0$ equation (26.17) gives

$$\psi = F_1[\sqrt{2l} + u].$$

Also on the wall $(x=-l)$ $u=0$; from the relationship $x = ut - \frac{d\psi}{du}$ we have $\frac{\partial \psi}{\partial u} = l = F_1'(\sqrt{2l})$. After integrating between the limits $l_{\text{н}}$ to l we obtain

$$F_1(\sqrt{2l}) = l(\sqrt{2l} - \sqrt{2l_{\text{н}}}).$$

Thus, function ψ will have the form

$$\psi = l(\sqrt{2l} - \sqrt{2l_{\text{н}}} + u). \tag{27.6}$$

Also it is possible to determine the pressure p_1 at the wall after the advent of the rarefaction wave. For this purpose, starting from (27.6) we determine that

$$\frac{\partial \psi}{\partial l} = t = \frac{l}{\sqrt{2l}} = \frac{l}{c}.$$

Because $c \sim p^{\frac{n-1}{2n}}$, then

$$\frac{c}{c_*} = \left(\frac{p}{p_*}\right)^{\frac{n-1}{2n}},$$

which at $n=3$ leads to the following relationship:

$$\frac{p_1}{p_*} = \left(\frac{l}{c_* t}\right)^3, \tag{27.7}$$

i.e. the pressure p_1 at the wall usually decreases as the inverse third power of t. For other values of n very much more cumbersome relationships are obtained for p_1.

We will now estimate the pressure p_2 at the points (on the line) of the join of the reflected wave to the incident wave. On the basis of (27.3), the following relationship holds on this line

$$u = \frac{2}{n-1}(c_* - c). \tag{27.8}$$

The equation of this line which is a C_+ characteristic can be found from the condition

$$\frac{dx}{dt} = u + c.$$

Substituting here the values of u and c from (25.9) we find that

$$\frac{dx}{dt} = \frac{4}{n+1} c_* + \frac{3-n}{n+1} \frac{x}{t}. \tag{27.9}$$

Integrating (27.9) and taking into account that the integral line should pass through the point $x = -l$ at $t = \frac{l}{c_*}$, we find that

$$x = \frac{2}{n-1} c_n t - \frac{n+1}{n-1} l \left(\frac{c_n t}{l}\right)^{\frac{3-n}{n-1}}. \tag{27.10}$$

For a travelling rarefaction wave

$$x = (u - c)\, t. \tag{27.11}$$

From (25.7), (27.10) and (27.11) it follows that

$$t = \frac{l}{c_n} \left(\frac{c_n}{c}\right)^{\frac{n+1}{2(n-1)}}. \tag{27.12}$$

This expression determines the time of the encounter of the reflected wave with the incident wave. Expressing c and c_n [illegible], we find that

$$\frac{p_2}{p_n} = \left(\frac{l}{c_n t}\right)^{\frac{4n}{n+1}}, \tag{27.13}$$

In the case of $n = 3$

$$\frac{p_2}{p_n} = \frac{p_1}{p_n} = \left(\frac{l}{c_n t}\right)^3, \tag{27.14}$$

i.e. the pressure in the reflected wave does not depend on the co-ordinates but only on the time, which is an important fact that simplifies all calculations in the solution of a number of concrete problems connected with the motion of detonation products of condensed explosives (reflection of a detonation wave from a wall, etc.).

It is interesting to determine the pressure p_2 at the section $x = 0$ i.e. at time $t = t_2$, when the reflected wave reaches the origin of the co-ordinates. For this moment on the basis of (25.10) we obtain

$$\frac{c_н}{c} = \frac{n+1}{2}$$

and

$$t_2 = \frac{l}{c_н}\left(\frac{n+1}{2}\right)^{\frac{n+1}{2(n-1)}}.$$

Whence it follows that

$$\frac{p_2}{p_н} = \left(\frac{2}{n+1}\right)^{\frac{2n}{n-1}}, \tag{27.15}$$

which for $n = 3$ gives $\frac{p_2}{p_н} = \frac{1}{8}$.

Below, the values of $\frac{p_2}{p_1}$ (for $t = t_2$) are given for various n, obtained as a result of exact solutions.

n	3	5/3	7/5	1
$\frac{p_2}{p_н}$	1.000	0,925	0,923	0,910

These data show that in the reflected wave the pressure and consequently the velocity of sound c varies little with the co-ordinates for any values of n.

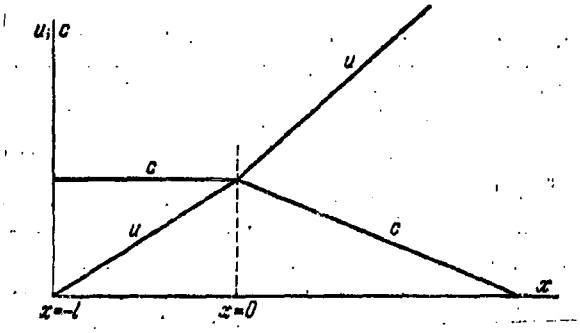


Fig. 41. Distribution of u and c in a gas during reflection of a centered rarefaction wave from a wall.

The distribution of u and c in the gas for the case under consideration is given in Fig. 41.

In the case $n=3$, as has already been said, p and c are only functions of time and do not vary at all with x.

The solution for a reflected wave in the general case $(n \neq 3)$ is extremely complicated and unsuitable for a number of transformations. By considering the slight variation of pressure with x, STANYUKOVICH obtained a simple approximate solution for the reflected wave which guaranteed good accuracy. For this purpose the pressure acting on the wall in the reflected wave is expressed approximately as a function of time by the relationship

$$\frac{p}{p_n}=\left[\frac{1+\frac{c_n\bar{t}}{l}}{\frac{c_n t}{l}+\frac{c_n\bar{t}}{l}}\right]^{k_1}, \tag{27.16}$$

where k_1 and $\bar{t}$ are constants.

Omitting the corresponding deductions, we will only state that these constants are determined by comparing the results of the exact and approximate solutions according to the formulae

$$\left.\begin{aligned} k_1&=\frac{1}{1-\frac{1}{4h\left[\theta\sqrt{\frac{2n}{n-1}}-1\right]}},\\ \frac{c_n\bar{t}}{l}&=\frac{1}{\frac{4n}{n+1}-\frac{1}{\theta\sqrt{\frac{2n}{n-1}}-1}}-1. \end{aligned}\right\} \tag{27.17}$$

Below, the values of k_1 and $\frac{c_n\bar{t}}{l}$ are given for various n.

n	3	5/3	7/5	1
k_1	3	1.80	1,55	1
$\frac{c_n\bar{t}}{l}$	0	−0,28	−0,83	−0,5

For a comparison of the accuracy of the results we will carry out an estimate of the impulses acting on the wall during the outflow of gas into a vacuum in an infinitely long tube:

$$I=\int_0^{p_n} p\,dt=\frac{p_n l}{c_n}\,\frac{k_1+\frac{c_n\bar{t}}{l}}{k_1-1}. \tag{27.18}$$

Also, taking into account the well-known thermodynamic relationship $\frac{pv}{n-1}=E$ which in the given case gives $p_n l=E_n(n-1)$ (where E_n is the total energy of the gas and l its initial volume, because the cross-sectional area of the tube is unity) and writing c_n in the form

$$c_n=\sqrt{n\frac{p_n l}{\rho_n l}}=\sqrt{\frac{(n-1)E_n}{nM_n}}, \tag{27.19}$$

where M_n is the total mass of gas, we reduce equation (27.18) to the form

$$I=\sqrt{2E_n M_n}\sqrt{\frac{n-1}{2n}}\,\frac{k_1+\frac{c_n\bar{t}}{l}}{k_1-1}.$$

Denoting

$$\frac{k_1+\frac{c_n\bar{t}}{l}}{k_1-1}\sqrt{\frac{n-1}{2n}}=\xi_1$$

and carrying out calculations for various n, we find values for ξ_1

n	3	5/2	7/2
ξ_1	0,866	0,850	0,839

which are very close to the corresponding values of ξ obtained as a result of exact solutions.

The application of this approximate method facilitates the solution of a number of complicated problems of an applied character.

In conclusion we note that the problem of the interaction of two identical centered rarefaction waves emerging simultaneously (at $t=0$ from the points $x=0$ and $x=2l$ and propagating towards one another is evidently equivalent to the problem considered above of the reflection of a rarefaction wave from a wall at distance l from the open end of a tube (Fig. 42).

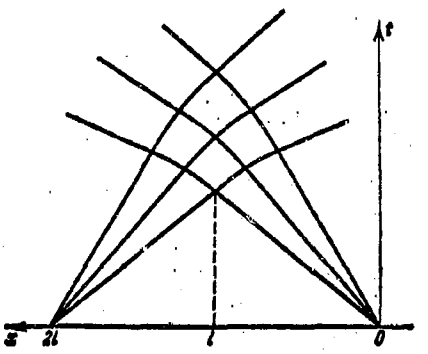


Fig. 42. Interaction of two identical centered rarefaction waves, emerging simultaneously and progressing towards one another.

§ 28. Bilateral outflow of gas from a cylindrical vessel into a pipe.

The preceding problem is generalised as follows.

At the moment $t=0$ the gas begins to flow out of the right-hand

end of a cylindrical vessel of length l into a tube of the same diameter. Within some interval of time $\tau\ \left(0<\tau<\frac{l}{c_н}\right)$, i.e. after the first rarefaction wave reaches the left-hand side of the vessel, outflow of gas begins from the left-hand side. During the interval of time $0\leqslant t\leqslant\tau$, the whole process reduces to the propagation of a simple wave moving to the left from the right-hand side.

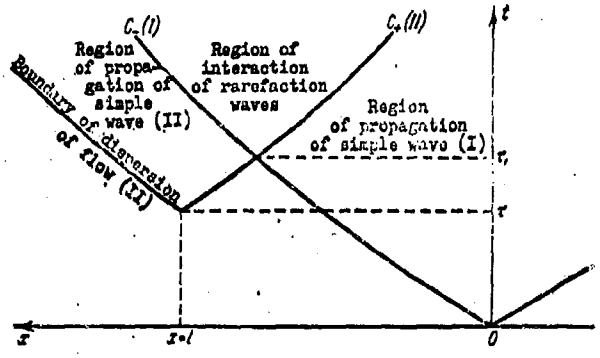


Fig. 43. Interaction of rarefaction waves during the bilateral outflow of gas into a tube occurring non-simultaneously.

At the moment $t=\tau$, the propagation of the second rarefaction wave begins from the left-hand end to the right. Let $t=\tau_1$ be the moment of encounter of these waves, while it is evident that $\tau<\tau_1<\frac{l}{c_н}$. During the interval of time $\tau\leqslant t<\tau_1$, we have an undisturbed medium between the fronts of the approaching waves, i.e. we will be concerned only with the motion of simple waves.

At time τ_1, as a result of the interaction of waves I and II, a new complicated wave arises which will be described by the general solution, since its left and right fronts will propagate through the

disturbed gas. The general picture of the phenomena under consideration is given schematically in Fig. 43 with the help of C characteristics.

The problem of bilateral outflow of gas into a tube was first solved by STANYUKOVICH. The results of the corresponding calculations are given below.

The masses M, the impulses I and the energies E of the gas flows to right and left are determined from the following relationships:

$$M_1 = \frac{M_0}{2}\left[1 + \frac{c_0 \tau}{l}\frac{(2R+1)!}{R!\,(R+1)!\,2^{2R+1}}\right],$$
$$M_2 = \frac{M_0}{2}\left[1 - \frac{c_0 \tau}{l}\frac{(2R+1)!}{(R+1)!\,2^{2R+1}}\right], \quad R = \frac{3-n}{2n-3}.$$

For $n = 3$ we have

$$M_1 = \frac{M_0}{2}\left(1 + \frac{c_0 \tau}{2}\right), \quad M_2 = \frac{M_0}{2}\left(1 - \frac{c_0 \tau}{2}\right). \tag{28.1}$$
$$I_1 = \frac{M_0 c_0}{2}\left[\frac{c_0 \tau}{l}\frac{1}{(2R+1)(2R+3)} + \frac{(2R+1)(2R)!}{2(R+1)!\,(R!)^2 R^{2R}}\right],$$
$$I_2 = \frac{M_0 c_0}{2}\left[\frac{c_0 \tau}{l}\frac{1}{(2R+1)(2R+3)} - \frac{(2R+1)(2R)!}{2(R+1)!\,(R!)^2 R^{2R}}\right].$$

At $n = 3$ we will have

$$I_{1,2} = \frac{M_0 c_0}{2}\left[\frac{c_0 \tau}{3l} \pm 1\right] \tag{28.2}$$

or substituting $c_0 = \sqrt{n(n-1)\varepsilon_0}$ where ε_0 is the specific energy of the gas, we obtain

$$I_{1,2} = \sqrt{2E_0 M_0}\left[\frac{\tau}{l}\sqrt{2\varepsilon_0} \pm 1\right]. \tag{28.3}$$

The energies are calculated from the formula

$$E_{1,2} = \frac{M_0 c_0^2}{4}(2R+1)^2\left[\pm\frac{c_0 \tau}{l}\frac{(2R+1)!}{2^{2R+1}R!\,(R+2)!} + \frac{1}{2R+3}\right].$$

which at $n=3$ gives

$$E_{1,2}=\frac{M_n c_n^2}{4}\left[\pm\frac{c_n\tau}{4l}+\frac{1}{3}\right]. \tag{28.4}$$

The indices 1 and 2 refer to the right and left flows, respectively.

§ 29. Conditions for the origination of shock waves.

In § 23 it was shown that during the propagation of a simple compression wave a shock wave arises which is characterized by an infinitely steep front.

In fact, let some disturbance of arbitrary amplitude be given which runs, for example, in the positive direction of the x axis. We shall find the velocity of propagation of any given state of the medium. Let us recall that for simple waves all the parameters of state (p, ρ, c) are connected with the velocity u by a single-valued functional variation.

At some time t_1 at the point x_1 let us assume the values $u=\bar{u}$; $c=\bar{c}$. These values should satisfy the solutions obtained i.e.

$$x_1=(\bar{u}+\bar{c})t_1+F(\bar{u}). \tag{29.1}$$

We will now determine at what point x_2 the values of $\bar{u}$ and $\bar{c}$ are the same at some time $t_2>t_1$. It is evident that the point x_2 should satisfy the equation

$$x_2=(\bar{u}+\bar{c})t_2+F(\bar{u}). \tag{29.2}$$

From (28.1) and (28.2) we find that

$$\frac{x_2-x_1}{t_2-t_1}=\bar{u}+\bar{c}. \tag{29.3}$$

From this it follows that the velocity of motion of the given state of the medium is $\bar{u}+\bar{c}$. Any two states, characterized by different values of u and c will be propagated at constant but different velocities. Because of this, the disturbance cannot be propagated unchanged; points characterizing the parameters of state of the medium for which $u+c$ is greater, for example, the wave crests, i.e. the places where the density is a maximum, will move more rapidly than other points for which the values of $u+c$ are considerably less. This is evidently explained physically by the fact that in a more compressed gas the velocity of sound is greater; a more compressed gas also possesses a greater mass velocity in the same direction as the propagation of sound.

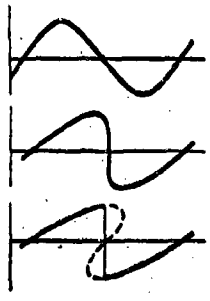


Fig. 44. Deformation of a wave of finite amplitude.

As a result of such a propagation of the disturbance, the wave will be deformed. The regions of compression (wave crests) will be displaced forward, the regions of rarefaction, on the other hand, will lag behind the general average flow of the gas - the wave crests will become steeper and steeper until finally its front becomes vertical (moment of formation of shock wave). The intersection of the characteristics, shown in Fig. 35, also reflects this phenomenon.

If, however, the pressures are calculated at later moments of time, then many-valued functions are obtained, according to which one and the same point x can have simultaneously three different values of pressure

and density, which is absurd from the physical viewpoint.

The character of the deformation of a sinusoidal wave of finite amplitude, derived from the obtained solutions, is shown schematically in Fig. 44.

The reason for such results being obtained with no physical meaning is because the original differential equations in gas-dynamics which we used only hold until discontinuities occur (Fig. 35). In fact, the occurrence of jumps and of surfaces of discontinuities (pressure, density, temperature) indicates a change in entropy of the system and in deriving the solutions we neglected thermal conductivity, i.e. we assumed constant entropy.

When the temperature gradient $\left(\frac{\partial T}{\partial x}\right)$ increases without limit in the motion of a wave, then even for a low coefficient of thermal conductivity λ the flow of energy $\lambda \frac{\partial T}{\partial x}$, transferable by thermal conductivity, should also increase without bound. From this it is evident that for the processes connected with the origination of large temperature gradients it is surely necessary to take into account the thermal conductivity of the medium.

The occurrence of discontinuities thus leads to an increase in entropy, i.e. to a dissipation of energy and consequently implies a powerful damping of the wave.

Bibliography.

1. L.D. Landau and E.M. Lifshitz. Mekhaniki sploshnykh sred (Fluid Mechanics). Translation published by Pergamon Press (1959).
2. L.I. Sedov, Metody podobiya i razmernosti v mekhanike (Similarity and dimensional methods in mechanics). Gostekhizdat (1957).
3. K.P. Stanyukovich. Neustanovivshiyesya dvizheniya sploshnoy sredy (Unsteady flow of a continuous medium). Gostekhizdat (1955).
4. Ya. B. Zel'dovich. Teoriya udarnykh voln i vvedeniye v gazodinamiky (Theory of shock waves and introduction to gas dynamics). Izd. Akad. Nauk USSR (1946).
5. N. Ye. Kochin, I.A. Kibel' and N.V. Roze. Teoreticheskaya gidromekhanika (Theoretical hydromechanics). Gostekhizdat (1948).
6. G.I. Abramovich. Prikladnaya gazovaya dinamika (Applied gas dynamics). Gostekhizdat (1953).
7. R. Courant and K.O. Friedricks. Supersonic flow and shock waves. Interscience Publishers, New York (1948).
8. Ia. B. Zel'dovich and A.S. Kompaneyets. Teoriya detonatsii (Theory of detonation). Gostekhizdat (1955).
9. G. Birkhoff. Hydrodynamics. Princeton Univ. Press (1950).
10. K.P. Stanyukovich. Teoriya neustanovivshikhsya dvizheniy (Theory of unsteady flow). Izd. Byuronovoy tekhniki, Moscow (1948).

CHAPTER VI

ELEMENTARY THEORY OF SHOCK WAVES

30. Basic Relations

Shock waves play a very important part in the propagation of detonation waves; they are of major interest in relation to the mechanical effects of explosions. The theory of shock waves was founded in the second half of the 19th century by RANKINE and others; RANKINE'S work, in which he made allowance for thermal conduction, was the earliest, in which the basic differential equations were derived. This system of equations has, so far, been solved only for the special case of a steady-state planar stepwise density change. The basic relationships for steady shock waves may be derived directly from the conservation laws. The following is a deduction of the basic equations.

First of all I consider the general conditions at the front of a general shock wave, which need not be moving uniformly. The front is the surface at which there are discontinuities in the parameters for the state and motion of the medium; the basic laws for this front in general are found by considering the behavior of an element of the surface during an indefinitely small interval. I employ a rectangular coordinate system that moves with the element, the x axis being normal to the surface (Fig. 45). The speed of the wave is then the speed at which the element moves along the x axis.

The laws of conservation (of mass, momentum, and energy) apply to the surface; the law of conservation of mass implies that any flux of matter must be continuous across the element. That flux, referred to

unit area, is ρu_1, in which ρ is density and u is the component of the flow velocity along the x_1 axis. Let subscripts 1 and 2 respectively denote the unperturbed and perturbed sides; then the law of conservation of mass, as applied to the front, is

$$\rho_1 u_1 = \rho_2 u_2. \tag{30,1}$$

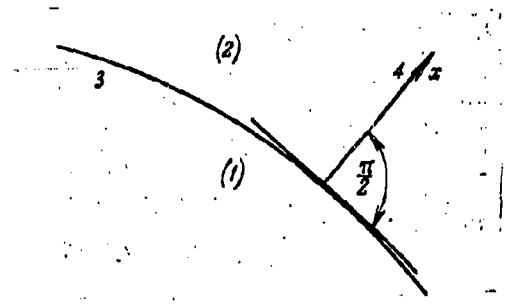


Fig. 45. Deduction of the relationships at the surface of discontinuity.

The law of conservation of momentum is used as follows. The condition for continuity in the x component of the momentum flux is

$$p_1 + \rho_1 u_1^2 = p_2 + \rho_2 u_2^2. \tag{30,2}$$

The conditions for continuity in the y and z components are

$$\rho_1 u_1 v_1 = \rho_2 u_2 v_2, \tag{30,3a}$$

$$\rho_1 u_1 w_1 = \rho_2 u_2 w_2. \tag{30,3b}$$

The condition for continuity in the energy flux is

$$\rho_1 u_1 \left(\frac{q_1^2}{2} + i_1\right) = \rho_2 u_2 \left(\frac{q_2^2}{2} + i_2\right), \tag{30,4}$$

$$q_1 = \sqrt{u_1^2 + v_1^2 + w_1^2}, \quad q_2 = \sqrt{u_2^2 + v_2^2 + w_2^2}, \tag{30,5}$$

in which q_1 and q_2 are the total velocities and $i = E + pv$ is the enthalpy. Then (30,1) gives (30,4) the form

$$\frac{q_1^2}{2} + i_1 = \frac{q_2^2}{2} + i_2. \tag{30,6}$$

To these six equations we add the equation of state

$$p = f(\rho, T), \tag{30,7}$$

which is assumed to be known.

The above equations define the conditions at the front completely; we may use them to find the parameters for the state and motion of the perturbed medium in terms of the parameters for the unperturbed medium.

There is no flow of the medium through the surface if $u_1 = u_2 = 0$; (30,2) implies that $p_1 = p_2$. The density, and the tangential components v and w, may undergo any changes across the surface. The discontinuity is called tangential if the values on the two sides are

unequal for one (or both) of the tangential components; the density may or may not change across the front. The discontinuity is called special if $v_1 = v_2$ and $w_1 = w_2$ but $\rho_1 \neq \rho_2$.

A flow of matter through the front must imply that

$$u_1 \neq u_2 \neq 0; \tag{30,8}$$

then (30,3a), (30,3b), and (30,1) imply that

$$v_1 = v_2; \quad w_1 = w_2, \tag{30,9}$$

(the tangential velocity components are continuous across the surface). The pressure, density, and other thermodynamic parameters then have discontinuities at the front; the above system of equations becomes

$$\rho_1 u_1 = \rho_2 u_2, \quad p_1 + \rho_1 u_1^2 = p_2 + \rho_2 u_2^2, \quad \frac{u_1^2}{2} + i_1 = \frac{u_2^2}{2} + i_2. \tag{30,10}$$

The flow is normal to the front, and we have a straight shock wave, if $u_1 \neq u_2 \neq 0$ but $v_1 = v_2 = 0$ and $w_1 = w_2 = 0$; the wave is spatially oblique if $v_1 \neq v_2 \neq 0$ and $w_1 \neq w_2 \neq 0$. The wave is called simply oblique if one of the tangential velocity components is zero. The above relations are applicable to a front of any shape.

The front (surface of discontinuity) moves at a speed D along the normal to the surface. It is always possible to choose a coordinate system such that the motion of the surface occurs along that normal; that system is called fixed, to distinguish it from the system in which our element of the front is at rest. The velocities u_{10} and u_{20} in the fixed system are

$$u_{10} = u_1 + D, \quad u_{20} = u_2 + D, \tag{30,11}$$

so (30,10), with $v_1 = v_2 = w_1 = w_2 = 0$, becomes

$$\rho_1 (u_{10} - D) = \rho_2 (u_{20} - D), \quad p_1 + \rho_1 (u_{10} - D)^2 = p_2 + \rho_2 (u_{20} - D)^2,$$
$$i_1 + \frac{1}{2}(u_{10} - D)^2 = i_2 + \frac{1}{2}(u_{20} - D)^2. \tag{30,12}$$

Now I turn to the basic properties of shock waves, which are considered in relation to a plane straight shock wave.

31. Plane Straight Shock Wave

Consider a density step propagating from left to right at a speed D

in a cylinder of unit cross-section. Figure 46 indicates the parameters, of which $u_1 \neq 0$. This motion u_1 is superimposed on the motion of the front, so the effective speed of the step in the medium is $D-u_1$ and the flow speed behind the front is u_2-u_1. Consider a coordinate system moving in the opposite sense at a speed D; the entire medium must be assigned a velocity $-D$ (one from right to left), which leaves the front AB in a fixed position. The conservation laws then give us the relationships we need.

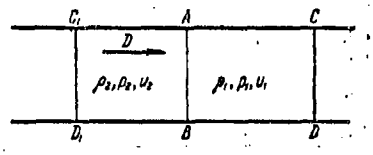


Fig. 46. Motion of a plane shock wave.

The medium to the right of AB moves to the left with a speed $D-u_1$; the medium compressed by the wave moves to left and right at speeds $D-u_1$ and $D-u_2$ respectively. In one second a mass of gas that initially took up a volume $D-u_1$ acquires a volume $D-u_2$; its right boundary CD moves up to AB, while its left boundary AB moves to C_1D_1. The masses in these two volumes are the same, so

$$\rho_1(D-u_1)=\rho_2(D-u_2). \tag{31,1}$$

which is simply the law of conservation of matter. NEWTON's second law is

$$Ft=Mu, \tag{31,2}$$

in which F is force, t is time, and Mu is change of momentum. Here the force is produced by the pressure difference p_2-p_1; the time is taken to be unity, so the law of conservation of momentum becomes

$$p_2-p_1=\rho_1(D-u_1)(u_2-u_1). \tag{31,3}$$

The internal energy of unit mass of the medium is E; the kinetic energy of unit mass is $\frac{u^2}{2}$. The motion of the medium requires an intake of work equal to $(p_2u_2-p_1u_1)$ in unit time, which, referred to unit mass,

becomes

$$\frac{p_2u_2-p_1u_1}{(D-u_1)\rho_1}.$$

The work done by the pressure goes to change the internal and kinetic energies; the energy-balance equation is

$$\frac{p_2u_2-p_1u_1}{(D-u_1)\rho_1}=(E_2-E_1)+\left(\frac{u_2^2}{2}-\frac{u_1^2}{2}\right). \tag{31,4}$$

This may be transformed by putting (31,1) in the form

$$\frac{D-u_1}{v_1}=\frac{D-u_2}{v_2}, \tag{31,5}$$

in which $v=1/\rho$ is the specific volume. We multiply both sides by v_1v_2 to get that

$$(D-u_1)v_2=(D-u_2)v_1,$$

and so

$$D=\frac{u_2v_2-u_1v_1}{v_2-v_1}.$$

Subtracting u_1 from both sides, we have

$$D-u_1=v_1\frac{u_2-u_1}{v_1-v_2},$$

whence

$$M=\frac{D-u_1}{v_1}=\frac{u_2-u_1}{v_1-v_2}. \tag{31,6}$$

Further, (31,3) gives us that

$$M=\frac{D-u_1}{v_1}=\frac{p_2-p_1}{u_2-u_1}.$$

Comparison of the last two expressions shows that

$$u_2-u_1=\sqrt{(p_2-p_1)(v_1-v_2)}. \tag{31,7}$$

The speed of the wave is then readily found as

$$D-u_1=v_1\sqrt{\frac{p_2-p_1}{v_1-v_2}}. \tag{31,8}$$

Then (31,6) and (31,8) enable us to put the energy equation as

$$E_2-E_1=\frac{1}{2}(u_2-u_1)\left[2\,\frac{p_2u_2-p_1u_1}{p_2-p_1}-(u_1+u_2)\right]=\frac{1}{2}(u_2-u_1)^2\left(\frac{p_2+p_1}{p_2-p_1}\right),$$

which gives us that

$$E_2-E_1=\frac{p_2+p_1}{2}(v_1-v_2). \tag{31,9}$$

This is called HUGONIOT's equation; it is used to relate the parameters of the medium on the two sides of the front.

For an ideal gas, and for any medium that obeys the polytropic law

pv^k = constant, we have that

$$\left.\begin{aligned} E &= c_v T = \frac{pv}{k-1}, \\ E_1 &= \frac{p_1 v_1}{k_1 - 1}, \quad E_2 = \frac{p_2 v_2}{k_2 - 1}. \end{aligned}\right\} \tag{31,10}$$

Simple manipulations give us that

$$\frac{p_2}{p_1} = \frac{\frac{k_2+1}{k_2-1}\frac{\rho_2}{\rho_1} - 1}{\frac{k_1+1}{k_1-1} - \frac{\rho_2}{\rho_1}}, \qquad \frac{\rho_2}{\rho_1} = \frac{\frac{k_2+1}{k_2-1}\frac{p_2}{p_1} + 1}{\frac{k_1+1}{k_1-1} + \frac{p_2}{p_1}},$$

which become

$$\frac{p_2}{p_1} = \frac{(k+1)\rho_2 - (k-1)\rho_1}{(k+1)\rho_1 - (k-1)\rho_2}, \quad \frac{\rho_2}{\rho_1} = \frac{v_1}{v_2} = \frac{(k+1)p_2 + (k-1)p_1}{(k+1)p_1 + (k-1)p_2}. \tag{31,11}$$

if $k_1 = k_2 = k$ (if the change is not too large). These equations express the shock adiabatic or HUGONIOT's adiabatic; this adiabatic represents the law of conservation of energy and is applicable to shock waves in polytropic media (it is analogous to the ordinary adiabatic).

Properties of shock waves. The above relations are

$$\left.\begin{aligned} u_2 - u_1 = u &= \sqrt{(p_2 - p_1)(v_1 - v_2)}, \\ D - u_1 = D &= v_0 \sqrt{\frac{p_2 - p_1}{v_1 - v_2}}, \\ E_2 - E_1 &= \frac{p_2 + p_1}{2}(v_1 - v_2), \\ p &= f(\rho, T). \end{aligned}\right\} \tag{31,12}$$

This is a system of four equations in five unknowns; we can determine four of the parameters if the fifth is given. Table 49 gives the parameters for shock waves in air for various values of $\frac{p_2}{p_1}$; it is convenient for future use to express the basic parameters u_2, p_2, and v_2 as functions of c_1, the velocity of sound in the unperturbed medium. We put $u_1 = 0$, $u_2 = u$, and use the equation of state for ideal gases to transform (31,3) to

$$p_2 - p_1 = R(\rho_2 T_2 - \rho_1 T_1) = \rho_1 D u. \tag{31,13}$$

Table 49

Parameters of Shock Waves in Air

Initial state:

$p_1 = 1$ atm, $\rho_1 = 1{,}293 \times 10^{-3}$ g/cm^3, $T_1 = 273°$ K, $c_1 = 333$ m/sec.

p_2, kg/cm^2	$\frac{T_2}{T_1}$	T_2, °K	$\frac{\rho_2}{\rho_1}$	u, m/sec	c_2, m/sec	D, m/sec
2	1,23	336	1,63	175	368	452
5	1,76	482	2,84	452	439	608
8	2,26	618	3,53	627	497	875
10	2,58	705	3,88	725	528	978
20	4,12	1126	4,81	1095	661	1369
30	5,57	1522	5,38	1364	763	1676
40	6,95	1898	5,76	1594	847	1930
50	8,28	2260	6,04	1795	920	2150
60	9,53	2660	6,30	1978	984	2350
80	11,76	3210	6,70	2300	1080	2705
100	14,15	3860	7,06	2590	1180	3020
200	23,71	6475	8,43	3715	1490	4220
300	31,6	8630	9,48	4590	1700	5160
400	38,5	10520	10,38	5330	1860	5900
500	44,8	12200	11,15	5980	1930	6570
600	50,4	13760	11,91	6570	2100	7140
700	55,6	15190	12,58	7130	2200	7730
800	60,6	16540	13,2	7620	2300	8260
900	55,2	17810	13,8	8100	2380	8730
1000	70,0	19100	14,3	8560	2460	9210
1300	81,6	22330	15,9	9800	2640	10450
1600	92,7	25310	17,3	10850	2800	11550
2000	106,2	29900	18,8	12210	2990	12900
2500	120,4	32860	20,8	13700	3160	14350
3000	134,4	36700	22,3	15050	3340	15750

Here we insert the ρ_2 of (31,5) and the T_2 of (31,10), with $k_1 = k_2 = k$, to get finally that

$$u = \frac{2}{k+1} D\left(1 - \frac{c_1^2}{D^2}\right). \tag{31,14}$$

(here $c_1^2 = \frac{kp_1}{\rho_1}$). The u of (31,14) is inserted in (31,13) to give us that

$$p_2 - p_1 = \Delta p = \frac{2}{k+1} \rho_1 D^2 \left(1 - \frac{c_1^2}{D^2}\right). \tag{31,15}$$

Further, (31,5) gives us that

$$\frac{v_1 - v_2}{v_1} = \frac{2}{k+1}\left(1 - \frac{c_1^2}{D^2}\right). \tag{31,16}$$

These equations give us the basic relationships for sound waves; if

$p_2 \to p_1$ and $v_2 \to v_1$,

$$D = v_1 \sqrt{-\frac{dp}{dv}} = \sqrt{\frac{dp}{d\rho}} = c_1.$$

Here $u = 0$ (the medium is at rest), and (31,9) becomes

$$dE = -p\,dv,$$

which is the usual adiabatic law pv^k = constant for an ideal gas. The previous relationships imply that $D > c_0$ and $u > 0$, with $u < D$, for a shock wave; the medium is displaced in the direction of motion of the front, but at a lower speed. The shock adiabatic plays a very important part in the theory of shock waves; the relation may be represented as a p–v diagram (Fig. 47), which provides a simple and convenient means of examining the behavior of shock waves. Through A (which represents the state of the unperturbed medium) and B (which represents the state behind the front) we draw a straight line, for which

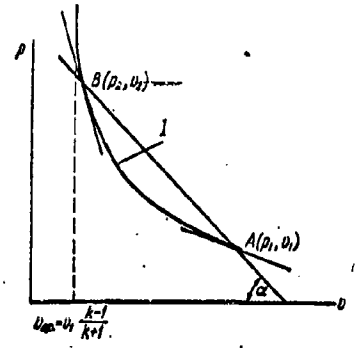


Fig. 47. Hugoniot curve (shock-wave adiabatic).

$$\frac{p_2 - p_1}{v_1 - v_2} = \tan\alpha,$$

in which α is as shown. This shows that α defines D and u completely. Any point above A on the curve corresponds to a shock wave, because $D > 0$ and $u > 0$; whereas below A we have that $(p_2 - p_1) < 0$ and $(v_1 - v_2) < 0$, so $D > 0$ and $u < 0$. This means that the medium is displaced in a sense opposed to that in which the perturbation propagates; that is, we have a wave of rarefaction. Now $p_2 \to p_1$ and $v_2 \to v_1$ at the limit for a weak shock wave, so

$$D = v_1 \sqrt{\tan\alpha} = v_1 \sqrt{-\frac{dp}{dv}},$$

which means that the shock adiabatic becomes an ordinary one; the two have a common tangent at A.

The entropy increases as we pass from A to B along the shock-wave curve; for an ideal gas

$$dQ = p\,dv + c_v\,dT, \tag{31,17}$$

so

$$\frac{dQ}{T} = dS = \frac{p}{T}\,dv + c_v\frac{dT}{T},$$

which gives us that $$dS = R\,d\ln v + c_v\,d\ln T.$$

The integral is

$$S - S_0 = R\ln v + c_v\ln T = \ln\left(v^R T^{c_v}\right). \tag{31,18}$$

We replace T by p and v to get that

$$\frac{1}{c_v}(S - S_0) = \ln\left(\frac{pv^k}{R}\right),$$

and so

$$pv^k = Re^{\frac{1}{c_v}(S-S_0)} = c. \tag{31,19}$$

Now $\sigma_1 = p_1 v_1^k$ for the unperturbed medium, and $\sigma_2 = p_2 v_2^k$ for the perturbed medium; inserting the v_2 of (31,11), we have that

$$\sigma_2 = p_2 v_2^k = \sigma_1\frac{p_2}{p_1}\left[\frac{(k-1)p_2 + (k+1)p_1}{(k+1)p_2 + (k-1)p_1}\right]^k > \sigma_1. \tag{31,20}$$

That is, the larger p_2 the greater the entropy increase. It can be shown that $\left(\frac{\partial^2 p}{\partial v^2}\right)_S > 0$ is the condition for a shock wave in any medium.

To the above relations we may add one for the temperature at the front for an ideal gas. Here $pv = RT$, so

$$\frac{T_2'}{T_1} = \frac{p_2}{p_1}\left(\frac{\rho_1}{\rho_2}\right)^k = \frac{p_2}{p_1}\,\frac{\frac{k_1+1}{k_1-1} + \frac{p_2}{p_1}}{\frac{k_2+1}{k_2-1}\frac{p_2}{p_1} + 1}, \tag{31,21}$$

in which the prime denotes the parameters of the medium for the shock wave. Shock compression causes the temperature to increase with the pressure more rapidly than for normal adiabatic compression; the reason, as we shall see, is that the density at the front remains finite at 10-12 times its initial value even when $p_2 \to \infty$. A normal adiabatic process obeys the laws

so $$T \propto c^2 \propto p^{\frac{k-1}{k}}; \quad \rho \propto p^{\frac{1}{k}}.$$

and $$\frac{T_{2a}}{T_1} = \left(\frac{p_2}{p_1}\right)^{\frac{k-1}{k}}$$

$$\frac{T_2'}{T_{2a}} = \left(\frac{p_2}{p_1}\right)^{\frac{1}{k}} \left(\frac{\rho_1}{\rho_2}\right)' = \left(\frac{\rho_2}{\rho_1}\right)_a \left(\frac{\rho_1}{\rho_2}\right)' = \left(\frac{p_2}{p_1}\right)^{\frac{1}{k}} \frac{\frac{k_1+1}{k_1-1}+\frac{p_2}{p_1}}{\frac{k_2+1}{k_2-1}\frac{p_2}{p_1}+1}. \qquad (31,22)$$

in which subscript a denotes parameters for normal adiabatic compression; (31,21) and (31,22), with $k_1 = k_2 = k$, become

$$\frac{T_2'}{T_1} = \frac{p_2}{p_1} \frac{(k+1)p_1+(k-1)p_2}{(k+1)p_2+(k-1)p_1}, \qquad (31,23)$$

$$\frac{T_2'}{T_{2a}} = \left(\frac{p_2}{p_1}\right)^{\frac{1}{k}} \frac{(k+1)p_1+(k-1)p_2}{(k+1)p_2+(k-1)p_1}. \qquad (31,24)$$

Equations (31,14), (31,15), (31,21), (31,23), and (31,24) take particularly simple forms if $p_2 \gg p_1$:

$$u' = \frac{2}{k+1} D' \qquad (31.25)$$

$$p_2 = \frac{2}{k+1} \rho_1 D^{12} \qquad (31.26)$$

$$\frac{\rho_2}{\rho_1} = \frac{k+1}{k-1}, \qquad (31.27)$$

$$\frac{T_2'}{T_1} = \frac{p_2}{p_1} \frac{k-1}{k+1}, \qquad (31.28)$$

$$\frac{T_2'}{T_{2a}} = \left(\frac{p_2}{p_1}\right)^{\frac{1}{k}} \frac{k-1}{k+1}. \qquad (31.29)$$

Equation (31,27) shows that the density does tend to a definite limit, which is dependent on k. Table 50 gives values computed for air by Burkhardt on the basis of revised values for the specific heats (with allowance for dissociation and ionization in the shock wave); for example, $T_2 = 30\,000°\,\mathrm{K}$ and $\frac{\rho_2}{\rho_1} = 9.5$ for $\frac{p_2}{p_1} = 3000$. Figures 48 and 49 compare these results with those given by classical formulas based on the assumption of constancy in the specific heats. These results show that D and p_2 vary little with k if the gas is ideal. Further, the classical methods give the T_2 for a given $\frac{p_2}{p_1}$ $(= \pi)$ too large if the

Table 50

Parameters of Shock Waves Producing Dissociation and Ionization

Initial state of air: $p_1 = 1$ atm, $T_1 = 273°$ K, $\rho_1 = 1.293 \cdot 10^{-3}$ g/cm^3

$\frac{p_2}{p_1}$	$\frac{T_2}{T_1}$	T_2, °K	$\frac{\rho_2}{\rho_1}$	u, m/sec	D, m/sec
216	20.5	5600	9	3870	4350
266	22.0	6000	10	4320	4800
384	26.0	7000	11	5220	5750
1040	48.0	13100	11	8600	9470
1620	75.0	20500	10	10680	11860
2990	114.0	31200	9.5	14500	16200
4080	140.0	38000	9.0	16900	19000

heat capacity is assumed to be a linear function of temperature; for example, T_2 comes out 20% larger than BURKHARDT's value for a π of 3000.

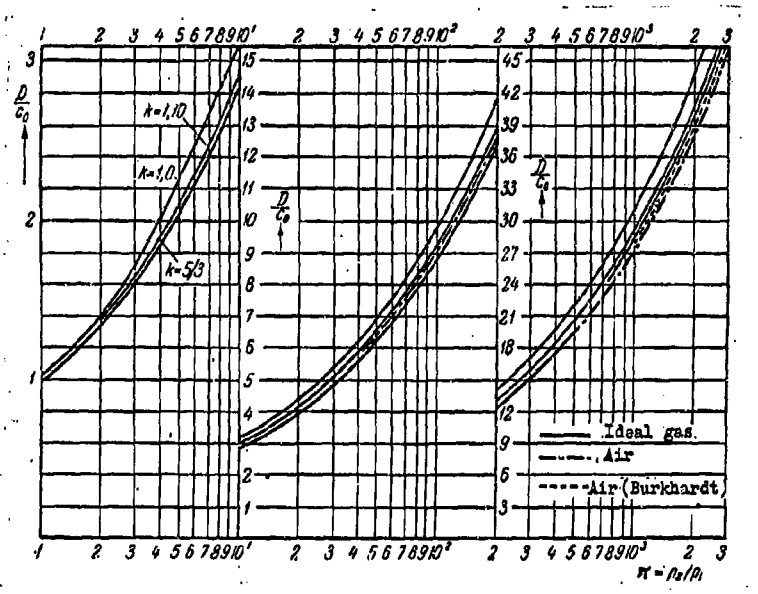


Fig. 48. Ratio of the speed of a shock wave to the speed of sound as a function of the pressure ratio for an ideal gas and for air.

The really large discrepancies occur in $\frac{\rho_2}{\rho_{2'}}$, though; dissociation

and ionization are very important at high temperatures. The number of particles increases, so the density tends to decrease. The density

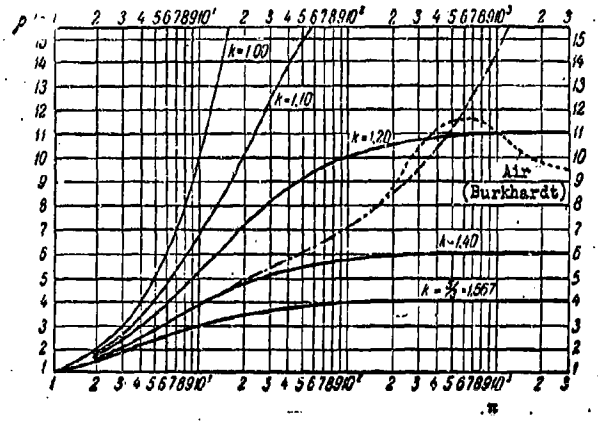


Fig. 49. Ratio of the densities as a function of the pressure ratio for shock waves in an ideal gas and in air.

given by the classical formulas is 2.3 times that found by BURKHARDT for a π of 3000, for example. Figure 49 shows that the density may even fall as π increases at the higher π, because dissociation becomes very important. Table 50 indicates that $\frac{\rho_2}{\rho_1} \approx 9.5$ for air at the limit, so $k_2 \approx 1.23$. (The theory of dissociation and ionization in shock waves is dealt with in section 35.)

The conclusions to be drawn are as follows.

1. The speed of a shock wave is always greater than that of sound in the unperturbed medium.

2. The parameters for the state and motion of the medium show stepwise changes at the shock front.

3. The medium behind a shock wave is displaced in the sense of motion of that wave.

4. The speed is dependent on the amplitude, which is not so for sound waves.

5. The entropy increases ($dS_2 > 0$) when a shock wave is formed.

6. A shock wave propagates as a single step in de sity; it is not oscillatory.

So far we have considered a shock wave as representing discontinuities in pressure, density, and temperature (Fig. 50); we have considered the parameters on either side of the front, but we have not

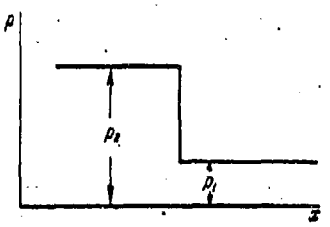


Fig. 50. Pressure in an ideal shock wave.

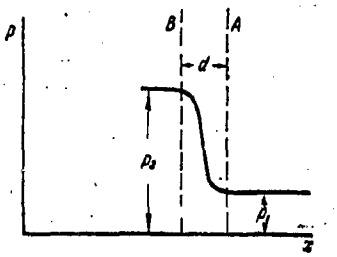


Fig. 51. Pressure in a real shock wave.

examined the structure of the front itself. The viscosity and thermal conductivity prevent the gradients from being indefinitely large; the front itself takes somewhat the form shown in Fig. 51, and there is a very narrow transition zone between the planes A and B. This zone contains only a very small amount of matter, and its thickness remains constant, so we were justified in neglecting the processes in this zone in the above treatment. The shock adiabatic uniquely defines the final state behind the front, but it tells us nothing about the changes in the frontal zone. These changes cannot be considered unless we introduce the viscosity and thermal conductivity, which have no effect on the relation of the final state to the initial state. For example, the equation

$$D^2 = v_1^2 \frac{p_2 - p_1}{v_1 - v_2},$$

was derived from the laws of conservation for mass and momentum; it is

correct except when viscosity effects are present (as at the front), for these alter the equation of conservation for the momentum.

A study of the differential equations as corrected for the viscosity and thermal conductivity reveals that the width d of the front is of the order of the mean free path for the initial state. ZEL'DOVICH has shown from the kinetic theory of gases that

$$d \approx l \frac{p}{\Delta p} \approx l \frac{c_1}{u},$$

in which l is the mean free path; TAYLOR has assumed that the ratio of the kinematic viscosity to the thermal diffusivity is one, in which case d for air is

$$d = 4 \times 10^{-5} \frac{1}{\Delta p} \text{ cm},$$

(Δp in atm). These expressions show that d is of the order of l for strong shock waves ($\Delta p \gg p_1$).

Finally, equations based on the assumption of continuity describe the behavior correctly only if the parameters change relatively little within a mean free path. This means that the results they give represent only a first approximation. A more detailed examination involves a study of the behavior of the various internal degrees of freedom of the gas.

The specific heat for very rapid changes (as in shock waves) may be appreciably less than that for slow changes. A gas molecule carries energy of rotation, vibration, and forward motion; all those increase with the temperature, and additional degrees of freedom associated with excited electronic states become significant at high temperatures. The various degrees of freedom do not take up energy equally readily; the forward motion and rotation do so almost instantaneously, but the vibrations respond relatively slowly. For example, the time needed to reach vibrational equilibrium is about 10^{-6} sec for CO_2. One result of

this is that the velocity of sound increases with frequency; this is equivalent to a reduction in the specific heat, which itself implies an increase in k, because $c_1^2 = \frac{kp_1}{\rho_1}$. The slow response of the internal degrees of freedom affects the structure of the front, because the compression is very rapid. Dissociation is also a process that takes an appreciable time. Zel'dovich states that a strong shock wave starts with a discontinuity, which has a width of the order of the mean free path and which shows no appreciable excitation of the internal degrees of freedom. Following this there is a fairly gradual rise over a length of the order of $D\tau$ (in which τ is the excitation time); Fig. 52 shows the structure. A detailed quantitative study confirms this; the front consists of two parts, one having very large gradients over a distance of a few times the mean free path, and the other (a few mm wide) having comparatively small gradients. Töpler photographs confirm these theoretical deductions.

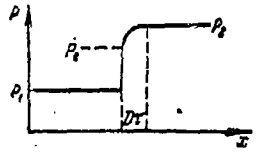


Fig. 52. Structure of a strong shock wave in a gas showing slow response in its degrees of freedom.

32. Oblique Shock Wave

This type may arise when a flow whose speed is constant strikes an inclined plane (Fig. 53). At the junction k of the two planes there

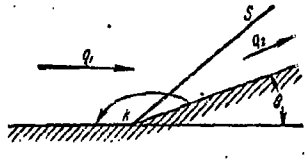


Fig. 53. Formation of an oblique plane shock wave; S is the front.

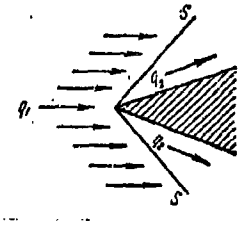


Fig. 54. Supersonic flow around a wedge; two shock waves.

arises an oblique shock wave; the flow is turned abruptly through the angle θ between the planes, whereupon it continues with a fixed speed This occurs if θ is less than some limit. Again, a flow around a wedge (Fig. 54) produces two shock waves; this type may be derived by combining two flows, one for each side of the wedge. Let us consider first a plane oblique shock wave, in which the incident flow makes an angle with the front (Fig. 55). Let q_1 and q_2 be the speeds of the flow on the two sides, and let u_1 and u_2 be the projections of those speeds on an axis parallel to the front. The equations for the laws of conservation then become

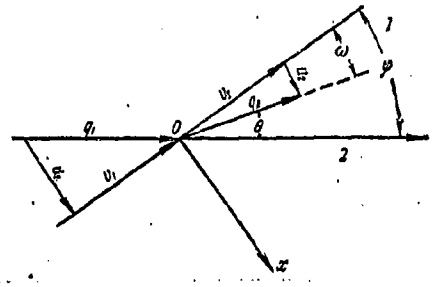


Fig. 55. Rotation of the flow after passage through an oblique shock front. 1) Front; 2) flow direction.

$$\left.\begin{aligned} \rho_1 u_1 &= \rho_2 u_2, \quad i_1 + \frac{u_1^2}{2} = i_2 + \frac{u_2^2}{2}, \\ p_1 + \rho_1 u_1^2 &= p_2 + \rho_2 u_2^2, \quad v_1 = v_2. \end{aligned}\right\} \tag{32,1}$$

Here (30,8) and (30,9) imply that $v_1 = v_2$ and $w_1 = w_2 = 0$ (two-dimensional case). The direction of the flow is altered, because $v_1 \neq v_2$ but $u_2 < u_1$, as (32,1) shows directly:

$$\frac{u_2}{u_1} = \frac{\rho_1}{\rho_2} < 1.$$

Let ω be the angle between the front and the flow direction behind the front (Fig. 55); then

$$\left.\begin{aligned} u_1 &= q_1 \sin\varphi, \quad v_1 = q_1 \cos\varphi, \\ u_2 &= q_2 \sin\omega, \quad v_2 = q_2 \cos\omega, \end{aligned}\right\} \tag{32,2}$$

in which q_1 is the resultant of u_1 and v_1, and q_2 is the same for u_2 and v_2. From (32,2) we have that

$$\frac{u_1}{v_1} = \tan\varphi, \quad \frac{u_2}{v_2} = \tan\omega,$$

but $v_1 = v_2$, so

$$\frac{v_2}{u_1} = \frac{\rho_1}{\rho_2} = \frac{\tan\omega}{\tan\varphi}, \tag{32,3}$$

which means that $\omega < \varphi$. The angle turned through by the flow is $\theta = \varphi - \omega$, so (32,3) may be put as

$$\frac{u_2}{u_1} = \frac{\rho_1}{\rho_2} = \frac{\tan(\varphi - \theta)}{\tan\varphi} \tag{32,4}$$

whereupon (32,1)-(32,3) give us that

$$p_2 - p_1 = \rho_1 u_1^2\left(1 - \frac{\rho_1}{\rho_2}\right) = \rho_1 q_1^2 \sin^2\varphi\left(1 - \frac{\rho_1}{\rho_2}\right). \tag{32,5}$$

The energy equation for a polytropic medium gives us that

$$\frac{\rho_1}{\rho_2} = \frac{(k+1)p_2 + (k-1)p_2}{(k+1)p_2 + (k-1)p_1}. \tag{32,6}$$

Then the $\frac{\rho_1}{\rho_2}$ of (32,5) gives us that

$$p_2 = \frac{2\rho_1 q_1^2}{k+1}\left[\sin^2\varphi - \frac{k-1}{2\rho_1 q_1^2}p_1\right] \quad p_2 - p_1 = \frac{2\rho_1 q_1^2}{k+1}\left[\sin^2\varphi - \frac{c_1^2}{p_1}\right]. \tag{32,7}$$

We may find a relation between φ and θ by combining (32,4), (32,5), and (32,7), which give us that

$$\sin^2\varphi\left(1 - \frac{\tan(\varphi-\theta)}{\tan\varphi}\right) = \frac{2}{k+1}\left[\sin^2\varphi - \frac{c_1^2}{q_1^2}\right]; \tag{32,8}$$

and this may be transformed to

$$\frac{2}{k-1} = \left(\frac{q_1}{c_1}\right)^2 \sin^2\varphi\left[\frac{k+1}{k-1}\frac{\tan(\varphi-\theta)}{\tan\varphi} - 1\right]. \tag{32,9}$$

This gives us $\theta = f(\varphi)$, so ρ_2 and u_2 may be found. That is, we have a complete solution for the parameters of the flow behind the front if p_1 , ρ_1 , u_1 , and φ are given.

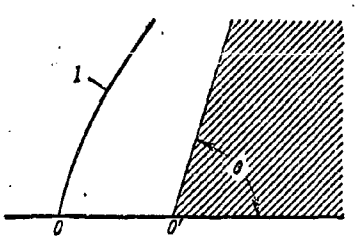


Fig. 56. Shock wave detached from vertex of cone.

1) Front.

A necessary condition for a shock wave to arise as in Fig. 53 is $u_1 > c_1$; that is, the normal component of the speed must be supersonic, not merely the speed itself. Then $q_1 > c_1$ in every case, because $v_1 > 0$. It can be shown that there is a limit θ_0 such that for $\theta > \theta_0$ the shock wave becomes

detached (Fig. 56); the shock wave becomes straight on the axis of symmetry. Further (purely adiabatic) compression occurs in the region OO'; the pressure at O' is given by

$$i_2' = i_2 + \frac{u_2^2}{2}, \quad \frac{i_2'}{i_2} = \frac{c_2'^2}{c_2^2} = \left(\frac{p_2'}{p_2}\right)^{\frac{k-1}{2}}, \tag{32,10}$$

in which i_2' and p_2' are the enthalpy and pressure at O'. Now

$$i_2 = \frac{k}{k-1}\frac{p_2}{\rho_2},$$

so we have that

$$\frac{p_2'}{p_2} = \left(1 + \frac{k-1}{2k}\frac{\rho_2 u_2^2}{p_2}\right)^{\frac{k}{k-1}}. \tag{32,11}$$

The u_2, p_2, and ρ_2 appearing here are given by the formulas for straight fronts $(v_1 = v_2 = 0)$; (32,1) and (32,6) give us that

$$u_2 = \frac{\rho_1}{\rho_2}u_1, \quad \frac{\rho_1}{\rho_2} = \frac{(k-1)p_2 + (k+1)p_1}{(k+1)p_2 + (k-1)p_1}$$

$$\frac{\rho_2 u_2^2}{p_2} = \rho_1 u_1^2 \frac{(k-1)p_2 + (k+1)p_1}{(k+1)p_2 + (k-1)p_1} = \frac{(k-1)\rho_1 u_1^2 + 2kp_1}{2\rho_1 u_1^2 - (k-1)p_1}, \tag{32,12}$$

and so

$$\frac{p_2'}{p_2} = \left[1 + \frac{k-1}{2k}\frac{(k-1)u_1^2 + 2c_1^2}{2u_1^2 - \frac{k-1}{k}c_1^2}\right]^{\frac{k}{k-1}}. \tag{32,13}$$

If $u_1 = c_1$, $p_2 = p_1$, and

$$\frac{p_2'}{p_2} = \left(1 + \frac{k-1}{2}\right)^{\frac{k}{k-1}} = 1 + \frac{k}{2} + \frac{k}{8} + \frac{k(2-k)}{48} + \dots$$

If $u_1 \gg c_1$,

$$\frac{p_2'}{p_2} = \left(1 + \frac{(k-1)^2}{4k}\right)^{\frac{k}{k-1}} = 1 + \frac{k-1}{4} + \frac{(k-1)^2}{32k} + \dots \tag{32,14}$$

At the limit, $\frac{p_2'}{p_2} = \frac{p_2'}{p_1} = e^{\gamma_2}$, when $k = 1$, in the first case; in the second, $\frac{p_2'}{p_2} = 1$. That is, the pressure increases only slightly within the adiabatic zone if the shock wave is sufficiently strong. The angle θ_0 is given by (32,9), which we put in the form

$$\frac{\tan(\varphi - \theta)}{\tan\varphi} = \frac{k-1}{k+1} + \frac{2c_1^2}{(k+1)q_1^2\sin^2\varphi}.$$

Then, because

$$\tan(\varphi - \theta) = \frac{\tan\varphi - \tan\theta}{1 + \tan\varphi\tan\theta}, \tag{32,15}$$

we have that

$$\tan^3\varphi\left(\frac{k-1}{2}\beta+1\right)-\tan^2\varphi\cot\theta(\beta-1)+\tan\varphi\left(\frac{k+1}{2}\beta+1\right)+\cot\theta=0,$$

$$\beta=\frac{q_1^2}{c_1^2}=M_1^2 \qquad (M_1 = \text{Mach No.}). \tag{32,16}$$

For simplicity, we put $\cot\theta=\alpha$ and $\tan\varphi=y$, with $k=7/5$, which gives us that

$$y^3(\beta+5)-5\alpha y^2(\beta-1)+(6\beta+5)y+5\alpha=0. \tag{32,17}$$

This shows that $y^2=1/(\beta-1)$ for any k when $\theta=0$, so

$$\sin\varphi=\frac{c_1}{q_1},$$

which is so for sound waves. This y is always positive, because the physically significant range in φ is

$$0\leqslant\varphi\leqslant\frac{\pi}{2}.$$

Equation (32,16) becomes, when $\beta\gg1$,

$$y^2-\frac{2}{k-1}\alpha y+\frac{k+1}{k-1}=0, \tag{32,18}$$

and so

$$y=\frac{\alpha}{k-1}\pm\sqrt{\frac{\alpha^2}{(k-1)^2}-\frac{k+1}{k-1}}. \tag{32,19}$$

The solution is physically meaningful if $\alpha\geqslant k^2-1$, so

$$y\leqslant\sqrt{\frac{k+1}{k-1}}. \tag{32,20}$$

The relation of β to y for a given angle $\theta=\theta_1$ is

$$\beta-1=\frac{\frac{k+1}{2}y^3+\frac{k+3}{2}y+\alpha_1}{\alpha_1y^2-\left(\frac{k-1}{2}y^3+\frac{k+1}{2}y\right)}, \tag{32,21}$$

in which $\alpha_1=\cot\theta_1$. Figure 57 shows $\beta=f(y)$ for $\alpha>\alpha_0$, in which

$$\alpha_0=\sqrt{k^2-1},$$

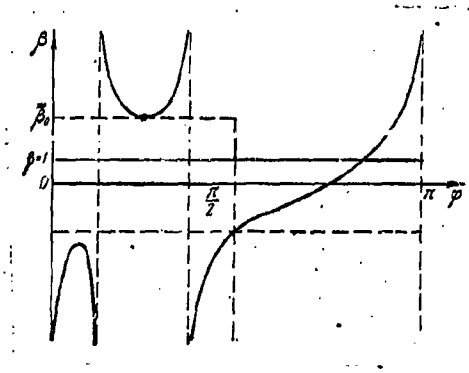


Fig. 57. The relation $\beta=f(y)$.

This shows that there are two values of y for every $\beta>\beta_0$: the actual process usually corresponds to the smaller value of y (the weaker shock wave); the third value of y for $\beta>\beta_0$ is negative and has no physical significance.

The limit $\beta_0 = \left(\frac{q_1}{c_1}\right)^2_0$ defines the smallest $\frac{q_1}{c_1}$ that can occur for a given θ_1. The two positive roots of (32,16) coincide when $\beta = \beta_0$. The flow conditions alter when $\theta > \theta_0$ and $\omega > \varphi_0$; the shock wave becomes detached. We can find $\theta_0 = f(\varphi_0)$ from (32,21) and, by equating the derivative to zero, we can find the condition for minimal β:

$$a_0^2 - a_0\left[\frac{k+1}{4}\frac{1+y_0^4}{y_0^4} - \frac{3-k}{2}y_0\right] + y_0^2 = 0. \qquad (32,22)$$

The results for oblique shock waves are best presented by means of graphs based on shock polars, which relate the parameters of the medium behind the front to q_1 and c_1. Here we need the components of q_1 and c_1 along the x and y axes, the x axis being the direction of the incident flow. Figure 55 shows that

$$\left.\begin{aligned} u_{1x} &= q_1, \quad u_{1y} = 0, \quad u_{2x} = u_2 \sin\varphi + v_2 \cos\varphi, \\ u_{2y} &= v_2 \sin\varphi - u_2 \cos\varphi. \end{aligned}\right\} \qquad (32,23)$$

We eliminate φ, v_2, and v_1 from these equations to get the equation for the shock polar as

$$u_{2y}^2 = (q_1 - u_{2x})^2 \frac{\frac{2}{k+1}\left(q_1 - \frac{c_1^2}{q_1}\right) - (q_1 - u_{2x})}{(q_1 - u_{2x}) + \frac{2}{k+1}\frac{c_1^2}{q}}. \qquad (32,24)$$

This is shown in graph form in Fig. 58. This polar enables us to construct the oblique front (the line OB) as follows. The direction of q_2 is given by $\tan\theta = \frac{u_{2y}}{u_{2x}}$ (Fig. 58 corresponds to $q_1 > c_k$); from O we draw a straight line at an angle θ to the horizontal axis to meet the curve at A and B. This result means that two modes of flow are, in principle, possible for the given θ, c_1, and q_1, as we have seen previously. The usual mode is that corresponding to B; vector OB defines q_2. The line of the front, which lies

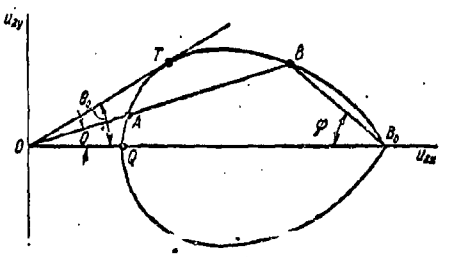


Fig. 58. The shock polar in the u_{2x}, u_{2y} plane.

at an angle φ to q_1 (i.e., to OB_0), is normal to the line joining B_0 to B, because the vector (q_2-q_1) is normal to the front. It is also clear that $\theta<\varphi$ (this has also been demonstrated above). Now A cannot exceed the limit θ_0 for a given c_1 and q_1; this limit corresponds to the tangent OT. Now θ_0 increases with $\frac{q_1}{c_1}$ and tends to the limit

$$\sin\theta_0=\frac{1}{k}, \tag{32,25}$$

when $\frac{q_1}{c_1}\to\infty$. A normal front (straight shock wave) corresponds to the point where the polar cuts the u_{2x} axis; then $u_{1x}=u_{2x}=c_k^2$.

This polar gives us directly only relations between the velocities; the pressure behind the front is given by (32,7) and (32,8), and the density by (32,6).

33. Acoustic Theory of Shock Waves

If $\frac{\Delta p}{p}\ll 1$ (weak shock wave), there is very little change in entropy, so we may consider the wave as being almost a simple compression wave having a discontinuity at its front (the entropy is then constant). Let the wave transfer the gas from the state (p_1, v_1, u_1) to the state (p_2, v_2, u_2); it is readily shown that the quantities for the final state after a weak shock wave differ from those for a simple wave only as regards terms of order higher than the second. To this end we put the equations for shock waves in the form

$$\left.\begin{aligned} u_2-u_1&=\sqrt{(p_2-p_1)(v_1-v_2)},\\ p_2-p_1&=\rho_1(u_2-u_1)(D-u_1),\\ \frac{p_2v_2-p_1v_1}{k-1}&=\frac{p_1+p_2}{2}(v_2-v_1);\end{aligned}\right\} \tag{33,1}$$

and so, for $\frac{(u_2-u_1)}{u_1}\ll 1$, we have

$$\left.\begin{aligned} c_2-c_1&=\frac{k-1}{2}(u_2-u_1),\\ u_2+c_2&=u_1+c_1+\frac{k+1}{2}(u_2-u_1)+\dots,\\ p_2-p_1&=\rho_1c_1(u_2-u_1)+\frac{k+1}{4}\rho_1(u_2-u_1)^2+\dots\end{aligned}\right\} \tag{33,2}$$

Further, we expand $D'=D-u_1$ in powers of (u_2-u_1) to get

$$D'=u_1+c_1+\frac{k+1}{4}(u_2-u_1)+\frac{(k+1)^2}{32}\frac{(u_2-u_1)^2}{c_1}+\dots \tag{33,3}$$

Substitution for (u_2-u_1) from the previous expansion gives us that

$$D' = u_1 + c_1 + \frac{1}{2}(u_2 + c_2 - u_1 - c_1) + \frac{1}{8}\frac{(u_2 + c_2 - u_1 - c_1)^2}{c_1} + \dots \qquad (33,4)$$

That is, the speed of the shock wave is, to a first approximation, simply the mean of the speeds for small perturbations on the two sides:

$$D = \frac{1}{2}(u_1 + c_1 + u_2 + c_2). \qquad (33,5)$$

If the initial state (u_1, c_1) for a simple wave is a steady flow, we have that

$$u_2 - u_1 = \frac{2}{k-1}(c_2 - c_1). \qquad (33,6)$$

Then (33,2), with $\frac{p_2}{p_1} = \left(\frac{\rho_2}{\rho_1}\right)^{\frac{1}{k}}$, $\frac{c_2}{c_1} = \left(\frac{\rho_2}{\rho_1}\right)^{\frac{k-1}{2}}$, gives us that

$$\left.\begin{aligned} p_2 &= p_1\left[1 + \frac{k-1}{2}\frac{u_2-u_1}{c_1}\right]^{\frac{2k}{k-1}}, \\ c_2 &= c_1 + \frac{k-1}{2}(u_2 - u_1), \\ u_2 + c_2 &= u_1 + c_1 + \frac{k+1}{2}(u_2 - u_1). \end{aligned}\right\} \qquad (33,7)$$

We expand (p_2-p_1) in terms of (u_2-u_1) to get that

$$p_2 = p_1 + \rho_1 c_1 (u_2 - u_1) + \frac{k+1}{4}\rho_1 (u_2 - u_1)^2 + \dots \qquad (33,8)$$

and so, if $\frac{\Delta p}{p_1} \ll 1$, the parameters of the two waves are the same up to quantities of the second order. This means that our future calculations for weak shock waves may be based on the approximate formulas

$$\left.\begin{aligned} D' &= \frac{u_1 + c_1 + u_2 + c_2}{2}, \\ \Delta p &= \rho_1 c_1 (u_2 - u_1), \\ \Delta \rho &= \frac{\rho_1 (u_2 - u_1)}{c_1}. \end{aligned}\right\} \qquad (33,9)$$

The error resulting from the use of these formulas is very small even when $\frac{\Delta p}{p_1}$ is somewhat greater than one; for example, if $k = 1,4$ and $\frac{\Delta p}{p_1} = 1.5$, the exact formulas give us that

$$\frac{u_2 - u_1}{c_1} = 0.71, \quad \frac{c_2 - c_1}{c_1} = 0.15$$
$$\frac{D'}{c_1} = 1.51$$

while the approximate ones give us that

$$\frac{u_2 - u_1}{c_1} = 0.70; \quad \frac{c_2 - c_1}{c_1} = 0.14;$$
$$\frac{D'}{c_1} = 1.52,$$

This enables us to use the acoustic approximation for waves of $\frac{\Delta p}{p_1}$ somewhat greater than one in certain theoretical treatments (in particular, for the reflection of a detonation wave from a wall; see section 58).

34. Energy Dissipation in Shock Waves

The motion is isentropic if the state of the medium changes slowly during an adiabatic process. The thermodynamic criterion here is that the rate of approach to equilibrium should be substantially in excess of the rate of any external perturbation. The rate of approach to equilibrium is correlated with the speed of elastic vibrations in the medium; compression by a piston or a blow on a surface is isentropic if the speed of the piston or striker is less than the speed of sound, for example.

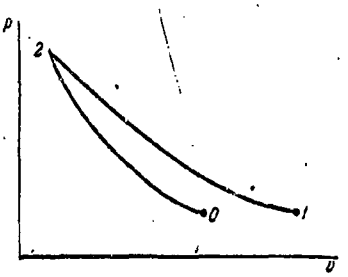


Fig. 59. Shock adiabatic and isentropic line.

The entropy is increased by the passage of a shock wave; physically, this means that the organized energy of the flow is in part converted to unorganized thermal energy. The kinetic energy decreases, and the internal energy increases, as we see from

$$i_2 - i_0 = \frac{p_2 - p_0}{2}(v_0 + v_2) \tag{34,1}$$

$$E_2 - E_0 = \frac{1}{2}(p_2 + p_0)(v_0 - v_2), \tag{34,2}$$

in which subscripts 0 and 2 denote the states before and at the front. The irreversible loss of energy is defined by

$$E_2 - E_2^* = \frac{1}{2}(p_2 + p_0)(v_0 - v_2) - \int_{v_2}^{v_0} v\,dp. \tag{34,3}$$

whereas the energy in state 2 after an isentropic compression is

$$E_2^* = E_0 + \int_{v_0}^{v_2} p\,dv. \tag{34,4}$$

The expansion from state 2 to state *1* is isentropic (Fig. 59), so

$$E_2 - E_1 = \int_{v_2}^{v_1} v\,dp. \tag{34,5}$$

Then (34,3)-(34,5) give us the irreversible loss as

$$\Delta E = E_1 - E_0 = \frac{p_2 + p_0}{2}(v_0 - v_2) - \int_{v_2}^{v_1} v\,dp. \tag{34,6}$$

This energy goes to produce the increased temperature found when the expansion is complete, so (34,6) gives us that temperature. For example, for an ideal gas we have that

$$\frac{p_2}{p_1} = \left(\frac{v_1}{v_2}\right)^k,$$

and so

$$\int_{v_2}^{v_1} p\,dv = \frac{p_2 v_2 - p_1 v_1}{k-1},$$

which implies that for $p_1 = p_0$ (which means that $v_1 > v_0$) we have that

$$\Delta E = c_v \Delta T = \frac{p_2 + p_0}{2}(v_0 - v_2) - \frac{p_2 v_2 - p_0 v_1}{k-1}. \tag{34,7}$$

in which v_1 is given by

$$\frac{p_2}{p_0} = \left(\frac{v_1}{v_2}\right)^k.$$

The temperature after the passage of the shock wave is then given by (34,7).

35. Shock Waves in Air: Allowance for Dissociation and Ionization

A strong shock wave produces a pronounced temperature rise; the number of particles tends to increase, on account of dissociation and ionization. The change in the number of particles alters the forms taken by the equation of state and by the shock adiabatic; the effects are reflected to varying extents in all parameters. These factors are exceptionally important in a nuclear explosion; the shock wave produces partial dissociation and ionization out to great distances from the center. Radiation plays an important part in energy transfer also, at least for rather shorter distances. The law of mass action applies to ionization and dissociation; the equilibrium constants for these

processes enable us to determine the composition and hence the number of particles. Developments in spectroscopy and theoretical physics have provided us with means of computing thermodynamic functions with an accuracy far exceeding that of methods normally used in chemical thermodynamics. These calculations can be extended to the very highest temperatures for a variety of reactions; they are based on quantum statistics, and can be applied with advantage to shock waves.

Statistical method for thermodynamic functions. The total energy of a gas molecule is made up of the energy of forward motion E_f, the energy of rotation E_r, the energy of vibration E_v, and the energy of electronic excitation E_e. Consider one mole of the substance, which contains N particles, of which $N_0, N_1, N_2, \ldots$ are respectively in the energy states $E_0, E_1, E_2, \ldots$; then the Boltzmann distribution implies that

$$N_i = \frac{N}{z} g_i e^{-\frac{\varepsilon_i}{kT}}, \qquad (35,1)$$

in which g_i is the statistical weight of the i-th state (the number of differing quantum states having the energy ε_i) and z is the sum over states:

$$z = \sum g_i e^{-\frac{\varepsilon_i}{kT}}. \qquad (35,2)$$

The summation is performed for all possible states from $i=0$ (the lowest level) to $i=\infty$; this z is an important parameter that appears in all later calculations.

This sum is calculated on the assumptions a) that the molecule behaves as a rigid rotor (that interaction between rotation and vibration is negligible); b) that quantization of the rotational energy can be neglected, because many vibrational states are already excited at room temperature; and c) that the vibrations are harmonic. Then the energy may be represented as the sum of the energies corresponding to the various degrees of freedom, while the statistical sum becomes the

product of the corresponding factors:

$$E_f + E_r + E_v + E_e, \tag{35,3}$$

$$z_f \cdot z_r \cdot z_v \cdot z_e. \tag{35,4}$$

The degrees of freedom for the forward motion are three, so

$$E_f = \frac{3}{2}kT, \tag{35,5}$$

while for diatomic and linear polyatomic molecules

$$E_r = kT \tag{35,6}$$

($E_r = \frac{3}{2}kT$ for nonlinear molecules).

The statistical sum for an atom consists of two factors (one for the forward motion, one for the electronic energy). Statistical mechanics gives us for the forward motion that

$$z_f = \int_{p=0}^{\infty} e^{-\frac{p^2}{2mkT}} 4\pi p^2 dp \frac{V}{h^3} = \frac{(2\pi mkT)^{\frac{3}{2}}}{h^3} V, \tag{35,7}$$

in which m is the mass of the particle, whose momentum is p, h is Planck's constant, and V is the volume of the system. The sum for the electronic states is

$$z_e = \sum_0^n g_e e^{-\frac{h\nu_n}{kT}} = \sum_0^n g_e e^{-\frac{\varepsilon_{n-1}}{kT}}, \tag{35,8}$$

in which ν_n is frequency;

$$\sum_0^n g_e e^{-\frac{\varepsilon_e}{kT}} = g_0 e^{-\frac{\varepsilon_0}{kT}} + g_1 e^{-\frac{\varepsilon_1}{kT}} + g_2 e^{-\frac{\varepsilon_2}{kT}} + \ldots. \tag{35,9}$$

The absolute E_e are unknown; all that can be measured are the differences $\Delta E_e = E_e - E_0$, which are found direct from spectroscopic measurements. For the purpose of calculating z_e we take E_0 as 0, which is equivalent to reckoning the energy from that level; then z_e is replaced by

$$z'_e = \sum_0^n g_e e^{-\frac{\Delta\varepsilon_e}{kT}} = g_0 + g_1 e^{-\frac{\Delta\varepsilon_1}{kT}} + g_2 e^{-\frac{\Delta\varepsilon_2}{kT}} + \ldots \tag{35,10}$$

Comparison of (35,9) with (35,10) shows that

$$z_e = z'_e e^{-\frac{\varepsilon_0}{kT}}. \tag{35,11}$$

It is usual to find that even $\Delta\varepsilon_1$ is very large, in which case

$\exp\left(-\frac{\Delta\varepsilon_1}{kT}\right)$ becomes appreciable only at very high temperatures; then the second and subsequent terms in (35,10) can be neglected, so

$$z'_e = g_0 = 2J+1, \tag{35,12}$$

in which J is the internal quantum number of the ground state.

We consider a system consisting of particles of one kind only, so the choice of zero state is unimportant; ε_0 does not appear in the calculations. Several types of particles may be present in a chemical reaction, and each has its own ε_0, in which case the energies must be referred to a zero common to all particles. Here z_e must appear in the statistical sum, not z'_e. Then the total sum over states for an atom is

$$z_A = z_f \; z'_e e^{-\frac{\varepsilon_0}{kT}} = z'_1 e^{-\frac{\varepsilon_0}{kT}}. \tag{35,13}$$

We do not know ε_0 for the various molecules, but $\Delta\varepsilon_0$ is readily found for reacting molecules; the sum of these differences is the heat yield of the reaction at absolute zero per particle. For one mole,

$$\Delta\varepsilon_0 N = \Delta E_0 = -Q_0 \tag{35,14}$$

so (35,13) becomes

$$z = z'_1 e^{-\frac{\Delta E_0}{kT}} = z'_1 e^{\frac{Q_0}{RT}}. \tag{35,15}$$

Statistical sum for a diatomic molecule. Here (35,7) gives z_f, m being the mass of the molecule; the internal degrees of freedom introduce their own factors, that for the rotation being

$$z_r = \frac{8\pi^2 kTI}{h^2 S}, \tag{35,16}$$

(in which I is the moment of inertia about an axis normal to the line joining the nuclei and S is the symmetry number) on the assumption that many rotational states are excited at room temperature. The number of degrees of rotational freedom is two for a diatomic or linear polyatomic molecule; the total number of degrees of freedom for a molecule consisting of n atoms is $3n$, so a linear molecule has $3n-5$ vibrational

degrees of freedom, while a nonlinear one has $3n-6$. The z_v of (35,2) requires the quantum-mechanical expression for the energy of a harmonic oscillator

$$\varepsilon_v = \left(n+\tfrac{1}{2}\right)h\omega, \tag{35,17}$$

in which n is the vibrational quantum number (0 to ∞), ω is the proper frequency of the oscillations, and $h\omega/2$ is the zero-point energy. This last is commonly included in the total zero-point energy ε_0, which is, in effect, a change in the level from which the energy is reckoned. Then

$$\varepsilon_v = nh\omega. \tag{35,17a}$$

The g_v for a solid is one for solids, diatomic molecules, and most polyatomic molecules, so (35,17a) gives us that

$$z_v = \sum_{n=0}^{\infty} e^{-\frac{nh\omega}{kT}} \approx \frac{1}{1-e^{-\frac{h\omega}{kT}}}. \tag{35,18}$$

The z_e is as for an atom, so the over-all statistical sum is

$$z = z_f\ z_r\ z_v\ z_e\ e^{\left(-\frac{\varepsilon_0}{kT}\right)}. \tag{35,19}$$

Thermodynamic functions. One gram-molecule of gas contains N particles; then the number in any given energy state is

$$N_i = \frac{N}{z} g_i e^{-\frac{\varepsilon_i}{kT}}. \tag{35,20}$$

The internal energy at temperature T is

$$E_T = \varepsilon_0 \frac{N}{z} g_0 e^{-\frac{\varepsilon_0}{kT}} + \varepsilon_1 \frac{N}{z} g_1 e^{-\frac{\varepsilon_1}{kT}} + \varepsilon_2 \frac{N}{z} e^{-\frac{\varepsilon_2}{kT}} + \ \ldots = \frac{N}{z} \sum \varepsilon_i g_i e^{-\frac{\varepsilon_i}{kT}}. \tag{35,21}$$

and

$$z = g_0 + g_1 e^{-\frac{\varepsilon_1}{kT}} + g_2 e^{-\frac{\varepsilon_2}{kT}} + \ \ldots = \sum g_i e^{-\frac{\varepsilon_i}{kT}}. \tag{35,22}$$

But

$$\frac{d\left(ge^{-\frac{\varepsilon}{kT}}\right)}{dT} = \frac{\varepsilon}{kT^2} ge^{-\frac{\varepsilon}{kT}},$$

$$\frac{\varepsilon_1}{kT^2} g_1 e^{-\frac{\varepsilon_1}{kT}} + \frac{\varepsilon_2}{kT^2} g_2 e^{-\frac{\varepsilon_2}{kT}} + \ \ldots = \frac{1}{kT^2} \sum \varepsilon_i g_i e^{-\frac{\varepsilon_i}{kT}} = \frac{dz}{dT}. \tag{35,23}$$

From (35,21) and (35,23) we have that

$$E_T = \frac{dz}{z\,dT} NkT^2 = RT^2 \frac{d\ln z}{dT}, \tag{35,24}$$

in which z is the over-all statistical sum. That is, once z is known

we can use (35,24) to find the total internal energy as a function of temperature, and hence the thermal capacity. Thermodynamics gives us that

$$T\left(\frac{\partial F}{\partial T}\right)_v = F - E \tag{35,25}$$

$$\frac{E}{T^2} = -\left(\frac{\partial \frac{F}{T}}{\partial T}\right)_v, \tag{35,26}$$

in which F is the free energy; (35,24) and (35,26) give us that

$$-\left(\frac{\partial \frac{F}{T}}{\partial T}\right)_v = \frac{R\, d\ln z}{dT}, \tag{35,27}$$

and so

$$F = -RT\ln z. \tag{35,28}$$

This gives us a thermodynamic interpretation of the statistical sum.

Equilibrium constant. The composition must be known before the energy, density, and so on can be calculated. The composition is governed by the equilibrium constants for dissociation and ionization; the values of these constants for very high temperatures may be expressed in terms of statistical sums to a very high order of accuracy. Thermodynamics gives as the free energy as

$$F = F^0 - RT\ln v. \tag{35,29}$$

so (35,28) gives us that

$$F^0 = -RT\ln\frac{z}{v}. \tag{35,30}$$

All energies must be reckoned from absolute zero when z is calculated (they must include the chemical energy the substance possesses when it is cooled to absolute zero). This means that z and F do not have fixed values; we can assign numerical values to them by specifying an individual zero of energy, which may be taken as the energy of the substance at absolute zero. Then (35,30) gives us that

$$F^0 = -RT\ln\frac{z'}{v} + E_0$$

or

$$F^0 - E_0 = -RT\ln\frac{z'}{v}. \tag{35,31}$$

The equilibrium constants are now readily found in terms of statistical

sums, for

$$\Delta F_v = -RT \ln K_c,$$

in which K_c is the equilibrium constant in terms of the concentrations of the reactants. This may be put in the form

$$\ln K_c = -\frac{\Delta(F^0 - E_0^0)}{RT} - \frac{\Delta E_0^0}{RT}. \tag{35,32}$$

The $(F^0 - E_0)$ of (35,31) gives us that

$$\ln K_c = \Delta \ln \frac{z'}{v} + \frac{Q_v}{RT}, \tag{35,33}$$

in which $\Delta E_0^0 = Q_0 v$ is the heat of reaction at absolute zero. Transferring from concentrations to partial pressures, we have

$$p_i = \frac{n_i}{v} RT,$$

in which n_i is the number of moles of a given species in the equilibrium mixture; then

$$\ln K_p = \Delta \ln \left(\frac{RT}{v} z'\right) + \frac{Q_p}{RT}. \tag{35,34}$$

That is, K can be expressed in terms of $\frac{z'}{v}$ and $\frac{RT}{v} z'$ for any species in the reaction, the rule being the same as for the expression in terms of the concentrations or partial pressures in the law of mass action. In the general case of a reaction

$$\nu_1 L_1 + \nu_2 L_2 + \ldots \rightleftarrows \nu_1' M_1 + \nu_2' M_2 + \ldots + Q,$$

$$\ln K_c = \ln \frac{n_{M_1}^{\nu_1'} n_{M_2}^{\nu_2'} \ldots v^{-\Delta\nu}}{n_{L_1}^{\nu_1} n_{L_2}^{\nu_2}} = \ln \frac{z_{M_1}'^{\nu_1'} z_{M_2}'^{\nu_2'} \ldots v^{-\Delta\nu}}{z_{L_1}'^{\nu_1} z_{L_2}'^{\nu_2}} + \frac{Q_v}{RT}$$

or

$$K_c = K_z v^{-\Delta\nu} e^{\frac{Q_v}{RT}}. \tag{35,35}$$

which gives us that

$$\frac{n_{M_1}^{\nu_1'} n_{M_2}^{\nu_2'} \ldots}{n_{L_1}^{\nu_1} n_{L_2}^{\nu_2} \ldots} = K_z e^{\frac{Q_v}{RT}}, \tag{35,36}$$

$$K_z = \frac{z_{M_1}'^{\nu_1'} z_{M_2}'^{\nu_2'} \ldots}{z_{L_1}'^{\nu_1} z_{L_2}'^{\nu_2} \ldots}. \tag{35,37}$$

Energy. There is no special difficulty in calculating the total energy once we have established the statistical sums and the numbers of

the various species. Consider 1 mole of gas, which consists of $N_0 = 6.02\times10^{23}$ particles at normal temperature. Let N be the number of particles for the equilibrium state at temperature T, where in general

$$N = N_m + N_a + N_{a^+} + N_e, \tag{35,38}$$

in which N_m is the number of undissociated molecules, N_a is the number of atoms produced by dissociation, N_{a^+} is the number of positive ions (from atoms), and N_e is the number of free electrons. We neglect molecular ions, because the ionization energy of a molecule is much higher than the dissociation energy; almost all the molecules are dissociated at temperatures at which ionization becomes appreciable.

Equation (35,3) gives us the total energy as the sum $E_T = \frac{3}{2}RT\frac{N}{N_0}(=E_f)$

$$+RT\frac{N_m}{N_0}(=E_r)+RT^2\left(\frac{N_m}{N_0}\frac{d\ln z}{dT}\right)(=E_v)+RT^2\left(\frac{N_a}{N_0}\frac{d\ln z_{a\,e}}{dT}+\frac{N_{a^+}}{N_0}\frac{d\ln z_{a^+\,e}}{dT}\right)(=E_e) \tag{35,39}$$

$$+\frac{N_a}{2N_0}Q_d+\frac{N_{a^+}}{N_0}Q_i\ (=E_d+E_i)$$

The dissociation energy E_d is calculated on the assumption that the molecules are diatomic and of one kind; the composition becomes more troublesome to calculate if the gas consists of more than one compound (as for air). Again, the above formulas become much simpler if the gas consists of atoms and ions only.

These results are applied to shock waves by means of the equation

$$E_1 - E_0 = \tfrac{1}{2}(p_1+p_0)(v_0-v_1) = \tfrac{1}{2}p_0v_0\left(1+\frac{p_1}{p_0}\right)\left(1-\frac{v_1}{v_0}\right).$$

The equation of state for the unperturbed gas, per mole, is

$$p_0v_0 = RT_0. \tag{35,40}$$

while that for the gas behind the front is

$$p_1v_1 = NkT_1, \tag{35,41}$$

in which k is Boltzmann's constant. The $\frac{v_1}{v_0}$ of (35,40) and (35,41) gives us that

$$E_1 - E_0 = \tfrac{1}{2}p_0v_0\left(1+\frac{p_1}{p_0}\right)\left(1-\frac{NT_1}{T_0}\frac{p_0}{p_1}\right). \tag{35,42}$$

Here $E_0 = \frac{5}{2}RT_0$ if the unperturbed gas consists of diatomic molecules at normal temperatures; in general, the gas may consist of any particles and may be heated to a high temperature, in which case the initial

energy is

$$E_0 = \psi R T_0,$$
$$\psi = \psi(T). \qquad (34,43)$$

This E_0, with (35,42), gives us that

$$E_1 = \frac{1}{2} R T_0 \left[\left(1 + \frac{p_1}{p_0}\right)\left(1 - \frac{N T_1}{T_0}\frac{p_0}{p_1}\right) + \psi \right] = E_T'. \qquad (35,44)$$

This equation may be used to compile curves of E_1 as a function of T_1 for various $\frac{p_1}{p_0}$; the point where the curve of (35,44) for a given $\frac{p_1}{p_0}$ meets the curve of (35,39) defines uniquely the temperature T_1' behind the front. This T_1' is inserted into (35,41) to get ρ_1', which enables us to find u, D, and c for the wave.

Some results on the composition of air at high temperatures are given below; Table 50 gives results for shock waves in air, with allowance for ionization and dissociation.

Composition of air at high temperatures. The mixture consists of molecules, atoms, and ions of oxygen and nitrogen, and also free electrons; compounds such as NO, N_2O, and NO_2 may be present. I shall consider only NO, because this has the largest energy of dissociation. One mole of air at room temperature consists of N_0 ($= 6.02 \times 10^{23}$) molecules; let there be N_1 molecules of oxygen and N_2 of nitrogen, with

$$\frac{N_1}{N_2} = \alpha = \frac{21.2}{78.8} = 0.269.$$

Let A be number of neutral atoms divided by N_0, A^+ being the same for positive ions, for electrons, and M for other species. Subscript 1 applies to oxygen, subscript 2 to nitrogen, and subscript 1 2 to nitric oxide. The equations for the equilibria are

1. Dissociation

$$\frac{A_1^2}{M_1} = c_1, \quad \frac{A_2^2}{M_2} = c_2, \quad \frac{A_1 A_2}{M_{12}} = c_3. \qquad (35,45a)$$

2. Ionization

$$\frac{A_1^+ \theta}{A_1} = c_4, \quad \frac{A_2^+ \theta}{A_2} = c_5. \qquad (35,45b)$$

The initial number of molecules is known, so

$$\left.\begin{aligned} \frac{N_1}{N_0} &= M_1 + \tfrac{1}{2}(A_1 + A_1^+ + M_{12}), \\ \frac{N_2}{N_0} &= M_2 + \tfrac{1}{2}(A_2 + A_1^+ + M_{12}), \qquad 0 = A_1^+ + A_2^+. \end{aligned}\right\} \tag{35,45c}$$

These eight equations define the eight unknowns. The equilibrium constants $c_i = \left(\frac{K_i}{N_0}\right) \exp\left(-\frac{\lambda}{kT}\right)$ are readily found; we put z_{if} as

$$z_{if} = \frac{(2\pi k m_i T_1)^{\frac{3}{2}} v}{h^3 N_0} = \frac{(2\pi k m_i)^{\frac{3}{2}} v_0 N_0 T_1^{\frac{5}{2}}}{T_0 h^3 N_0} \left(\frac{p_0}{p_1}\right). \tag{35,46}$$

whereupon the c_i become

$$\left.\begin{aligned} \log c_1 &= -\lambda_{a_1}\frac{5040}{T_1} + \frac{5}{2}\log T_1 - \log T_0 - \log z_{\text{in},M_1} + \\ &\qquad + 2\log z_{\text{in},A_1} + c_1 - \log\left(\frac{p_1}{p_0}\right), \\ \log c_2 &= -\lambda_{a_2}\frac{5040}{T_1} + \frac{5}{2}\log T_1 - \log T_0 - \log z_{\text{in},M_2} + \\ &\qquad + 2\log z_{\text{in},A_2} + c_2 - \log\left(\frac{p_1}{p_0}\right), \\ \log c_3 &= -\lambda_{a_{12}}\frac{5040}{T_1} + \frac{5}{2}\log T_1 - \log T_0 - \log z_{\text{in},M_{12}} + \\ &\qquad + \log z_{\text{in},A_1} + \log z_{\text{in},A_2} + c_3 - \log\left(\frac{p_1}{p_0}\right), \\ \log c_4 &= -\lambda_{r_1}\frac{5040}{T_1} + \frac{5}{2}\log T_1 - \log T_0 - \log z_{\text{in},A_1} + \\ &\qquad + \log z_{\text{in},A_1^+} + c_4 - \log\left(\frac{p_1}{p_0}\right), \\ \log c_5 &= -\lambda_{r_2}\frac{5040}{T_1} + \frac{5}{2}\log T_1 - \log T_0 - \log z_{\text{in},A_2} + \\ &\qquad + \log z_{\text{in},A_2} + c_5 - \log\left(\frac{p_1}{p_0}\right). \end{aligned}\right\} \tag{35,47}$$

Here

$$\left.\begin{aligned} c_1 &= \log\frac{(\pi m_1 k)^{\frac{3}{2}} v_0 N}{h^3 N_0} = 2.20 \qquad c_2 = \log\frac{(\pi m_2 k)^{\frac{3}{2}} v_0 N}{h^3 N_0} = 2.18 \\ c_3 &= \log\frac{\left(2\pi\frac{m_1 m_2}{m_1+m_2}\right)^{\frac{3}{2}} v_0 N}{h^3 N_0} = 2.15 \quad c_4 = c_5 = \log\frac{2(2\pi\mu k)^{\frac{3}{2}} v_0 N}{h^3 N_0} = 3.75 \end{aligned}\right\} \tag{35,48}$$

It is assumed for c_4 and c_5 that the mass of the ion is the same as that of the parent atom, m_j; μ is the mass of an electron, v_0 is the volume of 1 gram-mole at NTP (22.410 liters), λ_{a_i} is dissociation potential, λ_{r_i} is ionization potential, and z_{in} is the z for the internal degrees of freedom; $z_{in} = z_{el}$ for atoms or $z_r z_v z_e$ for molecules.

It is convenient to take θ as the independent variable in order to solve (35,45); then the last equation in (35,45c) and the two first in

(35,45a) give us that

$$A_2 = \frac{\theta^2}{c_5} - A_1 \frac{c_4}{c_5}.$$

We eliminate the number of molecules from the two penultimate equations to get that

$$\frac{A_1^2}{c_1} + \frac{A_1}{2} + \frac{A_1}{2\theta} c_4 + \frac{A_1 A_2}{2c_3} = \alpha \left[\frac{A_2^2}{c_2} + \frac{A_2}{0} c_5 + \frac{A_1 A_2}{2c_3} \right].$$

Substitution for A_2 gives us A_1, which is

$$A_1 = \frac{b}{2a}\left(\sqrt{1 + \frac{4ac}{b^2}} - 1\right),$$

$$a = \frac{1}{c_1} - \frac{c_4}{c_5}\left[\frac{1}{2c_3}(1-\alpha) + \frac{c_4}{c_5}\frac{a}{c_2}\right],$$

$$b = \frac{1}{2} + \frac{c_4}{2\theta}(1+\alpha) + \frac{\theta^2}{2c_2c_5}(1-\alpha) + \frac{a}{2}\frac{c_4}{c_5}\left(1 + \frac{4\theta^2}{c_2c_5}\right),$$

$$c = \frac{a}{2}\theta + \frac{a}{2}\frac{\theta^2}{c_5}\left(1 + \frac{2\theta^2}{c_2c_5}\right).$$

It is generally permissible to neglect the effect of the NO on A_1; then

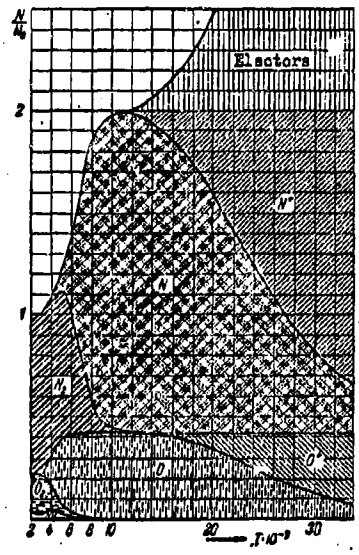


Fig. 60. Composition of air for $\frac{\rho}{\rho_0} = 1$; $\frac{N}{N_0}$ is the ratio of the number of particles to the number at 0°C.

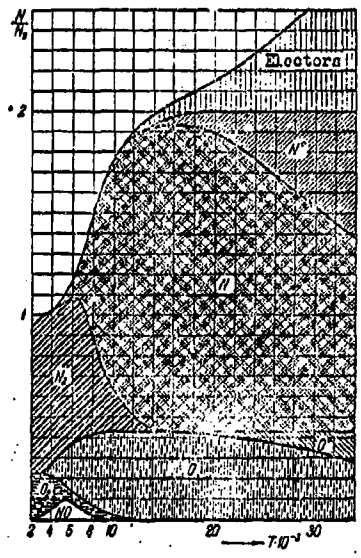


Fig. 61. Composition of air for $\frac{\rho}{\rho_0} = 20$.

all factors containing c_3 may be omitted. The A_1 for high temperatures (complete dissociation) is

$$A_1 = \frac{c'}{b'},$$

$$b' = \frac{1}{2} + \frac{c_4}{2c_5}(1+a) + \frac{a}{2}\frac{c_4}{c_5},$$

$$c' = \frac{a}{2}\theta + \frac{a}{2}\frac{\theta_2}{c_5}.$$

This gives A_1 as a function of θ, whereupon all other quantities, and hence N also, can be calculated as functions of θ, with T as parameter. We calculate θ as a function of temperature for a given N_1 to get the numbers of all other species.

Figures 60 and 61 gives results from these rather tedious calculations for the composition of air for $\frac{\rho}{\rho_0}$ of 1 and 20 for the temperature range 2000 to 30 000°K. We see that N increases fairly rapidly and

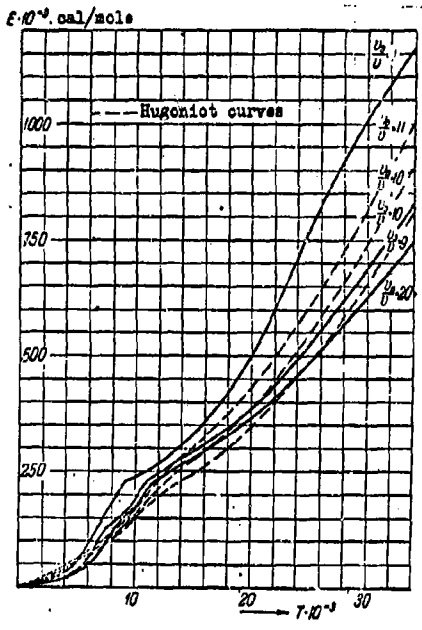


Fig 62. Internal energy of one gram-molecule of air at constant density.

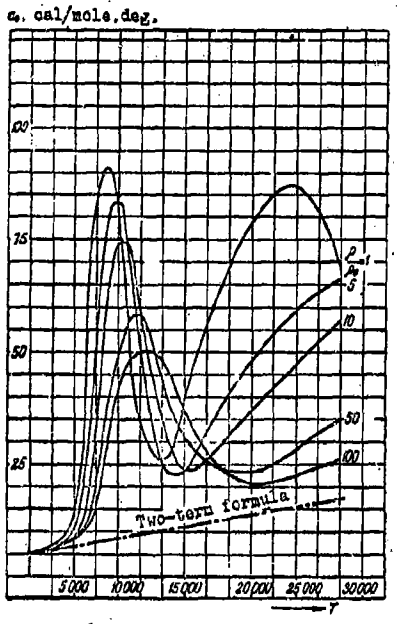


Fig. 63. Specific thermal capacity of nitrogen at constant volume.

also that dissociation and ionization are appreciably dependent on the density. The total energy per mole is

$$
\begin{aligned}
E_M &= \tfrac{3}{2} RT_1 (M_1 + M_2 + M_{12} + A_1 + A_2 + 2\theta) \\
&+ RT_1 (M_1 + M_2 + M_{12}) \\
&+ RT_1^2 \left(M_1 \frac{d}{dT} \ln z_{v\,,M_1} + M_2 \frac{d}{dT} \ln z_{v\,,M_2} + M_{12} \frac{d}{dT} \ln z_{v\,,M_{12}} \right) \\
&+ RT_1^2 \left(A_1 \frac{d}{dT} \ln z_{e\,,A_1} + A_2 \frac{d}{dT} \ln z_{e\,,A_2} \right. \\
&\qquad \left. + A_1^+ \frac{d}{dT} \ln z_{e\,,A_1^+} + A_2^+ \frac{d}{dT} \ln z_{e\,,A_2^+} \right) \qquad (35,49) \\
&+ N_0 \left(\frac{A_1 + A_1^+}{2} \lambda_{a_1} + \frac{A_1 + A_1^+}{2} \lambda_{a_2} + A_1^+ \lambda_{r_1} + A_2^+ \lambda_{r_2} - M_{12} \lambda_{r_3} \right).
\end{aligned}
$$

in which λ_{a_i} and λ_{r_i} apply to the corresponding elementary reactions. Figure 62 gives Burkhardt's results for air for various $\frac{v_0}{v}$; Fig. 63 gives the thermal capacity derived from these results, since $\left(\frac{\partial E}{\partial T}\right)_v = c_v$.

Bibliography

1. Ya. B. ZEL'DOVICH. Theory of Shock Waves: an Introduction to Gas Dynamics [in Russian]. Izd. AN SSSR, 1946.
2. L. D. LANDAU and E. M. LIVSHITS. Mechanics of Continuous Media [in Russian]. Gostekhizdat, 1953.
3. R. COURANT and K. O. FRIEDRICHS. Supersonic Flow and Shock Waves [Russian translation]. IL, 1950.
4. K. P. STANYUKOVICH. Transient-State Motion of a Continuous Medium [in Russian]. Gostekhizdat, 1955.
5. W. Y. M. RANKINE. Trans. Roy. Soc. Lond., 160, 277 (1870).
6. H. HUGONIOT. Journal de l'école polytechnique, 58 (1889).
7. R BECKER. Z. Phys., 8, 321-362 (1922).
8. R. H. COLE. Underwater Explosions [Russian translation]. IL, 1950.

CHAPTER VII

THEORY OF DETONATION WAVES

36. General Features and Basic Relationships

Explosion processes vary widely in rate and type in accordance with the initiation conditions, nature of the explosive, and so on. All such processes may be divided into two essentially distinct groups, namely those of burning and those of explosion proper. Burning has a rate dependent on external factors (especially the pressure), whereas the rate of an explosion process is almost independent of such factors. Theoretical studies show that a strict quantitative distinction can be drawn; the rate of burning is always less than the speed of sound in the unreacted material, whereas the rate of explosion is always greater than that speed. The laws of thermal conduction are decisive in burning; those of shock waves, in explosions. Burning can pass over suddenly to explosion under certain critical conditions; detonation, the limiting form of explosion, occurs under suitable circumstances, and here the rate is constant at the maximum rate possible for the given explosive. That is, detonation is a special steady-state form of explosion; the detonation rate is a very important characteristic of any explosive. We may say that explosion represents a transient process, which either goes over to detonation or dies away. This transient state is usually found around the site of initiation. Explosion in the wide sense covers the detonation (steady-state) and transient-state forms, which have no essential difference in mechanism of propagation.

The fullest study has been made on detonation processes, which are exceptionally important for detonators and high explosives; most of the theoretical work relates to gas mixtures, which form the simplest explosion systems. This work has given rise to a rigorous mathematical treatment of detonation waves; the main features of that treatment are applicable also to liquid and solid explosives. Detonation in gases was discovered in 1881 independently by BERTHELOT and by LE CHATELIER in the course of work on the propagation of flames in tubes. It was very soon discovered that the rate of propagation of a detonation wave under fixed conditions soon becomes constant; values of 3500-4000 m/sec were recorded for certain gas mixtures, which speeds are very much in excess of the speed of sound in those mixtures at ordinary temperatures and pressures.

The hydrodynamic theory of detonation made a major contribution to our understanding of detonation processes; it gave a satisfactory means of calculating all the parameters (speed, pressure, etc.) of a detonation wave. One of the founders of this theory was the Russian physicist MIKHEL'SON, who put forward the basic concepts in 1889; other major advances were made by CHAPMAN (1899), JOUGET (1905), and KRUSSAR (1907). Recent leading Russian workers in this field, who have applied the theory to condensed explosives especially, are LANDAU, ZEL'DOVICH, GRIB, STANYUKOVICH, and NEYMAN. The cause of detonation is that a shock wave propagates through the substance; if the amplitude of the wave is sufficient, there arises behind the front a very violent chemical reaction, which serves to maintain the wave parameters at a steady level. The rate of detonation can then be calculated as the rate of propagation of a shock wave.

The motion of an ordinary shock wave is composed of the propagation

of a pressure step and of the displacement of the mediu- A detonation wave is more complicated in structure, because the motion of the shock wave is associated with motions of the reaction zone and of the ultimate products. The steady state may be considered merely in terms of the initial state and of the final products; the reaction zone need not be considered. This zone remains fixed in a coordinate system that moves in the sense opposed to the motion of the wave (Fig. 64). Symbols to be used are D, the detonation rate, which equals the speed at which the reaction zone moves; u, the speed of the products behind the front; p_1, ρ_1, and T_1, parameters for the state behind the reaction zone; p_0, ρ_0, and T_0, the same for the region in front; E_1, the specific energy in the rear zone; E_0, the specific energy of the initial material; and Q, the specific energy release in the reaction.

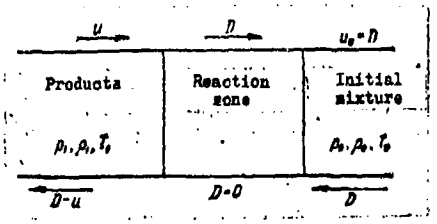


Fig. 64. Derivation of the basic relationships for a detonation wave.

The basic equations for shock waves apply also to detonation ones; we have that

$$u = (v_0 - v_1)\sqrt{\frac{p_1 - p_0}{v_0 - v_1}}, \qquad (36,1)$$

$$D = v_0\sqrt{\frac{p_1 - p_0}{v_0 - v_1}}. \qquad (36,2)$$

But D = constant here, so the latter equation gives a straight line in the variables p and v:

$$p = p_0 + \frac{v_0 - v}{v_0^2}D^2, \qquad (36,3)$$

The origin A may be taken at (p_0, v_0), which lies on this

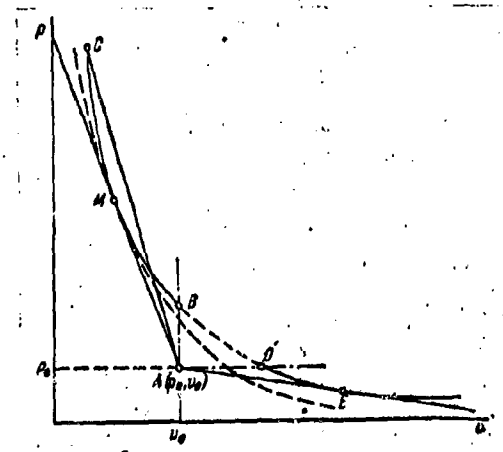


Fig. 65. HUGONIOT curve for a detonation wave.

line; the line is known as the MIKHEL'SON line. HUGONIOT's equation becomes

$$E_1 - E_0 = \frac{1}{2}(p_1 + p_0)(v_0 - v_1) + Q_v, \qquad (36,4)$$

in which the first term on the right is the change in internal energy resulting from the compression. Figure 65 shows the Hugoniot curve for a detonation wave; it lies above the corresponding curve for a shock wave on account of the energy acquired from the reaction.

The only significant part of the curve is CB, because here $D > 0$ and $u > 0$, as (36,1) and (36,2) show; part DE has $D > 0$ and $u < 0$, and it corresponds to burning, whose characteristic feature is that the products move in a sense opposed to that of the burning zone. Part BD does not correspond to any real steady process, because here $(p_1 - p_0) > 0$ and $(v_1 - v_0) < 0$, which imply imaginary values for D and u.

From A we draw a line at an angle α_1, which meets the HUGONIOT detonation curve at two points; here we have the condition

$$D = v_0 \sqrt{\tan \alpha},$$

which implies that a given D can correspond to two distinct states of the decomposed material at the front, which is physically absurd. CHAPMAN and JOUGET have demonstrated in different ways that any detonation corresponds to the unique state of the products specified by the point M (the point at which the MIKHEL'SON line touches the HUGONIOT adiabatic). Here $\tan \alpha$, and hence D, are minimal; $D = D_{min}$. The following is a proof that the state corresponding to M is one in which D is equal to the speed of propagation for a perturbation in the products (relative to a fixed observer), i.e. that

$$D = u + c, \qquad (36,5)$$

and that $dS = 0$, (i.e., S = constant) on the HUGONIOT curve. Now

(36,5) implies that

$$D-u=v_0\sqrt{\frac{p_1-p_0}{v_0-v_1}}-(v_0-v_1)\sqrt{\frac{p_1-p_0}{v_0-v_1}}=\sqrt{-p_1v_1}=c,$$

so

$$\frac{p_1-p_0}{v_0-v_1}=\tan\alpha=k\frac{p_1}{v_1}. \tag{36,6}$$

The proof that $D=u+c$ at M is given from the first law of thermodynamics:

$$T\,dS=dE+p\,dv.$$

The two sides are divided by p_0v_0 to make all quantities dimensionless. Let $\frac{E}{p_0v_0}=s$, $\frac{p}{p_0}=\pi$ and $\frac{v}{v_0}=\mu$; then

$$\frac{T}{p_0v_0}dS=ds+\pi\,d\mu.$$

Further, (36,4) in the same dimensionless terms is

$$s-s_0=\frac{\pi+1}{2}(1-\mu)+\frac{Q_v}{p_0v_0},$$

and so

$$ds=\frac{1}{2}[(1-\mu)\,d(\pi+1)+(\pi+1)\,d(1-\mu)].$$

We substitute for ds in the transformed thermodynamic law, in conjunction with the substitutions $d\mu=d(1-\mu)$ and $d(\pi+1)=d(\pi-1)$, to get that

$$\frac{T}{p_0v_0}dS=\frac{(1-\mu)\,d(\pi-1)-(\pi-1)\,d(1-\mu)}{2}.$$

The two sides are divided by $(1-\mu)^2$ to get that

$$\frac{T}{p_0v_0}dS=\frac{(1-\mu)^2}{2}\left[\frac{d(\pi-1)}{1-\mu}-\frac{(\pi-1)\,d(1-\mu)}{(1-\mu)^2}\right]. \tag{36,7}$$

Again, (36,6) in terms of π and μ is

$$\tan\alpha_1=\frac{\pi-1}{1-\mu}, \tag{36,6a}$$

in which

$$\tan\alpha_1=\frac{v_0}{p_0}\tan\alpha.$$

But

$$d\tan\alpha_1=\frac{d(\pi-1)}{1-\mu}-\frac{(\pi-1)\,d(1-\mu)}{(1-\mu)^2},$$

so comparison with (36,7) gives us that

$$\frac{T}{p_0v_0}dS=\frac{(1-\mu)^2}{2}d\tan\alpha_1.$$

Further,

$$d\tan\alpha_1=\frac{d\alpha_1}{\cos^2\alpha_1}=(1+\tan^2\alpha_1)\,d\alpha_1,$$

so

$$\frac{T}{p_0 v_0} dS = \frac{(1-\mu)^2 + (\pi-1)^2}{2} d\alpha_1. \qquad (36,7a)$$

Now S = constant for a steady-state detonation, so

$$\frac{(1-\mu)^2 + (\pi-1)^2}{2} d\alpha_1 = 0. \qquad (36,8)$$

This is possible only if $d\alpha_1 = 0$, because the factor before the differential is always positive; but $d\alpha_1 = 0$ at the point where α_1 has its minimum, which is the point where the MIKHEL'SON line touches the HUGONIOT adiabatic. Clearly, α_1 does not have a maximum at any point on the branch corresponding to detonation.

Point M is also the point at which the Hugoniot adiabatic touches the ordinary adiabatic, which is the line of constant entropy ($dS = 0$); AB is a common tangent to both adiabatics, so

$$\tan\alpha = \frac{p_1 - p_0}{v_0 - v} = \left(-\frac{dp}{dv}\right)_S = k\frac{p_1}{v_1},$$

which is a direct consequence of our assumption that $D = u + c$.

Another important feature is as follows. Expression (36,7a) shows that $dS > 0$ for points on the HUGONIOT curve on both sides of M, because $\alpha_1 > 0$ and the associated factor is always positive. This means that the entropy increases at the detonation front for any state in the products corresponding to a point other than M.

ZEL'DOVICH has given a more rigorous physical demonstration that M must correspond to a steady-state detonation and that any other state for the products gives rise to an unstable process; his demonstration is based on a study of the conditions for the reaction at the front.

37. Effects of Reaction Kinetics on the Formation and Behavior of a Detonation Wave

The reactions in a detonation wave are not instantaneous; the reaction time is governed by ν, the mean number of collisions needed to perform one act of reaction. Since $\nu \gg 1000$, the width of the front

in a detonation wave is very much greater than that in a shock wave; the gradients are much smaller, so effects from viscosity and thermal conduction are negligible. The role of heat conduction in transmitting the detonation is small, because the temperature gradients are low. The material is compressed so rapidly that its composition does not have time to change; the compression initiates the reaction, which produces heat; this results in subsequent expansion of the hot products. The pressure at the front is affected by this.

The speed of the detonation wave is not dependent on Q, being given by (36,2), which is a consequence of the equations for the conservation of matter and momentum. The viscous forces are negligible for the transition zone of a detonation wave (but not of a shock wave), so (36,2) is directly applicable to any state in which only part of the total Q has been released (or none at all, i.e. to the initial state). The process cannot be steady unless the parts of the reaction zone move at the same speed; any other situation would cause the detonation wave to become deformed as it moves, so the process would not be steady. The condition D = constant can occur only if all the parameters of the state vary in accordance with the MIKHEL'SON line

$$p = p_0 + \frac{D^2}{v_0^2}(v_0 - v).$$

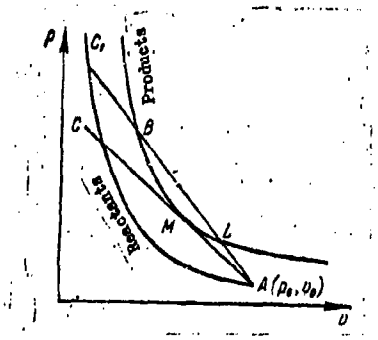


Fig. 66. Formation of a steady detonation wave.

Figure 66 illustrates the formation of such a wave. The explosive is compressed by a shock wave, whose speed is D, to the state C in which the reaction starts; the material is gradually converted to final products, and the transition from state C to the final state M proceeds along the line $4C$

(the expansion consequent upon the heating keeps the speed constant). The speed is constant, but p and v are variable; state M lies on the HUGONIOT adiabatic for the products, being the special point at which $dS=0$ and $D_0=u+c$, (the point for the steady state). Figure 67 illustrates the behavior of the pressure and density behind the front; here point M corresponds to point M on the HUGONIOT curve.

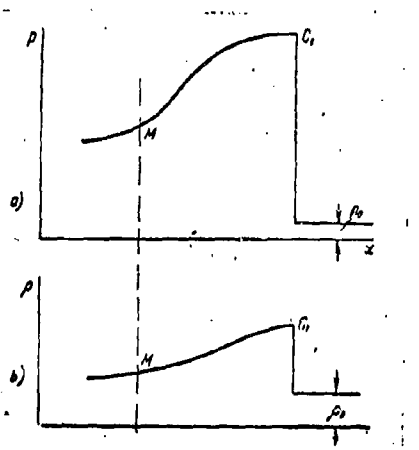


Fig. 67. Distribution of a) pressure and b) density in a detonation wave.

Consider now a detonation initiated by a shock wave having a speed $D_1>D$ and which compresses the material to state C_1; the above argument shows that the reaction must then take the course corresponding to the line AC_1, and the final state corresponds to point B of Fig, 66. This detonation wave cannot be stable, for a wave of rarefaction occurs in the products, and the head of this wave moves with the speed of sound for the products, namely $u+c$. This wave will not arise, and the products will not expand, only if we bring up behind the detonation wave a piston moving with a speed u (the speed of the products behind the front), which is impossible.

We have seen above that S increases to both sides of point M on the HUGONIOT curve. Now I shall show that $u+c>D_1$ for the upper part of the curve (for $v<v_1$ and $p>p_1$), the converse being true for the lower part (for $v>v_1$ and $p<p_1$). All parameters corresponding to point M are here denoted by subscript 1.

The first inequality is put as

$$v\sqrt{-\frac{dp}{dv}} = c > D - u = v\sqrt{\frac{p-p_0}{v_0-v}},$$

which implies that

$$-\frac{dp}{dv} > \frac{p-p_0}{v_0-v}. \tag{37,1}$$

We put HUGONIOT's equation in the form

$$E - E_0 = \frac{p+p_0}{2}(v_0-v) + Q$$

which gives the increment

$$dE = \frac{(v_0-v)\,dp - (p+p_0)\,dv}{2}, \tag{37,2}$$

in which

$$dE = T\,dS - p\,dv,$$

so simple manipulations give us that

$$-\frac{dp}{dv} = \frac{p-p_0}{v_0-v} - \frac{2T}{v_0-v}\frac{dS}{dv}. \tag{37,3}$$

Now $dS > 0$ and $dv < 0$, so $\frac{dS}{dv} < 0$; then

$$-\frac{2T}{v_0-v}\frac{dS}{dv} > 0,$$

i.e.

$$-\frac{dp}{dv} > \frac{p-p_0}{v_0-v},$$

which demonstrates that $u + c > D$.

Again, for the lower branch

$$dv > 0, \quad \frac{dS}{dv} > 0.$$

so

$$-\frac{dp}{dv} < \frac{p-p_0}{v_0-v}, \quad \text{i.e.} \quad u + c < D.$$

Now I turn to the stability or otherwise of the state represented by 3; here $u + c > D$, so the head of the rarefaction wave catches up with the detonation wave; the pressure at the front falls. The state at the front can be altered only by moving along the HUGONIOT curve for the products, because the reaction is already completed; the motion along this curve will continue until the pressure falls to p_i (that for point M), at which point $u + c = D_i$, which corresponds to stability.

An initial state with $D_1 > D_i$ (point B) can arise when an explosive is ignited by a detonator having a higher D_i; the normal speed D_1 is

attained only at a certain distance from the detonator, and so there is an initial transient zone. The above discussion is strictly correct only if the detonator and charge are identical in density and compressibility, because the speed of a shock wave changes discontinuously at the interface between two media that differ in either of these parameters (see chapter IX). The line of equal speeds, AC_1, meets the HUGONIOT adiabatic at a point L on the lower branch, but this point is inaccessible for physical reasons. The parameters of a wave of speed D_1 could correspond to L only if the material were first compressed to state C_1 by a shock wave; then the state of the products immediately after the reaction would correspond to B, but the further transition to B along AC_1 is not possible, because this would require energy in excess of Q (ZEL'DOVICH first directed attention to this point.) Further, should L be reached for a given D_1 by any means, the detonation wave would then be unstable, because $u+c<D$ at this point. This means that an elastic wave in the products will always lag behind the detonation wave, which makes it impossible for energy released behind the front to be transmitted to the front; the detonation wave then soon becomes an ordinary shock wave in an inert medium (one that dies away).

The mechanisms of the reactions initiated by the compression are such as to indicate that a stable state of detonation can exist only for the single state of the products that corresponds to point M. Thermodynamic arguments lead to the same conclusion; S must increase as heat is released in the reaction and becomes maximal on the MIKHEL'SON line at point M, which defines the parameters at the front for the instant when the reaction has gone to completion.

This statement is demonstrated as follows. The thermodynamic

relation

$$T\,dS = dE + p\,dv$$

may be modified by inserting the dE found from (36,4):

$$2T\,dS = (v_0 - v)\,dp + (p - p_0)\,dv. \tag{37,4}$$

The expression for the MIKHEL'SON line gives us that

$$(v_0 - v) = \frac{v_0^2}{D^2}(p - p_0),$$

and so

$$2T\frac{dS}{dp} = (p - p_0)\left(\frac{v_0^2}{D^2} + \frac{dv}{dp}\right). \tag{37,5}$$

Now $\frac{dS}{dp} = 0$ at the point of maximum S on that line, so

$$(p - p_0)\left(\frac{v_0^2}{D^2} + \frac{dv}{dp}\right) = 0,$$

whence

$$\frac{D^2}{v_0^2} = \frac{p - p_0}{v_0 - v_1} = \tan\alpha = -\frac{dp}{dv},$$

which corresponds to the point M at which AC touches the Hugoniot adiabatic; this demonstrates the above statement, because

$$\frac{d^2p}{dv^2} = -\frac{\frac{dp}{dv}(v_0 - v) + (p - p_0)}{(v_0 - v)^2} = -\frac{dp}{dv}\frac{1}{v_0 - v} - \frac{p - p_0}{(v_0 - v)^2} < 0$$

when

$$p = p_1 \text{ and } v = v_1.$$

38. Calculation of Detonation-Wave Parameters for Gas Mixtures

A detonation is described by p_1, ρ_1, T_1, u_1, and D_1, which are given by

$$E_1 - E_0 = \frac{p_1 + p_0}{2}(v_0 - v_1) + Q_v, \tag{38,1}$$

$$D = v_0\sqrt{\frac{p_1 - p_0}{v_0 - v_1}}, \tag{38,2}$$

$$u = (v_0 - v_1)\sqrt{\frac{p_1 - p_0}{v_0 - v_1}}, \tag{38,3}$$

$$\frac{p_1 - p_0}{v - v_1} = \left(-\frac{dp}{dv}\right)_S = \frac{kp_1}{v_1}, \tag{38,4}$$

$$p = f(S, T). \tag{38,5}$$

The last is the equation of state, whose form is dependent on the nature of the explosive material (gas, solid, or liquid). We may use $pv^k =$ constant for gas mixtures, whereupon HUGONIOT's equation becomes

$$\frac{p_1 v_1}{k-1} - \frac{p_0 v_0}{k_0 - 1} = \frac{p_1 + p_0}{2}(v_0 - v_1) + Q_v, \tag{38,6}$$

in which k_0 (for the initial mixture) usually differs somewhat from k (for the products). We eliminate p_1 and v_1, and put $k_0 = k$, to get a relation for D. (38,4) gives us that

$$\frac{v_0}{v_1} = \frac{\rho_1}{\rho_0} = \frac{k+1}{k} - \frac{p_0}{k p_1}. \tag{38,7}$$

This, with (38,2), gives us that

$$D_1^2 = v[(k+1)p_1 - p_0]. \tag{38,8}$$

We eliminate v_1 from the energy equation to get that

$$D_1^4 + k^2(k-1)^2 c_0^2 T_1^2 - 2(k^2-1) D_1^2 c_v T_1 - 2(k^2-1) D_1^2 Q_v = 0,$$

and so

$$D_1 = \sqrt{\frac{k^2-1}{2} Q_v + c_0^2} + \sqrt{\frac{k^2-1}{2} Q_v}, \tag{38,9}$$

in which c_0^2 is the speed of sound in the initial mixture; if D_1 is known, p_1 and v_1 are then readily found, for

$$\left.\begin{aligned} p_1 - p_0 &= \frac{\rho_0 D_1^2}{k+1}\left(1 - \frac{c_0^2}{D_1^2}\right), \\ v_0 - v_1 &= \frac{v_0}{k+1}\left(1 - \frac{c_0^2}{D_1^2}\right), \\ u_1 &= \frac{D_1}{k+1}\left(1 - \frac{c_0^2}{D_1^2}\right). \end{aligned}\right\} \tag{38,10}$$

The equation of state for ideal gases gives us that

$$T_1 = \frac{p_1 v_1}{R} = \frac{(kD_1^2 + c_0^2)^2}{k(k+1)RD_1^2}. \tag{38,11}$$

These expressions show that all the parameters of interest are dependent on T_1 (but not explicitly), because k is dependent on the temperature at the detonation front. This feature makes the final solutions rather cumbrous.

However, the expressions (and the calculations) become much simpler if we calculate k on the basis of the reaction temperature T_r and neglect p_0 relative to p_1. Results for typical cases show that neglect of p_0 has very little effect on the result if p_1 exceeds 10 atm, which is always so for detonations in the usual gas mixtures; then (38,7) becomes

$$\frac{v_0}{v_1} = \frac{\rho_1}{\rho_0} = \frac{k+1}{k}. \tag{38,12}$$

and the energy equation gives us that

$$p_1 = 2(k-1)\rho_0 Q_v. \tag{38,13}$$

which, inserted in (38,2) with p_0 neglected, gives us that

$$D = \sqrt{2(k^2-1)Q_v}. \tag{38,14}$$

The equation of state gives us that

$$T_1 = \frac{p_1 v_1}{p_0 v_0} T_0 = \frac{p v_1}{c_v (k-1)}.$$

We substitute for p_1 and v_1 from (38,13) and (38,12) to get that

$$T_1 = \frac{2k}{k+1} T_r, \tag{38,15}$$

We use (38,10) and (38,14) by neglecting c_0 as being small relative to D_1, which gives us that

$$u = \sqrt{\frac{2(k-1)}{k+1} Q_v}. \tag{38,16}$$

The Q_v appearing here must be referred to unit mass of the products; D and u are usually expressed in m/sec and p_1 in kg/cm^2, so Q_v must be expressed in mechanical units. Then $Q_v = 427gQ$ m^2/sec^2 (in which g is the acceleration due to gravity and Q is the heat of reaction in kcal/kg). But

$$Q_v = c_v T_1 = \frac{p_1 v_1}{k-1}$$

and (38,15) gives us T_1, so (38,14) may be put as

$$D = \frac{k+1}{k}\sqrt{knRT_1} \tag{38,17}$$

or, since

$$nR = \frac{1000}{M} \times 0.848 \times 9.81$$

(in which M is the mean molecular weight of the products), we have

that

$$D_i = \frac{k+1}{k}\sqrt{\frac{8310k}{M}T_i}. \qquad (38,18)$$

Then (38,17) shows that D exceeds the speed of sound in the compressed products by a factor [illegible]. It increases with the number of molecules per unit mass of the products, other things being equal. The factor cannot exceed two for gas mixtures.

(31,15) and (38,10) enable us to calculate the ratio of pressures for shock and detonation waves having the same speed D; for the shock wave

$$p' - p_0 = \frac{2}{k+1}\rho_0 D^2\left(1 - \frac{c_0^2}{D^2}\right).$$

and for the detonation one

$$p_i - p_0 = \frac{\rho_0 D^2}{k+1}\left(1 - \frac{c_0^2}{D^2}\right).$$

so

$$\frac{p' - p_0}{p_i - p_0} = 2 \quad \text{or} \quad p' \approx 2p_i$$

Further, (31,16) and (38,10) give us that $v' = 2v_i - v_0$.

These results again show that the products expand, which is the reason for the fall in pressure behind the reaction zone to about half the pressure produced in the initial mixture by the shock wave. Table 51 gives JOUGET's calculated results for detonation fronts in certain

Table 51

Parameters of Detonation Waves in Gas Mixtures

Mixture	T, °K	$\frac{\rho_0}{v_i}$	$\frac{p_i}{p_0}$	D_i, m/sec	
				calc.	meas.
$2H_2 + O_2$	3960	1.88	17.5	2630	2819
$CH_4 + 2O_2$	4080	1.90	27.4	2220	2257
$2C_2H_2 + 5O_2$	5570	1.84	54.5	3090	2961
$(2H_2 + O_2) + 5O_2$	2600	1.79	14.4	1690	1700

gas mixtures; JOUGET used here some not very precise results for the

thermal capacities as functions of T, but the calculated D_i are in very good agreement with the measured ones. LEWIS and FRIAUF have performed similar calculations for explosion mixture containing various other gases; they made allowance for the dissociation occurring at T_i. Table 52 gives their results, which show that the added gas affects D substantially; nitrogen and oxygen reduce D, whereas hydrogen increases it

Table 52

Detonation Speeds for Explosion Mixture Containing Other Gases

Mixture	$\frac{\rho_i}{\rho_0}$	T_i °K	D_i m/sec	
			calc.	meas.
$2H_2 + O_2$	18.0	3583	2856	2819
$(2H_2 + O_2) + O_2$	17.4	3390	2302	2314
$(2H_2 + O_2) + 4H_2$	16.0	2976	3527	3527
$(2H_2 + O_2) + N_2$	17.2	3357	2273	2267
$(2H_2 + O_2) + 3N_2$	15.6	3053	2053	2055
$(2H_2 + O_2) + 1.5\ Ar$	17.6	3412	2117	1950

greatly, although it reduces T_i. These observations are in agreement with the theory, which shows that D is dependent on the mean molecular weight as well as on T_i. Hydrogen and helium fall below H_2O in molecular weight, so they increase D to a certain extent.

An example of this effect is found for stoichiometric methane-oxygen mixtures:

$$CH_4 + 2O_2 + 8N_2 = CO_2 + 2H_2O + 8N_2 + 191.8 \text{ kcal}$$

Here T_i = 2200°K = $\frac{Q_v}{\sum c_v}$, in which $\sum c_v$ is given by figures listed in chapter III as

$$\sum c_v = 86.88 \text{ cal}$$

$$\sum c_p = 86.88 + 11R = 86.88 + 11 \times 1.986 = 108.74 \text{ cal}$$

Then

$$k = \frac{\sum c_p}{\sum c_v} = 1.25.$$

and (38,15) gives T_i as

$$T_i = \frac{2k}{k+1} T_r = 2440° \text{K}.$$

Also

$$M = \frac{44 + 2\times 18 + 8\times 28}{11} = 27.6.$$

so (38,18) gives us that

$$D = \frac{k+1}{k}\sqrt{\frac{k\cdot 8310}{M}T} = \frac{2.25}{1.25}\sqrt{\frac{1.25\times 8310}{27.6}\times 2440} = 1720 \text{ m/sec},$$

$$\rho_0 = 1.17\times 10^{-3} \text{ g/cm}^3; \quad \rho_i = 2.10\times 10^{-3} \text{ g/cm}^3,$$

$$u = \sqrt{\frac{2(k-1)}{k+1}Q_v} = 764 \text{ m/sec}$$

$$p_i - p_0 = \rho_0 u D_i = 15.7 \text{ kg/cm}^2.$$

39. Effect of the Density on the Detonation Rate

The above calculations are based on the equation of state for an ideal gas; this describes correctly the behavior of a gas mixture in its initial state at atmospheric pressure, because the density is doubled (at most) in the detonation wave, while the pressure at the front does not greatly exceed 10 atm. In this case, though, the initial density has no effect on D, u, and T_i; experiment shows that this is so for gas mixtures whose initial pressures are relatively low. For example, D for explosion mixture increases only from 2821 to 2872 m/sec when the initial pressure is raised from 760 to 1500 mm Hg. However, CLAPEYRON's equation is not applicable to gases of high initial pressure; the initial density starts to affect D substantially. For example, LE CHATELIER's results show that D increases from 1000 to 1600 m/sec for acetylene mixtures when the initial pressure is raised from 5 atm to 30 atm.

If we use ABEL's equation of state,

$$p(v-\alpha) = \frac{RT}{M}, \tag{39,1}$$

in which α is the covolume, on the assumptions that M is independent of ρ and that α = constant (as for ideal gases), then $\left(\frac{\partial E}{\partial v}\right)_T = 0$. Thermodynamics gives us that

$$dE = c_v\,dT + \left(\frac{\partial E}{\partial v}\right)_T dv,$$

but

$$\left(\frac{\partial E}{\partial v}\right)_T = T\left(\frac{\partial p}{\partial T}\right) - p, \tag{39,2}$$

so

$$dE = c_v\,dT + \left[T\left(\frac{\partial p}{\partial T}\right)_v - p\right]dv. \tag{39,3}$$

Now $\left(\frac{\partial E}{\partial v}\right)_T = 0,$ for an ideal gas, so

$$dE = c_v\,dT, \quad T\left(\frac{\partial p}{\partial T}\right)_v = p. \tag{39,4}$$

It is readily seen that ABEL's equation gives the same result, for its derivative gives us that

$$\left(\frac{\partial p}{\partial T}\right)_v = \frac{R}{M(v-\alpha)} = \frac{p}{T},$$

so

$$\left(\frac{\partial E}{\partial v}\right)_T = 0.$$

This means that Hugoniot's equation here takes the form applicable to an ideal gas:

$$E_i - E_0 = c_v(T_i - T_0) = Q + \tfrac{1}{2}(p_i - p_0)(v_0 - v_i).$$

Then (38,12) becomes

$$\frac{v_0 - \alpha}{v_i - \alpha} = \frac{k+1}{k}. \tag{39,5}$$

and

$$D = \frac{v_0}{v_0 - \alpha}\sqrt{2(k^2-1)Q_v} = \frac{1}{1-\alpha\rho_0}\sqrt{2(k^2-1)Q}, \tag{39,6}$$

in which ρ_0 is the mass (kg) per liter; (38,15) and (38,16) remain unchanged.

This shows that ABEL's equation, if used with α = constant, implies that D increases with ρ_0 although T_i and u remain unchanged. This effect of the density is actually observed, as Fig. 68 shows for explosion mixture for $\alpha = 0.75$ cm^3/g; the experimental points fit the curve well, and D increases from 3000 to 4400 m/sec when ρ_0 increases from 0.1 to 0.5 g/cm^3.

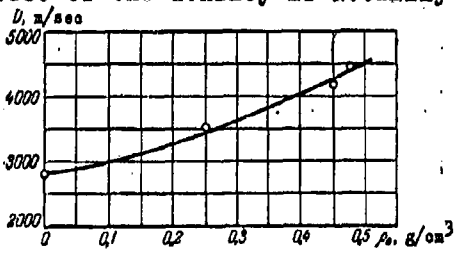


Fig. 68. Relation of D to density for explosion mixture.

TAFFANELLE and D'AUTRICHE, followed by SCHMIDT, have attempted

to apply the above equations to condensed explosives; the principal difficulty here is that α is not known for the products at the very high pressures produced by such explosives. They attempted to obviate this difficulty by deducing α from the measured D by means of (39,5) and (39,6); theory gives us for an ideal gas that $D_i = \frac{k+1}{k}\sqrt{knRT}$.

$$D_p = \frac{1}{1-\alpha\rho_0}\frac{k+1}{k}\sqrt{knRT}$$

so for a practical explosive

$$\frac{D_p}{D_{i_2}} = \frac{1}{1-\alpha\rho_0}. \qquad (39,7)$$

which gives us α if D_p is known and D_{i_2} is calculated. In this way SCHMIDT found α for various explosives; in particular, α for TEN decreases from 0.79 to 0.44 liters per kg when ρ_0 increases from 0.5 to 1.6 kg/liter. Similar results were obtained for trotyl, picric acid, and tetryl. Table 53 gives detonation-wave parameters SCHMIDT calculated in this way.

Table 53

Parameters of Detonation Waves in Trotyl (SCHMIDT)

ρ_0, kg/l	ρ_{i_2}, kg/l	D_p, m/sec	α, kg/l	p_{i_2}, atm	T_{i_2}, °K
1.0	1.23	4700	0.58	41 600	3250
1.29	1.53	5900	0.52	67 600	3530
1.46	1.70	6500	0.48	84 000	3550
1.59	1.53	6900	0.45	96 500	3630

The results are essentially in conflict with the assumptions made in deriving them; the formulas are applicable only if α is constant. A condensed explosive has $\left(\frac{\partial E}{\partial v}\right)_T \neq 0$, so (39,5) and (39,6) are not applicable.

The above method also gives the incorrect result that u is independent of ρ_0 and D, which is, physically speaking, absurd. All the same, the D_i calculated in this way are often in agreement with experiment; this is not really surprising, because the α are found from the measured D for

explosives of similar compositions.

40. Theory of Detonation for Condensed Explosives

LANDAU and STANYUKOVICH have shown that the main features of the hydrodynamic theory apply to condensed explosives; they have deduced the parameters of the detonation front from the equation of state for the highly compressed products. The argument is as follows. The initial density is higher (greater than that of water), so the pressure at the front becomes very high (often in excess of 10^5 atm), and the density of the compressed products is substantially in excess of the initial density. These features indicate that the ideal-gas equation and VAN DER WAALS's equation are not applicable, because they both neglect the forces of repulsion between particles, which forces are very important.

LANDAU and STANYUKOVICH's general deductions are as follows (detailed results are not given). A suitable general equation of state is

$$p = \Phi(v) + f(v)T. \qquad (40,1)$$

The forces of repulsion and attraction between molecules are represented respectively as

$$\Phi(v) = av^{-n} - bv^{-m}, \qquad (40,2)$$

The theory of solids indicates that $n > m$ and that $m \geq 2$, so $\Phi(v) \to 0$ when the distances r between molecules are large; the attraction is initially dominant as v decreases, so $\Phi(v) \to 0$. The repulsion exactly balances the attraction at a critical distance r_0; then $\Phi(v) = 0$ and the system is in equilibrium. Repulsion predominates if $r < r_0$, and $\Phi(v) > 0$. Figure 69 indicates the relation

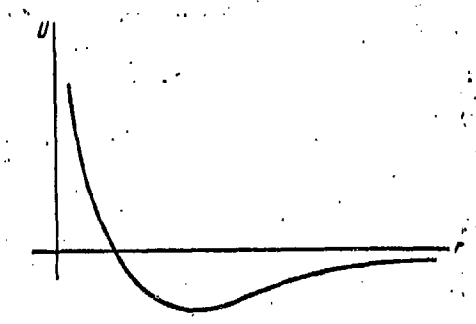


Fig. 69. Relation of interaction energy to separation for molecules.

between r, and the interaction energy U for two molecules; this and (40,2) imply that the attraction can be neglected in relation to the highly heated products, so the equation of state becomes

$$p = Av^{-n} + f(v)\,T, \tag{40,3}$$

in which A is a constant. BORN's lattice theory gives $p = Av^{-n}$ for the elastic component of the pressure, but this is not applicable for the very small separations considered here; a power-law representation of the repulsion is only a mathematically convenient approximation.

The term in $f(v)T$ represents the ratio of the total volume to the inherent volume of the molecules; $p = \frac{RT}{v}$ when v is large, and $\Phi(v) \to 0$, so $(f/v) \to \frac{R}{v}$ as $v \to \infty$. The molecules become deformed at very high pressures, so it is not possible to put $f(v)$ in the form $\frac{R}{v-\alpha}$, in which α is a constant. If $\alpha \propto v$ to a certain degree of approximation, then $f(v) = \frac{B}{v}$, in which B is a slowly varying function of v; B = constant for high pressures and $B \to R$ as $v \to \infty$. Then the final form for the equation of state is

$$p = Av^{-n} + \frac{BT}{v}. \tag{40,4}$$

Statistical physics gives us the free energy of a solid (or liquid) as

$$F = F_1(v) + RLT \ln \frac{\omega}{2\pi kT}, \tag{40,5}$$

in which $F_1(v)$ is the temperature-independent part of F, L is the mean number of degrees of freedom for a molecule, k is BOLTZMANN's constant, and ω is the mean vibrational frequency of the atoms (allowance being made for the rotational and vibrational degrees of freedom). But

$$p = \left(-\frac{\partial F}{\partial v}\right)_T,$$

so

$$p = -F_1'(v) - RLT\frac{\omega'}{\omega} = Av^{-n} + \frac{BT}{v} \tag{40,6}$$

Then

$$\frac{\omega'}{\omega} = -\frac{B}{RLv},$$

and so

$$\omega \sim v^{-\frac{B}{RL}}.$$

It can be shown that (40,6) corresponds to the isentropic equation

$$p = M(S)\, v^{-2\left(\frac{B}{RL}-\alpha\right)+1}, \qquad (40,7)$$

in which $M(S)$ is a function of the entropy whose form is governed by the conditions at the detonation front. This equation, with the conditions for contact between the MIKHEL'SON line and the shock adiabatic, gives us that

$$\left(\frac{\partial p}{\partial v}\right)_S = \frac{p}{v_0 - v} = \frac{\left[2\left(\frac{B}{RL}-\alpha\right)+1\right]p}{v} = k\,\frac{p}{v}$$

if we neglect p_0 relative to p; then B is related to k by

$$\frac{B}{RL} = \frac{k-1+2\alpha}{2} \qquad (40,8)$$

and (40,7) may be put as

$$p = M(S)\, v^{-k}. \qquad (40,9)$$

This k is given by

$$\left(-\frac{\partial \ln D}{\partial \ln v_0}\right)_Q = \frac{k-1}{2\left[\frac{2c_v}{B}k-1\right]} = a \qquad (40,10)$$

which is a consequence of (40,7) and the basic relationships for detonation waves.

The B of (40,8) is inserted in (40,10) to give

$$(\beta-1)k^2 - k[(2\alpha+1)\beta - 2\alpha - (\alpha+1)] + \alpha(2\alpha-1) = 0, \quad (40,11) \qquad (40,11)$$

in which

$$\beta = \frac{2c_v}{RL}, \quad \alpha \approx \frac{1}{6}.$$

That is, k may be found if α and β are known. The medium resembles a solid body in its behavior when the pressure is very high, and then $\beta = 2$, because $c_v = RL$. At low pressures, $\beta = 1$, because $c_v = \frac{RL}{2}$ for an ideal gas; k increases with α and β. Of course, the state of the highly compressed products is not exactly that of a solid; it approaches more closely that of a liquid at the high temperatures involved, so $c_v > RL$, and β may be somewhat greater than 2. Values of β near 2.2 are typical of standard high explosives.

We may deduce a from the relation of D to ρ_0, which is linear on a log-log plot for $\rho_0 = 1.2$ g/cm^3; then

$$\left(\frac{\partial \ln D}{\partial \ln \rho_0}\right)_Q = \text{const}$$

and a is almost constant; the range is 0.70-0.75 for most high explosives at reasonably high densities, so we may reasonably use an average value for a.

The A and n of (40,4) are to be found from the formula for the temperature T_1 at the front, which is deduced from the equations of energy and isentropy as

$$\Delta Q_n = c_v \Delta T = \frac{n-1}{n-m}\left(Q - \frac{D^2}{2(k+1)^2}\right)\left(\frac{2k}{k-1} - 1\right), \qquad (40,12)$$

in which ΔQ_n is the heat produced at the front and

$$m = 1 + \frac{B}{c_v} = 1 + \frac{k-1+2a}{\beta}.$$

If

$$D^2 = \frac{2(k-1)^2 Q(n-1)}{2k+1-n}, \quad c_v \Delta T = 0$$

(since $\Delta Q_n = 0$), and also $k = n$; then the limit D_1, at which $\Delta T = 0$, is given by

$$D_L^2 = 2(n^2-1)Q. \qquad (40,13)$$

Now k rises gradually to the limit n as ρ_0 increases, so (40,12) implies that T_1 falls from $2\frac{k}{k+1}T_2$ to $\frac{2k}{k+1}$, in which T_2 is the reaction temperature, to the initial temperature of the explosive as the density increases (the latter limit is unattainable in practice). The reason for this fall is as follows. The elastic forces between and within molecules become more important as the density

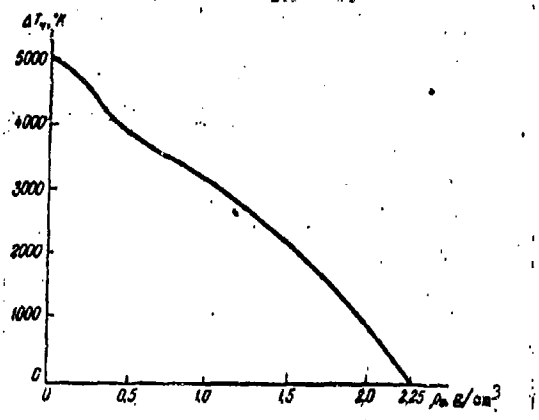


Fig. 70. Temperature rise at the front in a detonation wave as a function of density of explosive for Q_v = 1 kcal/g and M = 30.

increases, so the energy released by the reaction is in part used up in overcoming these forces (of repulsion); less is available for the energy of thermal motion, and so T_{k_1} falls. Figure 70 illustrates this.

The limit to k, namely n, is given by (40,4) and (40,7), which become the same for $T = 0$, for $M(S)$ = constant = M and so

$$p = Av^{-n} = Mv^{-\left[1+2\left(\frac{B}{RL}-\alpha\right)\right]} \tag{40,14}$$

whence

$$n = 2\left(\frac{B}{RL}-\alpha\right)+1 = k_1. \tag{40,15}$$

(k_1 is the limiting k). This gives us D_1, and hence, by extrapolation of the relation of ln D to ln ρ_0 (see Fig. 86, section 44), we get the limit to ρ_0, which is given by

$$p_1 = \frac{\rho_{0_1} D_1^2}{n+1}$$

and

$$\rho_1 = \rho_{0_1} \frac{n+1}{n}.$$

Then (40,14) gives us that

$$A = p_1 \rho_1^{-n} = \frac{D_1^2}{n+1} \rho_{0_1}^{1-n} \left(\frac{n}{n+1}\right)^n. \tag{40,16}$$

The k and m corresponding to any given ρ_0 and Q are calculated from the above formulas; Table 54 gives the final results for the case Q = 1 kcal/g, which corresponds to n = 3.6 and a limiting ρ_0 of 2.25 g/cm^3; these give β = 2.2. It has also been assumed that α increases linearly from zero at $\rho_0 = 0$ to 1/6 at $\rho_0 = 2.25$, then $\alpha = \frac{\rho_0}{16.5}$.

Table 54

Detonation-Wave Parameters

ρ_0, g/cm3	0	0.1	0.25	0.32	0.50	0.75	1.00	1.25	1.70	2.25
α	0	0.01	0.16	0.23	0.45	0.70	0.76	0.76	0.76	0.76
D, m/sec	2180	2500	2800	2950	3300	4300	5350	6500	8000	10 000
k	1.25	1.30	1.62	1.78	2.22	2.80	3.05	3.21	3.40	3.60
m	1.25	1.29	1.35	1.38	1.42	1.50	1.75	1.90	2.10	2.40
β	1.00	1.10	1.24	1.33	1.42	1.50	1.58	1.66	1.84	2.22

The above expressions give us that

$$p = \frac{Av_0^{-n}}{n-1}\left(\frac{k+1}{k}\right)^n \frac{n-m}{1-\frac{m-1}{2k}} + \frac{(m-1)Q\,\frac{k+1}{k}}{v_0\left[1-\frac{m-1}{2k}\right]}. \qquad (40,17)$$

But $D^2 = v_0^2 \frac{p}{v_0 - v}$, so (40,17) gives

$$D^2 = \frac{2(k+1)^2}{2k-(m-1)}\left[\frac{A}{n-1}\rho_0^{n-1}\left(\frac{k+1}{k}\right)^{n-1}(n-m) + (m-1)Q\right] \qquad (40,18)$$

which defines D in terms of ρ_0 and Q; in cgs units it becomes

$$D^2 = \frac{A}{1,16}b_1(\rho_0)\rho_0^{n-1} + b(\rho_0)Q = 10^{10}b_1\rho_0^{2,6} + bQ, \qquad (40,19)$$

in which $A = 1.16 \times 10^{10}$. We may put (40,4) in the form

$$p = A\rho^n + \frac{B}{M}\rho T = 1,16 \times 10^{10}\rho^{2,6} + \frac{B}{M}\rho T, \qquad (40,20)$$

in which M is the mean molecular weight and

$$\frac{B}{R} = \frac{k-1+2\alpha}{2}L.$$

Table 55 gives b, b_1, and β, as well as other parameters, as functions of ρ_0 for $Q = 1$ kcal/g and $M = 30$; the mean L for the products is 6, n and

Table 55

Parameters for the Equation of State and for the Detonation Front (Q = 1 kcal/g)

ρ_0, g/cm³	D, m/sec	ρ_i, g/cm³	$10^{-4}p_H$, kg/cm²	u_i, m/sec	ΔQ_i, cal/g	C_{v_i}, cal/mole-deg	ΔT_i, °K	$\frac{B}{R}$	b	b_1	A_0
0	2 180	0	0	910	490	6,0	5000	1,0	1,12	30	1.25
0,1	2 500	0.17	0,26	1040	487	7,0	4900	1,0	1,37	30	1,30
0,25	2 800	0.40	0,72	1020	480	7,5	4000	1,8	1,64	29	1,38
0,32	2 950	0.52	1.00	1060	466	8,0	4200	2,4	1,80	17,5	1,42
0,50	3 300	0,73	1.70	1030	453	8,5	3850	3,90	2,05	15,0	1,52
0,75	4 300	1,02	3.60	1130	435	9,0	3500	6,00	3,05	14,0	1,78
1,00	5 350	1,50	7.00	1330	416	9,5	3150	7,27	4,30	10,0	2,10
1,25	6 500	1,65	12,50	1540	381	10,0	2750	8,0	5,9	9,7	2,45
1,70	8 000	2,20	24,80	1800	265	11,0	1750	8,1	7,8	7,7	2,93
2,25	10 000	2,67	49,50	2200	0	12,0	0	8,7	10,0	7,0	3,60

A being as above.

The properties of the products gradually approach those of an ideal gas as the expansion proceeds; (40,9) cannot be used to discuss this

transition, for it represents the behavior accurately only for very high pressures. Instead, we use the energy equation,

$$E=\frac{p_i v_i - p_k v_k}{k-1}+\Delta Q, \tag{40,21}$$

in which subscript i denotes the initial state (that at the front) and subscript k some intermediate state, ΔQ being the residual heat in that state (the state in which the mixture becomes effectively an ideal gas). Any subsequent expansion obeys the law

$$pv^{\gamma}=p_k v_k^{\gamma}=\text{const}, \tag{40,22}$$

in which

$$\gamma=\frac{c_p}{c_v} \quad \text{for} \quad p<p_k \text{ and } v>v_k$$

and

$$\Delta Q_k=\frac{p_k v_k}{\gamma-1}. \tag{40,23}$$

Now (40,9) is the isentropic equation for the first stage of expansion, so

$$p_k v_k^k = p_i v_i^k, \tag{40,24}$$

The energy equation is

$$E=Q+\frac{p_i}{2}(v_0-v_i)=Q+\frac{D^2}{(k+1)^2}. \tag{40,25}$$

Comparison of (40,21) with (40,25) gives us

$$\Delta Q_k=\frac{p_k v_k}{\gamma-1}=Q+\frac{D^2}{2(k+1)^2}+\frac{p_k v_k}{k-1}-\frac{p_i v_i}{k-1},$$

which, when the $p_k v_k$ of (40,23) is inserted, becomes

$$\frac{RT_k}{\gamma-1}=\Delta Q_k=\frac{k-1}{k-\gamma}\left[Q-\frac{D^2}{2(k^2-1)}\right]. \tag{40,26}$$

That is, we replace

$$pv^{\eta(p,v)}=\text{const}$$

(an equation of isentropy with η variable) by (40,9) and (40,22), which are matched to ensure that the law of conservation of energy is obeyed.

It is very convenient here to introduce the k_0 defined by

7

This is an approximation, and (40,26) shows that this k_0 corresponds to $\Delta Q=0$; then we use a single formula $p=M(\rho)\rho^{\gamma}$ for the entire range of the expansion. Table 55 shows that $k_0=3$ for ρ_0 of 1.55 to 1.63 (the

usual range for high explosives). This means that we may use a mean value $\bar{k}$ of 3 in approximate calculations on detonation-front parameters and on the expansion of the products; precise calculations require the k_i of Table 54, of course. The basic relations for detonation waves then become

$$\left.\begin{aligned} p_i &= \frac{\rho_0 D^2}{k+1} = \frac{\rho_0 D^2}{4}; \quad c_i = \frac{k}{k+1} D = \frac{3}{4} D, \\ u &= \frac{1}{k+1} D = \frac{1}{4} D; \quad \frac{\rho_i}{\rho_0} = \frac{k+1}{k} = \frac{4}{3}. \end{aligned}\right\} \tag{40,27}$$

(here and henceforth, by k is meant k_0).

ZEL'DOVICH and KOMPANEYETS have given a more rigorous treatment based on the above assumptions; their results are

$$p = B v^{-n} (1 + y),$$

$$D^2 = Q \frac{\left\{ n + 1 + \left[2 + \frac{1}{\xi} \left(\frac{n}{2} - \frac{1}{3} \right) y \right] \right\}^2}{\left(\frac{1}{n-1} + \frac{6\xi y}{3n-1} \right) \left\{ n + \left[1 + \frac{1}{\xi} \left(\frac{n}{2} - \frac{1}{3} \right) \right] y - \frac{1}{2} (1+y)^2 \right\}} \tag{40,28}$$

$$y = \frac{c_v T_v^{n-1}}{R} \left(\frac{n}{2} - \frac{1}{6} \right) = \frac{p_m}{p_e} \tag{40,29}$$

is the ratio of the temperature component of the pressure to the elastic component, $\xi = \frac{c_v}{c_{v1}}$ (in which c_{v1} is the specific heat associated with the vibrational motion, which is converted to forward motion or rotation as the expansion proceeds), n is as above, and B is a constant dependent on the nature of the explosive. The relation of D to ρ_0 for TEN gives $B/Q = 0.473$ and $\xi = 4.8$; n is 2.8 to 3.0, which is almost exactly LANDAU and STANYUKOVICH's value. Calculations from (40,19) and (40,29) also give similar results. The D for a condensed explosive may be calculated approximately from

$$D_2 = D_1 \sqrt{\frac{Q_2}{Q_1}}, \tag{40,30}$$

in which subscript 1 relates to some standard explosive (say, trotyl) whose D is known accurately as a function of ρ_0. This gives D in terms of Q for a given density; the results are in agreement with experiment.

Example. Determine D for hexogene for $\rho_0 = 1.6$; $Q_2 = 1360$ kcal/kg. The D_1 for trotyl for this density is 7000 m/sec ($Q_1 = 1000$ kcal/kg), so (40,30) gives

$$D_2 = 7000\sqrt{\frac{1.36}{1}} \approx 8160 \text{ m/sec.}$$

Measurements give D for hexogene at 1.6 g/cm^3 as 8200 m/sec.

The following is a simple method of deducing k, which was described by POKROVSKIY and STANYUKOVICH. The perpendicular to the axis of a long charge makes a certain angle φ with the direction of maximum density for the fluxes of energy and momentum; we may assume that

$$\tan\varphi = \frac{u_1}{w},$$

in which u_1 is the speed of the products along the axis behind the front and w is the speed of the products escaping from the surface of the charge along the normal to the axis. Now

$$u_1 = \frac{D}{k+1}, \quad w = \frac{2kD}{k^2-1}, \text{ so}$$

$$\tan\varphi = \frac{k-1}{2k}, \quad k = \frac{1}{1-2\tan\varphi}.$$

This means that we have only to measure φ; various methods are available. For example, a curved charge may be detonated on an aluminium plate, in which case the damage is most pronounced along an arc of radius r that lies near the center of curvature. A simple geometrical construction shows that

$$\tan\varphi = \frac{1}{\sqrt{\frac{R^2}{r^2}-1}}, \quad \text{so} \quad k = \frac{1}{1-\frac{2}{\sqrt{\frac{R^2}{r^2}-1}}}.$$

DOKUCHAYEV has made many measurements of this kind, which have given k of 2.85 to 3.0 for R between 2.5 and 11 cm; R appears not to affect k at all, so we may say that the direction of escape is established very close to the charge, where the density is high and so k is effectively constant.

BAUM and SCHACHTER have used an entirely different method to test

the compression law for condensed explosives. Here use was made of the kinematic parameters of the shock waves set up in certain media in order to test the law for pressures up to 2 x 10^5 kg/cm^2. [illegible] is very convenient for this purpose, because the region in the shock wave becomes opaque; the motion of the wave can be recorded photographically.

If the charge is in contact with the water, we must have that $p_x = p'$ and $u_x = u_i'$ when the detonation wave reaches the interface (here p_x is the pressure in the gas, p' is the initial pressure of the shock wave in the water, u_x is the speed of the interface, and u_i' is the initial flow speed behind the shock front in the water). The compressibility of water is very much larger than that of the highly compressed products, so a rarefaction wave appears in the latter; then

$$u_x = u_i + \int_{p_x}^{p_i} \frac{dp}{\rho c}$$

(ρ is density), which, with the equation of isentropy $p = A\rho^k$, gives us that

$$u_x = \frac{D}{k+1}\left\{1 + \frac{2k}{k-1}\left[1 - \left(\frac{p_x}{p_i}\right)^{\frac{k-1}{2k}}\right]\right\}. \qquad (40,31)$$

Then

$$u' = \sqrt{(p_x - p_0)(v_{0w} - v_{xw})}, \qquad (40,32)$$

in which v_{0w} and v_{xw} are the specific volumes of water in the unperturbed state and at the front respectively. But $p_x \gg p_0$, so (40,32) may be put as

$$u' = \left[\frac{p_x}{\rho_{0w}}\left(1 - \frac{\rho_{0w}}{\rho_{xw}}\right)\right]^{\frac{1}{2}}. \qquad (40,33)$$

The relation of p to ρ for water is given for a wide range of pressures by

$$p_w = A\left[\left(\frac{\rho_{xw}}{\rho_{0w}}\right)^n - 1\right]. \qquad (40,34)$$

COLE gives A = 3047 kg/cm^2 and n = 7.15 for fresh water on the basis of BRIDGMAN's results for the compressibility as a function of temperature;

(40,33) and (40,34) give us that

$$u' = \sqrt{\frac{p_\infty}{\rho_{0\infty}}(1-\beta)}, \qquad \beta = \frac{\rho_{0\infty}}{\rho_{x\infty}} = \left(\frac{p_\infty}{A}+1\right)^{-\frac{1}{n}}. \tag{40,35}$$

The shock wave has a speed

$$D' = \frac{u'}{1-\frac{\rho_{0\infty}}{\rho_{x\infty}}} = \frac{u'}{1-\beta} = \sqrt{\frac{p_\infty}{\rho_{0\infty}}\frac{1}{1-\beta}}. \tag{40,36}$$

SCHACHTER has measured the initial speeds of shock waves produced in water by trotyl and by retarded hexogene; the speeds were measured in the direction of propagation of the detonation wave in the charge (Table 56).

Table 56

Initial Parameters of Shock Waves in Water

Explosive	ρ_0, g/cm^3	D_1, m/sec	D', m/sec	p_∞, kg/cm^2	u', m/sec
Trotyl	1.61	7000	5560	129 000	2300
Hexogene	1.60	8000	6100	166 000	2665

Here D' is experimental, while p_∞ and u' are from (40,35) and (40,36).

Equation (40,27) enables us to put (40,31) as

$$u_\infty = u' = \frac{D}{k+1}\left\{1+\frac{2k}{k-1}\left[1-\left(\frac{p_\infty}{\rho_0 D^2}(k+1)^{\frac{k-1}{2k}}\right)\right]\right\}; \tag{40,37}$$

The only unknown is k, which is the quantity required. The results given by the parameters of Table 56 are satisfactory if n is taken as 3.17 for retarded hexogene and as 3.20 for trotyl; that is, these two very different explosives have almost the same equation of isentropy, which is

$$pv^{3,2} = \text{const}, \tag{40,38}$$

in which k (= 3.2) is close to the value of 3 assumed previously.

In 1958 COOK criticized the hydrodynamic theory on the ground that thermal conduction is not negligible for a detonation wave; he considered that a heat flux can move at a speed substantially in excess of

the speed of a normal detonation wave. The consequence of this is that he rejects the parameter distributions for the reaction zone implied by the ZEL'DOVICH-DÖRING theory (section 37). As confirmation of this he quotes his experiments on the spread of the emission region in tetranitromethane before the normal detonation conditions have become established (speed in excess of 30 km/sec). There is, however, no justification for equating the spread of the emission to the speed of the heat flux; other effects may be responsible. In particular, COOK's tetranitromethane charge was detonated from both sides simultaneously by symmetrically placed charges isolated by layers of lucite. There is always a delay before the detonation becomes normal under these conditions; a weak wave is generated initially, which releases only part of the chemical energy. This wave does not produce a strong emission. Two such waves interact to increase the parameters (especially the temperature) very substantially; the reaction proceeds much more rapidly in the reflected waves. This means that the delay before the emission becomes strong will vary from one part of the charge to another; it will be least in the plane in which the waves meet. This means that, under suitable conditions, the phase velocity of the emission can be indefinitely large; it has no relation to the rate of spread of heat.

The hydrodynamic theory has received an important confirmation in the recently published work of ZEL'DOVICH, TSUKERMAN, and RIVIN, in which short X-ray pulses were used to measure the density distribution. COOK's criticism of the hydrodynamic theory is not convincing; his deductions are based on an incorrect interpretation of his results.

41. Limiting Conditions of Stability

Any gas mixture will detonate stably only within certain limits of concentration. Table 57 collects limits as given by various workers.

Table 57

Concentration Limits for Detonation at Room Temperature and Atmospheric

Mixture	% H_2, etc.		D_L	D_U
	LL	UL	m/sec	m/sec
$H_2 + O_2$	20	90	1457	3550
H_2 + air	18.2	58.9	1500	2100
$CO_2 + O_2$ (moist)	38	90	—	1473
C_2H_4 + air	5.5	11.5	1675	1801
$C_2H_4 + O_2$	3.5—3.6	92—93	1607	2423
$C_2H_6 + O_2$	3.2	37	1587	2210
$C_4H_{10} + O_2$	2.9	31.3	1595	2188
$(C_2H_5)_2O + O_2$	2.7	40	1593	4323

These limits apply for tubes 10-20 cm in diameter under laboratory conditions; they are somewhat wider for larger tubes. KOGARKO and ZEL'DOVICH have found that H_2 in air has limits of 15 and 63.5% H_2 for a tube 305 mm in diameter, for example. The lower limit is a result of the fall in D and of the relative rise in the importance of heat loss.

If the above relationships apply to the entire reaction zone, then D cannot be less than would correspond to point M on the Hugoniot curve no matter how low the reaction rate may be. Two conditions basic to those relations must be complied with, namely a) there must be no loss of heat by conduction to the cold tube and no friction at the wall of the tube; b) the tube must be absolutely rigid. Then the front remains straight, and all parameters are functions only of a coordinate whose axis is that of the wave. These conditions do not apply to real tubes, of course; the reaction cannot persist at all unless the rate of production of heat exceeds the rate of loss, and, in the limit, $\eta = Q_w/Q \to 1$, in which Q_w is the energy used by the wave and Q is the chemical energy. The balance between production and loss moves unfavorably as the reaction rate falls; η decreases, with the result that D does the same. The energy balance as defined by HUGONIOT's equation is altered if $\eta < 1$;

the wave propagates as though the chemical energy had been reduced by the amount of the heat loss.

ZEL'DOVICH and LEYPUNSKIY have shown that the ignition conditions at a detonation front are essentially the same as those for ignition by rapid adiabatic compression. They ignited the explosive mixture by means of a bullet from a special small-caliber rifle; a shock wave having the speed of the bullet was formed at the tip. Speeds of 1700-2000 m/sec were sufficient to ignite $2H_2 + O_2 + 5Ar$, although the gas was compressed for no more than 10 μsec.

VENDLAND has calculated the temperature at the front of a shock wave moving in a limiting mixture with a speed equal to the limiting stable D; he finds it to be close to the ignition temperature as measured by adiabatic compression. Of course, the excitation mechanism for a condensed explosive is rather more complicated, for the temperature change in the compressed layer is comparatively small.

The above results show why D is reduced when the tube is of small diameter; much heat is lost to the wall. ZEL'DOVICH has considered the theory of the limits and D as affected by heat loss and friction; the detailed treatment is given in ZEL'DOVICH and Kompaneyets's book "Theory of Detonation".

Similar effects, which may retard or suppress the detonation, can occur if the tube or casing ruptures during the process; this occurs mainly for condensed explosives, which produce very high pressures. The products then escape from the sides; the resulting rarefaction wave enters the reaction zone and may cause the pressure at the front to fall very greatly. The precise effect is dependent on the ratio of the width l of the reaction zone to the diameter d_2 of the charge. Let τ_1 be the reaction time, and let τ_2 be the time needed for the wave to

propagate back to the axis of the charge (a distance $d_3/2$); then

$$\tau_1 = \frac{l}{D} \qquad \tau_2 = \frac{d_3}{2c}, \tag{41,1}$$

in which c is the speed of that wave (the speed of sound in the products). If $\tau_1 > \tau_2$, the wave reaches the zone before the reaction is complete, in which case the pressure at the front will fall below that corresponding to point M on the HUGONIOT curve; the products start to expand rapidly before the reaction is complete, so not all of the energy is utilized and D is reduced. Figure 71 illustrates the general behavior of the rarefaction wave.

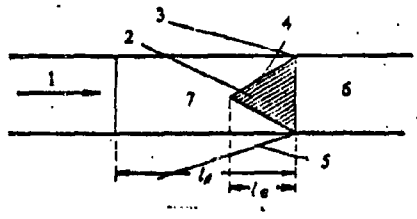


Fig. 71. Detonation in an open cylindrical charge. 1) Detonation direction; 2) rarefaction wave; 3) region unaffected; 4) rarefaction front; 5) front of escaping products; 6) explosive; 7) zone of products.

Here D is a function of l_e/l_p, in which l_e is the effective length of the reaction zone. The D corresponding to point M is then the maximum speed; the minimum diameter of charge d_m that can ensure this speed is given by $\tau_1 = \tau_2$ or $\frac{l}{D} = \frac{d_3}{2c}$ as

$$d_m \approx l, \tag{41,2}$$

because $c \approx \frac{D}{2}$ (see section 42). This applies to a charge of unlimited length.

COOK and others have drawn the same conclusion from the effects of particle size on D and on the radius of curvature of the detonation front. This enables us to evaluate the reaction rate if d_m is known. Figure 72 illustrates the situation in a charge of this diameter; the hatched area represents the zone that remains unaffected by the rarefaction wave during the reaction. The central zone of the detonation

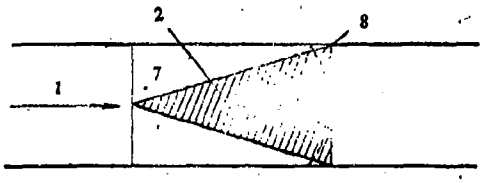


Fig. 72. Detonation in a charge of diameter d_m; 8) profile of wave front; other notation as for Fig. 71.

wave moves with a speed D, whereas parts nearer the edge [illegible] lower speeds. The result is a curved detonation front of the shape shown in Fig. 72. The radius of curvature R is roughly equal to l_e if d_1 lies between d_m and d_c (the critical diameter); the speed of any given point on the front varies as the sine of the angle between the axis of the charge and the tangent at that point. The process is steady, so the front moves without change of shape.

BELYAEV has recorded the motion of such fronts and has demonstrated that the central part does move appreciably faster than the edge. COOK has made systematic studies for various explosives; he finds that the front is spherical and that $0.5 < R_{max}/d_3 \leq 3.5$ for all the explosives he examined (apart from NH_4NO_3).

D starts to fall if d is reduced below d_m and reaches a limit D_c at d_{c_1}. This represents a limit to the stable state; below it, no shock wave can excite a self-sustaining reaction leading to a stable detonation wave. If D_1 and hence the pressure of the shock wave, falls below this limit, the explosion wave dies away. The critical shock-wave parameters are characteristic of the explosive. Other things being equal, the higher the reaction rate, the lower d_m and d_c; the casing has an effect here, because it restricts or prevents the escape of the products.

KHARITON formulated the stability criterion in the form $\tau_1 < \tau_2$; he

considered that no steady detonation was possible for $\tau_1 > \tau_2$. The measured d_m agree closely with those given by (41,2), which tends to confirm this view. If we assume that D is a function of $l_e/l_{p\,m} = \varphi$, being maximal for $\varphi = 1$, we can establish a relation between D and d for the range $d_c \leqslant d \leqslant d_m$ for charges of constant density and particle size. We assume that Q_x, the energy taken up by the front, is proportional to l_e ($Q_x = Q$, the total energy of reaction, when $l_e = l_{p\,m}$), so $\frac{Q_x}{Q} = \frac{l_e}{l_p}$. But $D' \propto Q$ and $l_e = \frac{1}{3}$, so

$$\frac{D_x}{D_m} = \sqrt{\frac{d_x}{l_{p.\,m}}}, \qquad (41,3)$$

d_x being the diameter and D_m the maximum D. Now l_x increases as d_x decreases, on account of energy losses and reduced temperatures; l_p can be deduced from kinetic considerations. Here $l_x = \tau D_x$ and $\tau = \frac{1}{v_x}$, in which v_x (the reaction rate) is proportional to $\exp(-E/RT_x)$. These relations imply that

$$\frac{l_x}{l_{p.\,m}} = \frac{D_x}{D_m} e^{\frac{E}{RT_{max}}\left(\frac{T_{max}}{T_x} - 1\right)}, \qquad (41,4)$$

in which T_x is the temperature corresponding to Q_x, T_{max} being the same for Q. Then (41,3) and (41,4) imply that

$$D_x = D_m \frac{d_x}{d_m} e^{-\frac{E}{RT_{max}}\left(\frac{T_{max}}{T_x} - 1\right)}. \qquad (41,5)$$

We need $T_x(d_x)$ in order to calculate D_x as a function of d_x; this presents some difficulty. However, $D_x(d_x)$ is known from experiment, so we can find $T_x(d_x)$; in this way we can find the temperature corresponding to the condition of limiting stability. In this connection, we may take the T of (41,5) to represent the mean temperature in the reaction zone.

JONES and EYRING have dealt with the theory of detonation for charges with $d < d_m$; the two treatments, although rather different, give almost precisely the same form for $\frac{D_m}{D_x} = f\left(\frac{a}{d}\right)$. , in which a is the width of the reaction zone. JONES's theory is based on representing the

charge as a material issuing from a nozzle (in a moving system of coordinates). Hydrodynamic relationships are deduced for the expanding products (the PRANDTL-MEYER problem). EYRING's theory differs from JONES's in the assumption that the wave front would be flat but becomes curved as a result of lateral escape of products. The relation of curvature to speed is deduced. Both theories deal with charges with and without cases; the case, if thin, is assumed to start moving before the reaction is complete, so its effects are determined by its inertia. On the other hand, the shock wave is taken to be responsible for the expansion if the case is very heavy; here lateral escape of products is mainly a result of the compressibility of the material.

The two theories often give good agreement with experiment; their main disadvantage is their assumption that the reaction zone is of constant width when $d < d_m$. KHARITON has claimed that any system in which an exothermic reaction is possible can be detonated under suitable conditions, no matter what the reaction rate; the slower the reaction, the greater d_m. This definition of capacity to detonate is not sufficiently precise, because it neglects the critical conditions associated with initiation at the detonation front. In fact, if Q is small, and if the D_m corresponding to that Q is less than the critical speed D_c (the speed needed to initiate the reaction), then no d however great can give rise to a steady detonation wave. (I. Ya. PETROVSKIY first directed attention to this point.) This means that we can assume that a system can be detonated only if it can give an exothermic reaction such that D can exceed D_c.

The above arguments as to the limits are dealt with in detail in chapter VIII, which presents experimental results.

42. Parameters of the Products Behind the Front

The detonation wave is always associated with a rarefaction wave, which appears as soon as the reaction is complete; the reason is that the products move with a speed u in the detonation direction immediately behind the reaction zone, where they are under high pressure. The products come to rest, and the pressure falls, if the charge is contained in an indefinitely strong tube closed at the starting end. It is readily demonstrated that the law of conservation of energy is violated if the rarefaction wave is neglected. The entropy at the detonation front remains constant, and behind the front we have an isentropic expansion, so the effect can be described in terms of the first two equations of gas dynamics. All parameters depend only on x and t (see section 22) if the wave is plane; the equations then become

$$\frac{\partial u}{\partial t}+u\frac{\partial u}{\partial x}+\frac{2}{k-1}c\frac{\partial c}{\partial x}=0, \tag{42,1}$$

$$\frac{2}{k-1}\frac{\partial c}{\partial t}+\frac{2}{k-1}u\frac{\partial c}{\partial x}+c\frac{\partial u}{\partial x}=0 \qquad (dS=0). \tag{42,2}$$

and these give us that

$$\frac{\partial}{\partial t}\left(u\pm\frac{2}{k-1}c\right)+(u\pm c)\frac{\partial}{\partial x}\left(u\pm\frac{2}{k-1}c\right)=0. \tag{42,3}$$

If

$$u=\pm\frac{2}{k-1}c+\text{const.} \tag{42,4}$$

(42,3) is satisfied exactly, so the initial system of equations can be put as

$$\frac{\partial u}{\partial t}+(u\pm c)\frac{\partial u}{\partial x}=0, \tag{42,5}$$

which enables us to put the solution as

$$x=(u\pm c)t+F(u). \tag{42,6}$$

This describes propagation in one direction only (a feature characteristic of detonation waves); the positive sign is taken if the propagation is from left to right in the direction of x increasing, and vice versa.

Then the parameters are given by the solutions

$$\left.\begin{aligned} x &= (u \pm c)\,t + F(u), \\ u &= \pm \frac{2c}{k-1} + \text{const}. \end{aligned}\right\} \qquad (42,7)$$

Let us suppose that the detonation starts at the closed end of the tube $(x=0)$ at time $t=0$ and propagates from left to right; the plus sign is then used in (42,7). The position for $t=0$ is defined as $x=0$, so $F(u)=0$, and

$$x = (u+c)\,t. \qquad (42,8)$$

For a strong detonation wave,

$$u_i = \frac{D}{k+1}, \quad c_i = \frac{k}{k+1} D.$$

Then the constant in (42,4) is

$$\text{const} = -\frac{D}{k-1}. \qquad (42,9)$$

Thus the rarefaction wave is described by

$$\frac{x}{t} = u + c, \quad u = \frac{2c-D}{k-1}. \qquad (42,10)$$

The tube is closed at $x=0$, so these equations apply only for x for which u is not zero; all parameters remain constant back as far as $x=0$ from the point at which $u=0$.

The products from condensed explosives, which give strong detonation waves, have $k=3$; then (42,10) takes the very simple form

$$\frac{x}{t} = u + c, \quad -\frac{D}{2} = u - c, \qquad (42,11)$$

so

$$c = \frac{x}{2t} + \frac{D}{4}, \quad u = \frac{x}{2t} - \frac{D}{4}. \qquad (42,12)$$

At the front, $\frac{x}{t} = D$, $u_i = \frac{1}{4}D$, and $c_i = \frac{3}{4}D$; when $u=0$,

$$\frac{x}{t} = \frac{D}{2}, \quad c_2 = \frac{D}{2}. \qquad (42,13)$$

Then (42,12) implies that u and c vary linearly in the range $\frac{D}{2} > \frac{x}{t} < D$; $u = 0$ and $c = \frac{D}{2}$ for $0 < \frac{x}{t} < \frac{D}{2}$.

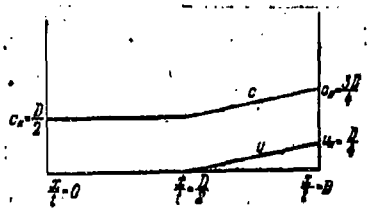


Fig. 73. Variations in u and c behind a plane wave with $k=3$.

Figure 73 shows u and c as functions of time; the point of transition from expansion to rest lies half-way between the detonation front and the point of initiation.

If $k=3$,

$$p=p_i\left(\frac{\rho}{\rho_i}\right)^3, \qquad c=c_i\frac{\rho}{\rho_i},$$

so for the point at which $u=0$,

$$p_x=\frac{8}{27}p_i, \quad \rho_x=\frac{2}{3}\rho_i=\frac{8}{9}\rho_0. \tag{42,14}$$

That is, the pressure follows a power law, while the density varies linearly. Figure 74 shows this. All parameters are functions of $\frac{x}{t}$ only, so the wave gradually becomes broader but does not change in shape (a self-modeling process). Table 58 gives results for various values of k; the pressure ratio clearly is little affected by k.

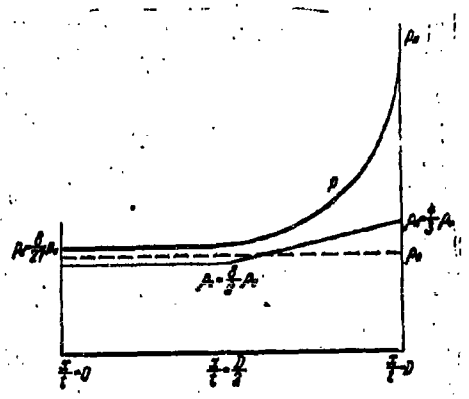


Fig. 74. Variation in p and ρ behind a plane wave with $k=3$.

Similarly, a spherical charge detonated at the center gives a wave whose parameters are functions of r/t only; ZEL'DOVICH has given the detailed argument, of which only the main results are presented here. Figure 75 shows the parameters for $k=3$. Here c is somewhat less than $D/2$ for the point at which $u=0$. A characteristic feature of spherical waves is that the pressure falls very sharply behind the front; the pressure and density at the front and at the center are as for the corresponding points on a plane wave.

Table 58

Density and Pressure in the Zone of Rest as Functions of k

k	$\frac{p_x}{p_i}$	$\frac{\rho_x}{\rho_i}$
3.0	0.30	0.67
1.66	0.33	0.51
1.40	0.34	0.46
1.20	0.35	0.42
1.0	$0.369=\frac{1}{e}$	0.369

The first result of a detonation in a closed space is a pressure p_{op} (the same at all points), the density being still ρ_0. This pressure is given by $\frac{p_{av}v_0}{k-1} = Q_v$, so

$$p_{av} = (k-1)\rho_0 Q_v. \qquad (42,15)$$

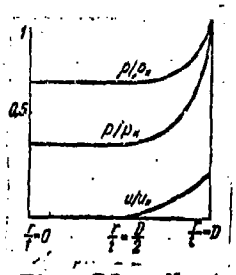


Fig. 75. Variation of p, ρ, and u behind a spherical detonation wave.

The pressure at the detonation front is

$$p_f = 2(k-1)\rho_0 Q_v. \qquad (42,16)$$

so $p_f/p_{av} = 2$. The increased pressure at the front is balanced by reduced pressures elsewhere, because $p_s = 0.6p_{av}$. The maximum pressure would be p_{av}, if the reaction was simultaneous at all points; that is, the local effect of a simultaneous explosion would be less than that of a normal detonation, although the total effect, being governed by the energy release, would be the same.

The above results show that a detonation causes substantial changes in the energy content and other parameters of the products; we shall see (in chapter XIII) that this feature occurs also for the processes of escape from the surface of the charge.

Bibliography

1. K. P. Stanyukovich. Transient-State Motion of a Continuous Medium [in Russian], Gostekhizdat, 1955.
2. Ya. B. Zel'dovich and A. S. Kompaneyets. Theory of Detonation [in Russian], Gostekhizdat, 1955.
3. R. Courant and K. O. Friedrichs. Supersonic Flow and Shock Waves [Russian translation], IL, 1950.
4. R. Cole. Underwater Explosions [Russian translation], IL, 1950.
5. Ya. B. Zel'dovich. Theory of Shock Waves: an Introduction to Gas Dynamics [in Russian], Izd. Akad. Nauk SSSR, 1946.

6. V. A. Mikhel'son. Collected Works [in Russian], vol. 1. Izd. Novgy Agronom, 1930.

7. Ya. B. Zel'dovich. Theory of Combustion and Detonation in Gases [in Russian], Izd. Akad. Nauk SSSR, 1944.

8. Ya. B. Zel'dovich. Zh. Éksper. Teoret. Fiz., 10, 542 (1940).

9. G. N. Abramovith and L. A. Vulis. Dokl. Akad. Nauk SSSR, 55, 111 (1947).

10. Ya. B. Zel'dovich and I. Ya. Shlyapintokh. Dokl. Akad. Nauk SSSR, 65, 871 (1949).

11. V. Rozing and Yu. Khariton, Dokl. Akad. Nauk SSSR, 26, 360 (1939).

12. A. F. Belyaev. Dokl. Akad. Nauk SSSR, 18, 267 (1938).

13. A. Ya. Apin. Dokl. Akad. Nauk SSSR, 50, 285 (1945).

14. L. D. Landau and K. P. Stanyukovich. Dokl. Akad. Nauk SSSR, 46, 399 (1945).

15. E. Jouget. Mechanique des Explosifs. Doin et Fils, Paris, 1917.

16. B. Lewis and G. Elbe. Combustion, Flame, and Explosion in Gases [Russian translation]. IL, 1948.

17. Collection of Articles on the Theory of Explosives [in Russian], Oborongiz, 1940.

18. M. A. Cook. The Science of High Explosives, New York, 1957.

CHAPTER VIII

EXCITATION AND PROPAGATION OF DETONATIONS

43. Excitation

Thermal or mechanical shock, or the direct action of a detonator, is the usual means of initiating an explosion. The initiation conditions are dependent on the method used, on the type of explosive, and on the parameters of the charge. Heating or local ignition almost always produce a period during which the material burns at an increasing rate; the duration of this phase is dependent on the density and diameter of the charge, the initial temperature, the external pressure, the strength of the casing, and so on. The process may develop rapidly or not at all (in the latter case, the charge merely burns). Some detonators detonate almost instantaneously no matter what the conditions.

Section 6 deals with initiation by impact; the typical features are as follows. The hot spots produced by the blow are the active centers; the reaction in these spots goes to completion long before the blow is over, and so it propagates into the material with the speed characteristic of explosions. These conditions are very different from those of thermal initiation; all transient effects are restricted to a thin layer of material deformed by the blow and last only a hundred microseconds or so. The subsequent propagation is dependent on the extent of the process in the primary layer; a powerful blow causes the charge to detonate, whereas a light one may cause a local spark that dies away.

Initiation by a detonator was discovered by NOBEL in 1864; he observed that nitroglycerine or dynamite was readily caused to explode completely by means of a small charge of mercury fulminate. Subsequent research revealed detonators even better than mercury fulminate; these are principally certain inorganic azides, and, in particular, lead azide, which has largely displaced mercury fulminate. High explosives with little tendency to detonate are nowadays commonly detonated by means of more sensitive explosives (TEN, hexogene, tetryl), which themselves are initiated by a detonator.

Much experimental work has been done on detonators, but the initiation mechanism was long neglected; major studies have been made only since the war, in particular by BELYAEV, KHARITON, PETROVSKIY, and SHEKHTER in the USSR. The mechanism is now considered to be as follows.

The detonator is in close contact with the charge, as in Fig. 76.

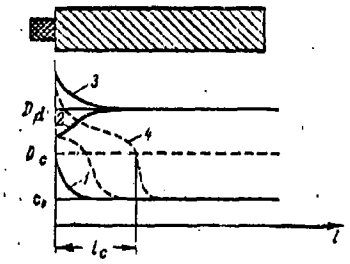


Fig. 76. Development of an explosion in a charge.

A shock wave starts to propagate through the charge when the detonator explodes; for simplicity, we assume that the density and compressibility of the two materials are the same, which means that the speed of the wave does not alter as it passes through the interface. No detonation can arise directly via the impact mechanism if the initial speed of the shock wave is below the speed of sound; for example, consider an attempt to detonate a charge of trotyl of density 1.60 g/cm^3 by means of ammotol 90/10. If the latter is used in a diameter close to the critical diameter, the detonation speed will be about 1600 m/sec, which is too low to excite an explosion directly in trotyl,

because the speed of sound for trotyl of that density is (according to REMPEL') about 1900 m/sec; for $\rho_0 = 1.665$ (a monocrystal of TNT), the speed is 2700-2800 m/sec.

Of course, the hot products from the detonator may ignite the charge, and the burning may go over to detonation under favorable conditions.

The following cases are possible if the speed of the initiating wave is greater than c_0 but close to D_e.

I. The shock wave cannot produce a self-sustaining reaction; it rapidly dies away, much as it would in an inert substance. The charge does not detonate, but it may be scattered. This corresponds to curve 1 of Fig. 76.

II. The wave ignites the charge, and the burning passes over into a detonation.

The detonation may also be initiated directly by the shock mechanism; the shock wave travels at a relatively low speed in the first part of the charge. The explosion is then delayed by some microseconds. Such conditions are close to the critical ones, and, in practice, the process is liable to die out.

The first necessary condition is then that the initiating wave should have a speed in excess of some limit; this is readily ensured if the detonator explodes with sufficient speed, as is usually the case. The second necessary condition is that the energy release should be sufficient to maintain the pressure at the front. The proportion of the energy so used has already been calculated (section 41) as a function of l_p/l_e (Fig. 71). The speed D_r of the rarefaction wave in an open charge is almost constant; $D_r \approx D/2$, so l_e/l_p determines the reaction rate, other things being equal. An increase in rate reduces

l_p and so increases the proportion of the energy that is used at the front.

The l_e for the steady state is dependent on the diameters of charge and casing. The initial width of the wave is very much dependent on the parameters of the detonator; the area of contact increases with the diameter of the detonator, and this has the effect of increasing the effective depth of the reaction zone. The detonator is most effective, other things being equal, when its diameter is the same as that of the main charge. An increase in length for a given diameter also tends to increase l_e, because the layer of products will tend to prevent the rarefaction wave from entering the reaction zone. However, not all of the products move along the line of propagation of the detonation, and the limiting effect is attained when the length is about twice the diameter (for open charges). That is, the effective depth is proportional to the active length of the detonator, l_a, other things being equal. The duration of the action also increases with l_a, and this prevents an early fall in the parameters of the initiating wave.

The following factors favor detonation in a charge of a given density.

1. Smaller crystal size. The less the size, the more numerous the active centers, and the more rapidly the reaction goes to completion. The result can be a substantial increase in the ease of detonation, as LEITMAN has observed (section 9).

2. Detonator buried in charge. The rarefaction wave is largely suppressed, and the area of action is increased.

3. Increased charge diameter and the presence of a casing. These restrict the effects of rarefaction waves.

If l_e/l_p is small in the initiation layer, on account of a low

reaction rate, the process at first propagates with a reduced speed. Autocatalysis may then raise the rate to the normal detonation speed (case 2 of Fig. 76), as is often observed.

If the detonation rate of a detonator of optimal length is much in excess of that rate for the main charge, the speed of the wave in the first part of the charge (several cm) may be in excess of the normal rate (curve 3 of Fig. 76).

The above discussion shows that the detonation region is always preceded by a region of transient conditions; the length of the latter region is dependent on many features of the charge and detonator. The normal rate can be attained almost at once if conditions are favorable, especially if the detonator produces a powerful pulse. Unfavorable conditions may cause the process to die out, especially so after the speed of the initiating wave has fallen below a certain limit (curve 4 of Fig. 76). This becomes more likely as the density increases, other things being equal, because e_0 increases, and with it D_c; SHEKHTER finds that an increase from 1.4 to 1.6 g/cm^3 for retarded hexogene causes a rise from 2300 to 2600 m/sec in D_c. (REMPEL' gives e_0 as about 7000 m/sec for 1.6 g/cm^3.) Moreover, the proportion of air spaces decreases, which means that less hot spots are produced by the initiating wave. Experiments in fact show that charges are less readily detonated at the higher densities, the effects being most pronounced for ammonites.



Fig. 77. Charge for measuring l_c: 1) charge; 2) electrical detonator; 3) brass plate; 4) steel plate.

The curve for a decaying explosion has two parts. In

the first, the speed falls slowly to D_c; this corresponds to a critical length l_c. In the second, the reaction is no longer excited, so the speed falls very rapidly; the length corresponding to this part is only 5-10 mm. It is found that l_c increases with the initiating capacity of the detonator and also with the sensitivity of the charge. These properties are used in the Artillery Academy test for detonators, in which l_c is used as the criterion. A charge of low susceptibility (e.g., TNT mixed with DNT, or ammonium-nitrate mixtures of high density) is used, the length l of the charge being such that $l_c < l$. The charge is used as shown in Fig. 77; the explosion leaves a clear impression on the plate (Fig. 78). Figure 79 shows l_c as a function of height of detonator for tetryl (d = 24.5 mm, ρ_0 = 1.6 g/cm^3; after PETROVSKIY). The limit is reached when the height is 50 mm, which is about 2d

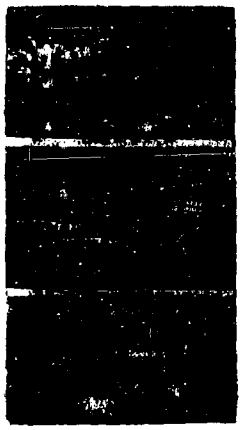


Fig. 78. Impressions on brass plates.

Figures 80 and 81 illustrate the effects of detonator diameter at constant weight (20 g; tetryl detonators). Clearly, l_c increases with d, although h becomes less than optimal; this shows that d is the more

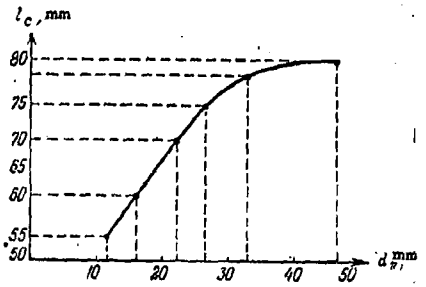


Fig. 79. Relation of l_c to height of detonator.

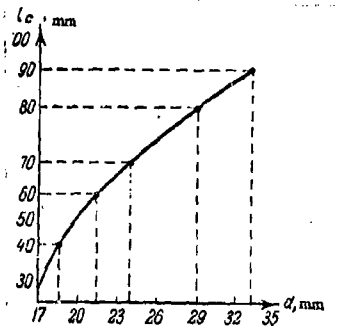


Fig. 80. Relation of l_c to detonator diameter.

important factor, l_c being a linear function of d_{ic}/d. As one would expect, l_c increases greatly when the detonator is enclosed in the charge.

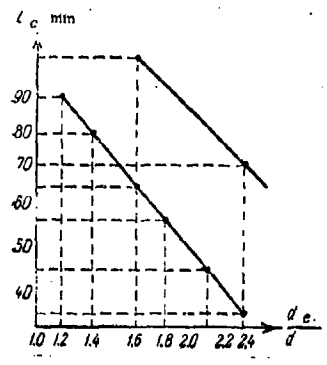


Fig. 81. Relation of l_c to d_{ic}/d; the top line is for a detonator enclosed in the charge.

44. Propagation of Detonation Processes

BERTHELOT and others made detailed studies for gas mixtures in 1881-1890, followed later by DIXON and others. The principal work in the USSR has been done by SHCHELKIN, ZEL'DOVICH, and SOKOLIK. The results are as follows.

1. D varies from 1000 to 3500 m/sec, which speeds are rather higher than the speed of sound at ordinary pressures and temperatures.

2. D is not appreciably dependent on the position of the tube (vertical or horizontal), on the material and thickness of the wall, and on the diameter (provided that this exceeds a certain limit).

3. D is not dependent on the initiation conditions (open or closed end of tube, spark or flame initiation, etc.), which affect only the length of the transition region.

4. D varies little with the initial temperature (Table 59), which affects only the ignition conditions. The slight fall at the high temperature is caused by the reduction in density (the tests were done at atmospheric pressure).

Table 59

Effect of Initial Temperature on Detonation Rate

T_0	$2H_2+O_2$	CH_4+3O_2
	D m/sec	D m/sec
10°	2821	2581
100°	2790	2538

5. D generally increases

with ρ_0 (pressure), slowly at low pressures and more rapidly at high ones.

6. D is dependent on the composition; every pair of gases has a best ratio (the one giving the highest D; Fig. 82).

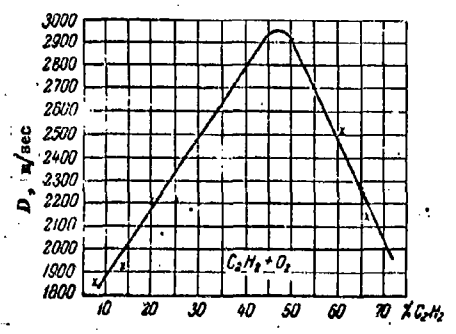


Fig. 82. D for acetylene-oxygen mixtures as a function of composition.

Dilution with either component results ultimately in a mixture that will not give a stable detonation wave; for example, one limit for hydrogen-air mixtures lies at 18.5% hydrogen. This limit corresponds to $D = D_c$. The lower limit for ordinary combustion, for comparison, is 4.1% hydrogen. Similarly, the upper concentration limit for detonation lies well below the upper limit for ignition.

Inert gases also affect D, but the effects are very much dependent on the nature of the diluent. For example, excess of hydrogen (which remains unused) within certain limits actually increases D, although the temperature of the explosion is reduced (Table 60). The increase is associated with the decrease in the mean molecular weight in this case; (38,18) shows that D^2 is inversely proportional to the density of the products, so helium added to $2H_2 + O_2$ also increases D, whereas an equal

Table 60

Effects of Diluting Explosion Mixture with Hydrogen

	T_c, °K	D
$2H_2 + O_2$	3583	2819
$(2H_2 + O_2) + 2H_2$	3314	3273
$(2H_2 + O_2) + 4H_2$	2976	3527
$(2H_2 + O_2) + 6H_2$	2650	3532

molar proportion of argon reduces D (Table 61), although both gases affect the temperature identically.

Table 61

Effects of Helium and Argon on D, for Explosion Mixture

	T_e, °K	D
$2H_2 + O_2$	3583	2819
$(2H_2 + O_2) + 3He$	3265	3130
$(2H_2 + O_2) + 5He$	3097	3160
$(2H_2 + O_2) + 3Ar$	3265	[illegible]
$(2H_2 + O_2) + 5Ar$	3097	[illegible]

The theory shows that D for a condensed explosive is primarily dependent on Q, other things being equal, although the physical parameters of the charge are important. The major factors here are the diameter, density, phase state, crystal size (for solids), and casing (if any). Some of these determine whether a detonation will occur at all under certain conditions. Many studies have been made of the effects of charge diameter d; BELYAEV and BOBOLEV in the USSR, and COOK abroad, have made the most systematic investigations. It is found that D increases with d up to some limit d_m, which varies from one explosive to another. Figure 83 shows the general form of the relation.

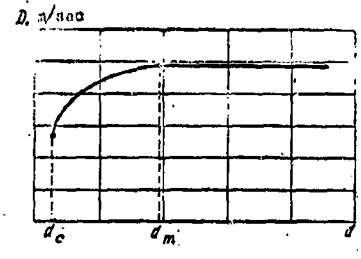


Fig. 83. Relation of D to diameter of charge.

Published results indicate that d_m is about 30 mm for dynamite and cast TNT, or 10 mm for TNT pressed to a ρ_0 of 1.60 g/cm^3. Hexogene with a ρ_0 of 1.0 g/cm^3 has a d_m of only 3-4 mm, whereas cast 50/50 ammotol has a d_m of about 120 mm. No steady-state detonation is possible unless $d > d_c$; the process simply dies away after a certain distance. This d_c corresponds to the D_c for the given conditions. BELYAEV has measured d_c for ammonites, and BOBOLEV for other explosives; d_m and d_c are found to be functions of density, grain size, and casing

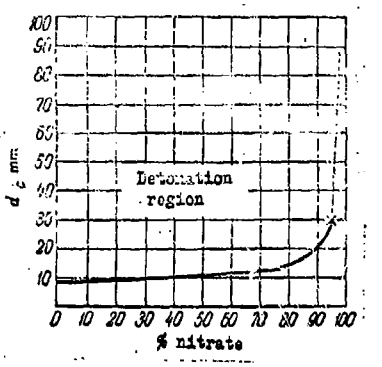


Fig. 84. Relation of critical diameter to composition for ammotol.

conditions even for a given explosive. In particular, d_c is very sensitive to composition, as Fig. 84 shows for ammotol (ammonium nitrate mixed with TNT; after BELYAEV). Here the density varied only from 0.83 to 0.85 g/cm^3; the powders were sieved to give a maximum grain size of 0.4 mm before use. Clearly, d_c rises very sharply above the 80/20 composition, although D falls only from 1300 to 1100 m/sec between compositions 80/20 and 97/3. (The d_c for the pure nitrate of density 0.7-0.8 g/cm^3 is 80-100 mm, and D_c is 1100 m/sec.) Table 62 gives BOBOLEV's results for some explosives; these relate to charges in thin-walled glass tubes.

Table 62

Critical Diameters for Charges

Explosive	ρ, g/cm^3	Crystal size, mm	d_c, mm
TNT	0.85	0.2 -0.07	11.2
Picric acid ..	0.95	0.75-0.1	9.2
Solid nitroglycerine	1.00	0.4	2.0
Hexogene	1.00	0.15-0.025	1.2
TEN	1.00	0.1 -0.025	0.9

Some explosives, especially ones very readily detonated, have very small d_c; for example, d_c = 0.05 mm for a stoichiometric mixture of tetranitromethane with nitrobenzene (HOLBINDER's value), while BOWDEN gives a d_c of about 20 μ for lead azide of nearly maximal density; here

$d_{in} \approx 400$ μ. The corresponding D for the last case are 2000 and 5500 m/sec. The azide merely decomposes slowly if $d < d_c$. The d_c for typical homogeneous explosives are much smaller than those for compositions containing NH_4NO_3, on account of differences in the reaction rates. The D_c for typical high explosives are 2200-3000 m/sec.

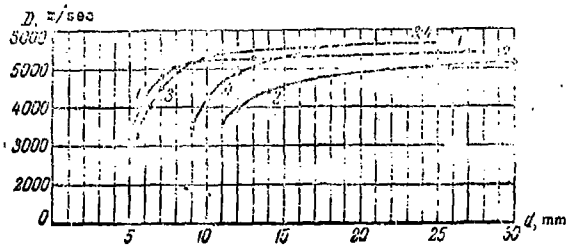


Fig. 85. Relation of D to charge diameter; effects of grain size.

The limits d_m and d_c increase with the grain size and tend to diverge, on account of change in the width of the reaction zone. This trend is common to homogeneous and mixed explosives. Figure 85 (after BOBOLEV) gives some results. Curve 3 relates to picric acid (ρ_0 = 0.95 g/cm^3, grains of sizes 0.1 to 0.75 mm), while curve 4 relates to the same material but of rather smaller grain size. The effects may be summarized as follows. For picric acid:

Grain size, mm	d_c, mm	d_m, mm	ρ_0, g/cm^3
0.1-0.75	9.0	17.0	0.95
Small	5.5	11.0	0.95

and for trotyl (curves 1 and 2);

Grain size, mm	d_c, mm	d_m, mm	ρ_0, g/cm^3
0.2 -0.07	11.0	30.0	0.85
0.05-0.01	5.5	9.0	0.85

The grain size does not affect the D_m for a given ρ_0; it affects only the rate of approach to that limit. Further, it does not affect D_c.

These rules apply also to mixtures, but d_c and d_m are usually much larger than for homogeneous explosives. For example, BELYAEV's results show that even very fine-grained dynamon (12% peat and 88% NH_4NO_3) gives a D that is very much dependent on d when the latter is 80 mm. This shows that many practical charges have $d < d_m$.

Some observations by FRIEDERICHS for TEN are relevant here. Finely powdered TEN was pressed (3000 kg/cm^2), and the product was broken up into pieces 4-5 mm in size, which were packed into a copper tube 15 mm in diameter to a mean density of 0.753 g/cm^3. Here D was 7924 m/sec, whereas the normal D for that density is only 4740 m/sec. Trotyl and other less sensitive explosives do not give anomalous D under these conditions. It is claimed that here the detonation propagates with the rate characteristic of the individual pieces, not as a continuous front, but this leaves the question open, for TEN and hexogene show the effect, whereas explosives such as trotyl do not. ROBOLEV has solved the problem by applying KHARITON's stability criteria. The pieces detonate independently if their size exceeds d_c; then the detonation is transmitted from piece to piece at a rate characteristic of the density of the pieces. The pieces cannot detonate in this way if their size is less than d_c, so a continuous front is formed, and the normal D is found. Now 4 mm is less than d_c for trotyl, so this gives no anomalous D. We would expect anomalous D for certain detonators whose d_c is less than their grain size, and FRIEDRICHS has actually observed this for lead azide and mercury fulminate at medium densities. For example, D is 4423 m/sec for lead azide of ρ_0 1.60 g/cm^3, which is

almost the D for 3.25 g/cm^3 (4500 m/sec).

The casing affects D because it restricts the lateral rarefaction waves and so favors complete use of Q in the detonation. This would indicate that the casing should have a more marked effect for an explosive that reacts slowly; in fact, it has often been observed that explosives based on ammonium nitrate give much higher D when they are enclosed in strong casings. The casing has little effect for a detonator. In general, the effect on D is appreciable for a high explosive only if d and ρ_0 are small, as Table 63 shows. Similar results have been obtained for pressed trotyl, picric acid, and so on. BELYAEV, BOBOLEV, and others have found 1) that the strength of the casing is without effect on D if $d > d_m$; 2) that no casing and no size of detonating pulse has any appreciable effect on the D_c for a given ρ_0; and 3) that d_c and d_m for a cased charge are much less than those for an open one, the effect being the greater the higher the inertial resistance of the casing. This last illustrates the most important aspect of the casing, although the strength is also important for low explosives. The casing acts in much the same way as an increase in D; BELYAEV finds, for example, that the stable D for 88/12 ammotol as charges 5 mm in

Table 63

Effects of Casing on D for Trotyl of Density 1.59 g/cm^3

d, mm	t, mm	D, m/sec
21	3	6555—6700
29	10	6700
75	14.5	6705
160	25	6750
300	50	6770

Table 64

Critical Diameters for Ammotol

Mixture		d_c, mm	
% trotyl	% nitrate	water	no case
100	0	—	9
22	72	4	12
12	88	5	15
6	94	8	21
3	97	14	30
0	100	40	160

diameter enclosed in water is 1650 m/sec, whereas this D is obtained with open charges only when d is 16-17 mm. Table 64 gives some of BELYAEV's results; in every instance the water shell had a thickness of $2d$ to $3d$, ρ_0 being 0.8-0.85 g/cm^3. Further, BELYAEV found that ammonium nitrate would detonate stably at a d of only 7 mm when the charge was enclosed in a steel tube of wall thickness 2 cm; here D was 1500 m/sec.

Only Q_v and ρ_0 affect D if $d > d_{кр}$; all other factors affect only the transient state. The increase in D with ρ_0 is at first rapid, but the rise continues up to the maximum ρ_0 attainable. Table 65 gives FRIEDRICHS's results, which agree with other findings.

Table 65

Relation of D to Charge Density

Picric acid		Tetryl		TEN		Pb azide	
ρ_0 g/cm^3	D, m/sec	ρ_0, g/cm^3	D, m/sec	ρ_0, g/cm^3	D, m/sec	ρ_0, g/cm^3	D, m/sec
0.7	4020	0.52	3040	1.03	5615	1.06	2664
0.97	4963	0.69	4444	1.22	6357	1.18	3322
1.32	6190	0.96	5387	1.37	970	2.56	4478
1.41	6510	1.22	6291	1.50	7418	3.51	4745
1.62	7200	1.42	7373	1.62	7913	3.96	5123
1.70	7483	1.68	7740	1.73	8350	4.05	5276

SHEKHTER has measured D for trotyl and hexogene (the latter retarded by 5% paraffin wax); Table 66 and Fig. 86 give these results, which fit the relation

$$D = B\rho_0^a. \qquad (44,1)$$

in which B = 5060 and a = 0.67 for trotyl, while B = 5720 and a = 0.71 for retarded hexogene. This relation applies to many other explosives over a wide range in ρ_0; a is close to

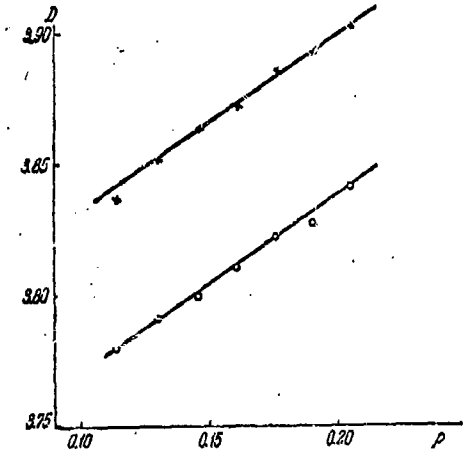


Fig. 86. Relation of D to ρ.

0.7. This is an indirect proof of the isentropic expansion of the products from condensed explosives at high pressures ($p = A\rho^3$); this type of law was used in deducing the equation of state. The exponent is close to 3 if the [illegible] of (44,1) is 0.7.

Table 66

Relation of D to Density for Trotyl and Retarded Hexogene

Trotyl		Hexogene	
ρ_0, g/cm^3	D, m/sec	ρ_0, g/cm^3	D, m/sec
1.30	6025	1.25	6660
1.35	6260	1.30	6975
1.40	6315	1.35	7125
1.45	6480	1.40	7315
1.50	6610	1.45	7470
1.55	6735	1.50	7640
1.60	6960	1.55	7820
1.61	7000	1.60	7995

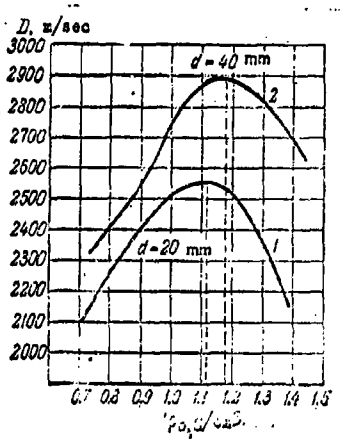


Fig. 87. Relation of D to ρ for cheddite.

The above relation between D and applies for any $d > d_m$ for homogeneous explosives; mixtures of two components give D that increase with ρ only up to some limit, beyond which there is a rapid fall and ultimately a failure to detonate. D'AUTRICHE has demonstrated this for cheddite (Fig. 87), and URBANSKIY and others have done the same for explosives based on NH_4NO_3. The point of maximum D moves to higher ρ as d increases, and the D generally become higher. Smaller grain size and improved mixing have much the same effect.

The effect is usually discussed in the specialist literature as one specific to mixtures, but we shall see that it is actually one that appears only when $d < d_m$ (the above results are for charges of this

type). BOBOLEV and others have found that d_m and d_c decrease rapidly and become more nearly equal as ρ_0 increases; Fig. 88 shows BELYAEV's results for pressed trotyl, in which curve 1 is for grains of size 0.2-0.7 mm and curve 2 is for grains of size 0.01-0.05 mm. Clearly, d_c is reduced to a third when ρ_0 increases from 0.85 to 1.5 g/cm^3; the d_c for cast trotyl of large grain size and for liquid trotyl (ρ_0 = 1.46, temperature 100°C) are both about 31 mm. This great increase in d_c is directly related to the lower sensitivity of these materials.

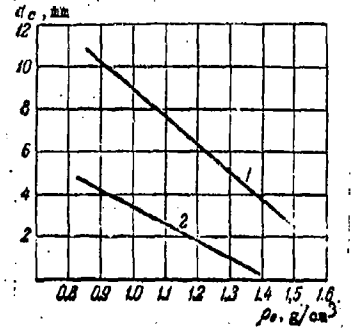


Fig. 88. Relation of d_c to ρ_0 for pressed trotyl.

The fall in D when $d < d_m$ is at first slow, but the drop to D_c becomes very rapid as d_c is approached; this is especially characteristic of high explosives at the higher densities. This makes it difficult to measure D_c accurately by varying d, and many of the D_c given in the literature are undoubtedly too high. On the other hand, a decaying explosion may be produced by suitable means in a charge, whereupon a photographic recording will give an accurate reading of the speed at which the detonation terminates. This speed may be taken as D_c; a charge of varying diameter is convenient for this purpose. D_c increases somewhat with ρ_0, on account of the increase in c_0; the increase is especially pronounced near the maximum ρ_0, and D_c approaches D_{max}. The latter increase is not associated with change in c_0, which does not exceed 3000 m/sec for typical high explosives of maximum density; the cause is that the mechanism of the initiation at the front is altered. The hot spots are the most important when ρ_0 is small, on account of the numerous pores and points of friction,

whereas the medium becomes more nearly homogeneous as the maximum ρ_0 is approached. Here the temperature rise produced by the shock wave is important; the adiabatic compressibility of an explosive is low (comparable with that of water), so the temperature needed to initiate and complete the reaction in a short time is attainable only from a shock wave much stronger than that needed for low ρ_0.

For example, if we take the compression zone for hexogene to be 10^{-6} cm wide, which implies that the zone is acted on by the wave for about 10^{-10} sec, we find that the temperature must be 1000-1100°K. Rough calculations show that this temperature can be produced in a monocrystal only by a wave whose D exceeds 6000 m/sec.

BELYAEV has observed a different relation between d_c and ρ_0 for mixtures containing NH_4NO_3; d_c increases with ρ_0, expecially for high ρ_0. Figure 89 gives results for 80/20 ammotol and for dynamon (88% NH_4NO_3 and 12% peat). Here d_c becomes 70 mm even when ρ_0 is only 1.2 g/cm^3 (curve 1); the rise is very pronounced. On the other hand, ammotol 80/20 (curve 2) shows comparatively little effect from ρ_0. Figure 90 shows the effect observed for mixtures containing more TNT (50/50 mixture, components passed through a No. 16 sieve). The behavior up to 1.1 g/cm^3 is much as for poor mixtures consisting largely of NH_4NO_3, whereas it becomes as for TNT and other homogeneous explosives at higher densities.

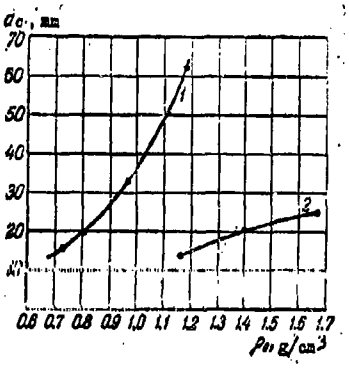


Fig. 89. Relation of d_c to ρ_0 for ammotol and dynamon.

The shape of the curves in Fig. 87 can now be explained. Clearly,

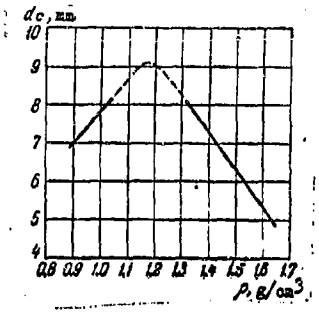


Fig. 90. Relation of d_c to ρ_0 for 50/50 ammotol.

D can increase no further.

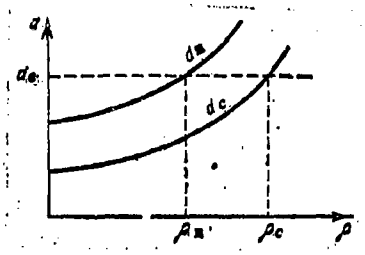


Fig. 91. Relation of d_m and d_c to diameter of experimental charge (schematic).

it is easy to ensure that $d > d_m$ for homogeneous explosives at all densities, so D is found to increase with ρ_0. The same should be found for d sufficiently large for mixtures; if it is not, and the curve has a peak instead, this means that $d > d_m$ only for the lower densities, as Fig. 91 shows schematically. Here D increases with ρ until ρ_m is reached, at which point $d_c = d_m$; then conditions become less favorable, and at some point Thereafter there is a fall until the point ρ_c is reached; here $d_{cr} = d_c$, and a charge of any higher density cannot be detonated.

This shows that the relation of D to ρ_0 must be as for a homogeneous explosive provided that $d > d_m$; Fig. 92 (after PETROVSKIY) demonstrates this for ammotol 90/10 (uncased charges; components passed through a No. 38 sieve). Clearly, there is no tendency for D to fall as ρ_0 increases if d is 40 mm.

Effects of other components. Combustible organic and inorganic

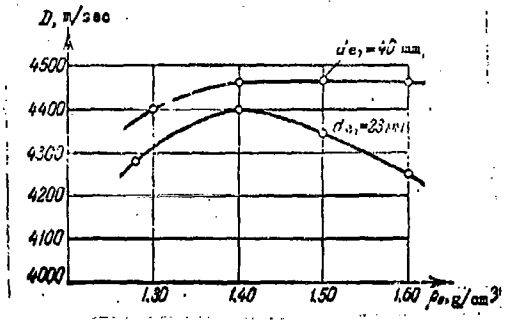


Fig. 92. Relation of D to ρ_0 for ammotol 90/10.

compounds affect D, the effects being dependent on the compound and on the explosive. For example, D for hexogene is reduced appreciably by 5% paraffin wax (from 7900 m/sec for pure hexogene at 1.50 g/cm^3 to 7640 m/sec for the retarded material at the same density). On the other hand, 3-5% of beeswax or paraffin wax increases the D for mercury fulminate somewhat. The reasons are as follows. The M for the products from mercury fulminate is very large; the paraffin reduces M and increases the volume of the products, so D increases, although the energy release is somewhat lower. On the other hand, the effect in the case of hexogene is largely one of reduction in Q.

Table 67

Effects of Other Components on D for Trotyl

	ρ_0, g/cm^3	D, m/sec
Trotyl	1.61	6850
50% trotyl + 50% NaCl	1.85	6010
75% " + 25% $BaSO_4$	2.02	6540
85% " + 15% $BaSO_4$	1.82	6690
74% " + 26% Al	1.80	6530

As a rule, an inert diluent tends to reduce D, though not as much as one might expect from the reduction in Q, as Table 67 shows. Large amounts of NaCl and $BaSO_4$ have little effect on D; these diluents act mainly as mechanical obstacles to the transmission of the detonation through the mixture. Even aluminium has this effect on trotyl, although it increases Q by up to 40%; the effect is very much the same as that of $BaSO_4$. The reason is that the aluminium reacts slowly, and most of

the reaction occurs in the zone affected by the rarefaction wave, so the extra energy is not available to the detonation front.

Two detonation rates. It has long been known that liquid nitrates (nitroglycerol, nitroglycol, methyl nitrate) can detonate at two very different rates. The higher one, which corresponds to Q, usually occurs when d is large and the initiating pulse is strong; here D is 6000-8000 m/sec. The lower D (about 1500 m/sec) occurs when d is small, but it can occur when d is large if the initiating pulse is weak. Again, a narrow tube connected to a wide one at first gives the high D when the wave enters it, but the speed suddenly drops to the low D after a certain distance. Recent work has shown that this effect is not confined to liquids; it can occur also for solids if d is close to d_c. BOBOLEV has observed the low D for powdered nitroglycerine and picric acid under these conditions, while LAWRENCE has found that the small D increases as ρ_0 decreases (the large D increases with ρ_0). RATNER has demonstrated that the effects are not associated with modifications or isomeric forms of the compound.

TSIBUL'SKIY has found that two distinct values of D can occur for explosives based on nitroglycerol, the strength of the initiating pulse being the decisive factor. The high D is 6000-8000 m/sec, and the low one up to 3000 m/sec. Each of these D has been measured as a function of d; each has its own d_c. The same effect has been observed for D5 dynamite for $d \geq 20$ mm, and for DIS dynamite for $d \geq 18$ mm. The high D does not occur for smaller d no matter how strong the detonator.

The low D is associated with incomplete decomposition (with a reduced Q_v), as analysis of the products has shown.

45. Initiation and Reaction Mechanisms for the Detonation Front

The relationships demonstrated above are very much dependent on

the reaction conditions at the front. It is very difficult to examine the kinetics of the reactions, and little is known at present. The ignition conditions in a detonation wave in a gas are very much as for ignition by adiabatic compression; the reaction is produced directly by the sharp rise in temperature. The pressure at the front in a liquid explosive is usually somewhat over 10^5 atm, the temperature being 900-1000°K. This is sufficient (see section 10) to cause the reaction to go to completion in the compressed zone even when no air bubbles are present; the time needed for complete reaction in typical high explosives is 10^{-6} to 10^{-7} sec.

The conditions at the front in a solid are not essentially different from those produced by mechanical shock, apart from the much greater rate of deformation; the stresses are extremely high, and intensely heated spots appear, which act as reaction centers. The number of these centers is much larger than that produced by an ordinary blow. A solid (pressed) material is more readily detonated than the same material in the liquid state; the difference in the critical diameters is a result of the higher temperatures and more numerous reaction centers in the solid.

The reaction conditions in a detonation wave are very much dependent on the composition and physical properties of the explosive. KHARITON considers that the mechanisms may be divided into impact, ballistic, and mixed types. A mechanism is of impact type if the material is compressed and heated before the reaction occurs; in this case the material is homogeneous, and the reaction occurs throughout the volume of the material in the reaction zone. This mechanism is characteristic of gases and of bubble-free liquids; the reaction time τ may be deduced as follows. The shock wave brings the material almost

instantly to the state represented by p_i and T_i, and so

$$\tau = \tau(p_i, T_i) = \frac{1}{w} \qquad (45,1)$$

in which w is the reaction rate. This formula is not generally applicable, on account of lack of data on the kinetic characteristics of the explosive for detonation conditions.

The ballistic mechanism is one in which the products are formed by the burning of individual particles; the reaction occurs only in the surface layers of the burning particles. The combustion process resembles that of gunpowder grains confined in a closed space and so is also called explosive burning. This is the basic mechanism for homogeneous solid explosives; the gaseous products from the active centers engulf the grains, which burn rapidly at these high temperatures and pressures. The number of active centers increases as the grain size decreases, while the mean burning time for a particle decreases, so the reaction zone becomes narrower; the result is that d_m and d_c decrease.

Consider the simplest case (a monomolecular reaction); here the rate w is given as a function of T by

$$w = Ze^{-\frac{E}{RT}} \qquad (45,2)$$

in which Z is 10^{11} to 10^{14} sec^{-1}. If the reaction were isothermal, then

$$\tau = \frac{1}{w_T} l \qquad (45,3)$$

but the high reaction rate makes the process adiabatic. The resulting increase in temperature raises the reaction rate, and so on. The theory of explosions for gases (section 51) shows that, under adiabatic conditions,

$$\tau = \tau_{\min} \approx \frac{1}{w_T} \frac{RT_i^2}{ET_e}, \qquad (45,4)$$

in which T_e is a temperature close to the reaction temperature. Now

d_m is related to τ by

$$d_m = \tau D,$$

and so we have that

$$d_m = \frac{DRT_i^2}{ZET_0} e^{\frac{E}{RT_i}}, \qquad (45,5)$$

in which D applies for the density used.

A rise in density raises the detonation pressure, which intensifies the local heating; moreover, an increase in density resulting from increased forming pressure is associated with a reduction in particle size. This size affects d_m and d_c more noticeably at the lower densities, though.

The reaction time for explosive burning is simply the time for a single particle to burn, which is

$$\tau_1 = \frac{l}{v}, \qquad (45,6)$$

in which $2l$ is the diameter of a grain and v is the linear burning rate. Then

$$d_m = D\tau_1 = l\frac{D}{v}. \qquad (45,7)$$

This relation may be used to find d_m if v is known as a function of pressure for relatively high pressures.

The mixed mechanism occurs when the reaction involves two or more substances not in molecular contact; it is characteristic of heterogeneous systems, especially solid ones. KHARITON considers that the reaction here occurs only at the interfaces, but it is difficult to suppose that the original components react directly, the more so since they are solid. The most likely sequence for explosives of dynamon type is as follows.

1. The nitrate decomposes to produce oxidizing agents; the primary reaction here appears to be

$$2NH_4NO_3 \longrightarrow 4H_2O + N_2 + 2NO + 29.2 \text{ kcal},$$

2. The other components, or their decomposition products, react with the NO_2; most of the heat is produced in this stage, and this heat serves to accelerate the reactions.

It is essential to mix the components thoroughly in order to ensure that the reactions occur rapidly and completely. Failure to do this may retard the reactions, especially those in stage 2, which in practice means incomplete combustion (the products contain oxides of nitrogen in large amounts).

The d_c of an ammonite increases rapidly with ρ_0, which implies that the reaction rate falls as p_i increases. The rate-limiting step is the decomposition of NH_4NO_3. (The effect is even more pronounced for pure ammonium nitrate.) BOBOLEV's observations on d_c for ammotols containing much TNT may be explained as follows. The rate of decomposition of the NH_4NO_3 remains high while ρ_0 and p_i are low, so the reaction sequence is basically as above; but the reaction with the TNT becomes the primary step at higher densities, the second step being decomposition of the NH_4NO_3 (in part caused by the first step) and reaction between decomposition products. The entire process requires a special study, especially as regards the decomposition kinetics of ammonium nitrate at high pressures.

All of the above schemes for detonation processes fall within the framework of the hydrodynamic theory, because it is assumed that the initiation and propagation of the reaction are directly associated with the passage of a shock wave. APIN has taken a very different view on this; he considers that the detonation in a condensed explosive propagates by a jet-breakdown mechanism. The layers ahead of the reaction zone are assumed to be broken down and ignited by the reaction products, the process being assisted by pores in solids and by bubbles in liquids.

The detonation rate is then the speed of the reaction products in the material.

This mechanism would appear not to be characteristic of detonations, for a detonation is readily transmitted through a layer of metal, water, etc.; no ignition by hot gases is possible here, and the shock-wave mechanism must be operative. One may presume that the same applies when there is no layer of metal, the more so because the strength (i.e., the initiating capacity) will be greater in the absence of the barrier. All the same, APIN's mechanism may apply to a charge consisting of fairly large pieces of explosive; but here we do not find the usual relation of D to ρ_0.

It may be that APIN's mechanism corresponds to burning at comparatively low rates; the flame penetrates through the gaps, the burning front ceases to be straight, and the process is not truly steady. Unstable burning of this type may pass over into detonation under certain conditions.

46. Methods of Measuring Rates of Explosion Processes

Methods for this purpose are now fairly well developed; the various types of apparatus may be divided into two groups. The first group covers various types of chronograph and oscillograph (instruments for measuring short times). A chronograph records the time taken for the process to pass between fixed points, which gives the mean speed between the points. The second group covers various types of optical recorder. If the process does not of itself emit light, use is made of the effects on the light from an accessory source.

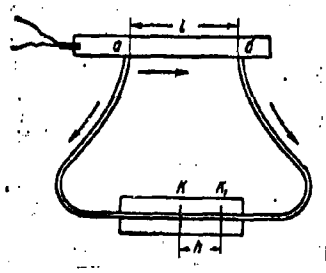


Fig. 93. D'AUTRICHE's method of measuring a detonation rate.

Optical methods have certain advantages; in particular, there is no lag in the recording, and there are no transducers to introduce errors. The recording is continuous, so the instantaneous speed can be measured. On the other hand, recent pulse oscilloscopes can measure speeds over distances of only a millimeter or two, which is very difficult to do photographically.

No special equipment is needed in the chronograph method; Fig. 93 illustrates D'AUTRICHE's system, in which the speed is compared with a known and constant speed of detonation, which acts as the time source. The charge is made up as a cylinder 30-40 cm long contained in a metal tube. The detonating fuse (about 1 m long) is inserted at two fixed points a and b, which are 10-20 cm apart. Sometimes the ends are fitted with detonator capsules. The middle is fixed to a thin lead or brass plate. A line K is marked exactly at the center. The charge is fired with a detonator and ignites the fuse; the detonations from the two ends meet at a point K_1 somewhat to the right of K. This point K_1 is readily visible on the plate.

Let D' be the detonation rate of the fuse, and let the time t_1 for the detonation to reach K_1 along the path aKK_1 from a be

$$t_1 = \frac{L}{2D'} + \frac{h}{D'},$$

in which L is the length of the fuse and h is the distance KK_1. Let D be the detonation rate for the charge; then the time t_2 for the detonation to reach K_1 along the path abK_1 is

$$t_2 = \frac{l}{D} + \frac{L}{2D'} - \frac{h}{D'}.$$

But $t_1 = t_2$, so

$$\frac{h}{D'} = \frac{l}{D} - \frac{h}{D'},$$

whence

$$D = \frac{lD'}{2h}. \qquad (46,1)$$

The errors are governed by the variation in D' and by uncertainty in h

and l. The maximum relative error in D is given by

$$d \ln D = d \ln l + d \ln D' + d \ln h.$$

The derivative is

$$\frac{dD}{D} = \pm \left(\frac{d}{l} + \frac{dD'}{D'} + \frac{dh}{h} \right).$$

D' is known to 1.5-2%; l (commonly 200 mm) is measurable to 1 mm (greater accuracy is not possible, as the explosive may penetrate into the recesses). Then

$$\frac{dl}{l} = \frac{1}{200} \times 100 = 0.5\%.$$

The h for a given l is dependent on D/D'; $h = l/2$ if they are equal, so $l = 200$ mm and $h = 100$ mm. The measurement of h is not very accurate, because the marks are not very clear and the center of the fuse may not be located exactly. The probable error is $dh/h = 2\%$, and so the maximum error is

$$\frac{dD}{D} = \pm (2 + 0.5 + 2) = \pm 4.5\%.$$

This result is in agreement with experiment, which indicates that the average error is about 1% and the maximum about 5%. This substantial range of error has sometimes been overlooked, as in FRIEDRICHS's measurements on the variations in D.

The above method is simple and convenient; moreover, it is directly applicable to charges as actually used, which is often not so for other methods. The main disadvantage is that the error is relatively high, particularly in view of the fact that only a mean speed over a fair length (some 30 cm) is obtained.

A pulse oscilloscope can be used for the same purpose, which provides a very precise time measurement (error only 10^{-8} to 10^{-7} sec). The simplest form of detector is provided by two leads inserted in the charge and connected to a charged capacitor. The detonation wave acts as a conductor and so produces at the first detector a pulse that serves

to trigger the beam; the second detector deflects the beam. The trace on the screen is photographed, together with the time marks. (Figure 94 shows the circuit, and Fig. 95 shows a typical result.) Then D is deduced from the length l on the trace corresponding to given time marks:

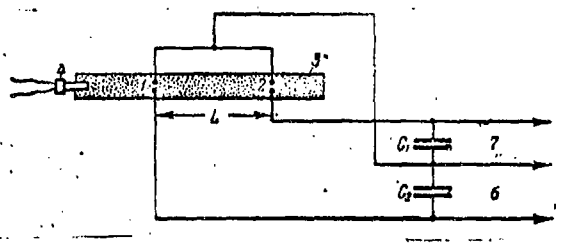


Fig. 94. Pulse-oscilloscope system for measuring D: 1) and 2) detectors; 3) charge; 4) detonator; 6) to trigger; 7) to deflection system; C_1 and C_2, capacitors.

$$D = \frac{L}{t},$$

in which L is the distance between the detectors and $t = lM$ is the time taken for the wave to pass between them, M being a scale factor for the trace.

The error can be diminished by using a spiral time-base, which enables one to measure t very precisely even when L is only 10-20 mm.

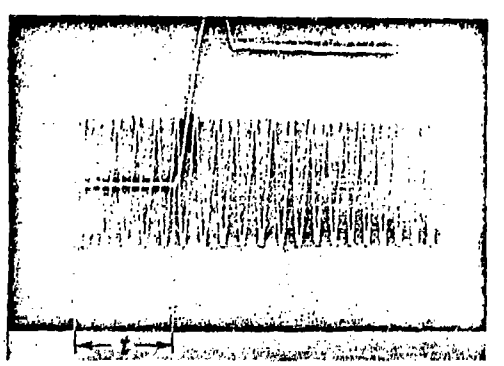


Fig. 95. Oscillogram of a detonation process.

Optical methods have been used extensively in studies on processes that accompany detonations. The path traversed is recorded as a function of time is recorded on a film; the film may move, or the image may be swept over it by a mirror.

Electron-optical converters may be used. Moving-film systems are divided into drum and disc types; in the first, the film is held on the outside or inside of a rotating drum (Fig. 96), or on a rotating disc in the second type.

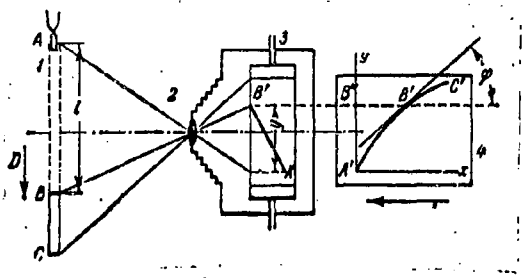


Fig. 96. Drum recorder.

The lens 2 forms an image on the drum 3, whose speed is measured. Let us assume that the detonation front acts as a luminous point; if the drum were not rotating, the image would trace out the line $A'B''$ as the front passes along AB. If the drum turns with a surface speed v, the image traces out a curve $A'B'C'$, which will be a straight line if D is constant. Then the speed D at a distance l from the start is

$$D=\frac{dl}{dt}. \qquad (46,2)$$

The projection of the corresponding part of the curve on the Oy axis is $A'B''$; from Fig. 96,

$$y=\beta l, \quad dl=d\left(\frac{y}{\beta}\right),$$

in which β is the magnification (usually $\beta < 1$). The distance moved through by the film (speed v) in the time t corresponding to l is

$$x=vt, \quad dt=d\left(\frac{x}{v}\right).$$

Then dl and dt are inserted in (46,2); β and v are constants, so

$$D=\frac{v}{\beta}\operatorname{tg}\varphi, \quad v=2\pi rn, \qquad (46,3)$$

in which φ is the angle as made by the tangent at B', r is the radius of the drum, and n is the angular speed; the slope is found by dividing y by x if D is constant.

The front is not a point, so the line is broad; the tangent cannot be drawn very exactly. The error can be minimized by restricting the width of the luminous spot with a slit, which may be inside or outside

the recorder, e.g., at the surface of the charge, but in that case it is damaged by the explosion and must be replaced frequently. Moreover, it reduces the light-gathering power of the objective very much. An internal slit is placed directly above the surface of the drum; it has none of the disadvantages of the other slit. On the other hand, β is 0.05 to 0.25 for most such recorders, which is a major disadvantage, because a charge 100 mm long produces a trace 5-25 mm long; no very exact measurements of change in D can be made.

Moving-film systems have the disadvantage that the linear speed is low; the film on the outside of a drum cannot be driven at more than 100 m/sec, on account of breakage under centrifugal forces. Speeds of 200 m/sec are attainable with the film inside the drum, but then the drum must be very carefully balanced, the system must be evacuated, and so on. Higher speeds are not accessible, because the emulsion starts to flow under the centrifugal forces.

The maximum relative error is given by (46,3) as

$$\frac{dD}{D} = \pm\left(\frac{d\beta}{\beta} + \frac{dr}{r} + \frac{d\omega}{\omega} + \frac{2d\varphi}{\sin 2\varphi}\right).$$

The factor that contributes most to the error is φ; the error is minimal if $D\beta/v = 1$, but this is very difficult to ensure for drums. For example, $\beta = 1/35$ if $D = 7000$ m/sec and $v = 200$ m/sec; this is not usable, because it demands charges of length 1 m or more. This shows that drum recorders are best used with slow processes, e.g. burning.

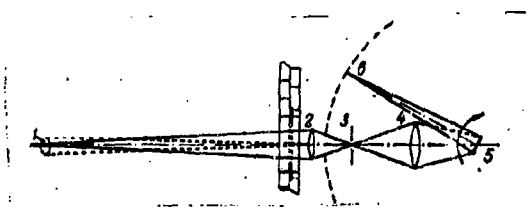


Fig. 97. Optical system of a mirror recorder: 1) charge; 2) and 4) lenses; 3) slit; 5) rotating plane mirror; 6) films.

Reasonable values of β are 0.25 to 0.5, so $D\beta/v = 1$ implies that v is to be

2000-3000 m/sec. These speeds are attainable with a mirror system working into a fixed film. The principal units are the optical system, the synchronizing unit, and the sweep device. The optical system (Fig. 97) consists of two lenses having a common focal plane, which provides a large radius of sweep and high image intensity if lenses of long focal length are used. Moreover, the charge can then be placed well away from the front lens. The full aperture of the first lens is used only if all the light entering it passes to the second lens and thence to mirror.

A slit placed in the common focal plane of the two lenses restricts the width of the image. The mirror is front-surface silvered and is made of thick glass or metal, in order to prevent distortion at high speeds. The synchronizing unit (Fig. 98) is used to start the detonation when the mirror is in a specified position. The rectifier 4 charges the capacitor 5; the spark gap 6 breaks down when the mirror is in the required position, and the current from the capacitor runs to ground via the synchronizer disc 7 and detonator 9. Disc 7 is rigidly coupled to the mirror 8. The axis of the mirror is parallel to the charge. The voltage (3-5 kV) at the capacitor is adjusted by means of the rheostat in the primary circuit of the transformer.

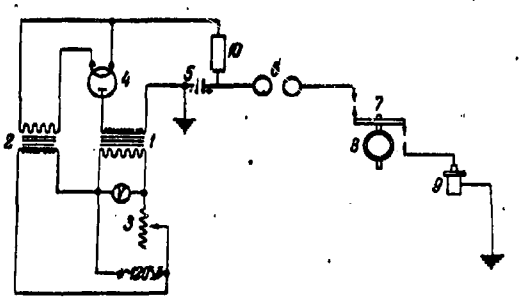


Fig. 98. Mirror synchronizing unit: 1) and 2) transformers; 3) rheostat; 4) rectifier; 5) capacitor; 6) discharge gap; 7) synchronizing disc; 8) mirror; 9) detonator; 10) resistor.

The angular speed of the mirror must be measured in order to determine the linear speed of the sweep; the measurement should be made to 0.5% or better. This speed v is related to $\omega = d\varphi/dt$ (Fig. 99) by $v = \omega_1 R = 2\omega R$, because $\psi = 2\varphi$; then (46,3) gives us that

$$D = \frac{4\pi R n}{\beta} \tan\varphi,$$

in which tan φ is the slope of the tangent and $4\pi R/\beta$ is a constant of the instrument, which may be denoted by C. Then

$$D = C n \tan\varphi.$$

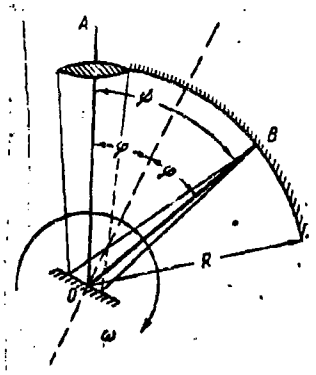


Fig. 99. Reflection of a ray from a rotating plane mirror.

For, example, we may have R as 1.5 m, β as 1/2 or 1/3, and n as 6000 rpm, in which case u = 1890 m/sec; this is very much larger than the maximum speed available from a drum recorder. Moreover, β is comparatively large, so the error of measurement is much less; instantaneous speeds can be measured, and changes occurring in distances of 1-3 cm are detectable. A charge only 100 mm long is quite sufficient.



Fig. 100. Detonation of a hexogene charge.

The maximum error is determined as for drum recorders; the result for a steady process comes out as ±0.8%, and for a process of variable speed as ±2.5%. Figure 100 shows a recording for a hexogene charge; the rate is clearly constant.

The rotating-mirror system has other advantages, because it enables one to combine a variety of methods,

e.g. for effects that do not produce light (for example, the flight of fragments and motion of shock waves in transparent media). The TOPLER effect is used, as shown in Fig. 101. Any perturbation in an optically homogeneous medium causes a change in the refractive index. The light from the source 1 forms a real image at the lens 3 after reflection at the mirror 2 if there is no perturbation; the result is a uniformly illuminated circle on the film 5. A perturbation 6 in the *AB* plane deflects the rays; the knife-edge 4 is placed in the image plane in order to reveal this perturbation. This edge blocks out the rays and prevents them from reaching the film, which results in an image of the perturbation. (The lens-holder has the same effect if the deviation is very great.)

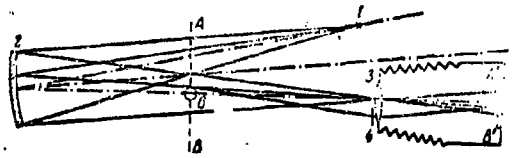


Fig. 101. Recording by means of transmitted light: 1) source; 2) spherical mirror; 3) lens; 4) knife-edge; 5) film; 6) object.

The perturbation may not cause the deflected rays to be cut off; instead, it may render the medium opaque. The result is then a shadow of the perturbation. This image may be restricted by a slit as in the method above, and the mirror may be rotated, in which case the film records the position of the perturbation as a function of time.

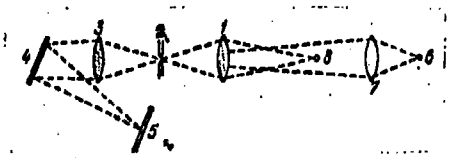


Fig. 102. Optical system with rotating mirror.

The light may be provided by an exploding wire; SOBOLEV has made a detailed study of this. The light may be collected by a high-aperture lens instead of by a spherical mirror. Figure 102

illustrates the use of a mirror. The detonation and the flash from the wire are synchronized electrically to the rotation of the mirror.

Very high recording speeds are accessible with electron-optical converters; Fig. 103 shows COURTNEY-PRATT's system. The line AB is the image of the slit placed directly by the charge; this gives rise to a line on the fluorescent screen. The position of this image line is controlled by a magnetic deflecting system. As the luminous point moves along the line AB, the vertical magnetic field (whose strength varies linearly in time) produces a deflection; the result is an image line whose slope is directly related to the speed of the luminous point. The slope of the line relative to the vertical axis AB is given by

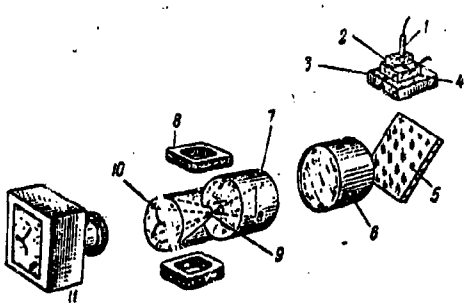


Fig. 103. Electron-optical converter used to photograph an explosion: 1) detonator; 2) charge; 3) slit; 4) safety glass; 5) plane mirror; 6) lens; 7) sensitive screen in converter; 8) deflecting device; 9) electron lens; 10) fluorescent screen; 11) camera.

$$\operatorname{tg}\varphi = \frac{v}{D\beta},$$

or

$$D = \frac{v}{\beta}\operatorname{ctg}\varphi,$$

in which v is the transverse speed of the electron beam at the screen when the luminous spot is stationary. The image line is recorded by a normal camera.

BOWDEN and JOFFE have estimated the time resolution of this system as 10^{-9} sec, although BUTSLOV and FANCHENKO's theoretical study

indicates that a resolution of 10^{-14} sec should be accessible.

A major advantage of the system is that it needs no synchronizing unit or special detonator. Electron-optical converters may be used to record fast processes generally; rates up to 10^8 frames per second are accessible, although the total number of frames is not large. SIMONOV and KUTUKOV have been able to record 6-10 frames each with an exposure of 0.05 to 0.5 μsec by means of a special pulse-shaping circuit.

Bibliography

1. Yu. B. Khariton, "Detonation capacity of an explosive"; A. F. Belyaev, "Effects of physical factors on the stability of detonations in explosives based on ammonium nitrate"; Ya. I. Leytman, "Effects of grain size on the sensitivity of high explosives to initiating pulses". Voprosy teorii vzryvchatykh veshchestv [Theory of Explosives], No. 1, issue 1. Izd. Akad. Nauk SSSR, 1947.
2. V. K. Bobolev. "Physics of explosions". Experimental Studies on the Physics of Explosions, Collection No. 2. Izd. Akad. Nauk SSSR, 1953.
3. Collection of Papers on the Theory of Explosives. Oborongiz, 1940.
4. W. Jost, "Explosion and Combustion Processes in Gases" [Russian translation], IL, 1953.
5. M. Patri, Burning and Detonation of Explosives . Oborongiz, 1938.
6. A. F. Belyaev and A. E. Belyaeva. Dokl. Akad. Nauk SSSR 50, 295 (1945).
7. V. K. Bobylev, Dokl. Akad. Nauk SSSR 57, 789 (1947).
8. A. Ya. Apin and V. K. Bobylev. Zh. Fiz. Khim. 20, 1367 (1946).
9. Idem., Dokl. Akad. Nauk SSSR 58, 241 (1947).
10. S. B. Ratner and Yu. B. Khariton. Dokl. Akad. Nauk SSSR 41, 307 (1943).

11. R. Kh. Kurbangalina, Zh. Fiz. Khim. 22, 49 (1948).

12. H. Eyring and R. E. Powell, Chem. Rev. 45, 69 (1949).

13. R. W. Cairns, Ind. Eng. Chem. 36, 79 (1941).

14. J. S. Courtney-Pratt, Research 2, 287 (1949).

15. Collection of Papers on High-Speed Cinematography in Science and Technology. IL, 1955.

CHAPTER IX

INITIAL PARAMETERS OF A SHOCK WAVE AT AN INTERFACE

47. Reflection of a Shock Wave at a Rigid Plane Wall

The pressure exerted by a shock wave on a barrier can be considerably in excess of the pressure at the front, on account of the reflection. The following is IZMAYLOV's treatment of the reflection of a plane steady-state shock wave by a rigid barrier. The state of the gas at the wall ahead of the incident wave is specified by p_0, ρ_0, and $u = 0$; the state behind the incident front, by p_1, ρ_1, and u_1; and that behind the reflected front, by p_2, ρ_2, and $u = 0$ (the wall is fixed). Figure 104 shows the situation in (t, x) coordinates, in which the various zones are denoted by 0, 1, and 2.

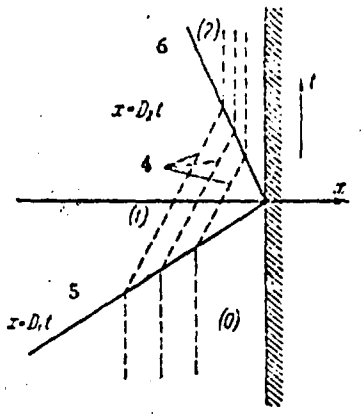


Fig. 104. Reflection of a shock wave by a rigid plane wall: 4) paths of gas particles; 5) incident front; 6) reflected front.

The reflected wave must be steady if the incident wave is. There is a stagnation region ($u = 0$) between the reflected wave and the wall; this means that the gas must acquire a speed u_2 equal in magnitude but opposite in sign to u_1, so the condition for the wall to be fixed is

$$u_1 - u_2 = 0. \qquad (47,1)$$

Best Available Copy

The basic relations for shock waves give us that

$$\sqrt{(p_1-p_0)(v_0-v_1)}=\sqrt{(p_2-p_1)(v_1-v_2)}, \tag{47,2}$$

in which $v = 1/\rho$; then

$$\frac{p_1-p_0}{\rho_0}\left(1-\frac{\rho_0}{\rho_1}\right)=\frac{p_2-p_1}{\rho_1}\left(1-\frac{\rho_1}{\rho_2}\right). \tag{47,3}$$

HUGONIOT's equations for the two waves determine ρ_1/ρ_0 and ρ_2/ρ_1 for a polytropic gas:

$$\left.\begin{aligned}\frac{\rho_1}{\rho_0}&=\frac{(k+1)p_1+(k-1)p_0}{(k-1)p_1+(k+1)p_0};\\ \frac{\rho_2}{\rho_1}&=\frac{(k+1)p_2+(k-1)p_1}{(k-1)p_2+(k+1)p_1}.\end{aligned}\right\} \tag{47,4}$$

Let $p_1/p_0 = \pi_1$ and $p_2/p_1=\pi_2$; then (47,3), with ρ_0/ρ_1 and ρ_1/ρ_2 inserted, becomes

$$(\pi_1-1)^2=\frac{\pi_1[(k-1)\pi_1+(k+1)](\pi_2-1)^2}{(k+1)\pi_2+(k-1)}. \tag{47,5}$$

and so

$$\pi_2=\frac{p_2}{p_1}=\frac{(3k-1)p_1-(k-1)p_0}{(k-1)p_1+(k+1)p_0}. \tag{47,6}$$

If $p_1 >> p_0$

$$\frac{p_2}{p_1}=\frac{3k-1}{k-1},$$

and so $p_2 = 8p_1$ if $k = 1.4$; further, (47,6) gives us the ratio of the excess pressures as

$$\frac{p_2-p_0}{p_1-p_0}=1+\frac{2kp_1}{(k-1)p_1+(k+1)p_0}. \tag{47,7}$$

If $(p_1 - p_0) << p_0$,

$$p_2-p_0\approx 2(p_1-p_0),$$

which is the result found in acoustics.

We may put (47,6) in the form

$$p_2=p_1+\frac{2kp_1(p_1-p_0)}{(k-1)p_1+(k+1)p_0}. \tag{47,8}$$

The incident pressure is p_1, so the second term on the right in (47,8) represents the pressure resulting from the motion of the medium behind the incident front. Here (47,2) and (47,4) give us that

$$p_1-p_0=\frac{k-1}{4}\rho u_1^2\left[1+\sqrt{1+\frac{16k}{(k-1)^2}\frac{p_0}{\rho_1 u_1^2}}\right]. \tag{47,9}$$

This ($p_1 - p_0$) is substituted into (47,8) to give

$$p_2 - p_0 = (p_1 - p_0) + \frac{k+1}{2}\rho_1 u_1^2\left[1 + \frac{k-1}{2(k+1)}\left(1 + \sqrt{1 + \frac{16k}{k^2-1}\frac{p_0}{\rho_1 u_1^2}}\right)\right]. \qquad (47,10)$$

The speed D_2 of the reflected wave is

$$D_2 = -v_1\sqrt{\frac{p_2 - p_1}{v_1 - v_2}} + u_1. \qquad (47,11)$$

This, with (47,2), (47,4), and (47,6), gives us that

$$D_2 = -\sqrt{\frac{2}{\rho_0[(k+1)p_1 + (k-1)p_0]}}\,[(k-1)p_1 + p_0]. \qquad (47,12)$$

while (47,4), with the p_2 of (47,6), gives us that

$$\frac{p_2}{p_1} = \frac{kp_1}{(k-1)p_1 + p_0}, \qquad (47,13)$$

which means that $p_2 / p_1 = 3.5$ for $k = 1.4$ if $p_1 \gg p_0$ and that $p_2 / p_0 = 21$; this shows that the density is very much increased by the reflection.

Figure 105 gives results for an ideal gas for various k; the

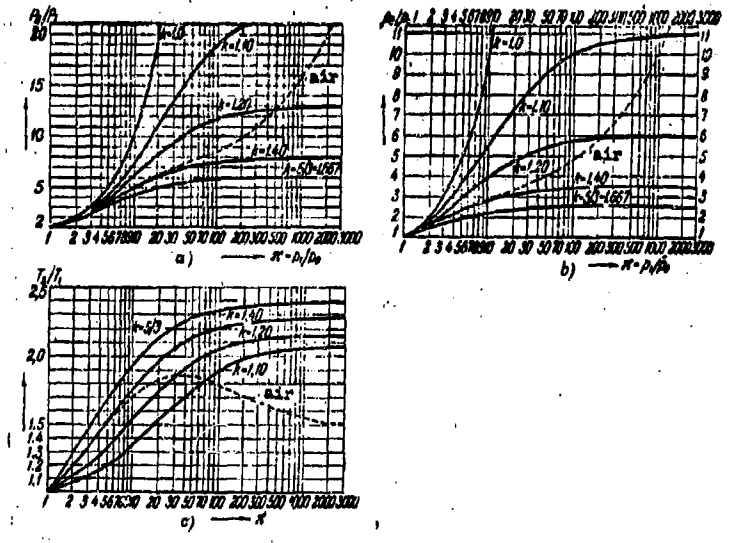


Fig. 105. Relation of a) the pressure ratio, b) the density ratio, and c) the temperature ratio for the reflected wave to the pressure ratio for the incident wave.

results apply to air for $\pi < 40$. The parameters of the reflected wave should be taken as initial ones if the wave is not steady.

The problem becomes much more troublesome if any attempt is made

to allow for the variation in the specific heat with temperature.

The problem is also more complicated if φ_0 (the angle between the incident front and the wall) is not zero. I shall consider the problem for an ideal gas only. The waves are as shown in Fig. 106; the parameters in region 0 (in front of the wave) are denoted by subscript zero, and so on. A moving coordinate system is used; the intersection between the wall and the wave is taken as being at rest. The velocity of the gas is denoted by q

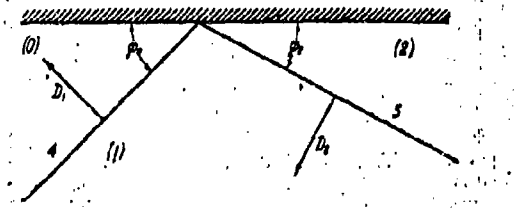


Fig. 106. Oblique incidence of a shock wave on a rigid wall: 4) incident front; 5) reflected front.

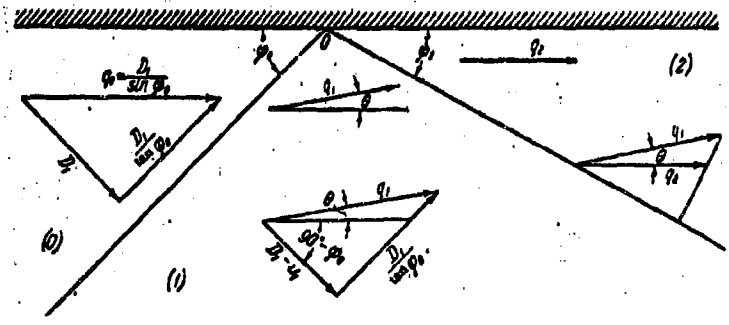


Fig. 107. Reflection of an obliquely incident shock wave at a rigid wall.

(Fig. 107); then

$$q_0 = \frac{D_1}{\sin\varphi_0}. \qquad (47,14)$$

The components normal and parallel to the front are respectively D_1 and $D_1/\tan\varphi_0$; q changes in magnitude and direction as the front is traversed, but the parallel component is not affected, because all forces are normal to the front. The normal component falls to $(D_1 - u_1)$, because the medium behind the front moves with a speed u_1.

Then

$$q_1 = \sqrt{(D_1 - u_1)^2 + \frac{D_1^2}{\tan^2 \varphi_0}}. \tag{47,15}$$

The angle between q_0 and q_1 is θ; the flow near the wall must be parallel to the wall, so q_2 must be turned through an angle θ in the reverse sense. This applies if the reflected front passes through O; in general, $\varphi_2 \neq \varphi_0$. Further, q_2 is defined by the fact that the component parallel to the front remains unchanged (Fig. 107):

$$q_2 = \frac{q_1 \cos(\varphi_2 + \theta)}{\cos \varphi_2}. \tag{47,16}$$

Here θ is given by

$$\tan(\varphi_0 - \theta) = \frac{D - u_1}{\frac{D_1}{\tan \varphi_0}}$$

or

$$\frac{\tan(\varphi_0 - \theta)}{\tan \varphi_0} = \frac{D - u_1}{D_1}.$$

But

$$\frac{D - u_1}{D_1} = \frac{\rho_0}{\rho_1},$$

so

$$\frac{\tan(\varphi_0 - \theta)}{\tan \varphi_0} = \frac{\rho_0}{\rho_1}. \tag{47,17}$$

HUGONIOT's equations relate p and v for adjacent regions:

$$\frac{v_0}{v_1} = \frac{(k+1)p_1 + (k-1)p_0}{(k-1)p_1 + (k+1)p_0} \tag{47,18}$$

$$\frac{v_1}{v_2} = \frac{(k+1)p_2 + (k-1)p_1}{(k-1)p_2 + (k+1)p_1}. \tag{47,19}$$

The q_i, p_i, and v_i for adjacent regions are related by

$$\left.\begin{aligned} v_0(p_1 - p_0) &= q_0(q_0 - q_1), \\ v_1(p_0 - p_1) &= q_1(q_1 - q_0), \\ v_1(p_2 - p_1) &= q_1(q_1 - q_2), \\ v_2(p_1 - p_2) &= q_2(q_2 - q_1). \end{aligned}\right\} \tag{47,20}$$

which define the q_i. A further condition is that

$$q_0 \times q_2 = 0, \tag{47,21}$$

which implies that q_0 is parallel to q_2. We can put (47,20)

$$\left.\begin{aligned}(v_0-v_1)(p_1-p_0)&=(q_0-q_1)^2=u_1^2,\\(v_0+v_1)(p_1-p_0)&=q_0^2-q_1^2,\\(v_1-v_2)(p_2-p_1)&=(q_1-q_2)^2=u_2^2,\\(v_1+v_2)(p_2-p_1)&=q_1^2-q_2^2.\end{aligned}\right\}\qquad(47,22)$$

This system of equations is readily solved, but the results are cumbrous; I give merely some final results in COURANT and FRIEDRICH's form:

$$\frac{\left(1-\frac{1}{\pi_1}\right)t_0}{1+\frac{\mu^2}{\pi_1}+\left(\frac{1}{\pi_1}+\mu^2\right)t_0^2}=\frac{(\pi_2-1)t_2}{1+\mu^2\pi_2+(\pi_2+\mu^2)t_2^2}=M,\qquad(47,23)$$

$$\frac{\left(1-\frac{1}{\pi_1}\right)^2}{\left(\mu^2+\frac{1}{\pi_1}\right)(1+t_0^2)}=\frac{(\pi_2-1)^2}{(\mu^2+\pi_2)(1+t_2^2)}=L,\qquad(47,24)$$

$$M^2(1-\mu^2)^2(t_0-t_2)+M[(1-\mu^2)^2-(t_0-t_2)^2-(\mu^2+t_0t_2)^2]-(t_0-t_2)=0,\qquad(47,25)$$

$$t_0=\operatorname{tg}\varphi_0,\quad t_2=\operatorname{tg}\varphi_2\quad\text{и}\quad\mu^2=\frac{k-1}{k+1}.$$

Now (47,25) gives two values for t_2 (namely, t_{2+} and t_{2-}) for any given π_1 and t_0, and also the corresponding quantities π_{2+} and π_{2-}. Figure 108a shows φ_2 as a function of φ_0 for various π_1; Fig. 108b shows π_2

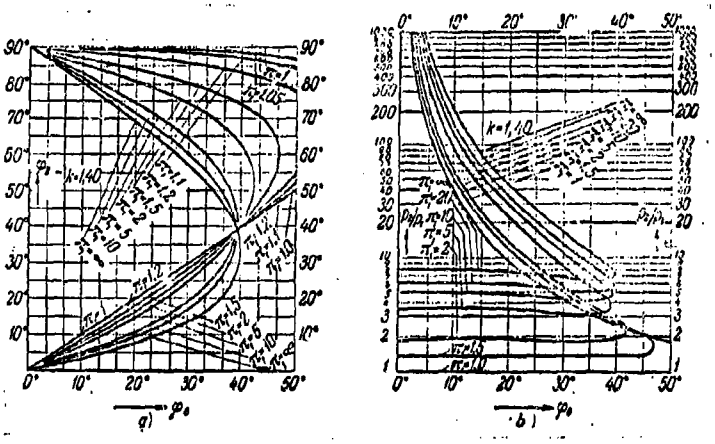


Fig. 108. Relation of *a*) φ_2 to φ_0 and *b*) π_2 to φ_0.

as a function of φ_0 for several π_1. The difference between π_{2+} and π_{2-} increases as φ_0 and π_1 decrease; π_{2+} becomes much larger than the π_2 for $\varphi_0 = 0$. This implies that π_{2-} is the more probable value, which corresponds to t_{2-}.

The lower branches of the curves of Fig. 108a imply that $\varphi_2 < \varphi_0$ if φ_0 is small; π_2 at first falls as φ_0 increases, but regains the initial level when $\varphi_0 = \varphi_0^*$. A notable point here is that φ_0^* is independent of π_1; $\varphi_0 = \varphi_2$ when $\varphi_0 = \varphi_0^*$. This φ_0^* is given by (47,25), with $t_0 = t_2$:

$$(1-\mu^2)^2 - (\mu^2 + t_0^2)^2 = 0,$$

or

$$\tan^2 \varphi_0^* = 1 - 2\mu^2,$$

so

$$\cos 2\varphi_0^* = \frac{\mu^2}{1-\mu^2} = \frac{k-1}{2}.$$

This means that $\varphi_0^* = 39°14'$ for air. Again, (47,24), with $t_0 = t_2$, shows that π_2 regains its initial value when $\varphi_0 < \varphi_0^*$:

$$\frac{(\pi_1 - 1)^2}{(\mu^2\pi_1 + 1)\pi_1} = \frac{(\pi_2 - 1)^2}{\mu^2 + \pi_2}.$$

The solution is

$$\pi_2 = \frac{(2\mu^2 + 1)\pi_1 - \mu^2}{\mu^2\pi_1 + 1}$$

or

$$\pi_2 = \frac{(3k-1)\pi_1 - (k-1)}{(k-1)\pi_1 + (k+1)}.$$

Further, π_2 becomes somewhat larger when $\varphi_0 > \varphi_0^*$; this is true, however, for $k = 1.4$ for $\pi_1 < 7.02$ (fairly weak waves). This φ_0^* is almost the limiting angle for regular reflection if π_1 is large, so such a wave cannot give a π_2 greater than that for $\varphi_0 = 0$.

The regular reflection described by the above relations is not possible for all φ_0 but only for $\varphi_0 \leqslant \varphi_{0m}$, in which φ_{0m} is dependent on π_1; the limit can be found from the condition that (47,25) must have a real root t_2 for given t_0 and π_1. Now $M = 0$ if $\pi_1 = 1$, and (47,25)

gives us that $l_2 = l_0$, so $\varphi_{0m} = 90°$, which is so for sound waves. Then $\varphi_{0m} < 90°$ if $\pi_1 > 1$ $(M > 0)$. Figure 109 shows φ_{0m} as a function of the pressure ratio for the incident wave. Irregular (MACH) reflection occurs for $\varphi_0 > \varphi_{0m}$; the speed of the reflected wave is greater than that of the incident wave, because the former travels through gas heated by the latter [the reflected wave is not appreciably retarded by the flow behind the incident front when φ_0 is large, since Fig. 107 shows that the component of the flow speed behind that front parallel to the reflected front is $u_1 \cos(\varphi_0 + \varphi_2)$]. This means that the reflected wave meets the incident wave at some distance from the surface; the result is a new wave (the head or MACH wave). There is also a contact discontinuity, which separates regions differing in density and temperature but identical in pressure and flow speed (Fig. 110). STANYUKOVICH and COURANT have made detailed studies of this type of reflection.

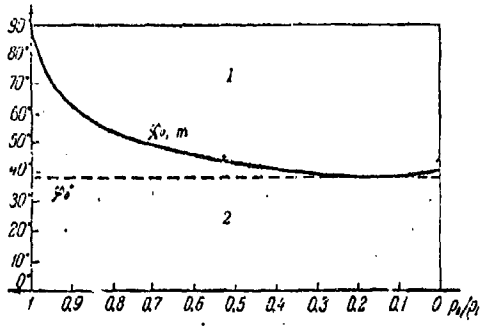


Fig. 109. Relation of φ_{0m} to pressure ratio for incident wave: 1) no regular reflection; 2) regular reflection possible.

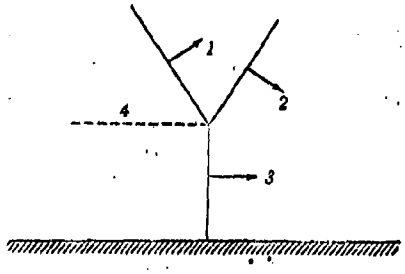


Fig. 110. Irregular reflection of a shock wave from a rigid wall: 1) reflected wave; 2) incident wave; 3) head wave; 4) contact discontinuity.

The principal feature of interest here is the ratio p_2/p_1, which

varies with φ_0 although π_1 is constant; for $\varphi_0 = 0$,

$$\frac{p_2}{p_1} = \frac{(3k-1)p_1 - (k-1)p_0}{(k-1)p_1 + (k+1)p_0}.$$

This π_2 at first decreases as φ_0 increases in regular reflection, but it regains its initial value when $\varphi_0 = \varphi_{0m}$, and, if π_1 is small, then somewhat exceeds the initial value. No such increase occurs in MACH reflection; π_2 for the head wave approaches one as φ_0 tends to 90°, because the wave slides along the surface instead of being reflected.

These various forms of reflection must be considered in order to estimate the loads that may act on the wall and also to determine the pressure at the front from experimental measurements of the force. A single shock wave can appear to give a variety of pressures at equal distances from the source, because the disposition of the instruments affects the result. Allowance must be made for the angle of incidence at the mounting of the instrument; the calculation becomes very troublesome if allowance must be made for flow around an obstacle comparable in size with the depth of the wave.

48. Initial Parameters of Shock Waves Produced by Efflux of Detonation Products

A shock wave is generated when the products from a detonation escape into any medium; the products themselves may contain a shock wave or a rarefaction wave. These shock waves may be examined if their initial parameters are known.

A shock wave is generated when the detonation wave reaches the interface between the charge and the medium; the parameters of this wave are determined by those of the detonation and by the mechanical characteristics of the medium. The effect on the products is dependent on the pressure difference at the interface; if $p_i < p_x$ (in which p_i is the pressure at the detonation front and p_x is the pressure at

the interface), a reflected shock wave will occur in the products. A rarefaction wave arises in the converse case.

There is no general analytic relation for the compressibility and density of an arbitrary medium, and so there is no general means of deducing which type of wave will arise in the products; but it is often possible to make the deduction for particular cases. For example, a reflected shock wave will occur if the medium is much more dense than the products (at the front); a rarefaction wave will occur if the reverse is the case. A reflected wave occurs if the products strike metals, while a rarefaction wave occurs if the products from a condensed explosive enter air, water, etc. A special study is needed if the two densities are similar.

The parameters of a wave generated at an interface may be derived from the laws for waves in the products and from the laws for shock waves in a medium in contact with a charge. Additional conditions imposed here are that the pressure and velocity must be continuous across the interface. Consider a plane detonation wave incident normally on an interface; there are two cases, namely $p_m < p_i$ and $p_m > p_i$. Figure 111 shows the pressures a) not long before the wave ($p_m < p_i$) strikes the interface and b) shortly afterwards. The condition at the interface is

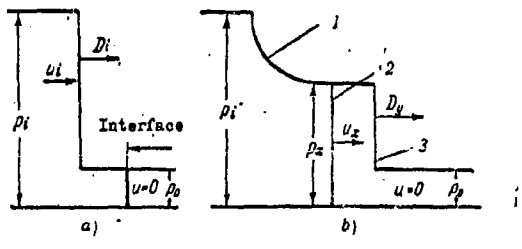


Fig.111. Determination of the initial parameters of a shock wave ($p_m < p_i$). 1) Rarefaction wave; 2) interface; 3) shock wave.

$$u_m = u_i + u_1, \qquad (48,1)$$

in which, u_x is the speed of the interface and u_1 is the change in the speed of the products in the rarefaction wave. The latter is

$$u_1 = \int_{p_\infty}^{p_i} \frac{dp}{\rho c} = \int_{v_i}^{v_\infty} \sqrt{-dp\,dv}, \tag{48,2}$$

in which ρ is density and c is the speed of sound (for the products). The relation of pressure to density for the products is

$$p\rho^{-k} = a, \tag{48,3}$$

in which $k = 3$ for high explosives of ρ_0 greater than one, and a is a constant.

Then, for a strong detonation wave,

$$\left.\begin{aligned} u_i &= \frac{D}{k+1}, \quad c_i = \frac{kD}{k+1}, \\ p_i &= \frac{k+1}{k}\rho_0 \quad\quad p_i = \frac{\rho_0 D^2}{k+1}. \end{aligned}\right\} \tag{48,4}$$

We may find u_1 from

$$c^2 = ak\rho^{k-1}, \quad \frac{c}{c_i} = \left(\frac{\rho}{\rho_i}\right)^{\frac{k-1}{2}} = \left(\frac{p}{p_i}\right)^{\frac{k-1}{2k}}, \quad \frac{\rho}{\rho_i} = \left(\frac{p}{p_i}\right)^{\frac{1}{k}}.$$

We insert ρ and c in (48,2) to get that

$$u_1 = \frac{p_i^{\frac{k+1}{2k}}}{\rho_i c_i} \int_{p_\infty}^{p_i} p^{-\frac{k+1}{2k}}\,dp = \frac{2kp}{(k-1)\rho_i c_i}\left[1 - \left(\frac{p_\infty}{p_i}\right)^{\frac{k-1}{2k}}\right].$$

But $kp_i / \rho_i = c_i^2$ and $c_i = kD/(k+1)$, so

$$u_1 = \frac{2kD}{k^2-1}\left[1 - \left(\frac{p_x}{p_i}\right)^{\frac{k-1}{2k}}\right] \tag{48,5}$$

or

$$u_1 = \frac{2}{k-1}(c_i - c_\infty). \tag{48,6}$$

The u_1 of (48,5) and the u_i of (48,4) are inserted in (48,1) to give us that

$$u_x' = \frac{D}{k+1}\left\{1 + \frac{2k}{k-1}\left[1 - \left(\frac{p_x}{p_i}\right)^{\frac{k-1}{2k}}\right]\right\}. \tag{48,7}$$

Now the speed u' of the medium behind the shock wave is

$$u' = u_\omega = \sqrt{(p_\omega - p_0)(v_{\omega 0} - v_{\omega\omega})}, \tag{48,8}$$

in which $v_{\omega 0}$ and $v_{\omega\omega}$ are the specific volumes of the medium on the two

sides of the shock wave and p_0 is the pressure in the medium ahead of the shock wave. Equations (48,7)and (48,8) define the initial parameters of the wave completely if the equation of state is known.

If the products escape into a vacuum, $p_\infty = 0$, so

$$u_\infty = u_{max} = \frac{3k-1}{k^2-1} D.$$

Then $u_{max} = D_i$ if $k = 3$, so the efflux speed cannot exceed D. Of course, this result does not correspond to experience; in fact, the leading section of the products escapes with a speed of almost $2D$ into a vacuum, and with a speed in excess of D even into air, although (48,7) implies that $u_\infty < D_i$ if $p_\infty > 0$. The reason for this discrepancy is that k cannot be taken as 3 if p_∞ is less than 20-30 thousand kg/cm^2. We shall see below that the initial p_∞ is of the order of p_i if the medium is dense (water, soil, etc.), so (48,7) then describes correctly the behavior of the products in those media.

If we assume that the detonation is instantaneous, (48,1), with $u_i = 0$, gives us that

$$u_\infty = u_i = \frac{2}{k-1}(\bar{c}_i - c_\infty),$$

in which $\bar{c}_i$ is the speed of sound in the products; then

$$u_\infty = \frac{2\bar{c}_i}{k-1}\left(1 - \frac{c_\infty}{\bar{c}_i}\right) = \frac{2\bar{c}_i}{k-1}\left[1 - \left(\frac{p_\infty}{\bar{p}_i}\right)^{\frac{k-1}{2k}}\right], \qquad (48,9)$$

in which $\bar{p}_i$ is the pressure in the products. But $\bar{c}_i = D[k/2(k+1)]^{1/2}$, so

$$u_\infty = \frac{2D}{k-1}\sqrt{\frac{k}{2(k+1)}}\left[1 - \left(\frac{p_\infty}{\bar{p}_i}\right)^{\frac{k-1}{2k}}\right]. \qquad (48,10)$$

For a vacuum, $p_\infty = 0$, so

$$u_\infty = \frac{2D}{k-1}\sqrt{\frac{k}{2(k+1)}},$$

which, with $k = 3$, gives us that

$$u_\infty = D\sqrt{\frac{3}{8}} = 0.61D.$$

This is substantially below the u_∞ found for actual detonations.

Now I consider the case $p_{w_1} > p_i$; Fig.112 shows the pressure immediately before and immediately after the wave reaches the interface. Here there is a reflected shock wave in the products (because $p_w > p_i$) and a shock wave in the medium. The condition at the interface is

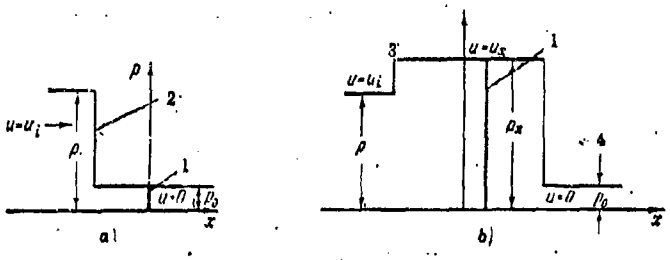


Fig. 112. Determination of the initial parameters of a shock wave ($p_{w_1} > p_i$): 1) interface; 2) detonation wave; 3) reflected shock wave; 4) shock wave.

$$u_w = u - u_1, \tag{48,11}$$

in which u_w is as shown and u_1 is the speed of the products behind the reflected shock wave; the latter is given by

$$u_1 = \sqrt{(p_w - p_i)(v_i - v_w)}, \tag{48,12}$$

in which v_i is the specific volume of the products at the front of the detonation wave and v_w is the same for the reflected wave. Then (48,3) transforms HUGONIOT's equation to

$$\frac{v_w}{v_i} = \frac{(k+1)p_i + (k-1)p_w}{(k+1)p_w + (k-1)p_i} = \frac{(k-1)\pi + (k+1)}{(k+1)\pi + (k-1)}, \tag{48,13}$$

in which $\pi = p_w / p_i$.

We transform (48,12) to

$$u_1 = \sqrt{p_i v_i (\pi - 1)\left(1 - \frac{v_w}{v_i}\right)}.$$

in which we insert the v_w / v_i of (48,13) to get that

$$u_1 = \sqrt{2 p_i v_i}\, \frac{\pi - 1}{\sqrt{(k+1)\pi + (k-1)}}.$$

Then (48,4) gives us that

$$\sqrt{2 p_i v_i} = \frac{D}{k+1}\sqrt{2k};$$

$$u_i = \frac{D}{k+1}\sqrt{2k}\,\frac{\pi-1}{\sqrt{(k+1)\pi+(k-1)}}.$$

We substitute for u_i and u_i from (48,11) to get that

$$u_\infty = \frac{D}{k+1}\left[1-\sqrt{2k}\,\frac{\pi-1}{\sqrt{(k+1)\pi+(k-1)}}\right]. \qquad (48,14)$$

Further, behind the shock wave in the external medium

$$u' = u_\infty = \sqrt{(p_\infty - p_0)(v_{00}-v_{0\infty})}, \qquad (48,15)$$

in which p_0 is the pressure (usually atmospheric) ahead of the shock wave; v_{p_0} and $v_{0\infty}$ are the specific volumes of the medium ahead of and behind that wave. But $p_0 \ll p_\infty$, so p_0 may be neglected, in which case (48,15) becomes

$$u_\infty = \sqrt{p_\infty (v_{00}-v_{0\infty})}. \qquad (48,16)$$

Equations (48,14) and (48,15) serve to define the initial parameters if the law of compression is known. Approximate solutions for certain media are given below.

Absolutely rigid wall. Here $u_\infty = 0$; then (48,14) is solved for as

$$\pi = \frac{5k+1+\sqrt{17k^2+2k+1}}{4k}. \qquad (48,17)$$

This π varies little with k, being 2.60 for the limiting case $\pi = 1$, 2.42 for $k = 1.4$, 2.39 for $k = 3$, and 2.28 for $k \to \infty$ (the root $\pi < 1$ for any k is physically meaningless). The $\rho_\infty / \rho_i = v_i / v_\infty$ are given by (48,13) as

$$k = 1 \quad (\pi = 2.60) \quad \frac{\rho_\infty}{\rho_i} = 2.60;$$
$$k = 1.4 \quad (\pi = 2.42) \quad \frac{\rho_\infty}{\rho_i} = 1.85;$$
$$k = 3 \quad (\pi = 2.39) \quad \frac{\rho_\infty}{\rho_i} = 1.33;$$
$$k \to \infty \quad (\pi = 2.28) \quad \frac{\rho_\infty}{\rho_i} = 1.00.$$

Then (48,13), with the π of (48,17) gives us that

$$\frac{\rho_\infty}{\rho_i} = \frac{v_i}{v_\infty} = \frac{9k^2+2k+1+(k+1)\sqrt{17k^2+2k+1}}{9k^2-1+(k-1)\sqrt{17k^2+2k+1}}. \qquad (48,18)$$

The initial speed of the reflected wave is

$$D_{\infty_1} = -v_i \sqrt{\frac{p_\infty - p_i}{v_i - v_\infty}} + u_i.$$

This may be put as

$$D_{\infty_1} = -\sqrt{\frac{p_i v_i (\pi - 1)}{\left(1 - \frac{v_{\infty_1}}{v_i}\right)}} + u_i.$$

We insert the v_∞ / v_i of (48,13) and use the relations

$$\sqrt{p_i v_i} = \frac{D_i}{k+1}\sqrt{k} \quad \text{and} \quad u_i = \frac{D}{k+1},$$

to get that

$$D_{\infty_1} = -\frac{D}{k+1}\left[\sqrt{\frac{k}{2}}\sqrt{(k+1)\pi + (k-1)} - 1\right]. \qquad (48,19)$$

Then $D_{\infty_1}/D_i = -0.31$ for $k = 1$ and $\pi = 2.60$, -0.78 for $k = 3$ and $\pi = 2.39$, and -1.28 for $k \to \infty$; that is, D_{∞_1} is very much dependent on k, but it is not very much dependent on π if k takes a fixed value close to 3, as the following values for $k = 3$ show:

$$\pi = 1.5 \quad \frac{D_{\infty_1}}{D_i} = -0.65$$

$$\pi = 2.0 \quad \frac{D_{\infty_1}}{D_i} = -0.74$$

$$\pi = 2.4 \quad \frac{D_{\infty_1}}{D_i} = -0.77$$

This fact enables us to measure k in terms of the speed of a shock wave reflected from a dense medium.

This measurement is one of some importance, because we have as yet no accurate method of measuring the pressures produced in detonations and in the reflection of detonation waves. Kinematic measurements can be made accurately, and these give us k, which enables us to calculate the parameters of a detonation wave with reasonable precision.

There is a small rise in the entropy of the products when the wave is reflected, which is caused by the small pressure change in the

reflected wave. We have that before reflection

$$S_i = \ln p\, v^k + \text{const};$$

and after reflection

$$S_\infty = \ln p_\infty v_\infty^k + \text{const}.$$

The entropy change is then

$$\Delta S = S_\infty - S_i = \ln \frac{p_\infty}{p_i}\left(\frac{v_\infty}{v_i}\right)^k = \ln \eta.$$

This η is given by (48,17) and (48,18) as

$$\eta = \frac{5k+1+\sqrt{17k^2+2k+1}}{4k}\left[\frac{9k^2-1+(k-1)\sqrt{17k^2+2k+1}}{9k^2+2k+1+(k+1)\sqrt{17k^2+2k+1}}\right]^k.$$

$$k=3 \qquad \eta = 1.08,$$

$$k=1 \qquad \eta = 1.00.$$

Thus ΔS is negligible, so we can perform the calculation for the reflected wave as for a set of sound waves. Here the RIEMANN solution gives us that

$$du = \pm c\, d\ln\rho. \qquad (48,20)$$

The isentropic law gives us that

$$\rho \sim c^{\frac{2}{k-1}},$$

so (48,20) becomes

$$du = \pm \frac{2}{k-1}\, dc.$$

The integral is

$$\Delta u = \pm \frac{2}{k-1}\Delta c$$

or

$$u_\infty - u_i = -\frac{2}{k-1}(c_\infty - c_i).$$

At the wall

$$u_\infty = 0,$$

so

$$c_\infty = c_i + \frac{k-1}{2}u_i = \frac{3k-1}{2(k+1)}D;$$

$$\frac{p_\infty}{p_i} = \left(\frac{\rho_\infty}{\rho_i}\right)^k = \left(\frac{c_\infty}{c_i}\right)^{\frac{2k}{k-1}}.$$

We substitute for c_m and c_i in the last expression to get

$$\frac{p_m}{p_i} = \left(\frac{3k-1}{2k}\right)^{\frac{2k}{k-1}}. \qquad (48,21)$$

The acoustic theory gives us that

$$D_m = \frac{u_i - c_i + u_m - c_m}{2} = -\frac{5k-3}{4(k+1)} D_i. \qquad (48,22)$$

For $k = 3$,

$$\frac{p_m}{p_i} = \left(\frac{4}{3}\right)^5 = 2.37; \quad \frac{\rho_m}{\rho_0} = \frac{4}{3} = 1.33; \quad c_m = D_i;$$

$$\frac{D_m}{D_i} = -\frac{3}{4} = -0.75.$$

These results are very close to the exact ones.

The theory enables us to determine the initial conditions at the contact between two colliding bodies (even liquid or solid ones); STANYUKOVICH explains this by saying that the formulation of the conservation laws for the instant of collision is not dependent on the phase states of the bodies. Moreover, no forces have yet arisen within the bodies when contact has just been made; the contact gives rise to shock waves.

Let subscript i and a denote the parameters before impact, primes and subscripts 1 and 2 denoting parameters after the impact. Consider a coordinate system in which the second medium is at rest; then the interaction is one between the first medium and an initially motionless barrier. The relative speed of collision is

$$u_{i1} = u_i \pm u_a, \qquad (48,23)$$

in which u_a is positive if the two media move in opposite senses and negative if they move in the same sense (the condition for collision is then $u_i > u_a$). The speed of the interface is u'; then

$$u' = u_1' = u_{i1} - u_1', \qquad (48,24)$$

and

$$p' = p_1' = p_2', \qquad (48,25)$$

The speeds of the media behind the shock waves originating from the point of contact are given by

$$u' = \sqrt{(p' - p_a)(v_a - v_1')} = u_{i1} - \sqrt{(p' - p_a)(v_i - v_1')},$$

in which p_a is the initial pressure; $p_a \ll p'$ if the speed of collision is high, so

$$u' = \sqrt{p'(v_a - v_2')} = u_{i1} - \sqrt{p'(v_i - v_1')}. \tag{48,26}$$

Let

$$v_a - v_2' = v_a\left(1 - \frac{v_2'}{v_a}\right) = \alpha_2 v_a = \frac{\alpha_2}{\rho_a},$$

and

$$v_i - v_1' = v_i\left(1 - \frac{v_1'}{v_i}\right) = \alpha_1 v_i = \frac{\alpha_1}{\rho_i},$$

Then

$$\frac{\rho_a}{\alpha_2} u'^2 = p', \quad (u_{i1} - u')^2 \frac{\rho_i}{\alpha_1} = p'. \tag{48,27}$$

so

$$p' = \frac{\rho_a}{\alpha_2} u'^2 = (u' - u_{i1})^2 \frac{\rho_i}{\alpha_1},$$

or

$$\frac{u' - u_{i1}}{u'} = \sqrt{\frac{\rho_a}{\rho_i}\frac{\alpha_1}{\alpha_2}};$$

the ratio of speeds being

$$\frac{u'}{u_{i1}} = \frac{1}{1 + \sqrt{\frac{\rho_a}{\rho_i}\frac{\alpha_1}{\alpha_2}}}. \tag{48,28}$$

This last defines the speed of the interface; the other initial parameters are readily found in terms of u', α_1, and α_2. For example, (48,27) defines the initial pressure at impact, while the speeds of the waves are

$$D_1' = -v_i\sqrt{\frac{p'}{v_i - v_1'}} + u_{i1},$$

$$D_2' = v_a\sqrt{\frac{p'}{v_a - v_2'}}.$$

The p' of (48,27) then gives us that

$$D_1' - u_{i1} = \frac{u' - u_1'}{\alpha_1}, \quad D_2' = \frac{u'}{\alpha_2}. \tag{48,29}$$

The equations of state (or of compressibility) are needed in order to find α_1 and α_2.

Equations (48,27) and (48,28) enable us to relate $u_{i\,1}$ to p':

$$p' = \frac{\rho_0 u_{i\,1}^2}{\left[\sqrt{a_2} + \sqrt{\frac{\rho_0}{\rho_i} a_1}\right]^2}. \tag{48,30}$$

A general relation between density and pressure for liquids and solids (not porous) is

$$p = A(S)\left[\left(\frac{\rho}{\rho_0}\right)^n - 1\right], \tag{48,31}$$

in which $A(S)$ is a function of the entropy; n may be taken as constant over a wide range of pressures. The change in S consequent upon impact can be neglected if the speed of impact does not exceed a few km/sec; then (48,31) is the equation of isentropy for a solid or liquid. Methods are available for measuring n and A; $n = 4$ for some metals, which agrees with JENSEN's result. We can calculate A from TATE's adiabatic equation of state for liquids and solids:

$$-\frac{1}{v}\left(\frac{\partial v}{\partial p}\right)_S = \frac{1}{n[p + A(S)]}, \tag{48,32}$$

which has the integral

$$p = A(S)\left\{\left[\frac{v(T;0)}{v(T;p)}\right]^n - 1\right\}. \tag{48,33}$$

But

$$-\frac{1}{v}\left(\frac{\partial v}{\partial p}\right)_s = \frac{1}{\rho c^2},$$

so (48,32) may be put as

$$p = \frac{\rho c^2}{n} - A. \tag{48,34}$$

Then $p = p_0$, $\rho = \rho_0$, and $c = c_0$ give us that

$$p_0 = \frac{\rho_0 c_0^2}{n} - A.$$

But

$$c^2 = c_0^2\left(\frac{\rho}{\rho_0}\right)^{n-1},$$

and so

$$p - p_0 = \frac{\rho_0 c_0^2}{n}\left[\left(\frac{\rho}{\rho_0}\right)^n - 1\right], \tag{48,35}$$

If we neglect p_0, which is here permissible, and compare this with

(48,30), we have that

$$A = \frac{\rho_0 c_0^2}{n}.$$

Table 68 gives calculated and experimental A for metals, for which

Table 68

Calculated and Measured Values of A for Metals

Metal	A_e kg/cm^2	A_c kg/cm^2	$\frac{A_c}{A_e}$
Iron	4.5×10^5	5.0×10^5	1.11
Copper	2.35×10^5	2.5×10^5	1.06
Duralumin	2.04×10^5	2.03×10^5	1.00

$n = 4$; the agreement is satisfactory, which confirms that (48,31) describes the behavior of a solid accurately. This equation gives us that

$$\alpha_1 = 1 - \frac{1}{\left(\frac{p'}{A_1} + 1\right)^{1/n}}, \quad \alpha_2 = 1 - \frac{1}{\left(\frac{p'}{A_2} + 1\right)^{1/n}}, \tag{48,36}$$

which is the final step in the solution. Table 69 gives some results,

Table 69

Parameters of Shock Waves Produced by Duralumin Striking Steel

u_{p1}, m/sec	p', kg/cm^2	α_1	α_2	u^d, m/sec
1 000	2.5×10^5	0.180	0.106	575
3 000	10^6	0.358	0.253	1 780
8 900	5×10^6	0.555	0.466	5 420
13 500	10^7	0.624	0.542	8 300
30 400	5×10^7	0.748	0.693	20 200

for which purpose the values adopted were $u_{p_1} = 0$, $\rho_1 = 7.8$ g/cm^3, $A_2 = 4.5 \times 10^5$ kg/cm^2, $\rho_1 = 2.73$ g/cm^3, and $A_1 = 2.04 \times 10^5$ kg/cm^2. The calculations are not very precise for $p' > 10^6$ kg/cm^2, because

the change in S cannot be neglected. The law of compressibility has not been tested experimentally for these ve high pressures.

We have made measurements of the A of ,31). Plates of various thicknesses were fitted with cylindrical charges (height equal to 5-6 diameters) standing on end. The wave reaching the plate was then almost plane. The other side of the plate was in contact with water in a transparent vessel; the wave in the plate gave rise to one in the water, which was recorded. The initial speed of the water wave gave u' for the interface with the water and hence the pressure. (These two parameters may be varied by using several different explosives.) The hydrodynamic theory then gives us the pressure and density for the wave in the metal, which may be treated as a liquid, because the stress produced by the explosion is well in excess of the yield point.

The equation is

$$u_\infty = u_i + u_1, \tag{48,37}$$

in which u_∞ relates to the interface, u_i the initial speed behind the wave in the metal, and u_1 to the change in that speed as a result of the reflection. The treatment of section 47 shows that

$$u_\infty = \sqrt{(p_\infty - p_0)(v_{w0} - v_{w\infty})}, \tag{48,38}$$

in which v_{w0} and $v_{w\infty}$ are specific volumes for the water ahead of and behind the shock wave. Now

$$u_i = \sqrt{p_i (v_{M0} - v_{Mi})}, \tag{48,39}$$

in which p_i relates to the incident wave in the metal and the v_M are specific volumes for the metal. Also,

$$u_1 = \int_{p_\infty}^{p_i} \frac{dp}{\rho c}. \tag{48,40}$$

If we use (48,31) for the law of compression, we can put (48,40) as

$$u_1 = \frac{2}{n-1} \sqrt{\frac{nA}{\rho_{M0}}} \left[\left(\frac{p_i}{A} + 1 \right)^{\frac{n-1}{2n}} - \left(\frac{p_\infty}{A} + 1 \right)^{\frac{n-1}{2n}} \right]. \tag{48,41}$$

Here p_∞ and u_1 are known, because water is used; the unknowns in (48,37) and (48,41) are then A, n, and p_i. Experiment can give us u_i, whereupon we have

$$p_i = \rho_{\infty 0} u_i D_i, \tag{48,42}$$

in which D_i is the speed of the shock wave, which is close to that of sound even if $p_i \geqslant 10^5$ kg/cm^2. There is no means of measuring D_i at a point; it can be measured only over a distance of several mm. (The values can be used without introducing great error, in view of the above.) Then (48,31) and (48,42) enable us to put (48,36) as

$$\frac{p_i}{\rho_{\infty 0} D_i^2} = \frac{\left(\frac{p_i}{A}+1\right)^{\frac{1}{n}} - 1}{\left(\frac{p_i}{A}+1\right)^{\frac{1}{n}}}. \tag{48,43}$$

Then the u_1 of (48,41) and the u_i of (48,42) give us from (48,37) that

$$u_\infty = \frac{p_i}{\rho_{\infty 0} D_i} + \frac{2}{n-1}\sqrt{\frac{nA}{\rho_{\infty 0}}}\left[\left(\frac{p_i}{A}+1\right)^{\frac{n-1}{2n}} - \left(\frac{p_\infty}{A}+1\right)^{\frac{n-1}{2n}}\right]. \tag{48,44}$$

The unknowns are as before; calculations show that p_i varies very little with n if $n > 3$, so we were able to put n as 4, and then to determine p_i and A for given p_∞ and D_i. We found that A remained nearly constant for $n = 4$ for a fairly wide range of plate thicknesses (i.e., for a wide range in p_i).

This work was done in 1955; later in the year, there appeared a paper on the same topic by WALSH and CHRISTIAN, who measured D_i for a metal with a free surface, and also u_∞ for that surface. Their assumption was that u_∞ would be twice u_i, because

$$u_\infty = u_i + u_1 \tag{48,45}$$

$$u_1 = u_i. \tag{48,46}$$

In fact, u_1/u_i varies from 0.96 to 1.03 for Zn, from 0.98 to 1.02 for Al, and from 0.98 to 1.01 for Cu for pressures up to 450 kbar (445 000 kg/cm^2); this introduces an error of $\pm 1\%$ in the v_m. Then (48,42) and (48,46) give p_i, which, with

$$\frac{v_{M0}}{v_{Mi}} = \frac{D_i - u_i}{D_i} \qquad (48,47)$$

gives v_{Mi}.

WALSH and CHRISTIAN's results for Al agree closely with ours; Table 68 gives the constants, and Table 70 gives the results. Their

Table 70

Compressibility of Aluminium as a Function of Pressure

p_i kbar	133.9	218.0	258.6	288.7	323.3	347.0	Source
$\frac{v_{Mi}}{v_{M0}}$	0.878	0.834	0.817	0.804	0.791	0.780	[10]
$\frac{v_{Mi}}{v_{M0}}$	0.880	0.830	0.813	0.801	0.788	0.777	Own results

results for Cu do not agree so well with ours, because their copper had a specific gravity of 8.903, whereas ours had one of 8.5.

AL'TSHULER and others in 1958 published some very important results on dynamic compressibility for metals at pressures up to 5×10^6 kg/cm^2. Their method was to measure the kinematic parameters of the waves excited in a target. In one case they measured the mean speed of the shock wave and the speed of the free surface, which latter was taken as twice the speed of the metal behind the front. This was shown to be so for pressures up to 3.5×10^6 kg/cm^2.

COOK denies that this relation is applicable; without good reason, he assumes that the measurements give the sum of the speed of the free surface and the speed of the body as a whole (instead of the first alone).

This would be so if the body were absolutely incompressible, in which case the acceleration would be indefinitely great. Such conditions do not occur, of course.

AL'TSHULER et al produced these very high pressures by allowing a body that had been accelerated slowly to strike a target at rest; if the striker and target are made of the same material, the speed of the interface should be

$$u' = \frac{1}{2}u,$$

in which u is the initial speed of the striker. This u and D' (the speed of the shock wave) must be measured in order to deduce the compressibility.

They found that D' is linearly related to u' if the latter is in the range 1 to 5.17 km/sec:

$$D' = C_0' + \lambda u'$$

in which C_0' and λ are empirical constants, which take the values 3.80 and 1.58 respectively for iron if the speeds are expressed in km/sec. This functional relation defines the dynamic adiabatic

$$p' = \frac{C_0'^2(\rho - \rho_0)\rho_0}{(\lambda-1)^2\left[\frac{\lambda}{\lambda-1}\rho_0 - \rho\right]^2}. \qquad (48,48)$$

AL'TSHULER et al consider that this is applicable for p' between 3×10^5 and 5×10^6 kg/cm^2 for iron. They found that this linear relation is applicable to all the metals whose C_0' and λ are listed below (but not for Sn); the adiabatics are of the form of (48,48).

	C_0', km/sec	λ	ρ_0, g/cm^3
Cu	3.90	1.46	8.93
Zn	3.20	1.45	7.14
Ag	3.30	1.54	10.49
Cd	2.65	1.48	8.64
Au	3.15	1.47	19.30
Pb	2.30	1.27	11.34
Bi	2.00	1.34	9.80

These general laws become much simpler if $p'/A \ll 1$; we may expand $\sqrt[n]{(1 + p'/A)}$ in series form and take only the first term, which gives us

$(1 + p'/nA)$. Then (48,36) gives us that $\alpha_1 = p'/(nA_1 + p')$ and $\alpha_2 = p'/(nA_2 + p')$; these are inserted in (48,30) to give us that

$$p' = \frac{u_{i1}\sqrt{(nA_2 + p')\rho_0}}{1 + \sqrt{\frac{\rho_0}{\rho_1}\frac{(nA_2 + p')}{(nA_1 + p')}}}. \qquad (48,49)$$

If now we neglect p' on the right, we get

$$p' = \frac{u_{i1}\sqrt{\rho_0 nA_2}}{1 + \sqrt{\frac{\rho_0 A_2}{\rho_1 A_1}}}, \qquad (48,50)$$

which is a linear relation of p_i to u_i. If now u_i is substantially less than the speeds of sound in the metal (c_0 and c_1), we can put (48,27) and (48,28) as

$$p' = \frac{\rho_1\rho_0 c_1' c_2'}{\rho_1 c_1' + \rho_0 c_2'} u_{i1}, \qquad (48,51)$$

$$u' = \frac{u_{i1}\rho_1 c_1'}{\rho_1 c_1' + \rho_0 c_2'}. \qquad (48,52)$$

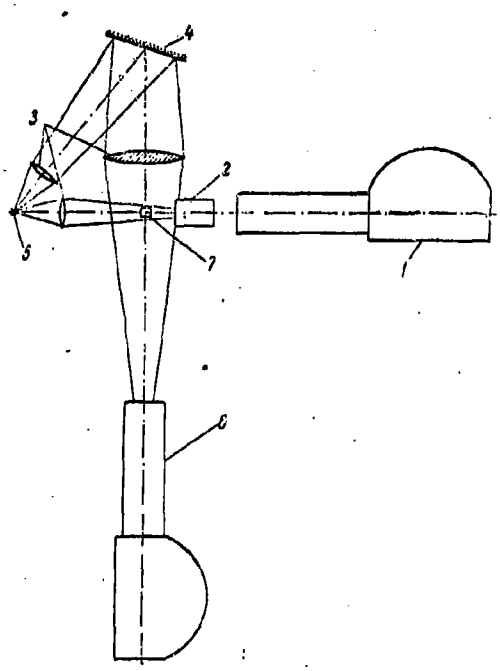


Fig. 113. Apparatus for measuring the displacement of the free end of a rod and the speed of a wave in the rod.

These expressions are correct only if the yield stress is exceeded by a considerable margin, as for lead and some alloys; other metals require a correction for the yield stress, which reduces u and increases p'. (This topic is considered in chapter XII.) A body that deforms in accordance with HOOKE's law can be used in measurements of compressibility if we have some means of

recording the displacement of the material in a thin rod. HOPKINSON first used rods in order to measure the pressure as a function of time; DAVIS described an electrical form of Hopkinson's method in 1948. Rods of HOPKINSON's original design have been used at the Institute of Chemical Physics in order t. measure the parameters of strong shock waves (see section 87). BAUM and STETSOVSKIY have improved the method by using a new technique for recording the motion of the end and the passage of the wave in the specimen (Fig. 113).

The two rotating-mirror recorders (type SFR-2M) were made at the Institute; the lens 2 and the recorder 1 produce photomicrographs (x 20) of the motion of the end of the rod 7, which lies normal to the

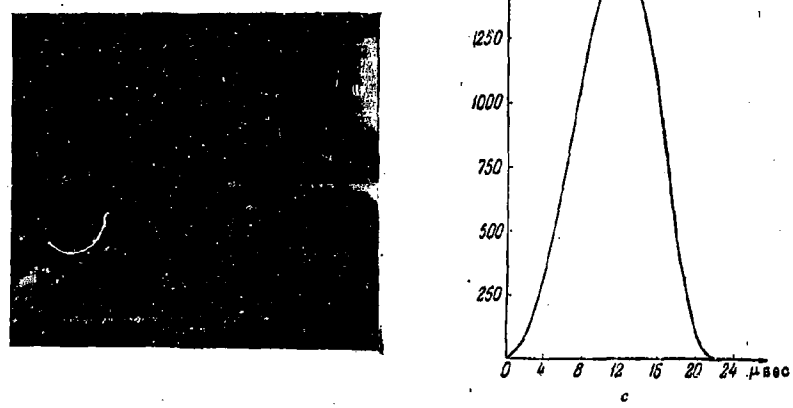


Fig. 114. a) Motion of the end of a rod after reflection of a compression wave; b) propagation of compression and tension waves in the rod; c) shape of stress wave.

plane of the figure. The second recorder 6 rec : s the progress of the wave excited in the specimen. The two recorders are synchronized with the light source 5 and with the explosion. The lenses 3 and

mirror 4 serve to direct the light to the recorder.

The pressure p_w in a compression wave approaching the free end is given by

$$p_w = \frac{1}{2}\rho_0 c_0 \frac{dx}{dt}, \qquad (48,53)$$

in which ρ_0 is density, c_0 is the speed of sound in the rod, and dx/dt is the speed of the free end. Experiment gives us $x = f(t)$, from which we find $p_w = \varphi(t)$, i.e. the form of the stress wave.

Figure 114a shows the motion of the end of a rod of plexiglas 200 mm long as excited by 200 mg of lead azide placed at the other end.

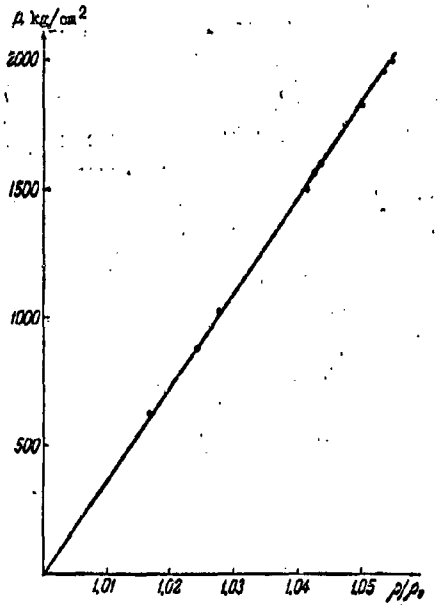


Fig. 115. Compressibility of plexiglas for dynamic loads.

Figure 114b shows the waves propagating in the rod, and Fig. 114c shows the stress wave. The recordings show that the tensile stresses resulting from the reflection at the free end are responsible for breaking the rod. The free end starts to move when the compression wave arrives; the rod breaks when the tensile stress exceeds the ultimate strength of the material.

The ultimate strength of plexiglas for dynamic loads is 1250-1350 kg/cm^2 (the value for static loads is only 650 kg/cm^2). The maximum speed of the material behind the shock wave is

$$u_{w\,max} = \frac{1}{2}\left(\frac{dx}{dt}\right)_{max},$$

so the law of compressibility can be deduced from the measured D and u_w, for which we have the basic laws

$$D = \frac{u_w}{1 - \frac{\rho_0}{\rho}} \tag{48,54}$$

$$p = \rho_0 u_{w\,max} D. \tag{48,55}$$

Figure 115 shows the result; the compressibility is linear up to 2000 kg/cm^2, which justifies our assumption that plexiglas obeys HOOKE's law, at least up to that limit.

49. Initial Parameters of Shock Waves in Media

Escape of detonation products into air. We have seen above that (48,7) cannot be applied to the shock wave and products when the latter escape into the air; LANDAU and STANYUKOVICH have proposed to incorporate a correction for the variation in k in order to perform the calculation. We do not know $k(p)$ in analytic form, so they used two isentropic laws in order to describe the process:

$$p_i v_i^k = p_k v_k^k \quad , \quad p_k v_k^\gamma = p v^\gamma, \tag{49,1}$$

in which subscript i refers to the detonation front, subscript k relates to the point where the two laws overlap, and γ is 1.2 to 1.4.

HUGONIOT's equation can be used to find p_k and v_k:

$$\frac{p_i v_i}{k-1} - \frac{p_k v_k}{k-1} + \Delta Q = \frac{p}{2}(v_0 - v_i) + Q_v, \tag{49,2}$$

in which ΔQ is the residual heat and Q_v is the heat of explosion. It is found that $p_k v_k$ is small relative to $p_i v_i$, so (49,2) can be put as

$$\frac{p_i v_i}{k-1} + \Delta Q = \frac{p v_0}{2}\left(1 - \frac{v_i}{v_0}\right) + Q_v. \tag{49,3}$$

But

$$p_i = \frac{\rho_0 D^2}{k+1}, \quad v_i = \frac{1}{\rho_i} = \frac{k}{k+1}\frac{1}{\rho_0},$$

so

$$\Delta Q = Q_v - \frac{D^2}{2(k^2-1)}. \tag{49,4}$$

Now ΔQ is thermal energy, so $\Delta Q = c_v T_k$; the products behave as an ideal gas for $p < p_k$, so

$$p_k v_k = R T_k = \frac{R \Delta Q}{c_v} = (\gamma - 1)\Delta Q. \tag{49,5}$$

We have two equations

$$p_k v_k = (\gamma - 1)\Delta Q \quad , \qquad p_i v_i^k = p_k v_k^k,$$

for p_k and v_k; γ can be found only if the composition of the products is known, but we may assume that $\gamma \approx 1.3$ for the usual high explosives. The velocity of escape is

$$u_\infty = u_1 + u_i, \tag{49,6}$$

in which u_1 is the change in the speed of the products resulting from the rarefaction wave; here

$$u_1 = \int_{p_\infty}^{p_i} \frac{dp}{\rho c}.$$

We divide the region of integration into two parts to get

$$u_1 = \int_{p_k}^{p_i} \frac{dp}{\rho c} + \int_{p_\infty}^{p_k} \frac{dp}{\rho c} = \frac{2}{k-1}(c_i - c_k) + \frac{2}{\gamma - 1}(c_k - c_\infty),$$

in which c is the speed of sound and $c_k = (\gamma p_k c_{1k})^{1/2}$. Then

$$u_\infty = u_i + \frac{2c_i}{k-1}\left(1 - \frac{c_k}{c_i}\right) + \frac{2c_k}{\gamma - 1}\left(1 - \frac{c_\infty}{c_k}\right). \tag{49,7}$$

Now

$$u_i = \frac{D}{k+1}, \quad c_i = \frac{kD}{k+1}, \quad \frac{c_k}{c_i} = \left(\frac{p_k}{p_i}\right)^{\frac{k-1}{2k}}$$

$$\frac{c_\infty}{c_k} = \left(\frac{p_\infty}{p_k}\right)^{\frac{\gamma-1}{2\gamma}},$$

so substitution gives us that

$$u_\infty = \frac{D}{k+1}\left\{1 + \frac{2k}{k-1}\left[1 - \left(\frac{p_k}{p_i}\right)^{\frac{k-1}{2k}}\right]\right\} + \frac{2c_k}{\gamma - 1}\left[1 - \left(\frac{p_\infty}{p_i}\right)^{\frac{\gamma-1}{2\gamma}}\right], \tag{49,8}$$

Further, $p_\infty = 0$ if the products escape into a vacuum, so

$$u_{\infty m} = \frac{D}{k+1}\left\{1 + \frac{2k}{k-1}\left[1 - \left(\frac{p_k}{p_i}\right)^{\frac{k-1}{2k}}\right]\right\} + \frac{2c_k}{\gamma - 1}. \tag{49,9}$$

The products produce a shock wave if they escape into the air, and this reduces the escape speed. Initially, the speed of escape coincides with u', the speed of the air behind the shock-wave front, which

we may take as strong. Then we have that

$$D' = \frac{\gamma_a + 1}{2} u' \; ; \quad p' = p_w = \frac{\gamma_a + 1}{2} \rho_a u'^2, \quad u' = u_w \qquad (49,10)$$

$$u_w = \sqrt{\frac{2}{\gamma_a + 1} \frac{p_w}{\rho_a}}, \qquad (49,11)$$

in which γ_a is γ for air (1.2 for strong shock waves) and ρ_a is the density of the air in front of the wave.

Equations (49,8) and (49,11) suffice to determine the initial parameters. Table 71 gives results for typical high explosives; the

Table 71

Initial Parameters of Shock Waves in Air

BB	ρ_e, g/cm³	D, m/sec	Q_v, kcal/kg	ΔQ, kcal/kg	$p_{p'}$, kg/cm²	$p_{x'}$, kg/cm²	$u_{x'}$, m/sec	D', m/sec	$u_{x=\infty}$, m/sec
Trotyl . . .	1.60	7000	1000	285	1350	570	6450	7100	10 500
Hexogene . .	1.60	8200	1300	310	1500	760	7450	8200	11 900
TEN	1.69	8400	1400	350	1800	810	7700	8450	12 400

last column is for escape into a vacuum, and here u_∞ is much larger than D' ($u_\infty \approx D'$ for escape into air). Experiment shows that these calculated values are somewhat too low, expecially for escape into vacuum. Moreover, the u_∞ (and the other parameters) for air are somewhat dependent on the density of the charge, as Table 72 shows for

Table 72

Speeds of Shock Waves in Air Near Charges

	ρ_e, g/cm³	D, m/sec	Mean speed, m/sec		
			0–30 mm	30–60 mm	60–90 mm
Trotyl	1.30	6025	6670	5450	4620
"	1.35	6200	6740	5670	4720
"	1.45	6450	6820	5880	—
"	1.60	7000	7500	6600	5460
Hexogene	1.40	7350	8000	—	—
"	1.60	8000	8600	6900	6400

charges 23 mm in diameter.

If we take the speed in the first section as D', we get u_0 for trotyl of density 1.60 g/cm^3 as $2D'/(\gamma_0 + 1) = 6800$ m/sec, so $p_0 = 640$ kg/cm^2, which are somewhat higher than the calculated values. Hexogene having a detonation rate of 8000 m/sec gives $p_\infty = 840$ kg/cm^2 and $u_\infty = 7850$ m/sec. The discrepancy can be reduced if we use the two laws

$$pv^k = \text{const} \quad , \quad pv^\gamma = \text{const}.$$

It is usual in calculations on the total effect of an explosive charge to assume that the detonation is instantaneous. We can evaluate the initial parameters of the shock wave in air for this case, for $u_i = 0$ and (48,7) becomes

$$u_\infty = u_1 = \int_{p_{k1}}^{\bar{p}_i} \frac{dp}{\rho c} + \int_{p_\infty}^{p_{k1}} \frac{dp}{\rho c} = \frac{2\bar{c}_i}{k-1}\left(1 - \frac{c_{k1}}{\bar{c}_i}\right) + \frac{2c_{k1}}{\gamma - 1}\left(1 - \frac{c_\infty}{c_{k1}}\right) \qquad (49,12)$$

or

$$u_\infty = \frac{2\bar{c}_i}{k-1}\left[1 - \left(\frac{p_{k1}}{\bar{p}_i}\right)^{\frac{k-1}{2k}}\right] + \frac{2c_{k1}}{\gamma - 1}\left[1 - \left(\frac{p_\infty}{p_{k1}}\right)^{\frac{\gamma-1}{2\gamma}}\right], \qquad (49,13)$$

in which the barred quantities apply to an instantaneous detonation, the others in subscript $k1$ being for the point of overlap:

$$\bar{p}_i = \frac{p_i}{2} \quad , \quad \bar{c}_i^2 = \frac{3}{8} D^2.$$

HUGONIOT's equation for this detonation is

$$\frac{\bar{p}_i v_0}{k-1} - \frac{p_{k1} v_{k1}}{k-1} + \Delta Q = Q_v;$$

so, if we neglect the second term as being small relative to the first, we have that

$$\Delta Q = Q_v - \frac{\bar{p}_i v_0}{k-1} = Q_v - \frac{p_i v_0}{2(k-1)} = Q_v - \frac{D^2}{2(k^2-1)}.$$

That is, the residual heat at this point is not dependent on the nature of the detonation. The parameters for this point of overlap are given by

$$\bar{p}_i v_0^3 = p_{k1} v_{k1}^3, \quad p_{k1} v_{k1} = (\gamma - 1)\Delta Q, \quad c_{k1} = \sqrt{\gamma p_{k1} v_{k1}}.$$

Table 73 gives results for instantaneous detonations. Exp[illegible]nt

Table 73

Initial Parameters of Shock Waves Produced in Air by Instantaneous Detonations

	ρ_0, g/cm³	Q_v, kcal/kg	p_{x1}, kg/cm²	p_φ, kg/cm²	u_φ, m/sec	D', m/s[illegible]	$u_{\varphi 1}$, m/sec
Trotyl	1.60	1000	1250	230	4100	4500	7750
Hexogene	1.60	1300	1300	300	4700	5150	8700
TEN	1.69	1400	1650	330	4900	5400	9000

shows that the initial parameters of actual shock waves in air are higher than the ones calculated for instantaneous detonation; this feature must be allowed for in any calculation on the local effects, but it is less important in relation to the general effects, for the actual and calculated parameters become very similar at fairly small distances from the source.

Shock wave in water. An underwater explosion from a charge whose density exceeds 1 g/cm³ has a rarefaction wave in the products, but here there is no need to consider the change in k, for there is no very large change in ρ or p. This means that we can use (48,7) and (48,8), so

$$u_\varphi = \frac{D}{k+1}\left\{1 + \frac{2k}{k-1}\left[1 - \left(\frac{p_\varphi}{p_i}\right)^{\frac{k-1}{2k}}\right]\right\} \qquad (49,14)$$

$$u_\varphi = \sqrt{(p_\varphi - p_0)(v_{v0} - v_{v\varphi})}. \qquad (49,15)$$

The relation of p to ρ for water for $p \geq 5000$ kg/cm² is

$$p = A\left[\left(\frac{\rho}{\rho_0}\right)^n - 1\right], \qquad (49,16)$$

in which A and n are empirical constants. Then (49,15) may be transformed by neglecting p_0, because $p_0 \ll p_\varphi$, and by replacing the specific

volumes by the densities:

$$u_x = \sqrt{p_x \frac{\rho_{0x} - \rho_{00}}{\rho_{0x}\rho_{00}}} = \sqrt{\frac{p_x}{\rho_{00}}\left[1 - \frac{\rho_{00}}{\rho_{0x}}\right]}, \qquad (49,17)$$

in which ρ_{00} is the density ahead of the shock wave and ρ_{0x} is the density in the shock-wave front. Formula (49,16) gives us that

$$\frac{\rho_{00}}{\rho_{0x}} = \frac{1}{\left(\frac{p_x}{A} + 1\right)^{\frac{1}{n}}} = \eta_x.$$

This ratio of the ρ is inserted in (49,17) to give that

$$u_x = \sqrt{\frac{p_x}{\rho_{00}}(1 - \eta_x)}. \qquad (49,18)$$

which, with (49,14), solves the problem. A graphical treatment is convenient; experiment gives the A and n for the range 0.03 to 0.2 Mkg/cm^2 as

$$A = 3940 \text{ kg/cm}^2, \quad n = 8,$$

i. e.

$$p_x = 3940\left[\left(\frac{\rho_{0x}}{\rho_{01}}\right)^8 - 1\right] \qquad (49,19)$$

$$\eta_x = \frac{1}{\left(\frac{p_x}{3940} + 1\right)^{0.125}}. \qquad (49,20)$$

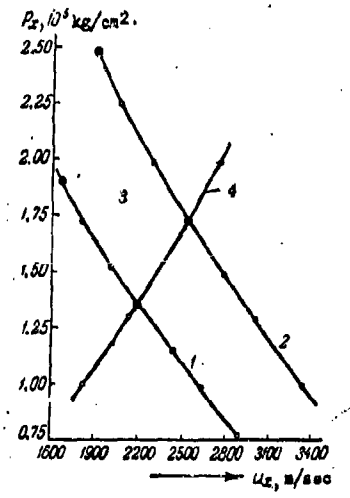


Fig. 116. Initial parameters of shock waves in water: 1) trotyl, ρ_0 = 1.61 g/cm^3; 2) retarded hexogene, ρ_0 = 1.60 g/cm^3; 3) rarefaction wave in products; 4) shock wave in water.

Figure 116 illustrates the graphical treatment for the explosives of Table 71. The curves for the rarefaction wave and for the shock wave in the water have been constructed from (49,14) and (49,17); these curves meet at a point that defines u_x and p_x, and so D' is given by

This D' is found from the ratio of the ρ and the u_x as given by (49,20) and (49,18) to be

$$D' = \sqrt{\frac{p_x}{\rho_{c0}(1-\eta_x)}}. \qquad (49,21)$$

Further, (49,16) gives us η_x and D_m from the known p_x.

The temperature change across the front in the water cannot be calculated exactly, because we lack reliable values for the thermal capacity of water at very high pressures; there is no information on the division of the internal energy between the thermal and elastic forms. We may, though, use the shock adiabatic

$$E_x - E_1 = \frac{p_x}{2}(v_{c0} - v_{cx}),$$

in order to determine the increase in the internal energy

$$\Delta E = E_x - E_0$$

during the compression; Table 74 gives results found in this way by means of (49,19). The initial pressure and speed are less than for

Table 74.

Initial Parameters of Shock Waves in Water

	ρ_0, g/cm³	D', m/sec	u_x, m/sec	$\frac{\rho_{cx}}{\rho_{c0}}$	p_x, kg/cm²	$\frac{D'}{G} \cdot 10^5$	ΔE, kcal
Trotyl	1.60	6100	2185	1.560	136 000	87.2	570
TEN	1.69	7020	2725	1.635	195 000	83.5	800

the charge itself; moreover, ρ_x/ρ_i and D_m/D' tend to decrease as D and p_i increase, which is a result of an increase in the compressibility at high pressures.

CHALLE has given comparable results for certain other liquids; he measured the density ratio by means of microsecond radiographs of waves generated by charges of TEN. His ρ_{0x}/ρ_{00} are: water, 1.75; ethanol, 2.05; acetone, 2.15; ethyl ether, 2.45. The first is close to our

value.

The parameters of the wave generated by an instantaneous detonation are given by

$$u_\infty = \frac{2\bar{c}_i}{k-1}\left[1-\left(\frac{p_\infty}{p}\right)^{\frac{k-1}{2k}}\right], \qquad (49,22)$$

$$u_\infty = u' = \sqrt{\frac{p_\infty}{\rho_{00}}\left[1-\left(\frac{p_\infty}{A}+1\right)^{-\frac{1}{n}}\right]}, \qquad (49,23)$$

in which subscript i denotes the initial values for the products; D' is given by (49,21), and $\rho_{0\infty}$ by (49,19). Table 75 gives some calculated results, which are substantially less than the actual values

Table 75

Initial Parameters of Shock Waves Produced in Water by Instantaneous Detonations

	ρ_0, g/cm^2	p_∞, kg/cm^2	u_∞, m/sec	D', m/sec	$\frac{\rho_{0\infty}}{\rho_{0i}}$
Trotyl . . .	1.60	43 000	1050	4000	1.37
TEN	1.69	62 000	1350	4500	1.43

(our results agree quite well with ones calculated by the KIRKWOOD-BETHE method). The accuracy of any such calculation is governed by the error in the relation of pressure to density, which is derived from measurements of the speeds of shock waves near explosions in water. Better methods of measurement are needed here, because results for isothermal compression (BRIDGMAN and others) cannot be used; water solidifies (seven forms of ice are known) when it is compressed slowly at very high pressures.

Shock waves in metals. The density of a metal or alloy is usually greater than that of the products from a detonation, while

the compressibilities usually stand in the reverse relation; this means that a metal tends to produce a reflected shock wave. The equations for the initial parameters are

$$u_x = \frac{D}{k+1}\left[1 - \sqrt{2k}\frac{\pi_x - 1}{\sqrt{(k+1)\pi_x + (k-1)}}\right], \tag{49,24}$$

$$u_x = u' = [p_x(v_{00} - v_{0x})]^{\frac{1}{2}}, \qquad \pi_x = \frac{p_x}{p_i}. \tag{49,25}$$

These enable us to find the parameters if $p(v)$ is known for high pressures. We have seen above that the relation of p to ρ for a metal is

$$p = A\left[\left(\frac{\rho}{\rho_0}\right)^n - 1\right]. \tag{49,26}$$

so (49,25) becomes

$$u_x = u' = \sqrt{\frac{p_x}{\rho_{00}}(1-\eta)}, \qquad \eta = \frac{\rho_{0x}}{\rho_{00}} = \left(\frac{p_x}{A} + 1\right)^{-\frac{1}{n}}. \tag{49,27}$$

Equations (49,24) and (49,27) give us the initial parameters of the shock waves in the metal if A and n are known.

Table 76 gives these initial parameters for certain metals exposed to the detonation waves from typical explosives; $p_x/p_i > 1$, and it increases with A, although it decreases as p_i increases. It is always substantially less than for reflection from an absolutely rigid wall (here $p_x/p_i = 2.4$). Further, ρ increases by 10-25% when the shock wave is strong; as one would expect, duralumin is found to be the most compressible, and steel the least.

The method described in section 48 for examining the stress wave is not applicable to the tail of the wave if the rod fractures; that method has been improved by BAUM and STETSOVSKIY as follows.

A narrow scratch is made on one of the side faces of the rod; passage of repeatedly reflected waves past this point is recorded as before, which enables one to use stress waves of any amplitude.

Table 76

Initial Parameters of Shock Waves in Metals

	ρ_0, g/cm³	Steel					Copper					Duralumin				
		p_x, kg/cm²	u_x, m/sec	D_x, m/sec	$\frac{\rho_x}{\rho_1}$	$\frac{\rho_{0x}}{\rho_{00}}$	p_x, kg/cm²	u_x, m/sec	D_x, m/sec	$\frac{\rho_x}{\rho_1}$	$\frac{\rho_{0x}}{\rho_{00}}$	p_x, kg/cm²	u_x, m/sec	D_x, m/sec	$\frac{\rho_x}{\rho_1}$	$\frac{\rho_{0x}}{\rho_{00}}$
Trotyl	1.30	207 000	505	5150	1.80	1.089	176 000	510	4000	1.53	1.15	154 000	830	6400	1.34	1.151
"	1.55	—	—	—	—	—	264 000	725	4250	1.50	1.20	—	—	—	—	—
Hexogene (retarded)	1.60	405 900	885	5750	1.83	1.174	356 000	900	4520	1.42	1.26	285 000	1400	7000	1.15	1.251
"	1.40	—	—	—	—	—	270 000	730	4260	1.47	1.21	—	—	—	—	—

This method has been applied to plexiglas to yield the $\varepsilon = \psi(\sigma)$ curve, in which ε is relative elongation and σ is tensile stress. The ε for an explosion wave is the ratio of the diaplacement of the line to the length of the section acted on by the wave. It is found that plexiglas, although usually considered as plastic, in fact obeys HOOKE's law up to the point of rupture for explosion conditions; it behaves as an ideally elastic body, and YOUNG's modulus E is 6×10^4 kg/cm^2. For comparison, the E given by $c = (E/\rho)^{1/2}$ is 6.05×10^4 kg/cm^2.

Bibliography

1. L. I. Sedov. The Methods of Similitude and Dimensions in Mechanics. Gostekhizdat, 1957.
2. Ya. B. Zel'dovich. Theory of Shock Waves: an Introduction to Gas Dynamics. Izd. Akad. Nauk SSSR, 1946.
3. Y. B. Zel'dovich and A. S. Kompaneyets. Theory of Detonation. Gostekhizdat, 1955.
4. R. Courant and K. O. Friedrichs. Supersonic Flow and Shock Waves [Russian translation]. IL, 1950.
5. L. D. Landau and E. M. Livshits. Mechanics of Continuous Media. Gostekhizdat, 1953.
6. L. D. Landau and K. P. Stanyukovich, Dokl. Akad. Nauk SSSR 47, No. 4 (1945).
7. Idem. Dokl. Akad. Nauk SSSR 47, No. 4 (1945).
8. Ya. B. Zel'dovich and K. P. Stanyukovich. Dokl. Akad. Nauk SSSR 55, 591 (1947).
9. K. P. Stanyukovich. Transient-State Motion of a Continuous Medium. Gostekhizdat, 1955.
10. J. M. Walsh and R. H. Christian, Phys. Rev. 97, No. 6 (1955).
11. P. W. Bridgman. Physics of High Pressure [Russian translation]. IL, 1948.
12. L. V. Al'tshuler, K. K. Krupnikov, B. N. Ledenev, V. I. Zhukov, and M. I. Brazhnik. Zh. Eksper. Teoret. Fiz. 34, No. 4 (1959).

Chapter X.

COMBUSTION OF EXPLOSIVES.

50. Basic Characteristics of Explosive Combustion Processes.

Under definite conditions most explosives are capable of undergoing stable combustion without transition to detonation. For powders rapid burning is the basic type of explosive transformation.

The results of theoretical and experimental studies show that the basic processes which are characteristic of combustion rather than detonation are included in the following:

1. During combustion energy enters the initial substance by heat conduction, diffusion of gaseous products, and irradiation. During detonation the energy and subsequent initiation of explosive reaction are provided for by the propagation of explosive pressure waves.

2. The rate of dissemination of combustion proc[illegible] is far and away less than the rate of detonation processes. The rate of combustion cannot exceed the speed of sound in the starting material, and is usually considerably less than this. This is a result of the comparatively slow rate of heat transfer and diffusion. It will be recalled that the rate of detonation processes always exceeds the speed of sound in the original substance, frequently by a considerable margin.

3. The combustion products formed directly at the front of the flame move in a direction opposite that of the flame front, whereas the opposite occurs during detonation. Consequently the pressure of combustion products in the flame zone is considerably less than at the front of a detonation wave.

4. The rate and character of the chemical processes occurring during the combustion of explosives depend to a considerable extent on the external pressure.

For example, combustion of pyroxylin and of some other esters of nitric acid at relatively low pressures (up to 30 - 50 atmos.) usually leads to the formation of nitrogen oxides and formaldehyde. This does not occur at higher pressures - of the order of hundreds or thousands of atmospheres. At very low pressures (close to the combustion unit) the combustion of many gaseous mixtures goes via a chain mechanism, whereas at sufficiently high pressures reactions going via a thermal mechanism become important.

The combustion of many liquid or solid explosives proceeds either in the gas phase, or simultaneously in the gas and condensed phases. The change to the final combustion products usually goes through a series of intermediate reactions.

It is characteristic of detonation in explosives that the chemical processes occur in both condensed and gaseous phases at very high pressures. Under these conditions behaviour of gases is virtually the same as that of liquids.

Investigation of the combustion of explosive systems had begun even in the second half of the last century. Gaseous mixtures were mainly concerned. The most important work on the combustion of gaseous mixtures during this period was carried out by Mallior and Le Chatelier, Dickson, and Michelson. Their investigations played an important role in the subsequent development of the theory of combustion of gaseous mixtures. The process of ignition and spread of the flame were studied for a long time in isolation from the chemical kinetics, and this led to some of the principal errors of the formal theories of combustion (Croy, Grimshaw, Letan, and others).

Considerable progress has been achieved in the development of the theory of combustion of gaseous and condensed explosives in the last ten years. This is a result of progress in the field of chemical kinetics, and in particular the theory of chain reactions which has been developed in the main by Hinshelwood and Semenov and their schools. The thermal and chain theories of auto-

ignition of gaseous mixtures, originated by Semenov, have served as a starting point for the theoretical work of Soviet scientists (Zel'dovich, Frank-Kamenetskii, Todes) on combustion.

Important results have also been achieved recently in the study of combustion processes in condensed phases and in the study of the conditions for transition from combustion to detonation. The most valuable studies in these fields have been carried out by Belyaev, Andreev, and Zel'dovich.

Combustion of gaseous explosive systems. Gaseous explosive systems are chiefly mixtures of combustible gases or vapours with oxygen or air. A gaseous mixture can be ignited either by heating the mixture or by localised ignition (electric spark, etc.).

In the first case the chemical reaction proceeds simultaneously throughout the volume of the vessel containing the gas; in the second case a flame arises at the ignition point and spreads through the initial material. The flame appears as a thin zone, which separates the unreacted starting material from the final reaction products, and in which chemical energy is converted into heat. Dissemination of the flame may occur by detonation or by normal combustion. The term "normal combustion" signifies the process by which ignition of each layer of the gaseous mixture proceeds by thermal conductive heating from the previous layer, or by diffusion of active intermediate reactive products into the starting mixture.

Thermal and chain ignition. Ignition and subsequent burning of gaseous mixtures can occur only in those cases in which the chemical reaction proceeds in conditions of progressive autoacceleration. The critical condition for ignition is therefore determined by the conditions for transformation from stationary to non-stationary reaction.

If at some value of the temperature and pressure stationary heating becomes impossible and the temperature of the reaction mixture begins to increase to an important extent in a non-stationary manner, the phenomenon

is designated thermal ignition. At sufficiently low pressures heat evolution by the reaction is compensated for by heat loss to the surroundings. As the pressure is increased heat evolution in the vessel is increased. This leads to an increase in the gas temperature and consequently to an increase in thermal radiation. However, the rate of reaction and of heat evolution also increase as a result of the rise in temperature.

Since the reaction rate (exothermic) increases exponentially with temperature whereas the heat loss increases more or less linearly with temperature, a continuously autocatalytic reaction occurs as the result of disturbance of the thermal equilibrium, and this leads to explosion (ignition). The limiting conditions for ignition depend notably on the dimensions of the vessel when a thermal reaction mechanism is involved. An increase in the size of the vessel leads to some decrease in the limiting ignition pressure because the relative size of the heat loss is decreased. Thermal combustion can be observed in any exothermic reaction, the rate of which increases sufficiently rapidly with increasing temperature.

If the concentration of active intermediate products begins to rise to an important extent in a non-stationary manner at some value of the external parameters, then the phenomenon is termed chain or diffusion ignition. Chain or diffusion combustion is possible only in autocatalytic reactions.

Ignition by a chain mechanism is principally encountered at comparatively low pressures. Most cases of ignition at atmospheric or higher pressures are of the thermal type. These are the reactions of most practical importance.

51. The Theory of Thermal and Chain Ignition of Gases

The basic ideas of autoignition were discussed by van't Hoff, according to whom the condition for an autoaccelerating reaction was that the heat input should exceed the heat loss. A quantitative theory of autoignition was first formulated by Semenov. The essence of this theory is that, under certain conditions (temperature, pressure, etc.) the heat of reaction becomes larger than the heat loss, and, as a result of this, the mixture becomes self-heating and the reaction autoaccelerating, so that an explosion ensues.

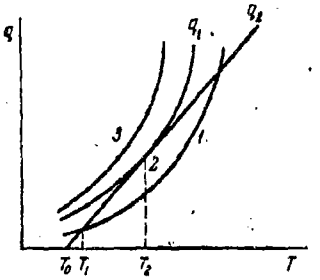


Fig. 117. Relation between the heat input q_1 and the heat loss q_2 at different pressures.

Let the gas mixture consist of molecules A and B which react together bimolecularly: $A + B = AB$. In this case the rate of reaction is described by the equation

$$W = Z[A][B]e^{-\frac{E}{RT}}, \qquad (51,1)$$

where A and B are concentrations. The quantity of heat liberated per second as a result of the reaction will be

$$q_1 = qW = qZ[A][B]e^{-\frac{E}{RT}} = Dp^2n(1-n)e^{-\frac{E}{RT}}, \qquad (51,2)$$

where q is the heat liberated by each elementary act of the reaction, n and $(1-n)$ are parameters which characterise the composition of the mixture, p is the total pressure of the mixture, and $D = qZ$.

Thus the heat, q_1, evolved by the reaction increases rapidly with temperature, and at a given temperature it is proportional to the second power of the pressure of the mixture.

In Fig.117 are shown curves which give the relation between q_1 and the temperature at different temperatures. The greater the pressure the higher lies the curve.

To a first approximation the heat loss per second, q_2, can be assumed to be proportional to the difference between the gas temperature and that of the surrounding medium

$$q_2 = \alpha(T - T_0), \tag{51,3}$$

where T is the temperature of the gas, T_0 is the temperature of the surrounding medium, and α is the coefficient of heat outflow.

The graphical representation of the relation between q_2 and T is a straight line. At low pressure, when the quantity of heat evolved is defined by curve *1*, the gas will initially heat up as a result of reaction because $q_1 > q_2$. The rate of reaction will increase until the temperature of the gas reaches T_1. At this point $q_1 = q_2$, and after this acceleration of the reaction ceases.

At higher pressures the heat evolution curve 3 lies completely above the heat loss line, $q_1 > q_2$; consequently the reaction rate rises continuously, leading to an explosion.

Curve *2* corresponds to a boundary case between "quiet reaction" and explosion. It only touches the heat loss line. A small change in either direction of the pressure or temperature T_0 would lead to an explosion or to a quiet reaction.

Evidently the pressure μ corresponding to this case would be the minimum pressure for self-ignition at the given temperature T_0.

This pressure can be defined in terms of the conditions for the curve and the straight to touch. Two conditions must be fulfilled at the point of contact

$$\left.\begin{aligned} qW &= \alpha(T_2 - T_0), \\ \frac{dq_1}{dT} &= \frac{dq_2}{dT}. \end{aligned}\right\} \tag{51,4}$$

The temperature T_2 can be determined from equation (51,4).

The solution, which we shall omit here, shows that T_2 is only a few degrees higher than T_0. Hence we may use the second equation of (51,4) on its own, putting $T = T_0$, to draw conclusions about the conditions for

thermal explosion. This equation gives

$$\frac{Dp^2n(1-n)E}{RT_0^2}e^{-\frac{E}{RT_0}}=a. \qquad (51,5)$$

Putting $\frac{aR}{Dn(1-n)E}=C$, we have $\frac{p^2}{T_0^2}=Ce^{\frac{E}{RT_0}}$

or $$\ln\frac{p}{T_0}=\frac{E}{2RT_0}+\frac{1}{2}\ln C,$$

whence finally $$\ln\frac{p}{T_0}=\frac{A}{T_0}+B, \qquad (51,6)$$

where $$A=\frac{E}{2R}$$

and $$B=\frac{1}{2}\ln C=\frac{1}{2}\ln\frac{aR}{Dn(1-n)E}.$$

It is easy to show that the limiting condition for self-ignition, as expressed by equation (51,6), remains correct in the case when the reaction is not bimolecular but goes via a more complex rule:

$$W=Z(A)^m(B)^le^{-\frac{E}{RT}}=Zp^{m+l}n^m(1-n)^le^{-\frac{E}{RT}}.$$

In this case $$A=\frac{E}{(m+l)R}$$

and $$B=\frac{1}{m+l}\ln\frac{aRE}{Dn^m(1-n)^l}.$$

Thus the logarithm of the ratio of the minimum pressure to the absolute temperature of autoignition should depend linearly on $1/T_0$. This rule was checked and confirmed by Zagulin and a number of other workers for a large number of gaseous mixtures.

Semenov's theory of thermal explosions, which is the basis for all later work in this field, was constructed from the assumption that the temperature may be assumed to be uniform throughout the vessel. This supposition is not in accord with the experimental data; ignition always occurs in a localised volume at a maximum temperature, and the flame then spreads through the gas.

A later development of the theory of thermal ignition was Frank-Kamenetskii's so-called stationary theory of thermal explosion, in which the distribution of temperatures in the gaseous reaction mixture is taken into account.

The stationary theory of thermal explosions starts from the discussion of the stationary equation of heat conduction for a system with a continuous distribution of energy sources:

$$\lambda \Delta T = -q', \qquad (51,7)$$

where Δ is the Laplace operator, q' is the volume rate of heat evolution, and λ is the thermal conductivity coefficient.

If the rate of reaction is related to the temperature by the Arrhenius relationship, then

$$q' = QZe^{-\frac{E}{RT}}, \qquad (51,8)$$

The equation (51,7) can now be put into the form

$$\Delta T = -\frac{Q}{\lambda} Ze^{-\frac{E}{RT}}, \qquad (51,9)$$

where Q is the heat effect of the reaction.

The problem reduces to the integration of the equation (51,9) with the boundary conditions: at the walls of the vessel, $T = T_0$.

According to this theory ignition of the gas should occur when a stationary distribution of temperature becomes impossible.

Without going into a detailed discussion of the mathematical conclusions, we shall look only at the end results of the theory in the form of a criteria which permit the limiting conditions of thermal ignition of the reacting gas to be established.

According to Frank-Kamenetskii this condition can be put in the form of a critical value of the dimensionless parameter

$$\delta = \frac{Q}{\lambda} \frac{E}{RT_0^2} r^2 Ze^{-\frac{E}{RT_0}}, \qquad (51,10)$$

where T_0 is the temperature of the walls of the reaction vessel, Q is the heat effect of the reaction, E is the energy of activation, R is the gas constant, r is the radius of the vessel, and $Ze^{-\frac{E}{RT_0}} = W$ is the rate of reaction at a composition of the reaction mixture corresponding to the maximum rate of reaction.

The parameter δ describes the aggregated properties of the system (the rate and heat effect of the reaction, thermal conductivity, size of the vessel). The critical condition for ignition has the form:

$$\delta = \text{const} = \delta_{кр}. \qquad (51,11)$$

If the corresponding parameter (which, when substituted into equation (51,10), characterises the experimental conditions) gives a value of δ less than the critical, then a stationary distribution of temperatures should be established; in the opposite case an explosion should ensue.

The critical value of δ depends on the geometric shape of the vessel. For a plane-parallel vessel $\delta_{кр} = 0{,}88$; for a spherical vessel $\delta_{кр} = 3{,}32$ and for a cylindrical vessel with length L and diameter d

$$\delta_{кр} = 2{,}00 + 0{,}843\left(\frac{d}{L}\right)^2.$$

Table 77

Decomposition of Azomethane (after Rice)

$(CH_3)_2N_2 = C_2H_6 + N_2$

p, mm Hg	T_{calc}, °K	T_{obs}, °K
191	619	614
102	629	620
55	638	631
31	647	643
18	656	659

Table 78

Decomposition of Methyl Nitrate (after Apin and Khariton)

$2CH_3ONO_2 = CH_3OH + CH_2O + 2NO_2$

p, mm Hg	T_{calc}, °K	T_{obs}, °K
163	531	520
107	538	521
33	555	534
9	578	567
4	590	597

Table 79

Decomposition of Nitrous Oxide (after Zel'dovich and Yakovlev)

$2N_2O = 2N_2 + O_2$

p, mm Hg	T_{calc}, °K	T_{obs}, °K
590	1110	1100
330	1175	1195
170	1255	1285

The theory permits the position of ignition limits to be calculated for reactions of known kinetics. The calculated results show excellent agreement with the experimental data in a number of reactions. Examples are shown in Tables 77 - 79.

Frank Kamenetskii showed that ignition had a thermal character if at the ignition limit δ exceeded the critical value. If ignition occurred at δ less than the critical value, then ignition of the gas had a chain character.

In the stationary theory of thermal auto-ignition only the distribution of temperature in the vessel is discussed. The change of this distribution with time is not taken into account. Todes, like Semenov, considered that the temperature was uniform throughout the reaction mixture. He discussed the relation between this temperature and time.

Non-stationary theory of thermal explosion. Starting from the assumption mentioned above, we shall discuss the heat balance of the whole vessel. The quantity of heat evolved by the chemical reaction in the total volume of the vessel in unit time is equal to

$$wQZe^{-\frac{E}{RT}}, \qquad (51,12)$$

where w is the volume of the vessel.

The quantity of heat lost from the walls of the vessel in the same time will be

$$\alpha S(T - T_0), \qquad (51,13)$$

where α is the coefficient of heat transfer, and S is the surface of the walls of the vessel. The difference between these quantities of heat, used in heating the gas, is, in unit time

$$c\rho w \frac{dT}{dt}, \tag{51,14}$$

where c is the heat capacity of the gaseous mixture, ρ is its density (number of moles per unit volume), and t is the time.

Comparing these equations, we obtain the heat balance equation

$$\frac{dT}{dt} = \frac{Q}{c\rho} Ze^{-\frac{E}{RT}} - \frac{\alpha S}{c\rho w}(T - T_0). \tag{51.15}$$

Putting $T - T_0 = \theta$, then

$$e^{-\frac{E}{RT}} = e^{-\frac{E}{RT_0}\left(\frac{1}{1+\frac{\theta}{T_0}}\right)},$$

It was shown earlier that $\theta \ll T_0$ close to the auto-ignition limit. Consequently, putting $\frac{1}{1+\frac{\theta}{T_0}}$ in the form of a geometric progression and omitting all terms of order greater than one, we obtain

$$e^{-\frac{E}{RT}} = e^{-\frac{E}{RT}\left(1-\frac{\theta}{T}\right)} = e^{-\frac{E}{RT}} e^{\frac{E}{RT_0^2}\theta}. \tag{51.16}$$

Transforming to dimensionless temperature

$$\Theta = \frac{E}{RT_0^2}\theta, \tag{51,17}$$

we get the equation (51,15) in the form

$$\frac{d\Theta}{dt} = \frac{Q}{c\rho}\frac{E}{RT_0^2} Ze^{-\frac{E}{RT_0}} e^{\Theta} - \frac{\alpha S}{c\rho w}\Theta \tag{51,18}$$

with the initial condition that $\Theta = 0$ at $t = 0$.

All the terms in equation (51,18) have the dimensions of reciprocal time. To convert this to the dimensionless form it is necessary to introduce a unitary scale of time. Equation (51,18) contains two parameters which could serve as such a scale:

$$\left.\begin{aligned} \tau_1 &= \left(\frac{Q}{c}\frac{E}{RT_0^2}\frac{z}{\rho}e^{-\frac{E}{RT_0}}\right)^{-1}, \\ \text{and} \quad \tau_2 &= \left(\frac{\alpha S}{c\rho w}\right)^{-1}. \end{aligned}\right\} \tag{51,19}$$

On this basis one can conclude that equation (51,18) should have the form

$$\theta = f\left(\frac{t}{\tau}, \frac{\tau_2}{\tau_1}\right), \qquad (51,20)$$

where τ can be either of the parameters τ_1 or τ_2.

Thus the relation between the dimensionless temperature and the dimensionless parameter, $\frac{\tau_2}{\tau_1}$, the value of which is determined by the form of the temperature-time curve. A sudden change in the course of the curve should occur at a definite critical value of the parameter $\frac{\tau_2}{\tau_1}$, i.e., the critical condition for ignition will be:

$$\frac{\tau_2}{\tau_1} = \text{const.} \qquad (51,21)$$

This result was first obtained by Todes. If one takes from the theory of thermal conduction the value

$$\alpha = \text{Nu}\,\frac{\lambda}{d},$$

where Nu -- the Nusselt criterion - is a constant value depending on the geometric form of the vessel, d is the characteristic linear dimension of the vessel, and λ is the thermal conductivity coefficient, it is not difficult to ascertain that, with a precision of a constant factor, the parameter $\frac{\tau_2}{\tau_1}$ coincides with the parameter δ introduced in the stationary theory. Thus both theories lead to a single form for the critical condition for auto-ignition.

Let us determine the physical meaning of the parameters τ_1 and τ_2. Let us write equation (51,18) in the form:

$$\frac{d\theta}{dt} = \frac{e^{\theta}}{\tau_1} - \frac{\theta}{\tau_2}. \qquad (51,22)$$

On the right hand side the first term is proportional to the amount of heat evolved in the reaction, whereas the second term is proportional to the amount of heat lost from the walls. At temperatures and pressures considerably above the limiting values, the first term will be much larger than the second. In these conditions heat loss can be neglected and a thermal explosion may be considered to be adiabatic. In this case the relation

between temperature and time should have the form

$$\Theta = f\left(\frac{t}{\tau_1}\right), \tag{51,23}$$

i.e., the time to reach some value of Θ will be proportional to τ_1. Consequently the induction period, i.e., the time during which the auto-ignition occurs, is proportional to the parameter τ_1 in adiabatic thermal explosions. An analytical solution shows that the proportionality constant is unity.

The parameter τ_1 is therefore termed the adiabatic induction period. From equation (51,19) it follows that the adiabatic induction period

$$\tau_1 = Be^{\frac{E}{RT}}, \tag{51,24}$$

where

$$B = \left(\frac{Q}{c}\frac{E}{RT_0^2}\frac{Z}{\rho}\right)^{-1} = \left[\frac{E}{RT_0^2}\frac{Z}{\rho}(T_m - T_0)\right]^{-1}, \tag{51,25}$$

($T_m = \frac{Q}{c} + T_0$ is the maximum explosion temperature) is calculated on the assumption that the heat capacity is constant.

The relation between the induction period and the self-ignition temperature (51,24) evidently has a more general value, and as has been noted (see Chapter II), it is found in experiments on most explosive systems studied both in the gas and in the condensed phase. Equation (51,25) establishes the theoretical relation between the pre-exponential factor B in equation (51,24) and the nature and basic kinetic characteristics of the gaseous mixture.

According to the theory developed above explosions principally arise in heated systems. However, many cases are known in which a slow reaction can, in certain conditions, become autoaccelerating, not as a result of heating, but as a result of the accumulation of catalytically active intermediate reaction products in the system. This occurs in conditions favouring the origin and branching of chains. In this case heating is the result of the explosion, not its cause.

The active intermediate products react with the starting materials and transform them into the end products of the reaction. These processes require a comparatively small activation energy, (especially when the active products) are free radicals or atoms) and t.y therefore go at a great speed. The initial formation of the active centres from the stable starting materials requires a high activation energy and hence cannot proceed at a high speed.

For an active centre reaction to proceed sufficiently fast it is necessary that the active centres should be regenerated during the reaction, i.e., the reaction of the active products with the starting materials should produce non active intermediate products as well as stable terminal reaction products.

Reactions in which regeneration of the active intermediate products occurs, are called chain reactions. Each active molecule (atom, radical) which is consumed during the reaction causes a prolongation of the chain in subsequent reaction steps.

In the last decade great progress has been made in the study of the kinetics and development of chain reactions, largely as a result of the work of Bodenstein, Hinshelwood, and the Soviet school under Semenov, who have particularly developed the important bases of the chain-theory of explosion for gaseous mixtures.

The chain theory of chemical reactions was first introduced to explain unusually large quantum yields (the number of reacted molecules arising from the absorption of one light quantum) in photochemical reactions - in certain cases the quantum yield reached 10^5 molecules per quantum.

As an example of a chain reaction the interaction between chlorine and hydrogen may be taken. According to Nernst this goes in the following way:

$$Cl_2 + h\nu = Cl + Cl,$$
$$Cl + H_2 = HCl + H,$$
$$H + Cl_2 = HCl + Cl + 45 \text{ kcal, etc.}$$

In this case a quantum of light causes the dissociation of a molecule of chlorine into chemically active atoms. In subsequent steps these atoms react with the starting materials to form new active centres (chlorine and hydrogen atoms) which ensure the continuation of the chain.

Other examples of reactions with chain mechanisms are the reactions between hydrogen and oxygen and between carbon monoxide and oxygen. The initial active centres in the former reaction are hydroxyl free radicals:

$$H_2 + O_2 = 2OH.$$

The process then proceeds further by the following scheme:

$$\begin{aligned} &1)\ OH + H_2 = H_2O + H, \\ &2)\ H + O_2 = OH + O, \\ &3)\ O + H_2 = OH + H \quad \text{etc.} \end{aligned}$$

In this process a single OH radical, many times regenerated, is capable of forming a large number of water molecules. The three intermediate products of reaction - OH, H, and O - are active centres and chain carriers.

Loss of one of the active centres, by a reaction which does not lead to regeneration, prevents the formation of many water molecules: such a process is called <u>chain termination</u>. In the case given the chain may be terminated as a result, for example, of the following reactions:

$$\begin{aligned} OH + OH &= H_2 + O_2, \\ H + H &= H_2, \\ O + O &= O_2. \end{aligned}$$

Chain rupture can also occur at the surface of the vessel walls either by reaction of the active centres with the material of the walls, or by simple absorption.

On the other hand, reactions (2) and (3) lead to an increase in the number of active centres; such processes are termed reactions with <u>chain branching</u>. If the rate of increase of active centres caused by chain

branching reactions exceeds the rate of their loss by chain termination reactions, then continuous autoacceleration occurs and finally the system explodes. In the opposite case ignition of the gas becomes impossible.

Limits of auto-ignition. The occurrence of upper and lower ignition limits may be explained in conditions in which chain reactions proceed. Upper and lower ignition limits have been established for mixtures of hydrogen, carbon monoxide, methane, and some other gases, with oxygen at sub-atmospheric pressures. A typical diagram of the ignition limits for
is given in Fig. 118.

The lower ignition temperature is characterised by the fact that for every temperature there is some minimum pressure, p_1, below which it is impossible for ignition of the gas to occur. When the pressure on the lower limit curve is lowered the auto-ignition temperature rises. However, in a certain temperature range ignition is impossible if the pressure exceeds some critical value, p_2. Thus the region in which explosive reaction occurs is shaped like a peninsula and this phenomenon is termed peninsular ignition.

Ignition limits may be determined in the following manner:

Let a gaseous mixture in a vessel be heated to the temperature and pressure required to exceed the pressure, p_2, corresponding to the upper limit. In these conditions a slow reaction will occur. A gradual pumping out of the mixture initially leads to a further decrease in the rate of reaction, but then at definite pressure, p_2, explosion occurs, indicated by a bright flash. The reaction retains its explosive character until some very low pressure, p_1, is reached when the mixture again ceases to ignite. As the temperature decreases the upper and lower limits approach one another and finally their ends coincide.

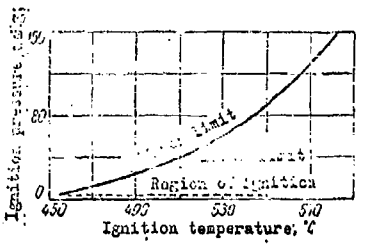


Fig.118 Region of ignition for a stoichrometric mixture of hydrogen and oxygen at low pressures.

The existence of an upper limit can serve as an undoubted demonstration of the chain mechanism of the reaction. In the given case a decrease in pressure leads to an increase in the rate of chain branching reactions in comparison with the rate of homogeneous chain termination. Consequently, below a certain critical pressure the process accelerates so much that an explosion ensues. This could not occur by a thermal mechanism.

According to Lewis and Alba, the existence of a lower limit for the hydrogen-oxygen explosive mixture is explained by the loss of active centres on the walls (heterogenous termination). At a sufficiently low pressure the part played by chain termination at the walls increases to such an extent that a further decrease in the reaction pressure finally causes the reaction to lose its explosive character. Studies by Kalbandyan and his co-workers showed that the principal heterogenous chain termination process in the $H_2 + O_2$ reaction is the loss of atomic hydrogen at the surface. This was explained by the fact that, because of its endothermicity, the slowest of the basic steps in the reaction is

$$H + O_2 = OH + O.$$

Consequently the concentration of atomic hydrogen in the reaction zone is considerably higher than the concentrations of the remaining active centres.

Study of the kinetics of chemical reactions above the upper ignition limit showed that, when the pressure was increased, the slow reaction was again transformed to an explosion, and this is linked with the existence of a third ignition limit. The curve of this limit is characterised by

the fact that, starting from a particular pressure, an increase in pressure leads to a sl ecrease in the auto-ignition temperature. Hence in a certain temperature range there exists not one, but three, limits and the relation between the ignition temperature and the pressure has the general form shown in Fig. 119.

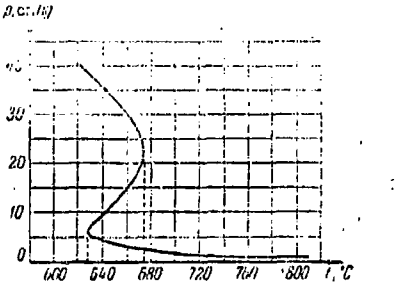


Fig.119. Change in the ignition temperature of a stoichiometric mixture of methane and oxygen with pressure.

Frank-Kamenetskii's calculations showed that the ignition of a hydrogen oxygen mixture in the region of the third limit had a thermal character.

It should be noted that, unlike auto-ignition, an upper limit does not exist for electric-spark initiated explosions.

Catalytic effect of impurities (additives). The large effects of additives in a gas on the conditions and rates of chain reactions is explained by the catalytic effects of the additives. Additives which appear to be positive catalysts are substances capable of giving rise to active centres of initiating chains, or of hindering the diffusion of active centres to the walls of the vessel. Negative catalysts on the other hand usually cause chain rupture by reacting with the active centres.

For example, small quantities of iodine or the other halogens strongly repress the oxidation of hydrogen in an explosive mixture by introducing the following processes:

$$H + I_2 = HI + I,$$

$$H + HI = H_2 + I.$$

The reaction between carbon monoxide and oxygen in the presence of traces of water vapour and hydrogen serves as an example of positive catalysis. Two types of reaction have been established for this mixture. One of these

occurs within an ignition peninsula at temperatures between 450 and 700°. The upper ignition limit corresponds to pressures from 70 mm to atmospheric pressure. Water vapour does not affect the position of the upper limit and hence does not take part in the mechanism of this reaction.

According to Lewis and Alba the active centres in this reaction are the CO_3 radical and the ozone molecule. However, this should lead to an almost complete suppression of the process at a sufficiently high temperature because of the thermal instability of CO_3 and O_3. It is known from experiments that a well dried mixture of CO and oxygen will not react even up to 700° at pressures of the order of atmospheric (i.e. above the upper limit). Above 700° only a slow heterogenous reaction is observed. Thus the homogenous (taking place in the body of the vessel) type of reaction discussed above is practically impossible outside the limits of the ignition peninsula.

In the conditions described above the process in a moist mixture is strongly accelerated, but the mechanism is changed considerably. According to Semenov and Zel'dovich, it can be described by the following scheme:

$$H + O_2 = OH + O,$$
$$OH + CO = CO_2 + H,$$
$$CO + O = CO_2,$$
$$O + H_2 = OH + H,$$
$$OH + H_2 = H_2O + H.$$

On the basis of a spectrographic study Kondrat'ev concluded that the limiting step in the combustion of CO in the presence of moisture is the process

$$OH + CO = CO_2 + H.$$

Stationary and non-stationary chain reactions. Depending upon the conditions, a chain reaction occurs in a stationary or in a non-stationary form. We shall discuss the simplest case in which only a single active intermediate takes part in the reaction. Let us call the concentration of the active

occurs within an ignition peninsula at temperatures between 450 and 700°. The upper ignition limit corresponds to pressures from 70 mm to atmospheric pressure. Water vapour does not affect the position of the upper limit and hence does not take part in the mechanism of this reaction.

According to Lewis and Alba the active centres in this reaction are the CO_3 radical and the ozone molecule. However, this should lead to an almost complete suppression of the process at a sufficiently high temperature because of the thermal instability of CO_3 and O_3. It is known from experiments that a well dried mixture of CO and oxygen will not react even up to 700° at pressures of the order of atmospheric (i.e. above the upper limit). Above 700° only a slow heterogenous reaction is observed. Thus the homogenous (taking place in the body of the vessel) type of reaction discussed above is practically impossible outside the limits of the ignition peninsula.

In the conditions described above the process in a moist mixture is strongly accelerated, but the mechanism is changed considerably. According to Semenov and Zel'dovich, it can be described by the following scheme:

$$\begin{aligned} H + O_2 &= OH + O, \\ OH + CO &= CO_2 + H, \\ CO + O &= CO_2, \\ O + H_2 &= OH + H, \\ OH + H_2 &= H_2O + H. \end{aligned}$$

On the basis of a spectrographic study Kondrat'ev concluded that the limiting step in the combustion of CO in the presence of moisture is the process

$$OH + CO = CO_2 + H.$$

Stationary and non-stationary chain reactions. Depending upon the conditions, a chain reaction occurs in a stationary or in a non-stationary form. We shall discuss the simplest case in which only a single active intermediate takes part in the reaction. Let us call the concentration of the active

product x. The change of this parameter with time is governed by the kinetic equation:

$$\frac{dx}{dt} = n_0 + fx - gx, \qquad (51,26)$$

where n_0 is the rate of chain initiation, f is the rate constant for chain branching processes, and g is the rate constant for chain terminating processes.

Under chain initiation are included the primary processes of intermediate product formation from the starting materials; under chain branching, those reactions in which one molecule of active intermediate reacts with starting material to give two or more active centres; and under chain termination, processes by which active centres are destroyed.

The solution of equation (51,26) has a different character, depending on the ratio between the parameters f and g. When $g > f$ we shall have a stationary regime. In this case the concentration of the active product, x, will, with time, approach a stationary value:

$$x = \frac{n_0}{g - f}. \qquad (51,27)$$

When this value has been reached the concentration of the active product will remain constant, and the reaction will go at a constant rate

$$v = kx, \qquad (51,28)$$

where k is the rate constant for chain transfer.

By chain transfer is meant the process by which one molecule (atom, radical) of intermediate product reacts with starting material to give the final reaction product; the active intermediate is regenerated.

The rate of chain transfer is not included in equation (51,26) because this reaction does not alter the quantity of active intermediate. It is formed as fast as it is consumed. However, the rate of chain transfer multiplied by the concentration of active intermediate does determine the

rate of the overall process for the conversion of starting materials into final reaction products.

The parameters n_0, f, and g depend on the concentration of the starting materials and change slowly as the reaction progresses. Consequently, according to equation (51,27), the parameter x changes. Hence it should not really be called stationary concentration of the intermediate, but a quasi-stationary one. However, the initial change in the parameter x (i.e. until it reaches its quasi-stationary value) occurs in a short time during which the concentration of the starting material does not undergo a notable change.

It is known from the theory of chain reactions that

$$g=\frac{\beta}{\Delta_1} \quad \text{and} \quad f=\frac{\delta}{\Delta_1}, \qquad (51,\ldots)$$

where δ is the probability of chain rupture, β is the probability of chain branching, and Δ_1 is the average time between two successive reactions in the chain.

By carrying out the respective substitutions, and by considering that the rate of reaction

$$W=\frac{x}{\Delta_1},$$

we can put equation (51,28) in the form

$$W=\frac{n_0}{\beta-\delta}=n_0\gamma,$$

where $$\gamma=\frac{1}{\beta-\delta}.$$

The parameter γ is termed the chain length and is the average number of elementary reactions or links in the chain arising from a single active centre in unit time.

With $f>g$ a non-stationary reaction is obviously obtained. In this case $\frac{dx}{dt}>0$.

Putting $f-g=\varphi$, we get the equation (51,26) in the following form:

$$\frac{dx}{dt}=\varphi\left(x+\frac{n_0}{\varphi}\right). \qquad (51,30)$$

Integration of this equation gives

$$\ln\left(x+\frac{n_0}{\varphi}\right)=\varphi t$$

or

$$x=\frac{n_0}{\varphi}\left(\frac{\varphi}{n_0}e^{\varphi t}-1\right). \qquad (51,31)$$

For times greater than $\frac{1}{\varphi}$ the concentration of active product and the reaction rate will increase exponentially with time, i.e. at a rate proportional to $e^{\varphi t}$. The initial period, when the active product concentration and reaction rate are small, is the induction or chain origin period. Its length is of the order of $\frac{1}{\varphi}$.

If we change the reaction conditions in such a way that the parameters g and f change, then at $g=f$ a sharp change in the character of the reaction will occur - a transition from a stationary to a non-stationary system. Thus the criterion that $g=f$ is the condition for chain auto-ignition.

We have discussed the case in which only one active intermediate product takes part in the reaction. When several intermediate products take part in the reaction the reaction can become much more complex, but the principal of the diagram does not change.

It follows from the theories discussed that auto-acceleration and ignition of a gas mixture, in which a chain reaction is taking place, can occur, not as a consequence of self-heating, but as a result of rapid chain branching. It is necessary to bear in mind that the increased rate of a chain reaction may in its turn lead to heating of the mixture, thus providing the prerequisite for an auto-accelerating reaction. This is because all the parameters of a chain reaction - the probability and rate of chain branching, the number of active centres, the rate of the chain reaction - depend extremely strongly on the temperature.

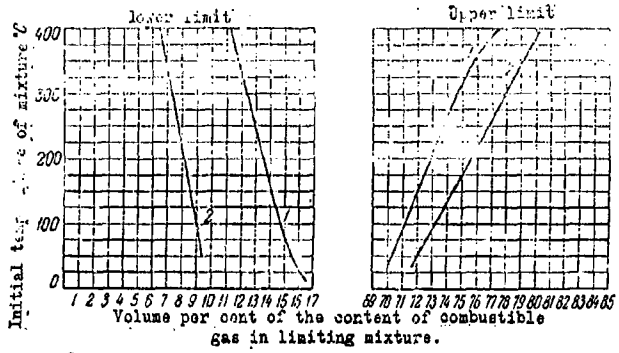


Fig.120. Relation between the ignition concentration limits and the initial temperature.

Combustion of a gaseous mixture is not possible at any percentage composition. When the composition is changed boundaries will be reached outside which it is not possible to cause a diffused flame to arise even with a very powerful spark. These boundaries are called concentration limits. The lower limit arises from a deficiency of oxygen in a mixture with an excess of the combustible component.

Concentration limits depend on the experimental conditions. With increasing power of the initiating impulse, of the initial temperature or pressure of the gaseous mixture the concentration limits are pushed farther apart.

The relation between the concentration limits and the initial temperatures for mixtures of carbon monoxide (curve 1) and hydrogen (curve 2) with air are shown in Fig.120.

It is evident from the figure that as the initial temperature is decreased the upper and lower limits approach one another, and it is evident that they will coincide at some particular temperature. This will evidently correspond to the mixture most likely to ignite in the conditions given.

The change in concentration limits with pressure is described by the curve shown in Fig. 121.

It is evident from the curve that the concentration limits are narrowed as the pressure is decreased, and on reaching some minimum pressure, p_0, the mixture becomes completely unable to burn. This pressure, p_0, corresponds to the most favourable ratio of components in the mixture. The explosion region at a given temperature is delimited by the curve acb.

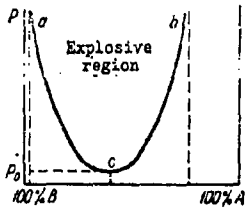


Fig.121. Relation between ignition concentration limits and the pressure.

The concentration limits also depend on where the gas is ignited. When the gas is ignited from below, i.e., when the flame spreads upwards, the concentration limits are always wider than when the flame spreads downwards. This is explained by the fact that the flame cannot move downwards when its rate of diffusion is slower than the rate of convention of the hot combustion products. Such a ratio of rates is established close to the concentration limits. From the point of view of safety techniques it is natural to consider as the index the possibility of ignition within the concentration limits with a spread of the flame from the bottom upwards.

Concentration limits for mixtures of various gases and vapours with are are cited in Table 80 (data from Lewis and Alba).

The concentration limits cited in Table 80 were determined at atmospheric pressure and room temperature with upward spread of the flame in tubes with a diameter of 10 cm. or more.

Concentration limits are determined not only by the concentration of components in the gaseous mixture but also by the diameter of the tube. Expansion of the concentration limits is observed in tubes with diameters of up to 5 cm. The same mixture will burn in a wide tube but not in tubes whose diameters are smaller than a critical value. This phenomenon was discovered

by Davy in 1816 and was the basis for the construction of the miner's safety lamp, in which a copper gauze with small holes prevents spread of the flame from the interior of the lamp into the atmosphere of the mine.

Table 80

Concentration limits for mixtures of gases and vapours with air.

Substance	Formula	Concentration limits, %	
		lower	upper
Hydrogen	H_2	4.00	74.20
Carbon monoxide	CO	12.50	74.20
Carbon disulphide	CS_2	1.25	50.00
Hydrogen sulphide	H_2S	4.30	45.50
Ammonia	NH_3	15.50	27.00
Methane	CH_4	5.00	15.00
Ethane	C_2H_6	3.22	12.45
Ethylene	C_2H_4	2.75	28.60
Acetylene	C_2H_2	2.50	80.00
Methanol	CH_4O	6.72	36.50
[illegible]nol	C_2H_6O	3.28	18.95
[illegible]ethyl ether	C_3H_8O	1.85	36.50
Methyl ethyl ether	C_3H_8O	2.00	10.10
Acetone	C_3H_6O	2.55	12.80
Benzene	C_6H_6	1.41	6.75
Toluene	C_7H_8	1.27	6.75
Xylene	C_8H_{10}	1.00	7.00
Dichloroethane	$C_2H_4Cl_2$	6.20	15.90

The origin of concentration limits is heat loss to the surrounding space by heat conduction through the walls of the tube and heat loss by irradiation.

When a flame is spreading through a narrow tube the limit of dissemination is connected with heat conduction at the walls. The concentration limits beyond which spread of a flame is impossible in a vessel of any diameter, is caused in its turn by radiative heat loss.

Zel'dovich developed the theory of the limits of flame spread.

52. Combustion of Gases.

Study of the processes of combustion in gaseous mixtures have been based principally on the use of photographic methods. Photography of flames may be carried out directly or by shadow or Schlieren methods which are based on differences in density between the non-combusted mixture and the products of combustion. Direct photography is possible when the luminescent intensity of the flame is sufficiently great.

The combustion of gaseous mixtures may occur in very different ways according to the experimental conditions. When combustion of the mixture occurs at constant pressure, the flame is observed to spread uniformly at a constant rate. This type of combustion can be brought about by igniting the gaseous mixture at the open end of a tube; in this case a continuous equalisation to atmospheric of the pressure at the flame front occurs. This condition (p = const) is observed in the cone of a bunsen burner flame, in which spread of combustion also occurs at a constant rate.

A uniform rate of flame diffusion can also be brought about by the soap bubble method (Stevens' method). A spherical flame front is formed by spark ignition of the gas in a soap bubble. As the flame front diffuses the diameter of the bubble increases as a result of the diffusion of combustion products. Because the resistance of a soap film is very small, the expansion of gases and the whole diffusion process goes at an almost constant pressure. The rate of diffusion of the flame in space is a combination of the rate of diffusion of the reaction zone relative to the gas and the movement of the expanding gases.

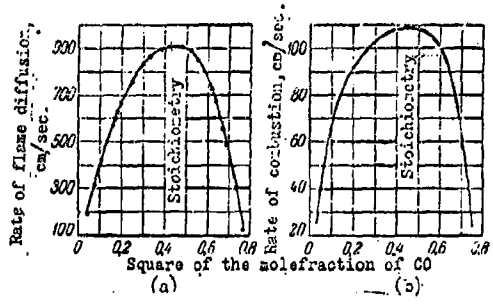


Fig.122. Relation between the rate of flame diffusion (a), or the rate of combustion (b) and the composition of a gaseous mixture.

The experimental results of various authors showed that the rate of combustion of gaseous mixtures depended strongly on the concentration of the components. Examples of this are shown in Fig. 122 and 123.

To give the curves a more symmetrical form, the abscissa in Fig. 122 is given in terms of the square of the molefraction of CO in the mixture. These data apply to moist mixtures of CO and O_2; the molefraction of H_2O is 0.033. The maximum rates of combustion for CO and CH_4 lie in the concentration region close to a stoichiometric ratio.

The effect of small concentrations of water on the combustion of a stoichiometric mixture of CO and O_2 is shown in Fig. 124, from which it can be seen that negligible quantities of water vapour lead to a very sharp increase in the rate of flame diffusion. This is in agreement with the catalytic role of water vapour. Water vapour appears to have no effect on the rate of combustion of a methane mixture.

The rate of diffusion of a flame depends markedly on the tube diameter. The corresponding data for a mixture of methane and air are shown in Fig. 125.

The greatest values measured correspond to a tube diameter of almost 100 cm. From the shape of the curve a rapid cessation of the rate of growth would not be expected on further increasing the tube diameter. This phenomenon can be explained by the fact that as the tube diameter is increased the flame front is distorted by convection currents. As a result the combustion surface is considerably increased and this is a continuous cause for an increase in flame velocity.

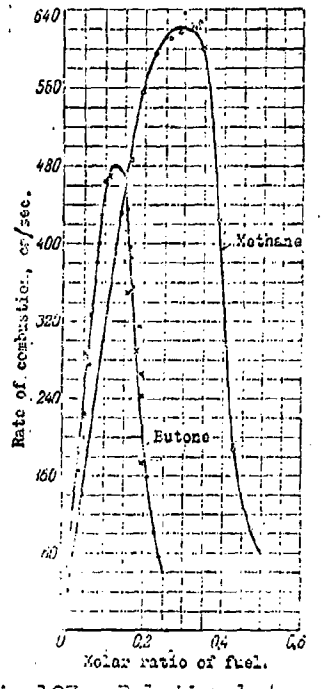


Fig.123. Relation between rate of combustion and the concentration composition of a gaseous mixture.

As a result of working up experimental data Coward and Hartwell showed that if the tube diameter is greater than a critical value, then the velocity of the flame (defined as the volume of gas burned in unit time at unit surface of the front) remains unchanged as the tube diameter changes.

The experimental results cited have a simple theoretical explanation. The basic lawsof combustion in a moving gas were established by Michelson in his work "The normal velocity of combustion in explosive gaseous mixtures". According to this law, if the normal to the surface of the flame front is at an angle φ to the direction of diffusion, then the rate of diffusion of the flame increases in inverse proportion to $\cos\varphi$. If the rate of diffusion of the flat front of the flame relative to the non-moving gas in a direction perpendicular to its surface is w, then the velocity v of the flame in the direction of its diffusion will be

$$v = \frac{w}{\cos\varphi}. \qquad (52,1)$$

The relation (52,1) is known as the cosine law. w is known as the normal or fundamental rate of diffusion of the flame.

The area rate gives a more general formulation. It is used for the curved flame front as well as planar ones. It follows from this rule that, for any size of flame front surface, the rate of diffusion increases as the ratio of surfaceof the flame front to its projection on a plane perpendicular to the direction of diffusion.

Let a flame diffuse in a tube of cross-sectional σ at a velocity v. The volume of the mixture being burnt in unit time will be:

$$V = v\sigma.$$

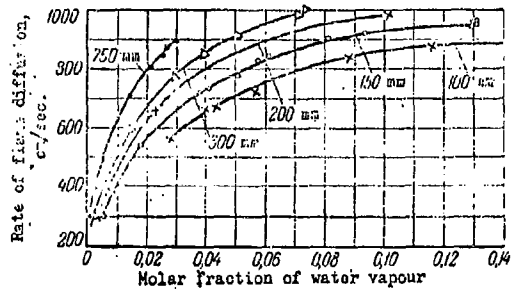


Fig.124. Effect of water vapour concentration on the rate of flame diffusion.

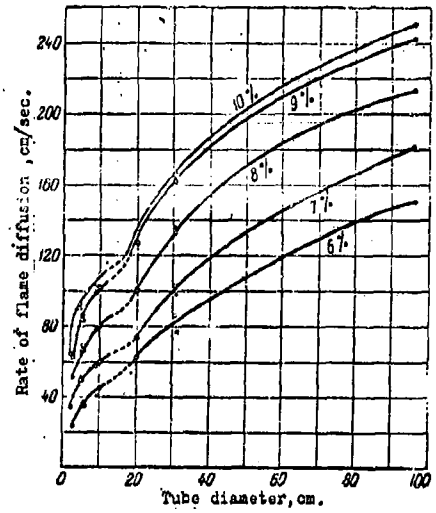


Fig.125. Relation between the rate of flame diffusion and tube diameter (methane and air mixture).

On the other hand, at each point on the surface the flame front is diffusing in a direction normal to this front at a fundamental velocity v. If the surface of any sort of curved flame front is designated S, then the volume of the mixture being burned in unit time is described by:

$$V = wS.$$

Hence

$$v = w\frac{S}{\sigma}, \qquad (52,2)$$

which is the equation for the area rule.

In certain cases of planar falme fronts we shall have

$$u = s\cos\varphi,$$

and the area rule will be transformed into the cosine law.

Theory of thermal diffusion of flames. If the chemical combustion reaction is not autocatalytic, then the cause of flame diffusion can only be transfe of heat from the combustion products to the unburned mixture. This type of flame diffusion is termed thermal.

A model of the distribution of temperature in a gaseous mixture caused by heat of reaction and thermal conductivity is shown schematically in Fig.126.

According to this scheme, chemical reaction (the combustion zone) begins only at a temperature T_i close to the temperature T_g of combustion of the gaseous mixture. In the zone limited by the temperatures T_i and T_0 (the initial temperature of the starting materials) reaction proceeds so lowly that heat evolution can be neglected. In this case the width of this (the heating zone) can be determined, starting from the differential equation for thermal conduction. For the one dimensional case this has the form

$$\frac{c\,dT}{dt} = \eta\frac{d^2T}{dx^2}, \qquad (52,3)$$

where c is the volume heat capacity and η is the coefficient of thermal conductivity.

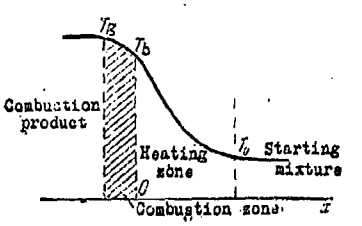


Fig.126. Temperature distribution in a burning gaseous mixture.

The solution of equation (52,3) has the form

$$T = T_0 + Ne^{-\frac{u/x}{\mu}}, \qquad (52,4)$$

where u is the rate of flame diffusion, N is a constant determined by the boundary conditions, and μ is the ratio of the thermal conductivity to the volume heat capacity and is called the coefficient of temperature conductivity

$$\mu = \frac{\eta}{c_p \rho}, \qquad (52,5)$$

where ρ is the mean density of the gas in the temperature range discussed.

Because at $x = \infty$ $T = T_0$, and at $x = 0$ $T = T_s$, then $N = T_s - T_0$ and (52,4) may be changed into the form

$$\frac{N}{T_\infty - T_0} = \frac{T_s - T_0}{T_\infty - T_0} = e^{\infty \frac{u}{\mu}}. \qquad (52,6)$$

Equation (52,6) makes it possible to judge the order of the width of the layer in which heating is important. This equation was first obtained by Michelson.

If as a scale for the width L of the zone we take the distance in which

$$L = \frac{\mu}{u} = \frac{\eta}{c_p \rho u}. \qquad (52,7)$$

Substituting in (52,6) the corresponding constants for a temperature of about 500°, we find: $L = 0.06$ cm. for a mixture of methane and air (u = 5 cm/sec.) and $L = 0.0003$ cm. for the explosive mixture $2H_2 + O_2$ (u = 1000 cm/sec).

In both cases the width of the heating zone is many times greater than the free path of a molecule. As a demonstration it is sufficient to substitute into (52,7) the molecular kinetic expression for coefficient of thermal conductivity

$$\eta = \frac{1}{3} c_p \rho \lambda c',$$

where λ is the longth of the free path of the molecule and c' is the mean velocity of thermal motion of a molecule.

The parameter c' is of the order of the velocity of sound in the gas, c_0; both these parameters are proportional to $\sqrt{T}$.

Thus, according to the order of parameters

$$L \approx \frac{1}{3} \lambda \frac{c'}{u}. \qquad (52,8)$$

For our examples $c' \gg u$.

Using the corresponding ratio of the kinetic theory of gases it is easy to establish in a general form the connection between the rate of flame diffusion and the speed of sound in the gaseous mixture.

As has been shown the width of the heating zone is given by the relation

$$L = \frac{\mu}{u}.$$

The width of the combustion zone L_r, i.e. the zone in which an intense chemical reaction is occurring (see Fig.126) will be

$$L_r = u\tau, \tag{52,9}$$

when τ is the time of a chemical reaction.

It is evident that L_r cannot be longer than L. In fact the combustion zone is always smaller than the heating zone. To observe its size it is necessary to conclude that L_r and L are proportional:

$$L_r = \Phi L, \tag{52,10}$$

where the coefficient $\Phi < 1$ and depends on the reaction kinetics and the temperatures T_0 and T_c.

By simultaneous solution of the equations (52,9) and (52,10) we obtain an expression for the rate of flame diffusion:

$$u = \sqrt{\Phi \frac{\mu}{\tau}}. \tag{52,11}$$

If λ is the length of the free path and γ is the average number of collisions necessary for an elementary act of the chemical reaction, then the time for the chemical reaction is

$$\tau = \frac{\lambda\gamma}{c'}, \tag{52,12}$$

where c' is the rate of motion of the molecules and $\lambda\gamma$ is the means of introducing the molecular thermal component by means of which it reacts.

Replacing τ by its value from equation (52,12) and the coefficient of temperature conductivity by its molecular kinetic expression, we get the formula (52,11) in the form

$$u = c' \sqrt{\frac{1}{3}\frac{\Phi}{\gamma}} \approx \frac{c}{\sqrt{\gamma}}\varphi, \qquad (52,13)$$

where c is the speed of sound in the combustion zone, and φ is a dimensionless factor smaller than unity.

A very important conclusion follows from formula (52,13): the rate of flame diffusion during combustion is always many times smaller than the speed of sound. This is because the rate of energy transfer in a gas by thermal conductivity is small compared to the rate of diffusion of elastic vibrations.

The Zel'dovich and Frank-Kamenetskii theory of combustion. These authors constructed their theory starting from calculations on the relation between the rate of chemical reactions and the temperature and the concentration of reacting substances.

The concentration of reactants at the flame front will change as a result of the chemical reaction and of diffusion. To calculate the rate of diffusion in thermal dissemination of a flame, it is necessary to find the connection between the temperature and the concentration of reactants in the flame zone. This connection can be defined by a simultaneous discussion of the equations for thermal conductivity and diffusion applied to stationary diffusion of a flame.

With the assumption that the coefficients of thermal conductivity and diffusion are independent of temperature these equations take the form

$$\mu \frac{d^2T}{dx^2} - u\frac{dT}{dx} + \frac{Q}{\rho c} f(n) Ze^{-\frac{E}{RT}} = 0 \qquad (52,14)$$

(thermal conductivity equation). Here $Qf(n)Ze^{-\frac{E}{RT}} = F(T)$ is the volume rate of heat evolution, $f(n)Ze^{-\frac{E}{RT}}$ is the rate of chemical reaction, and μ is the coefficient of temperature conductivity.

$$D\frac{d^2n}{dx^2} - u\frac{dn}{dx} - \frac{1}{\rho}f(n)Ze^{-\frac{E}{RT}} = 0 \qquad (52,15)$$

(diffusion equation) where D is the diffusion coefficient and n is the concentration of reactants. The boundary conditions for these equations are: at $x = +\infty$, $T = T_r$ and $n = 0$, and at $x = -\infty$, $T = T_0$ and $n = 1$.

From the kinetic theory of gases it is known that, if the molecular of the reactants and products are closely similar, the coefficient of temperature conductivity is close in value to the coefficient of diffusion. If the difference between these parameters is neglected equations (52,14) and (52,15) are the same. A simple transformation makes this clear. For this we introduce into equation (52,14) the identity

$$\vartheta = T_r - T. \qquad (52,16)$$

Then equation (52,14) takes the form

$$-\mu\frac{d^2\vartheta}{dx^2} + u\frac{d\vartheta}{dx} + \frac{Q}{\rho c}f(n)Ze^{-\frac{E}{R(T_r-\vartheta)}} = 0. \qquad (52,17)$$

The boundary conditions are: at $x = -\infty$, $\vartheta = T_r - T_0$; at $x = +8$, $\vartheta = 0$.

If equation (52,15) is multiplied by $-\frac{Q}{c}$ it takes the form

$$-D\frac{Q}{c}\frac{d^2n}{dx^2} + u\frac{Q}{c}\frac{dn}{dx} + \frac{Q}{\rho c}f(n)Ze^{-\frac{E}{R(T_r-\vartheta)}} = 0. \qquad (52,18)$$

Introducing the new transformation $\lambda = \frac{Q}{c}n$ into equation (52,18) we obtain

$$-D\frac{d^2\lambda}{dx^2} + u\frac{d\lambda}{dx} + \frac{Q}{\rho c}f(\cdot)Ze^{-\frac{E}{R(T_r-\vartheta)}} = 0, \qquad (52,19)$$

With $D = \mu$ this is identical with (52,17).

The boundary conditions for equation (52,19) are: at $x = -\infty$, $\lambda = \frac{Q}{c}$; at $x = +\infty$, $\lambda = 0$.

Assuming that c = Const., we get $\frac{Q}{c} = T_r - T_0$ and the boundary conditions if equation (52,19) coincide exactly with those of equation (52,17) and consequently

$$\lambda = \vartheta, \tag{52,20}$$

or

$$\frac{Q}{a} n = (T_r - T_0) n = T_r - T,$$

whence

$$n = \frac{T_r - T}{T_r - T_0}. \tag{52,21}$$

This equation immediately gives the concentration of the reactants at a point where the temperature is T. The contents of formula (52,21) can be formulated as the concentration and temperature fields in the flame zone. It is fulfilled when the rate of the chemical reaction depends only on the concentration of substances which are related to one another by a single stoichiometric ratio, and on the temperature.

Having established the connection between the reaction concentration and the temperature, we can in future limit our discussion to a single differential equation, e.g., the thermal conductivity equation.

We shall write the general thermal conductivity equation in the following form:

$$c_p \rho u \frac{dT}{dx} = c_p \rho \frac{dT}{dt} = \frac{d}{dx} \eta \frac{dT}{dx} + F(T), \tag{52,22}$$

where F is the volume rate of heat evolution.

Using the relation between the reactant concentration and the temperature according to (52,21), one can put the rate of chemical reaction (Arrhenius' Law), and consequently the parameter F, as functions of a single temperature.

An intensive chemical reaction occurs in a narrow chemical range, $\vartheta = T_r - T_u$, as shown in Fig. 126. The heat evolved by the reaction is used in heating the reacting mixture itself and in heating fresh mixture from T_0 to T_u.

The term $c_p \rho \frac{dT}{dt} = c_p \rho u \frac{dT}{dx}$ is the expenditure at heat in raising the temperature of the reaction mixture.

The term $\frac{d}{dx} \eta \frac{dT}{dx}$ is the loss of heat by thermal conductivity.

Because the temperature interval in which the reaction goes is narrow $(\vartheta < T_r - T_0)$ we can justifiably neglect the use of heat in heating the reacting mixture in the reaction zone; equation (52,22) then takes the form

$$\eta \frac{d^2T}{dx^2} + F(T) = 0. \qquad (52,23)$$

The thermal conductivity in the reaction zone can be counted as practically constant.

The solution of this equation has the form

$$\frac{dT}{dx} = \sqrt{\frac{2}{\eta} \int_{T_0}^{T_r} F(T)\, dT}. \qquad (52,24)$$

If we neglect the use of heat in heating the reacting mixture itself, then all the heat of reaction is dissipated by thermal conductivity.

Equating this heat loss from the reaction zone with the total heat evolved in the flame in unit time, we have

$$\eta \frac{dT}{dx} = u\rho Q, \qquad (52,25)$$

where Q is the volume calorific capacity of the mixture, and $u\rho$ is the mass velocity of the flame.

Comparing equations (52,24) and (52,25) we obtain as the final equation for the flame velocity:

$$u = \frac{1}{\rho Q} \sqrt{2\eta \int_{T_0}^{T_r} F(T)\, dT}. \qquad (52,26)$$

Cadovnikov compared the rates of combustion of explosive mixtures of carbon monoxide and air diluted with combustion products. The dilute mixture was heated beforehand so that the temperature of combustion would not differ from that of an undiluted mixture. This experiment confirmed with satisfactory precision the relation obtained from the theory, $u\rho Q = \text{const}$.

The parameter $F(T)$ in equation (52,26) can be expressed in the form

$$F(T) = Qn^m Ze^{-\frac{E}{RT}}, \qquad (52,27)$$

where n is the relative concentration of the reactant, and m is the order of the reaction.

If in (52,27) n is expressed in terms of the temperature as in (52,21) and $e^{-\frac{E}{RT}}$ is resolved into a series of degree $\frac{T_r - T}{T_r}$, and we take into account only first order terms (this is justifiable because the reaction rate is only large enough with T close to T_r), then we obtain

$$F(T) = Q\left(\frac{T_r - T}{T_r - T_0}\right)^m Ze^{-\frac{E}{RT_r^2}(T_r - T)}.$$

Making some further complications and taking account of the fact that at the lower integration limit the reaction rate becomes negligibly small, we get after integration of (52,26)

$$u = \sqrt{\frac{\mu}{\tau_r}\frac{2m!}{\theta_r^{m+1}}} = \sqrt{\frac{\eta_r 2m!}{c_p \rho_0 \tau_r \theta_r^{m+1}}}, \qquad (52,28)$$

Where $\theta_r = \frac{E}{RT_r^2}(T_r - T_0)$, η_r - is the coefficient of thermal conductivity at temperature T_r, τ_r is the characteristic time of the reaction at temperature T_r and the initial concentration of reaction products (reciprocal of the maximum rate of reaction).

Since the rate of reaction is

$$\left(\frac{dn}{dt}\right)_{max} = n_0^m Ze^{-\frac{E}{RT_r}},$$

where n_0 is the concentration of reactants in g/cm^3, then

$$\frac{1}{\tau_r} = \frac{1}{n_0^m Z} e^{\frac{E}{RT_r}}. \qquad (52,29)$$

In deducing the above result we started from the condition that the rate of reaction at the initial temperature T_0 was negligibly small. When this condition is not observed a stationary diffusion of the flame would

become quite impossible, because at any point the mixture would have reacted before the flame front arrived. The above conditions, which arise from the Arrhenius law, can be quantitatively formulated thus:

$$\theta = \frac{E}{RT_r^2}(T_r - T_0) \gg 1.$$

Substituting values of θ and τ_r in equation (52,28) and taking into account that $c_p(T_r - T_0) = Q$ (when c_p = const.), we obtain the corresponding equations for the rate of flame diffusion:

$$u = \sqrt{\frac{2\eta_r Z e^{-\frac{E}{RT_r}}}{\rho_0 Q (T_r - T_0)} \left(\frac{RT_r^2}{E}\right)^2} \qquad (52,30)$$

for first order reactions, and for second order reactions

$$u = \sqrt{\frac{4\eta_r n_0 Z e^{-\frac{E}{RT_r}}}{\rho_0 Q (T_r - T_0)^2} \left(\frac{RT_r^2}{E}\right)^2}. \qquad (52,31)$$

Belyaev's experiments on the combustion of methyl nitrate and nitroglycol (in the vapour phase) confirm the results of this theory well.

The important relation between the flame velocity and the temperature according to (52,30) and (52,31) is connected with Arrhenius law of chemical reaction rates, which states that, to a first approximation

$$u \sim e^{-\frac{E}{2RT_r}}, \qquad (52,32)$$

Consequently there should be a linear relation between $\lg u$ and $\frac{1}{T}$ The results of working up the data of Passauer and Sadovnikov (on CO/air mixtures) are shown in Fig. 127. They are in complete agreement with this requirement of the theory.

The relation between the rate of flame diffusion and the pressure with other conditions constant is determined by the characteristic relation of the chemical reaction rate and the pressure.

Because

$$F(T) \sim W \sim p^m,$$

then, according to (52,26)

$$\rho u \sim p^{\frac{m}{2}}, \qquad (52,33)$$

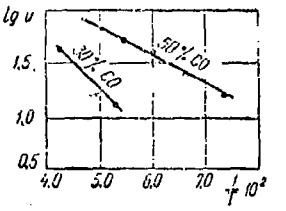


Fig.127. Relation between the rate of combustion and the temperature.

where W is the rate of the chemical reaction, p is the pressure of the gaseous mixture, and m is the order of the chemical reaction.

Thus, for a unimolecular reaction $\rho u \sim \sqrt{p}$ whereas for a bimolecular reaction $\rho u \sim p$.

Because the density of a gaseous mixture is proportional to the pressure, we get for a linear rate of combustion

$$u \sim p^{\frac{m}{2}-1}, \qquad (52,34)$$

which requires that u should be independent of pressure for a bimolecular reaction, and that $u \sim \frac{1}{\sqrt{p}}$ for a unimolecular reaction.

Ubbelohde and Kelliker's observation that the rate of flame diffusion in mixtures of different inflammable gases (petrol, benzene, methane) was related to the pressure at orders between $p^{-1/2}$ and p^0, corresponded to chemical combustion reactions of order between first and second.

53. Combustion of Condensed Explosives.

When explosion of a high explosive or detonator is brought about by a thermal impulse the formation of a detonation wave is always preceded by a more or less prolonged period of accelerating combustion. Transition from combustion into the detonation type of explosion only occurs in favourable conditions even in the case of non-stationary processes.

The combustion of detonators is usually very unstable and is easily transformed into detonation. On the other hand combustion of powders proceeds in a very stable manner and transition to detonation appears to be possible only under special circumstances which seldom occur in practice.

High explosives occupy an intermediate position between detonators and powders in their ability to undergo normal combustion.

The combustion of high explosives and detonators has been studied insufficiently. It has been investigated principally at low and constant pressures, close to atmospheric. It has been established that most of the explosives studied can undergo stable combustion at a constant rate in the defined conditions, and the rate was independent of the length of the charge.

Andreev observed that combustion of the explosives under discussion usually occurred with very weak luminescence in a gas layer which lay close to the surface of the condensed phase. Then what he called the combustion flame was a result of the combustion of hot reaction products in contact with the air.

The following factors can have a considerable effect on the character and rate of diffusion of the combustion processes: the properties of the explosive, the pressure, the initial temperature, the density of the charge, the diameter of the charge, the thickness and the kind of casing.

The possibility of a process and the rate of its diffusion are determined first and foremost by the kinetics of the chemical reaction, i.e., by the rate of heat evolution and the rate of heat transmission from the reaction zone into the starting material. The condition of heat transmission with a given reaction kinetics depends on the thermal conductivity of the explosive.

That lead azide only undergoes a detonation type of explosion, no matter what the conditions, can be explained by kinetic factors. The high rate of the chemical reaction in the conversion as a result of exceptionally rapid acceleration leads to diffusion processes by heat transmission being almost impossible.

On thecontrary, if the rate of a chemical reaction in given experimental conditions is small, then the loss of heat in consequence of heat diffusion to the surroundings would not be compensated by the source of heat, the process would be unstable and combustion would cease.

However, if the thermal conductivity of the explosive is high, then the heat of reaction may penetrate into the unreacted substance to a great depth, and consequently the temperature in the conversion zone would be insufficient to stimulate an intense chemical reaction capable of sustaining a self-diffusing process.

The specific peculiarity of the combustion of high explosives and detonators is the possibility of physico-chemical processes occurring simultaneously in the condensed and gaseous phases. In a very volatile substance combustion may occur exceptionally in the gas phase when its boiling or sublimation temperature is lower than the temperature at which the chemical reaction proceeds at a notable rate in the condensed phase.

In this case the general character of the combustion will be determined by two factors - the process of evaporation of the condensed phase and the conditions of development of the chemical reaction in the vapour; heat from the flame zone will pass to the condensed phase through a layer of hot, but not yet reacted, explosive vapour just as in gaseous mixtures. This type of combustion is characteristic for low boiling liquid explosives. The combustions of methyl nitrate and nitroglycol at comparatively low pressures are typical examples.

For non-volatile and poorly volatile substances, depending on its mechanism, the chemical reaction may occur either only in the condensed phase, or simultaneously in the condensed, smoke-gas, and gas phases. In the first case reaction leads almost directly to final combustion products, but in the second case combustion is a very complex process in which intermediate reactions are of definite importance. This type of

reaction is the most frequent in practice. Typical examples are the combustion of pyroxylin and

Pressure has the most important effect on the rate of combustion of explosives. As a rule the rate of combustion increases with pressure and at a sufficiently high pressure burning becomes unstable and changes into detonation.

Mercury fulminate is the most satisfactorily studied of detonators. Patri, who studied the combustion of non-pressed mercury fulminate in the open air, established that the process diffused at a rate of several tens of metres per second, that it was unstable and changed into a detonation. This is explained mainly by the easy diffusion of hot reaction products into the pores of the substance, thus continuously increasing the combustion surface.

A systematic investigation by Belyaev showed that mercury fulminate, which had been pressed into tablets (d = 4 mm; h = 7 mm) at a pressure of about 2000 Kg/cm^2 without cases, was able to undergo stationary combustion at atmospheric pressure at a rate of only about 1.5 cm/sec. Analogous data were obtained for some other detonators. Belyaev's results are cited in Table 81.

TABLE 81

Rate of combustion of some detonating explosives at atmospheric pressure

Name of explosive	Density g/cm^3	Linear velocity cm/sec.
Mercury fulminate	3.80	1.55
Trinitrotriazidobenzene	1.70	0.65
Diazodinitrophenol	1.45	2.15
Potassium picrate	1.83	1.50
Lead styphnate	exploded	-
Lead styphnate + talc(40/60)	--	14.50

It was concluded, from observations on the combustion of detonators at various pressures below atmospheric, that the rate of combustion over a wide range changes almost linearly with pressure.

$$u = a + bp. \qquad (53,1)$$

This circumstance is evidence of the important part played by combustion in the gas phase. If the rate of reaction in the gas phase depends on the number of collisions, then the rate of combustion should rise linearly with the pressure.

Results of experiments with mercury fulminate and trinitrotriazidobenzene are given in Table 82.

Mercury fulminate		Trinitrotriazidobenzene	
p, mm Hg	u, cm/sec	p, mm Hg	u, cm/sec
760	1.53	760	0.63
605	1.30	425	0.44
405	1.02	375	0.35
175	0.67	115	0.16
10	0.48	40	0.15

TABLE 82. Relation between the rate of combustion and pressure.

It is seen from these data that when the pressure is decreased to about a tenth the rate of combustion of mercury fulminate is decreased to about a third. With a pressure of 100 mm. or less the rate of combustion is practically independent of pressure. A similar pattern is observed for trinitrotriazidobenzene.

On the basis of these and other observations Belyaev concluded that reactions in the condensed phase played an important part in the combustion of detonators and especially of mercury fulminate. The intermediate products of mercury fulminate formed as the result of primary reactions react even at comparatively low temperatures in the gas phase; these reactions have a determining influence on the rate of

reaction at pressures close to atmospheric. At low pressures, considerably lower than atmospheric, the initial reaction in the condensed phase plays a determining role. This is confirmed by the fact that the rate of combustion is practically independent of pressure under these conditions. However, the initial reaction in the condensed phase causes the decomposition of only part of the mercury fulminate (10 to 20%); the rest volatilises undecomposed.

A characteristic feature of typical detonators is their ability to burn in a stable manner at very low pressures. Normal combustion of trinitrotriazidobenzene is not disturbed even at pressures below 10 mm. Muraour and Schumacher observed a stable auto-diffusion reaction in compressed mercury fulminate in high vacuum (p = 0.003 mm. Hg.)

Systematic experiments on the combustion of high explosives at various pressures, from 2 Kg/cm.^{2} downwards, were carried out by Andreev. He observed that the relation between the rate of combustion and the pressure was the same for most of the substances as for detonators. The results of some of these experiments are given in Table 83.

TABLE 83

Relation between the rate of combustion and the pressure for some high explosives

Explosive	$u=a+bp$ (cm/sec)
Methyl nitrate	0.008 + 0.102 p
Nitroglycol	0.003 + 0.025 p
Hexogen	0.009 + 0.05 p
Tetryl	0.011 + 0.034 p

In all these experiments combustion of the explosive was carried out in a glass tube ($d \sim 4-6$ mm) which was placed under the bell of a vacuum pump.

On the basis of these data it can be concluded high explosives considerably more slowly than detonators. The parameter b is considerably larger for the latter than for the former. Thus, according to Belyaev, $a = 0.4$ and $b = 1.1$ for mercury fulminate. This means that the acceleration of combustion under the influence of process proceeds considerably more slowly in high explosives than in detonators, because the former are capable of undergoing stable combustion (in the absence of factors causing increased acceleration) at relatively high pressures.

In most cases when the pressure is decreased below some minimum value normal combustion of explosives becomes impossible and the process ceases. The limiting pressure depends principally on the physico-chemical properties of the explosive and the mechanism of the chemical reaction in the combustion zone. According to Andreev's data this pressure is 250-400 mm. Hg. for nitroglycol, 600 mm. Hg. for hexogen, about 400 mm.Hg. for pyroxylin No.1, and less than 24 mm. Hg. for nitroglycerine.

The occurrence of a lower pressure limit for condensed explosives is evidence for the especially important role of reactions in the gas phase in the combustion of these substances. On decreasing the pressure the reaction rate and the rate of heat evolution in the gas phase decrease correspondingly, but the rate of heat loss in the condensed phase is practically independent of the pressure and remains constant. At a definite pressure this can lead to disturbance of the thermal equilibrium and cessation of the reaction.

If in the mechanism of combustion of an explosive under specified conditions, a reaction occurring in the condensed phase becomes of major importance, then the possibility of stable combustion on decreasing the pressure arises. A small value of the limiting pressure can indicate that a condensed phase reaction is controlling the self-diffusion process in the conditions given. The independence of the rate of combustion of mercury fulminate and pressure at $p < 100$ mm. Hg. and its ability to burn in high vacuum are in agreement with Belyaev's ideas on the combustion of this substance in the conditions discussed.

Baum has established for a whole series of solid explosive mixtures that their relative ability to undergo stable combustion at low pressures and strictly comparable conditions depends on the ratio between the solid and gaseous reaction products. If the reaction products at the combustion temperature are completely solid or liquid, then the rate of combustion is completely independent of pressure. Systems which are capable of this type of combustion are called gasless compositions. The expression for the rate of combustion of such mixtures takes a particularly simple form:

$$u = a = \text{const.}$$

Thus the term a in the equation $u = a + bp$ corresponds to the rate of the reaction controlling heat transmission and which occurs in the solid phase, whereas the coefficient b depends on the conditions for a process occurring in the gas phase.

The results of Andreev's studies showed that combustion of condensed explosives at high pressures goes in different ways depending on the physical state of the explosive. Explosives can be divided into three groups for discussion of this point, thus: non-porous explosives, porous (powdered and pressed explosives), and liquid explosive systems.

Besides the nitrocellulose powders, blasting gelatine, gelatine-dynamite and some other explosives are representative of the first class of explosives. The ability of these explosives to undergo stable combustion at high pressures is expressed most strongly. Thus, blasting gelatine does not lose its ability to burn normally in a closed system even at pressures of 1200 Kg/cm^2.

Typical representatives of the second group are the high explosive powders. According to Andreev's data, the limit of stable combustion for ten and heksogen is a pressure of about 25 Kg/cm^2, and for trotyl and picric acid a pressure of about 65 Kg/cm^2.

However, these explosives in a compressed state are able to burn stably in a closed tube at considerably higher pressures; for example, ten, at a density of 1.65 g/cm^2, burns normally even at 210 Kg/cm^2. Cast explosives behave in this manner when sufficiently compressed.

These facts can be explained thus: in powdered explosives at high pressures the burning gases can comparatively easily enter the pores between particles of explosive and ignite them. Consequently the surface of combustion increases sharply and a stationary process becomes impossible. The porosity of the explosive is decreased by increasing its density and this makes more difficult the entry of the flame deep into the substance.

The character of the combustion of liquid explosives in relation to the pressure is somewhat different from that of solid explosives. When nitroglycerine is ignited at atmospheric pressure it does not burn but flashes. When ignited in a sealed tube it detonates at a pressure of about 65 Kg/cm^2.

According to Andreev's data, relatively uniform combustion of nitroglycerine only occurs at pressures below 20 Kg/cm^2. At higher pressures the character of the combustion changes considerably. The surface of the

liquid is disturbed and the whole process occurs as a series of consecutive flashes. Theoretical and experimental investigations have shown that the disturbance of stable combustion in liquid and solid explosives is a result of an increase in the combustion surface. In the present case this occurs by boiling of the surface layer of liquid (Zel'dovich) or by disturbance of its gasodynamic stability (Landau) owing to the turbulence of the surface. Increased viscosity prevents the appearance of these phenomena.

On the basis of the results discussed, it is possible to conclude that the disturbance of stable combustion in condensed explosives depends not only on the acceleration of the process as a direct result of the rising pressure (this acceleration is small) but also on the cause which, at a certain pressure, produces a disturbance of the flame front and of the combustion surface.

For almost all the explosives studied the linear rate of combustion is decreased as the density (of the explosive) increases. This is shown for example in Andreev's data cited in Table 84.

TABLE 84

Effect of density on the rate of combustion of explosives in a glass tube

Density, g/cm^3	Rate of combustion, cm/min
	Tetryl (Inside dia. of the tube 24 mm)
0.65	Does not burn
0.74	5.41
0.85	4.83
1.04	4.46
1.07	4.27
	Hexogen (Inside dia. of the tube 6.3 mm)
0.68	Does not burn
0.89	3.46
0.85	3.19
1.05	2.19
1.16	2.49

The effect of density on the rate of combustion is evidence of the importance of changes in porosity of the substance. Density affects not only the rate of combustion but also whether it can occur at all.

The data in Table 84 show that the combustion of tetryl and heksogen ceases if the density is reduced below a certain level. Andreev explained this as a result of an increased rate of heat loss in the condensed phase caused by the ease with which the molten substance could penetrate between the particles of explosive. The limiting density depends on the experimental conditions (tube diameter, crystal size). The density limit for stable combustion is somewhat reduced by an increase in tube diameter and in the state of division of the explosive.

Pyroxylin, which has a cellulose-like structure, behaves quite differently from tetryl and heksogen. It burns energetically enough even at poured density, but it shows an upper density limit above which combustion does not diffuse (Table 85).

TABLE 85

Relation between the rate of combustion of pyroxylin No. 1 and density (internal diameter of the tube, 5.5 mm.)

Density, g/cm	Rate of combustion, cm/min
0.24	37.5
0.30	31.1
0.57	14.8
0.59	Extinguished

A satisfactory explanation for this peculiar phenomena has not yet been found.

For condensed explosives, just as for gaseous mixtures, there is a critical diameter below which combustion will not spread in the conditions of the experiment. Critical diameters at atmospheric pressure are shown in Table 86.

TABLE 86

Critical diameters for some high explosives

Explosive	Density g/cm^3	d_{cr}, mm.
Cast TNT	1.59	32.0
Cast Tetryl	1.60	5.7
Heksogen	1.0	6.0
Pyroxylin No.1	0.6	5.5
Nitroglycol	-	2.0

The critical diameter for an explosive is not constant. It changes considerably, varying with the density of the explosive, the material and thickness of the casing, and certain other factors.

The critical diameter depends on the heat loss. However, the conditions of heat output can differ considerably depending on whether the reaction occurs only in the gas phase or in both gas and condensed phases. In the latter case the combustion process would be accompanied by considerable heating of the condensed phase and the heat loss would increase sharply.

The limiting diameter also depends on the rate of combustion. The greater the rate of combustion the smaller will be the heat outflow and the critical diameter in otherwise identical conditions. TNT has its maximum limiting diameter at its lowest rate of combustion ($\sim$ 1 cm/min).

For volatile substances, in which the reaction occurs completely in the gaseous phase, the surface layer only of the condensed phase is heated to the boiling point and the heat loss consequent upon heat conduction in the condensed phase will be small. For this reason the limiting diameter of a nitroglycol charge is small even at low rates of combustion ($\sim$ 2 cm/min.).

The rate of combustion of explosives is increased relatively slightly by an increase in the initial temperature. The rate of combustion of a series of explosives studied by Andreev was not more than doubled by increasing the initial temperature by 100°. The results of some experiments are cited in Table 87.

TABLE 87

Effect of temperature on the rate of combustion of explosives at atmospheric pressure

Explosive	Experimental conditions.	Temperature coeff. of combustion rate (γ_u)
Nitroglycol	Liquid	1.52
Gelignite	-	1.82
Tetryl	ρ_0 = 0.9 g/cm^3	1.81
Heksogen	ρ_0 = 0.9 g/cm^3	1.45
Nitroglycerine powder containing 28% nitroglycerine.	ρ_0 = 1.6 g/cm^3	2.9

Similar results were obtained by Belyaev in experiments on the combustion of mercury fulminate. On changing the temperature from 16 to 105°C the rate of combustion of mercury fulminate increased 1.52 times. The data obtained permit one to conclude that the negligible acceleration of combustion with increasing temperature is a phenomenon which is general for high explosives and for detonators.

A study of the combustion of TNT and nitroglyc[illegible] temperatures close to the flash temperatures showed that in these conditions the acceleration of the process does not become large, as can be seen from the data cited in Tables 88 and 89.

TABLE 88

Effect of temperature on the rate of combustion of nitroglycol at atmospheric pressure

Initial temperature, °C	Linear rate of combustion mm/sec
20	0.20
60	0.31
100	0.41
145	0.57
180	0.87
184	0.62

From Table 88 it is seen that when the initial temperature was increased from 20 to 180°, i.e., almost to the flash temperature, the rate of combustion of nitroglycol increases approximately twice.

On the basis of his observations Belyaev concluded that at atmospheric pressure a temperature of 185° is limiting for normal combustion of nitroglycol in parallel layers.

TABLE 89

Effect of initial temperature on the rate of combustion of TNT at atmospheric pressure (internal diameter of the tube at 30 mm.).

Initial temperature, °C	Mass rate of combustion g/cm² .min	Remarks
112	1.42	
135	1.58	
200	1.65	
238	2.00	Combustion with pulsation
260	2.7	ditto
290	9.6	ditto

The combustion of TNT, which is initially even, becomes pulsating at temperatures of about 230 - 250° and is accompanied by spitting of the hot melt. This is one cause of the more rapid rate of growth of combustion under these conditions.

As will be shown below, it follows from the theory of combustion of condensed explosives that one would expect a linear relation between the logarithm of the rate of combustion and the reciprocal of the absolute temperature for condensed explosives (and also for gaseous systems).

The results from Andreev's and Belyaev's experimental data show that this requirement of the theory (in a stationary process) is in fact fulfilled and has a general character.

The Belyaev-Zel'dovich theory of the combustion of condensed explosives.

It is necessary to start from physical premises and the basic laws established in the theory of thermal diffusion of flames in gas to discuss the combustion processes in general and the combustion of condensed explosives in particular. However, it is also necessary to take into account those specific peculiarities which are linked with the mechanism of their combustion.

A number of authors (Letan, Shveikert, Yamaga, Kraw and Grimshaw, and others) have constructed theories of combustion on the premise that the chemical reaction proceeds only in the condensed phase. They started from the erroneous supposition that activation of the molecules and the transfer of energy in the combustion process occurs by bombardment of the surface layer of the explosive by the gaseous reaction products.

In 1938 Belyaev put forward a new theory of combustion for condensed explosives in which the basic role in energy transfer was played by thermal conductivity, and the kinetics of the chemical reaction were

taken into account. It differed from the theories discussed in that it assumed that the combustion of explosives took place in the gas phase, not the condensed phase.

According to Belyaev the energy at the surface of a volatile explosive would be used in evaporating the substance. According to Belyaev's calculation the probability of a molecule of nitroglycol at 200° having sufficient energy to evaporate is 10^{9} times as great as the possibility of it having sufficient energy for activation.

In fact the probabilities of these processes are respectively:

$$e^{-\frac{\lambda}{RT}} \quad \text{and} \quad e^{-\frac{E}{RT}},$$

where λ is the heat of evaporation and E is the energy of activation. For nitroglycol $\lambda = 14500$ cal/mole and $E = 35000$ cal/mole.

Thus the rate of evaporation should considerably exceed the rate of combustion and combustion can occur only in the gaseous phase. The heat set free in combustion would be used in heating the gases and in evaporating a new portion of the condensed phase. An increase in the rate of combustion and, consequently, an increase in the passage of heat to the condensed phase should lead to an automatic increase in the rate of evaporation, and this, by absorbing the energy from the combustion zone, would prevent reaction occurring in the condensed phase. Because of evaporation the surface of the explosive would be constantly changing, but the temperature of the surface of the condensed phase would remain at a constant value equal to the boiling point.

The explosive vapour should not ignite at once; some time should elapse while the gas is heated and the reaction spreads; consequently, combustion of the vapour would occur at some distance from the condensed phase, and between the combustion region and the condensed phase there would be a zone of gas awaiting combustion. Belyaev confirmed the

existence of such a zone (dark, non-luminous) experimentally in the case of nitroglycol. Thus we are led to the general diagram of combustion of explosives shown in Fig. 128.

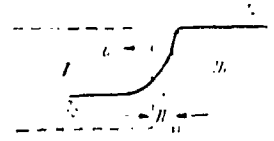


Fig. 128. Temperature distribution in a burning explosive.

Here / is the region of the condensed zone, // is the region of gas awaiting combustion, and /// is the region of hot reaction products. The curve $T_0 - T_k - T_r$ shows the temperature distribution. T_0 is the initial temperature of the explosive, T_k is the temperature at which the vapour pressure of the explosive is equal to the external pressure, i.e. for liquids, the boiling point, and T_r is the temperature of combustion.

It is clear than, when a stationary combustion system is established, the quantity of substance evaporating from 1 cm.^{2} of surface in 1 sec. should be equal to the amount of substance burning in 1 cm.^{2} in 1 sec; in other words, the mass rate of combustion should equal the mass rate of evaporation of the condensed phase.

Zel'dovich showed that the theory of combustion of gaseous mixtures developed by Frank-Kamenetskii and himself could, with some modification, be applied to some cases of interest to us. On going from the combustion of gaseous mixtures to the combustion of explosive vapours it is only necessary to take into account the energy used in evaporating the condensed phase. According to Zel'dovich, the mass rate of diffusion of combustion in explosive vapours is defined by the following expression:

$$\rho u = \sqrt{\frac{2\eta_r}{Q_r}\left(\frac{kT_r^2}{E}\right)^{m+1}(T_r - T_0)^{-m}(m+1)!W(T_r)}\ g/\text{sec}\cdot\text{cm}^2, \quad (53,2)$$

where η_r is the coefficient of thermal conductivity of the vapour at the combustion temperature, T_r is the combustion temperature, T_0 is the initial

temperature, $W(T_r)$ is the rate of reaction at temperature T_r, E is the activation energy, Q_r is the heat of reaction minus the heat of evaporation, and m is the order of the reaction.

In the particular case when the reaction is unimolecular, equation (53,2) can be put in the following form:

$$\rho u = \frac{RT_m^2}{E}\sqrt{\frac{2\tau_{r_0}Ze^{-\frac{E}{RT}}}{Q(T_r - T_0)}},$$

where ρ is the vapour density at temperature T_r.

From equation (53,2) it follows that the relation between the rate of combustion and the pressure is, in this case, of the same form as for gaseous mixtures: $u = kp^m$.

Since, according to the experimental study, the rate of combustion of nitroglycol depends linearly on the pressure, $m = 2$, i.e., the reaction which determines the rate of combustion of this substance is bimolecular.

The direct application of equation (53,2) to the calculation of rates of combustion is very difficult because the values of m, E and T_r are unknown for most explosives. However, if equation gives the correct connection between the basic kinetic constants and the rate of combustion, then the reverse problem can be solved - from the rate of combustion and its dependence on pressure the kinetic constants can be calculated. Belyaev carried out this type of calculation for nitroglycol; the calculated activation energy $E \approx 31{,}000$ cal/mole obtained by Apin from experiments on the thermal decomposition of nitroglycol. According to Belyaev, this confirms the correctness of his theory.

According to Belyaev combustion in the gas phase is only possible if the pressure does not exceed a certain critical value. As the pressure increases so does the boiling point, and consequently the temperature of the surface layer of the condensed phase. As a result, the "tail" of the

curve $T_k - T_0$ will reach further inside the substance. This increase in temperature may be very considerable. For nitroglycol t_k is 190°C at atmospheric pressure and 400°C at 100 atmospheres. At the same time the relation between the rate of evaporation and the rate of combustion changes considerably. At a sufficiently high pressure the heat liberated in the reaction would be only partly used in evaporation and combustion would occur in the condensed phase. However, in Belyaev's opinion such a combustion regime would not be stable and should change over to detonation almost instantaneously because of the direct bombardment of the unreacted molecules of the condensed phase by the gaseous products of explosive decomposition. It will be recalled that in the normal process of diffusion of combustion it is thought that the transfer of energy from the reaction zone to the starting material is by thermal conductivity.

Belyaev considered that the combustion mechanism described above was characteristic for most condensed explosives. If the boiling point is lower than the temperature at which intensive reaction occurs, and the heat of vaporisation is considerably less than the energy of activation, then combustion will occur in the gas phase. If the boiling point is considerably higher than the temperature at which intense decomposition begins, and the heat of vaporisation is close to the energy of activation, then decomposition will occur in the condensed phase. However, as a result of the initial reaction only vaporisation of the original substance and formation of hot products occurs. The further reaction of these products in the gas phase totally determines the rate of combustion.

The boiling points and the heat of vaporisation of some explosives are given in Table 90 (after Belyaev).

TABLE 90

Boiling points and heats of vaporisation of explosives

Explosive	Boiling point °C.	Heat of vaporisation cal/mole.
Methyl nitrate	66	9000
Nitroglycol	200	14 200
Nitroglycerine	250	18 500
TNT	335	17 000
Picric acid	320	21 000
TEN	270	23 000
Hekogen	340	26 000
Tetril	310	26 000
Trinitrobenzene	315	18 500
Trinitroxylene	305	18 000

The Belyaev-Zel'dovich theory is based on correct physical ideas. However, the theory schematizes excessively the process of combustion in condensed explosives and describes only the simplest case. This is characterised by the fact that the basic reaction (which determines the rate of reaction) occurs in the gas phase, and the mechanism and thermal effects of the reaction do not change with changing pressure.

Results of experimental studies have shown that, in most cases, the combustion of high explosives is much more complex and is accompanied by reactions in the condensed phase which contribute a considerable proportion of the heat of reaction. Moreover both the course of the reaction and the final reaction products do not remain constant in combustion conditions, and they change considerably with the pressure. At atmospheric pressure the decomposition of explosives is not complete and the nitrogen of the

explosive separates as nitric oxide, whereas at higher pressures (of the order of tens of atmospheres) no nitric oxide is observed.

54. COMBUSTION OF POWDERS

Normal combustion of high explosives and detonators is possible only under well-defined conditions, whereas for projectile explosives (powders) this type of explosive conversion is typical. The characteristic stable combustion of powders results from their ability to burn in parallel concentric layers even at high temperatures - 5000 - 6000 Kg/cm^2 in extreme cases.

The following three phases are normally distinguished in the combustion of explosives:

(1) ignition or localised origin of a self-diffusing reaction;

(2) inflammation or spread of the original process in the surface of the substance;

(3) proper combustion or diffusion of the reaction in the bulk of the substance.

Such a division of the process into three phases is in general conditional because they do not differ from one another in principle. However, it must be remembered that these processes occur at different rates in the conditions for the practical use of powders.

Ignition is the initial decomposition of the powder. This usually occurs as a result of local heating. It is the first stage of ignition.

The rate of inflammation of a powder depends on the nature of the powder, the state of its surface, and especially strongly on the pressure. The smokiness of a powder depends in the first place on its ability to burn.

The rate of ignition under otherwise equal conditions increases with increasing specific surface of the powder. According to this principle a powder with a rough porous surface as a rule ignites more easily than

a powder with a smooth surface.

The rate of ignition increases considerably with increasing pressure. This is because the increased pressure hinders the removal of the hot gaseous combustion products from the surface of the powder. Analogous data was also obtained for gelatinous nitroglycerine. According to the data of Levkovich and Arsh the rate of combustion of nitrocellulose powders in the open air fluctuates within the limits 20-40 cm/sec. When large quantities of powder are burned the rate of spread of the flame over the surface may reach several metres per second. When powders are burned in air the rate of spread over the surface is considerably greater than the rate of combustion. If a vertically suspended powder charge is ignited at its upper end, then in a certain time the surface of combustion of the charge will take the shape of a right-angled cone (Fig.129) because of the difference between the rates of ignition and combustion. The ratio between these rates can be defined in terms of the vertical angle of the cone

$$\sin\frac{\alpha}{2}=\frac{u_1}{u_2}, \qquad (54,1)$$

where u_1 is the rate of combustion and u_2 is the rate of ignition.

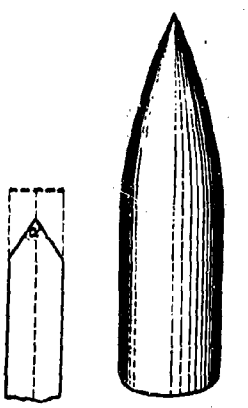


Fig.129. Combustion of a powder charge in air.

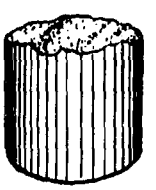


Fig.130. Combustion of a powder charge in an atmosphere of an inert gas.

When a charge is burned in an inert atmosphere these two rates are equal and consequently a crater is formed instead of a cone (Fig. 130). Hence it is clear that the great rate of combustion in open air is connected with the combustion of reaction products due to oxygen in the air.

Combustion of a powder proceeds at a definite rate normal to the surface. Equilibrium spread of the process is achieved thanks to the high density and uniform physical structure of the powder elements.

Other things being equal, the rate of combustion depends on the calorificity of the powder, the initial temperature of the powder elements, and the external pressure.

The rate of combustion increases with increasing calorificity. Consequently, for example, the rate of combustion of pyroxylin powder increases with increasing nitrogen content.

According to Murauer's investigations, at sufficiently high pressures the rate of combustion of nitrocellulose powders changes in an exponential manner with changes in the temperature. This is because there is a linear relationship between the logarithm of the linear rate of combustion and the temperature.

$$\lg u = A + BT. \qquad (54,2)$$

As the density of a powder decreases so its rate of combustion also falls. According to Weil's data, the time for complete combustion of standard cylindrical charges of smoke powder varies with increasing density of the charge as follows (Table 91).

TABLE 91

Charge density, g/cm^3	1.670	1.83	1.900	1.920	1.946
Time for combustion, sec.	0.00274	0.00392	0.01073	0.03802	0.05269

It follows from these data that a 17% increase in charge density led to the rate of combustion being lowered by a factor of more than 19.

This relationship is explained as follows: when the density is increased, the porosity of the powder is decreased, and thus the passage of hot reaction products into the body of the substance is hindred.

The rate of combustion increases with increasing initial temperature of the powder, but the effect of this factor in the case given is not large. According to Andreev's data, the ratio between the rates of combustion at 100° and 0° for a 28% nitroglycerine powder was 2.9.

The effect of pressure. The relation between the rate of combustion of powders and the pressure p has been the subject of many investigations.

According to Weil, the relation $u = f(p)$, is satisfied by the equation

$$u = Ap^{\nu}, \qquad (54,3)$$

where A and ν depend on the nature of the powder.

For smoky powders Weil put ν equal to 0.5. According to Zabudskom, $\nu = 0.93$ for pyroxylin powders.

Baum and Levkovich showed that ν was not constant for a particular powder. It changed considerably with the pressure. Thus for ignition of pipe powder in a manometric bomb, $\nu = 0.117$, whereas at atmospheric pressure $\nu = 0.505$.

Shapiro, from a treatment of other authors' data, considered that ν for smoky powder changes with increasing pressure as shown in the table.

Many authors believe that a simpler relation can be used for the rate of combustion of nitrocellulose powders:

$$u = Ap. \qquad (54,4)$$

This is a special case of (54,3) with $\nu = 1$.

$\frac{p}{p_0}$	ν
0.4	1.00
1.0	0.63
2.0	0.49
3.0	0.40
500	0.33

Gorst-Zlotowski experiments established that the relation (54,4) was satisfactorily observed only at high pressures (about 1000 atmos and above). For lower pressures (from 5 to 250 atmos) Shapiro found $\nu = 0.7$. Thus it can be seen that ν is not constant for nitrocellulose powders either.

The coefficient A in formula (54,4) is the rate of combustion at a pressure of 1 Kg/cm^2. The rate of combustion of a nitrocellulose powder at this pressure calculated from (54,4) was 0.07 mm/sec, whereas the actually observed rate was approximately eight times as large. Some authors believe that this difference arises because at the surface of the burning powder itself there is an increased pressure of about 8 atmos. However, Andreev and Varg by direct experiment showed that the excess pressure at the powder surface did not exceed 5 mm Hg.

This result also shows that equation (54,4) is not acceptable at relatively low pressures.

According to a number of workers (Graver, Wolff, Murauer) the relation between the rate of combustion and the pressure can be completely expressed by the two-termed formula:

$$u = a + bp, \qquad (54,5)$$

which was first used by S.P. Vukolov (1891).

However, more careful experiments showed that formula (54,5) gives sufficiently satisfactory results only at pressures lower than 400 Kg/cm^2.

According to Andreev the rate of combustion of nitrocellulose powders over a sufficiently wide range of pressures can be described by the general formula:

$$u = a + bp^{\nu}, \qquad (54,6)$$

where ν takes different values for different powders but is generally close to unity.

In conclusion it must be noted that not one of the formulae mentioned is able to describe the function $u(p)$ over a wide pressure interval because the mechanism of combustion and the thermal effects of reaction at high pressure are considerably different from those at pressures close to atmospheric. Thus experiments showed that the

thermal effect of burning a nitrocellulose powder at pressures below 40 Kg/cm^2 was only about 53% o heat of combustion of the powder at p 70 Kg/cm^2.

The sensitivity of different powders to pressure is not uniform. Thus smoky powders burn about ten time as fast as pyroxylin gunpowders at atmospheric pressure, whereas the reverse is observed at high pressures (2500 Kg/cm^2): the rate of combustion of pyroxylin powders is considerably greater than that of smoky powders.

By studying the combustion of various powders at pressures close to atmospheric, Baum established that as a rule the sensitivity of powders to pressure increased with increasing quantity of gaseous reaction products. In the absence of gaseous reaction products the rate of combustion is independent of the external pressure.

Mechanism of combustion of nitrocellulose powders. The mechanism of combustion of nitrocellulose powders remained almost unstudied until recently. This was a serious obstacle to the development of a complete theory of their combustion. Zel'dovich attempted to construct such a theory based on Belyaev's general ideas on the mechanism of combustion of condensed explosives, which have been discussed above.

The basic characteristic of this theory is the assumption that combustion of the powder is preceded by its vaporisation.

Combustion thus proceeds in the gas phase. If this is so it appears that the basic principles of the theory of combustion of gaseous mixtures can be applied to the combustion of powders. The chief difference between the combustion of powders and condensed explosives is that evaporation of the condensed phase is changed into gasification, which, according to Zel'dovich, is either weakly endothermic or weakly exothermic.

According to Zel'dovich the basic scheme for the combustion of nitrocellulose powders takes the following form. When heat is applied to the condensed phase the temperature in the surface phase (powder, gas) is raised to some temperature T_1 at which gasification of the heated layer of powder begins. The gaseous products are heated to the temperature at which chemical reaction begins by heat flow from the combustion zone. This leads to the final products of powder combustion. T_1 is practically independent of the initial temperature and pressure. T_1 has a tendency to rise as the rate of combustion increases but, because the rate of decomposition is exponentially related to the temperature, the expenditure of heat on gasification is increased and T_1 remains constant.

The greater the rate of combustion the thinner the heated layer of powder, but because T_0, T_1, T_2 remain constant, the temperature distribution curve increases in steepness. At low rates of combustion the curve will be gentle because a thicker layer of substance is heated with a longer time interval. With increase in pressure the rate of combustion increases but the thickness of the heated layer should decrease. This theoretical result was confirmed experimentally by Aristova and Leipunskii.

The basic principal conclusions of the Zel'dovich theory qualitatively reflect the regularities observed during the combustion of a powder, but the theory does not give quantitative agreement with experimental results. This is explained by the admitted simplifications of the complex mechanism of powder combustion.

Levkovich and Arsh showed from the analysis of experimental results that combustion of a powder is a considerably more complex process than allowed for in the Zel'dovich scheme. According to these authors combustion of a powder occurs in the condensed phase as well as in the gas phase. About 50% of the heat evolution occurs from reaction in the condensed phase, and it

follows that it must play an important part in the process of powder combustion. The intermediate oxidation-reduction processes, in which oxides of nitrogen take part (No, No_2) is very important in the combustion of the powder. The rates of oxidation-reduction processes depend markedly on the pressure. This explains the observation that combustion of nitrocellulose powders at low pressures is generally accompanied by considerable formation of nitric oxide.

Subsequent investigations supported some of the ideas of Levkovich and Arsh and led to further considerable definition of the mechanism of combustion of powders.

Rice and Genelle developed a quantitative theory for the combustion of nitrocellulose powders. They considered that the process took place in three stages: an exothermic reaction in the condensed phase, an intermediate reaction in the gas phase leading to the formation of nitric oxide, and reactions between nitric oxide and the products of incomplete combustion. The basic correlations in the theory of Rice and Genelle were obtained using the same assumptions and the same methods as were first used by Frank-Kamenetskii and Zel'dovich.

The special points of the Rice-Genelle theory are as follows. At very low pressures reaction in the condensed phase plays the decisive part in the dissemination of combustion. The rate of the reaction in the condensed phase is dependent on the temperature, but independant of the pressure. At higher pressures (up to a few atmospheres) the predominant place in the combustion process is gained by a bimolecular reaction which occurs in a second phase, for example the reaction between nitric oxide and carbon monoxide. The peculiarity of these reactions is that they have small activation energies and consequently their rates have little dependence on temperature, but depend strongly on pressure. The reactions of the

third phase (inflammation) occur only at pressures of 20 atmos. and above. The heat evolved in this zone is transferred into the adjoining intermediate reaction zone by thermal conductivity, and from the latter into the condensed phase. This leads to increased heating of its surface layers and to a corresponding increase in the rate of combustion. At high pressures the reactions in the third zone have a decisive influence on the rate of combustion.

The results of the Zel'dovich theory make it possible to define the basic parameters which characterise the ability of an explosive to ignite (the inflammability of an explosive).

If the surface of a powder (an explosive charge) is subjected to a heat source of a sufficiently high temperature, then the critical temperature at the surface of the explosive (the temperature at which ignition becomes possible) will not be reached immediately, but after some time τ_n. The time τ_n depends on the ratio between the rate of input of energy from heat transport and the rate of heat loss from the surface into the bulk of the material. When the critical temperature (T_{cr}) is reached on the surface of the explosive, the temperature distribution in the adjoining layers is set up according to the Michelson law, and this determines the thickness of the heated layer. The amount of heat in the heated layer at the moment of ignition (i.e. at the moment when T_{cr} is reached at the surface) can be determined from the equation

$$Q = \int_0^{x_0} c_p \rho (T - T_0)\, dx = \frac{\eta}{u} (T_k - T_0).$$

From this relation it follows that the so-called flash temperature (determined under defined standard conditions) cannot serve as a criterion of the inflammability of an explosive. This question is discussed in somewhat greater detail in Chapter XV.

55. THE TRANSITION FROM COMBUSTION TO DETONATION

The mechanism of the transition from combustion to detonation in gaseous mixtures. The conditions for transition from combustion to detonation are most simply established by a discussion of non-stationary processes of flame propagation in gaseous mixtures.

The equilibrium propagation of a flame at a constant rate occurs only when a gaseous mixture is ignited at the open end of a tube. On combustion in a closed tube the flame is propagated at a constantly increasing rate. The reason for this autoaccelerating process is the progressive compression of the gaseous mixture in front of the flame front. This was confirmed experimentally by Kirkby and Viler.

Thanks to the continuous increase in pressure (and, consequently, the increase in density and temperature) the reaction goes faster in each successive layer of gas and is finished in shorter time intervals. The increased pressure in front of the flame front is a consequence of the origin of a compression wave in the gas. The compression wave is formed as a result of expansion of the combustion products. The flame drives the gas before it like a piston. Each successive compression wave is propagated in a denser medium and catches up with its predecessor. As a result of the superposition of these elementary waves a sufficiently sharp pressure transition, characteristic of a shock wave, is progressively formed. The mechanism of formation of a shock wave from these elementary compression impulses was shown schematically in Fig. 35.

The curves *OD* describe the movement of a flame in time in the coordinates t, x. This curve starts from separate points (elementary compression

waves) the rate of propagation of which equals $u + c$ and the greater this is, the greater the velocity of the flame. This leads to the intersection of these characteristic curves and the formation of a sufficiently intense shock wave (see § 23).

The intensity of the shock wave increases with the propagation of the flame, and the rate of movement of the gas increases with it. Thus the rate of propagation of a flame in a relatively motionless mixture will be

$$u = u_1 + u_2, \qquad (55,1)$$

where u_1 is the velocity of the flame in a relatively moving gas and u_2 the velocity of the gas compressed by the shock wave.

The origin of compression waves in the initial gaseous mixture has been demonstrated by instantaneous photographs, taken by Tepler's method. One such photograph, taken while heating a mixture of $CH_4 + 2O$, is shown in Fig. 131. Here the sharp lines of the compression waves preceding the flame front are clearly seen.

An even more convincing demonstration of the formation of shock waves during the combustion of gaseous mixtures is the autoignition of the gas at a more or less considerable distance in front of the flame front.



Fig.131. Origin of compression waves in a burning gaseous mixture ($CH_4 + 2O_2$)

Thus the mechanism of transition of combustion into detonation comes to the following.

Combustion causes movement of the gas and the formation of shock waves of compression preceding the flame front. Consequently, propagation of the flame occurs in a compressed and moving gas. As the acceleration of the flame increases so does the amplitude of the shock wave, which causes acceleration of the flame, and so on. Detonation occurs when the intensity of the shock wave reaches some critical value, at which ignition of the gas and constancy of the regime at the wave front are assured as a result of the energy of reaction.

Under normal combustion conditions the velocity of a flame in a relatively motionless gas does not exceed 10 metre/sec. even in a very rapidly burning mixture. However, the transition from combustion to detonation is accompanied by acceleration of the flame. The rate of combustion passes through an intermediate value of the order of hundreds of metres per second. The movement of the flame at a velocity considerably greater than that for propagation by thermal conduction and considerably less than that for propagation by a detonation mechanism is easily explained from the condition of the processes proceeding in the moving gas.

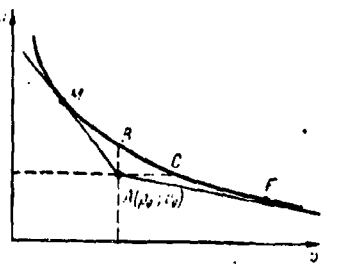


Fig.132. Hugoni's curve

This velocity intermediate between detonation and slow combustion corresponds to the region *BC* on Hugoni's curve. This region does not correspond to any material result (Fig. 132).

The point *M* corresponds to a process of stationary detonation. The point *F* corresponds to a process of slow stationary combustion, if the flame is propagated through a gas with the parameters of state p_0, v_0.

If one starts from the ideas on non-stationary flame propagation expressed above, then it is possible within the limits of hydrodynamic theory to construct a regime with any flame velocity; in particular with a velocity between slow combustion and detonation. Zel'dovich was the first to carry out a theoretical study of non-stationary combustion processes. We shall discuss the process of flame propagation in a long tube of constant cross-section with ignition of the gas at the closed end. In agreement with the mechanism of combustion established above we obtain the distribution of pressure in the gas, shown in Fig. 133 some intermediate time after ignition.

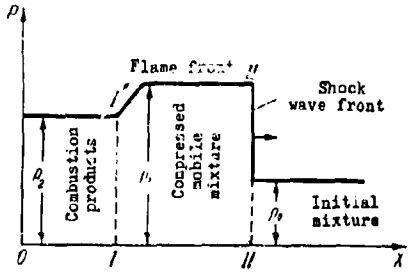


Fig. 133. Distribution of pressure in a burning gas

The volume limited by the sections $0-I$ is occupied by the reaction products, and the Volume $I-II$ by the compressed moving gas; the volume to the right of II contains the undisturbed mixture. With the passage of time the pressure, velocity, and other parameters of the zone $I-II$ increase, and they in their turn cause acceleration of the flame. However, as the velocity of the flame increases the difference between its velocity and that of the shock wave decreases and eventually they coincide at a velocity equal to the velocity of detonation. Let the parameters of state of the initial undisturbed mixture be p_0, v_0, $u_0 = 0$; the parameter of the shock wave being propagated in unreacted gas p_1, v_1, D_1 and u_1; and those of the products of combustion: p_2, v_2, D_2 and u_2 (Fig.134).

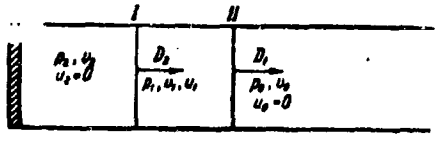


Fig.134. Distribution of parameters in a burning gas.

Let us write down for this case the corresponding relations which arise from

the laws of conservation. For the decomposition surface II we obtain the known relationships:

$$\left.\begin{aligned} p_1 - p_0 &= \frac{2}{k+1}\rho_0 D_1^2\left(1-\frac{c_0^2}{D_1^2}\right), \\ u_1 &= \frac{2}{k+1}D_1\left(1-\frac{c_0^2}{D_1^2}\right), \\ v_0 - v_1 &= \frac{2v_0}{k+1}\left(1-\frac{c_0^2}{D_1^2}\right), \end{aligned}\right\} \qquad (55,2)$$

where c_0 is the velocity of sound in the initial gas.

For the combustion zone (separation surfaces *I—II*) in which the heat of reaction Q is liberated, the corresponding equation take the form

$$p_2 - p_1 = \frac{\rho_1 (D_2-u_1)^2}{k+1}\left(1-\frac{c_1^2}{(D_2-u_1)^2}\right)(1+\eta), \qquad (55,3)$$

$$u_2 - u_1 = \frac{D_2-u_1}{k+1}\left(1-\frac{c_1^2}{D_2-u_1}\right)(1+\eta), \qquad (55,4)$$

$$v_1 - v_2 = \frac{v_1}{k+1}\left(1-\frac{c_1^2}{(D_2-u_1)^2}\right)(1+\eta), \qquad (55,5)$$

where

$$\eta = \sqrt{1-\frac{2(k^2-1)Q}{(D_2-u_1)^2\left[1-\frac{c_1^2}{(D_2-u_1)^2}\right]}}. \qquad (55,6)$$

The equations cited satisfy the boundary conditions. In the case when $Q=0$ and $\eta=1$ the equation has the general form for a shock wave. In the detonation case we have

$$D_2 - u_1 = \sqrt{2(k^2-1)Q + c_0^2}$$

and $\eta = 0$, i.e. we obtain the known relation for a process which is being propagated in a moving gas. This arises from the hydrodynamic theory of detonation.

If ignition of the gas started at the closed end of the tube, then

$$u_2 = 0. \qquad (55,7)$$

Thus in the cases of interest to us we have six equations with seven unknowns: p_1, v_1, u_1, D_1, p_2, v_2, and D_2. By fixing one of these parameters (for example the velocity of the flame which can be easily determined experimentally) the values of all the remaining parameters in the combustion zone can be calculated. The conditions of non-stationary combustion and

its transition to detonation can be more clearly established by graphical interpretation of the equations obtained (Fig. 135).

Curve *I* is the adiabatic Hugoni for the shock wave; curve *II*, the Hugoni for the final products of reaction. The transition from curve *I* to curve *II* corresponds to the evolution of the heat of reaction.

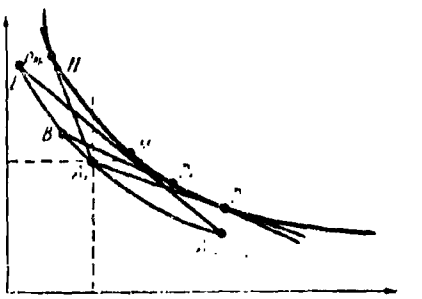


Fig.135. The transition from non-stationary combustion into detonation.

Let the gas in front of the flame front be compressed to a state corresponding to the point *B* as a result of the combustion process. At this state of the starting material the flame front acquires a point velocity corresponding to the state of the reaction products at D_1 on the adiabatic curve *II*. D_1 lies above the point *D*

If the pressure of the compressed mixture in front of the flame front remained at this level, then the point *D* would correspond to stationary propagation of the combustion process in the conditions given.

On further propagation of the process, the amplitude of the shock wave increases and this corresponds to a movement of the point *B* up the adiabatic curve *I*. It is plain that the point *D* will also move along the ascending branch of curve *II* until it coincided with the point M_1 and consequently the rate of combustion will increase accordingly.

Finally, when the pressure at the front of the shock wave reaches a critical value $p_{кр}$ at which its velocity becomes equal to the velocity of detonation, then autoignition of the compressed gas occurs and the state of the reaction products is represented by the point *M*. Only in this way does the propagation of the shock wave and of the reaction zone following it become stationary. During this predetonation period flame propagation in the relatively compressed moving gas is determined by the laws of heat transfer. With respect to the undisturbed and non-moving gas mixture

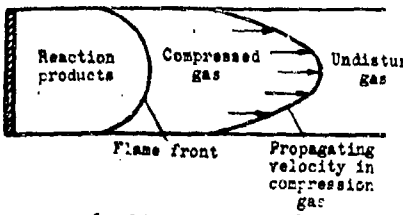


Fig.136. Distortion of the flame front.

propagation of the flame will possess combined "shock-heat" mechanism of energy transfer.

According to K.I. Shchelkin the layer of compressed gas lying along the side is decellerated and its movement in the centre of the tube is correspondingly accelerated; in this way turbulence of the gas arises. The distribution of velocities across the tube is not in equilibrium and this leads to a reorganisation of the profile of the flame front (Fig. 136) and an increase in the combustion process. The quantity of substance consumed in unit time is increased uniformly. The increased rate of combustion in its turn leads to an increase in the velocity of the moving gas and so on.

The condition for transition from combustion to detonation as a result of autoacceleration of the flame can be settled by photographing the process by a shadow (schleren) method on a moving film. One such photograph is shown in Fig. 137. The transition to detonation occurred at point *C* in front of the flame front. At this moment the flame front was at point *D*.

The mechanism of the transition from combustion to detonation for condensed explosives does not differ in principle from the mechanism for gaseous mixtures. However, this transition occurs under considerably different conditions. The origin of a shock wave and the movement of the substance in front of the flame front are practically excluded in the combustion of a condensed explosive; the formation of a shock wave occurs behind the flame front in the burning gaseous reaction products. A characteristic of the combustion of condensed explosives is the sharp increase in volume in the flame zone which results from the transformation of the explosive into gaseous products.

If these gases do not escape fast enough the pressure in the reaction zone will increase continuously, and the rate of combustion will increase.

When the rate of combustion reaches a critical value, stable combustion becomes impossible and the transformation to detonation occurs.

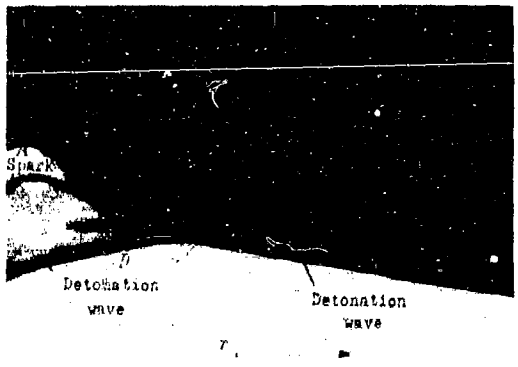


Fig. 137. Transformation of combustion of a gaseous mixture into detonation.

Disturbance of stationary combustion can also occur as a result of distortion of the flame front which results in an increase of the combustion surface.

Belyaev formulated the conditions for stable combustion of condensed explosives in a general form. According to Belyaev combustion can only be stable when the gas production (from the reaction) and the gas loss are in equilibrium. If the rate of gas production is greater than the rate of gas loss, then the process will accelerate. The disturbance of the gas balance is the most important cause of the transition from combustion into detonation. The critical rate of stable combustion can be determined from the equilibrium condition for the rates of gas formation and gas loss:

$$u_1 = u_2,$$

where u_1 is the rate of gas production which is equal to the rate of combustion in g/cm^2 sec., and u_2 is the rate of gas loss.

According to Belyaev's approximate calculation the critical rate of combustion at atmospheric pressure for normal explosives is of the order of 7 - 8 g/cm^2 sec. If $u_1 > 7-8$ g/cm^2 sec, the combustion will be non-stationary no matter what the initial pressure, and combustion will accelerate.

For most explosives the normal rate of combustion is considerably lower than the calculated critical rate. Nevertheless, disturbance of stationary combustion of those explosives is possible in certain conditions, in the first place when the flame front is distorted.

The work of Andreev has developed further the ideas outlined above. Andreev discussed in detail the relation between gas production and gas loss with various laws of combustion.

In Fig. 138 the lines describing gas loss as a function of pressure are designated u_2; the curves of gas formation are marked u_1.

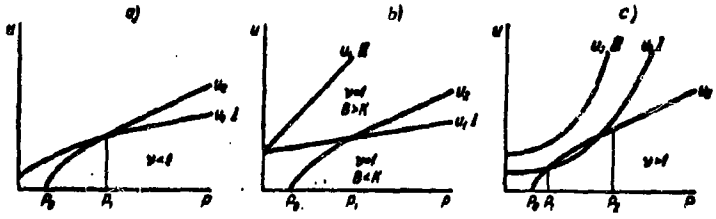


Fig. 138. Relation between gas production, gas loss, and pressure with various laws of combustion.

When $p = p_0$, i.e. when the pressure at the flame front is equal to the external pressure, the gas loss is zero. With increase in the pressure p, the gas loss increases as shown on the curve, and then, beginning at a pressure about twice as large as the external pressure, the gas loss increases in proportion with the pressure i.e.

$$u_2 = Kp_1,$$

where the coefficient of proportionality

$$K = \sigma\left(\frac{2}{k+1}\right)^{\frac{1}{k-1}} \sqrt{\frac{k}{k+1}} \sqrt{\frac{2T_0M}{22410\,p_0T_1}} = \sigma\sqrt{\frac{2\cdot 273M}{1{,}013\cdot 10^6\cdot 22410\,T_1}},$$

u_2 is the rate of gas loss, g/cm^2 sec.; k is the index of polytropy; σ is the cross-sectional opening for gas loss, cm^2; M is the molecular weight of the gases; and T_1 is the temperature of the gases.

For diatomic gases

$$\nu = \left(\frac{2}{k+1}\right)^{\frac{1}{k-1}} \sqrt{\frac{k}{k+1}} = 0.485$$

The form of the gas formation curve is determined by the character of the relation between the rate of combustion and the pressure. Let us assume that

$$u_1 = A + Bp^{\nu},$$

We shall discuss three cases: $\nu < 1$, $\nu = 1$ and $\nu > 1$.

Stationary combustion is possible and stable if the gas formation and gas loss curves intersect and the tangent of the angle of inclination touches the gas formation curve less than the tangent of the angle of inclination of gas loss line at the point of intersection.

We shall first discuss graph a (Fig. 138) where these conditions are fulfilled ($\nu < 1$). Let combustion start at pressure p_0 at this pressure gas loss is zero. The pressure at the flame front will rise until a pressure p_1 is reached, at which the gas loss and the gas formation are equal. From the graph it is seen that, with $\nu < 1$, the intersection of the gas formation and gas loss curves always permits stable combustion.

With $\nu > 1$ (graph c) for curve *II* stable combustion is generally impossible; it is easily shown that combustion is stable for curve *I*, if the pressure is less than p_2 and unstable at greater pressures.

If $\nu = 1$ (graph b), two cases are possible. If coefficient B is less than K (the tangent of the angle of inclination of the gas loss curve), then stable combustion is possible (line *I*). If B is greater than K (line *II*) then gas formation is greater than gas loss at any value of p, the pressure at the front will increase continuously and the process will finish as a detonation. Hence for the combustion law

$$u_1 = A + Bp$$

it is not the rate but the parameter $B = \frac{du}{dp}$, which is critical, i.e. the

derivative of the rate with respect to the pressure. Thus, with the usual linear dependence of the rate of combustion on the pressure, the condition for stable combustion is equivalent to the requirement that the acceleration of combustion $\left(\frac{du}{dp}\right)_{\omega p}$ should not exceed the value K. With $M = 28$ (CO; N_2), $T = 2730^{\circ}K$, $\psi = 0.485$ and $\varkappa = 1$, we get $K = 7.5 \frac{g/cm^2 \text{ sec.}}{Kg/cm^2}$.

Andreev's investigations showed that the acceleration of combustion in all the high explosives he studied was less than critical value even at temperatures close to the flash point, and hence their combustion was necessarily stable.

In fact this is only possible in those cases in which other additional possibilities of accelerating combustion are absent, e.g. in particular if the explosive retains the ability to burn in parallel layers at higher pressures as, for example, in characteristic of nitrocellulose powders.

In the case of pyroxylin and other porous substances, combustion can penetrate through the pores into the bulk of the substance under known conditions; the combustion surface increases rapidly and the gas formation is above the limit at which combustion is stable.

Landau showed that in the combustion of liquid explosives disturbance of the stability of combustion was produced by perturbation of the flame front by turbulence of the liquid. The flame front remained stable only if the mass rate of combustion did not exceed some limit defined by the equation

$$u_m = [4a_\kappa g \rho^2 \delta_\kappa]^{\frac{1}{4}}, \qquad (55,8)$$

where a_κ is the surface tension of the liquid at its boiling point, ρ is the density of the gaseous combustion products, δ_κ is the density of the liquid, and g is the accelerating force of gravity.

Since most organic explosives are liquid at their autoignition temperatures one can apply Landau's criterion to them.

Andreev noted that the parameters on the right hand side of equation (55,8) changed very little for different explosives. Consequently u_m is an approximately constant parameter at a given pressure, being approximately equal to 0.25 g/cm^2 sec at atmospheric pressure.

In Table 92 are cited approximate values for the rate of combustion of some explosives at the spark temperature. They were obtained by Andreev by extrapolation from results obtained at much lower temperatures.

TABLE 92

Rate of combustion of explosives at the spark temperature

Explosive	Rate of explosion at spark temp., g/cm^2 sec	Character of spark
Nitroglycerine	~ 0.5	Sharp sound, sample broke into small pieces.
Nitromannitol	0.7	
Nitroglycol	0.096	Weak sound, sample remained unbroken.
TEN	0.120	
Heksogen	0.084	
TNT	0.040	

It is seen from the table that, apart from the first two explosives, even at the spark temperature the rate of combustion is considerably less than the limiting value. These data agree with the character of the spark of the corresponding explosive and with the fact that disturbance of stable combustion at the usual beginning temperatures is observed at pressures considerably higher than atmospheric.

From this account the following conclusions can be drawn:

1. The basic principle for the transition from combustion to detonation is disturbance of the gas balance. This occurs if the rate or acceleration of combustion exceeds some critical value.

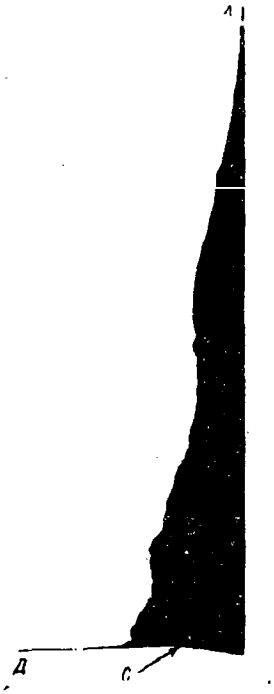


Fig.139. Transition from combustion to detonation with mercury fulminate.
A. Ignition point.
CD.. Detonation.

2. For most explosives which are capable of combustion the parameters u and $\frac{du}{dp}$ are considerably less than the critical values.

3. Disturbance of stable combustion of explosives in actual conditions is most frequently connected with curvature of the flame front and considerable increase in the combustion surface as a result of either combustion inside the substance (porous explosives) or perturbation of the flame front (liquid explosives).

High pressures facilitate the occurrence of these phenomena.

4. Growth of pressure at the flame front with a compensating gas loss is the cause of the formation of a shock wave (which increases in amplitude during combustion) in the reaction zone. Subsequent transition to detonation is similar to that in gaseous mixtures but it occurs at much higher critical pressures at the front of the shock wave.

5. These processes are accelerated by enclosing the explosive charge in a casing.

A photograph of the transition from combustion to detonation in mercury fulminate is shown in Fig. 139. Normal detonation starts at point C where the flame front coincides with the front of the pressure wave. In Fig. 140 a graphical interpretation of this photograph is given in terms of the coordinates D and l.

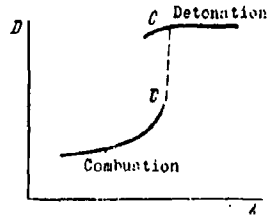


Fig.140. Diagram of transition from combustion to detonation in mercury fulminate.

It is seen from Fig. 140 that the origin of a detonation type of decomposition is connected with a sharply increased (discontinuous) rate of propagation of the process.

Bibliography

1. L. N. Khitrin. Physics of Combustion and Explosion, Moscow University Press, 1957.

2. Ya. M. Paushdin. Chemical Constitution and Properties of Reactive Fuels. U.S.S.R. Academy of Sciences Press, 1958.

3. K.K. Andreev. Thermal Decomposition and Combustion of Explosives. Gosenergoizdat, 1957.

4. N.N. Semenov. Chain Reactions. Goskhimtekhizdat, 1934.

5. A.F. Belyaev. Mechanism of Combustion of Explosives. Doctoral thesis. Moscow, 1946.

6. Ya.B. Zel'dovich. Theory of the Combustion and Detonation of Gases. U.S.S.R. Academy of Sciences Press, 1944.

7. M. Patri. Combustion and Detonation of Explosives, Oborongiz, 1938.

8. D.A. Frank-Kamenetskii. Diffusion and Heat Transfer in Chemical Kinetics. U.S.S.R. Academy of Sciences Press, 1947.

9. V. Iost. Combustion and Explosion in Gases. Foreign Lit. Publishing House, 1953.

10. B. Lewis and G. Albe. Combustion, Flames, and Explosion in Gases. Foreign Lit. Publishing House, 1948.

11. L.A. Vulis. The Thermal Regime of Combustion. Gosenergoizdat, 1954.

12. A.F. Belyaev and A.I.Korotkov. Physics of Explosions. Collected Vol.1 of the Scientific Studies in Explosion Physics. U.S.S.R. Academy of Sciences Press, 1952.
A.F. Belyaev and L.D. Komkova. The Combustion of nitroglycerin, nitroglycol, and methyl nitrate at high pressures; P.F. Pokhil, Mechanism of the combustion of smokeless powders; Z.I. Aristova and O.I. Leipunskii, The heating of powders before ignition. Physics of Explosions. Collected Vol. II of the Scientific Studies in Explosion Physics. U.S.S.R. Academy of Sciences Press, 1952.

13. Liquid and Solid Rocket Fuels. Collected Translations. Foreign Lit. Publishing House, 1959.

CHAPTER XI

BRISANCE OF EXPLOSIVES

§ 56. Methods of Estimating Brisance Theoretically.

Brisance - this is the ability of explosives to effect local destructive action, which is the result of the sudden shock of the detonation products through the material surrounding the explosive.

The brisance effect of explosives only appears at close distances from the site of the explosion, where the pressure and energy density of the explosion products is still sufficiently great. On moving away from the site of the explosion the mechanical effects are sharply reduced as a consequence of the steep drop in pressure, velocity and other parameters of the explosion products. Actually, it follows from theory that in the case of spherical symmetry the pressure in the explosion products is reduced inversely proportionally to R^9, where R is the distance from the explosion source. This follows from the fact that the highly compressed detonation products expand according to the law $pv^k = \text{const}$, where $k = 3$, and $v \sim R^3$.

The maximum brisance effect is manifested as a result of direct contact of the explosive with an obstacle disposed perpendicularly to the direction of propagation of the detonation wave.

The fragmentation effect of ammunition, the armour piercing effect of the detonation products and other forms of local destruction, for example, are explained by the phenomenon of the brisance effect of explosives.

Brisance, together with work capability, is one of the most important characteristics of an explosive, on which is based their relative evaluation and their choice for one or other tasks (fragmentation, blasting media, etc).

The brisance properties of explosives are not determined completely and identically by those parameters on which their work capability depends. The work capability depends mainly on the potential energy of the explosive, Q_v, the specific volume v_0 and the specific heat C of the gaseous explosion products. The work capability and fugacity effect of an explosive increases with increase of Q_v and v_0. The detonation velocity D and the detonation pressure p_i are the determining factors of brisance.

Trotyl and ammotol 80/20 possess approximately equal work capabilities. The brisance of trotyl significantly exceeds the brisance of ammotol, which is explained by its higher detonation velocity.

Variation of the charge density has a slight effect on the quantities Q_v and v_0, and consequently also on the work capability of the explosive, but on the other hand exerts a considerable influence on its brisance. This is explained by the fact that p_i and D depend strongly on the initial density of the explosive.

Experiments for evaluating brisance theoretically have been carried out by numerous investigators (BIKHEL', BEKKER, KAST etc.), which, however, were based on inadequately accurate physical grounds. As a consequence of this, the formulae proposed by them for a quantitative characteristic of brisance could find no practical application.

BIKHEL', assuming a definite velocity for the process, suggested that brisance could be evaluated by the quantity $\frac{1}{2} m D_i^2$ which he took for the kinetic energy of the detonation products. He assumed the initial velocity of the latter, for this, to be equal to the detonation velocity D of the explosive. It was established by theory and by experiments, however, that in fact the initial maximum velocity of dispersion of the explosion products for the majority of high explosives is higher than their detonation velocity. Moreover, it should be

borne in mind that different gas fractions do not possess identical velocities. On detonation, a considerable redistribution of velocities occurs of the gaseous explosion products according to their mass. Only a relatively small portion of the mass of gas possesses a high velocity ; the greater portion of the mass of gas possesses relatively low velocities (see para. 80).

REDL considered it more accurate to characterize brisance by the quantity mD, i. e. the momentum of the gaseous explosion products. Assuming, as a result of this, the same errors as BIKHEL, it did not, however, take into account the fact that on encountering an obstacle, the impulse of the explosion considerably increases as a result of reflection.

HESS and KAST assumed that brisance should be characterized by the power of the explosive. HESS, therefore, without taking into account the initial density of the explosive, related the power to unit weight of explosive. KAST, on the other hand, assigned a large importance to the density, and suggested that brisance should be evaluated by the power per unit volume of explosive.

KAST suggested that the power should be characterized by the expression

$$B = \frac{A_{max}\rho_0}{\tau}, \qquad (56.1)$$

where A_{max} is the maximum work done by the explosion products, τ is the time over which it takes place and ρ_0 is the density of the explosive.

According to KAST, τ is inversely proportional to the detonation velocity, and the work done, A_{max}, is proportional to the "power" F. As a result, the following formula was proposed by them for estimating the brisance of an explosive :

$$B_0 = FD\rho_0. \qquad (56.2)$$

K.K. SNITKO, assuming the absence of strict proportionality between A_{max} (equal to the potential energy of the explosive, Q_v) and F, and also assuming that $\tau = \frac{l}{D}$, where l is the charge length, suggested thatit was more accurate

to evaluate power by the relationship

$$B = \frac{Q_{exp} D}{l} \quad \text{cal/l.sec} \qquad (56.3)$$

He assigned this quantity to the energy stress as a result of the explosion. The values of B calculated according to formula (56.3) for certain explosives, are presented in Table 93.

Table 93

Energy Stresses of Certain Explosives

Name of Explosive	Density g/cm^3, ρ_0	Linear dimensions of charge l, m	Heat of explosion, kcal/kg	Detonation velocity, m/sec	Power kcal/l.sec
Ammotol 80/20	1.50	0.018	1010	5300	$74 \cdot 10^6$
Oxyliquite	1.00	0.100	2000	5000	$100 \cdot 10^6$
Trotyl	1.52	0.108	1010	6600	$93 \cdot 10^6$
Tetryl	1.55	0.108	1090	7500	$117 \cdot 10^6$
PETN	1.55	0.108	1400	7300	$156 \cdot 10^6$

Formulae (56.2) and (56.3) have found some application for the quantitative estimation of brisance of explosives and in general gives satisfactory agreement with that found in practise. Thus, in accordance with the data from Table 93 the brisance should increase with successive transition from ammotol to PETN, which is in fact verified by experimental results.

Nevertheless, Formulae (56.2) and (56.3) are, to a considerable extent, of an arbitrary nature. This is explained first of all by the fact that in the formulae mentioned the time τ, during which the explosion products do work, is assumed to be proportional to or equal to the time of traverse of the detonation through the charge, which is not true. Thus, for example, under conditions of simultaneous double-ended initiation of an explosive charge, its detonation time decreases by a factor of two. It is obvious, however, that this circumstance cannot, in itself, involve either an increase in the power or the brisance effect

of the explosive.

The duration of the work done by the explosion products is not determined uniquely by the detonation velocity, but it depends also on the nature of the obstacle and on certain other factors and it does not give an accurate quantitative determination.

From what has been suggested above, it follows that Formulae (56.2) and (56.3) cannot be proposed as the basis of any calculations associated with a quantitative evaluation of the local brisance effect of an explosion.

BEKKER, RUDENBERG and SCHMIDT, in order to interpret the concept of brisance, proceeded from accurate hydrodynamic representations of the process of detonation. For this, BEKKER and SCHMIDT assumed that brisance of an explosive should be characterised by a rapid change in pressure at the detonation wave front, which, as is well-known, is determined by the expression

$$\Delta p_i = \rho_0 u D. \tag{56.4}$$

RUDENBERG, proceeding from the representation, accurate in principle, that on encountering the obstacle, as a consequence of the movement of the detonation products to the wall, they will be compressed and the pressure will be increased, suggested that brisance could be characterised by the sum of the quantities

$$p_{imp} = \Delta p + \rho_1 u^2, \tag{56.5}$$

called by him the impulsive force. $\rho_1 u^2$ is the momentum of the detonation products in the region of the detonation wave.

For a strong detonation wave

$$\Delta p \approx p_i = \frac{1}{k+1}\rho_0 D^2$$

and

$$\rho_1 u^2 = \frac{\rho_0 D^2}{k(k+1)} = \frac{p_i}{k},$$

whence

$$p_{imp} = \frac{k+1}{k} p_i,$$

which for $k=3$ gives

$$p_{imp}=\frac{4}{3}p_i.$$

The expression proposed by RUDINBERG, is not sufficiently accurate. The actual pressure experienced by the wall at the site of encounter with the detonation wave, is determined by the conditions of its reflection from the wall and is easily determined by theoretical calculation (see para.48) .

§ 57. The Impulse resulting from Reflection of the Detonation Wave from the Wall.

The theoretical calculation of the impulse resulting from reflection of a detonation wave from a wall has been given by ZEL'DOVICH and STANYUKOVSKII. Let us consider this problem.

Suppose that a plane detonation wave is initiated at the left-hand open end of an explosive charge (at the origin of coordinates). The length of the charge is l ; a non-deformable wall is situated at the right-hand end for $x=l$. (Fig. 141).

The gas dynamic equations for uniform isentropic flow have the form

$$\frac{\partial}{\partial t}\left(u\pm\frac{2}{k-1}c\right)+(u\pm c)\frac{\partial\left(u\pm\frac{2}{k-1}c\right)}{\partial x}=0. \qquad (57.1)$$

We can write (57.1) for the case when $k=3$: as

$$\frac{\partial(u\pm c)}{\partial t}+(u\pm c)\frac{\partial(u\pm c)}{\partial x}=0. \qquad (57.2)$$

The solution of (57.2), in accordance with para.25 will be

$$\left.\begin{aligned} x&=(u+c)t+F_1(u+c),\\ x&=(u-c)t+F_2(u-c),\end{aligned}\right\} \qquad (57.3)$$

where F_1 and F_2 are arbitrary functions.

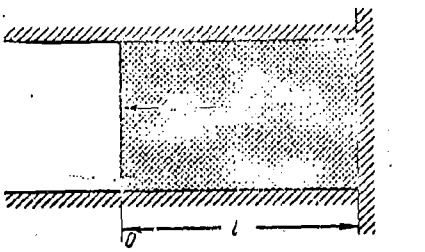
For the reflected wave the solution is finite for $t=\frac{l}{D}$, $x=l$. As a result of this, $u=0$, $c=D_i$; ; it follows from this that

$$F_1=l-\frac{D_i}{D_i}l=0, \qquad (57.4)$$

consequently,

$$x=(u+c)t. \qquad (57.5)$$

Figure 141. Derivation of the relationship for the impulse resulting from reflection of a detonation wave from a non-deformable wall.



The function F_2 is determined from the conditions that at the wall for $x=l$, $u\equiv 0$ for any value of t. Then

$$l=(0-c)t+F_2(0-c).$$

Assuming that for $t=\frac{l}{D}$ $c=D_i$, we obtain

$$l=-\frac{Dl}{D}+F_2(0-c), \text{ i.e. } F_2=2l. \qquad (57.6)$$

Consequently,

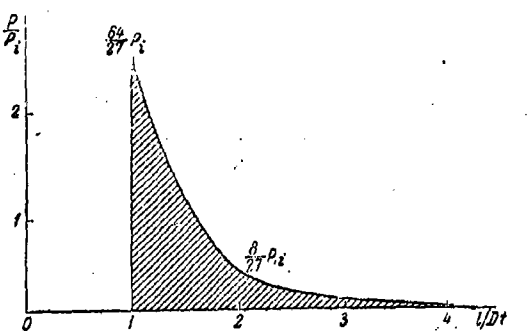
$$x=(u-c)t+2l. \qquad (57.7)$$

From equations (57.5) and (57.7) we determine u and c:

$$u=\frac{x-l}{t}, \quad c=\frac{l}{t}. \qquad (57.8)$$

The latter relationship enables us to establish easily the law of variation of the pressure acting on the wall with respect to time.

Figure 142. Fall in pressure acting on the wall as a result of reflection of a detonation wave.



From the isentropy equation $p=A\rho^3$ it follows that

$$\frac{p}{p_i}=\left(\frac{\rho}{\rho_i}\right)^3; \qquad (57.9)$$

since for $k=3$, $c \sim \rho$, then

$$\frac{p}{p_i} = \left(\frac{c}{c_i}\right)^3. \tag{57.10}$$

Substituting in equation (57.10) the value of c from (57.8) and assuming that $c_i = \frac{3}{4}D$, we obtain

$$p = \frac{64}{27} p_i \left(\frac{l}{Dt}\right)^3. \tag{57.11}$$

Equation (57.11) gives the law of variation of pressure at the wall. This relationship is presented graphically in Figure 142. The total impulse as a result of reflection of the detonation wave from the wall is

$$I = \int_{\frac{l}{D}}^{\infty} p\,dt = \frac{64}{27} S p_i \left(\frac{l}{D}\right)^3 \int_{\frac{l}{D}}^{\infty} \frac{dt}{t^3} = \frac{32}{27} S p_i \frac{l}{D}, \tag{57.12}$$

where S is the cross-sectional area of the explosive charge.

Since

$$p_i = \frac{1}{4}\rho_0 D^2,$$

then we have finally

$$I = \frac{8}{27} S \rho_0 l D = \frac{8}{27} m D, \tag{57.13}$$

where $m = S\rho_0 l$ is the mass of the charge.

It can be seen from Fig. 142 that the pressure at the wall falls exceedingly rapidly. It follows from this that the impulse, depending on the local action of the explosion(depicted on the graph by the hatched area), is imparted to the obstacle essentially after an extremely short interval of time $\tau \approx \frac{2l}{D}$, equal to the transit time of the rarefaction wave through the charge. $\frac{D}{2}$ is the velocity of the rarefaction wave.

In the case when $D = 8000$ m/sec and $l = 20$ cm, $t = 5 \cdot 10^{-5}$ sec.

After this time the pressure falls to the value $p_1 = \frac{8}{27} p_i$, which is still quite large and usually exceeds the elastic limit of deformation of the respective matarials.

It is necessary to take into account in calculations that the local explosion effect under conditions of direct contact of the charge with the obstacle is not entirely dependent on the impulse in a number of cases, but only upon a certain part of it, after the time of action of which the pressure does not fall below a certain critical limit, depending on the structure and mechanical characteristics of the obstacle material.

Moreover, in the same calculations one should take into account the actual maximum pressure originating at the boundary of separation of the media as a result of the reflection, which depends considerably on the relationship between the density and compressibility of the detonation products and of the medium itself. Methods of calculation of these pressures are considered in detail in Chapter IX.

However, in a number of cases for general estimation of the brisance effect of charges, it is sufficient to know the detonation pressure of the explosive and the specific impulse as a result of reflection of the detonation products from an absolutely non-deforming wall. Both these quantities are easily derived by theoretical calculation.

It follows from expression (57.13) that the specific impulse, depending (to a first approximation) on the local brisance effect of the explosive, depends not only on the detonation velocity and the density of the explosive, but also on the weight and geometrical parameters of the charge.

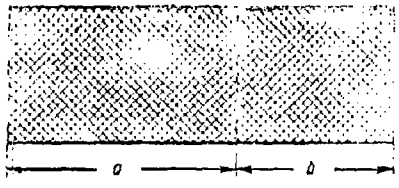
It also follows from expression (57.13) that the impulse, for approximately the same conditions, should increase linearly with increase in detonation velocity. Hence it follows that the impulse of a charge of a given explosive may be considerably increased as a result of an increase in density of the charge ; since $D = A\rho_0^n$, then the following relationship should consequently be achieved :

$$I = K\rho_0^n. \qquad (57.14)$$

Equation (57.13) assumes a linear relationship between impulse and charge length, which is not, in fact, observed. This is explained by the fact that in practice it is not possible to realise strictly one-dimensional motion of the detonation products and the complete exclusion of their sideways flight even for a closed charge in a sufficiently strong envelope.

However, relationship (57.13) can be used not only for the one-dimensional case but also for the three-dimensional case. For this it is necessary to substitute the mass of the active portion of the charge in place of the total mass of the charge, which can be calculated with sufficient accuracy in each individual case.

Figure 143. Dispersion of the detonation products from the ends of a cylindrical charge.



The theory of the active portion of a charge was worked out by O.E. VLASOV, G.I. POKHOVSKII and it received further development in the work of BAUM and STANYUKOVICH. By the active portion of a charge is meant that portion of a charge from which the detonation products are dispersed in a given direction. With increasing charge length for a given diameter, the active mass of the charge increases only up to a known limit. The limiting mass of the active portion of the charge can be calculated in the following manner.

Suppose that initiation of a cylindrical charge takes place in an arbitrary section dividing the charge into two parts (a and b), as shown in Fig.143.

From the theory of 'simultaneous' dispersion of the detonation products it is known that in this case, for the detonation products dispersing in opposite directions, the following relationships are valid :

$$m_1 = \rho_0 \frac{4a + 5b}{9} \qquad m_2 = \rho_0 \frac{5a + 4b}{9}, \tag{57.15}$$

where m_1 and m_2 are the masses dispersing to left and to right respecyively.

If the charge initiation is at the left-hand end, then 4/9 of the total mass of the charge is ejected to the side in which the detonation is propagated (to the right). However, as a consequence of the simultaneous flight of the detonation products from the side surface, the active mass of the charge is reduced.

If v is the velocity of the rarefaction wave propagated from the lateral surface towards the axis of the charge, and its radius is r, then the limiting length of the active portion of the charge l_a is determined from the condition

$$\frac{r}{v} = \frac{l_{lim}}{D}; \quad l_a = r\frac{D}{v}, \tag{57.16}$$

and the active mass will occupy a volume of a cone with a base radius of r and a height l_{lim}, i.e.

$$m_{lim} = \frac{1}{3}\pi r^2 \rho_0 l_a, \tag{57.17}$$

where m_{lim} is the limiting active mass of the charge.

Assuming that $v \approx \frac{D}{2}$, which is sufficiently close for practical application, and relating the active mass to the unit of surface of origin of the charge, we obtain

$$m'_{lim} = \frac{m_{lim}}{\pi r^2} = \frac{2}{3} r \rho_0. \tag{57.18}$$

It is obvious from (57.15) and (57.16) that the limiting value of the active mass for a given diameter of charge is attained for a charge length of $l = \frac{9}{2}r$. Hence it follows that the increase in specific impulse as a result of an increase in the charge length should only take place up to a known limit. By increasing the charge length above its optimum value $l_{opt} = \frac{9}{2}r$ (for this $l_a = \frac{4}{9}l_{lim}$) no increase of impulse should be observed (Fig.144).

If the charge length $l < \frac{9}{2}r$, then the active mass of the charge is determined by the volume of a truncated cone, the height of which is equal to

$\frac{4}{9}l$ (Fig.145).

The mass of the active portion of the charge is expressed in this case by the following relationship

$$\omega = \left(\frac{2}{3}l - \frac{1}{81}r^2 + \frac{1}{2187}r^4\right)\rho_0 \qquad (97.10)$$

Using the same considerations it can be shown that the active portion of the charge, and consequently also the specific impulse, should also increase with increase in charge diameter, asymptotically approaching a finite limit.

Figure 144. Active portion of an open charge for $l > l_{lim}$.

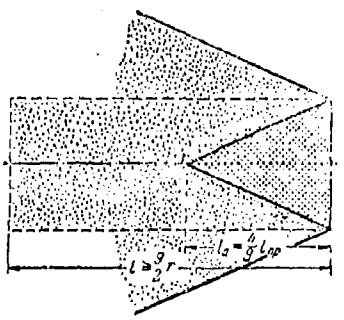
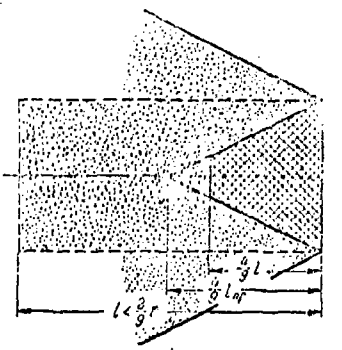


Figure 145. Active portion of an open charge for $l < l_{lim}$.



The theoretical relationships obtained above for the impulse resulting from an explosion, and the conclusions reached in relation to the estimation of the brisance of explosives are verified by the results of experimental investigations.

§ 58. Methods and Results of Experimental Determinations of Impulses.

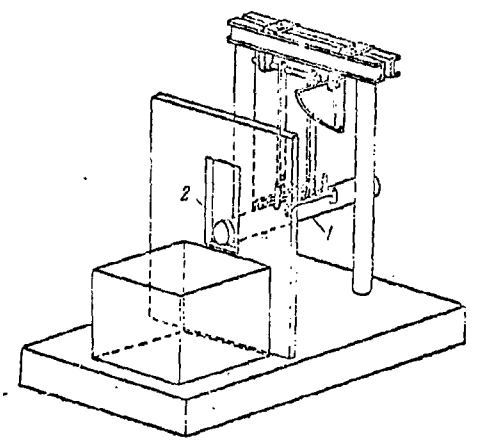
The most reliable instrument for determining impulses at the surface of detonating charges is the ballistic pendulum.

In order to determine the impulse, a metal plate is placed at the end surface

of a charge. The plate, as a result of detonation of the charge, transmits the momentum acquired by it to the pendulum. The impulse resulting from this is determined by the angle of deflection of the pendulum. In order that the pendulum completely acquires the whole of the impulse, it is essential that as a result of the explosion premature destruction of the plate should not occur; if the contrary is the case, fragments from it are ejected through random trajectories and they only partially strike the pendulum. A general view of the pendulum is shown in Fig.146. In order to measure impulses under conditions of direct contact between the charge and the pendulum, the "bob" 1 has removable anvils 2.

We shall derive the calculated formula for determining the impulse with respect to the measured angle of deflection of the pendulum.

Figure 146. Ballistic Pendulum



We introduce the following symbols : m is the mass of the plate projected at the pendulum, v is the velocity of the plate, R is the radius of impact of the plate, ω_0 is the angular velocity of the pendulum, K is the moment of inertia of the plate, L is the distance from the axis of suspension to the centre of gravity of the plate, and α is the angle of deflection of the pendulum.

On the basis of the Laws of Conservation of Momentum and Energy we have

$$mvR = (mR^2 + K)\omega_0, \tag{58.1}$$

$$\frac{1}{2}(K + mR^2)\omega_0^2 = g(ML + mR)(1 - \cos\alpha). \tag{58.2}$$

Solving simultaneously these two equations and substituting $1 - \cos\alpha = 2\sin^2\frac{\alpha}{2}$, we obtain

$$\frac{m^2v^2R^2}{mR^2 + K} = 4(M + m)gL\sin^2\frac{\alpha}{2},$$

whence

$$mv = \sqrt{(M + m)gL(mR^2 + K)}\,\frac{2\sin\frac{\alpha}{2}}{mR}. \tag{58.3}$$

Neglecting in equation (58.3) mR^2 and m in comparison with K and M respectively, we obtain

$$mv = \frac{2\sin\frac{\alpha}{2}}{R}\sqrt{MgLK}. \tag{58.4}$$

The period of small oscillations of a physical pendulum is

$$T = 2\pi\sqrt{\frac{K}{MgL}}. \tag{58.5}$$

Determining K from this expression and substituting in (58.4) we have

$$mv = \frac{2\sin\frac{\alpha}{2}}{R}\,\frac{TMgl}{2\pi} \tag{58.6}$$

or

$$I = mv = \frac{TMgL}{\pi R}\sin\frac{\alpha}{2}, \tag{58.7}$$

where the quantity $\frac{TQL}{\pi} = C$ is the pendulum constant ($Q = Mg$ is the weight of the pendulum).

By carrying out the experiment under conditions of direct contact between the charge and the pendulum, $R = L$. In order to determine the pendulum constant it is necessary to know the period of oscillation T and the static moment QL of the pendulum, which is easily determined by experiment.

The first systematic studies in determining impulses resulting from an

explosion and the establishment of the relationship between specific impulse and the compression of copper and lead crushers were carried out by M.A.SADOVSKII and P.F.POKHIL . The relationship between impulse, weight and geometrical parameters of the charge can be written by means of the formula

$$I = kP\frac{\omega}{\Omega}, \qquad (58.8)$$

where k is a coefficient, depending on the power of the explosive, P is the charge weight, ω is the base area of the charge in contact with the pendulum and Ω is the surface area of the charge.

Assuming that the momentum of the explosion products is proportional to the velocity of motion, which in its turn is proportional to the detonation velocity D, the authors derived formula (58.8) in the following form :

$$I = k_1 DM\frac{\omega}{\Omega}, \qquad (58.9)$$

where M is the charge mass.

Table 94 presents experimental data showing the effect of detonation velocity was achieved by varying the density of charges of trotyl and phlegmatized hexogen. The weight of the charges was 50g. and the diameter was 40mm.

Table 94

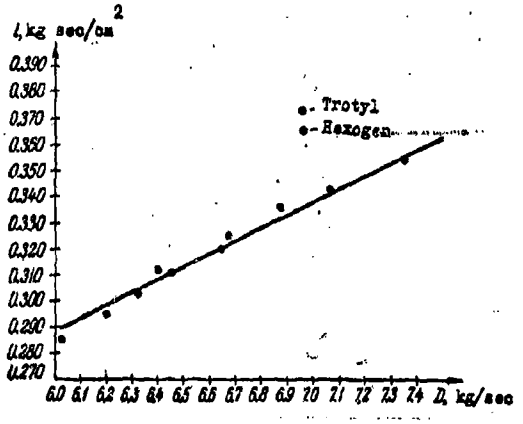
Relationship between specific impulse and detonation velocity

Charge density, g/cm^3	Trotyl		Phlegmatized hexogen	
	i, kg.sec/cm^2	D, m/sec	i, kg.sec/cm^2	D, m/sec
1.20	-	-	0.512	6400
1.25	-	-	0.525	6660
1.30	0.285	6025	0.536	6870
1.35	0.295	6200	0.545	7060
1.40	0.305	6320	0.555	7350
1.45	0.311	6440	-	-
1.50	0.320	6440	-	-

It can be seen from Fig.147 that for given charge characteristics

(constant weight and diameter) the relationship between impulse and detonation velocity for two essentially different explosives (trotyl and phlegmatized hexogen), as also required by theory, is expressed by one and the same linear relationship. This relationship, obviously, should be of a general nature.

Figure 147. Relationship between specific impulse and detonation velocity.



It can also be seen from Table 94 that with increase of density of the trotyl from 1.50 g/cm^3 to 1.50 g/cm^3 and for phlegmatized hexogen from 1.20 g/cm^3 to 1.40 g/cm^3, the specific impulse in both cases is increased by 12 - 13% .

Expression (57.14) , which results from theory, requires a linear relationship between log i and log ρ_0, which is well borne out by results of experiment (Fig.148).

With increase in charge diameter for constant height, the specific impulse, as also would be expected, increases, which for example can be seen from the data obtained by VERBOVSKII for trotyl, and presented in Fig.149.

Figure 148. Relationship between impulse and charge density ; 1 - Trotyl, charge weight 22.8g, 2 - Phlegmatized hexogen, charge weight 22.8g, 3 - Phlegmatized hexogen, charge weight 33.8g.

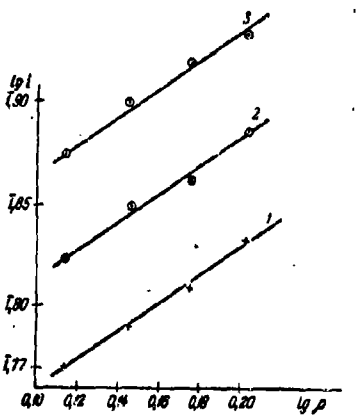
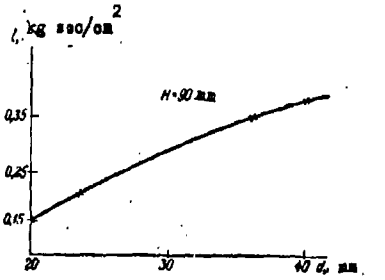


Figure 149. Relationship between specific impulse and charge diameter(height of charge H = 90mm)



The increase of impulse in the given case is explained by the substantial increase of the active portion of the charge with increase of its diameter.

On the basis of theory and from Fig. 149 it can be concluded that for a sufficiently large diameter of the charge the maximum increase will still have no noticeable effect on the specific impulse.

In Table 95 are presented values of impulses established experimentally and calculated according to formula (57.13) for trotyl charges, based on data concerning the active portion of the charge. As can be seen from the table, the calculated values are found to be in satisfactory agreement with the experimental values.

Table 95

Calculated and experimental values of specific impulses

Charge dimensions		Density	D, m/sec	Values of specific impulses	
H, mm	d, mm	g/cm^3		i, kg.sec/cm^2 (experiment)	i, kg.sec/cm^2 (calculated)
80	20.0	1.40	6320	0.162	0.178
80	23.5	1.40	6320	0.217	0.208
80	31.4	1.40	6320	0.305	0.280
80	40.0	1.40	6320	0.378	0.360
70	20.0	1.50	6640	0.205	0.200
70	23.5	1.50	6640	0.266	0.234
70	31.4	1.50	6640	0.325	0.314
43	40.0	1.50	6025	0.296	0.272
61	40.0	1.50	6025	0.316	0.305
67	40.0	1.50	6025	0.318	0.310

An example of the calculation of i is shown below. Suppose that for a charge of trotyl of height H = 80 mm and diameter d = 20 mm, $\rho_0 = 1.3$ g/cm^3 and D = 6025 m/sec.

Since $\frac{H}{d} > 2.25$, then the limiting active mass of the charge is

$$m_{ap} = \frac{2}{3}\pi r^3 \rho_0.$$

Since

$$\rho_0 = \frac{1.3 \cdot 10^3}{9.81} \text{ kg. sec}^2/\text{m}^4,$$

then

$$i = \frac{I}{S} = \frac{8}{27} \cdot \frac{2}{3} r \rho_0 D =$$

$$= \frac{8 \cdot 2 \cdot 2 \cdot 10^{-2} \cdot 1.3 \cdot 10^3 \cdot 6.025 \cdot 10^3}{27 \cdot 3 \cdot 9.81 \cdot 10^4} = 0.315 \text{ kg. sec/cm}^2$$

By enclosing the charge in a case, propagation of the lateral rarefaction waves in the detonating charge is limited to a greater or lesser extent, which leads to a corresponding increase of specific impulse at its end. With increase of density and thickness of the case, the impulse is noticeably increased. Some data illustrating the effect of these factors on the specific impulse are presented in Table 96.

It should be noted that the presence of a case leads to a considerable increase in brisance.

Table 96

Effect of a case on the specific impulse.

Explosive	Charge characteristics			i, kg. sec/cm^2			
	H, mm	d, mm	Density, g/cm^3	Steel case, thickness 8mm.	Steel case, thickness 3mm.	Aluminium case, thickness 1 mm.	No case
Trotyl	50	23.5	1.30	0.523	0.388	-	-
Trotyl	50	23.5	1.30	0.655	0.430	-	-
Trotyl	60	23.5	1.30	0.678	0.475	-	0.217
Phlegmatized hexogen	60	23.5	1.30	0.830	-	0.760	0.370

§59. Metods of Determining Experimentally the Brisance of Explosives.

The most simple methods for determining the characteristics of brisance are tests based on the compression of lead cylinders and copper crushers.

The test proposed by HESS in 1876, based on the compression of lead cylinders, is constructed in the following manner (Fig. 150). A cylinder a, made of refined lead, with a height of H = 60mm and a diameter d = 40mm, is placed on a

massive steel slab A. Above the cylinder is placed a steel plate b with a diameter of 41.5mm and thickness 10mm, on which is placed the explosive charge (c) with a weight of 50g. and a diameter of 40mm into which fits a No.8 capsule detonator (d). As a result of explosion of the charge, the lead cylinder is compressed and acquires a characteristic mushroom shape (Fig.151).

Figure 150. Test based on the compression of lead cylinders.

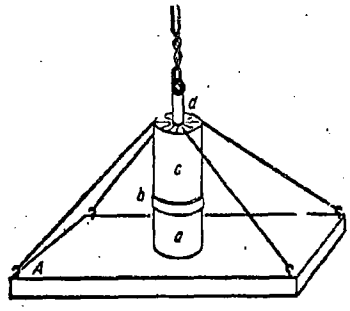


Figure 151. Compressed lead cylinder.



The reduction in height of the cylinder serves as a measure of the brisance

$$\Delta H = H_0 - H,$$

where H is the height of the cylinder after the explosion.

By exploding trotyl charges with a density of $\rho_0 > 1.5$ g/cm^3, and other charges with similar brisance properties, the lead cylinder is destroyed. In order to avoid this, a steel plate with a thickness of 20mm is used, or charges weighing only 25g. are exploded.

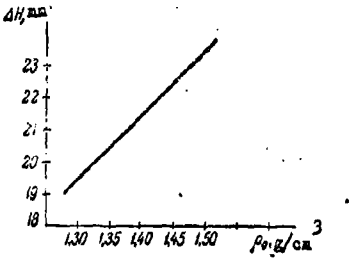
The results presented in Table 97 were obtained in this instrument of standard construction for certain explosives with a density of 1.2 g/cm^3 and using a TAT-8 capsule detonator.

For ammonites and similar explosive mixtures, the compression depends to a considerable extent on the degree of grinding and quality of mixing of the components. This is explained by the effect of these factors on the detonation

velocity and on the limiting diameter of these explosive systems.

With increase in charge density(for the same weight), the compression of lead columns increases linearly. Thus, for phlegmatized hexogen, by increasing its density from 1.2 to 1.5 g/cm^3 the compression was increased from 17.2 to 21.2mm (steel gasket with a thickness of 30mm). The relationship between compression and charge density is shown in Fig.152 for trotyl.

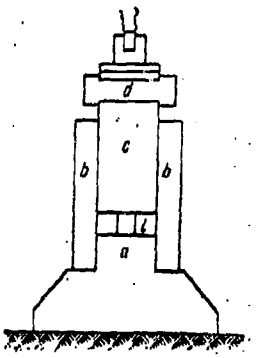
Figure 152. Relationship between compression of lead cylinders and charge density(trotyl).



A test based on the compression of copper crushers was proposed by KAST in 1895. An instrument for determining brisance by this test(brisance meter) is shown in Fig.153.

A hollow steel cylinder b, with a ground-in piston c of weight 680g. is fixed on a steel base a. On the piston there is a steel cover plate d with a thickness of 20mm and a weight of 320g, covered for protection from the direct action of the explosion products by two lead washers with a thickness of 4mm. Below the piston is a copper crusher l, usually with dimensions of 7 x 10.5mm. The test explosive charge, with a diameter of 21mm and fitted with a capsule-detonator, is placed on the lead washers. As a result of explosion of the charge, the piston receives a dynamic shock and compresses the crusher; the compression serves as a characteristic of the brisance.

Figure 153. Brisance meter.



The weight of the test charge was previously chosen equal to 10g. However, subsequent investigations have established that the results, up to a known limit, depend on the height of the charge. The limiting height of the charge for a diameter of 21mm amounts to about 70mm; experiments have been carried out with this height of the charge. Table 98 shows the results of experiments for certain explosives.

Table 98

Compression of Copper crushers.

Name of explosive	Compression of crusher, mm.
Fulminating jelly (Blasting gelatine)	4.8
Nitroglycerine	4.6
Tetryl	4.2
Melinite	4.1
Trotyl	3.6
Dinitrobenzene	2.1
Pyroxylin	3.0
Ammotol 50/50	2.5
Ammotol 70/30	1.6
62% Dynamite	3.9

Comparing the tests carried out on compression of lead cylinders and copper crushers, MEYER arrived at the conclusion that they give generally consistent results, and the average accuracy of both methods is approximately the same (about 3 - 4%).

One disadvantage of the test by compression of copper crushers is its small "resolution capability", since the compression of the copper crusher is relatively little changed by variation of charge density and height. Moreover,

the results of this test, in its standard form, are not representative in many cases. Thus for example, for a number of explosives the limiting diameter of which is considerably greater than 21mm (ammonites, mixtures of trotyl with dinitronaphthalene etc), brisance indices are obtained which are clearly too low.

HYDE and ZELLE, on the basis of the results of their investigations, came to the conclusion that the method of estimating the brisance of explosives, by direct comparison of the magnitude of compression of copper crushers, is not sufficiently accurate, since in the process of compression, the cross-sectional area of the crusher is increased and its resistance to deformation increases.

In order to establish the relationship between the resistance of the crusher and the magnitude of the compression they compressed simultaneously by explosion some crushers, then a number, n, of the crushers is selected such that the compression of each of them was equal to 1mm. In this case the effect of cross-section of the crusher can be neglected and the n - crushers compressed by 1mm may be taken as a measure of the brisance.

The data obtained by HYDE for certain explosives is presented in Table 99.

Table 99

Brisance of various explosives (according to HYDE)

Name of explosive	Density, g/cm^3	Charge weight, g.	Charge height, cm.	n
Dinitrobenzene	1.50	41	8	6.2
Trotyl	1.59	43	8	10.1
Picric acid	1.68	46	8	12.2
Tetryl	1.66	45	8	14.0
PETN	1.69	46	8	17.0

Notes: The charges were placed in a case of galvanised tin with a thickness of 0.3mm. The detonator was a No.8 capsule-detonator and 10g. of compressed picric acid.

BELYAYEV also occupied himself with the study of the dependence of the resistance of the crusher on its compression. In order to obtain an experimental relationship he subjected the same crusher to repeated compression by explosions of standard charges prepared from the same explosive.

The question of the relationship between compression of the crusher and the impulse from the explosion was first investigated by P.F. POKHIL and M.A. SADOVSKII. By establishing the operating conditions of a lead crusher under the action of an explosion, the authors referred to proceeded from the assumption that the resistance of the crusher is proportional to its cross-sectional area after deformation. By equating the volumes of the crusher before and after deformation we have

$$R = R_0 \frac{\omega}{H_0 - \Delta H}, \qquad (59.1)$$

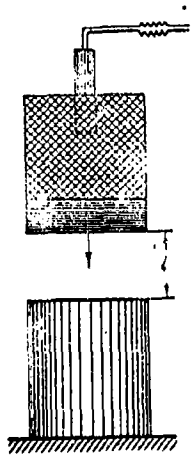
where H_0 is the original height of the crusher; ΔH its compression, R_0 is the initial resistance of the crusher, proportional to its area of cross-section, and ω is the volume of the crusher.

The equation for the work done in compression of the crusher has the following form

$$R\Delta H = R_0 \omega \frac{\Delta H}{H_0 - \Delta H} = \frac{I^2}{2M}, \qquad (59.2)$$

where I is the impulse of the explosion, acting on the base of the crusher, M is the mass set into motion after a time of explosion t. The mass M corresponds to that layer of metal which, after a time τ will be traversed by the deformation wave. In order to establish the quantity M, POKHIL and SADOVSKII carried out the following experiment. The steel plate and the explosive charge were placed coaxially at different distances l from the lead crusher (Fig.154).

Figure 154. Compression of a lead crusher by impact of a plate.



By detonating charges of explosive, a kinetic energy was imparted to the plate, depending on the magnitude of the impulse and the mass of the plate. Compression of the crusher occurred by the action of impact of the plate. Similar experiments were carried out by VEREŠČAGIN, the results of which are presented in Table 100.

It can be seen from the table that compression of the crusher is independent of whether or not the plate is in contact with the crusher. This indicates that after the time of action of the explosion, only the transmitting plate is set into motion. Hence it follows that in equation (59.2) M should be equated to the mass of the plate. Equation (59.2) establishes the relationship between compression of the crusher and the impulse.

Table 100

Compression of crushers by impact.

Charge			Plate		Compression (mm) of lead crusher, as a function of l.				
Explosive	Weight g.	Density g/cm³	Thickness, mm	Diameter mm.	$l=0$	$l=5$ mm	$l=10$ mm	$l=20$ mm	$l=100$ mm
Ammotol 80/20	50	1.2	10	41	16.1	16.0	16.0	-	-
Trotyl	50	1.3	10	41	22.5	23.0	23.0	-	23.0
Trotyl	50	1.3	16	41	20.0	-	20.0	20.0	-

By carrying out parallel measurements of impulses and compression of

crushers, POKHIL and SADOVSKII calculated, on the basis of equation (59.2), the resistance of the crusher for a variety of cases. It was established as a result of this that R varies within extremely wide limits (from 100 to 2000 kg/cm^2), rapidly increasing with increase of the initial velocity of the plate. This is mainly explained by the considerable increase in [illegible] of the lead which spills to the sides as a result of rapid deformations.

The initial velocity of the plate can be determined easily. According to data by VERBOVSKII, by exploding a charge of [illegible] with a weight of 50g at a density of 1.80 g/cm^3; the specific impulse I = 0.285 kg.sec/cm^2.

The velocity acquired by the plate with a diameter of 40mm and a height of 10mm (weight of plate 97.3g) will be, in the given case

$$v = \frac{sI}{M} = \frac{12{,}56 \cdot 0{,}285 \cdot 9{,}81}{97{,}3 \cdot 10^{-3}} = 362 \text{ m/sec},$$

where s is the area of the plate in contact with the explosive charge and M is the mass of the plate.

The initial velocity of the plate also characterises to some extent the initial velocity of deformation of the lead.

Direct application of equation (59.2) for calculating impulses by data obtained from compression of lead crushers (or solution of the reverse problem) presents difficulty, since the resistance of the crusher varies sharply with change of initial velocity of the plate and it does not afford an accurate determination. Moreover, the mass M in this equation is equated to the mass of the plate, which is true only up to a definite limit. If the deformation wave after the time of action of the explosion pressure on the plate has time to traverse a path greater than the height of the plate, then the mass M is indeterminate. In this case there will be no conformance between compression of the crusher, caused by the plate being projected by the explosion products, and compression under conditions of direct contact of the plate with the lead crusher.

This phenomenon can be observed in experiments with charges of powerful explosives with increased density and particularly in the presence of a thin transmission plate.

POHHIL and SADOVSKII have shown that equation (59.2) gives adequately satisfactory agreement with results of experiments by using data obtained from tests with compression of copper crushers. In order to accomplish this test, the initial velocity of the moving parts of the brisance meter are considerably less than the velocity of the plate used in tests carried out on compression of lead cylinders, which is dependent on the considerably greater weight of the mobile parts (1.25 kg) and the lower magnitude of the total impulse acting on the piston of the brisance meter.

Moreover, for copper crushers no toughening is observed. According to data by the above-mentioned authors, the numerical value of the resistance R_0 can be assumed with sufficient accuracy to be equal to the critical point of copper (3500 kg/cm^2), and the mass M is the mass of the moving parts of the brisance meter. Having used equation (59.2), the possibility is thus presented of determining the value of the impulse acting on the crusher according to data concerning its compression. For calculations, it should be based on the experimental results of brisance established by HYDE and ZELLE or EMLYAYEV's methods.

It was established above that with standardised equipment conditions (constant plate dimensions) compression of lead cylinders varies linearly with charge density :

$$\frac{\Delta H}{H_0} = k_1 \rho. \qquad (59.3)$$

On the other hand, the relationship between the specific impulse and the charge density (for constant mass of charge) is determined by the relationship

$$i = k_2 \rho^n, \qquad (59.4)$$

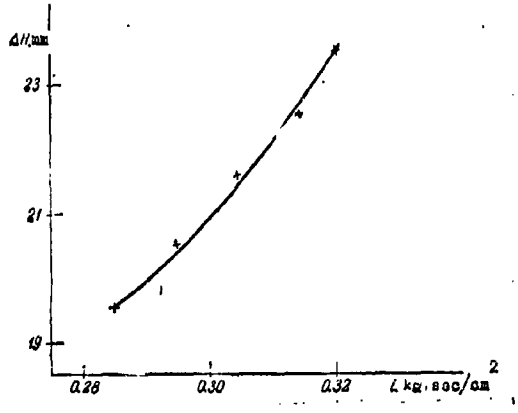
where $n < 1$, and for trotyl $n = 0.70$.

It follows from equations (59.3) and (59.4) that

$$\frac{\Delta H}{H_0} = \left(\frac{k_1}{k_2^{\frac{1}{n}}}\right) i^{\frac{1}{n}} = c i^{\frac{1}{n}}, \qquad (59.5)$$

i.e. that with increase in density of the charge, the compression of lead cylinders should increase somewhat more strongly than the specific impulse, which is verified by experimental data. Fig. 155 depicts the relationship between specific impulse and compression for trotyl charges with a weight of 50g. It can be seen from the graph that the compression increases with impulse more steeply than according to a linear law.

Figure 155. Relationship between compression of lead cylinders and specific impulse, for trotyl.



In addition to the methods described, the brisance of explosives is often assessed according to the results of practical tests of munitions equipped with explosives (missiles, mines), whereby the intensity and nature of fragmentation of the casing of the ammunition serves as criterion of brisance.

For these tests the munitions are usually exploded in an armoured pit,

and the casing fragments are collected and sorted out into definite groups according to weight. An assessment is carried out in each group of the number of fragments and by dividing by the total weight of all fragments collected in kilogrammes, a number of figures are obtained, a_1, a_2, a_3 ..... The value of these numbers and their sum

$$A = a_1 + a_2 + a_3 + \ldots$$

give the whole picture concerning the nature and intensity of fragmentation of the casing. The greater the number A, the greater the brisance of the explosive. For this, however, it is necessary to assume that fragmentation of the casing depends not only on the explosive charge, but to an even greater extent on the weight of the casing, and its shape and mechanical qualities. Because of the inevitable variations in these data, the method described for determining brisance is extremely approximate.

Moreover, the method described for estimating brisance cannot be admitted to be accurate, since the brisance effect of an explosive charge is determined not only by the intensity of fragmentation of the casing, but also by the kinetic energy acquired by the fragments as a result of the explosion. As a consequence of this, additional tests of munitions are sometimes carried out by exploding them in a circle of targets(sectors).

This method consists in the following: around the device to be exploded are disposed a number of wooden panels to definite specifications, in concentric circles with radii equal to 10, 20, 30, 40, 50 and 60 metres. After the devices have been exploded, the number of fragments are determined which have penetrated the panels and the number of fragments embedded in them.

The brisance of the explosive is assumed to be greater, the greater the radius of strike of the fragments. We note that the results of the test in a circle of targets characterizes to a greater extent the fragmentation effect of

the ammunition altogether, than the brisance effect of its explosive charge, since in a number of cas (for example for insufficiently thick and insuf - ficiently strong casin, the radius of strike for a more brisant explosive ; as a consequence of the more severe fragmentation of the casing, may appear to be less than for a less brisant explosive.

A more unbiased quantitative estimation of the possible fragmentation effects of charges can be carried out on the basis of data concerning the impulse, acting as a result of an explosion on the lateral surface of the case, since the predominant mass of fragments is formed as a result of shattering of just the cylindrical portion of the body of the ammunition. The initial velocity of the fragments , for approximately the same conditions, is entirely determined by the specific lateral impulse.

§60. Calculation of the Impulses acting on the Lateral Surface of the Charge Case.

The question of distribution of impulses along the lateral surface of a charge was investigated by BAUM and STANYUKOVICH.

In order to elucidate the method of calculation we shall consider two problems.

Problem I . Suppose that a detonation be initiated in the section $x=0$ of a cylindrical charge, placed in an infinitely strong tube, open at both ends. The length of the charge is l . The cross-sectional area of the charge is $s=1$. . As a result of this, a rarefaction wave originates simultaneously with the detonation wave in the section $x=0$. Both these waves, as is well-known, are described by the equations :

$$u+c=\frac{x}{t}, \quad u-c=-\frac{D}{2}, \tag{60.1}$$

whence

$$u=\frac{x}{2t}-\frac{D}{4},\quad c=\frac{x}{2t}+\frac{D}{4}. \tag{60.2}$$

We shall call this rarefaction wave the first rarefaction wave.

The pressure in this wave can be determined from the relationship

$$\frac{p_1}{p_i}=\left(\frac{c}{c_i}\right)^8, \tag{60.3}$$

where

$$p_i=\frac{\rho_0 D^2}{4},\quad c_i=\frac{3}{4}D. \tag{60.4}$$

Substituting in equation (60.3) the value of c_i from (60.4) and the value of c from (60.2), we obtain

$$\frac{p_1}{p_i}=\frac{8}{27}\left(\frac{x}{2t}+\frac{1}{2}\right)^8. \tag{60.5}$$

At the instant $t=\frac{l}{D}$ flow of the detonation products commences in the section $x=l$; a second rarefaction wave originates. The motion of this wave is determined by the general solution of the gas dynamic equations:

$$\left.\begin{aligned} x&=(u+c)\,t+F_1(u+c),\\ x&=(u-c)\,t+F_2(u-c). \end{aligned}\right\} \tag{60.6}$$

The arbitrary functions F_1 and F_2 can be determined from the condition that for $x=l$, $Dt=l$. As a result of this,

$$l=\left(\frac{1}{4}D+\frac{3}{4}D\right)\frac{l}{D}+F_1(u+c),$$
$$l=(u-c)\frac{l}{D}+F_2(u-c),$$

and hence

$$F_1=0\quad\text{and}\quad F_2=\frac{Dl-(u-c)\,l}{D}.$$

For the second wave, consequently, we have

$$u+c=\frac{x}{t},\quad u-c=D\,\frac{x-l}{Dt-l} \tag{60.7}$$

and

$$u=\frac{x}{2t}+\frac{D}{2}\,\frac{x-l}{Dt-l},\quad c=\frac{D}{2}\left(\frac{x}{Dt}-\frac{x-l}{Dt-l}\right). \tag{60.8}$$

The pressure in it is determined by the relationship

$$\frac{p_2}{p_1}=\left(\frac{c}{c_1}\right)^3=\frac{8}{27}\left[\frac{x}{Dt}-\frac{x-l}{Dt-l}\right]^3. \tag{60.9}$$

This wave is propagated through the gas of variable density and its front moves according to the law :

$$x=\frac{3}{2}l-\frac{Dt}{2}, \tag{60.10}$$

which is determined from the condition of simultaneous solution of equations (60.1) and (60.7). Hence, it is obvious that both rarefaction waves meet in the section x at the instant of time

$$t_2=\frac{3l-2x}{D}. \tag{60.11}$$

The specific impulse in the arbitrary section $0\leqslant x\leqslant l$ of the lateral surface of the charge will be

$$i=\int_{t_1}^{t_2}p_1\,dt+\int_{t_2}^{\infty}p_2\,dt, \tag{60.12}$$

where $t_1=\frac{x}{D}$, , p_1 and p_2 are determined from equations (60.5) and (60.9). On integrating, we obtain

$$\int_{t_1}^{t_2}p_1\,dt=\frac{i_0}{8}\left[\frac{3}{4}(1-\alpha)+\frac{3}{2}\alpha\ln\frac{3-2\alpha}{\alpha}+\frac{\alpha(1-\alpha)(36-21\alpha)}{(3-2\alpha)^2}\right],$$

$$\int_{t_2}^{\infty}p_2\,dt=\frac{i_0}{8}\left\{\frac{\alpha^3}{(3-2\alpha)^2}+6\alpha^2(1-\alpha)\left[\ln\frac{3-2\alpha}{2(1-\alpha)}-\frac{1}{3-2\alpha}\right]-\right.$$
$$\left.-6\alpha(1-\alpha^2)\left[\ln\frac{3-2\alpha}{2(1-\alpha)}-\frac{1}{2(1-\alpha)}\right]+\frac{1-\alpha}{4}\right\},$$

where $\alpha=\frac{x}{l}$ and $i_0=\frac{32}{27}\frac{p_1 l}{D}=\frac{8}{27}p_0 lD$ is the specific impulse on the end surface of the charge. Hence,

$$i=\frac{i_0}{8}\left[1+6\alpha(1-\alpha)+\frac{3}{2}\alpha\ln\frac{3-2\alpha}{\alpha}+\right.$$
$$\left.+6\alpha(1-\alpha)(2\alpha-1)\ln\frac{3-2\alpha}{2(1-\alpha)}\right]. \tag{60.13}$$

Carrying out the calculation for different sections of the lateral surface of the charge, we obtain :

$$\alpha = 0 \quad i = \frac{i_0}{8} = 0.125 i_0,$$
$$\alpha = \frac{1}{4} \quad i = 0.54 i_0,$$
$$\alpha = \frac{1}{2} \quad i = 0.48 i_0,$$
$$\alpha = \frac{3}{4} \quad i = 0.44 i_0,$$
$$\alpha = 1.0 \quad i = 0.125 i_0.$$

On analysing these results we can arrive at the conclusion that the maximum impulse is attained in the section $x = 0.7l$, i.e. at the place where approximately the two rarefaction waves meet.

Problem II. Suppose that detonation is initiated in the middle section of a cylindrical charge placed in an infinitely strong tube with open ends. Let us consider the impulses which will act on unit lateral surface of the tube at different distances from the detonation point. This problem is equivalent to the case when there is a wall in the middle section, so that at the wall $x = 0$.

The detonation wave within the interval of time $\frac{Dt}{2} \leqslant x \leqslant Dt$ is characterised by the equations

$$u + c = \frac{x}{t}, \quad u - c = -\frac{D}{2}, \tag{60.14}$$

whence

$$u = \frac{x}{2t} - \frac{D}{4}, \quad c = \frac{x}{2t} + \frac{D}{4}. \tag{60.15}$$

We shall call this wave the first wave. For this wave

$$\frac{p_1}{p_i} = \frac{8}{27}\left(\frac{x}{Dt} + \frac{1}{2}\right)^3. \tag{60.16}$$

Within the time interval $0 \leqslant x \leqslant \frac{Dt}{2}$ (see para. 43)

$$u = 0, \quad c = \frac{D}{2} \tag{60.17}$$

We shall call this wave the second wave. For this wave, as is well-known,

$$\frac{p_2}{p_i} = \frac{8}{27}. \tag{60.18}$$

At the instant of time $t=\frac{l}{D}$ (l — is the distance from the wall to the end of the charge) flow of the detonation products commences in the section $x=l$. The rarefaction wave originating as a result of this, as shown above, is described by the equations

$$u+c=\frac{x}{t},\quad u-c=D\frac{x-l}{Dt-l}, \tag{60.19}$$

whence

$$u=\frac{x}{2t}+\frac{D}{2}\frac{x-l}{Dt-l},\quad c=\frac{D}{2}\left[\frac{x}{Dt}-\frac{x-l}{Dt-l}\right]. \tag{60.20}$$

We shall call this wave the <u>third</u> wave. For this wave

$$\frac{p_h}{p_{H_1}}=\frac{8}{27}\left(\frac{x}{Dt}-\frac{x-l}{Dt-l}\right)^3. \tag{60.21}$$

The wave will move according to the law

$$x=\frac{3}{2}l-\frac{Dt}{2}. \tag{60.22}$$

The weak discontinuity in the detonation wave will be moving according to the law

$$x=\frac{Dt}{2}. \tag{60.23}$$

At the instant of time $t=\frac{3}{2}\frac{l}{D}$, and in the section $x=\frac{3}{4}l$, the rarefaction wave will meet the weak discontinuity dividing the detonation wave into two different regimes. This is established from simultaneous consideration of equations (60.22) and (60.23). A new <u>fourth</u> wave originates, which is a Riemann wave ($\rho_1=$ const). This wave is described by the equations :

$$u+c=\text{const}\quad\text{and}\quad u-c=D\frac{x-l}{Dt-l}. \tag{60.24}$$

At the conjugate point of this wave with the weak discontinuity we have :

$$u=0,\quad c=\frac{D}{2}\quad\text{or}\quad 0+\frac{D}{2}=\text{const},$$

whence

$$u+c=\frac{D}{2}, \tag{60.25}$$

and consequently,

$$u=\frac{D}{2}\left[\frac{1}{2}+\frac{x-l}{Dt-l}\right],\quad c=\frac{D}{2}\left[1-\frac{x-l}{Dt-l}\right]. \tag{60.26}$$

The right hand front will move according to the law

$$x=\frac{Dt}{2}. \tag{60.27}$$

and the left-hand front will move according to the law

$$x=\frac{3}{2}l-\frac{Dt}{2}. \tag{60.28}$$

For this wave we have

$$\frac{p_1}{p_2}=\frac{8}{27}\left[\frac{1}{2}-\frac{x-l}{Dt-l}\right]^3. \tag{60.29}$$

In the section $x=0$, at the instant of time $t=\frac{3l}{D}$, reflection of the rarefaction wave from the wall takes place, which is described by the equations

$$x=(u+c)t+F_1(u+c),\quad x=(u-c)t+F_2(u-c), \tag{60.30}$$

The function F_2 is determined by the expression

$$F_2=\frac{Dt-(u-c)t}{D},$$

as a consequence of which we can write that

$$x=(u-c)t+\frac{Dt-(u-c)t}{D}, \tag{60.31}$$

whence

$$u-c=D\frac{x-l}{Dt-l}. \tag{60.32}$$

In a similar manner, by substituting x by $-x$ and u by $-u$, we obtain for the left-hand end (of the charge)

$$u+c=D\frac{x+l}{Dt-l}. \tag{60.33}$$

For the wave reflected from the wall, equations (60.32) and (60.33) give

$$u=D\frac{x}{Dt-l},\quad c=D\frac{l}{Dt-l}. \tag{60.34}$$

We shall call this wave the fifth wave. It moves according to the law

$$x=\frac{Dt}{2}-\frac{3}{2}l, \tag{60.35}$$

which is established from a comparison of equations (60.33) and (60.25). For this wave we have

$$\frac{p_5}{p_2}=\frac{64}{27}\left(\frac{l}{Dt-l}\right)^6. \tag{60.36}$$

Let us now consider the region $0 \leqslant x \leqslant \frac{3}{4} l$. For the arbitrary quantity in this region, the pressure impulse is calculated according to the formula

$$i_1 = \int_{t_1}^{t_2} p_1\,dt + \int_{t_2}^{t_3} p_2\,dt + \int_{t_3}^{t_4} p_4\,dt + \int_{t_4}^{\infty} p_5\,dt, \qquad (60.37)$$

where

$$t_1 = \frac{x}{D}, \quad t_2 = \frac{2x}{D}, \quad t_4 = \frac{3l-2x}{D}, \quad t_5 = \frac{3l+2x}{D}. \qquad (60.38)$$

In the region $\frac{3}{4} l \leqslant x \leqslant l$, the impulse is determined by the formula

$$i_2 = \int_{t_1}^{t_2} p_1\,dt + \int_{t_2}^{t_3} p_3\,dt + \int_{t_3}^{t_4} p_4\,dt + \int_{t_4}^{\infty} p_5\,dt, \qquad (60.39)$$

where

$$t_1 = \frac{x}{D}; \quad t_2 = \frac{3l-2x}{D}; \quad t_3 = \frac{2x}{D}; \quad t_5 = \frac{3l+2x}{D}. \qquad (60.40)$$

Carrying out the calculation, which we shall omit here, we obtain finally

$$i_1 = \frac{i_0}{16}\left[\frac{16+23\alpha+8\alpha^2-18\alpha^3}{(1+\alpha)^3} + 3(1-\alpha)\ln\frac{1+\alpha}{1-\alpha} + 3\alpha\ln 2\right], \qquad (60.41)$$

which gives, for

$$\alpha = 0 \quad i = i_0,$$
$$\alpha = \frac{1}{4} \quad i = 0.94 i_0,$$
$$\alpha = \frac{1}{2} \quad i = 0.81 i_0,$$
$$\alpha = \frac{3}{4} \quad i = 0.64 i_0.$$

Expression (60.39) gives :

$$x = l \quad i = 0{,}25 i_0.$$

On analysing the results obtained, we see that the impulse begins to fall in the direction from the wall to the end of the charge, and that initially the fall is slow and then becomes more rapid.

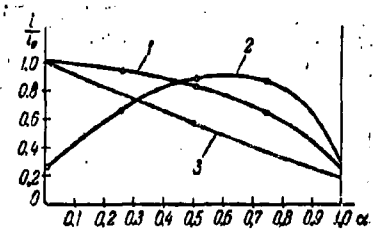
For a given mass of explosive, the presence of the wall may increase the impulse by a factor of two (since the wall is equivalent to twice the mass of explosive).

Figure 156 shows the distribution of specific impulses along the surface of a charge, obtained for various methods of initiation. Curve 1 depicts $i = i(\alpha)$, for the case of detonation from the wall. Curve 2 corresponds to the case considered in Problem I. Here, the impulse is converted for convenience of comparison for the doubled mass (the true value of i is less by a factor of two). Curve 3 is related to the case of detonation proceeding from the open end of the charge to the wall. The total impulse (I), acting on the entire lateral surface of the charge is

$$I = 2\pi R_0 \int_0^l i\,dx = 2\pi R_0 l \int_0^1 i\,d\alpha, \qquad (60.42)$$

where R_0 is the radius of the charge. If we assume that $2\pi R_0 = 1$, then the corresponding calculations give, for the case of detonation proceeding from the wall, $I = 0.75 i_0 l$, for instantaneous detonation in the presence of a wall $I = 0.77 i_0 l$, for detonation of the charge in an open tube $I = 0.66 i_0 l$, and for detonation proceeding towards the wall, $I = 0.54 i_0 l$.

Figure 156. Distribution of impulses along the lateral surface of a charge.



The latter case is equivalent to double-sided initiation of the charge, since the collision of the two contrary waves is equivalent to a reflection of the travelling detonation wave from the wall. This method of initiation is thus the least advantageous of all those considered.

§ 61. Determination of the Velocity of the Fragments scattered from the Lateral Surface of a Charge.

Under conditions of normal charge detonation, part of the total energy

is found in the form of kinetic energy of the detonation products. After completion of the process, the ratio of the kinetic energy $E_к$ to the total energy E_0 is equal to $\eta = \frac{E_к}{E_0} = 0.102$.

STANYUKOVICH showed that if the charge is enclosed in a tube, closed at both ends, then even after double reflection of the detonation wave from the walls, the parameters of the detonation products differ by 2% less from the parameters of the products of an instantaneous detonation.

When the explosive charge is enclosed in a case, the mass of which is greater than the mass of the explosive charge, then in order to calculate the velocity of the fragments it is necessary to use the hypothesis of instantaneous detonation, since reflection of the waves occurs several times prior to the case being significantly stretched and before the fragments, formed as a consequence of this, commence to fly apart.

The expansion velocity of the case u ,in the case of complete closure of the ends of the charge, if energy losses are neglected (expended on deformation of the casing), can be determined from the energy equation

$$\frac{Mu^2}{2} = m(Q - E_к) = mQ\left(1 - \frac{E_к}{Q}\right), \qquad (61.1)$$

where M is the mass of the case, m is the mass of the explosive, $E_к$ is the kinetic energy of the explosion products, and Q is the heat of explosive transformation of unit mass of explosive. For $\frac{M}{m} \gg 1$, $\frac{E_к}{Q} \ll 1$, and it can be assumed that

$$u_{lim} = \sqrt{2\frac{m}{M}Q}. \qquad (61.2)$$

Since the velocity of the detonation wave, on the average, is equal to $D = 4\sqrt{Q}$, it can be assumed with sufficient accuracy that

$$\frac{u_{lim}}{D} = \frac{1}{2}\sqrt{\frac{m}{2M}}. \qquad (61.3)$$

For example, for $\frac{M}{m}=4.5$ and $D=7000$ m/sec, $\frac{u}{D}=\frac{1}{6}$, and $u\approx1165$ m/sec.

In the case of a thick casing $\left(\frac{M}{m}\gg 1\right)$, the energy expended on deformation of the casing becomes considerable, which must be taken into account in relationship (61.1); in the contrary case, the difference between the calculated and measured velocities of the fragments will be substahtial.

We shall now consider how the difference in velocities of the casing or of the fragments may be observed, if the casing is considered as whole for the entire time and if it be assumed that it previously consisted of fabricated fragment-elements. This problem was solved by BAUM and STANYUKOVICH.

In the first case, considering a heavy casing $\left(\frac{M}{m}>1\right)$ and applying the Law of Conservation of Momentum, we can write

$$M\frac{du}{dt}=Mu\frac{du}{dr}=sp,\quad \frac{du}{dt}=\frac{du}{dr}\frac{dr}{dt}=u\frac{du}{dr}, \tag{61.4}$$

where s is the "current" area of the lateral surface of the cylindrical casing. It is obvious that

$$s=s_0\frac{r}{r_0}, \tag{61.5}$$

where s_0 is the initial area of the lateral surface of the cylinder. Since for the initial stage of expansion of the detonation products

$$pv^3=p(\pi r^2 l)^3=\text{const}, \tag{61.6}$$

then for $l=\text{const}$

$$p=\bar{p}_i\left(\frac{r_0}{r}\right)^6=\frac{\rho_0 D^2}{8}\left(\frac{r_0}{r}\right)^6, \tag{61.7}$$

where $\bar{p}_i$ is the initial pressure of the explosion products for instantaneous detonation.

Substituting the values of s and p in equation (61.4) we obtain :

$$Mu\frac{du}{dr}=\frac{D^2}{8}s_0\rho_0\left(\frac{r_0}{r}\right)^5=\frac{D^2}{4}m\frac{r_0^4}{r^5}$$

($m=\pi r_0^2 l\rho_0=\frac{s_0}{2}r_0\rho_0$ is the mass of the explosive charge) or

$$\frac{du^2}{dr}=\frac{D^2}{2}\frac{m}{M}\frac{r_0^4}{r^5}. \tag{61.8}$$

On integrating, we arrive at the following expression for the velocity of the casing :

$$\frac{u}{D}=\frac{1}{2}\sqrt{\frac{m}{2M}\left[1-\left(\frac{r_0}{r}\right)^4\right]}, \tag{61.9}$$

for

$$r\to\infty \quad \frac{u_{lim}}{D}=\frac{1}{2}\sqrt{\frac{m}{2M}}, \tag{61.10}$$

i.e. as we should expect, we have arrived at expression (61.3).

In the second case, $s=s_0$ and therefore integration of equation (61.4) leads to the following result :

$$\frac{u}{D}=\frac{1}{2}\sqrt{\frac{2m}{5M}\left[1-\left(\frac{r_0}{r}\right)^5\right]}, \tag{61.11}$$

which for $r\to\infty$ gives :

$$\frac{u_{lim}}{D}=\frac{1}{2}\sqrt{\frac{2}{5}\frac{m}{M}}. \tag{61.12}$$

Thus, the ratio of the velocities is

$$\frac{u_{lim}}{u_{lim}}=\sqrt{0.8}\approx 0.9. \tag{61.13}$$

This insignificant difference in the velocities is explained by the fact that the main part of the velocity of the casing or of the fabricated fragment-elements obtain at relatively small values of $\Delta r=r-r_0$, since the pressure falls inversely proportionally to r^6 $(pv^3\sim pr^6=\text{const})$.

The relationships obtained above for the main part of the casing or the prefabricated fragment-elements also hold good for detonation of explosives in a long cylinder, open at the ends. For a long charge, the length of which is several times greater than its diameter, the elements of the casing, being somewhat remote from the ends of the charge, are able to move to a considerable distance before the axial rarefaction wave is able to penetrate into the depths of the charge.

Let us consider another limiting case, when the length of the cylinder

with open ends is small in comparison with its diameter or is close to the diameter. It is obvious that as a result of this, before the casing (or fragments) is moved to a significant distance, the pressure has already fallen sharply; in order to calculate the velocity therefore, the following equation can be used :

$$Mu = I, \tag{61.14}$$

where I is the impulse:

$$I = Ai_0 \frac{2l}{r_0}, \tag{61.15}$$

the quantity A is chosen as a function of the cross-section of the tube and l is the length of the charge.

At the wall (or in the centre of the charge), $A = 1$ (or $A = 1/2$). Since

$$i_0 = \frac{8}{27} mD, \tag{61.16}$$

then

$$\frac{u}{D} = \frac{16}{27} A \frac{m}{M} \cdot \frac{l}{r_0}. \tag{61.17}$$

For example, in the case of detonation proceeding from the wall for $\frac{2l}{r_0} = 1$, $\frac{m}{M} = \frac{1}{8}$, $\frac{u}{D} = \frac{1}{27}$, which, for D = 7500 m/sec, gives u = 270 m/sec.

In the case of a long tube for $\frac{m}{M} = \frac{1}{8}$, $\frac{u_{lim}}{D} = \frac{1}{8}$, which, for D = 7500 m/sec, gives u_{lim} = 910 m/sec.

Thus, change in length of the tube leads to a change in velocity of a factor of $1.7 A \frac{l}{r_0} \sqrt{\frac{m}{M}}$.

It now remains to consider the general case, i.e. to explain how with change of length of the tube, the velocity of the fragments is changed. As above, we shall apply the hypothesis of instantaneous detonation, and we

carry out the calculation for fragments formed from the middle portion of the tube.

The rarefaction reaches the centre of the charge in a time

$$t_1 = \frac{l}{D}\sqrt{\frac{3}{8}}, \qquad (61.18)$$

where $2l$ is the length of the charge.

Assuming that the casing in the first stage (up to arrival of the rarefaction wave) is not shattered into fragments, in order to calculate the motion we apply formula (61.9) :

$$\frac{u}{D} = \frac{1}{2}\sqrt{\frac{m}{2M}\left[1-\left(\frac{r_0}{r}\right)^4\right]}.$$

Since $u = \frac{dr}{dt}$, then, introducing $\lambda = \frac{r}{r_0}$ and $\tau = \frac{Dt}{r_0}$, we arrive at the integral

$$\int_1^{\lambda} \frac{\lambda^2 d\lambda}{\sqrt{\lambda^4 - 1}} = \frac{1}{2}\sqrt{\frac{m}{2M}}\,\tau \qquad (61.19)$$

For $\tau = 0$, $\lambda = 1$; $\int_1^{\lambda} \frac{\lambda^2 d\lambda}{\sqrt{\lambda^4 - 1}}$ can be presented in the form of an elliptical integral.

It is sufficient for our purpose to approximate this integral by the expression

$$\int_1^{\lambda} \frac{\lambda^2 d\lambda}{\sqrt{\lambda^4 - 1}} \approx (\lambda^2 - 1)^{\frac{1}{2}}. \qquad (61.20)$$

From equations (61.19) and (61.20) we have

$$\lambda = \left(1 + \frac{1}{8}\frac{m}{M}\tau\right)^{\frac{1}{2}}. \qquad (61.21)$$

It is easy to arrive at the conclusion that the limiting velocity of flight of the fragments is

$$\frac{u_{\lim}}{D} = \frac{d\lambda}{d\tau} = \frac{1}{2}\sqrt{\frac{m}{2M}}, \qquad (61.22)$$

i.e. it corresponds to the velocity determined above.

At the instant of time $t = t_1 = \frac{x_1}{c_i}$ the rarefaction wave reaches the section $x = x_1$, after which the pressure of the detonation products begins to fall rapidly. In the case of one-dimensional flow the pressure varies according to the law

$$\frac{p}{p_i} = \frac{1}{8}\left(1 - \frac{x_i}{c_i t}\right)^3. \qquad (61.25)$$

At the instant of time $t_2 = \frac{l - x_1}{c_i}$ a rarefaction wave approaches the section $x = x_1$ from the centre of the charge, after which the pressure falls according to the law

$$\frac{p}{p_i} = \left(\frac{l}{c_i t}\right)^3. \qquad (61.26)$$

Since we shall have an interpolated, approximate solution determining the velocity of the fragments, then, arising from the fact that in the reflected wave the axial flow of gas will be predominant, it can be assumed that the lateral impulse arriving at the whole lateral surface as a result of the radial expansion of the casing is determined by the expression

$$\frac{I_1}{I_0} = \left(\frac{r_0}{r_1}\right)^6 = \lambda_1^{-6}, \qquad (61.25)$$

where $I_0 = \frac{8}{27} mD$.

As a result of this, and determining from equation (61.21) that $\lambda = \lambda_1$, we shall assume that $t = t_1 = \frac{l}{c_i}$ for $\tau = \tau_1 = \frac{lD}{r_0 c_i} = \frac{l}{r_0}\sqrt{\frac{2}{3}}$; then

$$\lambda_1 = 1 + \frac{1}{3}\frac{m}{M}\left(\frac{l}{r_0}\right)^2, \qquad (61.26)$$

$$\frac{u_1}{D} = \frac{d\lambda}{dt} = \frac{1}{4}\left[1 + \frac{1}{3}\frac{m}{M}\left(\frac{l}{r_0}\right)^2\right]^{-\frac{1}{2}} - \frac{m}{M}\frac{l_0}{r_0}\sqrt{\frac{2}{3}}. \qquad (61.27)$$

The total impulse arriving at the entire lateral surface is determined by the expression:

$$I = Mu_1 + I_1 = \frac{1}{2}\sqrt{\frac{1}{6}}\frac{l}{r_0} mD \frac{1}{\sqrt{1 + \frac{1}{3}\frac{m}{M}\left(\frac{l}{r_0}\right)^2}} + \frac{8}{27} mD \frac{1}{\left[1 + \frac{1}{3}\frac{m}{M}\left(\frac{l}{r_0}\right)^2\right]^3}. \qquad (61.28)$$

Best Available Copy

$$u_{1\infty}=\frac{I}{M}=u_1+\frac{I_1}{M}=\frac{1}{2}\sqrt{\frac{1}{6}}\frac{l}{r_0}\frac{m}{M}D\frac{1}{\sqrt{1+\frac{1}{3}\frac{m}{M}\left(\frac{l}{r_0}\right)^2}}+$$
$$+\frac{8}{27}\frac{m}{M}D\frac{1}{\left[1+\frac{1}{3}\frac{m}{M}\left(\frac{l}{r_0}\right)^2\right]^{2/3}}, \qquad (61.29)$$

for $l=0$, $u_{1\infty}=\frac{8}{27}\frac{m}{M}D$, for $l\to\infty$, $u_{1\infty}=\frac{1}{2}\sqrt{\frac{m}{M}}D$, (61.30)

Expression (61.29) does not take into account the distribution of the velocities of the fragments along the length of the charge. It is obvious that in the centre of the charge the velocities will be greater than at the periphery. Expression (61.29) gives only the average value of the velocity of the fragments, which is necessary for practical calculations. An accurate solution of the problem set, taking into account the distribution of velocities, can only be carried out by the method of characteristics.

Analysis of equation (61.29) shows that with increase in the length of the charge, the velocity of the fragments quite rapidly approaches to its limiting value and attains it for $2l\approx 8r_0$.

For axial initiation (radial detonation) the effect of the axial dispersion is reduced to a considerable extent, which is as if the length of the charge were increased.

This also leads to an increase of impulses and velocities of the fragments. The increase in impulses as a result of axial initiation has been verified by experiment.

§62. One-dimensional Projection of Bodies by the Detonation Products.

The theory of this problem was worked out by K.P.STANYUKOVICH.

Let us consider the motion of a body, projected by the detonation

Best Available Copy

products of a condensed explosive for the strictly one-dimensional problem (motion of the gas and the body in a tube).

Suppose that at the point $x=0$ a detonation has been initiated : the detonation products flow to the left into a space which may be assumed a vacuum (the presence of air does not, in practice, change the results of the calculation). A detonation wave proceeds to the right, which, for high explosives is characterized by an adiabatic law

$$p = A\rho^k. \qquad (82.1)$$

The one-dimensional motion of the detonation products is described by the equations :

$$u = \frac{2c - D}{k-1}; \qquad (82.2)$$

$$x = (u + c)\,t, \qquad (82.3)$$

where p is the pressure, ρ is the density of the detonation products, c is the local velocity of sound, and D is the velocity of the detonation wave.

Suppose that the length of the charge is l and that at the right hand side of it there is a body, the mass of which is M. Obviously, the mass of explosive is equal to $m = sl\rho_0$, where s is the cross-sectional area of the charge and ρ_0 is its initial density.

At the instant of time $t_1 = \frac{l}{D}$, the detonation wave reaches the body and, on being reflected from it, sets it into motion. Since, as is well-known, the entropy at the front of the reflected shock wave is increased very insignificantly, even for impact of a detonation wave against an absolutely solid wall, then the problem concerning the reflection of the wave from the solid body can be considered as an acoustic approximation, to an accuracy of a few percent.

Best Available Copy

For the third case (for $k=3$) we have :

$$\frac{\partial (u \pm c)}{\partial t} + (u \pm c)\frac{\partial (u \pm c)}{\partial x} = 0, \qquad (32.4)$$

which, as is known, gives

$$x = (u+c)t + F_1(u+c), \quad x = (u-c)t + F_2(u-c). \qquad (32.5)$$

Here $u+c$ and $u-c$ define the parameters of the reflected wave.

The boundary conditions for the given problem will be the condition of conjugation of the reflected wave with the wave described by equations (32.3) and (32.5), and the condition at the surface of the solid body :

$$M\frac{du}{dt} = sp; \quad u = \frac{dx}{dt}. \qquad (32.6)$$

The first case indicates that $F_1(u+c) = 0$; and consequently

$$x = (u+c)t. \qquad (32.7)$$

Taking into account that $p = p_1\left(\frac{c}{c_1}\right)^3$, where $p_1 = \frac{64}{27}p_2 = \frac{16}{27}\rho_0 D$ and $c_1 = D$, equation (32.6) can be reduced to the following form :

$$\frac{du}{dt} = \frac{s \cdot 16\rho_0 c^3}{M \cdot 27D} = \frac{\gamma c^3}{lD}, \qquad (32.8)$$

where

$$\gamma = \frac{16}{27}\frac{m}{M} \quad \text{and} \quad s\rho_0 = \frac{m}{l}.$$

Differentiating equation (32.7) with respect to t, we obtain

$$-\frac{du}{dt} = \frac{c}{t} + \frac{dc}{dt}. \qquad (32.9)$$

Comparing equations (32.9) and (32.8), we have

$$\frac{dc}{dt} + \frac{c}{t} + \frac{\gamma c^3}{lD} = 0. \qquad (32.10)$$

In order to solve equation (32.10) we shall use the substitution $c = \frac{z}{\sqrt{t}}$.

Then equation (32.10) will assume the form

Best Available Cop

$$\frac{dz}{d\ln t} = -\left(\frac{1}{2}z + \frac{\gamma}{lD}z^3\right)$$

or

$$\frac{dz^2}{z^2\left(1+\frac{2\eta}{lD}z^2\right)} = -d\ln t.$$

The solution of this equation does not present special difficulty. After elementary transformations we obtain :

$$z = \frac{l\theta}{\gamma}, \tag{32.11}$$

where

$$\theta = \left[1+2\eta\left(1-\frac{l}{Dt}\right)\right]^{-\frac{1}{2}}. \tag{32.12}$$

From equation (32.7) we find :

$$u = \frac{dx}{dt} = \frac{x-l\theta}{t}. \tag{32.13}$$

On integrating, we find

$$x = Dt\left[1+\frac{1-\sqrt{1+2\eta\left(1-\frac{l}{Dt}\right)}}{\eta}\right] = Dt\left[1+\frac{\theta-1}{\eta\theta}\right]. \tag{32.14}$$

Substituting the value found for x in equation (32.13), we obtain

$$u = D\left[1+\frac{\theta-1}{\eta\theta}-\frac{l}{Dt}\theta\right], \tag{32.15}$$

which gives the law of motion of the body.

We shall determine now the value of $u-c$. It is obvious that

$$u-c = \frac{x-2l}{t} = D\left[1+\frac{\theta-1}{\eta\theta}\right]-\frac{2l}{t}, \tag{32.16}$$

whence it follows that

$$F_2(u-c) = 2l. \tag{32.17}$$

Since

$$\frac{l}{Dt} = 1+\frac{\theta^2-1}{2\eta\theta^2}, \tag{32.18}$$

then

$$u-c = D\left[1+\frac{\theta-1}{\eta\theta}-\theta-\frac{\theta^2-1}{\eta\theta^2}\right] = D\left[1-2\theta+\frac{1-\theta}{\eta}\right]. \tag{32.19}$$

Hence it follows that

$$\theta = \frac{D(\eta+1) - \eta(a-c)}{D(2\eta+1)}$$

and

$$u - c = \frac{x - \frac{2l(\eta+1)}{2\eta+1}}{t - \frac{2\eta l}{(2\eta+1)D}}. \qquad (62.20)$$

Equations (62.7) and (62.20) completely solve the problem which has been posed. We shall now consider the two limiting cases. Let $M = 0$ and $\eta \to \infty$; then the problem boils down to a study of the motion of the interface produced as a result of their dispersion in vacuo. Equation (62.20) for this gives

$$u - c = \frac{x - l}{t - \frac{l}{D}}. \qquad (62.21)$$

Suppose now that $M \to \infty$ and $\eta = 0$, for this, the problem is analogous to that considered for the reflected wave from an absolutely solid wall :

$$u - c = \frac{x - 2l}{t}. \qquad (62.22)$$

This expression also results from the relationships which we determined earlier.

In conclusion we shall derive the limiting formulae which describe the law of motion of the projected body for $\frac{M}{m} < 1$ and $\frac{M}{m} > 1$.

For $\frac{M}{m} < 1$ and correspondingly large values of η, by using equations (62.14) and (62.15) and by means of expanding these equations into series with respect to powers of $\frac{1}{\sqrt{\eta}}$ we obtain :

$$\frac{x}{Dt} = 1 - \sqrt{\frac{2}{\eta}\left(1 - \frac{l}{Dt}\right)},$$

$$\frac{u}{D} = 1 - \sqrt{\frac{2}{\eta}\left(1 - \frac{l}{Dt}\right)} - \frac{\frac{l}{Dt}}{\sqrt{2\eta\left(1 - \frac{l}{Dt}\right)}}. \qquad (62.23)$$

Best Available Copy

For large values of $\frac{M}{m}$, expanding the expression in powers of η, we obtain

$$\frac{x}{l} = 1 - \eta + \frac{\eta}{2}\left(\frac{Dt}{l} + \frac{l}{Dt}\right), \quad \frac{u}{D} = \frac{\eta}{2}\left(1 - \frac{l^2}{(Dt)^2}\right); \tag{64.24}$$

for $t \to \infty$ $\frac{x}{l} = 1 - \eta + \frac{\eta}{2}\frac{Dt}{l}$, $\frac{u}{D} = \frac{\eta}{2}$.

It is obvious that for $M = 0$, the impulse of the projected body $I = 0$, for $M \to \infty$ $I = Mu = \frac{16}{27}\frac{mu}{\eta}$; for $t \to \infty$ $u = \frac{D\eta}{2}$; and consequently $I = \frac{8}{27}mD$, which, as we established earlier, corresponds to the total momentum of the detonation products as a result of their dispersion.

We can see that for large values of $\frac{M}{m}$, the absolute term is absent from the relationship between I and η; in order to determine the relationship between I and η, it is necessary to expand x with respect to η up to terms containing η^2.

On carrying out the calculation for u and I, we obtain, for $t \to \infty$:

$$\frac{u}{D} = \frac{\eta}{2}(1 - \eta); \quad I = \frac{8}{27}mD(1 - \eta).$$

In conclusion, we shall show that if the detonation products are dispersed in all directions (detonation of an open charge), then the relationships which we have derived will hold good, if by the quantity "mass of charge" m we understand the mass of its active portion m_a.

Table 101

Comparison of experimental and calculated velocities of plates, projected by the explosion of explosive charges.

m, g	ρ_0, g/cm³	D, m/sec	M, g	η	u_{exp}, m/sec	u_{calc}, m/sec	$\frac{u_{exp}}{u_{calc}} \cdot 100\%$
22.8	1.30	6880	6.60	2.04	2440	2670	91.6
22.8	1.40	7515	6.80	1.98	2540	2790	90.5
22.8	1.50	7690	6.82	1.87	2700	2450	91.5
22.8	1.60	8000	6.79	1.98	2830	3060	90.3
11.8	1.40	7515	6.91	1.18	2050	2170	93.5

The results of the experimental investigations verify the theory which has been developed quite well, as can be seen from Table 101, in which comparisons are made of the experimental and calculated (calculated according to relationship (62.15)) velocities of plates in the case of a charge of phlegmatized hexogen. The charge was installed in a thick steel tube.

.....

CHAPTER XII

CUMULATION *

§ 65. General Introduction

The cumulative effect is a substantial increase in the local effect of an explosion. This effect is obtained by using charges having a recess at one end - the cumulative recess. If such a charge be initiated from the opposite end, then the brisance effect in the direction of the axis of the recess turns out to be considerably greater than that resulting from normal charges. It has been established experimentally that if the surface of the cumulative recess be covered by a thin metallic casing, then the armour-piercing action of a cumulative charge is increased many times (Table 102).

Table 102

Effect on armour of normal and cumulative charges.

Charge characteristics	Obstacle	Nature of deformation of obstacle.
Solid, cylindrical; height 180mm, diameter 65mm	Armour plate, thickness 200mm	Indentation
Ditto, with conical recess, without casing	-Ditto-	"Crater", with depth 22mm
Ditto, recess has steel casing, thickness 2mm	-Ditto-	Through-puncture

The increased local effect of charges with recesses has been known for more than 100 years. However, for a long time no proper attention was paid to this phenomenon and cumulative charges were not used in military and peaceful technology.

The first systematic investigations of the phenomenon of cumulation were

* The generally accepted name for this phenomenon is charge shaping, and the effect is known as the shaped-charge effect

carried out during 1925 - 1926 by SUKHAREVSKII, who established the relationship between the armour-piercing action of cumulative charges(without casing) and the shape of the recess and a number of other factors.

Cumulative charges attained wide practical application only during the period of the Second World War. These charges were used in ammunition and in demolition agents designed for combatting tanks and fortifications.

Only during the years of the Second World War were serious experimental and theoretical investigations of cumulation initiated. The most outstanding work in this field is attributed to Soviet Scientists (POKREVSKII, LAVRENT'EV, et al).

The structural hydrodynamic theory of cumulation, based on accurate physical ideas, was worked out in 1945 by LAVRENT'EV and independently also by the American scientists Taylor, and Raechelberger et al.

On the basis of military experiments it can be concluded that cumulative munitions are effective agents of attack against armoured targets and engineering structures. They have also found wide application in technology, especially for extraction of petroleum.

The study of this problem must necessarily commence with a study of the cumulative effect in a pure form, i.e. in the absence of a metallic casing on the surface of the recess.

With the use of normal charges (not having recesses) we are concerned exclusively with the propagation of the divergent(chiefly spherical) explosion products and shock waves. The characteristic feature of such motion is the rapid decrease of the basic gas parameters (pressure, velocity, density) primarily as a consequence of the energy distribution of the explosion with respect to the motion of the detonation products and of the shock waves in a continuously increasing spherical volume.

On the contrary, as a result of the motion of the convergent stream of detonation products or of the shock waves, a considerable increase of the parameters of the medium occurs. The specific feature of such motion is the sharp increase in the energy density of the gas, which in its turn leads to a considerable increase in the local destructive effect of the explosion. Similar motions are attained as a result of the explosion of specially-shaped charges - cumulative charges.

Thus, the cumulative effect consists in the fact that it is associated with a considerable compression of the detonation products, an increase in their pressure, and also with a considerable increase in energy density of the dispersing detonation products, as well as in the shock waves originating as a result of the explosion.

A spherical, convergent shock or detonation wave serves as a classical example of cumulation. Pressures of around a million atmospheres may originate at the centre of convergence of such a wave. This form of cumulation, in particular, can be realized by the use of hemispherically-shaped charges with simultaneous initiation of explosion over the entire outside surface. However, the entire cumulative effect in the given case will be centred inside a cavity - in the zone adjacent to the centre of the sphere. This form is purely radial cumulation, which may find an extremely limited practical application. Nevertheless, it is of great scientific interest, since as a result of its consideration, certain features are revealed which apply generally for the cumulative effect as a whole.

The most important practical significance is that of directional axial cumulation. This form of cumulation can be achieved by exploding charges having a recess of one shape or another (hemispherical, conical, paraboloidal, hyperboloidal, etc). Axial cumulation is dependent on compression of the detonation

products and their acceleration along the axis of the recess. This form of cumulation, in contrast from radial cumulation, is always associated with the formation and directional motion of the so-called cumulative jet.

§64. Dispersion of Explosion Products from the Inclined Surface of a Charge.

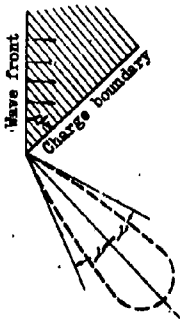
In order to determine the conditions for the formation of a cumulative jet as a result of axial directional cumulation, it is necessary to consider first of all the fundamental laws of discharge of the detonation products from a hollow cumulative recess, which in its turn leads to a review of the problem concerning the flow of detonation products from an inclined plane, i.e. it leads to the study of detonation of a linear charge in the case when the detonation wave approaches the surface of the charge at a certain angle.

In analyzing the diagram of the dispersion of the surface layer of the charge as a result of an inclined detonation wave, it can be proved that the main portion of the energy of this layer is radiated within quite a small angle, the bisector of which makes an angle γ with the normal to the surface of the charge, depending on α (Fig.157), where α is the angle between the detonation wave front and the surface of the charge. On the average, more than 70% of the energy of the surface layer is radiated within an angle of 10^0 : $\gamma = 15^0$ for $\alpha = \frac{\pi}{2}$; $\gamma = 10^0$ for $\alpha = \frac{\pi}{4}$.

We recall, that in calculating the dispersion of the detonation products, resulting from PRANDTL - MEYER's solution, we are correct in speaking only of the dispersion of the surface layer of explosive. Dispersion of the deeper layers will not conform with the law quoted; with increase of thickness of the charge, the thickness of the surface layer to which this solution applies, is

increased.

Figure 157. Dispersion of detonation products from an inclined plane.



Theory, as well as experiments, shows that the surface layer of a cumulative charge carries the main portion of the energy expended on destruction of the obstacle.

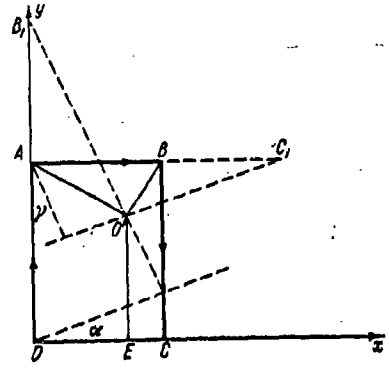
We shall analyse in detail the detonation of an extended linear charge. The experiments of POKROVSKII and DOBRYCHAYEV are in complete agreement with theory and have shown that the maximum effect on an obstacle are exerted by the detonation products making an angle of $7 \div 14^\circ$ with the normal to the surface of the charge. Since the main portion of the energy of a linear charge is concentrated within a small angle, then it is possible to construct geometrically the fronts of the dispersing detonation products of such a charge, given by any equation, i.e. a charge having the form of any arbitrary curve. Conversely, it is possible to determine the equation of the linear charge which produces at a given distance a given surface for the front of the detonation products.

Great interest is presented by a linear charge having a "Pi"-shape (Fig. 158). If such a charge be initiated at one of the ends, for example at the point O, then the following takes place: the front of the detonation products, proceeding from the line OA through an angle γ, and the front proceeding from the line AB through the same angle, meet along the line O'A ; as a result of this, $\angle OAO' = \frac{\pi}{4} + \gamma$. Similarly, we obtain the line O'B for AB and BC, and,

finally, the line of encounter O'E for OA and BC. It is obvious that the point O' has the coordinates

$$x = AB\cos^2(45° - \gamma) = \frac{AB}{2}(1 + \sin 2\gamma);$$
$$y = OA - \frac{AB}{2}\cos 2\gamma.$$

Figure 158. Detonation of a "Pi"-shaped charge.



If this charge be placed on a metallic plate, then maximum deformation of the metal will be observed just along the line AO', O'B and O'E. It is obvious that by measuring the angles OAO', ABO' and the coordinates of the point O', the angle γ can be determined with a high degree of accuracy, and also the quantity $\frac{D}{\bar{u}} = w$, since $\sin\gamma = \frac{\bar{u}}{D}$ (γ is the Mach angle in the given problem).

Suppose that the maximum action of the detonation products is moving with a velocity $\bar{u}$. Then, as a result of the detonation of the linear charge, the surface of propagation of the maxima will have a rectilinear shape. Since it is an envelope aggregate of the individual waves, then its angle of inclination to the surface of the charge will also be the Mach angle.

It should be noted that here $\bar{u}$ is not the velocity of the particles, but the velocity of motion of the maximum itself, which is several times less than the velocity of the particles. A similar case occurs with the one-dimensional dispersion of a gas issuing from a flask, when the velocity of motion ε_{max} is $\bar{u} = \frac{c_1}{\gamma}$, but the maximum velocity of the particles is

$$u_{max} = \frac{c_1}{\gamma}\frac{3\gamma - 1}{\gamma + 1} = \bar{u}\frac{3\gamma - 1}{\gamma + 1},$$

which for $\gamma = 3$ gives $u_{max} = 2\bar{u}$.

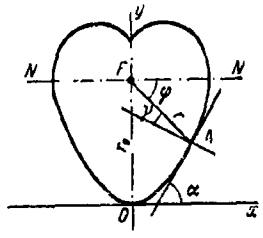
It is obvious that the very clear and sharp zone of action of the maximum $(\overline{\rho u^n})$ gives the possibility of focussing the stream of detonation products. This is possible as a result of the following conditions. The detonation products, proceeding from the different points of the detonating surface should converge simultaneously at the focal point; consequently, the front of the convergent wave of the detonation products should be spherical, and the angle between the tangent to the surface of the charge and the direction at the focus is constant. We shall derive the equation for such a "cumulating" surface. First of all we shall consider the plane problem and we shall derive the equation of the "cumulating" curve, giving a convergent circular wave. We shall arrange that the origin of the coordinates is at the focus of this curve. Suppose that a detonation be initiated at a certain point O (Fig. 159). Then, from the principle of tautochronism (Fermat's Principle) we have

$$\frac{\overline{OA}}{D}+\frac{AF}{\overline{u}}=\frac{OF}{\overline{u}}=\text{const.}$$

Hence, for the length of the arc OA we obtain the expression

$$\smile OA=\int_{\frac{\pi}{2}}^{\varphi}\sqrt{r^2+\left(\frac{dr}{d\varphi}\right)^2}\,d\varphi=(OF-AF)\frac{D}{\overline{u}}=\frac{D}{\overline{u}}(r_0-r), \tag{64.1}$$

Figure 159. Polarographic spiral.



where $\overline{u}$ is the velocity of motion of the maximum of action.

Differentiating expression (64.1) with respect to φ, we obtain

$$\frac{dr}{r}=-\frac{d\varphi}{\sqrt{\frac{D^2}{\overline{u}^2}-1}}. \tag{64.2}$$

Solving equation (64.2), we find

$$r=r_0 e^{\frac{\varphi+\frac{\pi}{2}}{\sqrt{\frac{D^2}{\overline{u}^2}-1}}}. \tag{64.3}$$

We have obtained the equation of a polarographic spiral.

By forming the surface of rotation(axis of rotation OF), we obtain the cumulating surface, giving a convergent spherical wave. As is well-known, a polarographic spiral satisfies the condition that : the angle between the tangent at any point A and the radius-vector is a constant value.

It is obvious from the construction that this angle is equal to $90°-\gamma$, and that $90°-\gamma=180°-(\alpha+\varphi)$, where α is the angle of slope of the tangent.

Hence,

$$\gamma=\alpha-90°+\varphi.$$

Since

$$\tan(90°-\alpha)=\cot\alpha=\frac{\frac{r'}{r}-\operatorname{tg}\varphi}{\frac{r'}{r}\operatorname{tg}\varphi+1}=\tan\left[\arctan\frac{r'}{r}-\varphi\right]=\tan[-(\varphi+\gamma)],$$

then

$$\arctan\frac{r'}{r}=-\gamma;\quad \frac{r'}{r}=-\tan\gamma,$$

but, as we have established

$$\frac{r'}{r}=-\frac{1}{\sqrt{\frac{D^2}{\bar{u}^2}-1}},$$

therefore

$$\tan\gamma=\frac{1}{\sqrt{\frac{D^2}{\bar{u}^2}-1}}\quad\text{and}\quad\sin\gamma=\frac{\bar{u}}{D}. \tag{64.4}$$

Thus, the basic relationship for a rectilinear charge also holds good in the case being considered. The polarographic spiral is the only curve which as a result of focussing the detonation products, simultaneously possesses the property of tautochronism and the property of directing from every element of its surface to the focus, the detonation products with precisely identical parameters through the very same angle. Experiments with detonating cord give good agreement with theory. For detonating cord

$$\frac{\bar{u}}{D} = \frac{1}{5}, \quad \gamma = 14°.$$

The maximum deformation of the plate on which rests the spiral made of detonating fuse, occurs at the theoretical focus of the spiral to an accuracy of a few percent.

The "volume" charge, formed by rotating the polarographic spiral round the axis OF and which gives a convergent wave from the detonation products is of great interest from the principle point of view, since such a charge with sufficiently large dimensions will create extremely high pressures at its focus, which may attain a million atmospheres. The initial average pressure of the detonation products is equal to 100,000 atm.

The surface formed by rotation of the polarographic spiral will be the "cumulative" surface of the charge guaranteeing simultaneous focussing of the detonation products only in the case when the detonator is located close to the point O. If the layer of explosive between the detonator and the cumulative surface(at the point O) is of sufficient thickness, then the shape of the cumulative surface already considered will not possess the specified properties, since it will no longer satisfy simultaneously tautochronism and discharge of the detonation products through the specified angle to the surface of the charge (for a specified angle between the detonation front and the surface). By cutting out a portion of the charge, formed by rotation of the polarographic spiral (for example through the plane NN), we obtain an actual cumulative charge which is capable of guaranteeing an extremely high pressure in the zone of convergence of the elementary jets. However, the armour-piercing capability of a charge like this will be small; this is explained by the fact as a result of its detonation the normal cumulative axial jet action does not develope. This problem will be considered below in more detail.

The theory of an open cumulative charge , guaranteeing directional axial

cumulation, presents considerably greater difficulty than the theory of a closed charge, since the stream of detonation products will possess not central (point) symmetry, but axial symmetry, which increases the number of independent variables of the problem by one. However, the laws established above enable a number of useful qualitative conclusions to be drawn relative to the nature and process of formation of a cumulative jet and to carry out certain approximate calculations of its parameters.

Process of Formation of a Cumulative Jet. It was established above that the main portion of the energy of the detonation products, adjacent to the boundary of the exploded charge, is radiated within a small angle, the bisector of which forms an angle γ with the surface of the charge. Hence it follows that for discharge through the surface of the cumulative recess, the detonation products will deviate from their initial trajectory, so that the maximum effect will be in the direction almost perpendicular to this surface. Abnormal refraction of the detonation products occurs and a shock wave front is created ahead of them. As a result of this motion of elementary jets, a stream of detonation products will be formed, converging along the axis of the cumulative recess and possessing increased density and velocity in relation to the detonation products, which are dispersed in other directions. The process of formation of a cumulative jet is shown diagrammatically in Fig.160.

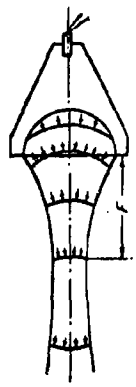


Figure 160. Formation of a Cumulative Jet.

Individual elementary jets will move normal to the surface of the

recess only in the vicinity of the recess itself. As a result of the further motion, the jets are straightened in accordance with the general laws of gas dynamics. At a certain distance from the base of the recess, maximum compression of the cumulative jet takes place. This distance F also determines the point of location of the so-called cumulative focus. At a distance exceeding the focal distance, the cumulative jet rapidly degenerates as a consequence of the radial flight of the detonation products, which are compressed to a high pressure.

It is known that the cumulative effect is manifested quite clearly only in the immediate vicinity of the charge. With increasing distance from the charge, the cumulative effect is sharply reduced and then dies out completely. It can be concluded from this that the action of a cumulative charge is conditioned principally by the shock of the detonation products(cumulative jet), which, at close distances from the explosion focus , possess a considerably higher density than the density of the air in the shock wave moving ahead of them. Even for normal discharge of detonation products, as we established in Chapter IX, the air density at the shock front is approximately 20 - 30 times less than the density of the stream of detonation products. The difference in the densities of the air and the cumulative stream is even more considerable.

Thus, we arrive at the conclusion that by studying the phenomenon of cumulation, it is necessary to pay particular attention to the consideration of the motion of the explosion products, and especially to that portion of them which, in particular, forms the cumulative jet . Problems associated with motion of the shock wave are of secondary importance in the given case.

Results of experiment have shown that the maximum velocity of the cumulative jet (the velocity of its leading portion) for high explosive charges amounts to 12 - 15 km/sec. The focal distance depends first and foremost on the shape of the recess : the less the curvature of the cumulating surface,

the less is the refraction undergone by the explosion products in discharging through this surface and the less is the corresponding focal distance.

In principle, the recess can be assigned such a shape that the cumulative focus will be located at a distance exceeding the zone of direct action of the explosion products.

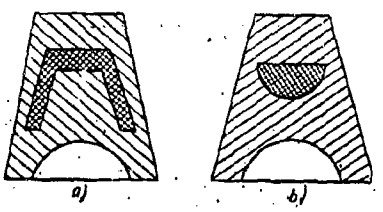
In this particular case, the cumulative effect will be chiefly dependent on the convergence of the shock waves. However, the action of similar cumulative charges will be considerably inferior to the action of a normal cumulative charge.

The focal distance for a given shape of recess varies in relation to the detonation velocity of the explosive charge. We shall analyse this situation by the example of a charge with a hemispherical recess. If the detonation wave arrives simultaneously at the entire surface of the hemisphere, then the cumulative focus will be found only a little beyond the centre of the hemi- hemisphere. The non-coincidence of the focus with the centre of the hemisphere is explained by the fact that for axial cumulation the elementary jets are straightened according to its proximity to the axis of the charge. The simultaneous arrival of the shock front at the entire surface of the recess, obviously, is possible only for an infinitely large detonation velocity. Hence it follows that the lower the detonation velocity of the explosive charge, the greater is the corresponding focal distance. This circumstance is one of the reasons for the considerable decrease in the cumulative effect as a result of detonating cumulative charges of low-brisance explosives (ammonites, etc).

For a given shape of recess and given properties of the explosive charge, the focal distance can be varied by introducing inside the charge specially selected "lenses" of an inert material, or of another explosive. These "lenses"

enable the detonation process to be directed, thus ensuring in particular, simultaneous arrival of the detonation wave at the surface of the recess. Figure 161 shows charges with "lenses". In case *a*, regulation of the time of arrival of the detonation wave at the surface of the recess is ensured by changing the direction of the detonation front; in case *b*, the lens is of an explosive with a lower detonation velocity.

Figure 161. Cumulative charges, with lenses.



In order to elucidate the influence of the shape and dimensions of the recess on the destructive action of a cumulative charge, and also in order to compute the energy and mass of the cumulative jet, it is necessary first of all to establish which part of the explosive charge, in particular, forms the cumulative jet. We shall call it the "active portion of the cumulative charge".

§ 65. Active Portion of a Cumulative Charge.

In order to assess the active portion of a cumulative charge, we shall use the system of instantaneous detonation. In this case the rarefaction waves proceed from all sides of the charge with uniform velocity, which permits the shape to be determined simply of the surface of the two convergent rarefaction waves, coming from any two surfaces, in this case when these surfaces are specified (Fig. 162).

Let the equation for the surface of revolution *1* be

$$y_1 = f_1(x_1). \qquad (65.1)$$

The equation for surface of revolution 2 is

$$y_2 = f_2(x_2). \qquad (65.2)$$

We shall write the unknown equation in the form

$$y = f(x). \qquad (65.3)$$

It is obvious from the construction that

$$x = x_1 - z, \quad y = y_1, \quad x = x_2, \quad y = y_2 - z. \qquad (65.4)$$

Eliminating z, from equation (65.4), we arrive at the relationship

$$y - y_2 = x - x_1. \qquad (65.5)$$

Since

$$x_1 = \varphi_1(y_1) \quad \text{and} \quad y_1 = y,$$

and

$$y_2 = f_2(x_2) \quad \text{and} \quad x = x_2,$$

then relationship (65.5) assumes the form

$$y + \varphi_1(y) = x + f_2(x). \qquad (65.6)$$

Figure 162. Active portion of a cumulative charge.

This equation determines the unknown surface of encounter of the two rarefaction waves. It is obvious that the line $y = f(x)$ should be equal to the departure of the lines $y_1 = f_1(x_1)$ and $y_2 = f_2(x_2)$. It is not difficult in principle to find the equation of this line. However, since inside the recess the stream of detonation products is dispersed more slowly than from the external face, a relatively large portion of the detonation products will issue from the external face. Therefore the line $y = f(x)$ is displaced close to the line $y_2 = f_2(x_2)$.

If the distance from the rear surface of the charge (Fig. 162) to the

point O is not less than the distance from it to the apex of the recess(not less than r), then the line of encounter of the rarefaction waves will be approximately the line of separation of the bulk of the explosion products, dispersing in different directions. It is obvious that the volume of the active portion of the charge v_a, of the portion moving in the direction of the cumulative recess, is determined - if the displacement of the line $y=f(x)$, is not taken into account because of the somewhat different conditions of flow of the detonation products from the external and internal surfaces - by the integral

$$v_a = \pi \int_0^{r+h} y^2 dx - \pi \int_h^{r+h} y_1^2 dx_1. \qquad (65.7)$$

As a result of this

$$y = y_1; \quad dx = dx_1 + dy_1 - dy_2,$$

which follows from equation (65.5).

It is necessary to know

$$x_1 = \varphi_1(y_1),$$

then

$$dx_1 = \frac{d\varphi_1}{dy_1} dy_1$$

and

$$v_a = \pi \int_0^{r_0} y_1^2 \left(dy_1 + \frac{d\varphi_1}{dy_1} dy_1 - dy_2\right) - \pi \int_0^{r_0} y_1^2 \frac{d\varphi_1}{dy_1} dy,$$

which gives

$$v_a = \frac{\pi r_0^3}{3} - \pi \int_0^r y_1^2 dy_2. \qquad (65.8)$$

It remains to find y_2 as a function of y_1, which is not difficult, since

$$y_1 = f_1(x_1) \qquad \text{and} \qquad y_2 = f_2(x).$$

On the other hand,

$$x = \varphi_1(y_1) = \varphi_2(y_2),$$

which gives

and

$$y_2 = \Phi(y_1)$$

$$v_a = \frac{\pi r_0^3}{3} - \pi \int_0^{r_0} y_1^2 \frac{d\Phi}{dy_1} dy_1. \qquad (65.9)$$

In the particular case when

$$y_2 = r_0 = \text{const}$$

(cylindrical charge), equation (65.6) assumes the form

$$y + \varphi_1(y) = x + r_0$$

and the volume of the active portion is determined by the formula

$$v_a = \frac{\pi r_0^3}{3}, \qquad (65.10)$$

since in equation (65.9) the expression under the integral sign is equal to zero, i.e., the active portion depends only on the calibre of the charge. As a result of this, it is assumed that the radius of the base of the recess is equal to the semi-diameter of the charge. From this, one must draw the conclusion that the active portion of the charge is reduced by varying the diameter of the base of the recess. Consequently, in order to obtain a large active portion in a charge of given diameter, it is essential that the diameter of the base of the recess be made as large as possible.

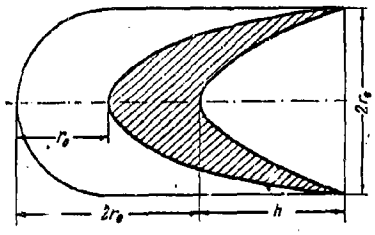


Figure 163. Active portion of a cylindrical cumulative charge.

For an example we shall consider a cylindrical charge with a hemispherical end section and a recess of arbitrary shape (Fig.163). The height of the charge is equal to $2r_0 + h$. The volume of this charge is equal to

$$v_0 = \pi r_0^2 (r_0 + h) + \frac{2}{3}\pi r_0^3 - \pi \int_0^{r_0} \frac{y_1^2 dy}{y_1'} =$$

$$= \frac{5}{3}\pi r_0^3 + \pi r_0^2 h - \pi \int_0^{r} \frac{y_1^2 dy}{y_1'}. \qquad (65.11)$$

The ratio

$$\frac{v_0}{v_a} = 5 + 3\frac{h}{r_0} - \frac{3}{r_0^3}\int_0^{r_0} \frac{y_1^2 dy}{y_1'}, \qquad (65.12)$$

where

$$y_1' = \frac{dy_1}{dx}. \qquad (65.13)$$

For a conical recess

$$\pi \int_0^{r_0} \frac{y_1^2\,dy}{y_1'} = \frac{\pi}{3} r_0^2 h, \quad v_0 = \frac{5}{3}\pi r_0^3 + \frac{2}{3}\pi r_0^2 h, \tag{65.14}$$

$$\frac{v_0}{v_a} = 5 + 2\frac{h}{r_0}. \tag{65.15}$$

Hence it is obvious that for actual charges $(h \approx 2r_0)$

$$\frac{v_0}{v_a} \approx 9,$$

i.e. the mass of the active portion of the charge will comprise 11% of the mass of the whole charge. The charge shown in Fig.165 has the minimum possible volume, for which the whole of it is used for calculating the active portion.

The active portion of a flat(non-cumulative charge) is determined as before by the relationship

$$v_a = \frac{\pi}{3} r_0^3.$$

The minimum volume of a similar charge is

$$v_0 = \pi r_0^3 + \frac{2}{3}\pi r_0^3 = \frac{5}{3}\pi r_0^3. \tag{65.16}$$

Therefore $\frac{v_0}{v_a} = 5$, which can be obtained directly from formula (65.14) by substituting $h = 0$ in it. Similarly, a cylindrical non-rounded charge will have

$$v_0 = 2\pi r_0^3 \text{ and } \frac{v_0}{v_a} = 6. \tag{65.17}$$

STANYUKOVICH, having likewise investigated the propagation of rarefaction waves for detonation products dispersing under actual conditions, showed that the relationshipsderived above for the active portion of any charge, are applicable, for instantaneous detonation, with an accuracy of 5% for calculating the active portion in the case of an actual detonation.

On analysing the results obtained, we can arrive at the following conclusions. The minimum height of charge for which its active portion attains its limiting value is equal, for a cylinder, to $H_{lim} = 2r_0 + h$, which, for actual cumulative charges with a conical recess without casing, corresponds approximately to 2 diameters. By reducing the length of the charge, the weight of the

active portion is reduced more slowly than the weight of the whole charge. This permits charges with a height of $H < H_{lim}$ to be used in cumulative munitions, without noticeably reducing the cumulative effect.

It follows from equation (65.10), that with increasing diameter of the base of the cumulative recess, the cumulative effect should increase considerably, since the mass of the active portion is proportional to the cube of the calibre.

We shall study now the effect of a casing and of a lining for a cumulative charge on the size of the active portion. We shall consider the following one-dimensional problem : Suppose that in an infinite non-deformable tube two bodies of masses M_1 and M_2 move in opposite directions under the action of an expanding gas(detonation products). The mass M_1 is moving to the right and M_2 is moving to the left. It is required to determine the velocities(u_1 and u_2) of motion of the masses, and also the mass of the detonation products moving to right and to left (m_1 and m_2). The following relationships are obvious :

$$u = \frac{x}{t}; \quad m = m_1 + m_2; \quad \rho = \frac{m_1 + m_2}{t(u_1 - u_2)}. \tag{65.18}$$

Assuming that the velocity of the gas is distributed linearly with respect to its masses m_1 and m_2, then from the Law of Conservation of Momentum we obtain

$$\frac{m_1 u_1}{2} - \frac{m_2 u_2}{2} + M_1 u_1 - M_2 u_2 = 0. \tag{65.19}$$

The Law of Conservation of Energy gives

$$\frac{m_1 u_1^2}{6} + \frac{M_1 u_1^2}{2} + \frac{m_2 u_2^2}{6} + \frac{M_2 u_2^2}{2} = mQ = \frac{m\bar{c}_l^2}{6}. \tag{65.20}$$

where $\bar{c}_l$ is the velocity of sound in the detonation products(for the case of instantaneous detonation). It is further obvious, that since

$$u = \frac{x}{t}, \text{ then } \quad \frac{u_1}{m_1} = \frac{u_2}{m_2}. \tag{65.21}$$

Solving simultaneously equations (65.19), (65.20) and (65.21), and taking into account that $m = m_1 + m_2$, we obtain

$$m_1 = \frac{m}{2}\left(1 + \frac{M_2 - M_1}{M_1 + M_2 + m}\right), \quad m_2 = \frac{m}{2}\left(1 + \frac{M_1 - M_2}{M_1 + M_2 + m}\right); \tag{65.22}$$

$$\left(\frac{u_1}{\bar{c}_i}\right)^2 = \frac{2m\,(m+2M_2)^2\,(M_1+M_2+m)}{(m+2M_2)^2\,[m\,(m+2M_2)+6M_1\,(M_1+M_2+m)]+(m+2M_1)^2} \times$$

$$\times \frac{1}{[m\,(m+2M_1)+6M_2\,(M_1+M_2+m)]}, \tag{65.23}$$

$$\left(\frac{u_2}{\bar{c}_i}\right)^2 = \frac{2m\,(m+2M_1)^2\,(M_1+M_2+m)}{(m+2M_2)^2\,[m\,(m+2M_2)+6M_1\,(M_1+M_2+m)]+(m+2M_1)^2} \times$$

$$\times \frac{1}{[m\,(m+2M_1)+6M_2\,(M_1+M_2+m)]}. \tag{65.24}$$

We now determine the unilateral impulse

$$I_1 = -I_2 = u_1\left[M_1 + \frac{m_1}{2}\right] = -u_2\left[M_2 + \frac{m_2}{2}\right]. \tag{65.25}$$

In the particular case when $M_2 = 0$,

$$I_1 = -I_2 = -\frac{m_2 u_2}{2} = \frac{u_1}{2}[2M_1 + m_1]. \tag{65.26}$$

Since for $M_2 = 0$

$$M_1 = \frac{m^2}{2(m+M_1)}, \quad \frac{u_1}{\bar{c}_i} = \frac{m}{\sqrt{(m+4M_1)\,(m+M_1)}},$$

then

$$I_1 = -I_2 = \frac{m\bar{c}_i}{4}\,\frac{(m+2M_1)^2}{(m+M_1)\sqrt{(m+M_1)\,(m+4M_1)}}; \tag{65.27}$$

for $M_1 \to 0$ $I_1 = \frac{m\bar{c}_i}{4}$; for $M_1 \to \infty$ $I_1 = \frac{m\bar{c}_i}{2}$. These results are obvious, since as a result of reflection from an absolutely solid wall $(M_1 \to \infty)$ the impulse is doubled.

If $M_1 = M_2 = M$, then

$$m_1 = m_2 = \frac{m}{2}, \tag{65.28}$$

$$u_1 = -u_2 = \bar{c}_i\sqrt{\frac{m}{m+3M}}, \tag{65.29}$$

$$I_1 = -I_2 = \frac{\bar{c}_i}{4}(m+2M)\sqrt{\frac{m}{m+3m}}. \tag{65.30}$$

If $M \to 0$, то $I_1 = \frac{m\bar{c}_i}{4}$; for $M \to \infty$ $I_1 = \frac{m\bar{c}_i}{2}\sqrt{\frac{Mm}{3}} \to \infty$, which is quite naturally so, since for $M_1 = M_2 = M \to \infty$, the pressure at the wall will

act for an infinitely long time.

This same scheme can be used with a high degree of accuracy for studying the disintegration of the active portion of a cumulative charge, assuming that m is the mass of the explosive enclosed between the casing and the lining units, and that M_1 and M_2 are the masses of these units. The distance between the casing and lining units is chosen with respect to the shortest straight line.

§ 66. Cumulation with Metallic Lining of the Recess.

In the presence of a metallic lining, as already noted, a very sharp intensification of the cumulative effect is observed at the surface of the recess. Notwithstanding this circumstance, the same physical peculiarities are maintained in this case which are characteristic of an explosion of a cumulative charge without lining of the recess. However, the picture of the phenomenon under discussion as a result of this is considerably altered.

It has been established as a result of experimental and theoretical investigations that the intensification of the cumulative effect in the presence of a lining is associated with the extremely powerful and unique redistribution of energy between the explosion products and the material of the metallic lining, and the conversion of part of the metal into a cumulative jet. The main part of the energy of the active portion of a cumulative charge is " pumped over" into the metal of the lining so that a thin layer is concentrated in it, which really forms the cumulative jet. As a consequence of this, a considerably greater energy density is attained in the jet than by the explosion of a charge without lining of the recess. The maximum " squeezing", determined by the ratio of the diameter of the recess to the diameter of the jet, for a charge without lining is equal to 4 - 5. For a charge with a metallic recess lining, the "squeezing"

is considerably greater, since the diameter of the cumulative jet is equal to 1 - 3mm.

The nature of the cumulative jet and the mechanism of its formation has been successfully established by methods of instantaneous X-ray techniques, spark photography etc, in comprehensive experimental investigations. The method of instantaneous X-ray photography is particularly fruitful for investigating the phenomenon of cumulation in the presence of a metallic lining.

The process has been studied in the most detail on charges with hemispherical and conical recess linings. To sum up these investigations, it was established that a metallic lining, under the action of the explosion products, is squeezed, as a result of which its sections are "slammed together" with the formation of a fine metallic jet, which possesses a high velocity.

The overall picture of the process of deformation of the metallic lining and the formation of a cumulative jet is shown in the two series of X-ray photographs (Figs, 164 & 165). They fix the process of squeezing of the lining and the motion of the jet with respect to time. On processing the experimental data it was proved that the maximum velocity of radial deformation of a steel cone with a wall thickness of 1 - 2mm, depending on the type of explosive charge, amounts to 1000 - 2500 m/sec. As a result of such rapid compression , the lining is transformed into a compact monolithic mass - a pestle (Fig.166), giving rise initially to the formation and subsequent development of the cumulative jet. As a result of the compression of each section of the lining, its thickness is increased, but the energy is mainly concentrated in its outer layer. The jet is formed exclusively on account of the stream of metal adjacent to the inner surface of the lining, which appears as a consequence of the rapid collision of its sections at the instant of "slamming together".

Figure 164 Formation of a cumulative jet by compression of a hemispherical lining : a - charge prior to explosion, b - charge 6 msec after explosion, c - after 8 msec, d - after 12 msec, e - after 24 msec.

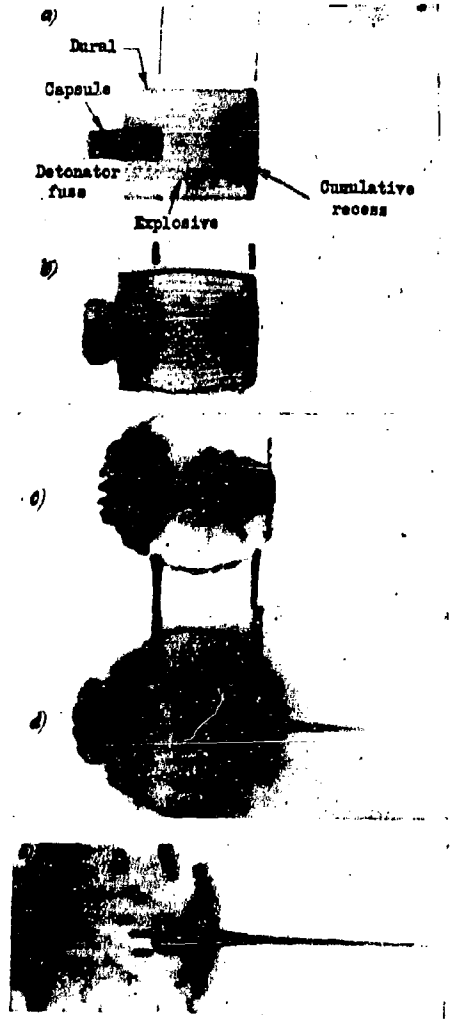
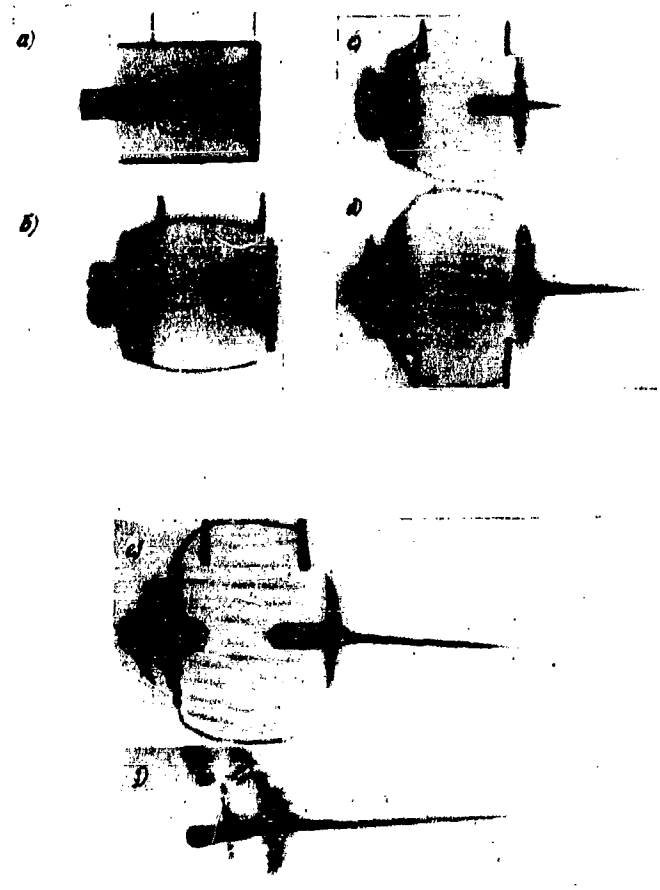


Figure 165. Formation of a cumulative jet by compression of a conical lining : a - prior to explosion, b - charge 6 msec after explosion, c - after 12 msec, d - after 15 msec, e - after 17 msec, f - after 24 msec.



The mass of metal transformed into the cumulative jet, amounts on the average to 6 – 11% of the mass of the lining.

Confirmation of the fact that the cumulative jet is associated with the stream of metal, in addition to the results given, is afforded by the following data. If a layer of copper, with a thickness of 0.05mm, be deposited on the inside surface of a steel cone by means of galvanising, then no trace of copper can be found at all in the pestle. If, however, the layer of copper is deposited on the outer surface of the cone, then streaks of copper oxide are discovered in the pestle. On inspection of the pestle, a narrow channel can be found along its axis, the presence of which is an indication that the inner layers of metal have a sharp increase in velocity in relation to the outer layers. The results of metallographic examinations of pestles in sections at different distances from the axis also afford information concerning the nature of the deformation of a metallic lining during the process of its compression.

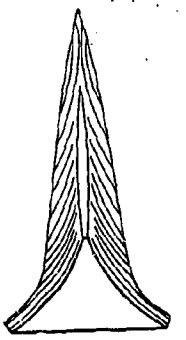


Figure 166. Pestle.

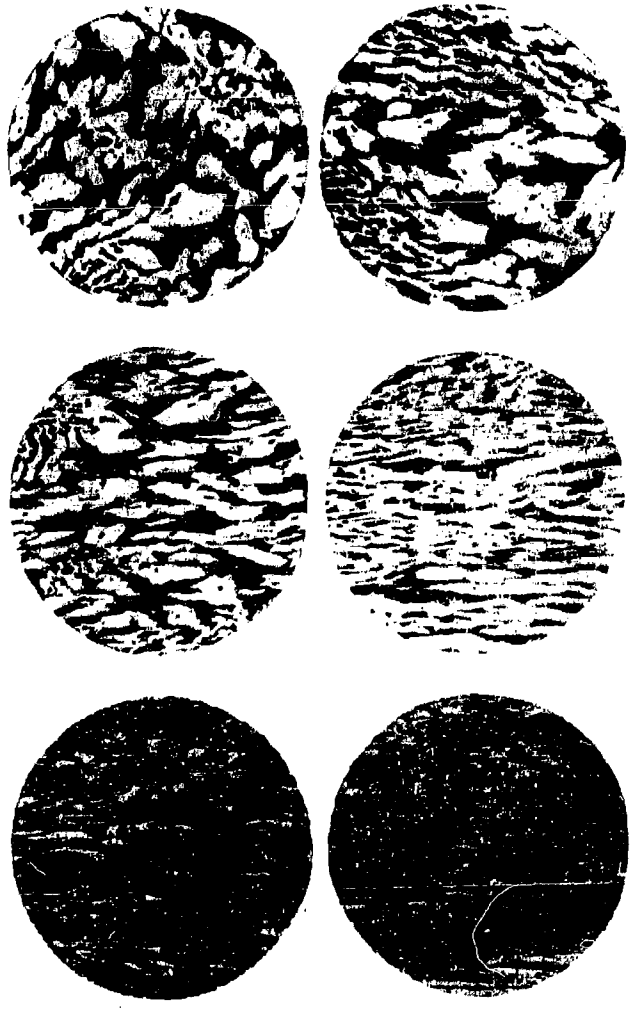
The orientation and stretching of the structural constituents can easily be seen in all the microstructure photographs (Fig. 167), in the axial direction.

The orientation and stretching are increased according to the extent of the proximity of the respective layers to the axis.

The formation and motion of a cumulative jet can be divided into two stages. The physical and mechanical characteristics of the metal of the lining have a considerable influence on these stages.

First Stage. The first stage characterizes the formation of the jet in the process of compression of the lining. During this period, the pestle and the jet comprise a single structure(see Figs. 164 & 165); however, their motion is accomplished with different velocities.

Figure 167. Microphotographs of thin sections of the pestle (brass)



The pestle moves relatively slowly(with a velocity of 500 - 1000 m/sec). The jet, on the other hand, has an extremely high velocity of forward motion. However, this velocity is different in different parts along the jet; the leading portion of the jet has the maximum velocity, and the velocity of the tail section is close to the velocity of the pestle. Depending on the shape and nature of the lining metal, the properties of the explosive charge and other factors, the velocity of the leading portion of the jet may vary within wide limits. For an aluminium lining of hyperbolic shape, the velocity of the leading portion attains, for example, approximately 11,000 m/sec.

Figure 168. Motion of a cumulative jet before and after piercing armour plate.



Some data on the velocity of the leading part of a cumulative jet are presented in Table 105.

The Cumulative charges are prepared, in all cases, from a mixture of trotyl and hexogen ($D = 7600$ m/sec).

The velocity gradients along a cumulative jet were established by direct experiment, namely by means of mirror scanning using a method of step-by-step

"chopping" of differents sections of the jet with obstacles of different thickness (Fig.168). This method was first developed and used in 1946 by BAUM and SHEKHTER. Subsequently it attained wide application for investigating the process of cumulation.

Table 103

Dependence of the velocity of the leading portion of a cumulative jet on certain factors.

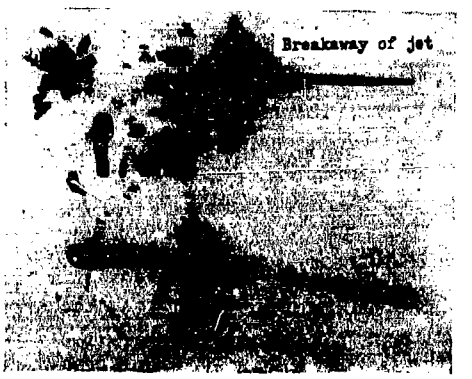
Charge dimensions		Nature of lining		Shape of recess	Parameters of recess		Velocity of leading portion of jet, m/sec	Velocity of leading* portion of jet, m/sec.
Diameter, mm	Height, mm	Material	Thickness, mm		Diameter of depression, mm	Angle of flare of cone, deg		
30	70	Steel	1	Hemispherical	28	-	5000	6050
30	70	"	1	Conical	27.2	60	6500	7650
30	70	"	1	"	27.2	55	7500	8500
30	70	"	1	"	27.2	27	7400	9000
30	70	"	1	Hyperbola	27.2	-	9500	-
42	85	"	4	"	57.2	-	7150	10700

*) Data for charges with an aluminium lining, thickness 1 mm.

Second Stage. During a certain interval of time after compression of the lining, the jet, because of the presence of velocity gradients, breaks away from the pestle(Fig.169). It can be assumed that the maximum effective action of a cumulative charge is achieved in the case when the jet is severed, subsequent to the supply of metal to it from the pestle being discontinued, which prior to a definite instant of time represents a unique reservoir, maintaining the supply for the jet. This may take place up to the time when the inertial

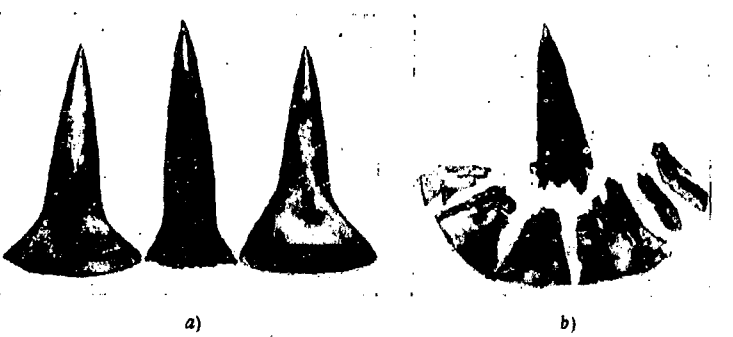
forces, under the action of which the flow of metal takes place, will no longer be in equilibrium with the cohesive forces between the metallic particles. From this point of view, a high plasticity of the material is a decisive factor.

Figure 169 Breakaway of the jet from the pestle.



This factor is of particularly important significance for the normal process of compression of the lining. In the process of deformation, no frangible breakdown of the lining should occur, since if the contrary is the case, the transfer coefficient of metal into the jet is sharply reduced, and its armour-piercing action is correspondingly reduced. Figure 170 shows linings in various stages of deformation, prepared from low-carbon and tempered steels.

Figure 170. Compression of linings of (a) soft and (b) tempered steel.



It can be seen from the figure, that compression of the first three specimens is not accompanied by brittle fracture (Figure 170 a); the lining made from tempered steel is shattered as a result of compression (Fig. 170 b).

It is obvious that the conditions for breakaway of the jet from the pestle are determined by the velocity gradient and the physico-mechanical characteristics of the metal from which the lining is made, and upon which depends the maximum elongation of the jet. On the basis of what has been stated, it may be concluded that the most effective action of a cumulative jet may be ensured only by a definite combination of the physico-mechanical properties of the lining metal. For this, it should be borne in mind that the properties of a metal under conditions of rapid deformation may differ considerably from its properties defined for normal deformation velocities. For example, cast iron, which is brittle under normal conditions, behaves as a metal with a relatively high plasticity as a result of the explosion of a cumulative charge.

As a result of investigations carried out by BAUM and SKLYAROV, the following was established.

The conditions of formation of a cumulative jet are determined by the microstructure of the lining metal and the ability of its structural constituents towards plastic deformation.

However, the plasticity of a metal under compression conditions, brought about by the action of an explosion, is not determined solely by its normal characteristics. The relationship between the ability of the metal towards rapid compression and the type of crystal lattice should be mentioned. The best compression is observed with linings of metal with a cubic lattice (Al, Fe, Cu); the worst compression is observed with metals having a hexagonal lattice(Cd, Co, Mg). The best armour piercing effect is attained for linings of copper and iron.

By catching a cumulative jet in certain loose media followed by metallographic analysis, it has been established that in the process of formation of a jet, melting of the metal does not occur. However, the temperature of the jet may exceed 900 ÷ 1000°C.

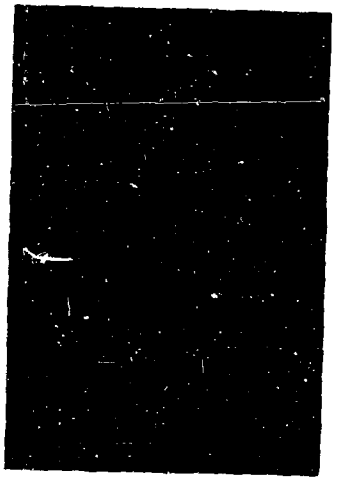


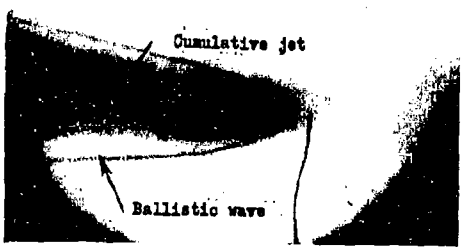
Figure 171. Photo-scan of the motion of the leading portion of a cumulative jet.

Motion of the jet in air is accompanied by considerable oxidation of the metal, which is associated with the elevated temperature of of the surface layers, because of air friction. As a result of this, intense luminescence of the cumulative jet is observed, especially in the case when the lining is made from duralumin or aluminium. This permits the motion of the jet to be photographed in its own light, with the aid of photo-scans, and to determine from the photographs the velocity of its motion. A typical photo-scan of the motion of a jet is shown in Figure 171.

A cumulative jet maintains its monolithic property only in the first stages of its motion. Before long, under the influence of the velocity gradients, its dispersion into particles takes place. The initial stage of destruction of a jet is shown in Fig. 172, which is a photograph obtained by an exposure of about 10^{-8} sec. This exposure was achieved by means of an electro-optical shutter, based on the Kerr effect. The equipment for the electro-optical shutter was devised by B.A.IVANOV. The formation of a "neck" can be clearly distinguished in

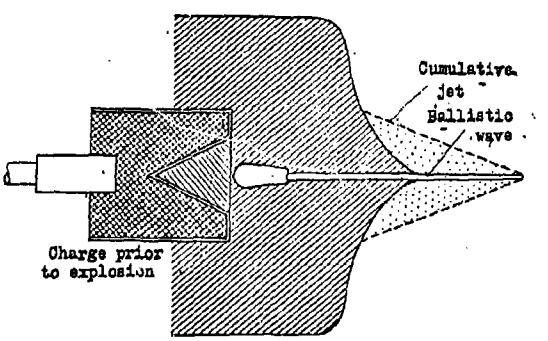
the photograph, along which breakup of the jet takes place into individual particles.

Figure 172. Spark-photograph of a dispersing cumulative jet(45 msec after commencement of the explosion).



The use of this method, combined with microsecond- X-ray photography, enables a complete picture to be reconstructed of the explosion of a cumulative charge in the presence of a metallic cumulative recess (Fig.175).

Figure 175. Explosion of a cumulative charge (diagrammatic)



The physical concepts developed above concerning the phenomenon of cumulation in the presence of a lining have served as the basis for an analytical interpretation of this phenomenon. For this, the classical theory of convergent jets has been used to advantage.

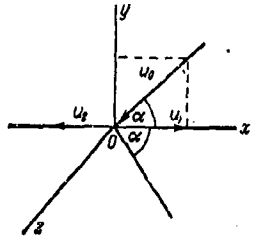
G.I.POKROVSKII first used this theory to describe the process of cumulation in the presence of a conical lining. The assumption is made in the theory that as a result of compression of the lining, the elastic and viscous forces can be neglected in comparison with the inertial forces, under the action of which compression of the lining takes place. The justification for this assumption is substantiated in the work of M.A.LAVRENT'YEV, creator of the hydrodynamic theory of cumulation. From consideration of this case, the metal of the lining, on compression, may be likened to an ideal incompressible liquid.

In order to arrive at the results of this theory, it is necessary to consider the fundamental aspects of the theory of convergent jets.

§ 67. Elements of the Theory of Convergent Jets.

We shall now consider the laws of motion of an incompressible liquid, as a result of the convergence of two identical plane jets (i.e. we shall consider a two-dimensional problem).

Figure 174. Collision of Jets.



It is well-known, that as a result of the convergence of two identical jets(identical in velocity and delivery) through a certain angle (2α), two jets are again formed, the liquid in which moves to opposite sides, in the direction of the bisector of the angle of convergence(Fig.174). As a result

of this, as follows from the Law of Conservation of Mass, Momentum and Energy, the velocities of the diverging jets are equal to each other with respect to magnitude, but opposite in sign and equal to the velocities of the original converging jets. The masses of liquid moving in the diverging jets are different. In the jet, in which the direction of motion of the liquid coincides with the projection onto the x - axis of the direction of motion of the initial jets, the mass of liquid is greater than in the jet oppositely directed. We shall now prove the validity of these statements.

It is obvious that the problem being considered is analagous to the problem of divergent jet colliding through an angle α with an ideal solid surface, coinciding with the plane xOz.

Suppose the supply of liquid per second in the impacting jet be m_0; let the velocity of the liquid in the jet be u_0. Denoting the jets diverging to right and left, simdlarly, by m_1, m_2, u_1, u_2 (supplies and velocities), we arrive, on the basis of the Laws of Conservation of Mass, Momentum and Energy, at the following relationships :

$$m_1 + m_2 = m_0, \quad -m_1u_1 + m_2u_2 = m_0u_0, \tag{67.1}$$

$$m_1u_1 + m_2u_2 = -m_0u_0\cos\alpha, \tag{67.2}$$

$$\frac{m_1u_1^2}{2} + \frac{m_2u_2^2}{2} = \frac{m_0u_0^2}{2}. \tag{67.3}$$

Hence, it follows that

$$-u_1 = u_0 = u_2, \tag{67.4}$$

$$\frac{m_1}{m_0} = \frac{1-\cos\alpha}{2} = \sin^2\frac{\alpha}{2}, \tag{67.5}$$

$$\frac{m_2}{m_0} = \frac{1+\cos\alpha}{2} = \cos^2\frac{\alpha}{2}. \tag{67.6}$$

It is assumed here that the original jet flows from right to left and from above to below.

Since the density of the liquid remains unchanged, then the masses can be substituted by the cross-section of the jet ; as a result of this,

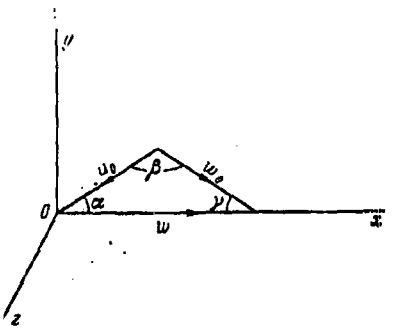
$$\frac{\delta_1}{\delta_0} = \sin^2\frac{\alpha}{2}, \quad \frac{\delta_2}{\delta_0} = \cos^2\frac{\alpha}{2},$$

where δ_0, δ_1 and δ_2 are the cross-sectional dimensions of the original and divergent jets ($m = \rho\delta|u|$, where ρ is the density of the liquid).

Suppose now that the point of intersection of the jet with the plane xOz is moving along the x-axis in the positive direction(to the right)with a certain velocity w, , then the velocity of the jet, diverging to the right (jet I) and to the left (jet II), will be

$$\left.\begin{aligned} w_1 &= u_1 + w, \\ w_2 &= u_2 + w. \end{aligned}\right\} \qquad (67.7)$$

Figure 175. Collision of jet(point of intersection of the jet with the plane is moving along the plane)



Here and in future $u_2 < 0$. In this case, in the system of coordinates in which the point of intersection is statioary, the resulting velocity w_0 and the direction (angle β) of motion of the original jet are determined from the relationship (Fig.175)

$$w_0^2 = u_0^2 + w^2 - 2u_0 w\cos\alpha, \qquad (67.8)$$

$$\sin\beta = \frac{w}{w_0}\sin\alpha, \qquad (67.9)$$

In this system of coordinates , the motion of the plane stream is observed, having a finite thickness through the front and intersecting the plane xOz through a certain angle $\gamma = 180° - (\alpha + \beta)$.

If the velocity of the liquid w_0 and the angle β between the direction of motion and the front of the stream, moving towards the plane xOz , and also the angle α , are given, then it is always possible to transfer to the system of

coordinates in which the point of intersection of the plane with the front of the liquid remains stationary.

It is of interest to consider three cases of motion of the liquid.

1. Let the angle $\beta = \frac{\pi}{2}$ (direction of motion of the liquid perpendicular to its front).

Then,

$$w_0 = w \sin\alpha = \sqrt{w^2 - u_0^2} \tag{67.10}$$

Hence we obtain

$$w = -\frac{u_0}{\cos\alpha}, \quad w_0 = -u_0 \tan\alpha, \quad w_1 = -u_0 \frac{1+\cos\alpha}{\cos\alpha}.$$

Taking into account relationship (67.7), we find

$$w_1 = w_0 \frac{1+\cos\alpha}{\sin\alpha} = \frac{w_0}{\operatorname{tg}\frac{\alpha}{2}}, \quad w_2 = -u_0 \frac{1-\cos\alpha}{\cos\alpha} \tag{67.11}$$

or

$$w_2 = w_0 \frac{1-\cos\alpha}{\sin\alpha} = w_0 \operatorname{tg}\frac{\alpha}{2}. \tag{67.12}$$

2. Let the angle $\beta = \frac{\pi}{2} - \alpha$ (direction of motion of the liquid perpendicular to the x-axis).

Then

$$w_0 = w \tan\alpha = \sqrt{u_0^2 - w^2}. \tag{67.13}$$

Hence,

$$w = u_0 \cos\alpha, \quad w_0 = -u_0 \sin\alpha, \quad w_1 = -u_0(1+\cos\alpha)$$

or

$$w_1 = w_0 \frac{1+\cos\alpha}{\sin\alpha} = \frac{w_0}{\tan\frac{\alpha}{2}}, \tag{67.14}$$

$$w_2 = -w_0 \frac{1-\cos\alpha}{\sin\alpha} = -w_0 \tan\frac{\alpha}{2}. \tag{67.15}$$

3. Let $w_2 = 0$, which corresponds to the plane of the retarded jet II. Then, from the conditions of (67.7), (67.8) and (67.9) we obtain :

$$-u_0 = w, \quad w_0 = -u_0\sqrt{2(1-\cos\alpha)} = -u_0 \sin^2\frac{\alpha}{2}, \tag{67.16}$$

$$w_1 = -2u_0 = \frac{w_0}{\sin\frac{\alpha}{2}}, \tag{67.17}$$

$$\sin\beta = -\sin\alpha\frac{u_0}{w_0} = \cos\frac{\alpha}{2}, \tag{67.18}$$

whence

$$\beta = \frac{\pi - \alpha}{2}. \tag{67.19}$$

Analysis of these simple relationships show, that on intersection with the stream of the plane xOz, redistribution of the mass and energy of the original stream takes place, between the two streams formed. As a result of this, jet I, moving to the right, has small mass but large energy, and jet II, on the contrary, has a large mass but small energy.

For given velocity w_0 and angles α and β, u_0, w, w_1 and w_2 are determined in the general case from the relationships

$$\left.\begin{aligned} -u_0 &= w_0 \frac{\sin(\alpha+\beta)}{\sin\alpha}, \\ w &= w_0 \frac{\sin\beta}{\sin\alpha}, \\ w_1 &= w_0 \frac{\sin\beta + \sin(\alpha+\beta)}{\sin\alpha}, \\ w_2 &= w_0 \frac{\sin\beta - \sin(\alpha+\beta)}{\sin\alpha}. \end{aligned}\right\} \tag{67.20}$$

The length of each jet, obviously, is equal to the length of the original jet. This follows from the fact that in the stationary system of coordinates the velocities, and consequently the lengths of all the jets are identical. The mass to energy ratio of these streams, as shown by relationships (67.5), (67.6) and (67.20), are determined by the formulae

$$\frac{m_1}{m_2} = \tan^2\frac{\alpha}{2}, \tag{67.21}$$

$$\frac{E_1}{E_2} = \frac{m_1 w_1^2}{m_2 w_2^2} = \left[\tan\frac{\alpha}{2} \cdot \frac{\sin\beta + \sin(\alpha+\beta)}{\sin\beta - \sin(\alpha+\beta)}\right]^2. \tag{67.22}$$

Hence it follows, that for $\alpha < \frac{\pi}{2}$

$$\frac{m_1}{m_2} < 1, \quad \frac{E_1}{E_2} > 1.$$

When $\beta = \frac{\pi - \alpha}{2}$ and $w_2 = 0$ (Fig.176), the entire energy transfers to jet I and, consequently, the energy density in it, in comparison with that originally, increases considerably. Since the energy density calculated per unit mass is $\frac{w^2}{2}$.

then

$$\frac{w_1^2}{w_0^2} = \frac{1}{\sin^2 \frac{\alpha}{2}}. \qquad (67.25)$$

For $\beta > \frac{\pi - \alpha}{2}$, the liquid in jet II will move to the right; for $\beta < \frac{\pi - \alpha}{2}$ it will move to the left; consequently, the energy density in jet I is reduced in comparison with the value as determined by relationship (67.25).

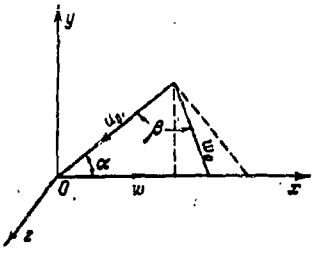


Figure 176 Collision of jets. Case of formation of a single jet after collision $\left(\beta = \frac{\pi - \alpha}{2}\right)$.

When the length of the original jet in the stationary system of coordinates, or the length of the stream front in a system of coordinates in which the point of intersection of the jet and the plane xOz, is stationary, is small, its leading portion will not be described by the relationships given above, since the liquid in this portion will have a non-stationary motion, being subject to a more complex law. The consideration of the effect of two non-identical jets colliding through a certain angle is somewhat more complex than for identical jets. We shall not study this problem, since the primary interest in the phenomenon of cumulation has already been presented in the problem being considered.

Collision of jets, taking into account the compressibility of the medium, can be studied for relatively slow plane motions. The basic equations for this can be written in the same form as for an incompressible medium. This is essentially, that for supersonic jets as a result of impact and divergence of the jet, in the plane xOz, one or several oblique compression discontinuities are formed. This leads to an increase in the entropy of the medium, and consequently, as a

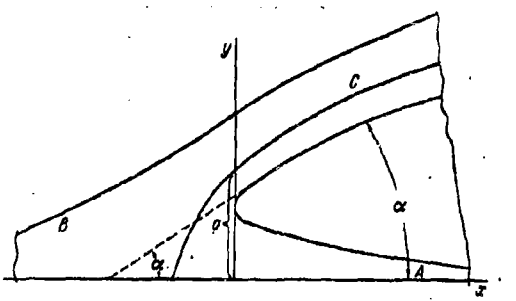
result of its expansion to its initial(atmospheric) pressure, it leads to the fact that its density will be less than the original for the gas, but the temperature will be higher. As a result of expansion of the liquid jets, phenomena may take place which are similar to the phenomenon of cavitation, i.e. disruption of the jet may occur.

§68. Elements of the Theory of Cumulation in Presence of a Metallic Lining.

The theory of the cumulative effect in the presence of a metallic lining has been most fully developed for charges with a conically shaped recess.

M.A.LAVRENT'EV has considered in detail the following problem : the sections of a conical lining with constant wall thickness instantaneously acquire a velocity which is normal to that forming it. The compression velocity is constant along the cone generatrix This statement of the problem can be boiled down to a consideration of the problem of collision of jets for an axi-symmetrical steady stream of an ideal liquid. Figure 177 shows a cross-section of such a stream, obtained by approximation methods.

Figure 177. Convergence of jets (steady stream of an ideal liquid). C - original jet, A and B - diverging jets.



At the origin of the coordinates, the velocity of the stream is equal to zero. For $x \to -\infty$ the stream is a cylindrical jet with radius r_1 and velocity $-u_0$. For $x \to \infty$ the stream is a cylindrical jet with radius r_0 and velocity u_0. The sections at the borders of the "shroud" have the general asymptote

$$y = x \tan \alpha + a, \tag{68.1}$$

whereupon

$$\tan \frac{\alpha}{2} = \frac{r_0}{r_1}. \tag{68.2}$$

From the condition that at the free surface of the "shroud" the stream velocity is equal to u_0, the supply of liquid into the "shroud" is equal to

$$\pi (r_0^2 + r_1^2) u_0 = 2\pi y \, \delta u_0, \tag{68.3}$$

where δ is the thickness of the "shroud".

Hence, it is not difficult to find an approximate expression for the thickness of the "shroud" δ in terms of the coordinate y and the radii of the jets r_0 and r_1:

$$\delta = \frac{r_0^2 + r_1^2}{2y} = \frac{r_0^2}{2y}\left(1 + \cot^2 \frac{\alpha}{2}\right). \tag{68.4}$$

Formula (68.4) is accurate for $y \to \infty$.

In order to calculate the parameters of a cumulative jet, we shall consider the motion of the liquid as a result of collision of the jets in the system of coordinates moving uniformly to the right with a velocity

$$v_0 = \frac{u_0}{\cos \alpha},$$
$$\xi = x - v_0 t.$$

In the new system of coordinates ξ, y, the conical shroud C will have a velocity w_0, orthogonal for $x \to \infty$ to the asymptotic cone A, which is formed, and which corresponds to the case of compression being considered (the sections of the cone have a velocity normal to the generatrix). As a result of this,

$$w_0 = u_0 \tan\alpha, \tag{68.5}$$

the velocity of the cumulative jet is

$$w_1 = w_0 \frac{1+\cos\alpha}{\sin\alpha}, \tag{68.6}$$

and the velocity of the shroud

$$w_2 = w_0 \frac{1-\cos\alpha}{\sin\alpha}. \tag{68.7}$$

It is not difficult to see that relationships (68.6) and (68.7) are identical with the corresponding relationships for the jet velocities, obtained by considering the plane problem $\left(\beta = \frac{\pi}{2}\right)$. As a result of this, and arising from the theory of collision of plane jets, the length of the cumulative jet is equal to the length of the cone generatrix, and the radius of the jet $r_0 = \text{const}$.

In actual cumulative charges, the velocity of compression of the lining is not constant, since the impulse imparted to the lining by explosion of the charge, is also not constant along the line of its formation, which leads to the appearance of velocity gradients along the cumulative jet and to its disruption. Moreover, as a result of compression of the sections of the lining and the formation from them of the corresponding sections of the jet, there occurs a change in the angle α.

LAVRENT'YEV calculated the parameters of the cumulative jet for charges with a conically shaped recess and close to conical, taking into account these factors.

We shall now derive the solution of this problem for the particular case of a conical recess with constant lining thickness.

We consider the motion of an element of the cone having the abcissa x at a specified instant of time t (Fig.178).

In this case

$$y = x\tan\alpha. \tag{68.8}$$

We denote

$$u = 2\delta y = 2\delta x \tan\alpha. \qquad (68.9)$$

In addition, assuming a linear law for the distribution of impulse along the cone generatrix, we obtain for the velocity of compression w of the lining

$$w = w_0(1 - kx). \qquad (68.10)$$

The length of the normal between the element A of the lining and the axis is equal to $\eta = \frac{y}{\cos\alpha}$.

The element under consideration, with abcissa x at the instant of time $t_1 > t$ forms an element of the jet at the point with abcissa x_0, equal to

$$x_0 = x + y\tan\alpha. \qquad (68.11)$$

It is obvious that

$$t_1 = \frac{\eta}{w}. \qquad (68.12)$$

In virtue of the non-constant velocity w, after a time $t_1 - t$, the element is turned at an angle $\Delta\alpha$, so that

$$\Delta\alpha = -\frac{\eta}{w}\frac{dw}{dx}. \qquad (68.13)$$

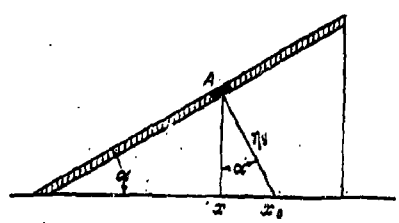


Figure 178. Motion of the elements of a conical lining.

Hence, assuming that

$$\bar{\alpha} = \alpha + \Delta\alpha \qquad (68.14)$$

and using relationships (68.6) and (68.10), we obtain for the velocity of the element of the jet,

$$w_1 = w_0(1 - kx)\frac{1 + \cos\bar{\alpha}}{\sin\bar{\alpha}}. \qquad (68.15)$$

The angle

$$\bar{\alpha} = \alpha + \Delta\alpha = \frac{\alpha + kx\tan\alpha}{1 - kx}. \qquad (68.16)$$

In accordance with formula (68.4), we have for the radius of the jet

$$r_0^2 = \frac{2\delta y}{1 + \cot^2\frac{\bar{\alpha}}{2}} = \frac{2\delta x\tan\bar{\alpha}}{1 + \cot^2\frac{\alpha}{2}}, \qquad (68.17)$$

which, after simple transformations gives

$$r_\omega = \sqrt{\delta x(\tan\bar{\alpha} - \sin\bar{\alpha})}, \qquad (68.18)$$

where x is distance from the leading portion of the jet.

In the proposed theory, the relationship has not been established for the velocity of compression of a cumulative lining as a function of the perameters of the explosive charge. Without this relationship, it is impossible to determine numerically the value of the basic parameters of the cumulative jet. In addition, in LAVRENT'YEV's theory, the strength characteristics of the metal of the lining, which in a number of cases may have an effect on the condition of formation of the cumulative jet.

We shall discuss the method for determining theoretically the parameters of a cumulative jet, taking into account the mass and energy of the active portion of a cumulative charge. This method has been developed by BAUM and STANYUKOVICH, who have also considered the problem of the limiting conditions of formation of a cumulative jet as a function of the strength characteristics of the lining metal.

We shall consider first of all the motion of the casing as a whole (the motion of the centre of gravity of the casing) as a result of the action on it of the dispersing detonation products, without taking into account its compression. This problem is easily solved on the basis of the general theory of a body projected by the detonation products.

The equation of Conservation of Energy for one-dimensional, uni-directional discharge of the detonation products in a hypothetical instantaneous detonation with synchronous projection of any body of mass M as a result of total expansion of the explosion products, can be written down in the form

$$\frac{Mu_m^2}{2} + \frac{s}{2}\int_0^{u_m} \rho u^2\, dx = mQ_v. \qquad (68,19)$$

Here u_m is the limiting velocity of the projectile, s is the cross-sectional area of the body, m is the mass of the explosion products.

Expression (68.19) is easily obtained, if it be assumed that the energy remaining in the detonation products is equal to

$$\frac{1}{2}\int_0^{u_m} u^2\,dm,$$

where $dm = s\rho\,dx$.

As the theory of one-dimensional discharge of the detonation products shows, for total expansion of the explosion products, i.e. when $p = p_a$, where p_a is the atmospheric pressure,

$$u = \frac{x}{t}, \quad \rho = \frac{m}{su_m t}. \tag{68.20}$$

Therefore,

$$\frac{1}{2}\int_0^{u_m} u^2\,dm = \frac{m}{2}\int_0^{u_m} \frac{x^3\,dx}{u_m t^3} = \frac{mu_m^2}{6}; \tag{68.21}$$

hence, taking into account that for an isentropy index of $\gamma = 3$ $D^2 \approx 16\,Q_v$, we obtain from equation (68.19)

$$\frac{u_m}{D} = \frac{1}{2\sqrt{2\left(\frac{M}{m}+\frac{1}{3}\right)}}. \tag{68.22}$$

This is the limiting velocity of the projectile and of the explosion products at the boundary with the projectile.

Dispersion of the explosion products, as we know, does not occur one-dimensionally, but, by introducing the concept of mass of the active portion of the charge $m = m_a$, (see para. 65), it can be assumed that the explosion products move along the axis of the charge. Consequently, in formulae (68.19) to (68.22), it should be understood that m is the active mass, m_a, of the charge. Strictly speaking, relationship (68.19), and consequently also (68.22) are valid for the case of instantaneous detonation.

Since the detonator is inserted in the portion of the charge opposite from that in which is located the cumulative recess, the energy density for an actual detonation, calculated per unit mass of the active portion of the charge, is greater than Q_v. We shall denote this energy density by

$$Q^* = \beta^2 Q_v, \tag{68.23}$$

where $\beta > 1$. As a result of this, relationship (68.22) assumes the form

$$\frac{u_m}{D} = \frac{\beta}{2\sqrt{2\left(\frac{M}{m_a} + \frac{1}{3}\right)}}. \tag{68.24}$$

We shall calculate the value of β.

The energy density at the detonation wave front for $\gamma = 3$ is equal to

$$Q_1 = \frac{1}{2}\left[u_1^2 + \frac{p_1}{\rho_1}\right]. \tag{68.25}$$

Since

$$u_1 = \frac{D}{4}, \quad p_1 = \frac{\rho_0 D^2}{4}, \quad \rho_1 = \frac{4}{3}\rho_0,$$

then

$$Q_1 = \frac{D^2}{8} = 2Q_v. \tag{68.26}$$

We now calculate the energy density Q_0 for that portion of the charge in which $u = 0$ (prior to dispersion). It is obvious that in this case

$$Q_0 = \frac{p_k}{\rho_k(\gamma - 1)} = \frac{p_1}{6\rho_0} = \frac{D^2}{24} = \frac{2}{3}Q_v, \tag{68.27}$$

since for $\gamma = 3$, $p_k = \frac{8}{27}p_1$ and $\rho_k = \frac{8}{9}\rho_0$.

It can be assumed with sufficient degree of accuracy that

$$Q^* = \frac{1}{2}(Q_1 + Q_0) = \frac{4}{3}Q_v. \tag{68.28}$$

There is no point in calculating the distribution of energy of the active portion of the charge more accurately, although, knowing its configuration, this is easily done.

It is well-known from the theory of one-dimensional dispersion, that a mass comprising 4/9 ths of the entire charge mass goes in the direction of

dispersion of the active portion of the charge, the energy of which comprises 16/27ths of the entire energy of the charge, and in the opposite direction there goes 5/9ths of the mass and 11/27ths of the energy. Consequently, in the first case the energy density will exceed the average by a factor of 4/3. On the basis of our calculations, we shall take $\beta^2 = \frac{4}{3}$, hence we finally obtain the relationship

$$\frac{u_m}{D} = \frac{1}{\sqrt{6\left(\frac{M}{m_a} + \frac{1}{3}\right)} \cdot \sqrt{\frac{M}{m_a} + \frac{1}{3}}} \approx \frac{0{,}41}{\sqrt{\frac{M}{m_a} + \frac{1}{3}}}. \qquad (68.29)$$

The centre of gravity of the lining will move with this velocity, without taking into account its compression. For an actual detonation, the average density of the explosion products of the active portion of the charge ρ^* is greater than the original density ρ_0 of the cumulative charge. The value of ρ^* may be assumed, with sufficient practical accuracy, to be equal to

$$\rho^* = \frac{1}{2}\left(\frac{4}{3}\rho_0 + \frac{8}{9}\rho_0\right) = \frac{10}{9}\rho_0. \qquad (68.30)$$

Relationship (68.30) can be used for calculating the active mass m_a. For a steel conical lining of a 76-mm missile, thickness 2mm for $h/d = 1.58$, we obtain

$$M = 130\ g \quad m_a = \frac{\pi r_0^3}{3}\rho_0 \approx 45\ g.$$

For $D = 7600$ m/sec (mixture of trotyl-hexogen), $u_m = 1750$ m/sec.

We shall now consider the motion of the casing simultaneously with its compression. In order to calculate the basic laws, observed as a result of this, we shall consider the following scheme.

Suppose that detonation takes place instantaneously. A plane plate of mass M moves under the action of the expanding detonation products, such that

its lower portion slides along the axis of symmetry (Fig. 179). It is obvious, that in the scheme of instantaneous detonation, the velocity of the plate will be normal to its surface, i.e. $u_m = w_{0max}$. This velocity corresponds to the maximum velocity of "slamming" of the lining. However, the different points of the plate(lining) will actually have a different velocity of motion relative to the axis of symmetry.

This is explained by the fact that the distance to the axis of symmetry for different elements of the lining will be different, since any body does not acquire its limiting velocity instantaneously, but over the path of its motion. Moreover, the angle of inclination of the lining to the axis of symmetry will be changed (increased) during the process of its compression. Therefore, the average velocity of compression of the lining will be

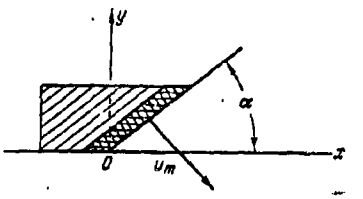


Figure 179. Motion of a plane plate under the action of detonation products.

$$\bar{u} = \bar{w}_0 = \eta \frac{0.41D}{\sqrt{\frac{M}{m_0} + \frac{1}{3}}}. \quad (68.51)$$

The coefficient η takes into account the uncomplete utilisation of the energy of the active portion of the charge and the error in the average increase of the angle of inclination of the lining to the axis as a result of its compression. We shall consider this problem in more detail below, and we shall calculate the coefficient $\bar{\eta}$.

Assuming in the case being considered that the direction of motion of the lining is perpendicular to its generator $\left(\beta = \frac{\pi}{2}\right)$, we obtain finally, in the scheme for an ideal liquid, an approximate relationship determining the

velocity of motion of the jet

$$\overline{w_1} = \overline{\eta}\frac{0.41D}{\sqrt{\frac{M}{m_a}+\frac{1}{3}}}\frac{1}{\tan\frac{\alpha}{2}}. \qquad (68.32)$$

As we shall see below, $\overline{\eta} = 0.67$ (for the example being considered); therefore $w_1 \approx 7500$ m/sec, which is close to the experimentally established value.

It follows from the theory that with reduction of the angle of flare of the cone, the velocity of the jet should be increased. This corresponds with experimental data (Table 103).

It follows also from equation (68.32), that by observing geometrical similarity in relation to the shape of the charge and of the recess, constancy of the ratio $\frac{M}{m_a}$ and approximately equal conditions(quality of the explosive, lining material), the velocity of the cumulative jet should be independent of the diameter of the charge and of the recess, which in fact is observed in experiment (Table 104).

Table 104

Effect of $\frac{M}{m_a}$ on the velocity of the leading portion of a cumulative jet.

(Shape of recess - conical, angle of flare 35°)

Lining material	Diameter of charge, mm	Velocity of leading portion of jet, m/sec
Steel	22	7400
"	30	7500
"	42	7400
Duralumin	22	8800
"	30	8500
"	42	8600

If the thickness of the lining δ is not too small (if the opposite is the case the usual jet is not formed), then with reduction of δ the velocity of the jet should increase up to a certain limit, which is confirmed by the data of Table 105.

Table 105

Effect of thickness of lining on the velocity of the leading portion of a cumulative jet

(Charge dimensions : h = 85mm, d = 42mm)

Lining material	Thickness of lining, mm	Velocity of leading portion of jet, m/sec
Steel	2	6700
"	3	6050
"	4	5250
Duralumin	1	8690
"	2	7600
"	3	7500
"	4	7150

We shall consider qualitatively the effect of the compressibility of the metal of the lining and its structural resistance on the compression process and on the formation of the cumulative jet.

Since the height and thickness of a layer of the active portion of a charge decrease from the axis to the base of the recess, then the velocity of compression also falls for the peripheral portions of the lining as compared with the inner portions. Since only the pressure, developed as a result of collision of the corresponding portions of the lining, falls to a value p_{lim}, i.e. to

a certain limiting value, the process of jet formation finishes. As a result of this, p_{lim} corresponds to the internal pressure, proportional to the cohesive forces.

As a consequence of the non-constancy of the velocity of compression of the different sections of the lining, a velocity distribution also makes its appearance along the cumulative jet, so that the leading portion of the jet attains a velocity greater than that of the rear portion. The substantial velocity gradients lead to stretching of the jet and its breakdown into a number of separate parts.

We shall now undertake certain considerations related to the description of the phenomenon. The maximum pressure resulting from the impact of two identical bodies is, as is well-known, independent of the angle of impact, and is described by the relationship

$$p_m = \frac{\rho_0 u_0^2}{4\left(1-\frac{\rho_0}{\rho_m}\right)}, \qquad (68.33)$$

where ρ_0 and ρ_m are the density of the body prior to impact and at the shock front(compression wave) resulting from their impact, u_0 is the impact velocity.

Relationship (68.33) is a particular case of the more general relationship(see para.73).

Applying the law of compressibility,

$$p = f(\rho) \approx A\left[\left(\frac{\rho_m}{\rho_0}\right)^n - 1\right], \qquad (68.34)$$

ρ_m can be eliminated from equations (68.33) and (68.34) and $p_m = \varphi(\rho_0, u_0^2)$ can be determined.

Since, as we have already shown, u_0 has a different value for every

section of the lining, then the value of $p_m \sim u_m^2$ will also vary.

If we assume that the active mass of the explosive, arriving at each element of the lining, depends approximately on the distance r of a given element from the axis of symmetry, then

$$m_{ar} = m_{a0}\left(1 - b\frac{r}{r_0}\right), \qquad (68.35)$$

where r_0 is the radius of the base of the cumulative recess, m_{a0} is an element of mass of the active portion of the charge at the axis of symmetry, $b < 1$.

Then, approximately

$$\frac{p_{xr}}{p_{x0}} = \frac{u_{mr}^2}{u_m^2} = \frac{m_{ar}}{m_{a0}} = 1 - b\frac{r}{r_0}. \qquad (68.36)$$

Here p_{xr}, p_{x0}, u_{mr} and u_m are the pressure and velocity at the axis and at a distance r from it. Hence it follows that in fact, a radius $r = r_{lim}$ can always be found for any charge, for which $p_{xr} = p_{lim}$. The material of the lining elements for $r > r_{lim}$, having been compressed, will not always give rise to a cumulative jet.

It is obvious that the limiting velocities of compression should be less than the armour-piercing velocity of the jet.

The conditions of formation of a cumulative jet have a substantial influence on the laws governing its motion and the effect on an obstacle. We note that for a value of the angle α, approaching $\frac{\pi}{2}$ the cumulative jet will not always be formed, since the velocity of compression, proportional to $\cos\alpha$, is small and the compressive pressure is less than p_{lim}. In view of the fact that the pressure, developed by the shock of the detonation wave around the lining,

$$p_s = p_i(1 + 1.4\sin^2\alpha) \qquad (68.37)$$

increases with increase of the angle α, the lining should split up into a number of fragments. These fragments, dispersed with an angle $\alpha \leqslant \frac{\pi}{2}$, will move directly with a velocity

$$u_{mr} = u_m \sin\alpha \sqrt{1 - b\frac{r}{r_0}} = 0.41 D \sin\alpha \sqrt{\frac{1 - b\frac{r}{r_0}}{\frac{M}{m_0} + \frac{1}{3}}}. \qquad (68.38)$$

As a result of this, only fragments proceeding from the central portion of the lining will have a substantial velocity.

We shall determine approximately the optimum thickness of the cumulative lining, and we shall carry out the calculation for a cone. Let the length of the jet be equal to $l = l_0\psi$, where ψ is the extension coefficient of the jet under armour-piercing conditions.

The mass of the jet is

$$M_1 = \pi l_0 \psi \bar{r}_0^2 \delta \rho_0, \qquad (68.39)$$

where $\bar{r}_0$ is the mean radius of the jet.

In accordance with formula (67.5), the mass of the lining is

$$M = \frac{M_1}{\sin^2\frac{\alpha}{2}} = \frac{\pi l_0 \psi \bar{r}_0^2 \delta \rho_0}{\sin^2\frac{\alpha}{2}} = \frac{2}{3}\pi R_k h \delta \rho_0. \qquad (68.40)$$

Here R_k is the base radius of the cone, h is the height of the cone ($h = l\cos\alpha$, where l is the cone generatrix, approximately equal to the initial length of the jet l_0).

From equation (68.40) we obtain

$$\bar{r}_0 = \sqrt{\frac{2}{3}\frac{R_k \delta \cos\alpha}{\psi}} \sin\frac{\alpha}{2}. \qquad (68.41)$$

Bearing in mind that the maximum effective length of the jet, for which maximum armour-piercing is achieved, is

$$l_{eff} = l_0 \psi_{eff}$$

(ψ_{eff} is the maximum extension for which the jet still retains its monolithic nature), and solving equation (68.41) relative to δ, the optimum thickness of the lining can be determined approximately:

$$\frac{\delta_{opt}}{R_k} = \frac{3\psi_{eff}\bar{r}_0^2}{2R_k^2 \cos\alpha \sin^2\frac{\alpha}{2}}. \qquad (68.42)$$

If we assume, on the basis of experiment, that for a steel lining

$\psi_{opt} \approx$! and $\bar{r}_0 =$ 0.80mm ($\bar{r}_0$ changes little with change of δ), then for the case we are considering (R = 30mm, $2\alpha = 55^\circ$, we obtain $\delta_{opt} =$ 2.20mm, which is close to the experimentally established value(2 - 2.5mm).

In conclusion we shall establish the limiting ratio of the mass of the lining to the mass of the active portion of a cumulative charge, for which jet formation ceases.

For this, we shall assume (see equation (68.53)) that the limiting pressure at which jet formation ceases is

$$\bar{p}_{lim} \leqslant \frac{\rho_a \bar{u}^2_{0\,lim}}{4\left(1 - \frac{\rho_a}{\rho_\infty}\right)}. \qquad (68.43)$$

If $\bar{p}_{lim}$, and the value of ρ_a/ρ_∞ corresponding to it are known for a given material, then u_{lim} can be determined.

For values of $u_0 < u_{lim}$ as we have already shown, further flow of metal and formation of a cumulative jet ceases.

Using expression (68.51) and taking into account the coefficient η, we obtain

$$\left(\frac{M}{m_a}\right)_{lim} = \left(\frac{0.41 D\eta}{\bar{u}_{0\,lim}}\right)^2 - \frac{1}{3}. \qquad (68.44)$$

$\left(\frac{M}{m_a}\right)_{lim}$ can be determined by experiment. In experiments carried out by BAUM, with a 56mm charge of ammotol 90/10 of density 1.2 g/cm^3 (D = 3400 m/sec) and with a copper conical lining (d_{base} = 45 mm ; angle of flare of cone $2\alpha = 37^\circ$, δ = 3mm, M = 429g.), jet formation was completely absent. As a result of this, $\left(\frac{M}{m_a}\right)_{lim} \approx$ 4.57 and $\bar{u}_{0lim} =$ 420 m/sec. Using formula (68.43), we obtain $\bar{p}_{lim} \approx$ 70,000 kg/cm^2.

Knowing the value of $\bar{u}_{0\,lim}$, $\left(\frac{M}{m_a}\right)_{lim}$ can be determined and also the limiting thickness of the lining for a cumulative charge prepared from any explosive.

For a charge of trotyl/hexogen mixture, $\left(\frac{M}{m_a}\right)_{lim}$ = 0.21, and the limiting

thickness of the copper cone δ_{11m} = 16.0 - 17.0 mm.

We note finally that the value of $\bar{p}_{11m_n}$, established for the given material under conditions of compression of the lining, should be considerably less than the value of p_{11m}, which is characteristic for this same material under armour-piercing conditions of the cumulative jet. This is explained by the fact that the strength characteristics of materials are not constant, but depend substantially on the nature of application of the stress to the obstacle and on the conditions of its deformation.

For example, for a steel lining, the limiting velocity of the cumulative jet $w_{1\,crit}$ as a result of its action on a steel obstacle, is equal to 2000 m/sec, which corresponds to the value $p_{11m} \approx 4.8 \cdot 10^5$ kg/cm^2. For $w_1 < w_{1\,crit}$ the armour-piercing characteristics practically cease. The large value of p_{11m} in the given case is explained by the instability of the cumulative jet and its continuous breakdown in the process of armour piercing.

§69. The Effect of the Non-uniformity of Compression of the Lining on the Distribution of Velocities in a Cumulative Jet.

From the theory of the active portion of a cumulative charge, it is possible to establish the nature of the lining compression and distribution of velocities along the cumulative jet, which is of considerable interest.

In view of the fact that the ratio $\left(\frac{M}{m_a}\right)_i$ is not constant for the individual elements of the lining, but is reduced from the vertex to the base of the cumulative recess, the velocity of compression of the individual elements of the lining will also be changed, in accordance with expression (68.51). As a result of this it should be taken into account that the angle of slope α_i of

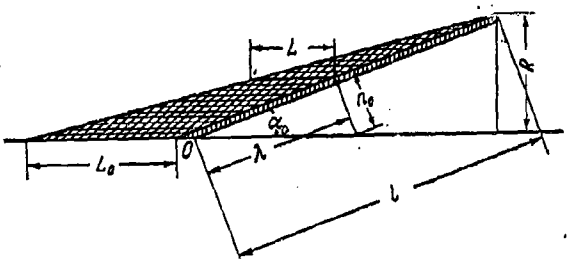
the individual elements of the lining to the axis of the charge will also be changed during the process of their compression. The net effect of these factors (non-constancy of u and α) will have its effect on the non-uniform distribution of velocities w_{ij} along the cumulative jet. The magnitudes of the active portions of individual elements of the lining may be determined geometrically (Fig. 180). For this, it is sufficient to know the shape of the lining and of the charge, and also the weight of the lining and the weight if the charge casing.

Since we are considering the action of the explosion products from the active portion on the lining, then the process of their expansion may be assumed to be one-dimensional, as before. In this case, the following relationship will be valid for an instantaneous detonation system :

$$M_i \frac{du_i}{dt} = M_i u_i \frac{du_i}{dn_i} = M_i \frac{du_i^2}{2dn_i} = Sp, \qquad (69.1)$$

where M_i is the mass of the i-th lining element, u_i is its velocity, S is its area, n_i is the path length of the i-th element to the axis of symmetry.

Figure 180. Compression of the conical lining of a cumulative charge.



Since the mass of the i-th element of the active portion of the charge is equal to $m_i = SL\rho_0$, and

$$p = \bar{p}_i \left(\frac{L}{L+n}\right)^3, \qquad (69.2)$$

where

$$\bar{p}_i = \frac{\rho_0 D^2}{8},$$

then

$$M_i = \frac{du_i^2}{2dn_i} = \frac{S\rho_0 D^2}{8}\left(\frac{L}{L+n}\right)^3 = \frac{m_i D^2}{8L}\left(\frac{L}{L+n}\right)^3. \qquad (69.3)$$

Hence

$$\frac{d\left(\frac{u_i}{D}\right)^2}{d\left(\frac{n}{L}\right)} = \left(\frac{m}{M}\right)_i \frac{1}{4\left(1+\frac{n}{L}\right)^3}. \qquad (69.4)$$

Integrating expression (69.4) for the conditions that $u = 0$ for $n = 0$, we arrive at the relationship

$$\frac{u_i}{D} = \frac{1}{2}\sqrt{\frac{1}{2}\left(\frac{m}{M}\right)_i\left[1-\left(\frac{L}{L+n}\right)^2\right]}. \qquad (69.5)$$

Since

$$\frac{L}{L_0} = \frac{m}{m_0} = f\left(\frac{\lambda}{l}\right), \qquad (69.6)$$

where m_0 and L_0 are the mass and length of the element of the active portion lying immediately next to the axis of the charge, then

$$\frac{u_i}{D} = \frac{1}{2}\sqrt{\frac{f\left(\frac{\lambda}{l}\right)}{2}\frac{m_0}{M_i}\left[1-\left(\frac{L}{L+n}\right)^2\right]}. \qquad (69.7)$$

The function $f\left(\frac{\lambda}{l}\right)$ can easily be determined geometrically for any given shape of recess. The mass of any element of lining is also known ; in the most general case

$$M_i = M_0\varphi\left(\frac{\lambda}{l}\right).$$

Assuming that the angle through which any element of the lining approaches the axis of the charge is not changed (this angle is equal to $90^\circ - \alpha_0$), we can easily determine the "slam" velocity of an arbitrary element of the lining.

Actually,

$$n_i = \lambda\tan\alpha_0, \qquad (69.8)$$

and therefore equation (69.7) can be written in the form

$$\frac{u_i}{D} = \frac{1}{2}\sqrt{\frac{m_0}{2M_0}\frac{f}{\varphi}\left[1-\left(\frac{L}{L+\lambda\tan\alpha_0}\right)^2\right]}. \qquad (69.9)$$

In the case of a conical recess with a lining of constant thickness

$$f\left(\frac{\lambda}{l}\right)=1-\frac{\lambda}{l};\quad \varphi\left(\frac{\lambda}{l}\right)=1,\quad L=L_0\left(1-\frac{\lambda}{l}\right).$$

For this

$$\frac{m_0}{M_0}=\frac{L_0}{\delta}\frac{\rho_0}{\rho_1}\sin\alpha_0,\quad l=\frac{R_0}{\sin\alpha_0}\ \text{and}\ \ L_0=R_0,$$

where δ is the thickness of the lining, ρ_0 is the density of the explosive, ρ_1 is the density of the lining metal, R_0 is the base radius of the cone.

Now equation (69.5) assumes the form

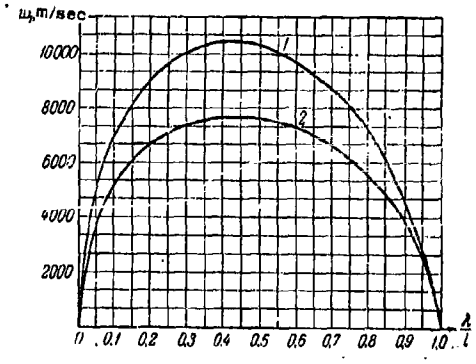
$$\frac{u_l}{D}=\frac{1}{2}\sqrt{\frac{R_0\rho_0\sin\alpha_0}{2\delta\rho_1}\left(1-\frac{\lambda}{R_0}\sin\alpha_0\right)}\times \times\sqrt{1-\left[\frac{R_0\left(1-\frac{\lambda}{R_0}\sin\alpha_0\right)}{R_0\left(1-\frac{\lambda}{R_0}\sin\alpha_0\right)+\lambda\tan\alpha_0}\right]^2} \tag{69.10}$$

The value of w_{1l}, as before, is determined by the expression

$$w_{1l}=\frac{u_l}{\tan\frac{\alpha_0}{2}}. \tag{69.11}$$

For the actual example presented above (R_0 = 30 mm, δ = 2 mm, α_0 = 17°30', ρ_0 = 1.6 g/cm^3, ρ_1 = 7.8 g/cm^3 and D = 7600 m/sec), having used equations (69.10) and (69.11), we determine the corresponding values for u_l and the velocity distribution w_{1l} in the cumulative jet. The results of the calculation are presented in Fig. 181 (curve 1).

Figure 181. Velocity distribution along a cumulative jet.



It can be seen from the figure that the maximum velocity gradients in the cumulative jet arise on account of the lining elements lying towards the apex and base of the recess. This should have as its consequence the rapid breakaway of the jet from the pestle and the intense dispersion of the leading portion of the jet. What has been said is found to be in accordance with the results of experimental investigations.

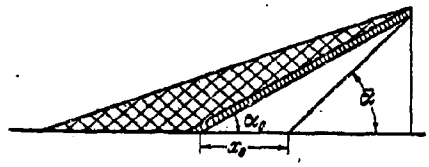


Figure 182. Compression of a conical lining, taking into account the non-instantaneity of detonation of the charge.

In actual charges, detonation does not take place instantaneously; therefore we should take into account the time during which the detonation wave traverses the distance from the vertex to the base of the cone. After this time the vertex of the lining travels a certain path x_0, as a consequence of which the angle of slope of the lining is changed (Fig. 182). Since for the vertex of the lining

$$\frac{u}{D} = \frac{1}{2}\sqrt{\frac{m_0}{2M_0}\left[1-\left(\frac{x}{L_0+x}\right)^2\right]} = \frac{1}{D}\frac{dx}{dt}, \qquad (69.12)$$

where

$$\frac{m_0}{M_0} = \frac{L_0\rho_0 \sin\alpha_0}{\delta\rho_1},$$

then

$$\int_0^{x_0} \frac{dx}{\sqrt{1-\frac{x^2}{(L_0+x)^2}}} = \frac{D\tau}{2}\sqrt{\frac{1}{2}\frac{L_0\rho_0\sin\alpha_0}{\delta\rho_1}}. \qquad (69.13)$$

Here τ is the time during which the detonation wave travels the path from the vertex to the base of the cone. It is obvious that

$$\tau = \frac{l\cos\alpha_0}{D}.$$

Since

$$\int_0^{x_0} \frac{dx}{\sqrt{1-\frac{x^2}{(L_0+x)^2}}} = \int_0^{x_0} \frac{(L_0+x)\,dx}{\sqrt{L_0^2+2L_0x}} \approx$$

$$\approx \frac{L_0}{6}\left(1+2\frac{x_0}{L_0}\right)^{\frac{3}{2}} + \frac{L_0}{2}\left(1+2\frac{x_0}{L_0}\right)^{\frac{1}{2}} - \frac{2}{3} = f(x_0) \qquad (69.14)$$

(for $\frac{x_0}{L_0} < 1$ this solution is quite accurate), then

$$f(x_0) = \frac{l\cos\alpha_0}{2}\sqrt{\frac{1}{2}\frac{L_0\rho_0}{\delta\rho_1}\sin\alpha_0}. \qquad (69.15)$$

We determine x_0 from expressions (69.14) and (69.15).

Knowing x_0, it is easy to determine $\bar{\alpha}$, the angle of slope of the lining to the axis of the charge at the instant of termination of the detonation:

$$\frac{x_0}{l} = \frac{\sin(\bar{\alpha}-\alpha_0)}{\sin\bar{\alpha}} = \cos\alpha_0 - \sin\alpha_0\cot\bar{\alpha}, \qquad (69.16)$$

where $\bar{\alpha}-\alpha_0$ is the increment of the angle.

In solving the neutralized problem it can be assumed that the average value of the angle is

$$\alpha_{av} = \frac{\bar{\alpha}+\alpha_0}{2} = \alpha_0 + \frac{\Delta\alpha}{2}. \qquad (69.17)$$

In solving the problem by elements, it can be assumed with sufficient accuracy that

$$\frac{\Delta\alpha_i}{\Delta\alpha} = 1 - \frac{\lambda}{l}. \qquad (69.18)$$

Therefore, in formulae (69.10) and (69.11), in calculating u_i and w_{1i}, the angle α_0 should be replaced by the angle

$$\alpha_i = \alpha_0 + \Delta\alpha_i.$$

For the example considered above $\frac{m_0}{M_0} \approx 1$, $f(x_0) = 0.25\,l$, whence $\frac{x_0}{L_0} = 1$, $\frac{x_0}{l} = 0.3$ and $\Delta\alpha \approx 6°$.

For the solution of the neutralised problem (for calculating w_{1av}), the error in the angle gives the coefficient

$$\eta_{1,av} = \frac{\tan\frac{\alpha_0}{2}}{\tan\left(\alpha_0 + \frac{\Delta\alpha}{2}\right)}. \qquad (69.19)$$

In our case $\alpha_0 = 17^\circ 30'$ and $\eta_{1,av} \approx 0.70$.

In order to find the velocity distribution along the jet, it is necessary, having been given λ, to calculate the value of $\Delta\alpha_i$ according to relationship (69.18).

In our example

$$\Delta\alpha_i = 6^\circ\left(1 - \frac{\lambda}{l}\right).$$

The nature of the velocity distribution by calculating the change in angle is shown in Fig. 181 (curve 2). For $\frac{\lambda}{l} = 0.5$, $w_1 = 7200$ m/sec, which is very close to the maximum velocity of the cumulative jet, established for a similar charge by experiment.

We shall now calculate the coefficient η, applicable to formula (68.52). the volume of the active portion of the charge $v_a = \frac{\pi}{3} l^3 \sin^2 \alpha_0$; ; the limiting volume, in which the explosion products from the active portion of the charge expand in the process of compression of the lining is $v = \frac{\pi}{3} l^3 \frac{\sin^2 \alpha_0}{\cos \alpha_0}$ (see Fig. 180); taking into account that

$$\frac{v_a}{v_a + v} = \frac{\bar{\rho}}{\rho_a} = \frac{\bar{c}}{c_1}, \qquad (69.20)$$

so that $\rho \sim \bar{c}$, where $\bar{c}$ is the mean velocity of sound in the explosion products, we obtain

$$\frac{v_a}{v_a + v} = \frac{\cos \alpha_0}{1 + \cos \alpha_0}, \qquad (69.21)$$

$v_a + v$ is the limiting volume occupied by the explosion products from the active portion of the charge at the end of compression of the lining.

The ratio of the energy remaining at this instant in the explosion products to their initial energy is

$$\frac{E}{E_1}=\left(\frac{\bar{c}}{c_1}\right)^2=\frac{\cos^2\alpha_0}{(1+\cos\alpha_0)^2}. \qquad (69.22)$$

The kinetic energy acquired by the lining is

$$E_{\text{к}}=E_1-E=E_1\left[1-\frac{\cos^2\alpha_0}{(1+\cos\alpha_0)^2}\right],$$
$$\frac{E_{\text{к}}}{E_1}=1-\frac{\cos^2\alpha_0}{(1+\cos\alpha_0)^2}=\frac{1+2\cos\alpha_0}{(1+\cos\alpha_0)^2}=\eta_2^2, \qquad (69.23)$$

where η_2 is a coefficient which takes into account the incomplete utilization of energy in determining $\bar{w}_1$ according to equation (68.32).

For the example being considered, $\eta_2 \approx 0.95$. Since, as we have established above, consideration of the error in the mean variation of the angle α gives $\eta_1 = 0.70$ for this case, then by determining $\bar{w}_1$ according to formula (68.32) $\bar{\eta} = 0.95 \cdot 0.7 \approx 0.67$.

Since the velocity in the cumulative jet is increased from the front to the rear elements and then falls again towards the end of the jet, redistribution of velocities will take place, namely, the leading portion of the jet as a result of this will be accelerated, and the middle portion will be retarded. The diameter of the jet, as a result of this, increases somewhat.

In order to describe the final velocity distribution in the jet and to determine its diameter, we make use of the Laws of Conservation.

Let us consider the simple case. Suppose that the velocity of the jet at the interval $0<l\leqslant\bar{l}$ increases linearly from zero to $\bar{w}_{1\max}$ (for $x=l-\bar{l}$), and at the interval $\bar{l}\leqslant x\leqslant l$ it falls linearly to zero (for $x=l$).
We shall superimpose the origin of the coordinate at the end of the jet. Over a certain time, a new regime is established, for which the velocity of the leading portion of the jet is equal to $w_{1\max}$. The velocity distribution will be linear (from $w_{1\max}$ to zero for $x=C$). The length of the jet is equal to $l-\bar{l}$,

and the ratio of the mean areas of cross-section of the jet prior to redistribution and after distribution will be equal to $\frac{l-\bar{l}}{l}$.

We shall now prove this. Prior to redistribution of the velocities

$$m_1 = s_1\rho\,\bar{l}, \quad m_2 = s_1\rho\,(l-\bar{l}), \quad m = m_1 + m_2 = s_1 l\rho.$$

Neutralizing the velocity in the jet, we obtain

$$I_1 = \frac{m_1 w_{1\max}}{2}, \quad I_2 = \frac{m_2 w_{1\max}}{2},$$

$$I = I_1 + I_2 = \frac{m w_{1\max}}{2},$$

$$E_1 = \frac{m_1 w_{1\max}^2}{6}, \quad E_2 = \frac{m_2 w_{1\max}^2}{6},$$

$$E = E_1 + E_2 = \frac{m w_{1\max}^2}{6}$$

[ρ is the density of the jet, s_1 is the area of cross section (average), l is the length of the jet].

After redistribution of velocities

$$m = s_2\rho\,(l-\bar{l}),$$

$$I = \frac{m w_{1\max}}{2}, \quad E = \frac{m w_{1\max}^2}{6},$$

which proves our hypothesis.

It follows from these relationships that

$$\frac{s_2}{s_1} = \frac{l}{l-\bar{l}}$$

or

$$\frac{r_2}{r_1} = \sqrt{\frac{l}{l-\bar{l}}}. \tag{69.24}$$

The time after which redistribution occurs can be estimated from the relationship

$$\tau_0 = \frac{2l}{c_0}, \tag{69.25}$$

where c_0 is the velocity of sound in the jet material. The path of the compression and rarefaction waves in both directions is taken into account by these relationships.

Towards the end of compression of the lining, the length of the jet is

$$l_1 = \overline{l}_0 + w_{1\max}\tau_0. \qquad (69.26)$$

where $\overline{l}_0 = l - l_0$.

Actually, the initial velocity distribution in a cumulative jet is not linear (see Fig.181). Consequently, a precise solution of the problem is more complex. However, the jet can always be divided into several intervals and it can be assumed that in each one of them the velocity distribution is linear.

§ 70. Theory of the Armour-piercing Action of a Cumulative Jet.

The theory of the armour-piercing action of a cumulative jet was first developed by LAVRENT'YEV. It originated from the hypothesis that as a result of the impact of the jet with armour plate, high pressures are developed, at which the strength resistance of the metal may be disregarded, and the armour plate may be considered as an ideal incompressible liquid. In accordance with this, LAVRENT'YEV considered the following problem in detail.

Suppose that the jet is in the shape of a cylinder with radius r_0; the velocity of all its elements is identical and equal to w_1. In addition, let us assume that the jet penetrates into a cylinder with radius r_1, coaxial with the jet. In this setting the problem is equivalent to the problem we have considered of the collision of two jets; by changing the signs of the jet velocities, the mode of formation of the jet as a result of compression of the lining reduces to the mode of operation of the jet as a result of its penetration into a medium with the same density.

In this case, Fig.177 may be considered as the mode of penetration of a jet A into an obstacle B if we assume that the obstacle B (pestle) for $x \to -\infty$ has zero velocity. Hence the relationship follows for the penetration velocity of the jet (armour-piercing velocity):

$$u = \frac{w_1}{2}. \qquad (70.1)$$

It follows from relationship (70.1) that as a result of penetration of the jet to a depth L, a portion of the jet, also equal to L, is expended, i.e. the maximum depth of armour penetration is equal to the length of the cumulative jet.

If the jet and the armour plate have different densities, then the penetration velocity is determined by the formula

$$u = w_1 \frac{1}{\sqrt{\frac{\rho_2}{\rho_1} + 1}}, \tag{70.2}$$

and the depth of penetration by the formula

$$L = l \sqrt{\frac{\rho_1}{\rho_2}}, \tag{70.3}$$

where ρ_1 and ρ_2 are the densities of the jet metal and of the armour plate, and l is the length of the jet, equal to the length of the generatrix of the cone.

LAVRENT'YEV showed that the original scheme proposed by him is valid, if the pressure resulting from collision of the jet with the armour plate exceeds $2 \cdot 10^5$ kg/cm^2, i.e. if $w_1 > w_{crit} \approx 4 \cdot 10^3$ m/sec.

Results of verification have shown that velocities and depths of penetration calculated by LAVRENT'YEV are different from the experimental values in a number of cases.

The principal reason for the variance between theory and experiment is in neglecting the compressibility of metals at high pressures and, in particular, the structural resistance of obstacle material.

The structural resistance of metals, as is well-known, increases in general with increase of dynamic loading and, as we shall show below, under definite conditions it becomes commensurate with the pressure generated by the cumulative jet.

In this case, the depth of armour penetration should depend not only on the length of the jet and the ratio of the densities of the metals, but also on the velocity of the jet and the structural characteristics of the armour plate.

The structural resistance p_{st} of metals, under conditions of dynamic stresses acting on them, cannot be determined with sufficient accuracy theoretically, in view of the absence of reliable data concerning the variation of the parameters of the crystal lattice of metals at high pressures.

The value of p_{st} may be established, however, on the basis of experimental data for the limiting velocity of a cumulative jet w_{1crit}, at which the armour-piercing action ceases.

It is obvious that for this velocity, the pressure of the jet will be balanced by the total resistive forces of the obstacle, which is compounded from the inertial force p_{in} and the structural resistance p_{st}.

However, since in the vicinity of the limit of penetrability the velocity of motion of the metal of the obstacle is negligibly small, the quantity p_{in} can be quite reasonably neglected, and the value of p_{st} can be determined from the theoretical relationship between the pressure and the velocity of the cumulative jet.

Table 106

Critical Velocity of armour-piercing

Obstacle material	Brinell hardness	Material of cumulative jet	Critical velocity of jet, m/sec
Duralumin	115	Duralumin	2900
Steel	125	Duralumin	3300
Steel	125	Steel	2050
Tempered steel	$R_c \approx 50$	Steel	2200

Results of determination of w_{1crit} for certain metals, as obtained by BAUM and SHEKHTER, are presented in Table 106.

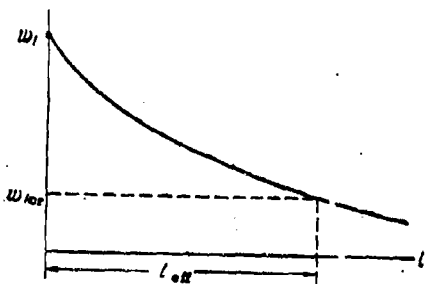
With the object of determining w_{1crit} for any material, the limiting

thickness of armour penetration was established accurately at 3 - 5 mm, and the exit velocity of a cumulative jet at this thickness was measured photographically.

Figure 168 shows a photograph on which the motion of the rear portion of a cumulative jet is recorded.

It follows from Table 106 that $w_{l\,crit}$ depends on the relationship between the densities of the metals of the jet and of the obstacle and their physico-mechanical characteristics.

Figure 183. Velocity distribution along a cumulative jet.



Thus, it may be concluded that not the whole of the jet possesses armour-piercing capabilities, but only a certain portion of it, which we shall call the effective length of the jet, l_{eff}.

The quantity l_{eff} is determined by the nature of the velocity distribution along the cumulative jet, as Fig.183 shows diagrammatically.

Naturally, in order to determine l_{eff}, it is necessary to consider the jet at the instant of its maximum extension, at which it still retains its monolithic character. It is obvious that in this state it will possess maximum armour-piercing capabilities. The value of l_{eff} can be calculated if we know the law of motion of the cumulative jet.

The theory of the armour-piercing action of a jet, taking into account the compressibility of the metals of the jet and of the obstacle and also its structural characteristics, has been developed by BAUM and STANYUKOVICH.

§ 71. Motion of a Cumulative Jet.

We shall consider first of all the motion of a cumulative jet in air. It is obvious that at relatively small distances from the charge(up to several metres), which are also of practical interest, the air resistance can be neglected and we can consider the motion of the jet as in a vacuum. Furthermore, it is obvious that the internal pressure in different portions of the jet is close to atmospheric and the pressure gradient $\left(\frac{\partial p}{\partial x}\right)_t$ is small in comparison with the velocity gradient $\left(\frac{\partial u}{\partial x}\right)_t$. It can be assumed that $\left(\frac{\partial p}{\partial x}\right)_t = 0$.

In this case, in order to describe the motion of the jet, Euler's equation for non-stationary, one-dimensional motion of liquids can be used:

$$\frac{\partial u}{\partial t} + u\frac{\partial u}{\partial x} + \frac{1}{\rho}\frac{\partial p}{\partial x} = 0. \qquad (71.1)$$

For $\frac{\partial p}{\partial x} = 0$ (in the given case $u = w_1$) the general solution of equation (71.1) is written in the form

$$x = ut + F(u). \qquad (71.2)$$

Knowing the law of distribution of the velocity u with respect to the coordinate x, at any finite instant of time, for example for $t = 0$, it is easy to determine the arbitrary function $F(u)$ (origin of the time reading and of the coordinate are entirely arbitrary, since in equation (71.1) t and x appear under the differential sign).

Suppose that for $t = 0$, $u = f(x)$ or $x = \varphi(u)$, where $\varphi(u)$ is a given function of the velocity; then it is obvious that

$$F(u) = \varphi(u),$$

i.e.

$$x = ut + \varphi(u). \qquad (71.3)$$

The isogonal motion is inertial; every particle of the jet has a constant velocity, determined by the initial conditions, and independent of time. Hence, it follows that

$$\left(\frac{\partial x}{\partial t}\right)_{x_0} = u = u_0(x_0), \tag{71.4}$$

where u_0 describes the velocity distribution as a function of the Lagrangian coordinate x_0. The value of x_0 defines the position of a particle at the instant of time $t = 0$.

At any arbitrary instant of time $t > 0$, the position of a particle is determined by the expression

$$x = x_0 + u_0(x_0)\, t. \tag{71.5}$$

Suppose that for $t = 0$ the length of a certain part of the jet is $l_{0\,(1,2)} = x_{2,0} - x_{1,0}$.

Then, for $t > 0$, the length of this part of the jet is determined by the expression

$$l_{t\,(1,2)} = l_{0\,(1,2)} + [u_{2,0}(x_{2,0}) - u_{1,0}(x_{1,0})]\, t. \tag{71.6}$$

We shall consider two possible cases of motion of the jet. In the first case we shall assume that the velocity depends linearly on the coordinate, i.e. for $t = 0$

$$u = u_0\left(1 - \alpha\frac{x_0}{l_0}\right), \tag{71.7}$$

where u_0 is the velocity of the leading portion of the jet, α is a dimensionless coefficient which depends on the velocity gradient and which can be determined by experiment from data concerning the velocity distribution along the jet, l_0 is the initial effective length of the jet.

For $x = l_0$,

$$u = u_0(1 - \alpha) = u_{crit},$$

where $u_{1\,crit} = w_{1\,crit}$.

Hence it follows that

$$\alpha = 1 - \frac{u_{crit}}{u_0}$$

$$\frac{u}{u_0} = \left[1 - \left(1 - \frac{u_{crit}}{u_0}\right)\frac{x_0}{l_0}\right]. \tag{71.8}$$

From expression (71.8) we obtain

$$\frac{x}{x_0} = \frac{1 - \frac{u}{u_0}}{1 - \frac{u_{crit}}{u_0}} \tag{71.9}$$

Using expressions (71.5) and (71.8), we obtain the relationship

$$\frac{x}{l_0} = \frac{ut}{l_0} + \frac{1 - \frac{u}{u_0}}{1 - \frac{u_{crit}}{u_0}} \qquad (t > 0).$$

Hence, we determine $u = u(x, t)$:

$$\frac{u}{u_0} = \frac{-\frac{x}{l_0} + \frac{u_0}{u_0 - u_{crit}}}{-\frac{u_0 t}{l} + \frac{u_0}{u_0 - u_{crit}}} \tag{71.10}$$

The position of every particle of the jet for $t > 0$ is determined by the relationship

$$x = x_0 + u_0 t \left[1 - \left(1 - \frac{u_{crit}}{u_0}\right) \frac{x_0}{l_0}\right]. \tag{71.11}$$

The effective length of the jet is determined by the relationship

$$l_{eff} = l_0 + (u_0 - u_{crit})\, t. \tag{71.12}$$

In the second case we assume that at $t = 0$, the velocity distribution along the jet is determined by the law

$$u = u_0 \left[\left(1 - \alpha \frac{x_0}{l_0}\right) + \beta \left(\frac{x_0}{l_0}\right)^2\right]. \tag{71.13}$$

Suppose that for $x = l_0$, $u = u_{crit}$. Then

$$\frac{u_{crit}}{u_0} = 1 - \alpha + \beta,$$

whence

$$\beta = \frac{u_{lim}}{u_0} + \alpha - 1,$$

which finally determines

$$\frac{u}{u_0} = 1 - \alpha \frac{x_0}{l_0} + \left(\alpha - 1 + \frac{u_{lim}}{u_0}\right) \left(\frac{x_0}{l_0}\right)^2, \tag{71.14}$$

whereupon the parameter α should be determined by experiment. It is easy to determine the value of x for $t>0$ from equation (71.14) :

$$x = x_0 + u_0 t\left[1 - \frac{\alpha x_0}{l_0} + \left(\alpha - 1 + \frac{u_{crit}}{u_0}\right)\left(\frac{x_0}{l_0}\right)^2\right]. \qquad (71.15)$$

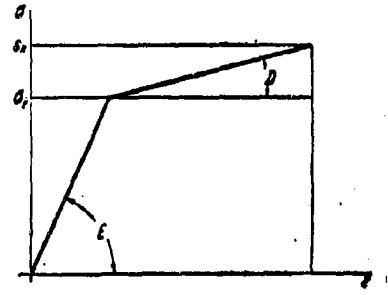
The total effective length of the jet as a result of this is determined, as before, by relationship (71.12).

During the process of motion, the jet, having extended, loses its monolithic nature in the course of a certain time t_{lim}. We shall determine t_{lim}.

In this case, when the velocity along the jet varies according to a linear law, the relative extension of the jet can be expressed directly by the relationship

$$\bar{\varepsilon} = \frac{u_0 - u_{crit}}{l_0} t_{lim} \qquad (71.16)$$

Figure 184. Diagram of true stresses.



If the process of extension of the jet is limited only by the region of elastic deformations, then in order to determine t_{lim} we can use the well-known relationship

$$\sigma_i = E\varepsilon \quad ,$$

where σ_i is the temporary resistance of the metal, ε is the relative extension, and E is the modulus of elasticity.

However, deformation of the jet is accomplished after the limits of the elastic region, in view of which Hook's Law cannot be used in the given case for calculating the relative extension of the metal. For this we must use fixed experimental relationships which establish the connection between the breaking load and the relative extension of the respective metals. In order to obtain

these relationships, diagrams of true stresses (Fig. 184) may be used, which include the region of plastic deformation as well as the elastic region, for which the law of increase of tension is characterized by the equation

$$\sigma - \sigma_0 = A(\varepsilon - \varepsilon_0).$$

Substituting this equation by the approximate equation

$$\sigma = D\varepsilon + \text{const}, \tag{71.17}$$

where D is the strength modulus, knowing the quantity S_k and neglecting elastic deformation, the relative extension can be determined approximately from the diagram

$$\bar{\varepsilon} \approx \frac{S_k - \sigma_1}{D}, \tag{71.18}$$

where S_k is the resistance of the metal at breakup.

We find from relationships (71.16) and (71.18) that

$$l_{11m} = \frac{l_0}{u_0 - u_{11m}} \frac{S_k - \sigma_1}{D}. \tag{71.19}$$

Substituting the value found for l_{11m} in expression (71.12), we find, finally, the relationship for the limiting effective length of jet

$$l_{eff} \approx l_0 \left(1 + \frac{S_k - \sigma_1}{D}\right). \tag{71.20}$$

It is not possible, meanwhile, to use this formula directly for numerical calculations, since the existing values of S_k and D are valid only at normal temperatures and small deformation velocities of metals. By increasing the temperature and velocity of deformation, these values are changed. The values of S_k and D at the temperatures and enormous deformation velocities which are attained by the motion of a cumulative jet, are not known at present.

Equation (71.20), however, leads us to the conclusion that in order to increase l_{eff}, and consequently also the armour-piercing effect, it is

necessary to ensure such a combination of the physico-mechanical properties of the lining metal, at which the ratio $\frac{S_k - \sigma_t}{D}$ attains the greatest possible value.

On the basis of data with respect to the armour-penetrability of cumulative charges and from X-ray photographs of cumulative jets, it may be assumed that for a lining made of mild steel

$$1 < \frac{S_k - \sigma_t}{D} \leqslant 2,$$

i.e., l_{min} amounts approximately to $3l_0$, where l_0 is about the length of the generatrix of the cumulative recess.

§ 72. Physical Principles of the Theory of the Armour-piercing Action of a Cumulative Jet

In constructing the theory of the armour-piercing action of a cumulative jet, it is not possible to proceed without clear ideas concerning the mechanism of destruction of the armour plate.

It is difficult to determine, without preliminary analysis, whether we are dealing in a given case with large-scale destruction of the material of the armour plate, or with some other phenomena.

Elementary calculation, generally speaking, indicate that even close to the limit of penetrability, the energy of a cumulative jet is sufficient to cause melting of the metal of the armour plate.

We shall determine the limiting velocity of the jet, for which complete fusion of steel can still be achieved, assuming that the lining, and consequently also the jet, consist of the same metal.

The kinetic energy of unit mass of the jet is

$$\varepsilon_1 = \frac{u^2_{lim}}{2}. \qquad (72.1)$$

The energy required for melting unit mass of the obstacle is

$$\varepsilon_2 = q. \qquad (72.2)$$

For steel at normal pressures, q = 0.5 kcal/g.

Comparing equations (72.1) and (72.2), we obtain for the case we are discussing, u_{lim} = 1600 m/sec.

The actual value of u_{lim} should be somewhat greater, since at the high pressures (around 10^6 kg/cm^2), experienced by the metal at the instant of impact, the melting point and the specific heat of the metal will be considerably higher than at normal pressure, i.e. u_{lim} will approximate to the value of u_{crit}, which for normal steel is equal to 2050 m/sec.

However, it is difficult to assume that under impact conditions of a cumulative jet, having a duration of a few millionths of a second, total excitation of all the degrees of freedom can occur, which determine the conditions of fusion of the metal of the obstacle.

We are also led to this same conclusion by the experimental fact that the depth of penetration for metals with very similar nature (with practically identical values of q and equal density), depends significantly on their strength characteristics.

For example, for steel with a hardness H_B = 125, u_{crit} = 2000 m/sec, but for tempered steel with Rc = 50, u_{crit} = 2200 m/sec.

Still more significant are the data concerning the effect of the strength of the respective metals on the depth of penetration. These data have been obtained by BAUM and SKALYAROV.

The results of their experimental determinations are presented in Table 107.

The experiments were carried out with charges of trotyl-hexogen 50/50, with a diameter of 42 mm and a height of 84 mm; the cumulative recess was

hyperbolic in shape with a lining of aluminium alloy of thickness 2 mm.

Table 107

Relationship between armour-piercing action of a jet and the hardness of the armour.

Material of obstacle	Brinell hardness	Depth of penetration, mm.
Steel	100	111
Steel	550	80
Aluminium alloy	50	527
Aluminium alloy	200	256

On the basis of what has been said, it may be concluded that the metal of the armour plate during the process of action of the cumulative jet, is evidently in a peculiar quasi-liquid state, the transition conditions for which depend substantially on its strength characteristics.

In future, we shall use the quantity ρ_{st} as a primary strength characteristic of the metal, which is easily derived by experimental determination.

The following physical factors should form the basis of structure of a more precise theory of the armour-piercing effect, as shown by the results of experiments which have been carried out :

1. At high pressures, arising as a result of the interaction of a cumulative jet with an obstacle, it is necessary to take into account the compressibility of the metal, which becomes considerable.

2. The strength characteristics of the metal of the obstacle have a considerable influence on the depth of penetration. Destruction of the armour plate is associated with the overcoming of the structural forces in the metal and

its transition to a quasiliquid state.

3. Taking into account the circumstance mentioned, the velocity of penetration can be computed as the velocity of motion of the boundary of separation between the metal of the jet and the metal of the armour plate.

4. The depth of penetration for approximately equal conditions is determined by the effective length of the cumulative jet l_{eff}, for which its velocity becomes equal to u_{crit}. Penetration ceases on the jet attaining this velocity.

§ 73. Velocity of Penetration and the Pressure as a Result of Impact of the Jet with an Obstacle.

As a result of the collision of the jet with an obstacle, a shock wave originates in the obstacle as well as in the jet. In order to determine the pressure developed on penetration of the obstacle by the jet and the velocity of penetration, the well-known relationships of the theory of shock waves can be used :

$$u_m = u - \sqrt{p_m (v_{1,0} - v_{1,m})} = \sqrt{p_m (v_{2,0} - v_{2,m})}, \qquad (73.1)$$

where u is the velocity of a corresponding element of the jet, u_m is the velocity of motion of the boundary of separation of the two media (armour-piercing velocity), p_m is the pressure at the boundary of separation of the media at the instant of impact, $v_{1,0}$; $v_{1,m}$ are the specific volumes of the impacting body (the jet), initially and at the instant of impact, $v_{2,0}$; $v_{2,m}$ are the specific volumes of the body subjected to the impact (the obstacle).

We shall suppose that $v_m = v_0 (1 - \alpha)$. After a few transformations, relationship (73.1) leads to the following formulae, which determine p_m and u_m :

$$p_m = \frac{\rho_{1,0} u^2}{\left(\sqrt{\alpha_1} + \sqrt{\alpha_2 \frac{\rho_{1,0}}{\rho_{2,0}}}\right)^2}, \qquad (73.2)$$

$$u_\infty = \frac{u}{1+\sqrt{\frac{a_1}{a_2}\frac{\rho_{2,0}}{\rho_{1,0}}}}. \qquad (73.3)$$

where $\rho_{1,0}$ and $\rho_{2,0}$ are the initial densities of the impacting body and of the body suffering impact.

In contrast from formula (70.2), established by LAVRENT'YEV, equations (73.2) and (73.3) take into account the effect of the compressibility of the impacting bodies on the armour-piercing parameters.

It follows from formula (73.3) that in the case when the jet and the obstacle consist of one and the same metal ($a_1 = a_2$, $\rho_{1,0} = \rho_{2,0}$), the velocity of penetration $u_\infty = \frac{u}{2}$.

In this particular case, formulae (73.3) and (70.2) lead to an identical result. It was shown in Chapter IX that at pressures of around 10^5 kg/cm^2 and higher, the relationship between p and ρ is established by the law

$$p_\infty = A\left[\left(\frac{\rho_\infty}{\rho_0}\right)^n - 1\right]. \qquad (73.4)$$

Expressing $\frac{\rho_\infty}{\rho_0}$ by a and using equation (73.4), we find

$$\frac{\rho_\infty}{\rho_0} = \frac{1}{1-a},$$
$$a = 1 - \frac{1}{\left(1+\frac{p_\infty}{A}\right)^{\frac{1}{n}}}. \qquad (73.5)$$

Substituting the relationship obtained for a in equation (73.2), we obtain

$$p_\infty = \frac{\rho_{1,0}u^2}{\left\{\sqrt{1-\frac{1}{\left(1+\frac{p_\infty}{A_1}\right)^{\frac{1}{n}}}}+\sqrt{\frac{\rho_{1,0}}{\rho_{2,0}}\left[1-\frac{1}{\left(1+\frac{p_\infty}{A_2}\right)^{\frac{1}{n}}}\right]}\right\}^2} \qquad (73.6)$$

The velocity of motion of the boundary of separation u_∞, calculated according to formula (73.3), corresponds to a medium, the strength of which is

not taken into account (water, lead, etc).

Under actual conditions of armour-piercing, it is necessary to take into account the structural resistance of the armour plate metal p_{st}, as a consequence of which the actual velocity of motion of the boundary of separation, equal to the penetration velocity, will be less than u_x. We shall denote this velocity by $u_{x,0}$.

The quantity $u_{x,0}$ can be determined by the formula

$$u_{x,0} = \sqrt{(p_x - p_{st})(v_{2,0} - v_{2,x})}. \tag{73.7}$$

Here p_{st} is interpreted as the initial "internal" pressure in the metal of the armour plate.

Transforming relationship (73.7), the following relationship can be written down for $u_{x,0}$:

$$u_{x,0} = \sqrt{\left[\frac{\rho_{1,0}u^2}{\left(\sqrt{a_1} + \sqrt{a_2\frac{\rho_{1,0}}{\rho_{2,0}}}\right)^2} - p_{st}\right]\frac{a_2}{\rho_{2,0}}} =$$

$$= u\sqrt{\frac{a_2\rho_{1,0}}{\rho_{2,0}}\left[\frac{1}{\left(\sqrt{a_1} + \sqrt{a_1\frac{\rho_{1,0}}{\rho_{2,0}}}\right)^2} - \frac{p_{st}}{\rho_{2,0}u^2}\right]},$$

or finally,

$$u_{x,0} = u\sqrt{\frac{1}{\left(1 + \sqrt{\frac{a_1}{a_2}\frac{\rho_{2,0}}{\rho_{1,0}}}\right)^2} - \frac{p_{st}a_2}{\rho_{2,0}u^2}}. \tag{73.8}$$

For $\rho_{2,0}u^2 \gg a_2 p_{st}$, relationship (73.8) transforms to relationship (73.3) and if the jet and the obstacle consist of one and the same metal, then $u_{x,0} = \frac{u}{2}$. At the velocities u of cumulative jets which we usually encounter in practice, the value of $\frac{u_{x,0}}{u} < \frac{1}{2}$.

For $p_\infty = p_{st}$, $u_{\infty,0} = 0$, which is attained for $u = u_{crit}$. The results obtained correspond to actual conditions of armour-piercing by cumulative charges.

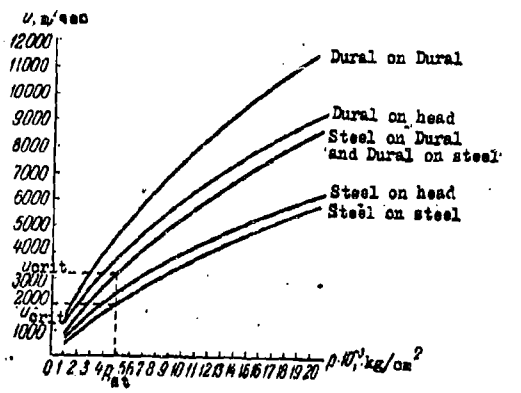
Knowing the value of u_{crit} by experiment for the appropriate metals, it is easy to calculate values of p_{st} for them. For this purpose relationship (73.6) is used, which, after substituting $u = u_{crit}$ and $p_\infty = p_{st}$ in it, assumes the form

$$p_{st} = \frac{\rho_{1,0} u_{crit}^2}{\left[\sqrt{1 - \frac{1}{\left(1 + \frac{p_{st}}{A_1}\right)^{\frac{1}{n}}}} + \sqrt{\frac{\rho_{1,0}}{\rho_{2,0}}\left(1 - \frac{1}{\left(1 + \frac{p_{st}}{A_2}\right)^{\frac{1}{n}}}\right)}\right]^2} = 0\rho_{1,0} u_{crit}^2 \qquad (73.9)$$

The calculation of p_{st} is conveniently carried out by a graphical method. For this purpose different values are assigned to p_∞ and the corresponding values of u are calculated. The results of the calculations are presented in the form of graphs of $p_\infty = f(u)$, which can be used to determine p_{st} according to the values of u_{crit} found experimentally.

The relationship between the pressure p and the velocity u of a cumulative jet is presented in Table 108 and in Figure 185.

Figure 185. Relationship between velocity and pressure as a result of the interaction of a cumulative jet with different obstacles.



It can be seen from Fig,185 that for steel with hardness $H_B = 125$, $p_{st} = 4.8 \cdot 10^5$ kg/cm^2, and for duralumin with a hardness $H_B = 115$, $p_{st} = 2.8 \cdot 10^5$ kg/cm^2.

We note that p_{st} for steel amounts to about 20 – 25% of the maximum (initial) pressure, which originates in the obstacle at the instant of its collision with the leading portion of the cumulative jet.

The calculation of the penetration velocity $u_{s,0}$, is carried out in the following manner. Using the graph (Fig.185), the corresponding value of p_0 is found for a jet velocity v and then a_1 and a_2 are determined according to formula (73.4). The values found for these quantities are substituted in relationship (73.8).

Table 108

Relationship between the pressure and velocity for penetration of a cumulative jet.

p, kg/cm^2	v, m/sec (duralumin jet through duralumin obstacle)	v, m/sec (duralumin jet through steel obstacle)	v, m/sec (steel jet through steel obstacle)
$1 \cdot 10^5$	1500	900	510
$2 \cdot 10^5$	2320	1640	970
$3 \cdot 10^5$	3200	2270	1380
$4 \cdot 10^5$	4000	2870	1760
$5 \cdot 10^5$	4670	5390	2120
$6 \cdot 10^5$	5310	3870	2450
$7 \cdot 10^5$	5930	4350	2785
$8 \cdot 10^5$	6520	4775	3070
$9 \cdot 10^5$	7060	5180	3350
$1 \cdot 10^6$	7570	5580	3630
$1.2 \cdot 10^6$	8540	6340	4110
$1.4 \cdot 10^6$	9450	7040	4640
$1.6 \cdot 10^6$	10250.	7660	5110
$1.8 \cdot 10^6$	11100	8290	5550
$2 \cdot 10^6$	11850	8890	5980

The results of a few calculations which have been carried out, and applicable to obstacles and cumulative jets of steel and duralumin, are presented in Table 109, where the relationship between $u_{x,0}$ and the jet velocity u is given.

Table 109

Relationship between penetration velocity and jet velocity.

Jet material – Duralumin Armour plate material – Steel		Jet material – Steel Armour plate material – Steel	
u, m/sec	$u_{x,0}$, m/sec	u, m/sec	$u_{x,0}$, m/sec
3300	0	2050	0
4000	610	3000	940
5000	1060	4000	1540
6000	1470	5000	2080
7000	1890	5500	2360
8000	2260	6500	2770
9000	2650	7000	3340

In Table 110 the values of the average prnetration velocities are compared, which have been established experimentally and calculated according to LAVRENT'YEV's formula and according to formula (73.8), for the initial stages of armour-piercing (thickness of armour 22 – 30 mm). The average velocity (u_{av}) of the element of a jet expended in the process of armour penetration was chosen for the claculations.

Table 110

Experimental and calculated armour-piercing velocities

Thickness of obstacle, mm.	Obstacle material	Jet material	Average velocity of element of jet u_{av}, m/sec.	$\frac{u_{x=0}}{u_{av}}$		
				By experiment.	By Formula (73.8)	By Lavrent'yev's Formula
30	Steel	Steel	6300	0.43	0.44	0.50
20	Duralumin.	Duralumin	8000	0.43	0.44	0.50
30	Duralumin	Steel	7100	0.57	0.60	0.65

It can be seen from the Table that the results of theoretical calculation by formula (73.8) and those by experiment are in complete agreement.

The results, calculated by LAVRENT'YEV's formula lead in all cases (even for the initial stages of penetration) to a higher value for the penetration velocity. Naturally, for greater depths of penetration, this discrepancy will be markedly increased.

§ 74. Determination of the Depth of Penetration

We shall consider the problem of motion of the boundary of the medium (penetrability) in general form. The penetration velocity of the jet is

$$u_{x,0} = \frac{dx}{dt} = u \sqrt{\frac{1}{\left(1+\sqrt{\frac{a_1}{a_2}\frac{\rho_{2,0}}{\rho_{1,0}}}\right)^2} - \frac{p_{st}a_2}{\rho_{2,0}u^2}}, \tag{74.1}$$

where u is a function of x and t.

Transforming the right hand side of equation (74.1), we obtain

$$\frac{dx}{dt} = u_0 \sqrt{\frac{u^2}{u_0^2\left(1+\sqrt{\frac{a_1}{a_2}\frac{\rho_{2,0}}{\rho_{1,0}}}\right)^2} + \frac{p_{st}a_2}{\rho_{2,0}u_0^2}}, \tag{74.2}$$

where u_0 is the initial velocity of the leading portion of the jet.

Introducing the notation

$$1+\sqrt{\frac{a_1}{a_2}\frac{\rho_{2,0}}{\rho_{1,0}}}=\beta_1,\quad \frac{\rho_{\text{вт}}a_2}{\rho_{2,0}u_0^2}=\frac{\beta_2}{\beta_1^2}, \tag{74.3}$$

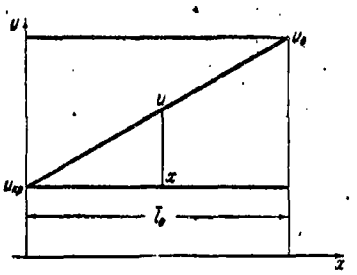
we can write equation (74.2) in the form

$$\frac{d\frac{x}{l_0}}{d\frac{u_0 t}{l_0}}=\frac{1}{\beta_1}\sqrt{\left(\frac{u}{u_0}\right)^2-\beta_2}, \tag{74.4}$$

where l_0 is the effective length of the jet for $t=0$.

Solving this differential equation for the initial conditions $x=0$, $t=0$, $u=u_0$ and $f(0,0)=1$, we find $x=F(t)$. Knowing that at the end of penetration $\frac{u}{u_0}=\frac{u_{\text{crit}}}{u_0}$, it can be determined that $x_t=L$, by simultaneous solution of the equations $x_t=F(t_t)$ and $f(x_t,t_t)=\frac{u_{\text{crit}}}{u_0}$, where L is the depth of penetration and t_t is the time to the end of penetration.

Figure 186. Linear distribution of velocities along a cumulative jet.



The solution of this problem leads to a cumbersome expression, from which the value of L can be determined by the method of successive approximation or by tables.

However, the depth of penetration can be determined more simply. For this, we require the velocity in the jet to be neutralized, so that the Law of Conservation of Energy for the jet is fulfilled. For a linear velocity distribution in the jet, which follows from simple geometrical considerations(Fig.186), we can write

$$\frac{u_0-u}{u_0-u_{\text{crit}}}=\frac{\bar{l}_0-x}{\bar{l}_0},$$

or,

$$u=u_0-\left(1-\frac{x}{\bar{l}_0}\right)(u_0-u_{\text{crit}}). \tag{74.5}$$

($\bar{l}_0$ is the length of the jet at the instant of arrival at the armour plate); the energy of the jet is

$$E = \frac{s\bar{l}_0\rho_0\bar{u}^2}{2} = \frac{sl_0\rho_0}{2}\int_0^1 u^2 d\frac{x}{l_0} = \frac{sl_0\rho_0}{2}\int_0^1 \left[u_{crit} + \frac{x}{t}(u_0 - u_{crit})\right]^2 d\frac{x}{l_0} =$$

$$= \frac{sl_0\rho_0}{2}\left[u_{crit}^2 + \frac{(u_0 - u_{crit})^2}{3} + u_{crit}(u_0 - u_{crit})\right], \tag{74.6}$$

and from equations (74.5) and (74.6) we can obtain that

$$\frac{\bar{u}}{u_0} = \sqrt{\frac{1 + \frac{u_{crit}}{u_0} + \frac{u_{crit}^2}{u_0^2}}{3}}, \tag{74.7}$$

where $\bar{u}$ is the neutralized velocity of the jet.

In order to calculate the depth of penetration, we obtain the equation

$$u_{\infty,0} = \frac{dx}{dt} = \frac{\bar{u}}{\beta_1}\sqrt{1 - \beta_2}.$$

Integrating this expression, we have

$$L = \frac{\bar{u}t_1}{\beta_1}\sqrt{1 - \beta_2}, \tag{74.8}$$

where L is the depth of penetration, t_1 is the time to the instant of completion of the penetration. It is obvious that

$$t_1 = \frac{\bar{l}_0 + L}{\bar{u}}, \tag{74.9}$$

whence

$$\frac{L}{\bar{l}_0} = \frac{1}{\dfrac{1 + \sqrt{\frac{\alpha_1}{\alpha_2}\frac{\rho_2}{\rho_1}}}{\sqrt{1 - \frac{p_{st}}{\rho_2\bar{u}^2}\frac{\alpha_2}{\left(1 + \sqrt{\frac{\alpha_1}{\alpha_2}\frac{\rho_2}{\rho_1}}\right)^2}}} - 1}. \tag{74.10}$$

For $p_{st} \to 0$,

$$\frac{L}{\bar{l}_0} = \sqrt{\frac{\alpha_2}{\alpha_1}\frac{\rho_{1,0}}{\rho_{2,0}}}. \tag{74.11}$$

If the compressibility coefficient of the metals of which consist the jet and the obstacle are identical ($\alpha_1 = \alpha_2$), then we arrive at LAVRENT'YEV's formula

$$L = \bar{l}_0\sqrt{\frac{\rho_{1,0}}{\rho_{2,0}}}. \tag{74.12}$$

From the relationships which have been obtained, it can be concluded that the armour-piercing capability of a cumulative jet, for approximately equal conditions, is proportional to the length of the generatrix of the lining. Therefore, for equal heights, a lining of hyperbolic shape is more advantageous than a conical lining. The use of a lining with a generatrix in the form of the branch of a logarithmic spiral is irrational, since it forms not a normal jet but a spherical bullet.

In order to achieve the maximum armour-piercing effect $(L = L_{max})$ it is essential that the quantity l_0 be chosen in such a manner that during the time of the entire subsequent process of penetration of the jet into the armour plate, the jet should maintain its continuity.

The optimum value for $\bar{l}_0 = l_0 + R_f$ (l_0 is the initial length of the jet; R_f is the focal distance) is equal to the optimum distance of the charge from the armour plate, at which the cumulative jet has the maximum penetration capability.

Consequently, in the case specified, the concept of "focal distance" has a completely different physical significance than for a cumulative charge without lining.

For approximately equal conditions, the focal distance will be greater for the charge having a cumulative lining of metal which has a greater capability of being stretched without breaking down.

For modern cumulative charges with a conical recess and iron lining,

$$\frac{l_{eff}}{l_0} \approx 3,$$

where l_0 is approximately equal to the length of the generatrix of the cone.

§ 75. Determination of the Diameter of the Hole

An accurate determination of the diameter of the hole is extremely complex. However, an approximate relationship for calculating the diameter of the hole can be obtained as a result of the following considerations.

It may be assumed that after the impact of the leading portion of the jet with the surface of the obstacle, transient high pressures p_m are formed (which we calculated above). These pressures are relieved very rapidly, as a consequence of which radial motion of the material of the obstacle takes place under the action of the inertial forces. Bearing in mind that the lateral shock wave is almost cylindrical, the following relationship can be written down :

$$\frac{p_{lat}}{p_m} = \sqrt{\frac{r_0}{R_h}}, \qquad (75.1)$$

where p_{lat} is the lateral pressure, p_m is the pressure in the axial direction, r_0 is the mean radius of the jet and R_h is the current radius of the hole.

Assuming that the radial motion of the metal ceases when $p_{lat} = p_{st}$ we can find the radius of the hole from equation (75.1)

$$(R_h)_{in} = r_0 \left(\frac{p_m}{p_{st}}\right)^2. \qquad (75.2)$$

At the instant of completion of penetration, i.e. when $p_m = p_{st}$, $R_{hm} = r_0$. In the example given, the maximum value for $p_m = 2.0 \cdot 10^6$ kg/cm^2, $p_{st} \approx 5.0 \cdot 10^5$ kg/cm^2. The mean radius of the jet, $\bar{r}_0$, is determined by the formula

$$\bar{r}_0 = \sqrt{\frac{2}{3}\frac{R_c \delta \cos\alpha}{\psi}} \sin\frac{\alpha}{2}.$$

Substituting the values $2R_c = 60$ mm, $\delta = 2$ mm, $\alpha = 35^0$ for our actual case and assuming that the maximum coefficient of extension for present-day steel casings $\psi \approx 5$, we find $\bar{r}_0 = 0.76$ mm.

Using equation (75.2), we find the maximum diameter of the hole $d_h = 2R_h \approx 24$ mm, which is in good agreement with experiment.

When the charge is exploded under such conditions that the process of normal jet formation is disrupted and its effective extension is not achieved (for example, if the charge is placed immediately on the armour plate), then the diameter of the hole may be considerably increased , which is, in fact, observed in practice. Naturally, the depth of penetration as a result of this is reduced(since the length of the jet $l < l_{min}$)

§ 76. Effect of Rapid Spin on the Stability of a Cumulative Jet and on its Armour-piercing Action.

It is well-known that the armour-piercing action of a spinning cumulative ammunition is less than that of non-spinning ammunition. With increase of angular velocity of a cumulative charge, the negative effect of spin motion is intensified. Systematic investigations of the effect of spin on the cumulative effect, as a function of the diameter and shape of the recess, the angular velocity of the charge and the distance from it to the obstacle, have been carried out by BAUM. Certain experiments in this direction were also carried out under the leadership of LAVRENT'YEV.

The Effect of Calibre(diameter of the base of the recess) of a Charge on the Armour-piercing Effect with Spin. For investigating the effect of this factor, charges of trotyl-hexogen 50/50 mixture were used in steel casings with a conical recess. The cumulative cavities(linings) were of steel. The experiments were carried out at spin velocities of 20,000 to 30,000 rpm. The charges were exploded at the focal distance from the armour plate. The results of these experiments are presented in Table 111.

It is obvious from the table that with increase of calibre of the charge, the negative influence of rotation is intensified, and to a large extent for charges with a deep conical recess. This is explained by the fact that in view of the Law of Conservation of Momentum, the elements of the jet will have an angular velocity determined by the moment of the momentum of the corresponding lining element relative to its instantaneous axis of spin as a result of "slamming". The maximum angular velocity of the jet is determined by the expression

$$\omega_{jet} = \omega_0 \left(\frac{R_0}{R_c}\right)^2, \qquad (76.1)$$

where ω_0 is the angular velocity of the charge, R_0 is the base radius of the cone, R_c is the base radius of the cone(pestle) after its total compression.

Table 111

Effect of spin on the armour-piercing action of cumulative charges.

Diameter of charge, mm	Parameters of cone		Wall thickness of lining, mm	Depth of penetration, mm.		Reduction in armour-piercing effect, %
	Diameter of base of recess, mm	$\frac{h}{d}$		Without spin	n = 20,000 r.p.m.	
32	26	1	1.0	45 ± 5	37 ± 4	20
55	44	1	1.5	77 ± 1	57 ± 2	26
76	56	1	2.0	132 ± 3	90 ± 5	32
32	26	2	2.0	74 ± 5	44 ± 5	41
76	56	2	2.0	205 ± 5	82 ± 2	60

Here R_c refers to the pestle and not to the jet, since at the instant of formation, the pestle and jet comprise a single body and, consequently,

they have identical angular velocity.

It follows from (76.1) that with increase in calibre of the charge, the angular velocity of the jet increases considerably, which, as we shall show below, has a negative influence on its stability.

Effect of Angle of Flare of the Cone on Armour-piercing Effect, as a Result of Spin. With the object of investigating the effect of this factor, tests were carried out with 76-mm cumulative charges, having conical recesses and an angle of flare of 60°, 35° and 27°. The results of these tests are presented in Table 112.

On the basis of the data in Table 112, we can draw the following conclusions.

1. A high cone with a stationary explosion guarantees greater armour-piercing effect than a low cone. This is explained for the most part by the fact that with a high cone, a greater length and greater velocity of the cumulative jet is attained.

2. The negative effect of spin, for approximately equal conditions, is intensified with decrease in the angle of flare of the cone. This is explained by the fact that a long jet, because of twisting under spin conditions, is less stable.

Table 112

Effect of the flare angle of the cone on the armour-piercing action of spinning cumulative charges

Shape of recess	Parameters of recess			Penetration effect, mm.		Reduction of armour-piercing effect by spin, %.
	α	d_b, mm.	$\frac{h}{d_b}$	Without spin	n = 20,000 r.p.m.	
Cone	27	56	2.0	205 ± 5	82 ± 2	60
Cone	35	56	1.2	160 ± 5	88 ± 8	46
Cone	60	56	1.0	150 ± 5	90 ± 5	52
Hyperbola	-	56	2.0	160 ± 5	85 ± 5	47

The effect of spin velocity on the armour-piercing effect is shown in Table 113.

Table 113

Effect of spin velocity on the armour-piercing effect of cumulative charges

Diameter of charge, mm	Shape of recess	Parameters of recess		Depth of penetration, mm				
		d_{base}, mm	h/d	Without spin	n = 5000 r.p.m.	n = 10,000 r.p.m.	n = 15,000 r.p.m.	n = 20,000 r.p.m.
76	Cone	56	2	205	120	115	98	82
76	Hyperbola	56	2	160	150	150	100	85

In Table 114, data are presented characterizing the effect of spin as a function of the distance of the charge from the armour plate. 76-mm charges

with conical recesses were tested.

It can be seen from the table, that by exploding charges with a conical recess ($h/d_{base} = 1$) under stationary conditions, the cumulative jet possesses a quite stable armour-piercing efficiency at distances between charge and armour plate equal to twice the calibre. However, the negative influence of spin on armour-piercing capability of a cumulative jet commences to be effective even at very short distances between the charge and the armour plate, which testifies to the rapid disruption and breakdown of the jet under spin conditions.

Table 114

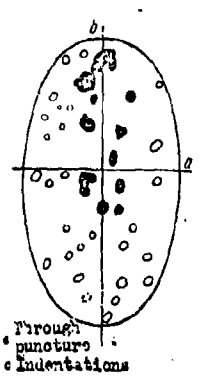
Relationship between armour-piercing action (depth of penetration, mm) and the distance between charges and armour plate.

Spin velocity	Distance between charge and armour plate, mm			
	10	40	76	152
Without spin	100	132	-	120
20,000 r.p.m.	70	90	70	40

In studying the question of structure and the reasons for disruption of a cumulative jet as a result of spin, it is particularly interesting from the point of view of principles, to determine the behaviour and operating regime at relatively far distances from the point of explosion of the charge, at which are observed quite distinct symptoms of disruption of the jet, even as a result of normal stationary explosion.

§77. Concerning the Stability of a Cumulative Jet

Figure 187. Effect of a 76-mm cumulative charge on a slab (distance between charge and slab 4.5 mm).



The results of investigations permit the conclusion to be drawn that the most important initial forms of disruption of the jet appear to be in the following :

1. In the breakdown of the monolithic nature of the jet under the action of velocity gradients, as a consequence of which disintegration of the jet takes place into a large or small number of elements. As a result of large gradients, intense disintegration of the jet may occur, and, as a consequence of this, it is converted into a stream of finely divided metallic particles.

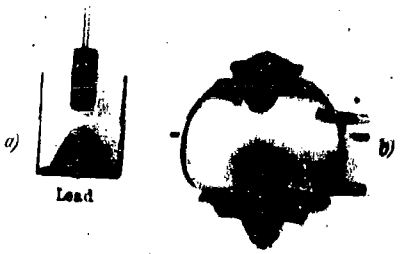
The fall in armour-piercing capability with distance in the given case is a consequence of the reduction in density and radial divergence of the jet because of the resistance of the air. Figure 187 shows the zone of lethality (holes and indentations) of 20-mm armour plate of a 76-mm cumulative charge at a distance of 4.5 m. from the site of explosion (this zone is elliptical in shape with semi-axes a = 18 cm and b = 58 cm).

2. In the expansion of the jet and its subsequent radial disintegration under the action of the energy of elastic compression, accumulated in the jet during the period of its formation. A similar type of disruption is distinctly observed with jets from lead, which has a large volume compressibility.

The nature of the jet formed by a lead lining is shown in Figure 188.

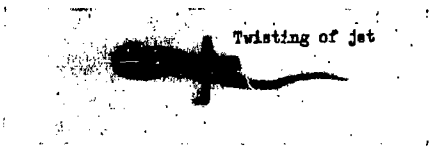
Figure 188. Lead cumulative jet :

a) - charge prior to explosion, *b*) - formation of lead cumulative jet, 12 microsec after explosion.



3. In the twisting of the jet as a consequence of asymmetry of the explosive impulse or of the cumulative crater, which leads to deviation of the individual elements of the jet from their normal trajectory and to a reduction in the armour-piercing efficiency (Figure 189). This form of instability for the appropriate conditions(in the case of a relatively large twisting of the jet and its destruction) may lead to the formation of two or more perforations in the armour plate.

Figure 189. Destruction of stability of a cumulative jet.



Under actual conditions of usage of cumulative charges, the possibility should not be excluded of the simultaneous appearance of all the factors which we have enumerated.

Under conditions of stationary explosion, disruption of the jet is only sufficiently noticeable at relatively large distances from the site of the explosion. However, as a result of rapid spin of the charge, the jet, under

Figure 190. Effect of a spinning cumulative charge on an obstacle (n = 20,000 r.p.m)



Figure 191. Effect of non-spinning cumulative charge on an obstacle.



the action of centrifugal forces may even undergo more profound disruption at once, associated with the increase in the extent of twisting of the jet and with the radial dispersion of its individual elements. The phenomena mentioned, at distances relatively close to the charge, should lead to an increase in the diameter of the hole, to breakup of the jet with simultaneous reduction of the depth of penetration, and at larger distances to practically total elimination of the armour-piercing effect.

Figure 192. Action of a non-spinning cumulative charge on an obstacle.



The considerations mentioned are found to be in complete agreement with the results of experiment. Thus, for example, Figure 190 shows the effect of a cumulative jet on an obstacle under conditions of explosion of a charge having a spin velocity of 20,000 r.p.m. In the given case, as a consequence of the disruption of the jet, several indentations were formed in the armour plate, which were spread over a relatively large area. The results of the action on armour plate of a similar charge as a result of stationary explosion and identical distance from the obstacle are shown in Figure 191.

A steel screen with a thickness of 20 mm was placed in the path of the cumulative jet from a 76-mm charge at a distance of 135 cm from the charge. The nature of the damage to the screen as a result of stationary explosion is shown Fig. 192, and the same with spin is shown in Fig. 193.

On the basis of the data presented, it can be concluded that the observed differences in disturbance of the stability of the jet as a result of spin and under conditions of stationary explosion are only of a quantitative nature. Disruption of the jet, observed with stationary explosion at relatively large distances from the charge, occurs at considerably smaller distances with spin.

The deformations of a cumulative charge as a result of possible asymmetries of the explosive impulse and of the lining were investigated theoretically by KREIN. From the results obtained by him, it follows that

even with slight asymmetry of the cumulative lining or of the explosive impulse, displacement of the centre of formation of the jet takes place relative to the primary axis of the charge. In connection with this, and also as a consequence of the change with respect to time of the direction of the initial velocities of the jet elements, twisting of the jet occurs.



Figure 193. Effect on an obstacle of a spinning cumulative charge.

According to LAVRENT'YEV, this type of disruption of a cumulative jet is more frequently encountered in practice and is the primary reason for the negative influence of spin on the armour-piercing properties of cumulative charges. As a result of this he proceeds to the following considerations.

Asymmetry of the explosive impulse, to some degree or other, almost always occurs in actual charges as a consequence of the deviation of the axis of the recess from the axis of the lining, incorrect positioning of the detonator, and a number of other reasons. However, under conditions of stationary explosion, the initial twisting of the jet will be reduced as a consequence of two stabilising factors : the effect of the air medium and the stresses in the jet, which originate because of its extension, as a result of which the jet will be straightened out.

Confining ourselves to an analysis of the second factor, the jet can be considered, to a first approximation, as a jet which is under a tension p_0 as a result of plastic flow. The frequency of oscillation of a string, and consequently also the jet, is determined by the well-known formula

$$\tau = \frac{\pi}{l}\sqrt{\frac{p}{\rho}}, \qquad (77.1)$$

where l is the length, p is the tension and ρ is the density.

If we assume that $p = 4 \cdot 10^3$ kg/cm^2 and $l = 3$ cm (the element of the jet with the most clearly defined antinode), then we obtain, in accordance with formula (77.1), that the time required for the antinode to die out is

$$t_0 < 5 \cdot 10^{-6} \text{ sec},$$

i.e. with a velocity of the rear portion of the jet $w_1 = 4 \cdot 10^3$ m/sec, the antinode will be wiped out when the element of jet being considered traverses a path $s = 2$ cm.

Thus, on the free-flight path of the rear portion of the jet to the armour plate, the stabilising factor under consideration may considerably reduce the amplitude of the jet. LAVRENT'YEV notes that for the asymmetries existing in actual charges and for angular velocities of the lining of 5000 - 15,000 r.p.m., the centrifugal forces are found to be greater than the stabilising forces from the tension of the jet.

As a result of the motion of a spinning jet, its antinode will increase; the rear portion of the jet will not strike the hole pierced by its leading portion; the energy of the rear portion will be expended on piercing a second hole.

In conclusion, we note that the factor we have considered cannot be recognised as the sole cause of the negative influence of spin on the cumulative effect. Side by side with twisting of the jet, and a no less important form

of disruption(as indicated by numerous photographs) is disintegration of the jet into discrete particles.

A simple calculation shows that under the action of the centrifugal forces , and during the process of motion of the spinning jet, quite considerable dispersion of it may occur radially.

In fact, the maximum centrifugal forces originating in the jet, can be determined by the formula

$$p = \rho_0 r_0 \omega^2 = \rho_0 r_0 \omega_0^2 \left(\frac{R_c}{r_0}\right)^2, \qquad (77.2)$$

where r_0 is the initial diameter of the cumulative jet, ρ_0 is the initial density of the jet.

The centrifugal forces, originating in a jet as a result of firing a 76-mm cumulative missile from a 15-calibre gun, calculated by the formula given are approximately equal to 1800 kg/cm^2.

Under the action of the centrifugal forces, divergence of the jet should occur, which is a function of time. The acceleration acquired by particles of the jet is determined by the expression

$$\frac{d^2r}{dt^2} = \omega^2 r, \qquad (77.3)$$

where r is the radius of the jet, t is the time and ω is the angular velocity of the jet.

On integrating this differential equation we obtain

$$\frac{r}{r_0} = \frac{1}{2}(e^{\omega t} + e^{-\omega t}). \qquad (77.4)$$

Knowing the value of ω_0 = 500 r.p.m., the ratio $\frac{r}{r_0}$ can easily be calculated for any instant of time.

The total time of motion of the elements of the jet in air (over a path of 50 mm) and of penetration into armour plate to 30 mm, amounts approximately

to $t = 3 \cdot 10^{-5}$ sec for the case we are considering.

The results of the calculation show that at this instant, the diameter of the jet is increased by 25%, and its lethality area by 56%. The average density of the jet is correspondingly reduced by 50%. This result is foundt to be in accordance with the reduction in penetrability (by 52%), which was laid down in our experiments on spin.

§78. Super High-speed Cumulation

It is of great interest in experimental physics to obtain gaseous and metallic jets which are moving with velocities of around several tens of kilometres per second. In addition to the use of powerful electrical charges, leading to similar velocities of motion in plasmas, it was shown by the work of I.V. KURCHATOV et al, that cumulation methods can be used for obtaining such high velocities.

By analyzing the basic relationship of the theory of cumulation

$$w_1 = \frac{w_0}{\tan \frac{\alpha}{2}}, \qquad (78.1)$$

it is easy to satisfy oneself that the velocity of a cumulative jet increases with decrease of the angle α. Hence it follows that if the velocity of "slam" w_0 of the elements of the lining is sufficiently large(which can be achieved by the correct choice of explosive, lining metal and other parameters of a cumulative charge), then for sufficiently small values of α an extremely high velocity can be achieved, in principle, for a cumulative jet. Such velocities can be attained, in particular, under conditions of achievement of cylindrical cumulation.

It has been shown in a series of works by American scientists that by using cylindrical tubes made of light metals as linings, the lateral surface

of which is enclosed in a quite thick lay of explosive, a velocity of around several tens of kilometres per second c... be ensured in the leading portion of the cumulative jet. The maximum velocity of the cumulative jet, equal to 90 km/sec, was attained by using tubes of beryllium, the specific gravity of which is 1.5. A shaped(cumulative) charge is shown diagrammatically in Fig.194.

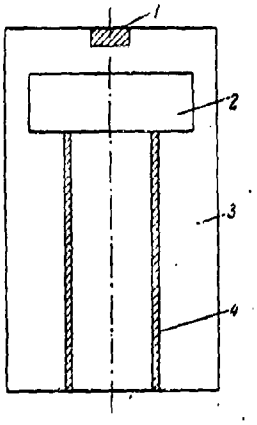


Figure 194. A Shaped (Cumulative) charge. 1 - Detonator, 2 - Heavy lens, 3 - Explosive charge, 4 - Cumulative lining.

As a consequence of the non-simultaneous arrival of the detonation wave at the different elements of the lining, its implosion shock, in spite of the cylindrical shape of the lining, will still occur all over at a certain angle, which will increase according to the extent of advancement of the detonation wave along the tube. By regulating the time of arrival of the detonation wave at the various elements of the tube in some way or other, the angle α can be altered within certain limits, and thereby a given velocity distribution in the cumulative jet can be assured, for the maximum possible velocity of its leading portion.

The parameters of a cumulative jet, in the case of cylindrical shaping, can be easily calculated. First of all we estimate the angle through which the elements of the lining converge towards the axis. We shall give the solution for the plane wave case, obtained by BAUM and STANYUKOVICH.

We shall employ for the calculation the scheme for which the detonation wave, curved by the "lens", begins to excite the active portion of the charge at a distance y_0 from the metallic lining (Fig. 195). The front of the detonation wave, commencing at the point y_0, reaches the point x_0 in a time

$$t_0 = \frac{\sqrt{x_0^2 + y_0^2}}{D}, \tag{78.2}$$

The motion of a given element of the lining commences exactly at this instant of time. We shall assume that every element of the lining is moving along the y - axis, so that the law of motion of an element of lining is determined by the expression

$$\frac{M}{s}\frac{d^2y}{dt^2} = p, \tag{78.3}$$

where $M = s\delta h$ is the mass of a given element of lining; s is its area; h is the thickness and δ is the density of the lining material. Hence,

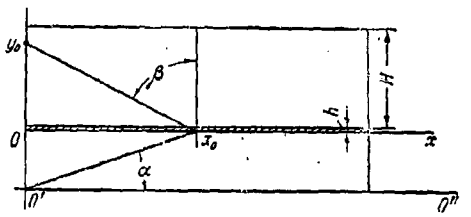
$$\frac{d^2y}{dt^2} = \frac{p}{\delta h}, \tag{78.4}$$

Integrating equation (78.4) with respect to time, we find that the velocity of motion of the given element of lining is

$$w_0 = \frac{dy}{dt} = \frac{1}{\delta h}\int_{t_0}^{t} p\,dt = \frac{I(t)}{\delta h}, \tag{78.5}$$

where $I = I(t)$ is the impulse (momentum) transmitted to a given element of lining and calculated per unit area of the element.

Figure 195. Derivation of the relationships for a cumulative charge with a cylindrical lining.



The pressure acting on the given element of lining can be determined approximately by the relationship

$$p = p_0\left(\frac{t_0 - t_1}{t - t_1}\right)^3, \qquad (78.6)$$

where the quantities p_0 and t_1 depend on the coordinate x_0 of the given lining element. It may be assumed for this that the impulse imparted by a given element of explosive to a given element of lining is constant and is independent of x_0. The momentum, which the detonation products develope in a given direction (without connecting masses), having a mass m, is determined, as we know, by the expression

$$I_0 = \frac{4}{27} mD. \qquad (78.7)$$

As a result of this, half the mass of the explosion products moves to one side, and half to the other side. The total momentum is equal to zero, since the forces acting as a result of the explosion are internal forces. On reflection from an absolutely solid wall

$$I_{refl} = 2I_0 = \frac{8}{27} mD. \qquad (78.8)$$

If the explosive is enclosed in a metal case, and the mass of the wall of the case corresponding to the mass of a given element of explosive is M_2,

and the mass of an element of lining is M_1; then we can calculate the corresponding momentum developed as a result of detonation and of the connecting masses of lining and wall which are projected.

The respective relationships are presented in para. 65.

In the particular case when $M_2 = 0$, the formula is considerably simplified :

$$I = I_0 \frac{(m+2M_1)^2}{\sqrt{(m+M_1)^2(m+4M_1)}}. \tag{78.9}$$

If $M_2 = M_1 = M$, then

$$I = I_0\left(1+\frac{2M}{m}\right)\sqrt{\frac{1}{1+\frac{3M}{m}}}. \tag{78.10}$$

The latter case is simple for calculation ; we shall also use it.

In the general case, we shall suppose that

$$I = \eta I_0. \tag{78.11}$$

In particular, η is determined from equations (78.9) or (78.10). Since $M = sh\delta$, then $m = sH\rho_0$ and $\frac{M}{m} = \frac{h\delta}{H\rho_0}$, where ρ_0 is the density of the explosive.

Then,

$$I = I_0\left(1+\frac{2h\delta}{H\rho_0}\right)\sqrt{\frac{1}{1+\frac{3h\delta}{H\rho_0}}} = \eta I_0. \tag{78.12}$$

From relationship (78.6) we find

$$I = \int_{t_1}^{\infty} p\,dt = \frac{p_0}{2}(t_0 - t_1). \tag{78.13}$$

The value of p_0 for normal reflection is determined by the relationship

$$p_0 = \frac{64}{27} p_1, \tag{78.14}$$

where $p_1 = \frac{\rho_0 D^2}{4}$, whence

$$p_0 = \frac{16\rho_0 D^2}{27}. \tag{78.15}$$

As a result of sliding of the detonation wave

$$p_0 = p_1. \tag{78.16}$$

It can be assumed in the general case that

$$p_0 = p_1 + \left(\frac{64}{27} - 1\right) p_1 \cos^2\beta, \tag{78.17}$$

where β is the angle between the front of the detonation wave and the lining. Expression (78.17) can be conveniently written in the form

$$p_0 = p_1\left[1 + \frac{37}{27}\cos^2\beta\right]. \tag{78.18}$$

Thus, since $\cos^2\beta = \frac{y_0^2}{x_0^2 + y_0^2}$, and $t_0 = \frac{\sqrt{x_0^2 + y_0^2}}{D}$, we have

$$p_0 = p_1 \frac{64y_0^2 + 27x_0^2}{27(x_0^2 + y_0^2)}. \tag{78.19}$$

Using relationships (78.7), (78.11) and (78.19) we obtain

$$\eta' = \eta/\eta_0 = \frac{4s\rho_0 HD\eta}{27} = \frac{s\rho_0 D}{8 \cdot 27} \frac{64y_0^2 + 27x_0^2}{x_0^2 + y_0^2}(\sqrt{x_0^2 + y_0^2} - Dt_1), \tag{78.20}$$

whence it follows that

$$Dt_1 = \sqrt{x_0^2 + y_0^2} - 32\eta H \frac{x_0^2 + y_0^2}{64y_0^2 + 27x_0^2}, \tag{78.21}$$

Thus, in the approximate law for the fall of pressure with time at the boundary of the explosion products and the lining, we know all the constants (p_0, t_0, t_1). In particular, if $x_0 = 0$, $y_0 = H$, $M_2 = 0$, $M_1 \to \infty$, then $\eta = 2$, and $Dt_1 = 0$, which follows from the theory of reflection of a detonation wave. Since

$$p = p_0\left(\frac{t_0 - t_1}{t - t_1}\right)^3,$$

where $p = p_0(x_0)$, $t_1 = t_1(x_0)$, (for a given y_0), then, on using equation (78.3), we find

$$w_0 = \frac{dy}{dt} = \frac{p_0}{2\delta h}\int_{t_1}^{t}\left(\frac{t_0 - t_1}{t - t_1}\right)^2 = \frac{p_0}{2\delta h}\left(t_0 - t_1\right)^3\left[\frac{1}{(t_0 - t_1)^2} - \frac{1}{(t - t_1)^2}\right] \qquad (78.22)$$

Integrating equation (78.22) with respect to time, we find the law of motion of the given element of lining :

$$y = \frac{p_0}{2\delta h}(t_0 - t_1)\left[t + t_1 - 2t_0 + \frac{(t_0 - t_1)^2}{t - t_1}\right]. \qquad (78.23)$$

Since

$$p_0 = p_1\frac{64y_0^2 + 27x_0^2}{27\left(y_0^2 + x_0^2\right)}, \qquad \text{and} \qquad t_0 - t_1 = \frac{32H\eta}{D}\frac{x_0^2 + y_0^2}{64y_0^2 + 27x_0^2}, \text{ then}$$

equation (78.23) assumes the form

$$y = \frac{16}{27}\frac{p_1 H\eta}{D\delta h}\frac{(t - t_0)^2}{t - t_1}, \qquad (78.24)$$

or

$$y = \frac{4}{27}\frac{H\eta p_0}{h\delta}\frac{D(t - t_0)^2}{t - t_1} \qquad (78.25)$$

Knowing $y = y(t, x_0)$, it is easy to determine the angle α, at which a given element of lining reaches the plane of symmetry.

It is obvious that

$$\tan\alpha = \left(\frac{\partial y}{\partial x_0}\right)_t. \qquad (78.26)$$

The velocity which the given element of lining will have as a result of this is,

$$w_0 = \left(\frac{\partial y}{\partial t}\right)_{x_0}. \qquad (78.27)$$

Since the velocity of the jet is $w_1 = \frac{w_0}{\tan\frac{\alpha}{2}}$ and for small angles (and it is precisely these small angles in which we are interested for obtaining high velocities) $\tan\frac{\alpha}{2} \approx \frac{1}{2}\tan\alpha$, then

$$w_1 \approx \frac{2w_0}{\tan\alpha} = 2\frac{\left(\frac{\partial y}{\partial t}\right)_{x_0}}{\left(\frac{\partial y}{\partial x_0}\right)_t} = 2\frac{\partial(y; x_0)}{\partial(t; y)} = -2\left(\frac{\partial x_0}{\partial t}\right)_y. \qquad (78.28)$$

Using expression (78.25), we find that

$$t = t_0 + Ay \pm \sqrt{2Ay(t_0 - t_1) + A^2y^2}, \tag{78.29}$$

where $A = \frac{27}{8}\frac{\delta}{\rho_0}\frac{h}{H\eta D}$,

and having written equation (78.28) in the form

$$w_1 = -\frac{2}{\left(\frac{\partial t}{\partial x_0}\right)_y}, \tag{78.30}$$

we find that

$$w_1 = \frac{2}{\frac{dt_0}{dx_0} \pm \frac{Ay\left[\frac{dt_0}{dx_0} - \frac{dt_1}{dx_0}\right]}{\sqrt{A^2y^2 + 2Ay(t_0 - t_1)}}}; \tag{78.31}$$

$$\operatorname{tg}\alpha = \frac{4}{27}\frac{H}{h}\frac{\rho_0 D}{\delta}\frac{t - t_0}{(t - t_1)^3}\left[(t - t_0)\frac{dt_1}{dx_0} - 2(t - t_1)\frac{dt_0}{dx_0}\right], \tag{78.32}$$

where

$$\frac{dt_0}{dx_0} = \frac{x_0}{D\sqrt{x_0^2 + y_0^2}},$$

$$\frac{dt_1}{dx_0} = \frac{x_0}{D}\left[\frac{1}{\sqrt{x_0^2 + y_0^2}} - \frac{64 \cdot 37\eta H y_0^2}{\left[64y_0^2 + 27x_0^2\right]^2}\right]. \tag{78.33}$$

It is obvious, that for $t = 0$ and $\alpha = 0$, the dispersing mass as a result of this however is equal to zero. In this case, both the oppositely-located parts of the lining are in contact, and the process of jet formation, in general, is not commenced. With increase of time, the angle α and the dispersing mass increases, but the velocity of the jet falls. As a result of this, for appreciable masses passing into the jet, enormous velocities of around 100 km/sec can be attained.

We find the limiting expressions for small angles, which correspond to small values of x_0, are

$$t_0 = \frac{y_0}{D}, \quad t_1 = \frac{y_0}{D} - \frac{\eta H}{2D}, \quad \frac{dt_0}{dx_0} = \frac{x_0}{Dy_0}, \quad \frac{dt_1}{dx_0} = \frac{x_0}{Dy_0}\left(1 - \frac{37\eta H}{64 y_0}\right),$$
$$\frac{w_0}{D} = \frac{4}{27}\frac{\rho_0}{\delta h}(\eta H)^2\left[\left(\frac{1}{\eta H}\right)^2 - \left(\frac{1}{2Dt - 2y_0 + \eta H}\right)^2\right], \tag{78.34}$$

$$y = \frac{4}{27}\frac{\rho_0 HD}{\delta h}\frac{\left(t - \frac{y_0}{D}\right)^2}{\left(t - \frac{y_0}{D} + \frac{\eta H}{2D}\right)}, \tag{78.35}$$

$$w_1 = -\frac{2Dy_0}{x_0}\frac{1}{1 + \frac{Ay\frac{37}{64}\frac{\eta H}{y_0}}{\sqrt{A^2y^2 + Ay\frac{\eta H}{D}}}}, \tag{78.36}$$

$$\operatorname{tg}\alpha = \frac{4}{27}\frac{H}{h}\frac{\rho_0}{\delta}\frac{x_0}{y_0}\frac{t - \frac{y_0}{D}}{\left(t - \frac{y_0}{D} + \frac{\eta H}{2D}\right)^2}\times$$
$$\times\left[\left(t - \frac{y_0}{D}\right)\left(1 - \frac{37}{64}\frac{\eta H}{y_0}\right) - 2\left(t - \frac{y_0}{D} + \frac{\eta H}{2D}\right)\right]. \tag{78.37}$$

It is obvious that the maximum velocities of motion of the jet which is formed will occur for small values of x_0. The maximum velocity will be for $x_0 = 0$. The energy of a given element of the jet is almost equal to the energy of motion of a given element of lining; this energy increases with time, and for $t \to \infty$ attains its maximum value. For $t \to \infty$,

$$\frac{w_0}{D} = \frac{4\eta\rho_0 H}{27\delta h}, \quad \frac{w_1}{D} = -\frac{2y_0}{x_0}, \quad \operatorname{tg}\alpha = -\frac{4H\rho_0 x_0}{27h\delta y_0}\left(1 + \frac{37}{64}\frac{\eta H}{y_0}\right). \tag{78.38}$$

The energy of a given element of the jet is

$$\overline{E}_1 = \frac{1}{2}\overline{m}_1\overline{w}_1^2. \tag{78.39}$$

where $\overline{w}_1$ is the velocity of the given element of the jet.

Since the mass of any given jet element is

$$\bar{m}_1 = \bar{m}_0 \sin^2 \frac{\alpha}{2} \approx \frac{\bar{m}_0}{4} \tan^2 \alpha, \tag{78.40}$$

where $\bar{m}_0$ is the mass of the given element of lining, we have

$$\bar{E}_1 = \frac{8\bar{m}_0 D^2}{27 \cdot 27} \frac{H^2 \rho_0^2}{h^2 b^2} \left(1 + \frac{37}{64} \frac{\eta H}{y_0}\right)^2. \tag{78.41}$$

This energy is independent of the quantity x_0 .

The momentum of a given element of the jet is

$$\bar{I}_1 = \bar{m}_1 \bar{w}_1 = \frac{8\bar{m}_0 D H^2 \rho_0^2 x_0}{27 \cdot 27 h^2 b^2 y_0} \left(1 + \frac{37}{64} \frac{\eta H}{y_0}\right)^2. \tag{78.42}$$

The momentum increases according to the extent of increase of x_0.

Since almost the maximum velocity of motion of the lining, w_0 , is attained for relatively small intervals of time, elapsed from the commencement of motion, there is no necessity to withdraw the lining from the plane, or in an actual case, from the axis of symmetry to a greater distance. It is sufficient to take for this distance a value around $(2 \div 5)\, y_0$.

The difference between the axi-symmetrical case and the chosen plane will be insignificant.

A similar elementary theory can be developed for linings with an arbitrary curvo-linear shape. The general expressions retain their form for this. It should also be taken into account that as a result of integrating expression (78.5), for

$$t_0 = t_0(x_0), \quad y = f(x_0), \tag{78.43}$$

i.e. y will be a given function of x_0.

Evidently it is profitable to choose a casing, nevertheless, with a rectilinear shape, but somewhat sloping towards the axis of symmetry on the side opposite from the compression (Fig. 196).

Let us now pass on to the determination of the pressure and temperature

resulting from the impact of a cumulative jet with a solid obstacle.

As a result of the collision of two cumulative jets, having velocities of around 100 km/sec, extremely high pressures and very considerable temperatures should originate, which considerably exceed those resulting from the collision of normal cumulative jets.

In order to explain which equation of state must be used in the given case for describing the collision process, we first of all make a rough estimate of the pressures originating as a result o f this.

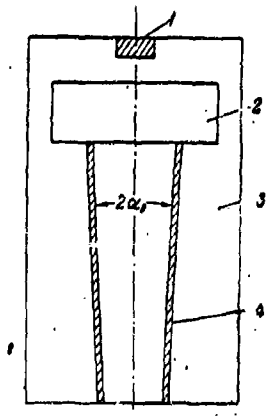


Figure 196. A Shaped charge ; 1 - detonator, 2 - heavy lens, 3 - explosive charge, 4 - cumulative lining.

The problem concerning the collision of two cumulative jets is equivalent to the problem of impact with an absolutely rigid obstacle. As a result of impact with the obstacle, a shock wave originates in the cumulative jet, which proceeds from the wall, the initial pressure in which, as we know, is determined by the relationship

$$p_* = \frac{\rho_0 u_0^2}{1 - \frac{\rho_0}{\rho_*}} = \frac{\rho_0 u_0^2}{\alpha}, \qquad (78.44)$$

where u_0 and ρ_0 are the velocity and density of the cumulative jet, p_* and ρ_* are the pressure and density at the shock front which has been formed.

It is obvious that the pressure p_* will be a minimum for $\alpha = 1$. The value of α is determined by the equation of state of the given material.

If, within the range of high pressures which are of interest to us, we assume the equation of state for the material of the jet to be of the form $p = A\rho^n$, then the limiting density ρ_* will be determined by the relationship

$$\frac{\rho_*}{\rho_0} = \frac{n+1}{n-1}.$$

As a result of this,

$$a_{\lim} = \frac{2}{n+1}, \quad p_* = \frac{n+1}{2}\rho_0 u_0^2. \tag{78.45}$$

Equation (78.45) gives the maximum pressure p_*, which originates as a result of the impact. At very high pressures (around 10^8 kg/cm^2), any medium is transformed into an electron gas, and for this the equation of state $p = A\rho^n$ actually holds good, so that $n = \frac{5}{3}$ (as for a monatomic gas) and relationship (78.45) assumes the form

$$p_* = \frac{4}{3}\rho_0 u_0^2. \tag{78.46}$$

For $u_0 = 100$ km/sec, $\rho_0 = 1.5$ g/cm^3 (beryllium), we obtain from relationship (78.46) that $p_* = 1.5 \cdot 10^8$ kg/cm^2, which confirms the validity of the estimate of the pressure which we have made, and which gives the basis for considering the material of the jet as a degenerate electron gas.

It is well-known from statistical physics that the equation of state for this gas is

$$p = \frac{1}{5}\left(\frac{6\pi^2}{g}\right)^{\frac{2}{3}}\frac{h^2}{4\pi^2 m_e}\left(\frac{N}{V}\right)^{\frac{5}{3}}, \tag{78.47}$$

where g is the statistical weight of the particles, N is the number of particles in one mole, m_e is the mass of an electron, h is Planck's constant, equal to $6.558 \cdot 10^{-27}$ erg.sec, V is the molar volume of the substance at the pressure p. For the case being considered, $g = 2$, $N = ZN_A$, where N_A is Avogadro's number and Z the number of electrons in an atom of the given metal (for beryllium $Z = 4$), $V = \frac{\mu}{\rho}$, where μ is the atomic weight of the metal and ρ is its density at the pressure p (for beryllium $\mu = 9$g/mole). Thus, for beryllium,

$$p = \frac{1}{5}(3\pi^2)^{\frac{2}{3}} \frac{h^2}{4\pi^2 m_e} \left(\frac{4N_A}{9}\right)^{\frac{5}{3}} \rho^{\frac{5}{3}}. \qquad (78.48)$$

We shall now calculate the temperature originating during the process of impact of a cumulative jet with an obstacle.

The first, extremely rough estimate of the temperature can be carried out for the following considerations. The internal energy of the medium at the shock front is

$$E = \frac{p}{2}(v_0 - v) = \frac{pv}{n-1}. \qquad (78.49)$$

For a degenerate electron gas, since $n = \frac{5}{3}$, we have

$$E = \frac{3}{2} pv. \qquad (78.50)$$

We now transcribe equation (78.50) in the form

$$E = c_v T = \frac{3}{2} p \frac{\mu}{\rho}. \qquad (78.51)$$

It is well-known that at high temperatures, the atomic specific heat of solids tends to $6 \frac{\text{cal}}{\text{gram-atom.deg}}$. If, in the given case, we assume that $c_v = 6 \frac{\text{cal}}{\text{gram-atom.deg}}$ for the material of the jet, then

$$T = \frac{3 \cdot 9 \cdot 1.35 \cdot 10^{11} \cdot 2.34 \cdot 10^{-5}}{2 \cdot 6 \cdot 6} \approx 1.1 \cdot 10^6 \,^\circ\text{K}. \qquad (78.52)$$

We must admit, however, that this temperature is clearly excessive, since the specific heat of substances existing in an electron gas state is an increasing function of temperature.

In accordance with this, and with the object of obtaining a more precise estimate of the temperature which is of interest to us, we shall proceed from the formula for the specific heat of a degenerate electron gas

$$c_v = \beta N T \left(\frac{V}{N}\right)^{\frac{2}{3}}, \qquad (78.53)$$

where

$$\beta = \left(\frac{9\pi}{6}\right)^{\frac{2}{3}} \frac{m_e k^2 4\pi^2}{h^2}$$

and k is Boltzmann's constant, equal to $1.38 \cdot 10^{-16}$ cal/deg.

For the case we are considering here, relationship (78.53) assumes the form

$$c_v = \left(\frac{2\pi}{6}\right)^{\frac{2}{3}} \frac{m_e k^2 \cdot 4\pi^2}{h^2} 4N_a T \left(\frac{\mu}{4\rho N_a}\right)^{\frac{2}{3}}.$$

Substituting in this expression the numerical values of the corresponding quantities, we obtain

$$c_v = 2{,}87\,T \quad \frac{\text{g.cm}}{\text{deg.}} \quad .$$

We now transform equation (78.51), and we obtain

$$c_v T = 2{,}87\,T^2 = \frac{3}{2} \cdot 1.35 \cdot 10^{11} \cdot \frac{9}{6} = \frac{9}{4} \cdot 1.35 \cdot 10^{11},$$

whence

$$T = 3.25 \cdot 10^5\ ^\circ\text{K}.$$

We have determined this temperature on the assumption that the material of the jet behaves, under impact conditions, as a degenerate electron gas.

We shall now verify the validity of this assumption.

As we know, the criterion for strong degeneration is $\theta \ll 1$, where

$$\theta = \frac{2^{\frac{5}{3}} \pi m_e k V^{\frac{2}{3}} T}{h^2 N^{\frac{5}{3}}}. \qquad (78.54)$$

Substituting the numerical values for the respective quantities in equation (78.54), we obtain

$$\theta = 4.73 \cdot 10^{-8} T, \qquad (78.55)$$

whence it is obvious that at temperatures of around $10^5 - 10^6\ ^\circ\text{K}$, $\theta \ll 1$, i.e. the material of the jet at the instant of impact can, in fact, be considered as a degenerate electron gas.

Thus, the second variant, which leads to a shock temperature of around 500,000°K for $u_0 =$ 100 km/sec, is evidently quite accurate.

It follows from this that at shock velocities of around several tens of km/sec, a cumulative jet will possess not only an armour-piercing action, but

also a powerful armour-burning capability.

At impact velocities of the jet of around 100 km/sec, the appearance of not only normal radiation may be expected, but also harder radiation.

CHAPTER XIII

EXPLOSION IN AIR

§ 79. Fundamental physical effects originating as a result of an explosion.

In the overwhelming majority of cases explosions are created with the objective of a specific effect on the medium surrounding the source of the explosion.

Let us analyse in more detail the effect of an explosion in air.

Explosive charges may have various shapes. It is difficult to describe the effect of charges with a complex shape, however, with the exception of the region in the immediate vicinity of the charge it is always possible, for practical application, to reduce the effect of the explosion of a similar charge with sufficient accuracy to the effect of a spherical, cylindrical or plane (one-dimensional) charge.

The effect of the explosion in the immediate vicinity of the charge must always be considered separately.

It is known from experiment that the explosion of a charge, not differing greatly in one dimension with respect to all the dimensions, at distances around the average dimension of the charge is equivalent to the effect of the explosion of a spherical charge of the same weight. In the case when the measurements of the charge in one dimension considerably exceed its size in the other two dimensions, the effect of the explosion at a distance around the mean value of the smaller dimensions is equivalent to the explosion of a cylindrical charge of the same weight, but at a distance of several of the larger charge sizes it is equivalent to the explosion of a spherical charge of the same weight.

As a result of this, in the regions distant from the charge end around the smaller dimension the effect of the explosion is equivalent to the explosion of a charge of somewhat less mass than the mass of the charge originating in a tube (plane explosion).

Let us investigate the fundamental physical effects originating from an explosion. If the explosion were to occur in a vacuum (for example, at the surface of the moon), then the products of the explosion, having a finite pressure (as a consequence of the fact that heat has been liberated in a finite volume) begin to expand unimpeded, being subject to the law of non-steady motion. As a result of this, at any given instant of time the distribution of pressure, density and velocity of the expanding explosion products at different distances from the origin of the explosion will be different. The pressure and density will be minima in the outer regions and maxima in the inner regions of the explosion products, but the velocity of the gas, on the contrary, will be a maximum in the outer regions and a minimum in the inner regions. In the case of a spherical charge, the velocity at the centre of the explosion will obviously be equal to zero; in the case of the explosion of an arbitrary charge a number of points of zero velocity are similarly always found in the inner regions.

Expansion of the explosion products in an infinite "empty" space will proceed unrestrictedly.

For an analytical description of the expanding explosion products, we shall introduce the concept of "explosion field". By the explosion field we shall imply the region of space, at each point of which all the parameters characterising the explosion products (pressure, density, temperature, velocity etc) can be uniquely defined. The explosion field will be transient, since at all points all parameters will be changing with respect to time.

It is essertial to note here also that the maximum velocity of dispersion of the explosion products will correspond to the velocity of propagation of the boundary of the explosion products, whereupon for dispersion of the explosion products in vacuo the density and pressure at the boundary of the explosion products will be equal to zero.

This maximum velocity, u_{max}, of outflow of gases depends on the shape of the exploding charge, on the inherent course of the explosion process itself, and also on the energy of explosive transformation Q. Between u_{max} and the energy of explosion in the case of a spherical charge, when the explosion products are a gas, there exists a simple relationship :

$$u_{max} = (3\bar{k} - 1)\sqrt{\frac{2Q}{\bar{k}^2 - 1}}, \qquad (79.1)$$

where $\bar{k}$ is the mean adiabatic index of the expansion process.

For typical explosives :

$$Q \approx 1 \text{ cal/g}, \quad \bar{k} = \frac{5}{4}, \quad u_{max} \approx 11\,000 \text{ m/sec}$$

By the hypothesis of instantaneous detonation

$$\bar{u}_{max} = 2\sqrt{\frac{\bar{k}}{\bar{k} - 1} Q}, \qquad (79.2)$$

which, for typical explosives gives

$$\bar{u}_{max} = 9000 \text{ m/sec}.$$

In the case of an explosion from condensed explosives, when the explosion products are not an ideal gas in the initial state, those simple formulae are changed into somewhat more complex ones. But the values of the maximum velocities of outflow remain practically invariable (cf. Chap. IX); thus, for a real detonation $u_{max} = 12\,000$ m/sec ; for an instantaneous detonation $u_{max} = 10\,000$ m/sec.

For the detonation of the most powerful explosives (for example, hexogen), the maximum velocities of outflow amount to 18 000 m/sec.

In the case of an explosion in any other medium, the process of dispersion of the explosion products will take place somewhat differently than for dispersion in vacuo.

Two regimes of dispersion, different in principle, may arise. As a result of dispersion the explosion products at the boundary of the charge begin to interact with the medium surrounding the charge. In the case of a very dense medium the line of demarcation between charge and medium begins to move slowly from the centre of the charge. If the explosion process occurred by detonation, then the detonation products, moving behind the front of the detonation wave will move more rapidly than the line of demarcation, and, on striking it, will be compressed. The pressure of the detonation products at the demarcation line will increase in the first instants of time after conclusion of the detonation ; only after the lapse of some time does the pressure of the detonation products commence to fall. If the medium is not very dense, then the line of demarcation between the detonation products and the medium will move more rapidly than the detonation products, and at the very beginning of the expansion process the pressure in the explosion products will fall.

In the first case considered with respect to the detonation products, a shock wave comes from within the line of demarcation, being the consequence of the impact of the detonation products with the medium; on reaching the centre the shock wave is "transformed" into a rarefaction wave, and then everywhere within the explosion products the pressure begins to fall. In the second case with respect to the explosion products a rarefaction wave issues; a shock wave propagates through the medium, immediately setting it in motion.

Thus, the study of the dispersion of the explosion products in any medium is considerably complicated in comparison with the study of dispersion

in vacuo and, speaking of the explosion field in the first case, it is necessary to determine the parameters not only of the detonation products but also of the medium set into motion.

However, even without developing the theory of dispersion of the explosion products it is possible to evaluate distances at which the effect of the explosion products will be practically no longer felt, and also to estimate the distances at which the shock wave will act, propagated in the medium surrounding the source of the explosion. First and foremost it is obvious that as a result of an explosion in an infinite medium the explosion products over a certain time after commencement of dispersion occupy a certain finite volume v_∞, corresponding to the residual pressure of the explosion products, and equal to the pressure of the surrounding medium p_a.

If the average initial pressure of the explosion products

$$\bar{p}_1 = \frac{\rho_0 D^2}{8} = 2\rho_0 Q \qquad (79.3)$$

(in this case the isentropy index for the explosion products $k = 3$) and the residual pressure

$$p_\infty = p_a \quad \text{for} \quad v = v_\infty,$$

then the finite volume is easy to determine from the following considerations: for typical explosives, up to a pressure $p_k \approx 2000$ kg/cm^2 the explosion products, as is well-known, expand according to the law:

$$pv^3 = \text{const} = \bar{p}_1 v_0^3 = p_k v_k^3, \qquad (79.4)$$

where v_k is the volume corresponding to the pressure p_k.

For $p < p_k$ we shall assume that expansion proceeds according to the law

$$pv^\gamma = \text{const} = p_k v_k^\gamma = p_a v_a^\gamma, \qquad (79.5)$$

where $\gamma = 1.2 - 1.4$.

By linking these two laws for $p_k \approx 2000$ kg/cm^2 we shall derive accordingly the equation of state of the explosion products and the equation of

conservation of energy (see Chap. VII).

Thus,

$$\frac{v_\infty}{v_0} = \left(\frac{\bar{p}_i}{p_k}\right)^{\frac{1}{3}} \left(\frac{p_k}{p_a}\right)^{\frac{1}{\gamma}}. \qquad (79.6)$$

Here, v_0 is the initial volume of the explosion products. Since for typical explosives $\rho_0 = 1{,}6$ g/cm^3; $D = 7000$ m/sec, then

$$\bar{p}_i \approx 100\,000 \text{ kg/cm}^2; \quad p_a = 1 \text{ kg/cm}^2; \quad \gamma = \frac{7}{5},$$

whence

$$\frac{v_\infty}{v_0} = 50^{\frac{1}{3}} \cdot 2000^{\frac{5}{7}} = 3.7 \cdot 220 = 800;$$

for

$$\gamma = \frac{5}{4} \qquad \frac{v_\infty}{v_0} = 50^{\frac{1}{3}} \cdot 2000^{\frac{4}{5}} = 1600.$$

Thus, the explosion products of typical explosives expand by approximately 800—1600 times. In the case of a spherical explosion, the limiting radius of the volume occupied by the explosion products will be 10 times greater than the initial radius of the charge. In the case of a cylindrical charge this ratio will be equal to approximately 30. Thus, it can be confirmed that the effect of the explosion products are confined to extremely small distances. To this it should be added, that as a consequence of the instability of the process of expansion of the explosion products they will attain a finite boundary by means of a number of damping oscillations near this boundary; at first, the explosion products, having expanded, occupy the maximum volume, in excess of the limiting (by 30—40%) so that their average pressure will be less than p_a; then, the external pressure compresses them to a pressure somewhat greater than p_a and so on. However, there is significance in analysing only the first expansion and first compression processes, after which the process practically dies away.

We note now that in reality the dividing boundary between the explosion products and the medium, being initially clearly expressed, over a time

become everywhere more and more diffuse, since behind the shock wave front the pressure will be turbulent; a turbulent region is created in neighbouring dividing boundaries, which, on intensifying will erase the dividing boundary. "Diffusion" of the explosion products in the medium, however, takes place quite slowly and only after completion of the dispersion process does total intermixing of the explosion products take place with the medium. For the first stage of dispersion, we are therefore justified in speaking of the initial dividing boundary. Knowing the finite volume, the energy (E_∞) can be determined which is "bound up" in the explosion products :

$$E_\infty = \frac{p_a v_\infty}{\gamma - 1}. \tag{79.7}$$

Since the initial explosion energy (E_i) is determined by the relationship

$$E_i = \rho_0 v_0 Q = mQ, \tag{79.8}$$

where m is the mass of explosive, then the energy transmitted to the medium (in the shock wave) will be

$$E_s = E_i - E_\infty = m\left[Q - \frac{p_a v_\infty}{(\gamma - 1)\rho_0 v_0}\right]. \tag{79.9}$$

whence

$$\frac{E_s}{E_i} = 1 - \frac{p_a}{(\gamma - 1)\rho_0 Q}\frac{v_\infty}{v_0}.$$

Taking for typical explosives $Q = 1$ kcal/g, $\frac{v_\infty}{v_0} = 800$, $\rho_0 = 1.6$ g/cm^3, we find that for $\gamma = \frac{7}{5}$ $\frac{E_s}{E_i} = 0.97$; for $\gamma = \frac{5}{4}$, $\frac{E_s}{E_i} = 0.91$.

The overwhelming portion of the explosion energy is transmitted to the medium surrounding the region of the explosion; of course, in consequence of the increase in entropy and a corresponding reduction of free energy in the shock wave, a considerably less portion of the explosion energy is transmitted than results from calculation. As we showed above, part of the explosion products will, prior to establishing a state of equilibrium, move towards the centre and will carry about 1/3 of the explosion energy. Consequently, about

two-thirds of the explosion energy is transmitted in the primary shock wave. Moreover, the surface layer of explosives in a number of cases "burns" with incomplete release of energy and therefore not all the energy E_l is released, but only about 0.9—0.8 E_l, which further reduces the energy transmitted in the shock wave.

In the case when the explosion products are represented by an ideal gas, the limiting volume is calculated according to the formula

$$\frac{v_\infty}{v_0} = \left(\frac{\bar{p}_i}{p_a}\right)^{\frac{1}{\gamma}},$$

whereupon

$$\bar{p}_i = (\gamma - 1)\rho_0 Q = \frac{\rho_0 D^2}{2(\gamma+1)}.$$

The energy transmitted in the shock wave is

$$E_i = mQ\left[1 - \frac{p_a}{(\gamma-1)\rho_0 Q}\left(\frac{(\gamma-1)\rho_0 Q}{p_a}\right)^{\frac{1}{\gamma}}\right].$$

The energy transmission coefficient for the shock wave will be

$$\frac{E_s}{E_l} = 1 - \left[\frac{p_a}{(\gamma-1)\rho_0 Q}\right].$$

In the case when $Q = 1$ kcal/g, $\rho_0 = 1.6$ g/cm^3, $\gamma = \frac{7}{5}$, we have

$$\frac{E_s}{E_l} = 0.94.$$

In the case when $\gamma = \frac{5}{4}$ $\frac{E_s}{E_l} = 0.86$.

Thus, the calculations carried out for a non-ideal and for an ideal gas are in practical agreement.

Let us pass on to the approximate evaluation of the range of observable effect of the shock wave for an explosion in air. As a result of the impact of the detonation products on the air, the initial pressure at the shock front at the [illegible] 1000 kg/cm^2, but this pressure falls rapidly with time.

It is well-known that the velocity of propagation of a shock front (D_s) and the velocity of outflow of gas behind the wave front (u_s) are connected by

the relationship

$$u_s = \frac{2D_s}{\gamma+1}\left(1-\frac{c_a^2}{D_s^2}\right),$$

where c_a is the velocity of sound in quiescent air. As a result of propagation of the shock wave, a regime is rapidly established, for which the velocity of outflow of the gas in the wave is almost linearly increased from the boundary of separation to the shock front. Assuming that for expansion of the explosion products the velocity of the wave front is $\frac{\gamma+1}{2}$ times greater than the velocity of the boundary of separation, we find the distance passed through by the shock front, which will be less than the actual, i.e. somewhat less than the actual dimensions of the region occupied by the shock wave, since the velocity of the shock front exceeds the velocity of the boundary of separation by a factor of more than $\frac{\gamma+1}{2}$. This reduced distance, obviously, will also be a factor of $\frac{\gamma+1}{2}$ greater than the distance traversed by the boundary of separation. The length of the shock wave will be $\frac{\gamma+1}{2}-1=\frac{\gamma-1}{2}$ times less than this distance. Consequently, for a spherical explosion, the volume $v_{s\infty}$ occupied by the shock wave will be defined, for $v=v_\infty$, by the relationship

$$v_{s\infty} \geqslant \left[1-\left(1-\frac{\gamma-1}{2}\right)^3\right]v_\infty;$$

whence, by expanding in series and neglecting terms of the 2nd and 3rd order we obtain

$$v_{s\infty} \geqslant \frac{3}{2}(\gamma-1)\,v_\infty = 0.6v_\infty \approx 500v_0$$
$$\left(\gamma=\frac{7}{5}\right).$$

The intrinsic energy of the air enclosed in this volume, by comparison with the explosion energy transmitted in the shock wave, can be neglected, since the explosion energy per unit volume is equal to $\frac{427 \cdot 1.6 \cdot 10^3}{k-1}$,

Best Available Copy

and the energy of the air in the entire volume (for $v_0 = 1$) is equal to

$$500 \cdot \frac{10^6}{\gamma - 1} = 500 \cdot 10^6 \cdot 2.5.$$

Thus, the ratio of the energy of the air to the explosion energy is equal to

$$\frac{500}{427 \cdot 160} \approx 0.0075.$$

The average air pressure in the shock wave (assuming all the energy to be turbulent) will be

$$\bar{p}_k \leqslant (\gamma - 1)\rho_0 Q \frac{v_0}{v_\infty} = 50 \text{ kg/cm}^2.$$

Thus, for a spherical explosion at distances from the centre of the explosion around $10-12\, r_0$, the average pressure in the shock wave will be around 50 kg/cm^2. Beyond this the pressure begins to fall approximately inversely proportional to the square of the distance ($p \sim r^{-2}$), which, at a distance of $25\, r_0$ gives $p_k \approx 10$ kg/cm^2.

Further out the fall in pressure will be less intensive, and the shock wave itself will no longer be strong. Therefore, if the destruction is determined by the pressure of the shock wave, then a distance of $225-50\, r_0$ can be regarded as the limit of strong effect on the medium surrounding the source of the explosion. The impulse of the shock wave (specific impulse) varies approximately as $\sqrt{r}$, since the duration of effect of the shock wave is proportional to r_0.

If the density and potential of the explosive be taken into account, then it can be said that the distance of finite effect of the shock wave, if the destruction is determined by the pressure, is proportional to $M^{\frac{1}{3}}Q$; and for impulsive demolition this distance is proportional to $M^{\frac{1}{3}}\sqrt{Q}$.

For a cylindrical explosion

$$v_{\infty r} \geqslant (\gamma - 1)\, v_\infty \approx 0.4 v_\infty \approx 300 v_0$$

at a distance of about $30-40\, r_0$ $\bar{p}_k \leqslant 80$ kg/cm^2.

The law of fall of pressure up to $\bar{p} \approx 10$ kg/cm^2 will be $p \sim r^{-\frac{5}{2}}$.

Thus, the pressure of 10 kg/cm^2 will be attained at a distance of around 150 r_0. The distance of finite action of the shock wave with respect to pressure is proportional to $\sqrt{MQ}$, and with respect to impulse to $M^{\frac{4}{3}}Q$.

In the case of a one-dimensional explosion

$$v_{s,\infty} \geqslant \frac{\gamma-1}{2} v_\infty = 0.2 v_\infty \approx 150 v_0.$$

At a distance of around 1000 r_0 the average pressure $\bar{p}_s \leqslant 150$ kg/cm^2, further out the fall in pressure, up to a pressure of about 30 kg/cm^2, will take place according to the law $p_s \sim r^{-1}$. Later, the pressure will fall more slowly $\left(p \sim r^{-\frac{1}{2}}\right)$. The distance of finite effect of the explosion with respect to pressure is proportional to MQ. The impulse of the shock wave in the one-dimensional case, as we shall see below, even for $r \to \infty$ remains finite.

In practice, because of energy losses, accumulating with time (mainly as a consequence of increase of entropy), the effect of the shock wave, especially in the one-dimensional case, will be manifested at distances considerably less than those calculated.

Let us consider the principal special features of the effect of an explosion in an unconfined liquid (in water). Expansion of the explosion products in water will take place more slowly than in air, in consequence of the greater resistance of water to compression. However, the overall dimensions of the cavity filled by the explosion products will not exceed the dimensions calculated for the explosion in air if the intrinsic pressure of the water is close to atmospheric.

For an explosion at some depth, for example at a depth of 100 m, where $p = 10 p_a$, the overall volume occupied by the explosion products is $v_\infty = 160 v_0$. Obviously, the initial pressure of the medium exerts a noticeable influence on the magnitude of v_∞. For a deep explosion the gaseous cavity (bubble)

Best Available Copy

will gradually float to the surface because of the marked difference of pressure acting on various parts of it. However, rate of ascent of the bubble is considerably less than the velocity of the processes brought about by the explosion ; the explosion itself and its visible consequences are already completed at the instant of emergence at the surface of the bubble. The field of the shock wave created will differ sharply from the field of an air shock wave. The cause of this difference is obvious : in the first place the initial pressure at the shock front, which in air for the most powerful explosives does not exceed 1500—2000 kg/cm^2, for typical explosives in water will be around 150,000 kg/cm^2 ; secondly, in consequence of the small (relative to air) compression of the water, its temperature will only be increased slightly ; as a result of this the increase in entropy also will be small and, consequently, the energy carried in the shock wave will be "usefully" expended in movement of the wave (in mechanical work, and not in heat).

Somewhat less energy will be transmitted in the shock wave of deep explosions than for explosions in air. Thus, for example, for an explosion at a depth of 100 m ($p = 10p_0$), 94% of the explosion energy is transmitted in the shock wave (for $\gamma = \frac{7}{5}$), whereas for an explosion in air (for $\gamma = \frac{7}{5}$) 97% of the explosion energy is transmitted in the shock wave. This difference is small. Consequently, the overall effect of the shock wave in water will be somewhat more powerful than the effect of the shock wave in air. In the initial stage of expansion of the detonation products the pressure in the shock wave will, in the case of a spherical and cylindrical explosion, [illegible] approximately according to the law $p \sim r^{-3}$, and in the second case according to the law $p \sim r^{-2}$. In the case of a one-dimensional explosion the drop in pressure initially will be very slow (up to $r \approx 20r_0$). Later, the pressure will drop according to the law $p \sim r^{-1}$

In attaining an average pressure in the explosion products of around 2000 kg/cm^2 the drop in pressure is retarded.

These data relate to the average pressures in an shock wave. The pressure at the shock front will fall, in the case of a spherical explosion, also according to the law $p_f \sim r^{-3}$, for a cylindrical explosion according to the law $p_f \sim r^{-2}$ and for a one-dimensional explosion according to the law $p_f \sim r^{-1}$. The shape of the shock wave in water will differ strongly from the shape of an air shock wave, in that the shock wave being considered will be, even in the first instants of time after its formation, characterized by a very sharp drop in pressure, density and velocity behind the shock front. It can be said that the maximum density of energy in the shock wave will be localized within a very narrow zone.

The change of density at the front of a powerful shock wave in water may be considerable, as for example, at a pressure of around 100,000 kg/cm^2 the density of water attains a value of 1.5 g/cm^3.

The limiting distances at which a significant effect from an explosion is manifested are of approximately the same magnitude as those for an explosion in air.

The powerful destructive effect of an explosion is manifested in the space occupied by the explosion products. The effect of a water shock wave in volumes larger than the volume occupied by the detonation products is quite insignificant, despite the large magnitude of the initial pressures, since the pressure drops extremely rapidly.

The effect of an explosion in unrestricted earth affects volumes comparable with the volume of expansion of the explosion products up to atmospheric pressure ; the effect of the explosion near the free surface , as is well-known, is accompanied by the appearance of a crater, the radius of

which $R \sim (mQ)^{\frac{1}{3}}$; as a result of this, bursting of the ground occurs at a distance in excess of one - two orders of the dimension of the crater.

The shock wave which is formed as a result of this in the earth, is not much different, with respect to its properties, from the shock wave propagated in water.

The effect of an explosion in an unrestricted metallic(crystalline) medium is manifested in volumes considerably less than the overall volume of the detonation products, and the volume is defined by the magnitude of the pressure, yet still producing noticeable plastic deformations of the metal. If we assume that this pressure for steel is roughly $p \geqslant 10{,}000$ kg/cm^2, we arrive at a volume which only exceeds the initial volume of the explosive by a factor of two or less. For an explosion near the free surface of the metal or within a thin metallic casing, part of the metal will becrushed and the effect of the explosion will be accompanied by a fragmentation effect.

§80. One-dimensional dispersion of Detonation Products.

The study of the dispersion of the detonation products in the simple one-dimensional case presents considerable interest and assists in the explanation of the fundamental laws of dispersion of the detonation products resulting from explosion of a spherical charge, and which will be discussed below.

The detonation wave, as we already know, may be determined from the special solution of the basic equations of gas dynamics. Since one can always assume that the detonation of any cylindrical charge is initiated in an arbitrary cross section $0 = x$ at an instant of time $t = 0$, , then for the wave, propagated to the right, the equation

$$x = (u + c)t + F(u)$$

will hold good, whereupon in the given case

Best Available Copy

$$F(u)=0 \quad \text{and} \quad u-\frac{2c}{k-1}=\text{const.}$$

For waves propagating to the left, the equations

$$x=(u-c)\cdot t,$$
$$u+\frac{2c}{k-1}=\text{const.}$$

will hold good.

Since at the front of the detonation wave

$$u_1=\frac{D}{k+1}, \quad c_1=\frac{kD}{k+1},$$

then for the "right-hand" wave

$$u-\frac{2c}{k-1}=-\frac{D}{k-1},$$

and for the "left-hand" wave

$$u+\frac{2c}{k-1}=\frac{D}{k-1}.$$

For future calculations it is advantageous to introduce the dimensionless quantities

$$\frac{u}{D}=w, \quad \frac{c}{D}=a, \quad \frac{x}{l}=\xi, \quad \frac{Dt}{l}=\tau,$$

where l is the length of the charge.

Finally, we shall write the equation for the right-hand detonation wave in the form

$$\frac{\xi}{\tau}=w+a, \quad w=\frac{2a-1}{k-1} \tag{80.1}$$
$$\text{for } \frac{1}{2}\leqslant\frac{\xi}{\tau}\leqslant 1; \quad \text{for } 0\leqslant\frac{\xi}{\tau}\leqslant\frac{1}{2} \quad a=\frac{1}{2} \text{ and } w=0.$$

For the left-hand detonation wave we have

$$\frac{\xi}{\tau}=w-a, \quad w=-\frac{2a-1}{k-1} \tag{80.2}$$
$$\text{for } -\frac{1}{2}\geqslant\frac{\xi}{\tau}\geqslant -1; \quad \text{for } 0\geqslant\frac{\xi}{\tau}\geqslant -\frac{1}{2} \quad a=+\frac{1}{2} \text{ and } w=0.$$

Let us investigate what happens to the wave propagated to the right at the instant when this wave reaches the boundary of the charge and the

detonation products commence to disperse. We shall study the dispersion of the detonation products in a vacuum.

Dispersion of the Detonation Products in a Vacuum. The characteristic special feature of this dispersion is that the velocity of motion of the particles at the front of the dispersing detonation products gradually attains its maximum value $u=\frac{3k-1}{k^2-1}D=(3k-1)\sqrt{\frac{2Q}{k^2-1}}$ defined, as we know, by the special solution

$$u=u_i+\frac{2(c_i-c)}{k-1};$$

for $c=0$, $u_i=\frac{D}{k+1}$, $c_i=\frac{kD}{k+1}$.

The density, or the local velocity of sound proportional to it, on the contrary, reduces in stages to zero. The distribution of velocity and density in the detonation products can be found only in the case when we apply the general solutions of the gas-dynamic equations. This becomes clear from the following. When the detonation wave reaches the boundary of the charge, two waves originate : one of these may be interpreted as a rarefaction wave issuing from within the boundary of the charge, and the other wave is propagated into space. Thus, a Riemann solution is no longer applicable here, since it holds good only for a wave travelling in one direction with constant parameters at the front, and the rarefaction wave travels from within the charge, the parameters of which are varying at the front(gradually decreasing). The general solution must satisfy boundary conditions, in particular the condition of coupling the new solution with the old special solution.

If the dispersion of the detonation products takes place in a vacuum, then for a complete description of this process the same two gas-dynamic equations will suffice, which we have used up till now . If the dispersion takes place in a medium of specified density, then ahead of the front of the detonation products a shock wave with variable amplitude is created, as a

consequence of which the entropy at its front will be continuously changing, and a complete solution of the problem can only be obtained from the three gas-dynamic equations.

We shall limit ourselves for the present to dispersion of the detonation products in a vacuum. The new solution, about which we have just spoken, will hold good up to the time when the front of the rarefaction wave does not reach the point of first order discontinuity of the special solution for the detonation wave. As a result of this, another solution arises. It is not difficult to see that it will again be a special solution, since behind the point of first order discontinuity the density, or the local velocity of sound, remain constant, but the velocity of motion of the particles is similarly equal to zero.

Consequently, the wave travelling from within the charge will possess constant parameters at its front, i.e. properties by which the Riemann wave is precisely characterised. This special solution gives the relationship between the velocity and the local velocity of sound no longer as a function of $\frac{x}{t}$ but by a more complex function of x and t.

A similar analysis can also be carried out for the left-hand end of the charge. As a result, we arrive at the fact that the two individual rarefaction waves, one of which travels from the right-hand end to the left, and the other from the left-hand end to the right, impact.

Then at the instant of impact a fifth solution will arise, which will not be singular and which can be found only from the general integral of the gas-dynamic equations. This general integral can be found arising from the two boundary conditions of its conjugate with the right- and left-hand individual waves. As a result, we shall have five solutions conjugate between themselves at four points. As we shall further see, it is easy to satisfy

ourselves of the fact that the waves defined by the extreme and mean general solutions will be propagated in the course of time at intervals increasing proportionally with time, but the mean individual solutions in the case of $k=3$ will continue at intervals, maintaining constant and finite values. On account of this, for $t\to\infty$ the masses found withing these intervals will tend towards zero, and we can exclude them from further considerations.

In the general case when $k<3$, the mass of gas found within the intervals, defined by the mean individual solutions, also tends towards zero for $t\to\infty$.

Thus, the complete solution consists of seven separate solutions. We shall find all the solutions mentioned above in the case of $k=3$, which corresponds on the average with the expanding detonation products of typical explosives.

Now, let the detonation of a charge be initiated in a certain plane passing through the origin of coordinates. We shall denote the length of the right-hand portion of the charge of explosive by l_1 and the left-hand portion by l_2. Then the detonation wave travelling to the right can be described by the following equations :

$$\left.\begin{aligned} &w+a=\frac{\xi}{\tau},\quad w-a=-\frac{1}{2} && \text{for} \quad \frac{1}{2}\leqslant\frac{\xi}{\tau}\leqslant 1,\\ &w=0,\quad a=\frac{1}{2} && \text{for} \quad 0\leqslant\frac{\xi}{\tau}\leqslant\frac{1}{2}. \end{aligned}\right\} \qquad (80.3)$$

At the instant of time $\tau_1=\lambda_1=\frac{l_1}{l}$ the detonation wave reaches the right-hand end of the charge, after which dispersion of the detonation products commences. It can be proved from the general solutions that the dispersion process will be characterized by these equations :

$$w_1+a_1=\frac{\xi}{\tau}; \qquad (80.4a)$$

$$w_1 - a_1 = \frac{\xi - \lambda_1}{\tau - \lambda_1}. \qquad (80.4b)$$

Equation (80.4a) is obvious; equation (80.4b) we find results from the general solution of the gas- dynamic equations :

$$x = (u - c)\,t + F_2(u - c).$$

For $\tau_1 = \lambda_1$ and $\xi_1 = \lambda_1$

$$F_2(u - c) = \lambda_1 [1 - (w_1 - a_1)],$$

whence, for $w_1 - a_1$ we obtain equation (80.4b).

The rarefaction wave, created by the dispersion, proceeding from right to left, at the instant of time $\tau_2 = \frac{3}{2}\lambda_1$ in the cross-section $\xi = \frac{3}{4}\lambda_1$ encounters the point of weak discontinuity, which is established from the simultaneous solution of equation (80.4b) and equation (80.3), which, for the point of weak discontinuity (for $w = 0$) takes the form $\frac{\xi}{\tau} = \frac{1}{2}$.

As a result of this a new solution is created. This solution will have the form

$$w_2 + a_2 = \frac{1}{2}. \qquad (80.5)$$

The solution for $w_2 - a_2$ is retained :

$$w_2 - a_2 = \frac{\xi - \lambda_1}{\tau - \lambda_1}. \qquad (80.6)$$

A similar picture will be presented for the left-hand end of the charge. In order to describe the corresponding equations it is only necessary to substitute λ_1 by $\lambda_2 = \frac{l_2}{l}$, $w + a$ by $w - a$, , $w - a$ by $-(w + a)$ and ξ by $-\xi$. We obtain

$$w + a = -\frac{\xi - \lambda_2}{\tau - \lambda_2},$$

$$w - a = -\frac{1}{2}.$$

At the instant of time $\tau_3 = \frac{3}{2}(\lambda_1 - \lambda_2)$, the right - and left-hand rarefaction waves meet, which is established from simultaneous solution of equations (80.5) and (80.6), and the analagous equations set down for the left-hand end. As a result of this a new solution will again be created :

$$w_3 + a_3 = \frac{\xi + \lambda_2}{\tau - \lambda_2}, \quad w_3 - a_3 = \frac{\xi - \lambda_1}{\tau - \lambda_1}. \qquad (80.7)$$

We now write down all the solutions for the right and left ends of the charge :

$$w_1+a_1=\frac{\xi}{\tau},\quad w_1-a_1=\frac{\xi-\lambda_1}{\tau-\lambda_1},\quad -w_1+a_1=\frac{\xi}{\tau},$$
$$w_1+a_1=+\frac{\xi+\lambda_2}{\tau-\lambda_2},$$
$$w_2+a_2=\frac{1}{2},\quad w_2-a_2=\frac{\xi-\lambda_1}{\tau-\lambda_1},\quad -w_2+a_2=\frac{1}{2},$$
$$w_2+a_2=+\frac{\xi+\lambda_2}{\tau-\lambda_2},$$
$$w_3+a_3=\frac{\xi+\lambda_2}{\tau-\lambda_2},\quad w_3-a_3=\frac{\xi-\lambda_1}{\tau-\lambda_1}.$$

Let us consider how the energy, momentum and masses of the detonation products will be distributed, dispersing in opposite directions, at a sufficiently large interval of time $\tau\ (\tau\to\infty)$. For this we can, as already mentioned above, exclude from our consideration the masses of gas determined by the individual solutions.

To this end we shall consider the relationship

$$I_\alpha=\frac{16}{9}lD^\alpha\rho_0\left[\int_{\frac{\tau}{2}}^{\tau}a_1w_1^\alpha\,d\xi+\int_0^{\frac{\tau}{2}}a_3w_3^\alpha\,d\xi\right]. \tag{80.8}$$

For $\alpha=0$, $I_0=M_1$ is the mass of the explosion products dispersing to the right, for $\alpha=1$, $I_1=I_1$ is the momentum of this mass, and for $\alpha=2$, $I_2=E_1$ is the energy of this mass.

Evaluating the integrals for the right and left ends of the charge, we have

$$\left.\begin{aligned}M_1&=\frac{M}{9}(4\lambda_1+5\lambda_2),\quad E_1=\frac{MD^2}{16\cdot27}(16\lambda_1+11\lambda_2),\\ M_2&=\frac{M}{9}(5\lambda_1+4\lambda_2),\quad E_2=\frac{MD^2}{16\cdot27}(11\lambda_1+16\lambda_2),\end{aligned}\right\} \tag{80.9}$$
$$I_1=I_2=\frac{4MD}{27}.$$

The initial mass of explosive $M=\rho_0 l$ (the cross-sectional area of the charge $S=1$).

The equality of the impulses(momenta) is obvious, since only internal forces act in the detonation process. The ratios of masses and energy are determined by the formulae

$$\frac{M_1}{M_2}=\frac{4l_1+5l_2}{5l_1+4l_2},\quad \frac{E_1}{E_2}=\frac{16l_1+11l_2}{11l_1+16l_2}, \qquad (80.10)$$

$$\text{for}\quad l_2=0\quad \frac{M_1}{M_2}=\frac{4}{5},\quad \frac{E_1}{E_2}=\frac{16}{11}.$$

Hence, it is obvious that for an end position of the detonator in the side of the charge less mass is involved than in the contrary position, but this mass carries with it the greater energy.

It can thus be said, that in the detonation process redistribution of energy takes place and this redistribution can be controlled by changing the location of the detonator, which agrees well with experimental data. The distribution of density and velocity of the detonation products for different cases is shown in Figures 197 - 201.

When the detonation is initiated at one end of the charge, the magnitude of the wave is considerably reduced : there remain only the rarefaction wave proceeding from the open end, which is described by equations (80.4a) and (80.4b), and the rarefaction wave proceeding from the end where detonation was initiated. It should be noted that this wave is described by the same equations as the detonation wave, i.e. by equations (80.5); as a result of this, the maximum velocity of discharge of the detonation products at the side opposite from the direction of detonation is determined from the expression

$$u=u_i+\frac{2}{k-1}(c-c_i)=\frac{-D+2c}{k-1},$$

which, for $c=0$, gives $u=-\frac{D}{k-1}$.

In the case when detonation is initiated in the middle of the charge, it can be assumed that it is initiated from the solid wall, and as a result of this the momentum received by the outflowing detonation products is equal to the

pressure a · on the wall (see Chapter XI).

Figure 197. Dispersion of detonation products for a centrally located detonator ($l_1 = l_2 = 9$ cm, $D = 9000$ m/sec).

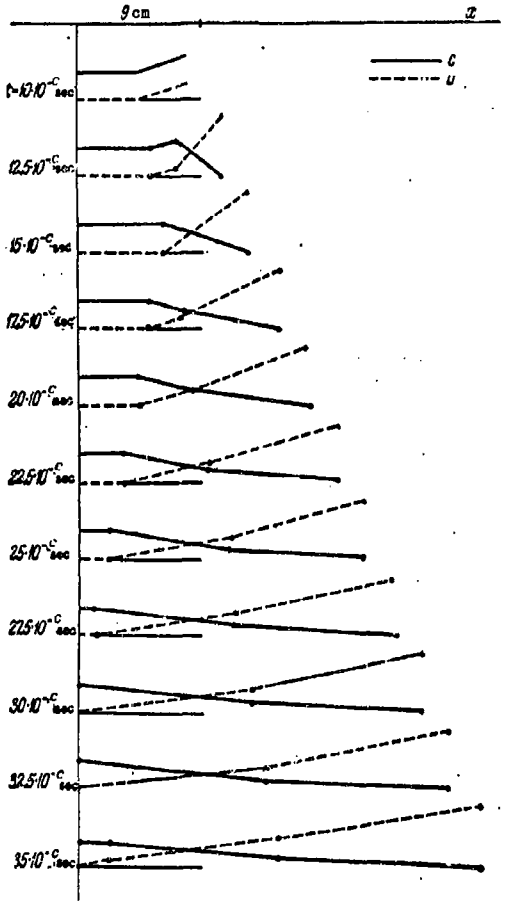


Figure 119 Dispersion of detonation products for an end-located detonator ($l_1 = 9$ cm, $D = 9000$ m/sec).

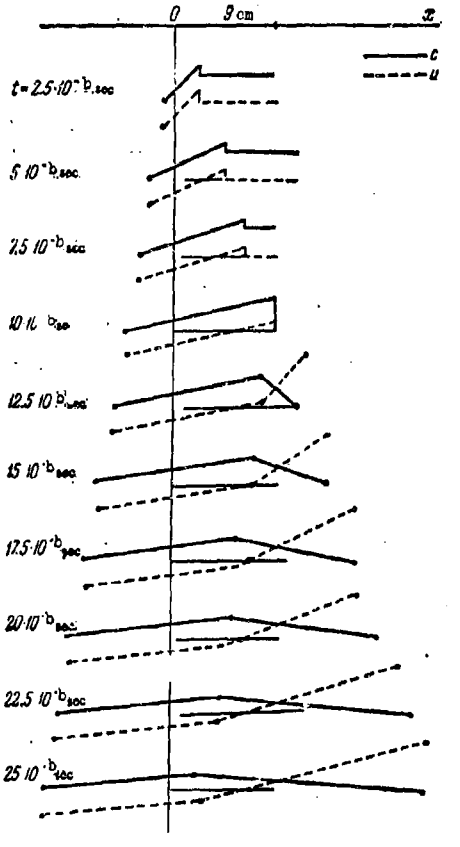


Figure 109

Dispersion of detonation products ($l_1 = 8$ cm, $l_2 = 4$ cm, $D = 8000$ m/sec).

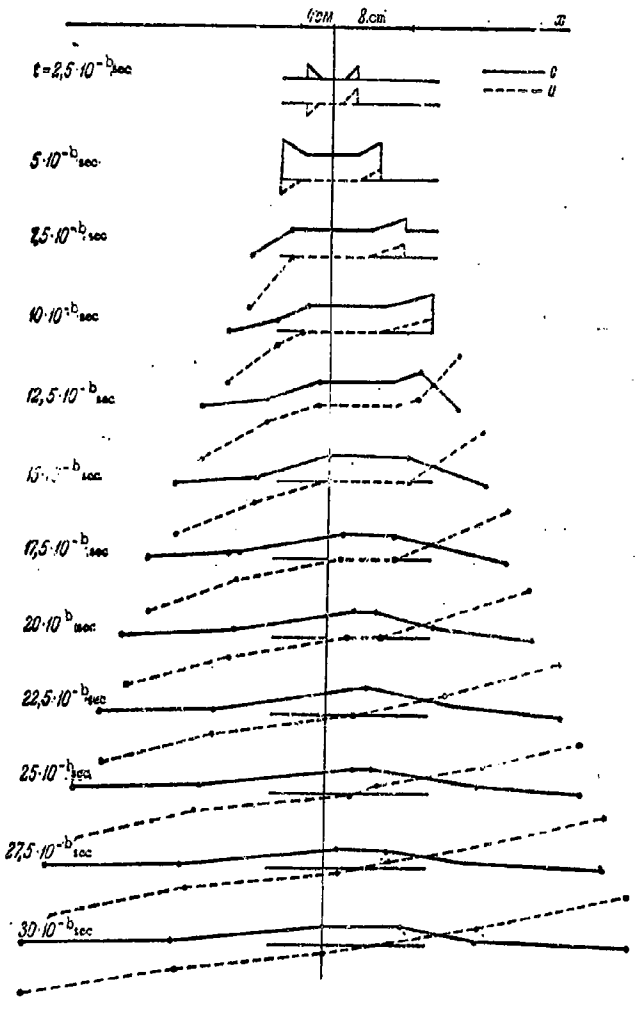


Figure 200 Motion of detonation products (path of particles : $l_1 = 9$ cm, $l_2 = 6$, , $D = 9000$ m/sec).

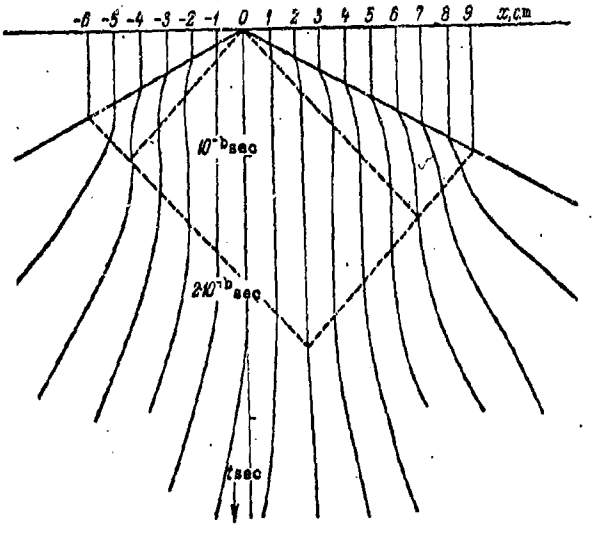
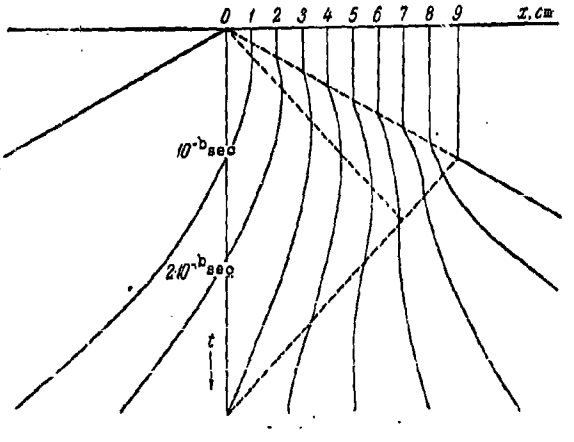


Figure 201 Motion of detonation products (path of particles : $l_1 = 9$ cm, $l_2 = 0$, $D = 9000$ m/sec).



This impulse is determined from relationship (80.9). If the velocity of detonation is expressed via the energy of decomposition of the explosive (Q), then

$$D^2 = 2(k^2-1)Q = 16Q$$

and the impulse is determined by the relationship

$$I = \frac{16}{27}\sqrt{ME} = \frac{32}{27}\sqrt{M_1E_1}, \tag{80.11}$$

where $E = MQ$, $M_1 = \frac{M}{2}$ is the mass of the detonation products discharging in this direction and $E_1 = M_1Q$.

Analysis of the wave system formed as a result of dispersion of the detonation products in those cases when the isentropy index $k < 3$, presents considerable analytical difficulty. However, here the problem can be solved for the case when $k = \frac{2n+3}{2n+1}$.

In this case

$$\left.\begin{aligned} M_1 &= M\left[1 - \lambda_2)\frac{[2(n+1)]!}{n!}\left(\frac{n+2}{2n+3}\right)^{2(n+1)}\sum_0 + \lambda_2\right], \\ M_2 &= M - M_1, \\ E_1 &= E\left[2(\lambda_1-\lambda_2)\frac{(n+2)^2}{n+1}\frac{[2(n+1)]!}{n!}\left(\frac{n+2}{2n+3}\right)^{2(n+1)}\sum_2 + \lambda_2\right], \\ E_2 &= E - E_1, \\ I_1 &= I_2 = 2\sqrt{\frac{ME}{n+1}}\,(n+2)\frac{[2(n+1)]!}{n!}\left(\frac{n+2}{2n+3}\right)^{2(n+1)}\sum_1. \end{aligned}\right\} \tag{80.12}$$

Here

$$\sum_0 = \sum_{\alpha=0}^{n}\left(\frac{n+1}{n+2}\right)^{n-\alpha}\frac{n!}{(n-\alpha)!\,(n+\alpha+2)!},$$

$$\sum_1 = \sum_{\alpha=0}^{n}\left(\frac{n+1}{n+2}\right)^{n-\alpha}\frac{n!\,(\alpha+1)}{(n-\alpha)!\,(n+\alpha+3)!},$$

$$\sum_2 = \sum_{\alpha=0}^{n}\left(\frac{n+1}{n+2}\right)^{n-\alpha}\frac{n!\,(\alpha+1)(\alpha+2)}{(n+\alpha)!\,(n+\alpha+4)!}.$$

In the limiting case when $k = 1$, for any position of the detonator, identical masses are disintegrated to left and to right carrying identical amounts of energy. The magnitude of the impulse as a result of this is determined by the

expression

$$I = \sqrt{\frac{ME}{\pi}}. \qquad (80.13)$$

We shall deduce the values of $\frac{M_1}{M_2}$ and $\frac{E_1}{E_2}$ for an end-located detonator, i.e. when $\lambda_2 = 0$, for different values of k. (Table 115)

Table 115

Ratio of mass and energy of the dispersing detonation products for different values of the isentropy index.

(one-dimensional dispersion)

n	0	1	2	∞
k	3	$\frac{5}{3}$	$\frac{7}{5}$	1
$\frac{M_1}{M_2}$	$\frac{4}{5}$	$\frac{297}{328}$	$\frac{49}{51}$	1
$\frac{E_1}{E_2}$	$\frac{16}{11}$	$\frac{21 \cdot 81}{89 \cdot 16}$	$\frac{8}{7}$	1

For $k = 3$ $I = \frac{16}{27}\sqrt{ME} = 0.592\sqrt{ME}$,

for $k = 1$ $I = \sqrt{\frac{ME}{\pi}} = 0.565\sqrt{ME}$.

We see that the impulse is considerably reduced by a reduction of k from 3 to 1. The redistribution of mass and energy as a result of this is also reduced, and for $k = 1$ the effect of redistribution tends to zero.

Analysis of the process of discharge of the detonation products presents considerable interest in the case when detonation takes place instantaneously, i.e. when explosion of an explosive takes place in a constant volume. The initial stage of discharge is characterized by a wave in one direction, which is described, obviously, by the special solution of the basic equations of gas-dynamics ; for example, for the detonation products discharging to the right :

$$u-c=\frac{x}{t},\quad u=\frac{2}{k-1}(\bar{c}_i-c). \tag{80.14}$$

At the front of the rarefaction wave, the velocity of the gas is equal to zero, the velocity of sound is equal to the initial velocity of sound, the arbitrary function of the special solution, obviously, can be equated to zero, assuming that the discharge process is initiated at the instant of time $t=0$ in the section $x=0$.

The initial parameters of the detonation products are determined by the relationships

$$\frac{\bar{c}_i^2}{k(k-1)}=Q,\quad \bar{p}_i=\frac{\rho_0\bar{c}_i^2}{k}=(k-1)\rho_0 Q=\frac{\rho_0 D^2}{2(k+1)}. \tag{80.15}$$

It should be noted that the pressure of the products of an "instantaneous" detonation are less by a factor of two than the pressure at the front of the detonation wave. At the instant of time $t=\frac{l}{2\bar{c}_i}$, the rarefaction wave proceeding from the right and left end of the charge converges at the centre of the charge, after which a reflected wave is formed which, in the case of $k=3$, is described by the equations

$$u-c=\frac{x}{t},\quad u+c=\frac{x+l}{t}. \tag{80.16}$$

This result ensues from the condition that for $t=\frac{l}{2\bar{c}_i}$ in the section $x=-\frac{l}{2}$ $u=0$ and $c=\bar{c}_i$, as a consequence of which the arbitrary function $F_1(u+c)$ in the equation $x=(u+c)t+F_1(u+c)$ is equal to $F_1=-l$.

The magnitude of the impulse acting on the wall located at the middle of the charge, is determined, for an arbitrary value of k, by the formula

$$I=\sqrt{2(2n+3)ME}\,\frac{(2n+1)!}{n!(n+1)!\,2^{2(n+1)}}, \tag{80.17}$$

where $k=\frac{2n+3}{2n+1}$.

For $k=1,\ n\to\infty$, the impulse is determined by the formula

$$I=\sqrt{\frac{ME}{\pi}}. \tag{80.18}$$

Values of impulse for different isentropy indices are presented in Table 116.

In comparing the magnitude of the impulses for a normal and for an instantaneous detonation, we arrive at the conclusion that for $3 > k > 1$ the impulse for an instantaneous detonation is considerably in excess of the impulse for a normal detonation. For $k = 1$ the impulses for both cases are the same.

Now let us analyse the results obtained. The principal special feature of a non-stationary discharge of gas is the redistribution of the energy density with respect to the mass of discharging gas.

A small portion of the mass has a velocity considerably in excess of the "mean velocity" $\sqrt{\frac{ME}{n}}$ corresponding to the initial energy density; the main portion of the mass moves with velocities less than the "mean velocity".

Table 116

Values of impulse for different values of the isentropy index

(one-dimensional dispersion, instantaneous detonation)

k	n	Impulse, I.
3	0	$\frac{1}{2}\sqrt{\frac{3}{2}ME} = 0.592\sqrt{ME}$
$\frac{5}{3}$	1	$\frac{3}{8}\sqrt{\frac{5}{2}ME} = 0.585\sqrt{ME}$
$\frac{7}{5}$	2	$\frac{5}{16}\sqrt{\frac{7}{2}ME} = 0.575\sqrt{ME}$
1	$n \to \infty$	$\sqrt{\frac{ME}{n}} = 0.565\sqrt{ME}$

Since $u = u(M)$, it is clear that the momentum(impulse) will be less than for stationary motion of this same mass of gas M with the same store of energy E.

Actually,

$$I = \int_0^M u\,dM, \quad E = \frac{1}{2}\int_0^M u^2\,dM, \tag{80.19}$$

where $u = u(M)$.

Let us find the condition for I_{max} if E is given.

We substitute the expression

$$\Phi = I + \lambda E = \int_0^M \left(u + \frac{\lambda u^2}{2}\right) dM,$$

where λ is a constant factor (Legendre factor).

Differentiating the expression $u + \frac{\lambda u^2}{2}$ with respect to u and equating the result to zero, we have $1 + \lambda u = 0$, whence $u = -\frac{1}{\lambda} = \text{const}$.

Thus, I attains a maximum for a given energy if the velocity of the gas is independent of M, i.e. in the case of stationary gas flow. As a result of this, since for flow in vacuo $E = \frac{Mu^2}{2}$, and $I = \frac{Mu}{2}$, we have

$$I = \frac{1}{2}\sqrt{2ME} = 0{,}71\sqrt{ME} \tag{80.20}$$

(the total momentum is $2I = \sqrt{2ME}$).

We shall denote the coefficients in the expressions determining the momentum, in the cases of normal and instantaneous detonation, by ξ_1, ξ_2 and we shall denote the coefficients indicating the ratio of these momenta to the momentum for stationary flow by $\theta_1 = \frac{\xi_1}{\sqrt{2}}$ and $\theta_2 = \frac{\xi_2}{\sqrt{2}}$. The calculated data are presented in Table 117.

Table 117

Ratio of the momenta for instantaneous and normal detonation to the momentum for stationary flow

(one-dimensional disperaion)

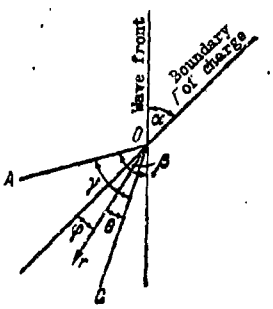
n	k	ξ_1	ξ_2	θ_1	θ_2
0	3	0.592	0.612	0.837	0.865
1	5/3	0.585	0.592	0.823	0.839
2	7/5	0.575	0.585	0.810	0.825
3	9/7	0.566	0.580	0.800	0.818
∞	1	0.565	0.565	0.795	0.795

As already mentioned above, the laws governing the discharge of the detonation products in a vacuum give true results in the case of discharge in air only in the vicinity of the charge, i.e. at those distances for which the mass of air set into motion by the detonation products is less than the mass of explosive. In the one-dimensional case this distance considerably exceeds the length of the charge.

§81. Dispersion of Detonation Products for an Inclined Section.

Let us consider the extremely interesting case of the flow of detonation products from the surface of an explosive charge, towards which the detonation wave converges through a certain angle α (Fig. 202).

Figure 202 Approach of detonation wave towards the surface of a charge at an angle.



In order to determine the parameters of the detonation products dispersing from the surface layers close to the charge, exact solutions of the gas-dynamic equations can be used. However, before analysing these relatively complex solutions we shall consider an approximate solution of the problem, with a view to explaining the physics of the phenomenon, the results of which

are, on the average, quite accurate.

We shall assume that on the average, dispersion of the detonation products takes place with respect to the normal to the surface of the charge, i.e. in the direction of maximum pressure gradient. Actually, as we shall see from the exact solution, dispersion takes place within a certain angle, the bisector of which almost coincides with the normal to the surface of the charge.

It can be seen from Fig. 205 that the resultant velocity is

$$q_k = \sqrt{u_i^2 + \left(\frac{2}{k-1} c_i\right)^2 + \frac{4}{k-1} u_i c_i \cos\alpha}, \qquad (81.1)$$

where u_i is the velocity of motion of the detonation products behind the front of the detonation wave, $\frac{2}{k-1} c_i$ is the velocity of dispersion of the detonation products in vacuo with respect to the normal and α is the angle between the front of the detonation wave and the surface of the charge.

Transforming relationship (81.1) and taking into account that $u_i = \frac{D}{k+1}$, and $c_i = \frac{kD}{k+1}$, we arrive at the relationship

$$q_k = \frac{D}{k^2-1} \sqrt{5k^2 - 2k + 1 + 4k(k-1)\cos\alpha}, \qquad (81.2)$$

which, for $k = 3$, gives

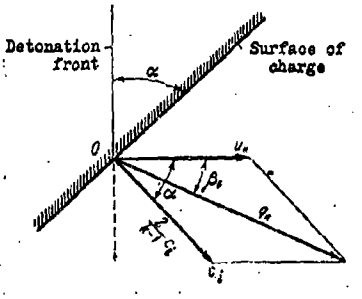
$$q_k = \frac{D}{4} \sqrt{10 + 6\cos\alpha}.$$

For $\alpha = 0$, $q_k = D$, and for $\alpha = \frac{\pi}{2}$ $q_k = \frac{D}{2}\sqrt{\frac{5}{2}}$.

The angle of rotation of the velocity vector β_0 (Fig. 205), obviously, can be determined from the relationship

$$\sin\beta_0 = \frac{2}{k-1}\frac{c_i}{q_k}\sin\alpha = \frac{2k\sin\alpha}{\sqrt{5k^2 - 2k + 1 + 4k(k-1)\cos\alpha}}, \qquad (81.3)$$

Figure 205 Dispersal of detonation products from the surface of the charge



Let us determine the limits of variation of the angle of rotation β_0 as a function of the variation of the angle α.

For $\alpha = 0$, $\beta_0 = 0$,

and for $$\alpha = \frac{\pi}{2} \quad \sin\beta_0 = \frac{2k}{\sqrt{5k^2 - 2k + 1}}, \qquad (81.4)$$

which, for $k = 3$, gives $\sin\beta_0 = \frac{3}{\sqrt{10}}$, whence $\beta_0 = 73°$. This corresponds to a deviation of the flow from the normal by 17°. We note that the exact solution gives, for the mean velocity vector, an angle of deviation from the normal equal to 12—14°, depending upon the polytropic index.

Actually, as we already know, as a result of dispersion of the detonation products, the pressure falls rapidly and the gas, as a result of expansion becomes ideal, and the index of polytropy approximates to the value $k = \frac{7}{5}$.

In this case, the relationships we have derived give for $\alpha = 0$, $q_k = \frac{10D}{3}$, $\beta_0 = 0$; for $\alpha = \frac{\pi}{2}$ $q_k = 2.8D$, $\beta_0 = 80°$, i.e. the deviation of the flow from the normal is obtained equal to 10°.

The true values of q_k and β_0 lie between those given for $k=3$ and $k=\frac{7}{5}$.

Let us turn to the derivation of more precise solutions.

In the polar system of co-ordinates, for which the point of intersection of the detonation wave with the surface of the charge is stationary the following equations are valid

$$\left.\begin{aligned} u\frac{\partial u}{\partial r}+\frac{v}{r}\frac{\partial u}{\partial \theta}-\frac{v^2}{r}+\frac{1}{\rho}\frac{\partial p}{\partial r}=0,\\ u\frac{\partial v}{\partial r}+\frac{v}{r}\frac{\partial v}{\partial \theta}+\frac{uv}{r}+\frac{1}{\rho r}\frac{\partial p}{\partial \theta}=0,\\ \frac{\partial}{\partial r}(\rho u r)+\frac{\partial}{\partial \theta}(\rho v)=0, \end{aligned}\right\} \qquad (81.5)$$

where r is the radius vector, θ is the polar angle, u is the radial velocity component, v is the tangential velocity component, ρ is the density and p is the pressure of the gas.

It is obvious that for the assumptions made, all the parameters, close to the line of intersection, depend slightly on r.

Then, for the condition such that p, ρ, u, and v depend only on θ, the equations take the form (Prandtl - Mayer solution):

$$\frac{du}{d\theta}=v, \quad \frac{1}{\rho}\frac{dp}{d\theta}+v\left(u+\frac{dv}{d\theta}\right)=0, \quad \rho u+\frac{d(\rho v)}{d\theta}=0. \qquad (81.6)$$

Introducing the velocity of sound and carrying out certain transformations we obtain

$$\left.\begin{aligned} \frac{du}{d\theta}=v,\\ c^2\frac{d\ln\rho}{d\theta}+v\left(u+\frac{dv}{d\theta}\right)=0,\\ u+\frac{dv}{d\theta}+v\frac{d\ln\rho}{d\theta}=0. \end{aligned}\right\} \qquad (81.7)$$

Multiplying the last expression termwise by v and comparing it with the previous expression, we arrive at the result that $v=c$.

We shall find that the solution of our actual problem results from this condition.

In order to determine the maximum velocity q_k of flow of the detonation products in a vacuum and the dependence of the flow velocity q on the angle θ we are justified in using Bernoulli's equation for steady flow (for the assumption we have made, that in the vicinity of the confines of the charge all the parameters are practically independent of r) :

$$\hat{q}_k^2 = q^2 + \frac{2c^2}{k-1} = \text{const}, \tag{81.8}$$

where $\hat{q}_k$ in the given case is the same for all stream lines.

Since $q^2 = u^2 + v^2$, where $v = c$, and the initial flow velocity q_i and the initial velocity of sound c_i are given, then from Bernoulli's equation it is easy to determine the maximum velocity q_k which the gas acquires flowing in vacuo, and also the dependence of the velocity on the angle θ :

$$\hat{q}_k^2 = q_i^2 + \frac{2c_i^2}{k-1} = u_i^2 + \frac{k+1}{k-1}c_i^2 = u^2 + \frac{k+1}{k-1}c^2. \tag{81.9}$$

Since

$$\frac{du}{d\theta} = v = c,$$

then

$$\frac{du}{d\theta} = \sqrt{\frac{k-1}{k+1}(\hat{q}_k^2 - u^2)}. \tag{81.10}$$

Hence it follows that

$$u = \hat{q}_k \cos\sqrt{\frac{k-1}{k+1}}\theta \tag{81.11}$$

(we shall read off the angles from the line where $u = \hat{q}_k$ in a counter-clockwise direction). In Fig. 202 this line is OC. Further, from equation (81.10) and (81.11) it follows that

$$v = c = \hat{q}_k\sqrt{\frac{k-1}{k+1}}\sin\sqrt{\frac{k-1}{k+1}}\theta. \tag{81.12}$$

The local Mach angle is determined by the equation

$$\tan M = \frac{v}{u} = \sqrt{\frac{k-1}{k+1}}\tan\sqrt{\frac{k-1}{k+1}}\theta. \tag{81.13}$$

Let us determine the region of existence of a solution for the case under consideration. In Fig. 202 this region is bounded by the lines OC and OA; above the line OA we have a region of constant velocity. The value of the angle γ, defining the region of existence of a solution, can be found from formula (81.13)

$$\tan M_{1\lim} = \sqrt{\frac{k-1}{k+1}} \tan \sqrt{\frac{k-1}{k+1}} \gamma. \qquad (81.14)$$

It can be seen from Fig. 204, that in the chosen moving system of coordinates having a velocity of $\frac{D}{\sin \alpha}$, we have

$$\frac{c_i}{\frac{D}{\tan \alpha}} = \tan M_{1\lim}.$$

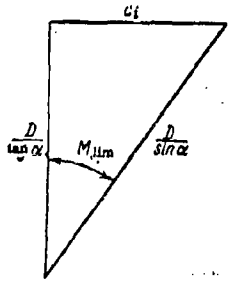
Substituting $c_i = \frac{kD}{k+1}$, we obtain

$$\frac{k}{k+1} \tan \alpha = \tan M_{1\lim}.$$

Hence it further follows that

$$\tan \sqrt{\frac{k-1}{k+1}} \gamma = \frac{k}{k+1} \tan \alpha. \qquad (81.15)$$

Figure 204 Relationship between velocities (dispersion from an inclined section)



In the region γ all the parameters are functions only of the angle ϑ. The line OC gives the limit of dispersion.

Obviously, for $\vartheta = \gamma$, $c = c_i$, whereupon using formulae (81.12) and

(81.5) we obtain

$$\dot{q}_k = \sqrt{\frac{k+1}{k-1}}\, c_i \operatorname{cosec} \sqrt{\frac{k-1}{k+1}}\,\gamma. \tag{81.16}$$

Hence, using (81.11) and (81.12) we obtain

$$u = c_i \sqrt{\frac{k+1}{k-1}} \operatorname{cosec} \sqrt{\frac{k-1}{k+1}}\,\gamma \cos \sqrt{\frac{k-1}{k+1}}\,\theta, \tag{81.17}$$

$$v = c = c_i \operatorname{cosec} \sqrt{\frac{k-1}{k+1}}\,\gamma \sin \sqrt{\frac{k-1}{k+1}}\,\theta. \tag{81.18}$$

Let us determine the values of the parameters in the usual (non-mobile) system of coordinates. The angle between the radius-vector and the initial confines of the charge is

$$\varphi = \beta - \gamma + \theta - \alpha. \tag{81.19}$$

We determine the total dispersion velocity. Knowing the angle of flight and taking into account the initial velocity $\frac{D}{\sin\alpha}$ we derive the vector sum. We obtain

$$\dot{q}_k = \frac{D}{\sin\alpha}\sqrt{\frac{k^2-\cos^2\alpha}{k^2-1}}. \tag{81.20}$$

The angle ψ between the confines of the charge and the velocity vector is determined by the formula

$$\tan(\psi - \varphi) = \frac{\bar{v}}{\bar{u}},$$

where $\bar{u}$ is the projection of the velocity onto the radius-vector and $\bar{v}$ is the projection of the velocity onto the perpendicular to the radius-vector.

The formulae obtained establish the dependence of the velocity and density of the dispersing detonation products upon the angle of flight and upon the angle of impact. Analysis of the solution shows that the maximum density of the impulse is proportional to $\rho\dot{q}$, where $\dot{q} = \sqrt{\bar{u}^2 + \bar{v}^2}$; the maximum energy is proportional to $\rho\dot{q}^2$ and the maximum power is proportional to $\rho\dot{q}^3$; they amount to practically one and the same angle with the normal to the surface of the charge. This angle depends on α and k.

With increase of k and α this angle is decreased.

Figure 205 Dispersion of detonation products from an inclined section $\left(k=3,\ \alpha=\frac{\pi}{2}\right)$.

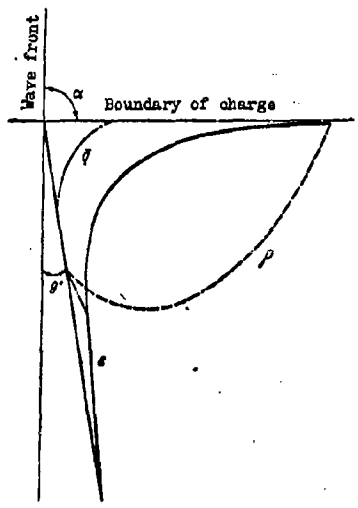
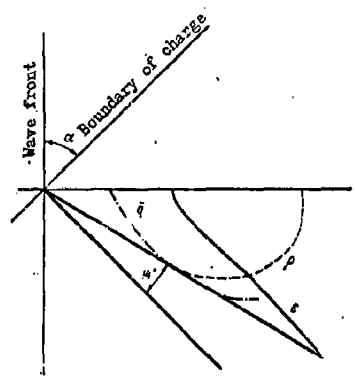


Figure 206 Dispersion of detonation products from an inclined section $\left(k=3,\ \alpha=\frac{\pi}{4}\right)$.



In the case of $k=3$ for $\alpha = 45^\circ$ it amounts to 8°; for $\alpha = 90^\circ$ the angle is equal to 14°, which is in good agreement with experimental data. Figs. 205 - 208 show the distribution of the quantities proportional to $\rho q^2 = \varepsilon$, ρ and q for $k=3$ and $k=\frac{7}{5}$ and for $\alpha = 45^\circ$ and $\alpha = 90^\circ$.

Figure 207. Dispersion of detonation products from an inclined section $\left(k = \frac{7}{5},\ \alpha = \frac{\pi}{2}\right)$.

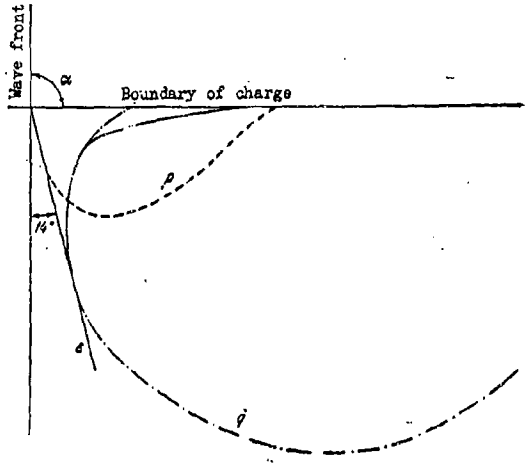
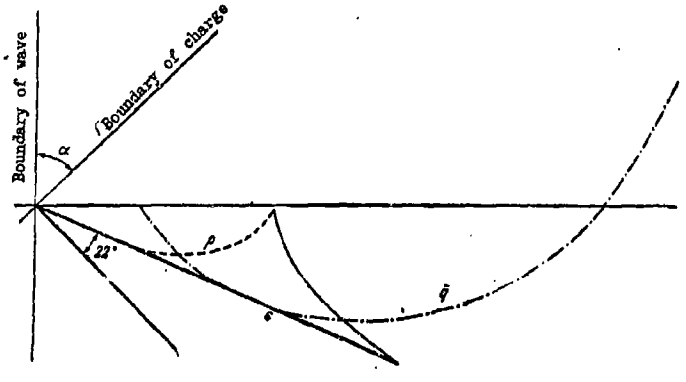


Figure 208. Dispersion of detonation products from an inclined section $\left(k = \frac{7}{5},\ \alpha = \frac{\pi}{4}\right)$.



The case of dispersion of the detonation products from the lateral surface of an explosive charge is of interest for more detailed consideration, i.e. when the angle $\alpha = \frac{\pi}{2}$.

In this case $\gamma = \frac{\pi}{2}$, $\beta = \pi$, , $\varphi = \theta$,

$$\left.\begin{aligned} &\tilde{q}_k = \sqrt{\frac{k+1}{k-1}}\, c_i = \frac{kD}{\sqrt{k^2-1}}, \quad u = \sqrt{\frac{k+1}{k-1}}\, c_i \cos\sqrt{\frac{k-1}{k+1}}\,\theta, \\ &v = c_i \sin\sqrt{\frac{k-1}{k+1}}\,\theta, \quad \bar{u} = D\left[\frac{k}{\sqrt{k^2-1}}\cos\sqrt{\frac{k-1}{k+1}}\,\theta - \cos\theta\right], \\ &\bar{v} = D\left[\frac{k}{k+1}\sin\sqrt{\frac{k-1}{k+1}}\,\theta - \sin\theta\right], \quad \tan(\psi-\theta) = \frac{\bar{v}}{\bar{u}}, \\ &\rho = \frac{k+1}{k}\,\rho_0\left(\frac{\sin\sqrt{\frac{k-1}{k+1}}\,\theta}{\sin\sqrt{\frac{k-1}{k+1}}\,\frac{\pi}{2}}\right)^{\frac{2}{k-1}}. \end{aligned}\right\} \qquad (81.21)$$

An approximate, but very graphical solution of this same problem is also possible (See p.....), based on the assumption that after the detonation wave has passed through a given section of the charge, dispersion of the surface layers under the action of the internal pressure takes place perpendicularly to the surface of the charge, in the system of coordinates moving together with the wave front. Then, in a non-mobile system of coordinates, it is obvious that dispersion of the detonation products will take place through an angle ψ to the surface of the charge, such that this angle is obtained from the ralationship

$$\tan\psi = \frac{u_i}{u_0} = \frac{k-1}{2k}, \qquad (81.22)$$

where $u_0 = \frac{2c_i}{k-1} = \frac{2kD}{k^2-1}$ is the velocity in a direction normal to the surface of the charge, and $u_i = \frac{D}{k+1}$ is the velocity in a direction along the surface of the charge. The total velocity of dispersion, obviously, is determined by the relationship

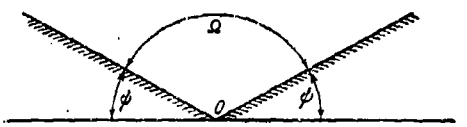
$$\bar{q} = \frac{D}{k+1}\sqrt{\frac{4k^2}{(k-1)^2}+1}. \qquad (81.23)$$

For typical explosives, assuming k = 3, we obtain from (81.22) and (81.23) that $\psi = 18^\circ$ and $\bar{q} = 0.8\ D$.

The laws as indicated are particularly clearly manifested for the detonation of any extended charge of explosive or for a detonating fuse.

If we wish to obtain, for example, the front of the dispersing detonation products as a plane surface, then it is necessary for this purpose to take an extended charge or a length of detonating cord in the form of an angle, such that the magnitude of this angle Ω, obviously, is determined by the relationship: $180^\circ - 2\psi = \Omega$ (Fig. 209).

Figure 209. Charge shape for obtaining a plane dispersion front for the detonation products.



In concluding the investigation of the processes taking place as a result of dispersion of the detonation products in vacuo, it should be noted that the use of the isentropy equation $pv^k = \text{const}$, where k = 3, as we know holds good only for pressures of $p > 2000$ kg/cm^2; for pressures of $p < 2000$ kg/cm^2 the isentropy equation $pv^\gamma = \text{const}$, must be used, where $\gamma = \frac{5}{4}$ to $\frac{7}{5}$. However, the leading portion of the detonation products, for which the isentropy equation $pv = \text{const}$, holds good, has extremely small mass, namely its mass amounts to not more than 5% of the total mass of the detonation products, which does not necessitate separate consideration of its effect.

§ 82. Dispersion of Detonation Products in Air.

Let us pass on to a study of the dispersion of detonation products in air. In order to simplify the problem we shall assume initially that the detonation is instantaneous, and we shall consider the distribution of the detonation products and of the shock wave as if in a tube.

Let, at an instant of time $t = 0$ in the section $x = 0$, a discharge of detonation products be initiated; as a result of the shock of the detonation products on the air in it, a stationary shock wave is formed, the initial parameters of which are

$$p = p_\infty, \quad u = u_\infty, \quad \rho = \rho_\infty, \quad c = c_\infty. \tag{82.1}$$

This shock wave will be propagated to the right, and to the left through the charge a rarefaction wave will proceed, such that the rarefaction wave at a time interval $c_i t \leqslant x \leqslant (u_\infty - c_\infty) t$ will be described by the well-known relationships

$$u - c = \frac{x}{t}, \quad u = \frac{2}{k-1}(\bar{c}_i - c). \tag{82.2}$$

At the time interval $(u_\infty - c_\infty) t \leqslant x \leqslant u_\infty t$ a stationary wave passes through the detonation products

$$u = u_\infty, \quad p = p_\infty, \quad \rho = \rho_{n\infty}, \quad c = c_{n\infty}. \tag{82.3}$$

The initial parameters of the shock wave and of the detonation products at the boundary of separation are determined from the equation

$$\frac{u_\infty}{\bar{c}_i} = 1 - \left(\frac{p_\infty}{\bar{p}_i}\right)^{\frac{1}{3}} = \sqrt{\frac{p_\infty}{\bar{p}_i}\frac{2\rho_0}{3(\gamma+1)\rho_\infty}}, \tag{82.4}$$

which, for

$$\gamma = \frac{5}{4}, \quad \rho_\infty = \frac{1}{770} \text{ g/cm}^3, \quad \rho_0 = 1.6 \text{ g/cm}^3, \quad D = 8000 \text{ m/sec}$$

gives

$$\bar{c}_i = 4880 \text{ m/sec}, \quad \bar{p}_i = 128{,}000 \text{ kg/cm}^2, \quad p_\infty = 320 \text{ kg/cm}^2.$$

The reflected rarefaction wave

$$u - c = \frac{x}{t}, \quad u + c = \frac{x + 2l}{t} \tag{82.5}$$

overtakes the stationary rarefaction wave at

$$\frac{x_1}{l} = 2\frac{u_x}{c_{n.0}}, \quad \frac{\bar{c}_1 t_1}{l} = 2\frac{\bar{c}_1}{c_{n.0}} \tag{82.6}$$

whereupon a new wave originates

$$u + c = \frac{x + 2l}{t}, \quad u - c = u_0 - c_{n.0} \tag{82.7}$$

which will be a compression wave. (In the case of a spherical explosion, as a result of the dispersion there is formed not a simple compression wave but a shock wave which passes through the explosion products). This compression wave overtakes the boundary of separation at

$$\frac{x_2}{l} = 2\frac{u_0}{c_{n.0}}, \quad \frac{\bar{c}_1 t_2}{l} = 2\frac{\bar{c}_1}{c_{n.0}}, \tag{82.8}$$

after which there originates in the air a new wave, within the zone of the shock wave, which overtakes the front of the shock wave at

$$x_3 = \frac{2c_0}{u_0 + c_0 - D_2} D_2 t_1, \quad t_3 = \frac{2c_0}{u_0 + c_0 - D_2} t_1 \tag{82.9}$$

(which corresponds to $\frac{x}{l} = 20 - 25$).

This wave will be a simple one :

$$u - c = u_0 - c_0, \quad x = (u + c)t + F(u), \tag{82.10}$$

so that an arbitrary function can be found knowing the law of motion of the boundary of separation. However, we shall not carry out these complex calculations since they are of no great practical value.

Now let us consider the problem of the initial phase of motion of the shock wave created by an actual detonation.

An accurate solution to this problem is not possible, however an approximate description of the properties of this wave can be given in the case when the isentropy equation for the detonation products takes the form

$$p = A\rho^5, \tag{82.11}$$

or

$$p = B\sigma^5 \tag{82.12}$$

and on the assumption that within the region of the shock wave the density is

$$\rho_{x0} = \rho_0 \frac{\gamma + 1}{\gamma - 1} \tag{82.13}$$

Behind the shock front, according to the extent of the pressure change, the air density changes (it is reduced), but we shall not take this into account in the approximate analysis.

On these assumptions the problem is solved analytically.

We shall present only the final results, omitting the rather unwieldly derivations.

The laws of variation of the shock wave parameters in the process of its propagation are determined by the relationships

$$\tau = \left(\frac{v_0}{v_\infty}\right)^{\frac{2}{5}} e^{\frac{2}{5}\alpha\left(v_0^{\frac{1}{2}} - v_\infty^{\frac{1}{2}}\right)} \qquad (82.14)$$

where

$$\tau = \frac{Dt}{l}, \quad v_\infty = \frac{u_\infty}{D}, \quad v_0 = \frac{u_0}{D} \qquad (82.15)$$

($u_0 = u_{\infty 0}$ is the initial velocity of motion of the boundary of separation).

$$a^2 = \frac{32}{27(\gamma+1)}\frac{p_0}{\rho_a}. \qquad (82.16)$$

The law of motion of the shock front is determined by the relationship

$$\frac{x}{l} = \xi = \frac{v_0^{\frac{5}{2}}}{a}\left(av_\infty^{\frac{1}{2}} + 1\right) e^{\frac{2}{5}\alpha\left(v_0^{\frac{1}{2}} - v_\infty^{\frac{1}{2}}\right)} \qquad (82.17)$$

(for $\tau = 1$, $v_\infty = v_{0x} = \left(\frac{d\xi}{d\tau}\right)_0$).

The pressure at the boundary of separation is equal to

$$\frac{p_\infty}{\rho_l} = 0{,}065 v_\infty^2. \qquad (82.18)$$

For D = 8000 m/sec

$$p_\infty = 970 v_\infty^2, \qquad (82.19)$$

if the pressure is measured in kg/cm^2. Results of the calculations are presented in Table 118 .

Table 118.

Shock wave parameters in air (one-dimensional charge)

$\tau=\frac{Dt}{l}$	$\xi=\frac{x}{l}$	$v_m=\frac{u_m}{D}$	$\frac{p_m}{p_0}$
1	1	0,89	780
1,73	1,63	0,84	680
2,65	2,38	0,80	620
4,12	3,53	0,76	560
5,18	4,32	0,74	530
5,80	4,79	0,73	510
120	69,0	0,50	240

The solution found is applicable in practice up to times for which the equation $p = A\rho^3$ is valid for the detonation products. Approximately it will be effective up to a distance of about ten times the charge length.

In the case of instantaneous detonation the reflected wave of the rarefaction wave overtakes the shock front at a distance of about 22 l.

At this same distance the pressure in the shock wave for an actual detonation is approximately the same as in the case of an instantaneous detonation, and the maximum drop in pressure in the shock wave in both caseswill take place according to one and the same law. We have already shown that the law governing the drop in pbessure may be represented approximately by formula (82.19).

For this case we write down the Law of Conservation of Momentum

$$\frac{d}{dt}(M_s u_m) = sp = sp_m\left(\frac{x_2}{x}\right) = u_m\frac{dM_s}{dt} + M_s\frac{du_m}{dt};$$

since $M_s = s\left(\rho_s x\frac{\gamma+1}{2} - \rho_0 l\right)$, then, by introducing dimensionless coordinates and neglecting the quantity $\frac{l}{x} = \frac{1}{\xi}$ relative to unity, we can arrive at the equation

$$\xi\ddot{\xi} + \dot{\xi}^2 = \frac{2}{\gamma+1}\frac{p_m}{\rho_s D^2}\left(\frac{\xi_2}{\xi}\right)^k. \qquad (82.20)$$

Here $\xi_2 = \frac{x_2}{l}$ is the dimensionless distance at which the reflected wave, or more precisely the compression wave (82.7), overtakes the boundary of separation.

Integration of this equation for the initial conditions

$$x = x_2, \quad t = t_2, \quad u = u_\infty \quad \text{or} \quad \xi = \xi_2, \quad \tau = \tau_2, \quad v = v_\infty$$

gives the approximate law of variation of the shock wave parameters for its maximum propagation.

The law of variation of velocity with distance has the form

$$v^2 = \frac{A}{\xi^3} - \frac{4}{\gamma+1}\frac{p_\infty}{\rho_0 D^2}\frac{1}{k-1}\frac{\xi_2^k}{\xi^{k-1}} \qquad (82.21)$$

for

$$\xi^{k-3} = \frac{4\xi_2^k}{A(\gamma+1)(k-1)}\frac{p_\infty}{\rho_0 D^2}, \quad v = 0,$$

i.e. this value of ξ determines the limiting expansion of the detonation products.

At greater distances from the point of explosion the pressure at the shock front will be greater than at the boundary of separation, which, in the course of time, leads to considerable inaccuracies in using equation (82.17).

Considerable interest is presented by examination of the limiting phase of propagation of the shock wave at distances where the change in entropy proves to be quite small. By neglecting this change the problem can be considered as an acoustical approximation.

§ 83. Limiting "acoustical" Phase of the Process.

Within the limit, for a sufficiently large interval of time after the beginning of the process (for $t \to \infty$ in an infinite tube), the explosion products will completely occupy a finite volume, since the final pressure should be p_∞.

This volume, for the detonation products of condensed explosives, is determined by the relationship

$$\frac{v_\infty}{v_i}=\frac{\rho_i}{\rho_\infty}=\frac{l_\infty}{l}=\left(\frac{p_i}{p_k}\right)^{\frac{1}{\gamma}}\left(\frac{p_k}{p_a}\right)^{\frac{1}{k}}, \tag{83.1}$$

where p_k is the pressure at the conjugate point.

The pressure of the air set into motion within the zone of the shock wave should also be close to p_a for large values of t (but not identically equal to p_k) in all regions, since the shock wave for these conditions degenerates into a sound wave which should be represented by a compression wave.

This sound wave should carry the entire determinate energy $\overline{E}_0 = E_a$, which is determined from the following considerations.

The detonation products, within thelimit, have an energy of

$$E_\infty=\frac{p_a v_\infty}{k-1}=\frac{p_a v_i}{k-1}\left(\frac{p_i}{p_k}\right)^{\frac{1}{\gamma}}\left(\frac{p_k}{p_a}\right)^{\frac{1}{k}}. \tag{83.2}$$

Thus, the energy given up to the atmosphere will be

$$\overline{E}_0=E_i-E_\infty=E_i\left[1-\frac{p_a v_i}{(k-1)E_i}\left(\frac{p_i}{p_a}\right)^{\frac{1}{\gamma}}\left(\frac{p_k}{p_a}\right)^{\frac{1}{k}}\right]. \tag{83.3}$$

This energy, for a sufficiently large value of t, is also propagated by a very extensive, but of small intensity, compression wave.

For a plane sound wave, the amplitude of which is not infinitely small, for $\Delta\rho=\rho-\rho_a\leq\rho_a$, as is well-known, the singular solution of the basic system of equations is valid:

$$\left.\begin{aligned} x&=(u+c)t+F(u+c),\\ u&=\frac{2}{\gamma-1}(c-c_a). \end{aligned}\right\} \tag{83.4}$$

If the quantity $u+c$ in the wave depends monotonically upon x, such that $\frac{\partial(u+c)}{\partial x}>0$, then in the course of time the quantity $u+c$ becomes a linear function of x, whatever the value of $F(u+c)$ was.

Actually, $\frac{\partial x}{\partial(u+c)}=t+\frac{\partial F}{\partial(u+c)}=t\left(1+\frac{\partial F}{t\,\partial(u+c)}\right)$,

for $t\to\infty$, $\frac{\partial x}{\partial(u+c)}\to t$, $\frac{\partial^2 x}{\partial(u+c)^2}=0$, which gives

$$x=(u+c)t+\text{const}. \tag{83.5}$$

We shall assume also that for $t < \infty$

$$x = (u + c)t + \text{const.}$$

whereupon this expression, for convenience in future use, will be written in the form

$$x = -x_0 + (u + c)(t + t_0). \tag{85.6}$$

Then, from the second relationship of (85.4) and (85.6) we obtain

$$u = \frac{2}{\gamma+1}\left(\frac{x + x_0}{t + t_0} - c_a\right), \quad c = \frac{2}{\gamma+2}\left(\frac{\gamma-1}{2}\frac{x + x_0}{t + t_0} + c_a\right). \tag{85.7}$$

The velocity of the front of the not infinitely weak sound wave is determined by the equation

$$D_s = \frac{dx}{dt} = \frac{u + c + c_a}{2} = \frac{\gamma+1}{4}u + c_a = \frac{x + x_0}{2(t + t_0)} + \frac{c_a}{2}. \tag{85.8}$$

Integrating (85.8) we arrive at the relationship defining the law of motion of the shock front :

$$x = -x_0 + c_a(t + t_0) + A\sqrt{t + t_0}, \tag{85.9}$$

where the constant of integration A is defined from the condition that at a certain time $\bar{t}$, the known coordinate of the wave $\bar{x}$ (or the velocity $\bar{D}_s$) is

$$A = \frac{\bar{x} + x_0}{\sqrt{\bar{t} + t_0}} - c_a\sqrt{\bar{t} + t_0}.$$

From (85.7) and (85.8), (85.9) we obtain for the wave front

$$\left.\begin{aligned} u_{s,f} &= \frac{2A}{(\gamma+1)\sqrt{t + t_0}}, \quad c_{s,f} = c_a + \frac{\gamma-1}{\gamma+1}\frac{A}{\sqrt{t + t_0}}, \\ D_s &= c_a + \frac{A}{2\sqrt{t + t_0}}. \end{aligned}\right\} \tag{85.10}$$

The total energy of the sound compression wave can be determined by the formula

$$E_0 = \int_{p_a}^{p_f}\left(\frac{p - p_a}{\gamma - 1} + \frac{\rho u^2}{2}\right)dx, \tag{85.11}$$

where p_f is the pressure at the wave front.

Since $\Delta p < p_a$, then the expression following the integral sign can be represented, accurate to terms of the second order, in the form

$$\frac{\Delta p}{\gamma-1}+\frac{\rho u^2}{2}=\frac{\Delta\rho c_a^2}{\gamma-1}+\frac{(\Delta\rho)^2 c_a^2}{2\rho_a}+\frac{\rho_a u^2}{2},$$

but to the same approximation $u=\frac{\Delta\rho}{\rho}c_a$, therefore

$$\frac{\rho_a u^2}{2}=\frac{(\Delta\rho)^2 c_a^2}{2\rho_a}.$$

From the first equation of (83.7) (expanding into series and discarding terms of the second order) we obtain

$$\Delta\rho=\frac{2}{\gamma+1}\frac{\rho_a}{c_a}\left[\frac{x+x_0}{t+t_0}-c_a\right]+\frac{3-\gamma}{(\gamma+1)^2}\frac{\rho_a}{c_0^2}\left(\frac{x+x_0}{t+t_0}-c_a\right)^2, \tag{83.12}$$

for

$$\Delta\rho=0 \quad x=-x_0+c_a(t+t_0);$$

for $\Delta\rho=\Delta\rho_s \quad x=-x_0+c_a(t+t_0)+A\sqrt{t+t_0},$

therefore

$$E_0=c_a^2\int_0^{\Delta\rho_s t}\left(\frac{\Delta\rho}{\gamma-1}+\frac{(\Delta\rho)^2}{\rho_a}\right)dx=\frac{A^2\rho_a c_a}{\gamma^2-1}\left[1+\frac{3\gamma-1}{3(\gamma+1)}\frac{A}{c_a\sqrt{t+t_0}}\right]. \tag{83.13}$$

Obviously, the excess mass of air M_0 contained within the wave is determined by the expression

$$M_0=\int_0^{\Delta\rho_s t}\Delta\rho\,dx=\frac{A^2\rho_a}{(\gamma+1)c_a}\left[1+\frac{3-\gamma}{3(\gamma+1)}\frac{A}{c_a\sqrt{t+t_0}}\right]. \tag{83.14}$$

Let us now determine the momentum I_0 of the air in this wave :

$$I_0=\int_{\rho_a}^{\rho_s t}\rho u\,dx=\rho_a\int_0^{\Delta\rho_s t}u\,dx+\frac{c_a}{\rho_0}\int_0^{\Delta\rho_s t}(\Delta\rho)^2\,dx,$$

hence

$$I_0=\frac{A^2\rho_a}{\gamma+1}\left[1+\frac{4}{3(\gamma+1)}\frac{A}{c_a\sqrt{t+t_0}}\right]. \tag{83.15}$$

If we express E_0 and I_0 via M_0 , substituting A by D_s :

$$\left.\begin{aligned}E_0&=\frac{M_0c_a^2}{\gamma-1}\left[1+\frac{2}{3}\frac{\gamma-1}{\gamma+1}\left(\frac{D_s}{c_a}-1\right)\right],\\ I_0&=M_0c_a\left[1+\frac{2}{3}\left(\frac{D_s}{c_a}-1\right)\right];\end{aligned}\right\} \tag{83.16}$$

for $t\to\infty$

$$M_0=\frac{A^2}{\gamma+1}\frac{\rho_a}{c_a},\quad E_0=\frac{M_0c_a^2}{\gamma-1}=M_0l_a,\quad I_0=M_0c_a. \tag{83.17}$$

The fall in energy with increase in time is associated with the fact that as a

result of the propagation of a non-infinitely weak sound wave, a portion of the energy is irreversibly transaformed into thermal energy, which "gets stuck" behind the wave passing through the given volume of air. This affect can also be studied : we know that in determining E_0, I_0 and M_0 the inaccuracies associated with neglecting change of entropy does not affect terms of the second order proportional to $(\Delta p)^2 \sim t^{-1}$, which, after integration become terms of the first order.

The inaccuracy associated with neglecting entropy only affects terms of the third order, which after integration become terms of the second order.

It is obvious that behind the wave for $p = p_a$, the condition $\bar{v} < v_a$ should be attained, which gives $\bar{c} > c_a$, where $\bar{v}$ and $\bar{c}$ are the specific volume and velocity of sound behind the wave, so that the quantities $\Delta\bar{v} = \bar{v} - v_a$ and $\Delta\bar{c} = \bar{c} - c_a$ should be proportional to the quantity $(\Delta p_{ударн})^2$.

Let us find these relationships. Since the volume density of the energy behind the wave is constant, $\Delta(\bar{\rho}\varepsilon) = 0$, where ε is the internal energy density, calculated per unit mass ; hence $\Delta\bar{\rho}\varepsilon + \rho_a \Delta\varepsilon = 0$. Since $\Delta\varepsilon = T_a \Delta S - p_a \Delta\bar{v}$, we arrive at the relationship

$$\frac{\Delta v}{v}(\varepsilon_a + p_a v_a) = \frac{\Delta\bar{v}}{v} i_a = T_a \Delta S, \qquad (85.18)$$

where i_a is the enthalpy of the air.

In order to determine the value of ΔS with respect to the rapid change of pressure at the wave front, we have the well-known relationship

$$T_a \Delta S = \frac{(\Delta p_i)^3}{12} \frac{\partial^2 v}{\partial p^2}. \qquad (85.19)$$

Therefore

$$\frac{\Delta\bar{v}}{v_a} = \frac{(\Delta p_i)^3}{12 i_a} \frac{\partial^2 v}{\partial p^2}. \qquad (85.20)$$

In the case of an ideal gas

$$i_a = \frac{\gamma p_a v_a}{\gamma - 1}, \quad \frac{\partial^2 v}{\partial p^2} = \frac{\gamma + 1}{\gamma^2} \frac{v_a}{p_a^2},$$

and (85.20) assumes the form

$$\frac{\Delta\bar{v}}{v_a} = \frac{\gamma^2 - 1}{12\gamma^2} \left(\frac{\Delta p_{ударн}}{p_a}\right)^3. \qquad (85.21)$$

Since for constant pressure $\frac{\Delta\bar{v}}{v_a} = \frac{2\Delta\bar{c}}{c_a}$, then

$$\frac{\Delta\bar{c}}{c_a} = \frac{\gamma^2-1}{24\gamma^2}\left(\frac{\Delta p_{s.f.}}{p_a}\right)^2. \qquad (85.22)$$

In order to satisfy the Law of Conservation of Energy, i.e. in order that the sum of the total energies of the air masses contained in the wave and behind the wave should be constant, it must be assumed that behind the wave the pressure $p_1 \neq p_a$.

Obviously, the difference

$$p_1 - p_a = \Delta p_1 \sim (\Delta p_{s.f.})^2;$$

a more accurate calculation gives

$$\Delta p_1 = \frac{\gamma(3\gamma-1)}{6(\gamma+1)^2}\frac{A^2}{c_a^2(t+t_0)^{\frac{2}{3}}}.$$

For $t \to \infty$

$$I_0 = \sqrt{(\gamma-1)M_0E_0}. \qquad (85.23)$$

Since the momentum of the air is equal to the pressure impulse acting on the wall for $t \to \infty$ (as a result of completion of the gas discharge process), then this impulse is determined by the formulas

$$I_0 = M_0c_a, \quad M_0 = (\gamma-1)\frac{E_0}{c_a^2}. \qquad (85.24)$$

Obviously, the value of E_0 is the sum of the energy of the gas $\bar{E}_0$ given up to the atmosphere and the energy E_d of the displaced mass of air, where

$$E_d = (v_\infty - v_1)\frac{p_a}{\gamma-1}. \qquad (85.25)$$

Substituting $\bar{E}_0$ from (85.5) and assuming that

$$E_0 = \bar{E}_0 + E_d$$

and $k = \gamma$, we arrive at the formula

$$I_0 = (\gamma-1)\frac{E_0}{c_a} = \frac{\gamma-1}{c_a}E_1 - \frac{p_a v_1}{c_a},$$

whence, after transformation, we have

$$I_0 = M_1\frac{p_a}{\rho_1}\frac{v_a}{\gamma}\left(\frac{\gamma-1}{k_0-1}\frac{p_1}{p_a} - 1\right) = (\gamma-1)\frac{E_0}{c_a}, \qquad (85.26)$$

where M_1 is the mass of explosive, $k_0 = 3$ for typical explosives.

Comparing the magnitude of the impulse I_0 with the impulse resulting

from discharge of the detonation products in vacuo (I_i') we find that

$$\frac{I_0}{I_i'} = \frac{(\gamma-1)}{c_*}\sqrt{\frac{3}{2}Q} \approx 3.$$

Comparing the mass of air in the shock wave with the mass of the detonation products, we have

$$\frac{M_0}{M_i} = \frac{(\gamma-1)Q}{c_*^2} \approx 40.$$

In the process of expansion of the gas, the instant comes when $p = p_*$, but $u > 0$ at the boundary of separation and the expansion of the gas is prolonged up to a value $p < p_*$, when the velocity u_x of the boundary of separation between the gas and the air becomes equal to zero. After this, reverse motion of the gas commences - it is compressed to a value $p > p_*$, then it again expands, and so on, until the condition $p = p_*$ is established everywhere. Damping oscillations of the gas column are set up. Obviously, it is sufficient to consider the first expansion and compression, after which the process practically ceases, as a result of which it is found that $p < p_*$ at the wall during a certain interval of time. Thus, the magnitude of the impulse also undergoes fluctuations around the value I_0.

The case which we have considered of the limiting shock wave gives an approximation for the value p_* above, and this signifies that for advancement of the shock wave, the pressure at the wall, being less than p_*, approaches the value p_*; after the first expansion, the process of compression of the gas will have the largest amplitude, corresponding to a weak shock wave. In the process of the first expansion the shock wave is relatively strong.

Compression of the gas takes place as a consequence of the fact that the pressure behind the shock wave, as we have shown, is greater than it was originally ($p > p_*$).

The laws which we have considered for the limiting phase of the shock wave are adequately understood from the physical point of view.

Let us now try to analyse approximately the basic laws associated with the pulsations of the gas, and to estimate the limits of its maximum expansion.

From the theory of non-stationary motion, it is known that the "non-stationary " impulse is, on the whole, only 20% less than the corresponding "stationary" impulse ; this difference can serve as a characteristic redistribution of energy. It may be thought that the difference between the internal energy of the gas for $t \to \infty$, $x = x_\infty$ and for $x = x_{max}$, where x_{max} is the maximum expansion, will be of the same order.

The energy for $x = x_\infty$ is

$$E_\infty = E_i \left(\frac{l}{l + x_\infty}\right)^{k-1}.$$

The energy for $x = x_{max}$ is

$$\bar{E} = E_i \left(\frac{l}{l + x_{max}}\right)^{k-1}.$$

The difference in energy is

$$\Delta E = E_i \left[\left(\frac{l}{l + x_\infty}\right)^{k-1} - \left(\frac{l}{l + x_{max}}\right)^{k-1}\right] \qquad (85.27)$$

or

$$\Delta E = E_i \left[\left(\frac{p_a}{p_i}\right)^{\frac{k-1}{k}} - \left(\frac{\bar{p}}{p_i}\right)^{\frac{k-1}{k}}\right], \qquad (85.28)$$

where $\bar{p}_i$ is the pressure for $x = x_{max}$.

Since $p_a - \bar{p} < p_i$, then, denoting $p_a - \bar{p} = \Delta p$, we arrive at the expression

$$\Delta E \approx E_i \frac{k-1}{k} \frac{\Delta \bar{p}}{p_a} \left(\frac{p_a}{p_i}\right)^{\frac{k-1}{k}} = E_\infty \frac{k-1}{k} \frac{\Delta \bar{p}}{p_a}.$$

Taking $\frac{\Delta E}{E_\infty} = \frac{1}{7}$, we see that $\frac{\Delta p}{p_a} = \frac{1}{2}$.

Thus, the value of the minimum pressure is 0.5 p_a and $\frac{x_{max}}{x_\infty} \approx 1.8$, and consequently the magnitude of the impulse is not very considerable.

Thus, the essential conclusion can be drawn that the momentum of the shock wave for $t \to \infty$ tends towards a completely finite limit. This momentum exceeds the momentum of the detonation products, which they should possess as a result of discharge in vacuo. The increase of momentum is explained by the fact

that the mass of air set into motion exceeds the mass of the detonation products by a factor of ten.

§ 84. Theory of a Point Explosion.

Similarity solution for a strong shock wave

The convergent strong wave.

A point explosion is the simplest case of the action of a shock wave, for which it is assumed that the mass of the detonation products are infinitely small (it tends to zero), but the quantity of energy liberated by the charge is finite.

Obviously, such a statement of the problem boils down to the discussion of the effect of only one shock wave.

At distances close to the source of the explosion, this shock wave will be strong. Therefore, in order to study its properties, the intrinsic energy of the air set into motion can always be neglected, i.e. the value of the atmospheric pressure p_0 in comparison with the pressure at the shock front.

As already shown in 1944 by SEDOV and STANYUKOVICH, the study of a point explosion is considerably more simple than the study of an actual explosion, and the results obtained from it may also be applied to suit the case of an actual explosion.

As a result of a point explosion, the motion of the air in the shock wave at close distances from the explosion origin follows a similarity solution, since it is independent of any of the linear initial parameters characterising the explosion.

By "similarity solution" motion we should understand motion such that the spatial distribution of any value is decreased similarly with itself in time.

In order to study a point explosion, the basic system of differential equations

$$\left.\begin{aligned} &\frac{\partial u}{\partial t}+u\frac{\partial u}{\partial r}+\frac{1}{\rho}\frac{\partial p}{\partial r}=0,\\ &\frac{\partial \ln \rho}{\partial t}+u\frac{\partial \ln \rho}{\partial r}+\frac{\partial u}{\partial r}+\frac{Nu}{r}=0,\\ &\frac{\partial \frac{p}{\rho^{\gamma}}}{\partial t}+u\frac{\partial \frac{p}{\rho^{\gamma}}}{\partial r}=0 \end{aligned}\right\} \qquad (84.1)$$

is transformed into a system of common differential equations, since all the parameters characterising the motion of the air in the shock wave can be expressed by the relationships

$$u=t^{a_1-1}\xi(z),\quad \rho=t^{a_2}\eta(z),\quad p=t^{2(a_1-1)+a_2}\sigma(z), \qquad (84.2)$$

where $z=r/t$ is an independent function, a_1 and a_2 are constants.

In order to obtain the unknown differential equation, we shall introduce the change $w=p/\rho$. Then equation (84.1) will assume the form

$$\left.\begin{aligned} &\frac{\partial u}{\partial t}+u\frac{\partial u}{\partial r}+w\frac{\partial \ln \rho}{\partial r}+\frac{\partial w}{\partial r}=0,\\ &\frac{\partial \ln \rho}{\partial t}+u\frac{\partial \ln \rho}{\partial r}+\frac{\partial u}{\partial r}+\frac{Nu}{r}=0,\\ &\frac{\partial \ln w}{\partial t}+u\frac{\partial \ln w}{\partial r}-(\gamma-1)\left(\frac{\partial \ln \rho}{\partial t}+u\frac{\partial \ln \rho}{\partial r}\right)=0. \end{aligned}\right\} \qquad (84.3)$$

From the second equation of (84.3) it follows that

$$\frac{\partial \ln \rho}{\partial t}+u\frac{\partial \ln \rho}{\partial r}=-\left(\frac{\partial u}{\partial r}+\frac{Nu}{r}\right).$$

Substituting the expression on the right hand side in the last equation of (84.3) we obtain

$$\frac{\partial \ln w}{\partial t}+u\frac{\partial \ln w}{\partial r}+(\gamma-1)\left(\frac{\partial u}{\partial r}+\frac{Nu}{r}\right)=0. \qquad (84.4)$$

Introducing $x=u\frac{t}{r}$, $y=w\frac{t^2}{r^2}$, we obtain the equations

$$\left.\begin{aligned} &\dot{x}-x+xx'+y'+x^2+2y+y\frac{\rho'}{\rho}=0,\\ &\frac{\dot{\rho}}{\rho}+x\frac{\rho'}{\rho}+x'+(N+1)x=0,\\ &\frac{\dot{y}}{y}+x\frac{y'}{y}+(\gamma-1)[x'+(N+1)x]+2(x-1)=0. \end{aligned}\right\} \qquad (84.5)$$

Here, for example,

$$\dot{x} = \frac{\partial x}{\partial \ln t},$$

$$x' = \frac{\partial x}{\partial \ln r}.$$

We shall now derive the solution of this system, assuming that

$$x = x(z), \quad y = y(z), \quad \rho = t^{a_1}\eta(z), \tag{84.6}$$

where

$$z = \frac{r}{t^{a_1}}.$$

Then

$$\dot{x} = -a_1 \frac{dx}{d\ln z},$$

$$x' = \frac{dx}{d\ln z}.$$

Equation (84.5) now takes the form :

$$dx(x - a_1 + 1) + dy + y\frac{d\eta}{\eta} + (2y - x)\,d\ln z = 0,$$

$$\frac{dy}{y}(x - a_1) + (\gamma - 1)\,dx + d\ln z\,[x[N(\gamma - 1) + \gamma + 1] - 2] = 0,$$

$$\frac{d\eta}{\eta}(x - a_1) + dx + [(N+1)x + a_2]\,d\ln z = 0,$$

hence we find that

$$\left.\begin{aligned} \frac{d\ln z}{dx} &= \frac{(a_1 - x)\frac{d\ln y}{dx} - (\gamma - 1)}{[N(\gamma - 1) + \gamma + 1]x - 2} = \\ &= \frac{(a_1 - x)^2 - \gamma y}{y[2(a_1 - 1) + a_2 + \gamma(N+1)x] - x(1-x)(a_1 - x)}, \\ -\ln\eta &= \ln(x - a_1) + \int \frac{a_2 + (N+1)x}{a_1 - x}\,d\ln z. \end{aligned}\right\} \tag{84.7}$$

We have one differential equation of the first order in the whole of the derivatives. Its solution will be $F_1(x;\ y;\ c_1) = 0$. z is determined by the quadrature

$$F_2(x;\ y;\ z;\ c_1;\ c_2) = 0,$$

and η is determined by the quadrature

$$F_3(x;\ y;\ z;\ \eta;\ c_1;\ c_2;\ c_3) = 0.$$

As a result we obtain a solution dependent upon six constants : three obtained by integration (c_1, c_2 and c_3), and three introduced the solution (a_1, a_2, τ) ; at the same time the constant τ can be introduced, since the

equations are unaltered by substituting $t + \tau$ for t.

Relationship (84.2) follows automatically from relationships (84.4) and (84.5), so that

$$\sigma = z^2 y \eta.$$

Since at the front of a strong shock wave conditions are achieved such that

$$p_i = \frac{2}{\gamma+1}\rho_0 D_s^2,$$
$$u_i = \frac{2}{\gamma+1} D_s,$$
$$\frac{\rho_i}{\rho_0} = \frac{\gamma+1}{\gamma-1}$$

(where D_s is the velocity of the shock front, and the suffix "i" refers to parameters at the shock front), and also

$$\left.\begin{aligned} z &= z_i, \\ r &= z_i t^{a_1}, \\ dr &= a_1 z_i t^{a_1-1}\, dt = a_1 \frac{r}{t}\, dt, \end{aligned}\right\}$$

then

$$D_s = \frac{dr}{dt} = a_1 \frac{r}{t}. \qquad (84.8)$$

It is easy to see that at the front of the wave $z = z_i = \text{const}$, since the distance travelled by the wave front, in the case of similarity solution motion, varies proportionally as t^{a_1}, which follows from definition of similarity solution motion itself, i.e. it is independent of z.

It follows from these conditions that

$$\left.\begin{aligned} x_i &= \frac{2}{\gamma+1} D_s \frac{t}{r} = \frac{2a_1}{\gamma+1}, \\ y_i &= \frac{p_i}{\rho_i}\frac{t^2}{r^2} = \frac{2(\gamma-1) D_s^2 t^2}{(\gamma+1)^2 r^2} = \frac{2(\gamma-1) a_1^2}{(\gamma+1)^2}. \end{aligned}\right\} \qquad (84.9)$$

Obviously, $\eta = \eta(z_i) = \text{const}$; the parameter a_1 is equal to 0, since at the front of a strong shock wave in an ideal gas

$$\frac{\rho_i}{\rho_0} = \frac{\gamma+1}{\gamma-1} = \text{const}.$$

The point with the coordinates

$$x_i = \frac{2}{\gamma+1} a, \quad y_i = \frac{2(\gamma-1)}{(\gamma+1)^2} a_1^2$$

lies on a curve, which is the solution of the equations for a strong shock wave from a point explosion. As a result of t[illegible], equation (84.7) takes the form

$$\left.\begin{aligned}\frac{d\ln z}{dx} &= \frac{(a_1-x)\frac{d\ln y}{dx}-(\gamma-1)}{[N(\gamma-1)+(\gamma+1)]x-2} = \\ &= \frac{(a_1-x)^2-\gamma y}{y[2(a_1-1)+\gamma(N+1)x]-x(1-x)(a_1-x)}, \\ -\ln\eta &= \ln(x-a_1)+(N+1)\int\frac{x}{x-a_1}d\ln z.\end{aligned}\right\} \qquad (84.10)$$

In order that the solution should be determinate, it is necessary to know the constant a_1. The constant τ_1, without limiting the generality of the solution, can be assumed equal to zero, on the assumption that the explosion takes place at time t = 0. In the given case, a_1 is determined from energy considerations.

We write down the expression for the total energy of the shock wave at any instant of time (as long as the wave is a strong one) :

$$E = A\int_0^{r_0}\left[\frac{p}{\gamma-1}+\frac{\rho u^2}{2}\right]r^N dr. \qquad (84.11)$$

Here $A = 2$ for N = 0 ; $A = 2\pi$ for N = 1 ; $A = 4\pi$ for N = 2. Expression (84.11) reduces to the form

$$E = A\int_0^{z_0}\left(\frac{z^2y\eta}{\gamma-1}+\frac{z^2x^2\eta}{2}\right)z^{N_1}dz\,t^{2(a_1-1)+a_1(N+1)+a_2}. \qquad (84.12)$$

Since the total energy is constant, then the integral should be independent of t , and therefore

$$2(a_1-1)+a_1(N+1)+a_2=0,$$

or

$$a_1(N+3)+a_2=2. \qquad (84.13)$$

In the case under consideration $a_2=0$ and

$$a_1=\frac{2}{N+3}. \qquad (84.14)$$

Consequently, for a plane wave $a_1=\frac{2}{3}$, for a cylindrical wave $a_1=\frac{1}{2}$, and for a spherical wave $a_1=\frac{2}{5}$.

Thus, equation (84.2) assumes the form

$$\left.\begin{aligned} u &= xzt^{(a_1-1)} = xz^{\frac{N+3}{2}} r^{-\frac{N+1}{2}}, \\ p &= t^{2(a_1-1)} z^2 y_\rho = z^{N+3} y_\rho r^{-(N+1)}. \end{aligned}\right\} \tag{84.15}$$

Thus, at the wave front

$$p_i \sim r^{-N} \tag{84.16}$$

and the velocity of the wave front is

$$D_s \sim u_i \sim r^{-\frac{N+1}{2}}. \tag{84.17}$$

This result was first obtained by LANDAU in 1945.

It was shown by SYEDOV that the solution of the first equation of (84.7) for the conditions of (84.14) can be written in a simple analytical form

$$y = \frac{\gamma-1}{2\gamma} x^2 \frac{a_1 - x}{x - \frac{a_1}{\gamma}}. \tag{84.18}$$

It can be easily seen that this solution satisfies the initial conditions of equation (84.9), i.e. the conditions at the wave front.

From the quadratures we determine that

$$z = c_1 x^{-a_1} \left(x - \frac{a_1}{\gamma}\right)^{\frac{\gamma-1}{2}\frac{a_1}{(\gamma-2)a_1+1}} \left[x + \frac{a_1}{a_1(\gamma-2)+1-\gamma}\right]^a = c_1 \varphi_1(x), \tag{84.19}$$

$$\eta = \rho = c_2 (a_1 - x)^{\frac{2}{\gamma-2}} \left(x - \frac{a_1}{\gamma}\right)^{\frac{1-a_1}{(\gamma-2)a_1+1}} \times$$

$$\times \left[x + \frac{a_1}{a_1(\gamma-2)+1+\frac{2}{\gamma}}\right]^{\frac{2a}{(\gamma-2)a_1+1}} = c_2 \varphi_2(x). \tag{84.20}$$

We determine further that

$$u = c_1 t^{(a_1-1)} x^{(1-a_1)} \left(x - \frac{a_1}{\gamma}\right)^{\frac{\gamma-1}{2}\frac{a_1}{(\gamma-2)a_1+1}} \left[x + \frac{a_1}{a_1(\gamma-2)+1-\gamma}\right]^a = \tag{84.21}$$

$$= c_1 \varphi_3(x),$$

$$p = \frac{\gamma-1}{2\gamma} c_1^2 c_2 t^{2(a_1-1)} x^{2(1-a_1)} (a_1 - x)^{\frac{\gamma}{\gamma-2}} \left[x + \frac{a_1}{a_1(\gamma-2)+1-\gamma}\right]^b = \tag{84.22}$$

$$= \frac{\gamma-1}{2\gamma} c_1^2 c_2 \varphi_4(x).$$

Here

$$a = \frac{a_1}{a_1(\gamma-2)+1-\gamma}\left[\frac{\gamma-1}{2}\frac{\gamma}{a_1(\gamma-2)+1}+1\right]+a_1,$$

$$b = 2a\left[1+\frac{1}{(\gamma-2)\,a_1}\right].$$

From equations (84.20) and (84.22) we determine the temperature

$$RT = \frac{p}{\rho} = (\gamma-1)\,c_v T = \frac{\gamma-1}{2\gamma}c_1^2 t^{2(a_1-1)}x^{2(1-a_1)}\times$$

$$\times(a_1-x)\left(x-\frac{a_1}{\gamma}\right)^{\frac{a_1-1}{(\gamma-2)a_1+1}}\left[x+\frac{a_1}{a_1(\gamma-2)+1-\gamma}\right]^{2a}. \qquad (84.23)$$

Equations (84.20) - (84.23) give the distribution of the primary parameters of the shock wave behind the shock front and the values of the parameters at the shock front as a function of time, or the path taken by the shock wave.

Let us analyse the solutions thus found. At the centre of a point explosion for

$$x = x_1 = \frac{a_1}{\gamma}, \quad y \to \infty, \quad z = 0$$

$$u = 0, \quad \rho = 0, \quad p = \text{const} = \bar{p}, \quad T \to \infty.$$

The quantity $\frac{p}{\rho_i} = \frac{\bar{p}}{\rho_i}$, is determined from equation (84.22)

$$\frac{\bar{p}}{\rho_i} = \theta = \left(\frac{\gamma+1}{2\gamma}\right)^{2(1-a_1)}\left(\frac{\gamma+1}{\gamma}\right)^{\frac{\gamma}{\gamma-2}}\left[\frac{\gamma+1}{\gamma}\frac{a_1\gamma+1-2a_1}{2a_1\gamma+3-(4a_1+\gamma)}\right]^b. \qquad (84.24)$$

Let us consider the limiting case ; for $\gamma = 1$ $\theta = \frac{1}{2}$ for any value of N. Table 119 gives the values of θ for various values of N and γ.

Table 119

Dependence of θ on the Isentropy Index

γ	1	9/7	7/5	5/3	2	3
$N=0$	0,5	0,45	0,39	0,35	0	0,18
$N=1$	0,5	0,42	0,36	0,32	0	0,16
$N=2$	0,5	0,39	0,34	0,30	0	0,15

For $\gamma \to 2$ $\theta = \frac{3}{2}\left(\frac{3}{4e}\right)^{\frac{2(N+1)}{N+3}}$. For N = 0, 1, 2 we have respectively

$\theta = \frac{3}{2}\left(\frac{3}{4e}\right)^{\frac{2}{3}}$, $\theta = \frac{9}{8e}$ and $\theta = \frac{3}{2}\left(\frac{3}{4e}\right)^{\frac{4}{5}}$.

Let us evaluate the integral in expression (84.12); using formula (8414) we obtain

$$E = A\int_0^{z_n} \eta z^{\frac{2}{a_1}}\left(\frac{y}{\gamma-1}+\frac{x^2}{2}\right)\frac{dz}{z}. \qquad (84.25)$$

It follows from equation (84.18) that

$$\frac{y}{\gamma-1}+\frac{x^2}{2} = \frac{x^2}{2}\left[\frac{a_1-x}{\gamma x-a_1}+1\right] = \frac{\gamma-1}{2\gamma}\frac{x^2}{x-\frac{a_1}{\gamma}},$$

and from equations (84.19) and (84.20) we obtain

$$z = z_i\frac{\varphi_1}{\varphi_{1i}}, \quad \eta = \rho_i\frac{\varphi_2}{\varphi_{2i}} = \rho_0\frac{\gamma+1}{\gamma-1}\frac{\varphi_1}{\varphi_{2i}},$$

where φ_{1i} and φ_{2i} the values of the functions φ_1 and φ_2 for $x = x$, $z = z_i$.

Thus,

$$E = A\int_{x_1}^{x_i}\frac{\gamma+1}{2\gamma}\rho_0 z_i^{\frac{2}{a_1}}\frac{x^2}{x-\frac{a_1}{\gamma}}\frac{\varphi_1^{\frac{2}{a_1}}\varphi_2\varphi_1'}{\varphi_{1i}^{\frac{2}{a_1}}\varphi_{2i}}dx.$$

If we denote

$$\int_{x_1}^{x_i}\frac{x^2}{x-\frac{a_1}{\gamma}}\frac{\varphi_1^{\frac{2}{a_1}}\varphi_2\varphi_1'}{\varphi_{1i}^{\frac{2}{a_1}}\varphi_{2i}}dx = \xi. \qquad (84.26)$$

Then

$$E = \frac{\gamma+1}{2\gamma}A\xi\rho_0 z_i^{\frac{2}{a_1}} = \frac{\gamma+1}{2\gamma}A\xi\rho_0 z_i^{N+2}. \qquad (84.27)$$

We shall transform this expression. Since

$$p_i = \frac{2}{\gamma+1}\rho_0 D_{z_1}^2 = \frac{2a_1}{\gamma+1}\rho_0 r_i^{\frac{2(a_1-1)}{a_1}} z_i^{\frac{2}{a_1}},$$

then

$$z_i^{\frac{2}{a_1}} = z_i^{N+2} = \frac{\gamma+1}{2}\frac{p_i}{a_1^2\rho_0}r_i^{N+1}, \qquad (84.28)$$

which gives

$$E\frac{\gamma+1}{2\gamma}A\xi\frac{\gamma+1}{2a_1^2}p_i r_i^{N+1} = \left(\frac{\gamma+1}{2a_1}\right)^2 A\xi\frac{p_i r_i^{N+1}}{\gamma}.$$

If we denote

$$\left(\frac{\gamma+1}{2a_1}\right)^2 \frac{\xi}{\gamma} = \frac{2\xi_0}{(\gamma-1)(N+1)},$$

then we arrive at the expression

$$E = \frac{2A\xi_0}{N+1}\frac{p_i}{\gamma-1} r_i^{N+1}. \qquad (84.29)$$

Here $\frac{A}{N+1} r_i^{N+1}$ represents the volume v_i occupied by the shock wave. If we designate $\frac{p_i}{\gamma-1} = \frac{E}{2}$, where E_i is the volume energy density at the shock front, then

$$E = \xi_0 v_i E_i. \qquad (84.30)$$

Since E can be represented in the form $E = v_i \bar{E}$ where $\bar{E}$ is the mean volume energy density, then $\xi_0 = \frac{\bar{E}}{E_i}$ denotes the ratio of the mean energy density to the energy density at the shock front.

The value of will be necessary for our further calculations. Since

$$p_i = \frac{2a_1^2}{\gamma+1}\rho_a z_i^3 t^{2(a_1-1)} = \frac{\gamma-1}{2}\frac{E(N+1)}{A\xi_0} z_i^{3-\frac{2}{a_1}} t^{2(a_1-1)},$$

then

$$z_i^3 = \left[\frac{\gamma-1}{2}\frac{E(N+1)(\gamma+1)}{A\xi_0 2a_1^2\rho_a}\right]^{a_1}, \qquad (84.31)$$

which determines the value of p_i by the relationship

$$p_i = \frac{2a_1^2}{\gamma+1}\rho_a t^{2(a_1-1)}\left[\frac{\gamma^2-1}{4}\frac{E(N+1)}{\rho_a A\xi_0 a_1^2}\right]^{a_1}.$$

If we designate

$$\frac{2a_1^2}{\gamma+1}\rho_a\left[\frac{\gamma^2-1}{4}\frac{E(N+1)}{\rho_a A\xi a_1^2}\right]^{a_1} = B. \qquad (84.32)$$

then

$$p_i = Bt^{2(a_1-1)} = Bt^{-\frac{2(N+1)}{N+2}}. \qquad (84.33)$$

The results of calculation for a spherical and cylindrical shock wave are presented in Figures 210 and 211.

Figure 210 Distribution of parameters at the front of a spherical similarity solution shock wave.

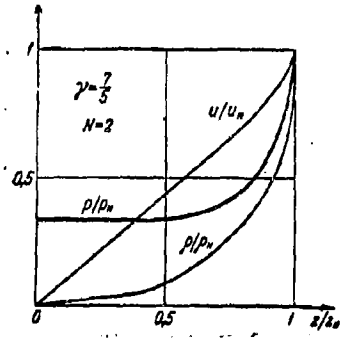
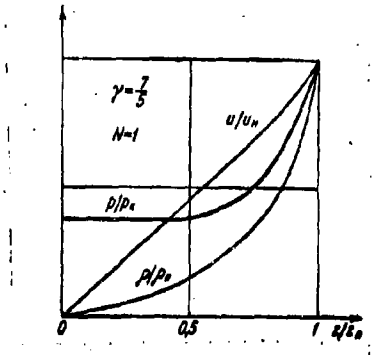


Figure 211 Distribution of parameters at the front of a cylindrical similarity solution shock wave.



Let us pass on to the determination of the impulse for a strong similarity solution shock wave. Obviously, the impulse acting on unit surface perpendicular to the wave velocity at a distance r_1 from the centre of the explosion is determined by the formula

$$I=\int_{t_1}^{\infty} p\,dt=B\int_{t_1}^{\infty} t^{-\frac{2(N+1)}{N+3}}dt. \qquad (84.54)$$

Here $t_1=z_n r_1^{1/n}$ is the time during which the wave front travels a distance r_1. Hence it is clear that in the one-dimensional case N = 0 for a plane wave

$$I\sim t_1^{\frac{1}{3}}\sim\sqrt{r_1},$$

for a cylindrical wave (N = 1)

$$I\sim\ln t_1\sim\ln r_1,$$

and for a spherical wave (N = 2),

$$I\sim\frac{5B}{t_1^{\frac{2}{5}}}\sim\frac{1}{\sqrt{r_1}}.$$

Thus, the impulse proves to be finite only for a spherical wave for $r_1 \to \infty$. But this is understandable, since in idealising the problem we assume that the external counter-pressure is equal to zero.

Actually, if the external counter-pressure is taken into account, then for a plane and a cylindrical wave the impulse acting on unit surface will always have a finite value at any distance.

We shall present a few calculations carried out for a more real case - a strong spherical, similarity solution wave ($N = 2$, $a_1 = \frac{2}{5}$, air density $\rho_1 = 1/770$ g/cm^3). On evaluating the integral in (84.26) we obtain $\xi_0 = \frac{1}{3}$ for $\gamma \approx \frac{5}{4}$ to $\frac{7}{5}$, i.e. for a heated air shock wave (evaluation of this integral is carried out numerically, since the integral is insolvable in the general form).

Hence, using formula (84.29) we obtain

$$E = \frac{8\pi}{9} \frac{\rho_1}{\gamma - 1} r_1^3,$$

which, for $\gamma = \frac{5}{4}$ gives

$$E = \frac{32\pi}{9} \rho_1 r_1^3. \qquad (84.55)$$

Further, taking equations (84.51) and (84.52) we obtain

$$B = \frac{1}{8} E^{\frac{2}{5}}, \quad z_1^2 = 25 E^{\frac{2}{5}},$$

whence

$$i = \frac{5E^{\frac{2}{5}}}{8\xi_1^{\frac{1}{5}}} = \frac{5E^{\frac{2}{5}} z_1^{\frac{1}{2}}}{8\sqrt{r_1}} = 1.4\sqrt{\frac{E}{r_1}} \qquad (84.56)$$

(in the C.G.S. system).

These formulae are valid only up to a definite distance (up to a pressure at the wave front of about 10 - 20 kg/cm^2).

Further on the density at the wave front is reduced, the wave readjusts to become a similarity solution wave. As a result of this the intrinsic

energy of the air set in motion by the shock wave commences to play a significant rôle. This factor also disrupts the similarity solution behaviour of the motion, since the flow of energy is not subject to the law of similarity.

Assuming that

$$E = mQ = \frac{4}{3}\pi r_0^3 \rho_0 Q$$

(m is the mass and r_0 the radius of the charge) we arrive at the conclusion that by taking into account the intrinsic energy of the air in the vicinity of the point of explosion, the energy balance (equation (84.29) will be determined by the relationship

$$\frac{24\pi r_i^3}{3\cdot 3}\frac{p_i}{\gamma-1} = \frac{4\pi r_0^3}{3}\rho_0 Q + \frac{4\pi r_i^3}{3}\frac{p_a}{\gamma-1}$$

(the second term of the right-hand portion of the equation allows for the intrinsic energy of the air set into motion). After transformation we obtain

$$\Delta p = \frac{3(\gamma-1)\rho_0 Q}{2}\left(\frac{r_0}{r_i}\right)^3 + \frac{p_a}{2}, \qquad (84.57)$$

where

$$\Delta p = p_i - p_a.$$

Neglecting p_a in comparison with Δp, since the wave is a strong one, and after substituting the values $\rho_0 = 1.6$ g/cm^3, $Q = 1000$ kcal/kg and $\gamma = 1.25$ we obtain

$$\Delta p = 25\,000\left(\frac{r_0}{r_i}\right)^3. \qquad (84.58)$$

This formula is valid for distances at which the wave is still strong. Consequently, a pressure of 25 kg/cm^2 is attained for $r_i \approx 10 r_0$, i.e. approximately at the same distances as for an actual explosion.

The theory of a strong point explosion which we have considered is valid only in the region in which the pressure ahead of the shock front can be neglected in comparison with the pressure at the shock front, i.e. at relatively small distances from the centre of the explosion.

At the same time, for the explosion in air of a spherical charge of

the usual explosives, the basic relationships at the shock front as a function of the characteristics of the charge and of the distance can only be established approximately at present. The impulse of the shock wave is determined by a more or less accurate calculation. However, this is inadequate for estimating the radius of the destructive effect of a normal or an atomic explosion. It is essential to know the characteristics of the explosion field (pressure, velocity head, impulse etc) in the region where, in the hydrodynamic sense, the wave is no longer strong, but is still capable of causing characteristic destruction.

The development of machine calculating techniques nowadays permits similar problems to be solved relatively simply. Thus, the problem of a powerful explosion in an infinite atmosphere of constant density has been solved by numerical integration with the aid of electronic computers. The results of the solution are presented in a report by Broud in the form of graphs and collective tabular data for the empirical formulae. The problem has been solved for three cases : a point explosion, an isothermal sphere, the density of the gas inside of which is equal to the gas density outside, the sphere, and an isobaric sphere, the inside temperature of which is equal to the gas temperature outside the sphere. The initial pressures in the isothermal spheres are 2000 and 121 atm. respectively.

The initial pressure of the medium outside the sphere and in the medium surrounding the point source were taken as equal to one atmosphere.

A similar calculation has also been carried out by D.E. OKHOTSIMSKII, I.L. KONDRASHEV, Z.P. VLASOV and R.K. KAZOKOV in the Mathematical Institute of the Academy of Sciences USSR for a somewhat more extended range of pressure at the shock front than in Broud's paper.

We shall give the primary results of the numerical solution to the

problem as stated. As primary variables we take the dimensionless distance

$$\lambda = \frac{r}{\varepsilon}$$

and the dimensionless time

$$\tau = \frac{tc_0}{\varepsilon},$$

where r is the distance from the explosion centre, ε is a quantity proportional to the explosion energy converted into the shock wave (dynamic length), t is the time and c_0 is the velocity of sound in the gas ahead of the shock front; ε is determined by the relationship

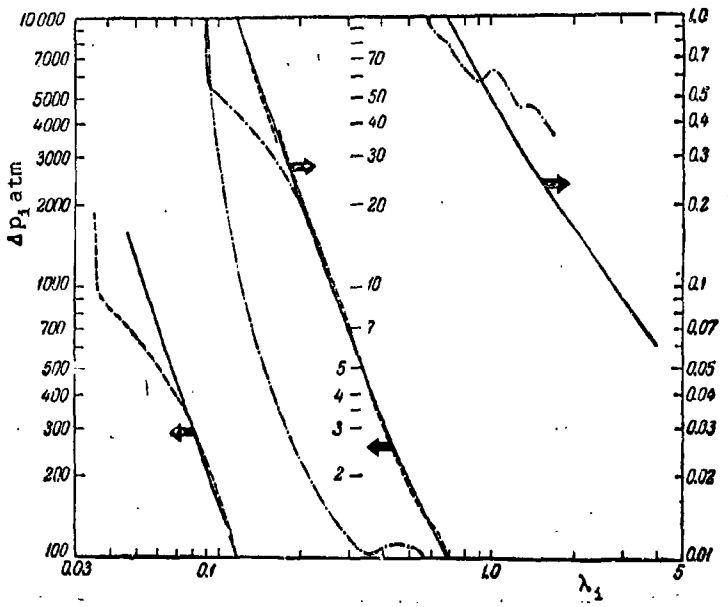
$$\varepsilon^3 = \frac{E_s}{p_0} = \frac{4\pi}{p_0}\int_0^{r_1} \rho\left(E_{int} + \frac{u^2}{2}\right) R^2\, dR - \frac{4\pi r_1^3}{3(\gamma-1)}, \qquad (84.59)$$

where E_s is the energy imparted to the gas by the explosion, p_0 is the atmospheric pressure (the pressure ahead of the shock front), ρ is the density of the gas behind the shock front, u is the velocity of the gas behind the shock front, E_{int} is the specific internal energy of the gas in the shock wave; γ is the adiabatic index of the gas, assumed to be constant in the problems to be solved, r_1 is the distance from the explosion centre to the shock front, $\frac{u^2}{2}$ is the specific kinetic energy of the gas in the shock wave.

The second term of the right hand portion of relationship (84.59) gives the initial internal energy of the gas.

The dependence of the over-pressure at the shock front on λ_1 $(\lambda_1 = r_1/\varepsilon)$ is shown in Fig. 212. The continuous curves give the dependence of $\Delta p_1(\lambda_1)$ for a point explosion, and the peaked curves depict the dependence of the over-pressure at the shock front on λ_1 for the case of isothermal spheres with an initial overpressure of 2000 atm. and 120 atm. The dot-dash curves depict the solution for an isobaric sphere.

Figure 212 . Dependence of overpressure at the shock front on dimensionless distance.



For a point explosion within the range $p_i \geqslant$ 10 atm, the results of the numerical solution are well-described by the empirical formula

$$\Delta p_i = 0.1567\ \lambda_i^{-3} + 1 \text{ atm.} \qquad (84.40)$$

For weak shock waves

$$\Delta p_i = 0.137\ \lambda_i^{-3} + 0.119\ \lambda_i^{-2} + 0.269\ \lambda_i^{-1} - 0.019 \text{ atm,} \qquad (84.41)$$

where

$$0.1 \leqslant \Delta p_i \leqslant 10 \text{ or } 0.26 < \lambda_i < 2.8 .$$

If the energy transformed into the shock wave is expressed in units of TNT equivalent and the distance r_i in metres, then relationship (84.40)

and (84.41) can be written thus :

$$\Delta p_i = 6.70 \frac{q_{eq.}}{r_i^3} + 1 \text{ atm} \qquad (84.42)$$

and

$$\Delta p_i = 0.975 \frac{\sqrt[3]{q_{eq}}}{r_i} + 1.455 \frac{\sqrt[3]{q_{eq}^2}}{r_i^2} + 5.85 \frac{q_{eq.}}{r_i^2} - 0.019 \text{ atm}, \qquad (84.43)$$

where $q_{eq.}$ is the TNT equivalent of the explosion with respect to the shock wave(for the case of an explosion in an unconfined infinite atmosphere).

It follows from Fig. 212 that the solution for isothermal spheres practically corresponds with the solution for a point explosion commencing at $r \geqslant 2r_0$, i.e. when the mass of gas set into motion by the shock wave exceeds the original mass of gas in the isothermal sphere by a factor of 10 or more.

The dependence of the maximum velocity head $Q_i = \frac{1}{2} \rho_i u_i^2$ (ρ_i is the density of the gas at the shock front and u_i is its velocity) on the dimensionless distance λ_i is shown in Fig. 213 (for a point explosion).

Figure 213. Dependence of maximum velocity head on dimensionless distance.

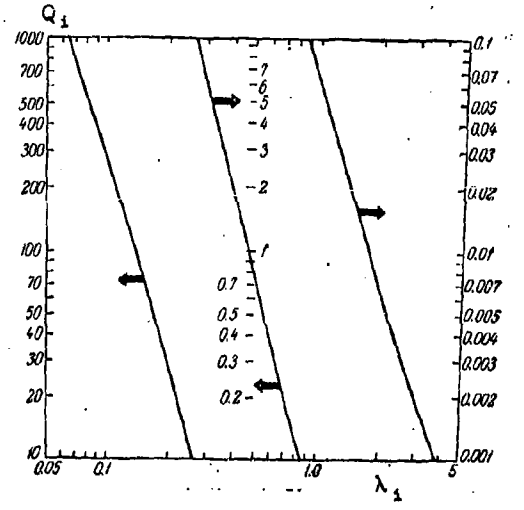
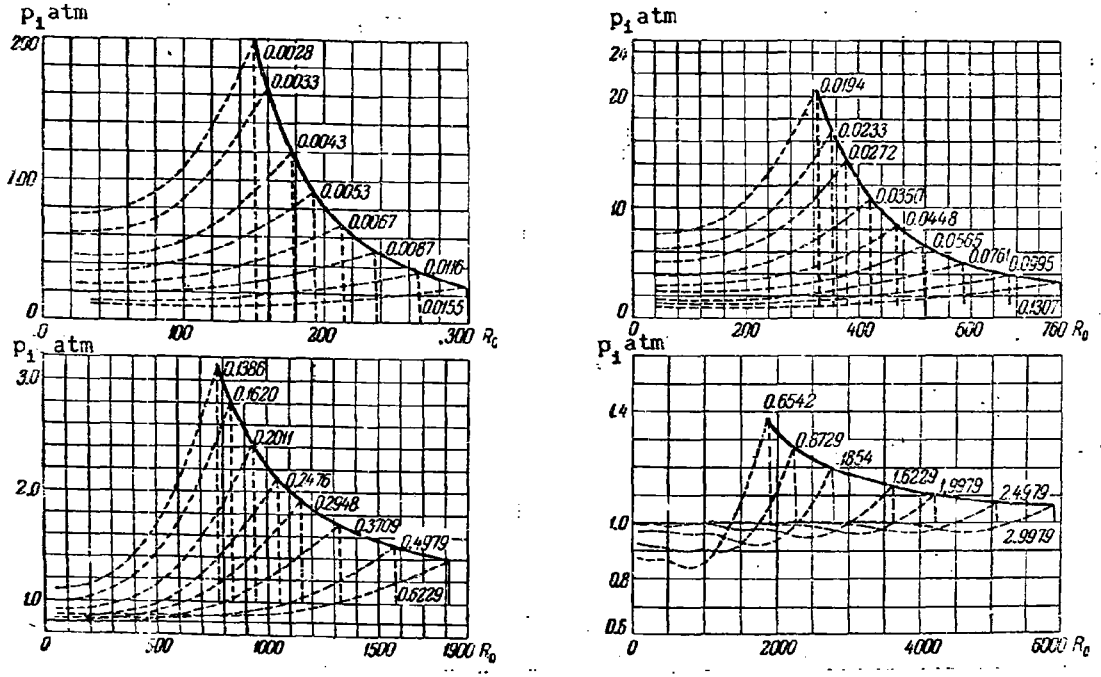


Figure 214. Change of pressure behind the shock front at various relative distances.



The dependence of u_i on λ_i within the range $\Delta p_i \geqslant 0.1$ atm. is well-described by the empirical formula

$$u_i = 0{,}30\lambda_i^{-\frac{1}{2}} = 3.66\sqrt{\frac{\sqrt[3]{q_{eq}^2}}{r_i^2}}. \qquad (84.44)$$

The change in pressure behind the shock front at different relative distances is shown in Fig. 214. The pecked lines show the change in pressure as a function of the coordinates and the numbers beside the peaks of the curves show the time after explosion in the dimensionless units $\tau = \frac{t c_0}{r}$. The dimensionless distance R_0 is related to the distance r_i up to the shock front by the relationship

$$r_i = s\frac{R_0}{1627{,}2}$$

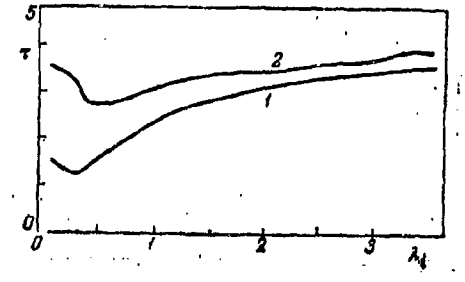
or

$$r_i = \sqrt[3]{\frac{Eq}{p_0}}\frac{R_0}{1627{,}2} = 2{,}15 \cdot 10^{-3} R_0 \sqrt[3]{q_{eq}}.$$

The envelope drawn through the vertices of the broken curves gives the dependence of the pressure at the shock front on the dimensionless distance R_0.

Fig. 215 shows the dependence of the time of action of the compression and rarefaction phases (curves 1 and 2 respectively) of the shock wave on distance (in dimensionless units).

Figure 215. Dependence of time of action of the compression and rarefaction phases of the shock wave on dimensionless distance.



For shock waves fromm normal explosives, according to Sadovskii, the time of action of the compression phase is equal to

$$t \approx 1.5 \cdot 10^{-3} \sqrt[6]{q}\,\sqrt{r_1},$$

where q is the weight of the charge. But $r_1 = \lambda_1 \sqrt[3]{\frac{E}{p_a}}$, $t = \frac{\tau \sqrt[3]{\frac{E}{p_a}}}{c_a}$ and $q = \frac{E}{4{,}27 \cdot 10^5}$, and $q = \frac{E}{4.27 \cdot 10^5}$, where E is the energy of explosive charge ; the specific energy is assumed to be equal to 1000 kcal/kg = $4.27 \cdot 10^5$ kgm/kg(TNT).

After substitution we obtain

$$\tau = 0{,}26 \sqrt{\lambda_1}.$$

Comparison of data with respect to time of action of the shock wave shows that the time of action of the compression phase for a point explosion, just as for a normal explosion, is described by the same laws, i.e. the time of action is proportional to $\lambda_1^{\frac{1}{2}}$.

The time of action of the rarefaction phase is practically independent of distance :

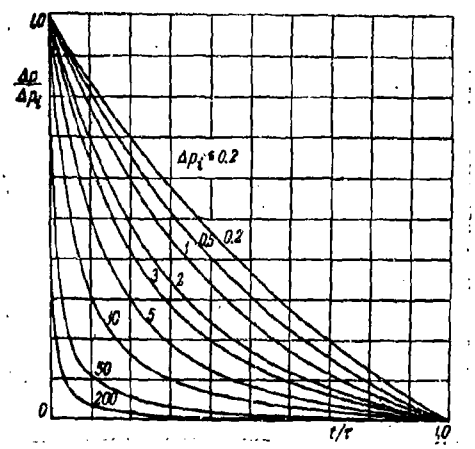
$$\tau_- = 1.22 = \frac{lc_a}{c}$$

and

$$t_- = 4.25 \frac{\sqrt[3]{q_{eq}}}{c_a} \text{ sec}.$$

Fig. 216 shows the change of pressure with time at different distances, characterising the overpressure at the shock front (τ is the time of action of the compression phase, where $0 \leqslant t \leqslant \tau$).

Figure 216 . Change of pressure with time for shock waves of different intensity (at different distances from the explosion centre).



The relationship $\frac{\Delta p}{\Delta p_i}\left(\frac{t}{\tau}\right)$ can be expressed by the empirical formula

$$\frac{\Delta p}{\Delta p_i} = \left(1 - \frac{t}{\tau}\right) e^{-\frac{\alpha t}{\tau}},$$

if $\Delta p_i \leqslant 1$ atm, then $\alpha = \frac{1}{2} + \Delta p_i$.

For shock waves with 1 atm. $\leqslant \Delta p_i \leqslant$ 5 atm.,

$$\alpha = \frac{1}{2} + \Delta p_i \left[1.1 - (0.13 + 0.20\,\Delta p_i)\frac{t}{\tau}\right].$$

A very similar relationship is also established for the velocity head :

$$\frac{Q}{Q_i} = \left(1 - \frac{t}{\tau}\right)^b e^{-\frac{\alpha t}{\tau}},$$

where for waves with $\Delta p_i < 1$ atm, b = 0.75 + 3.2 Δp_i.

It should be noted that in the region where the atmospheric pressure can be neglected in comparison with the pressure at the shock front, numerical solution gives results practically identical with the analytical solution of the problem for a strong point explosion, according to SEDOV and STANYUKOVICH. This holds good for the region where $\lambda_i \leqslant 0.2$.

What has been said is verified in Fig. 217, where the continuous curves show the variation of the gas parameters behind a similarity solution type of shock front, and the peaked curves show the same for a point explosion, taking into account the counter-pressure (for two time intervals).

For the numerical solution of the problem of a point explosion it has been assumed that the gas set into motion is ideal. This is valid if $\Delta p_i \leqslant 10$ atm, as applied to air.

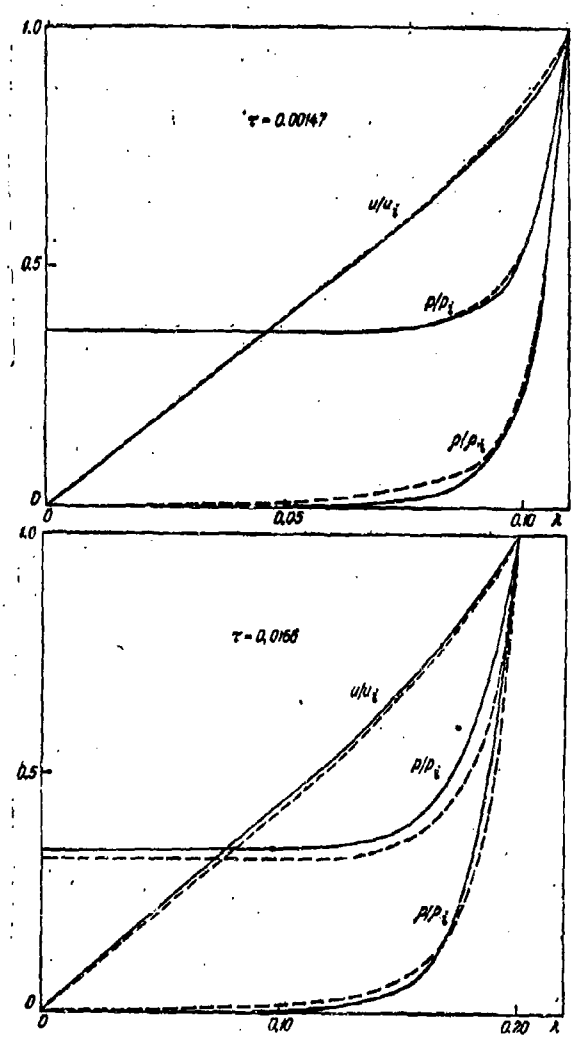
Since the mass of air compressed by the shock wave up to a pressure of $\Delta p \geqslant 10$ atm. amounts to only 5% of the mass of air compressed by the wave up to $\Delta p \geqslant 1$ atm., then the solution is valid with sufficient accuracy for air in the region where $\Delta p_i < 10$ atm. In the region where $\Delta p_i \geqslant 10$ atm., it is necessary to take into account the non-ideality of air. No account is taken in the solution of the transfer of explosion energy by radiation, which for very powerful explosions may be of considerable magnitude. Also, ionisation and dissociation processes are not taken into account, but these are significant only in the region close to the explosion focus.

Up to now we have considered the divergent shock waves which are formed by expansion of the detonation products. Now we shall consider a strong spherical shock wave travelling towards the centre of symmetry, and we shall assume that the medium in which the wave is propagated obeys the equation of polytropy

$$pv^{\gamma} = \text{const.} \qquad (84.45)$$

The theory of this motion has been developed by LANDAU and STANYUKOVICH in 1944. In order to study the properties of a shock wave converging from infinity towards a centre of symmetry, the results of the theory of a point explosion can be used, since the motion of the similar wave will be that of a similarity solution.

Figure 217. Distribution of gas parameters behind a shock front (similarity and non-similarity solution) for two time intervals.



The equations and the initial conditions at the wave front are the same as in the problem of a strong shock wave divergent from the centre of symmetry.

Our problem has been stated up to now as being equivalent to the problem of a strong shock wave diverging from the centre of symmetry. However, the region of existence of a solution in the latter case is defined as $0 \leqslant z \leqslant z_1$, since for the given $t = t_0$, r varies from $r = r_f$ to $r = 0$. In this case of the divergent wave the parameter a_1 is determined from the Law of Conservation of Energy and can be found from the relationship $a_1 = \frac{2}{N+3}$.

In the problem being considered, when the motion of the wave is also that of a similarity solution but the wave moves towards the centre from infinity, the region of existence of a solution is determined as $z_1 \leqslant z < \infty$. The value of the parameter a_1 cannot yet be determined from the Law of Conservation of Energy, since the total energy of the similar wave is infinite. It should be determined as a result of other considerations. z_1 should also be other than in the case of the divergent wave.

In order to simplify future calculations, the convergent wave can be considered as a divergent wave by replacing t with $-t$ and u with $-u$, i.e. as if the motion of the wave were reversed.

First of all we shall see if a solution exists within the range $z_1 \leqslant z < \infty$ for this $-\infty < t \leqslant 0$. Since the velocity behind the shock front should fall (or, in any case it should not increase), then by considering the process for any fixed instant of time $t = t_0$, the conclusion can be drawn that $x = u\frac{t_0}{r}$ falls behind the front and for $r \to \infty$, $x = 0$; thus u remains finite. Consequently, x should be determined within the range $0 \leqslant x \leqslant x_1$, and the value of the derivative is $\frac{d \ln z}{dx} < 0$ 0 (for a divergent wave $\frac{d \ln z}{dx} > 0$). Substituting in equation (84.10) the value of x and y at the point (x_1, y_1), we shall

have

$$\frac{d\ln z}{dx}=\frac{\gamma-1}{2}\frac{\frac{d\ln y}{dx}\frac{a_1}{\gamma+1}-1}{\left(N\frac{\gamma-1}{\gamma+1}+1\right)a_1+1}=\frac{(\gamma+1)^2}{2[4a_1\gamma+2N\gamma a_1+4a_1-3(\gamma+1)]} \tag{84.46}$$

Hence it follows that if

$$a_1(4\gamma+2N\gamma+4)-3(\gamma+3)>0, \tag{84.47}$$

then

$$\frac{d\ln z}{dx}<0.$$

The condition of (84.47) determines a certain finite value for the parameter a_1. By taking into consideration the inequality (84.47) the unknown solution actually exists. The value of the derivative should change monotonically, since change of its sign would be evidence of the fact that x is a multiple function of z or that u is a multiple function of z or r, and the latter is excluded by physical considerations. Consequently, it is necessary that in equations (84.46) or (84.10) the numerators and denominators of the fractions should vanish simultaneously. We require that the expressions

$$(a_1-x)^2-\gamma y \quad \text{and} \quad y[2(a_1-1)+(N+1)\gamma x]-x(1-x)(a_1+x);$$

should vanish simultaneously; then

$$\left.\begin{aligned}\bar{x}&=\frac{a_1\gamma(N+1)-\gamma+2(1-a_1)}{2\gamma N}+\\&+\frac{\sqrt{[a_1\gamma(N+1)-\gamma+2(1-a_1)]^2-8N\gamma a_1(1-a_1)}}{2\gamma N}\\ \bar{y}&=\frac{(a_1-\bar{x})^2}{\gamma}.\end{aligned}\right\} \tag{84.48}$$

The roots of

$$\bar{x}=\frac{a_1\gamma(N+1)-\gamma+2(1-a_1)}{2\gamma N}-\frac{\sqrt{[a_1\gamma(N+1)-\gamma+2(1-a_1)]^2-8N\gamma a_1(1-a_1)}}{2\gamma N}$$

and

$$\bar{x}=a$$

do not satisfy the unknown solution, since by this the values of a_2 are obtained less than the limiting value, which follows from equation (84.47). For $\bar{x}=a_1$, $y=0$ the wave is divergent. In this case the inequality (84.47) is not maintained and $\frac{d\ln z}{dx}>0$.

If the solution of equation (84.10) is written in the form

$$F(x, y, a_1) = c_1$$

(c_1 is the integration constant), then it is required that the line (84.48) passes through the points $\bar{x}, \bar{y}$ and x_1, y_1. Hence it follows that since $\bar{x}, \bar{y}$ and x_1, y_1 are in essence functions of a_1, then we can write

$$F_1(a_1) = c_1, \quad \bar{F}(a_1) = c_1,$$

whence

$$F_1(a_1) = \bar{F}(a_1),$$

which also determines unambiguously the value of a_1. Equation (84.10) has no analytical solution which will satisfy the conditions posed, and therefore the value of a_1 must be determined numerically. However, an approximate value of a_1 can be found by supposing that the expressions

$$(a_1 - x)^2 - \gamma y, \quad y[2(a_1 - 1) + \gamma(N+1)x] - x(1-x)(a_1 - x)$$

and

$$[N(\gamma - 1) + \gamma + 1]x - 2.$$

vanish simultaneously. Hence

$$\bar{x} = \frac{2}{N(\gamma-1)+\gamma+1}, \quad \bar{y} = \frac{(a_1 - x)^2}{\gamma},$$

$$a_1^2\{[N(\gamma-1)+\gamma+1]^2\} - (3-N)a_1[N(\gamma-1)+\gamma+1] - 2(N-1) - \gamma(\gamma-1)(N+1) = 0. \tag{84.49}$$

We note also that the radicand expression in (84.48) should be greater than zero, otherwise the roots of $\bar{x}$ will be imaginary. The other approximate value for a_1, determined from the conditions of inequality of the roots of x and $\bar{x}$, should also satisfy the conditions of the problem. We shall determine this value. Let the radicand expression in (84.48) be equal to zero; then

$$2(1-a_1) - \gamma + a_1\gamma(N+1) = \sqrt{8N\gamma a_1(1-a_1)}.$$

Hence

$$a_1^2\{[\gamma(N+1)-2]^2 + 8\gamma N\} - 2a_1\{(\gamma-2)[\gamma(N+1)-2] + 4\gamma N\} + (2-\gamma)^2 = 0. \tag{84.50}$$

One of the values of a_1 agrees approximately with the value determined by formula (84.49) ; the other, close to zero, does not satisfy the conditions of the problem.

In order to solve equation (84.10) it is essential to know the value of a_1 . As shown by analysis, a_1 is determined almost exactly by relationship (84.50), based on our calculations.

Let us see what values are assumed by a_1 for various values of N and γ . Analysis and calculation show respectively that for $\gamma = 1$ $a_1 = 1$ for $N = 0, 1, 2$; for $\gamma \to \infty$ (incompressible liquid) $a_1 = 1$ for $N = 0$, $a_1 = 2$ for $N = 1$ and $a_1 = \frac{5}{8}$ for $N = 2$. For a spherical shock wave ($N = 2$), consideration of which presents the greatest interest, the values of a_1 for $\gamma = \frac{7}{5}$ and $\gamma = 3$ have been calculated, as a result of which a_1 was found to be equal to 0.717 and 0.658 respectively.

In order to completely explain the properties of the phenomenon, the solution must be analysed in the vicinity of the point $\frac{1}{z} = 0$, which corresponds to an infinite distance from the centre for $r_1 > 0$ and to any finite distance from the centre for $r_1 = 0$, i.e. when the wave has reached the centre. For this, $\frac{z\,dx}{dz} \to \infty$, $x \sim \frac{1}{r} = 0$, $y \sim \frac{1}{r^2} = 0$ and equation (84.10) in the vicinity of the point $x = 0$, $y = 0$ assumes the form

$$\frac{dx}{dy} = \frac{x}{2y}, \quad \frac{dz}{dx} = \frac{z}{x}. \tag{84.51}$$

These expressions are obtained if terms of the second and higher orders are neglected in equation (84.10), i.e. the terms x^2, xy and $y \sim x^2$.

It follows naturally from these relationships that $y \sim x^2$ and $z \sim \frac{1}{x}$.

The second equation of (84.10) in this case assumes the form

$$-\ln \eta = \ln v = \ln a_1 + \frac{N+1}{a_1 z} = \text{const}. \tag{84.52}$$

We obtain (84.52) after substituting the value of x_1 as a function of z in

the second equation of (84.10), from the relationship

$$\frac{dz}{dx} = \frac{z}{x}.$$

Hence, $\rho = \rho_{lim} = \text{const}$, $u = u_{lim} = \text{const}$, $p = p_{lim} = \text{const}$, since

$$\ln v = \ln a_1 + \frac{(N+1)}{a_1 z} = \text{const}, \quad p = \rho y^2 \frac{l^2}{r^2} \sim \rho l^2, \quad u = x\frac{l}{r} \sim l.$$

We note that the velocity u is negative everywhere after substitution of l by $-l$ and of u by $-u$.

The limiting values of density, velocity and pressure may be found only by a numerical method. At the front

$$p = \rho_i y_i \frac{r^2}{l^2} = \rho_i y_i z_i^2 l^{2(a_1-1)},$$

i.e.,

$$p \sim l^{2(a_1-1)} \sim r^{\frac{2(a_1-1)}{a_1}} \sim r^{-b}, \tag{84.53}$$

$$u \sim r^{\frac{a_1-1}{a_1}} \sim r^{-\frac{b}{2}}, \tag{84.54}$$

where

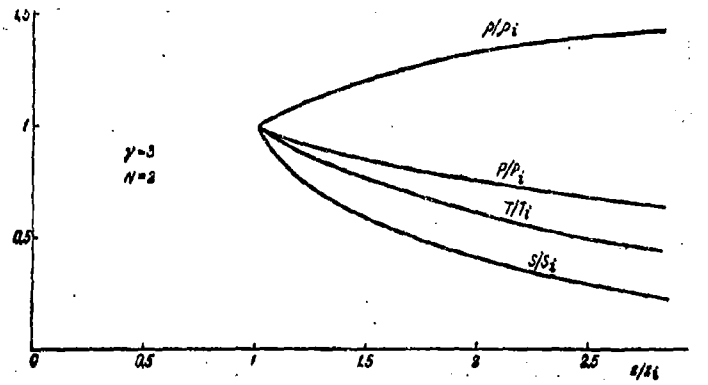
$$b = \frac{2(1-a_1)}{a_1}.$$

For a spherical wave, the values of the parameters b and of the limiting density ρ_{lim} can be given in a table.

γ	b	$\frac{\rho_{lim}}{\rho_i}$
1	0	2.72
7/5	0.8	2.70
3	1.1	1.45
∞	3.3	1

The results of calculations describing the nature of propagation of a spherical convergent detonation wave for $\gamma = 3$ are shown in Figs. 218 – 220.

Figure 218. Distribution of parameters behind the front of a spherical convergent detonation wave.



The considerations developed here concerning the properties of a strong convergent wave can be applied successfully to the study of convergent detonation waves. The entropy at the front of the similarity solution wave increases, the pressure also increases, being subject to the law which we have established for convergent shock waves.

The distribution of parameters behind the front of a detonation wave will be somewhat different from the case of a shock wave.

As a result of our investigations, the conclusion may be drawn that the pressure at the front of a shock wave converging towards the centre of symmetry increases approximately inversely proportionally with the distance from the centre ($p \sim \frac{1}{r}$). Therefore, for convergent shock waves, and even moreso for detonation waves, the pressure in regions close to the centre of symmetry may attain enormous magnitudes (of the order of millions of kg/cm^2).

Figure 219. Variation of pressure behind the front of a convergent detonation wave at different instants of time.

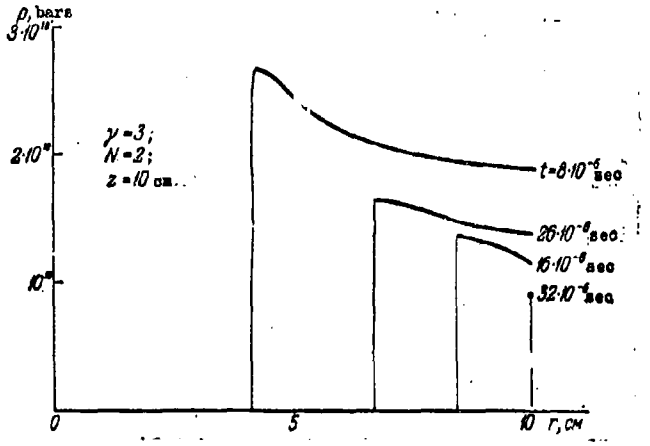
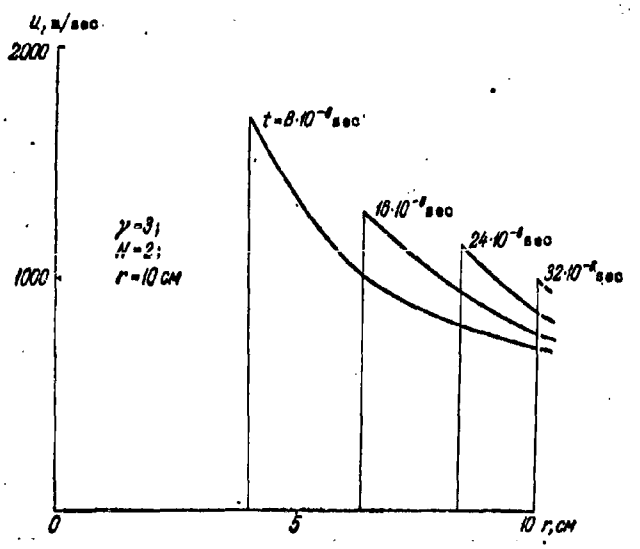


Figure 220. Variation of velocity behind the front of a spherical convergent wave at different instants of time.



For cylindrical waves, $p \sim \frac{1}{\sqrt{r}}$; thus, the pressure along the axis of symmetry may also be considerable.

Conformance to the laws as stated enables one to draw the conclusion that in convergent waves the energy will be concentrated everywhere in smaller and smaller volumes according to the degree of convergence, i.e. the energy density will increase. These considerations have an important significance for the basis and establishment of the special features of the process of cumulation and of certain similar processes.

§ 85. A Spherical Explosion.

The study of the one-dimensional disperaion of detonation products and the resulting shock waves has enabled a number of laws of motion to be established, which we shall apply here.

We now pass on to the study of the dispersion of the explosion products from a spherical charge in air. The explosion of a long cylindrical charge can be studied by similar methods and we shall not dwell separately on this. We shall present only the principal results at the end of this section for determining the pressures and impulses resulting from the explosion of a cylindrical charge.

We shall give here a few approximate analytical results for a spherical charge, and we shall now show that the explosion field resulting from a real detonation of a spherical charge can always be substituted by the explosion field of a spherical charge, assuming that it was detonated instantaneously just as in the case of a one-dimensional detonation.

Actually, we shall consider the first phase of dispersion of the explosion products for a real spherical detonation. It is obvious, first of all, that the pressure in the explosion products will fall more rapidly than

in the shock wave, since the isentropy index for the explosion products is considerably greater than for air, and this also leads to a rapid fall of pressure in the explosion products as a result of their expansion. Now, in the case of a one-dimensional explosion after several interactions of the reflected rarefaction wave, a compression wave originated which travelled in the opposite direction from the gas flow. As a result of explosion of a spherical charge, a similar compression wave is formed immediately after impact of the explosion products on the air, i.e. immediately after generation of the shock wave. Further, this compression wave travelling contrary to the gas flow from the explosion products and passing through a region of sharply-falling pressure may become a shock wave. Somehow or other this compression wave(or shock wave) begins to smooth out the pressure in the explosion products. The shock wave will travel, experiencing everywhere less and less impact pressure on the part of the explosion products. At a distance of about $10r_0$ theexplosion products will be almost stationary and they will give up practically all their energy to the air (to the shock wave), since the interactions between the wave itself will smooth out the pressure gradients in the explosion products .

The same picture will be presented also for the hypothesis of an instantaneous detonation.

In the one-dimensional case, the smoothing out of the field of a real detonation and its approximation to the case of an instantaneous detonation takes place at a distance of about $20r_0$, which corresponds to 20 initial volumes of explosive. For a spherical explosion this will correspond to approximately $5r_0$, i.e. it may be supposed that smoothing out of the field in the case of a real detonation takes place after the rarefaction wave, which is formed by the commencement of dispersion at the surface of the

explosive, arrives at the centre of the charge, is"reflected"from it and then reaches the boundary of separation between the explosion products and the shock wave, which actually occurs at a distance of about $3 - 4r_0$, i.e. considerably closer than for the complete expansion of the explosion products.

We have shown above that about 90% of the energy of the explosion products is transferred to the air. However, the energy of the air moving forward (from the centre of the explosion) is, as measurements show, less than this value and it amounts to 60 - 70% of the total explosion energy. This is explained by the fact that the process of expansion of the explosion products is non-stationary and the boundary of separation between the explosion products and the shock wave causes oscillations about the equilibrium position (when a pressure of $p = p_a$ is established in the explosion products). About 20 - 25% of the explosion energy is involved in these oscillatory movements. Therefore, from the boundary of separation between the explosion products and the air not only one wave radiates, but a series of extremely rapidly damping shock waves(apparently it is still essentially a second pulsation, since the wave originating from a third pulsation will be so weak that it will be practically similar to an ordinary sound wave). Therefore in the first shock wave travelling forward, not 90% of the total explosion energy is transformed, but 25 - 20% less, i.e. the shock wave will contain 65 - 70% of the total explosion energy.

Let us establish how the average pressure in the shock wave, the pressure at the shock front and in the explosion products will vary at different distances from the source of the explosion.

In order to study the pressure profile of a spherical explosion we shall use a hypothetical instantaneous detonation, as we agreed above. At a distance of $r \geqslant (3 - 4)r_0$ this pressure profile conforms with the pressure profile

for a real detonation.

We note that for a real detonation , at the instant of formation of the shock wave the initial pressure at the shock front is greater than in the case of an instantaneous detonation, but the rate of fall of pressure with distance is greater for a real detonation, which leads to equalisation of pressure for both cases at distances of (3 - 4)r_0 approximately.

Close to the site of the explosion the mass of air engulfed by the shock wave is

$$M_a = \frac{4}{3}\pi\rho_a (r_2^3 - r_0^3) = \frac{4}{3}\pi\rho_a \frac{\gamma+1}{\gamma-1}(r_2^3 - r_1^3), \qquad (85.1)$$

hence it follows that

$$M_a = \frac{4}{3}\pi\rho_a \frac{\gamma+1}{2}(r_1^3 - r_0^3), \qquad (85.2)$$

where r_1 is the distance from the centre of the explosion to the boundary of separation and r_2 is the distance from the centre of the explosion to the shock front. The Law of Conservation of Momentum can be written in the form

$$\frac{d(M_a u_1)}{dt} = s(p_1 - p_a), \qquad (85.3)$$

where $s = 4\pi r_1^2$ is the surface area of the boundary of separation and u_1 is its velocity.

Since

$$p = \bar{p}_i \left(\frac{c}{\bar{c}_i}\right)^3 \qquad (85.4)$$

and

in the vicinity of the site of the explosion

$$u + c = \bar{c}_i,$$

where $\bar{p}_i = \frac{\rho_0 D^2}{8}$ and $\bar{c}_i = \sqrt{\frac{3\bar{p}_i}{\rho_0}}$ is the average pressure and average velocity of sound in the explosion products for instantaneous detonation, then relationship (85.3) (neglecting the quantity p_a which is small in

comparison with p_1) assumes the form

$$\frac{d\left[u_1\left(r_1^3-r_0^3\right)\right]}{dt}=\frac{2}{\gamma+1}\cdot 3r_1^2\frac{\bar{p}_i}{\rho_a}\frac{\left(\bar{c}_i-u_1\right)^3}{\bar{c}_i^3}=\frac{r_1^2\rho_0}{\bar{c}_i\rho_a}\left(\bar{c}_i-u_1\right)^3,$$

since $\bar{p}_i=\frac{\bar{c}_i^2\rho_0}{3}$ (ρ_0 is the density of the explosive charge). Hence,

$$\frac{d\frac{u_1}{\bar{c}_i}}{dt}\left(r_1^3-r_0^3\right)+\frac{u_1}{\bar{c}_i}\frac{dr_1^3}{dt}=\frac{2}{\gamma+1}\frac{\rho_0}{\rho_a}\frac{\left(\bar{c}_i-u_1\right)^3}{\bar{c}_i^2}r_1^2. \tag{85.5}$$

Further, substituting

$$\frac{du_1}{dt}\text{ by }u_1\frac{du_1}{dr_1}\text{ and }\frac{dr_1^3}{dt}\text{ by }u_1\frac{dr_1^3}{dr_1}=3u_1r_1^2,$$

we arrive at the relationship

$$\frac{u_1}{\bar{c}_i}\frac{du_1}{\bar{c}_i}\frac{r_1^3-r_0^3}{dr_1^3}=\frac{2}{3(\gamma+1)}\frac{\rho_0}{\rho_a}\left(1-\frac{u_1}{\bar{c}_i}\right)^3-\frac{u_1^2}{\bar{c}_0^2},$$

whence

$$\frac{d\left(r_1^3-r_0^3\right)}{r_1^3-r_0^3}=\frac{\frac{u_1}{\bar{c}_i}\frac{du_1}{\bar{c}_i}}{\frac{2}{3(\gamma+1)}\frac{\rho_0}{\rho_a}\left(1-\frac{u_1}{\bar{c}_i}\right)^3-\frac{u_1^2}{\bar{c}_i^2}}. \tag{85.6}$$

The solution of this equation for the condition that for $r = r_0$ then $u=u_x$ does not present difficulty. Here u_∞ is the initial velocity with which the products of the instantaneous detonation escape into the air. The value of u_∞ is determined from the relationship

$$\frac{2}{3(\gamma+1)}\frac{\rho_0}{\rho_a}\left(1-\frac{u_\infty}{\bar{c}_i}\right)^3=\frac{u_\infty^2}{\bar{c}_i^2}. \tag{85.7}$$

If we write the general solution of equation (85.6) in the form

$$\int\frac{d\left(r^3-r_0^3\right)}{r^3-r_0^3}=\psi\left(\frac{r^3}{r_0^3}-1\right)=\int_{v_\infty}^{v}\frac{v\,dv}{a(1-v)^3-v^2}, \tag{85.8}$$

where

$$v=\frac{u_1}{\bar{c}_i},\quad a=\frac{2}{3(\gamma+1)}\frac{\rho_0}{\rho_a},\quad v_\infty=\frac{u_\infty}{\bar{c}_i}.$$

then it follows from this solution that the velocity and pressure falls rapidly with distance, approximately according to the law

$$\frac{u_1}{u_\infty}=\left(\frac{r_0}{r_1}\right)^4,\quad \frac{p}{p_\infty}\approx\left(\frac{r_0}{r_1}\right)^8. \tag{85.9}$$

These relationships are valid only at the very beginning of the motion. Later the explosion products no longer obey the law of isentropy $p = A\rho^{\gamma}$, since the pressure falls considerably below 1000 - 500 kg/cm^2. As a result of this it is necessary to use the equation for general isentropy $p = A_1\rho^{\gamma}$, where $\gamma \approx \frac{5}{4}$ to $\frac{7}{5}$ (for the detonation products).

However, instead of combining the two solutions evaluating the integral of the momentum in the two zones, the approximate relationship $u + \frac{2}{\gamma_1 - 1} c = \frac{2}{\gamma_1 - 1} c_1$ should not be used (which is satisfied accurately only for one-dimensional motion) but it must be assumed that since the density falls as r^{-3} then the pressure falls as $r^{-3\gamma}$, where $\gamma = 3$ up to $r = 2r_0$ and then $\gamma \approx \frac{5}{4}$. Equation (85.3) then assumes the form

$$\frac{d(Mu_1)}{dt} = u_1 \frac{d(Mu_1)}{dr} = 4\pi r_0^2 p_\infty \left(\frac{r_1}{r_0}\right)^3 \frac{p}{p_\infty} = 4\pi r_0^2 p_\infty \left(\frac{r_1}{r_0}\right)^{3-3\gamma}$$

(p_∞ is the initial pressure at the boundary of separation) and this immediately gives

$$\frac{du_1^2}{d\frac{r_1}{r_0}} = -6\,\frac{u_1^2}{\frac{r_1}{r_0}} + 3(\gamma+1)\frac{p_\infty}{\rho_\infty}\left(\frac{r_1}{r_0}\right)^{-3(\gamma+1)}. \qquad (85.10)$$

Hence for initial conditions as specified above

$$u_1^2 = \bar{A}\left(\frac{r_0}{r_1}\right)^6 + \frac{\gamma-1}{2-\gamma}\frac{p_\infty}{\rho_\infty}\left(\frac{r_0}{r_1}\right)^{3\gamma}, \qquad (85.11)$$

where the constant of integration

$$\bar{A} = u_\infty^2 - \frac{\gamma-1}{2-\gamma}\frac{p_\infty}{\rho_\infty}.$$

Finally we obtain

$$u_1^2 = u_\infty^2\left(\frac{r_0}{r_1}\right)^6 + \frac{\gamma-1}{2-\gamma}\frac{p_\infty}{\rho_\infty}\left[\left(\frac{r_0}{r_1}\right)^{3(\gamma-1)} - \left(\frac{r_0}{r}\right)^3\right]\left(\frac{r_0}{r_1}\right)^3, \qquad (85.12)$$

which at small distances gives $u_1 \sim \frac{1}{r_1^3}$ and at relatively large distances gives

$$u_1 \sim r_1^{-\frac{3\gamma}{2}} \sim r_1^{-2}.$$

We note once again that we are determining here the law of motion of the boundary of separation.

We shall now pass on to establishing some of the laws of motion of the

shock front. For this purpose we shall consider the total energy balance for the propagated shock wave. We shall introduce the concept of average "braking" pressure p_b. Assuming that all the energy of the shock wave at any instant of time is potential energy (the air in the shock wave is "braked"), this pressure p_b can be determined from the relationship

$$E_s = \frac{p_b}{\gamma - 1} \frac{4}{3} \pi (r_2^3 - r_1^3), \tag{85.13}$$

where E_s is the energy of the shock wave, r_2 is the distance of its leading edge from the explosion centre, and r_1 is the distance from the explosion centre to the boundary of separation. Obviously, the energy of the shock wave is compounded from the energy transferred to it by the detonation products (E_{s1}) and the intrinsic initial energy of the air (E_{s2}). These energies are determined from the relationships

$$E_{s1} = E_i \left[1 - \left(\frac{p_b^*}{p_i} \right)^{\frac{\gamma - 1}{\gamma}} \right] = E_i \left[1 - \left(\frac{r_0}{r_1} \right)^{3(\gamma - 1)} \right], \tag{85.14}$$

where p_b^* is average pressure in the explosion products,

$$E_i = \frac{4}{3} \pi r_0^3 \rho_0 Q$$

where E_i is the energy of the explosive charge (Q is the specific energy of the explosive) ;

$$E_{s2} = \frac{4}{3} \pi (r_2^3 - r_0^3) \frac{p_a}{\gamma - 1}, \tag{85.15}$$

whence

$$E_s = \frac{p_b}{\gamma - 1} \frac{4}{3} \pi (r_2^3 - r_1^3) = E_i \left[1 - \left(\frac{r_0}{r_1} \right)^{3(\gamma - 1)} \right] + \frac{4}{3} \pi \frac{p_a}{\gamma - 1} (r_2^3 - r_0^3)$$

or

$$p_b - p_a = \frac{(\gamma - 1) E_i \left[1 - \left(\frac{r_0}{r_1} \right)^{3(\gamma - 1)} \right]}{\frac{4}{3} \pi (r_2^3 - r_1^3)} = (\gamma - 1) \rho_0 Q \frac{r_0^3}{r_2^3 - r_1^3} \left[1 - \left(\frac{r_0}{r_1} \right)^{3(\gamma - 1)} \right] + p_a \frac{r_1^3 - r_0^3}{r_2^3 - r_1^3}. \tag{85.16}$$

This relationship is valid until total expansion of the detonation products has taken place, i.e. up to $r_1 = \alpha r_0 = (10 - 12) r_0$. After this the energy of the shock wave will be determined approximately by the relationship

$$E_s = E (1 - \alpha^{-3(\gamma - 1)}) + \frac{4}{3} \pi (r_2^3 - r_1^3) \frac{p_a}{\gamma - 1}. \tag{85.17}$$

which follows from the condition that

$$\frac{p_{i\,lim}}{p_i} = \left(\frac{r_0}{\alpha r_0}\right)^{3(\gamma-1)} = \alpha^{-3(\gamma-1)}.$$

The explosion products will no longer give up energy, and the portion of the air behind the tail end of the shock front will be braked, possessing the initial energy density for $p = p_a$. From equations (85.13) and (85.17) we have

$$p_b - p_a = (\gamma - 1)\rho_0 Q \frac{r_0^3}{r_2^3 - r_1^3}\left[1 - \alpha^{-3(\gamma-1)}\right] \qquad (85.18)$$

for $r_1 \geq \alpha r_0 \approx 10 r_0$.

For future calculations it is now necessary for us to know the value of r_2 for $r_1 = \alpha r_0$; we shall assume meanwhile that $r_2 = \beta r_0$. We shall establish the relationship between the potential and kinetic energies in the shock wave.

Since the pressure in the explosion products falls more rapidly than in the shock wave, then the rarefaction wave which follows at the rear along with the shock wave compels it to assume such a shape that the pressure and velocity in the leading portion of the shock wave becomes greater than at the rear. Assuming to a first approximation that the pressure (and density) and velocity in the shock wave are determined linearly along the r - axis for any fixed instant of time, we find that

$$E_s \approx \frac{p_f}{2(\gamma+1)} \cdot \frac{4}{3}\pi(r_2^3 - r_1^3) + E_{s.k}, \qquad (85.19)$$

where $E_{s.k}$ is the kinetic energy in the shock wave; $\frac{p_f}{2}$ defines the average pressure (not the braking pressure) of the shock wave, p_{if} is the pressure at the shock front. Since

$$E_{s.k} = \frac{4\pi}{2}\int_{r_1}^{r_2} r^2 \rho u^2\, dr,$$

then the average value of ρu^2 is $\frac{p_i u_i^2}{4}$ (for a linear distribution of ρ and u with respect to r). Therefore

$$E_{s.k} = \frac{p_i u_i^2}{8}\frac{4}{3}\pi(r_2^3 - r_1^3).$$

Substituting the value found for $E_{s.k}$ in (85.19) and comparing the expression obtained with (85.15) we obtain

$$\frac{p_b}{\gamma-1}=\frac{p_i}{2(\gamma-1)}+\frac{\rho_i u_i^2}{8}, \tag{85.20}$$

where ρ_i and u_i are the density and velocity at the shock front. For a strong shock wave (up to $r_1 \approx 10r_0$) we shall have the following relationships :

$$p_i=\frac{2}{\gamma+1}\rho_a D_s^2, \quad \rho_i=\frac{\gamma+1}{\gamma-1}\rho_a, \quad u_i=\frac{2D_{sa}}{\gamma+1},$$

therefore

$$p_b=\frac{\rho_a D_s^2}{\gamma+1}+\frac{1}{2(\gamma+1)}\rho_a D_s^2=\frac{3}{2}\frac{\rho_a D_s^2}{\gamma+1}. \tag{85.21}$$

Since $D_s=\frac{dr_2}{dt}$, then from relationships (85.21) and (85.16), neglecting p_a in comparison with p_b, we obtain

$$p_b=\frac{3}{2}\frac{\rho_a}{\gamma+1}\left(\frac{dr_2}{dt}\right)^2=(\gamma-1)\rho_0 Q\frac{r_0^3}{r_2^3-r_1^3}\left(\frac{r_0}{r_1}\right)^{3(\gamma-1)}. \tag{85.22}$$

Knowing the law of motion of the tail edge of the shock front (the boundary of separation between the explosion products and the shock wave) and solving equation (85.22) for the condition that $r_2 = r_0$ for $t = 0$, the law of motion of its leading edge can be determined. Assuming, on the basis of (85.12) that

$$u_1=\frac{dr_1}{dt}=u_\infty\frac{r_0^2}{r_1^2},$$

we find that

$$r_1^3=r_0^3+3u_\infty t r_0^2. \tag{85.23}$$

On the basis of equation (85.22) it can be assumed for an approximate estimation that

$$\frac{dr_2}{dt}=\sqrt{\frac{(\gamma^3-1)\rho_0 Q}{3\rho_a}}\left(\frac{r_0}{r_2}\right)^{\frac{3}{2}},$$

whence we find that

$$r_2^{\frac{5}{2}}=r_0^{\frac{5}{2}}+\frac{5}{2}\sqrt{\frac{\gamma^3-1}{3\rho_a}\rho_0 Q}\,t r_0^{\frac{3}{2}}. \tag{85.24}$$

For $r_1 = 10r_0$ we have, on the basis of equation (85.23)

$$t\approx\frac{r_0}{u_\infty}\frac{10^3}{3}\ \text{sec},$$

or since

$$u_\infty = 4000 \text{ m/sec} = 4 \cdot 10^5 \text{ cm/sec},$$

then $t = \frac{r_0}{1200}$ sec, so that for a typical explosive ($Q = 1$ kcal/g and $\rho_0 = 1.6$ g/cm^3) we obtain $\frac{r_2 - r_1}{r_0} \approx 10$. Thus, we have arrived at the well-known experimental fact by very rough calculations that the length of the shock wave to the instant of cessation of motion of the explosion products, i.e. to the instant of its so-called breakaway from the explosion products, is approximately equal to $10r_0$. Actually, it is evident that this value may vary from $10r_0$ to $15r_0$.

By length of the shock wave we understand the quantity $\lambda = r_2 - r_1$. We shall now determine the pressure at the shock front at the instant of breakaway from the explosion products. For this purpose we shall write the relationship (85.22) in the form

$$p_b - p_a = \frac{3}{4}(p_i - p_a) = (\gamma - 1)\rho_0 Q \frac{r_0^3}{r_2^3 - r_1^3}\left[1 - \left(\frac{r_0}{r_1}\right)^{3(\gamma-1)}\right]. \qquad (85.25)$$

This relationship also defines the pressure at the shock front for $r_1 \leqslant 10r_0$, i.e. for $r_2 \leqslant 20r_0 - 25r_0$.

An approximate relationship between r_1 and r_2 can be found from (85.23) and (85.24) by eliminating t and neglecting the quantity r_0:

$$\left(\frac{r_1}{r_0}\right)^5 = \left(\frac{r_2}{r_0}\right)^{\frac{5}{2}} \cdot \frac{6}{5} \frac{u_\infty}{\sqrt{\frac{2}{3}(\gamma^2 - 1)\frac{p_a}{\rho_0} Q}} \approx \left(\frac{r_2}{r_0}\right)^{\frac{5}{2}} \frac{u_\infty}{c_i} \cdot \frac{3}{25}$$

or

$$\frac{r_2}{r_0} = \left(\frac{r_1}{r_0}\right)^{\frac{6}{5}} \cdot 8^{\frac{2}{5}} \cdot \left(\frac{c_i}{c_\infty}\right)^{\frac{2}{5}} \approx 2 \cdot 3\left(\frac{r_1}{r_0}\right)^{\frac{6}{5}}.$$

For $r_1 = 10r_0$, $r_2 = 20r_0$, we determine from (85.24) that $p_i - p_a \approx 4$ kg/cm^2. This means that at these distances the wave is already weak. For the assumption made above, the rate of fall of pressure should be

retarded. This in fact actually occurs.

The velocity of motion of the tail end of the shock front becomes approximately equal to the velocity of sound c_a, and the velocity of the leading edge of the shock front is equal to $c_a + \frac{\text{const}}{r_2}$, therefore the length of the shock wave as a result of its further motion is changed only slightly and proportional to $\ln \frac{r_2}{r_0}$.

The relationship for determining p_b thus assumes the form

$$p_b - p_a \approx \frac{\gamma-1}{3} \rho_0 Q \frac{r_0^3}{\alpha r_2^3}, \tag{85.26}$$

since

$$r_2^3 - r_1^3 = (r_1 + \alpha r_0)^3 - r_1^3 \approx 3\alpha r_0 r_1^2,$$

where $\alpha = 10 - 15$. Later the relationship between p_b and p_a is altered. Actually, since

$$p_b - p_a = \frac{p_i - p_a}{2} + \frac{\gamma-1}{8} \rho_i u_i^2,$$

then approximately $p_b - p_a \approx \frac{p_i - p_a}{2}$,

$$\Delta p_i = p_i - p_a = \frac{2}{3} \frac{\gamma-1}{\alpha} \rho_0 Q \frac{r_0^3 \eta}{r_2^3}, \tag{85.27}$$

where $\eta = 1 - \alpha^{-3(\gamma-1)}$. If at the start of motion for a strong wave

$$p_i \sim \frac{r_0^3}{r_2^3} \sim \frac{M}{r^3}, \tag{85.28}$$

where M is the mass of the explosive charge, then we now have

$$\Delta p_i \sim \frac{r_0^3}{r_2^3} \sim \frac{M^{\frac{2}{3}}}{r_2^2}. \tag{85.29}$$

Relationship (85.27) shows that the rate of fall of pressure is actually retarded for $r_2 > 20 r_0$.

Let us express the pressure in terms of the shock wave velocity. Since

$$p_i - p_a = \frac{2\rho_a}{\gamma+1}(D_s^2 - c_a^2),$$

then

$$D_s^2 = c_a^2 + \frac{\gamma^2-1}{3a}\frac{\rho_0}{\rho_a} Q \frac{r_0^2}{r_2^2}\eta. \tag{85.50}$$

According as how the spherical shock wave is propagated, a rarefaction originates behind the wave, and the pressure becomes less than atmospheric; the pressure variations in the wave are observed to be of the type of pressure variations in a normal sound wave.

Consequently, within the limit (at a distance of about 30 - 40r_0 approximately) the average energy density in the shock wave will be determined, as before, by the relationship

$$\varepsilon_s = \frac{1}{3a}\rho_0 Q \frac{r_0^2}{r_2^2}\eta.$$

The expression for this energy in terms of Δp_i is modified and takes the form

$$\varepsilon_s = \frac{(\Delta p_i)^2}{\rho_a c_a^2}. \tag{85.51}$$

In the limit

$$\Delta p_i = \sqrt{\frac{\rho_0 \rho_a Q^2}{3a}\eta}\,\frac{r_0}{r_2}, \tag{85.52}$$

that is ,

$$\Delta p \sim \frac{r_0}{r_2} \sim \frac{M^{\frac{1}{3}}}{r_2}, \tag{85.53}$$

The development here of the general considerations may be made considerably more precise, but we have limited ourselves here only to the basic physical picture of shock wave propagation. Below we shall examine the question of the impulses acting as a result of a spherical explosion, and we shall see that this problem is solved quite accurately on the basis of the elementary relationships.

In accordance with the theory of detonation, for an impulse flux

passing through unit area at a distance equal to the radius of the charge is

$$i = \frac{16}{27}\frac{\sqrt{ME}}{4\pi r_0^2}, \qquad (85.34)$$

where $E = MQ$ is the total explosion energy.

It is well-known from mechanics that for a given energy, the momentum or impulse flux increases proportionally with the square root of the mass set into motion. Consequently, the flux of an impulse passing through unit area at a distance r from the charge, since air is set into motion, is determined by the relationship

$$i = \frac{16}{27}\frac{\sqrt{E(M+M_a)}}{4\pi r^2}, \qquad (85.35)$$

where M_a is the mass of air set into motion.

Since $E = MQ = \frac{MD^2}{16}$, where D is the detonation velocity, then

$$i = \frac{MD}{27\pi r^2}\sqrt{1+\frac{M_a}{M}}. \qquad (85.36)$$

For this it is assumed that the available (free) energy is conserved, since on the average the loss of free energy by the irreversible process of shock front formation are almost exactly compensated by the intrinsic energy of the air set into motion by the shock wave.

Since at distances of $r \leqslant 10 - 15r_0$

$$M_a = \frac{4}{3}\pi\rho_a(r^3 - r_0^3), \quad M = \frac{4}{3}\pi\rho_0 r_0^3,$$

then

$$1+\frac{M_a}{M} = 1+\frac{\rho_a}{\rho_0}\left(\frac{r^3}{r_0^3}-1\right) \approx 1+\frac{\rho_a}{\rho_0}\frac{r^3}{r_0^3};$$

and here the quantity $\frac{\rho_a}{\rho_0}$ can always be neglected as small compared with unity $\left(\frac{\rho_a}{\rho_0} = \frac{1}{1250}\right)$. Therefore at these distances

$$i = \frac{MD}{27\pi r^2}\sqrt{1+\frac{\rho_a}{\rho_0}\frac{r^3}{r_0^3}}. \qquad (85.37)$$

At distances greater than $10 - 15r_0 = \alpha r_0$, the shock wave, as we have already

shown "breaks away" from the explosion products (strictly speaking the explosion products break away from the shock wave) ; as a result of this

$$M_a = \frac{4}{3}\pi\rho_a\left[r^3 - (r - \alpha r_0^3)\right] \approx 4\pi\rho_a \alpha r_0 r^2 = 4\pi\rho_a \alpha r_0^3 \left(\frac{r}{r_0}\right)^2.$$

Therefore

$$1 + \frac{M_a}{M} = 1 + \frac{3\alpha\rho_a}{\rho_0}\left(\frac{r}{r_0}\right)^3,$$

and relationship (85.36) takes the form

$$t = \frac{MD}{27\pi r^2}\sqrt{1 + \frac{3\alpha\rho_a}{\rho_0}\left(\frac{r}{r_0}\right)^3}. \qquad (85.38)$$

Within the limit, for large values of $\frac{r}{r_0} \geqslant 40 - 50$, we obtain

$$t = \frac{MD}{27\pi r^2}\sqrt{3\alpha\frac{\rho_a}{\rho_0}\left(\frac{r}{r_0}\right)^3} = \frac{MD}{27\pi r r_0}\sqrt{3\alpha\frac{\rho_a}{\rho_0}}. \qquad (85.39)$$

Assuming that for typical explosives $D = 7200$ m/sec, $\rho_0 = 1.6$ g/cm^3, $\alpha = 12$, then

$$\frac{\rho_a}{\rho_0} = \frac{1}{1250} : 3\alpha\frac{\rho_a}{\rho_0} = \frac{3}{100}$$

and relationships (85.37), (85.38) and (85.39) in the C.G.S. system assume the form

$$\left.\begin{aligned} t &= 0.85\cdot 10^4\sqrt{1 + \frac{1}{1200}\frac{r^3}{r_0^3}}\,\frac{M}{r^2}, \\ t &= 0.85\cdot 10^4\frac{M}{r^2}\sqrt{1 + \frac{3}{100}\frac{r^2}{r_0^2}}, \\ t &= 1.5\cdot 10^3\frac{M}{r_0 r} = 2.7\cdot 10^3\frac{M^{\frac{2}{3}}}{r}. \end{aligned}\right\} \qquad (85.40)$$

In the M.K.S. system we shall have

$$\left.\begin{aligned} t &= 8.5\frac{M}{r^2}\sqrt{1 + \frac{1}{1200}\frac{r^3}{r_0^3}}, \\ t &= 8.5\frac{M}{r^2}\sqrt{1 + \frac{3}{100}\frac{r^2}{r_0^2}} = 27\frac{M^{\frac{2}{3}}}{r}\sqrt{1 + \frac{100 r_0^3}{3r^3}}, \\ t &= 1.5\frac{M}{r_0 r} = 27\frac{M^{\frac{2}{3}}}{r}. \end{aligned}\right\} \qquad (85,41)$$

As a result of reflection of the shock wave and of the explosion products from any obstacle, the pressures and impulses increase. In this case, the values for the impulses and average pressures should be multiplied by the quantity c_m, where for a very extensive obstacle $c_m = 2$.

We shall now derive the basic laws of propagation of cylindrical waves.

"In the vicinity" of the charge, up to $r \approx (30 - 50)r_0$

$$p \sim \frac{MQ}{lr^2}, \quad i = \frac{2MD}{27rl\pi}\sqrt{1+\frac{\rho_a r^2}{\rho_0 r_0^2}}, \tag{85.42}$$

where l is the length of the cylinder on which the mass of the explosive M fits.

At distances lying within the interval $(50 - 150)r_0$

$$p \sim \frac{MQ}{lrr_0}\frac{M^{\frac{2}{3}}Q}{lr_0},$$
$$i = \frac{2MD}{27lr\pi}\sqrt{1+2\frac{\rho_a}{\rho_0}\alpha\frac{r}{r_0}}, \tag{85.43}$$

where $\alpha \approx 50$.

At distances of around $200r_0$ and greater

$$p \sim \frac{M^{\frac{1}{3}}\sqrt{Q}}{\sqrt{lr}},$$
$$i = \frac{2}{27\pi}\frac{M^{\frac{5}{6}}D}{l\sqrt{r}}\sqrt{2\frac{\rho_a}{\rho_0}\alpha}. \tag{85.44}$$

Finally, we note that the relationships determining the impulses are verified experimentally, not only with respect to order of magnitude, but also in numerical coefficients with an accuracy of about 5 - 10%.

We note also that on the basis of comparison of the pressures and impulses, since $I \sim \bar{p}\tau$ (τ is the time over which the shock wave acts) for a spherical wave for $r < 50r_0$ $\tau \sim \frac{r}{\sqrt{Q}}$ and for $r > 50r_0$ $\tau \sim \frac{r_0}{c_a}$; for a cylindrical wave with $r < 100r_0$, $\tau \sim \frac{r}{\sqrt{Q}}$, and with $r > 100r_0$ $\tau \sim \frac{r_0}{c_a}$.

At present, no accurate theory of spherical and cylindrical explosions exists, although the construction of a similar theory is possible thanks to the development of gas-dynamic methods.

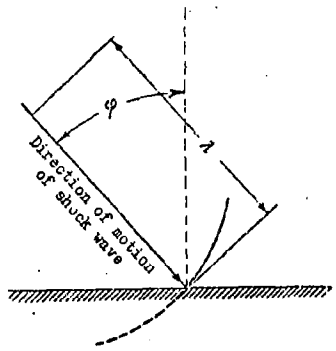
Concerning the Relationship between the Impulses for transmitted and incident shock waves.

The relationships obtained for the impulses resulting from an explosion are related to the case when the shock wave is reflected normally from an obstacle. However, under actual conditions of the effect of an explosion, the shock wave may fall on an obstacle, in particular on a measuring instrument (impulsometer), through various angles. Obviously, the impulse felt by the obstacle may, depending on the angle of impact of the shock wave, be considerably different from the impulse resulting from normal reflection of a wave from the obstacle.

A knowledge of the relationship between the discernable impulse and the angle of impact of the shock wave is important for an accurate estimation of the efficiency of action of an explosion on the basis of what has been shown, with various positions of the measuring instruments with respect to the shock front.

It is very difficult to carry out an accurate measurement of the impulse of a shock wave moving towards an obstacle at an angle φ (the angle between the normal to the obstacle and the direction of propagation of the shock wave (Fig. 221).

Figure 221. Approach of a shock wave to an obstacle, at an angle.



An account is given below of a method for solving approximately the problem, as proposed by BAUM and STANYUKOVICH. We shall introduce the following symbols :

i_N is the specific impulse for the normally reflected shock wave from the obstacle $(\varphi = 0)$.

i_τ is the specific impulse for the transmitted shock wave (glancing parallel with the obstacle) $\left(\varphi = \frac{\pi}{2}\right)$.

i_φ is the specific impulse for the shock wave moving towards the obstacle at an angle φ.

In determining i_φ we shall assume approximately that the total impulse of the shock wave is compounded from the impulse i_1 of the static pressure and the impulse i_2 of the mass of air flow ρu, moving with a velocity u.

It is essential to bear in mind that

$$i_1 = i_\tau \sin\varphi \qquad (35.45)$$

and

$$i_2 = i_N \cos^2\varphi. \qquad (35.46)$$

Relationships (35.45) and (35.46) are obtained from the following

considerations. It is obvious that

$$i_\tau = \int_0^\tau \Delta p \, dt,$$

so that the time of action of the shock wave as a result of its front moving parallel with the obstacle should be proportional to the length of the shock wave λ, and in the case of its approaching the obstacle at an angle φ it is proportional to the projection of φ on the horizontal axis, i.e. it is proportional to $\sin \varphi$ (see Fig. 221). By the length of the shock wave, we understand here the distance from the shock front to the rear limit (i.e. to the place where the pressure in the wave becomes equal to atmospheric).

Since the normal projection of the velocity u is proportional to $\cos \varphi$ and the mass flow, acting on unit area of the obstacle, is also proportional to $\cos \varphi$, then the normal component of the impulse if proportional to $\cos^2 \varphi$, which leads to relationship (85.46).

We arrive finally at the relationship

$$i_\varphi = i_1 + i_2 = i_N (\cos^2 \varphi + \beta \sin \varphi), \qquad (85.47)$$

where $\beta = \frac{i_\tau}{i_N}$.

The quantity β can be represented in the form

$$\beta = \frac{\int_0^\tau \Delta p \, dt}{2 \int_0^\tau \rho u^2 \, dt}.$$

The introduction of the factor 2 into the denominator takes into account that for a normal reflection of the flow from the obstacle, the momentum is doubled.

Since

$$\int_0^\tau \Delta p \, dt = \overline{\Delta p}\, \tau, \quad \int_0^\tau \rho u^2 \, dt = \overline{\rho u^2} \tau,$$

where $\overline{\Delta p}$ and $\overline{\rho u^2}$ are the average values of Δp and ρu^2 at an interval of the length of the shock wave, then

$$\beta = \frac{\overline{\Delta p}}{2 \overline{\rho u^2}}.$$

We shall assume that the velocity depends approximately linearly upon the

distance, i.e. that $u = rf_1(t)$.

As a result of this the following relationships will be valid

$$\rho = r^{\alpha} f_2(t), \quad p = r^{\alpha+2} f_3(t),$$
$$\overline{p} = \frac{p_1}{\alpha+3}, \quad \overline{\rho u^2} = \frac{\rho_1 u_1^2}{\alpha+3},$$

where p_1, ρ_1, u_1 are the values of p, ρ, and u at the shock front. Hence it follows that

$$\beta = \frac{p_1 - (\alpha+3)p_a}{2\rho_1 u_1^2}.$$

Assuming that $p_1 - (\alpha+3)p_a = \Delta p_1$ we obtain

$$\beta = \frac{\Delta p_1}{2\rho_1 u_1^2}.$$

The relationships for the shock front give

$$\beta = \frac{1}{2}\left[\frac{k-1}{2} + \frac{kp_a}{\Delta p_1}\right] = \frac{1}{2}\left[\frac{k+1}{2\left(1 - \frac{c_a^2}{D_*^2}\right)} - 1\right]. \qquad (85.48)$$

For a strong wave $\beta = \frac{k-1}{4}$, , which gives $\beta = \frac{1}{10}$ for $k = \frac{7}{5}$. But if it be taken into account that for strong shock waves, as a consequence of the development of dissociation and ionisation processes, $\frac{\rho_1}{\rho_a} = \frac{k+1}{k-1} \approx 9$, , then we obtain $k = \frac{5}{4}$ and $\beta = \frac{1}{16}$.

Relationship (85.48) holds good up to a pressure of $\Delta p_1 \geqslant p_a$, for smaller pressures it is essential to take into account the region behind the shock wave, where $\Delta p < p_a$. For $\frac{\Delta p_1}{p_a} = 1$ we have $\beta = \frac{3k-1}{4}$, which gives $\beta = \frac{4}{5}$. for $k = \frac{5}{7}$. For $\frac{\Delta p_1}{p_a} \ll 1$ the wave form is approximately sinusoidal. As a result of this $\int_0^\infty \Delta p\, dt \to 0$, and $\int_0^\infty \rho u^2 dt > 0$, since in the region of $\Delta p > 0$ $(\rho u^2)_+ = (\rho + \Delta\rho)u^2$, and in the region of $\Delta p < 0$, $(\rho u^2)_- = (\rho - \Delta\rho)u^2$ and

$$(\rho u^2)_+ - (\rho u)_-^2 = 2\Delta\rho u^2 > 0.$$

As a result of this $\beta \to 0$.

Thus, with reduction of pressure at the shock front, the value of increases initially and then it falls again for $\frac{\Delta p_1}{p_a} \ll 1$

We note that, depending upon the form of distribution of the parameters

behind the shock front, the value of β may vary.

We can write, that for any given distribution of p, ρ, and u

$$\beta = \theta \frac{\Delta p_1}{2\rho_1 u_1^2}, \qquad (35.49)$$

where θ depends on the form of the distribution.

For a similarity solution wave, for example, $\theta \approx 2$. If for a wave which is not very strong Δp and u depend linearly on r., and $\rho \approx \rho_0 = \text{const}$, then $\theta = \frac{3}{2}$ etc. For any distribution of the parameters behind the shock front, a value of β, can always be found for every real case, and which is a solution to the problem set.

The magnitude of the impulse, determined by formula (35.47), has a weakly expressed maximum. Actually, assuming that

$$\frac{dI_\varphi}{d\varphi} = \beta \cos\varphi - 2\cos\varphi \sin\varphi = 0$$

we find that the angle $\varphi = \varphi_0 = \arcsin\frac{\beta}{2}$.

§ 86. Effect of Intrinsic Velocity of Forward Motion of the Charge on the Explosion Efficiency

Modern military technology is associated as a rule with the use of moving explosive sources, which possess in many cases a large intrinsic forward velocity (around 3000 m/sec and more) , commensurate with the average velocity of dispersion of the detonation products.

At these velocities the energy of the moving explosive source increases considerably(by a factor of two or more) relative to its static energy, which in its turn leads to a more or less considerable change of the explosion field.

The law of propagation of an explosion as a result of the detonation of a moving explosive charge has been studied by POKROVSKII and independently also by BAUM and STANYUKOVICH

The principal results of the investigation are presented below. It is

obvious that if the explosive source is moving, then even for instantaneous detonation of the charge, the explosion field will not be one-dimensional; the parameters of the explosion will be changed, dependent on the angle φ between the specified direction and the velocity vector of motion of the charge. The maximum explosion effect will be in the direction of motion of the explosion source. All the relationships presented below are given for this case.

We shall consider first of all the effect of explosion of a spherical charge in a vacuum.

The basic formulae defining the ratio of the fluxes (falling on unit area) of the mass, impulse and energy of the moving explosion source $(m,\ i,\ \varepsilon)$ to these same parameters for a stationary explosion source $(m_0,\ i_0,\ \varepsilon_0)$ have the form

$$\left.\begin{aligned}\frac{m}{m_0}&=1+\frac{u_0}{c_i},\\ \frac{i}{i_0}&=\left(1+\frac{u_0}{c_i}\right)^2,\\ \frac{\varepsilon}{\varepsilon_0}&=\left(1+\frac{u_0}{c_i}\right)^3,\end{aligned}\right\} \tag{86.1}$$

where u_0 is the intrinsic velocity of motion of the charge, c_i is the average deduced velocity of sound in the detonation products ($c_i \approx 0.46D$, where D is the detonation velocity).

The values of $\frac{m}{m_0}$, $\frac{i}{i_0}$ and $\frac{\varepsilon}{\varepsilon_0}$ are given in Table 120 for different values of $\frac{u_0}{c_i}$.

Table 120

Ratio of fluxes of mass, momentum and energy of a moving explosion source to the same parameters for the case of a stationary explosion source.

$\frac{u_0}{c_1}$	0	1/3	2/3	1	4/3
$\frac{m}{m_0}$	1	4/3	5/3	2	7/3
$\frac{I}{I_0}$	1	16/9	25/9	4	49/9
$\frac{\varepsilon}{\varepsilon_0}$	1	64/27	125/7	8	343/27

For explosives of the hexogen type (D = 8000 m/sec, c_1 = 3700 m/sec) for u_0 = 5000 m/sec, $\frac{m}{m_0}$ = 2.33, $\frac{I}{I_0}$ = 5.5, $\frac{\varepsilon}{\varepsilon_0}$ = 12.7. For u_0 = 3000 m/sec $\frac{m}{m_0}$ = 1.8; $\frac{I}{I_0}$ = 3.2, $\frac{\varepsilon}{\varepsilon_0}$ = 6.0.

We shall show that for a cylindrical charge, the maximum value of the local effect of the explosion is found to be weaker than for a spherical charge.

As a result of an explosion in air, the initial pressure at the front of the shock wave created, for a moving charge, relative to the pressure for a stationary explosion source is determined by the relationship

$$\frac{p_x}{p_{x_0}} = \left(1 + \frac{u_0}{D_*}\right)^2, \qquad (86.2)$$

where p_x is the initial pressure of the shock wave in air for the moving explosion source, p_{x_0} is the initial pressure of the shock wave in air for a stationary explosion source.

$$p_{x_0} = \frac{\gamma+1}{2}\rho_a D_*^2,$$

where ρ_a is the density of the ambient air. Taking $\rho_a = \frac{1}{770}$ g/cm^3, D_* = 7200 m/sec, $\gamma = \frac{5}{4}$, p_{x_0} = 800 kg/cm^2 for u_0 = 3000 m/sec, we obtain

$$\frac{p_x}{p_{x_0}} \approx 2.0,$$

i.e. the initial pressure of the shock wave is increased approximately by a

factor of two.

We shall denote the initial velocity of the air behind the shock front from a stationary explosion by u_{∞_0} and for a moving charge by u_∞. The ratio of these velocities is defined by the formula

$$\frac{u_\infty}{u_{\infty_0}} = \sqrt{1 + \left(\frac{u_0}{D}\right)^2}. \qquad (86.3)$$

For u_0 = 3000 m/sec and D = 7200 m/sec, $\frac{u_\infty}{u_{\infty_0}} = 1.42$.

The air retards the flow of the detonation products. It can be shown from the Law of Conservation of Momentum that the velocity of motion of the centre of gravity of the explosion products relative to distance will vary according to the law

$$\frac{u_r}{u_0} = \frac{1}{1 + \frac{\rho_{ar}}{\rho_0}\left(\frac{r}{r_0}\right)^3}, \qquad (86.4)$$

where ρ_0 is the initial density of the explosive, ρ_{ar} is the density of the air behind the shock front at a distance r from the centre of the explosion, u_r is the velocity of motion of the centre of gravity of the explosion products for the moving charge at a distance r, and u_0 is the initial velocity of motion of the charge.

For $r \approx 10 r_0$ $\left(\frac{r}{r_0}\right)^3 \frac{\rho_{ar}}{\rho_0} \approx 1.$

For $r \approx 50 r_0$ $\left(\frac{r}{r_0}\right)^3 \frac{\rho_{ar}}{\rho_0} \approx 50.$

At greater distances we obtain the formula

$$\frac{u_r}{u_0} = \frac{\rho_0}{\rho_a}\left(\frac{r_0}{r}\right)^3. \qquad (86.5)$$

For

$$r = 20 r_0 \quad \frac{u_r}{u_0} \approx \frac{1}{20},$$

i.e. the intrinsic velocity of motion under real conditions becomes equal to several hundreds of metres per second.

The ratio of the energy of the air in the shock wave to the total

explosion energy for the moving charge is determined by the expression

$$\frac{E_a}{E_l} = \frac{c_a^2}{Q + \frac{u_0^2}{2}} \frac{1}{\gamma - 1} \frac{\rho_a}{\rho_0} \left(\frac{r}{r_0}\right)^3, \qquad (86.6)$$

where c_a is the velocity of sound ahead of the shock front, Q is the potential energy of the explosive, E_a is the energy of the air in the shock wave, E_l is the total explosion energy. For $\frac{u_0^2}{2} = Q = 427 \cdot 10^8$ reg/g, $\gamma = \frac{7}{5}$, $c_a = 330$ m/sec and $r = 40 r_0$

$$\frac{E_a}{E_l} \approx 1.3.$$

Thus, it can be assumed that the equalising process of the energy of the air is mainly completed for $r > 40 r_0$, and we arrive at a practically uniform distribution of parameters in the shock wave relative to the centre of mass. Consequently, at large distances from the point of explosion (around 40 – 50 r_0 and more), in order to determine the shock wave parameters we can use the limiting formulae

$$i \sim \frac{m^{\frac{2}{3}} \sqrt{E_l}}{r}, \quad p_{lim} \sim \frac{m^{\frac{1}{3}} E_l^{\frac{1}{2}}}{r}.$$

Comparing these expressions with the corresponding expressions for a stationary explosion, we can write

$$\left.\begin{aligned} \frac{i_{lim}}{i_{st}} &= \sqrt{1 + \frac{u_0^2}{2Q}}, \\ \frac{p_{lim}}{p_{st}} &= \sqrt{1 + \frac{u_0^2}{2Q}}. \end{aligned}\right\} \qquad (86.7)$$

For $\frac{u_0^2}{2} = Q$ ($u_0 = 3000$ m/sec) $\frac{i_{lim}}{i_{st}} = 1.4$ and $\frac{p_{lim}}{p_{st}} = 1.4$.

Since the dependence of i and p on energy is the same, then the radii of the destructive effects, estimated either with respect to impulse or pressure, will increase proportionally with the quantity $\sqrt{1 + \frac{u_0^2}{2Q}}$, and the area will increase proportionally with the quantity $1 + \frac{u_0^2}{2Q}$, which, for $u_0 = 3000$ m/sec gives a two-fold increase in area and for

u_0 = 5000 m/sec the increase in area is practically four-fold. This will occur at relatively large distances, when all the energy is more or less uniformly distributed throughout the entire volume occupied by the shock wave.

The following conclusions can be drawn from an analysis of the relationships we have presented.

In the case the explosion of a spherical charge at high initial velocities ($u \approx 3000$ m/sec), the maximum increase of explosion effect in the immediate vicinity of the charge exceeds by 5 - 10 times the effect of a stationary charge. However, the effect of the explosion, as a result of this, (in the case of a low altitude explosion) will be, for the most part, of a local nature (formation of a crater in the ground, etc). For a cylindrical charge, the maximum increase of the local effects of the explosion is found to be weaker than for a spherical charge.

At distances greater than 40 r_0 the excess impulse and pressure for a moving explosion source will be less significant (for u_0 = 3000 m/sec it is about 25 - 40% , which corresponds to an increase in the area of effect by a factor of 1.5 - 2).

§ 87. Some Results of Experimental Investigation of the Destructive Effects of an Explosion.

The destructive effect of an explosion, determined by the total work of the explosion products, is manifested in a different manner and at different distances from the source of the explosion depending upon the properties of the explosive, the charge weight and the nature of the medium in which the explosion takes place.

The work capability(efficiency) of an explosive, and the destructive

effect of the explosion associated with it for approximately the same conditions are increased with increase of the potential energy of the explosive and with increase of the specific volume of the gaseous explosion products.

For given properties of the explosive and the charge weight, the range of efficiency of action of the explosion also depends to a well-known extent on the geometrical shape of the charge and on the method of its initiation.

The work done by the explosion products can easily be determined theoretically from the assumption concerning the isentropic law for their expansion. In this case we can write

$$dA = -dE = -c_v\,dT, \tag{87.1}$$

whence, bearing in mind that

$$c_v = \frac{nR}{k-1},$$

we obtain

$$A = \frac{nRT_1}{k-1}\left(1-\frac{T_1}{T_1}\right).$$

Relating the work A to 1 kg of explosive and assuming that $pv^k = \text{const}$, $Tv^{k-1} = \text{const}$ and $T^k p^{1-k} = \text{const}$, we finally have

$$A = \frac{F}{k-1}\left(1-\frac{T_1}{T_1}\right) = \frac{p}{k-1}\left[1-\left(\frac{v_1}{v_1}\right)^{k-1}\right] =$$

$$= \frac{F}{k-1}\left[1-\left(\frac{p_1}{p_1}\right)^{\frac{k-1}{k}}\right], \tag{87.2}$$

where T_1, v_1, and p_1 are respectively the temperature, specific volume and pressure of the gaseous products at the instant of explosion, and T_1, v_1, and p_1 are the values of the same parameters during the process of expansion of the explosion products.

The quantity $F = nRT_1$ is the so-called "power" of the explosive, where n is the number of moles of gaseous explosion products formed as a result of the explosion of 1 kg of explosive.

It is obvious that the quantity F has the dimensions of energy.

Actually,

$$R = \frac{p_0 v_0}{273},$$

where p_0 is the atmospheric pressure, v_0 is the specific volume of one mole of gas at NTP. If p_0 is expressed in atmospheres and v_0 in litres, then F will be expressed in $\frac{\text{l.atm}}{\text{kg}}$.

For unrestricted expansion of the explosion products in the atmosphere

$$p_1 = p_0, \quad T_1 = T_0, \quad v_1 = v_0$$

and

$$A = A_{max} = lQ_v, \tag{87.3}$$

where l is the mechanical equivalent of heat.

The quantity $A_{max} = lQ_v$ is the potential energy of the explosive; it is usually taken to be a measure of the efficiency of an explosive.

Relationship (87.3) is obtained on the assumption that the explosion products consist entirely of gases. If, however, there are also solid and liquid substances in addition to the gases, then $A_{max} < lQ_v$. In this case, in order to determine theoretically the value of A_{max}, the heat exchange between the gaseous and condensed explosion products during the process of their dispersion must be particularly taken into account, since their rate of cooling differs significantly. Such a calculation presents considerable difficulties.

For an explosion in a closed volume (for example in a steel or lead bomb) or in dense medium (e.g. water, earth), the exchange of heat between the explosion products may be quite complete. In the latter case, the velocity of motion of the boundary of separation between the explosion products and the medium is relatively small, which ensures adequate duration of contact and interaction between the gaseous and condensed explosion products and a more complete conversion of the potential energy of the explosive into mechanical work of the explosion.

As a result of the explosion in air of explosive charges, breakaway of the shock wave from the front of the detonation products may, in a number of cases, occur earlier than the exchange of heat between the condensed and gaseous particulates is completes, which will have as its consequence an inadequately complete conversion of the explosion energy into a shock wave. However, the possibility must not be excluded as a result of this, of partial oxidation of solid combustible particles because of the oxygen in the air (for example, solid carbon formed by the explosion of trotyl).

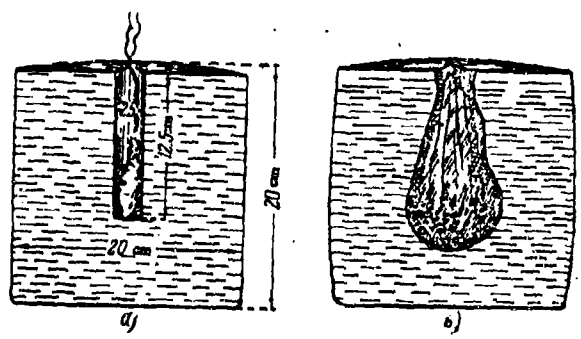
If the explosive is represented by a heterogeneous system (oxyliquite, a mixture of explosive with powdered metals etc.), then the explosive effect may be noticeably reduced depending on the conditions of the experiment and on the relationship between the sizes of the solid particles comprising the explosive system and the diameter of the charge itself.

It is well-known that the time of occurrence and the zone width of the chemical reaction at the front of a detonation wave increases according to the extent of reduction of the degree of dispersivity of these particles. Consequently, as a result of the presence of sufficiently coarse particles of an explosive system and the accomplishment of the explosion in air, the chemical reaction, because of the rapid dispersion of the reacting substances, is unable to be totally completed within the zone of effective action of the explosion products. This, as experiment shows, leads to an inadequately complete utilisation of the energy of the explosive system. If, however, the diameter of the charge is increases, then the extent of completion of the reaction increases and for a definite ratio of $\frac{d_{charge}}{d_{part.}}$ (where d_{charge} is the diameter of the charge and $d_{part.}$ is the mean diameter of the particles) a sufficiently complete conversion of energy of chemical reaction into an explosion wave (up to 70%) may be achieved in principle. This is confirmed by results of experiment.

By exploding similar heterogeneous explosives systems in a closed volume (lead bomb) or in dense media (water, earth), a fully completed reaction and efficient utilization of the explosive energy is achieved, just as one would expect, even under conditions for which quite small charges are used.

The energy losses may be dependent not only on an incomplete reaction between the components of the explosive system, but also on the partial scattering and incompleteness of reaction particularly of the surface layers of the explosive charge, which also appears as a shock wave of weakened intensity. A similar phenomenon is observed in using non-homogeneous as well as homogeneous explosives.

Figure 222. Lead Bomb.



It follows from Khariton's principle that the energy losses increase for approximately equal conditions with increase of the limiting diameter of the charge.

According to data by SADOVSKII, for charges of ammatol 40/60 with a weight of 25 kg. the losses may attain 38%, but for a weight of 500 kg. the losses are 13%. For charges of TNA, the limiting diameter of which is small, the energy losses are very insignificant. With increase of charge weight the

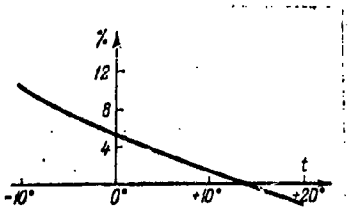
the energy losses are reduced. The charge casing also exerts a similar influence. However, in the latter case the conversion of energy into the shock wave is also reduced, since part of the potential energy of the explosive charge is converted into kinetic energy of the fragments. For small filling coefficients the fragments receive up to 75% of the explosion energy.

In order to evaluate practically the efficiency of an explosive under laboratory conditions, the so-called lead bomb expansion test is usually used. It consists in the following. A 10 gm batch of explosive is detonated by means of a detonator cap in a cylindrical channel in a massive lead block (Fig. 222a), made of pure lead. As a result of the explosion, the channel of the bomb is dilated (Fig. 222b) and the increase of its volume serves as a characteristic of the efficiency of the explosive.

The diameter and height of the bomb are 20 cms; the diameter of the bomb channel is 2.5 cm, with a depth of 12.5 cm, and has a volume of 61 - 62 cm^3. The bomb weighs about 70 kg.

In order to analyse the results of experiments one must take into consideration 1) the deviation of the bomb temperature from 15°C , for which a diagram can be used to determine this correction (Fig. 225) ;

Figure 325 Temperature correction (per cent) for lead bombs.



2) the capsule effect ; i.e. dilation of the bomb channel due to the explosion of the detonator cap itself ; 3) absence of strict proportionality between the efficiency of the explosive and the dilation of the bomb channel, as a

consequence of the reduction of the thickness and resistance of the walls of the bomb, due to the large dilation.

The results of this experiment for various high explosives are presented in Table 121.

Table 121

Lead Bomb channel dilation test.

Name of explosive	Dilation of lead bomb, ml.
Trotyl (TNT)	285
Picric acid	350
Tetryl	340
Hexogen	480
TEN (Tetra-erythritol nitrate)	500
Ammatol 80/20	360
Dynamite 83%	520

Another method which enables the efficiency of an explosive to be determined is the method of testing by means of a ballistic pendulum-mortar. (Fig. 224). This pendulum consists of a freely suspended mortar inside which is placed a charge (about 10 g.) of the test explosive. The explosion chamber is closed by a projectile B. As a result of the explosion the missile is ejected and the pendulum is deflected backwards by the powerful recoil. The angle of deflection of the pendulum serves as a measure of the efficiency of the explosive.

Actually, the total work done by the explosion products is

$$A = A_1 + A_2,$$

where A_1 is the work expended in raising the pendulum by a height h, corresponding to an angle of deflection of α. A_2 is the work expended on imparting a velocity v to the projectile.

Obviously,

$$A_1 = Qh = Ql(1 - \cos\alpha), \quad A_2 = \frac{qv^2}{2g},$$

where Q and q are the weights of the pendulum and projectile respectively, l is the length of the pendulum (from the axis of the pivot to the centre of gravity).

The value of v can be easily calculated from the equilibrium conditions for the momenta of the pendulum and of the projectile, i.e.

$$Qu = qv.$$

The velocity of swing of the pendulum, u, is determined by the relationship

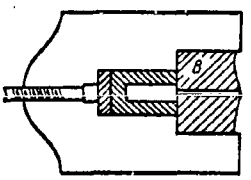
$$Ql(1 - \cos\alpha) = \frac{Qu^2}{2g}.$$

Thus, the efficiency of the explosive is determined by the relationship

$$A = Ql(1 - \cos\alpha)\left(1 + \frac{Q}{q}\right)\frac{1000}{a} \quad \text{kgm/kg.} \qquad (87.4)$$

where a is the weight of the explosive expressed in grams.

Figure 224 Ballistic pendulum mortar.



The experimental results show that the efficiency of an explosive, and consequently the destructive effect of the explosion, is practically independent of the density of the explosive charge, which is in accordance with theory.

Effect of the Explosion Products and of the Shock Wave. As a consequence of the high detonation pressure attained for modern explosives of around $2 - 2.5 \times 10^5$ kg/cm^2, the explosion is always accompanied by the impact of the detonation products through the medium in which the explosion has taken place, and by the formation later of the shock wave.

The initial parameters of the shock waves originating as a result of an explosion vary within wide limits, depending on the nature of the medium. Thus, for example, in metals (iron, steel, copper) which have low compressibility the initial pressure p_{m0} of the shock wave resulting from the explosion of typical high explosives, amounts to $1.6 - 1.8\ p_1$ (p_1 is the detonation pressure), in soils $p_{m0} \approx p_1$, for an explosion in water $p_{m0} = 0.6 - 0.7\ p_1$ and in air, which has a very strong compressibility and a low density p_{m0}, as a rule does not exceed 1300 - 1500 kg/cm^2.

In dense media (metals, concrete, earth) all the parameters of the shock wave, according to the extent of the distance from the explosion source, fall considerably more abruptly than in air. This is explained by the considerable losses of energy of the explosion products and of the shock wave, and also by transferrence to deforming the medium. As a consequence of this, the zone of effective action in such media is considerably less than for an explosion in air.

Resulting from a study of the effect of an explosion in air the observed destructive effects may be assumed to be divided into three groups :

1) strong, characterised by destruction of stone and brickwork,

2) medium, accompanied by destruction of walls and wooden structures,

3) weak, by which glass windows, for example, are broken.

Effect of an Explosion in Dense Media. Firings of explosives in dense

media, including earth, are usually accompanied by destruction and ejection of the medium. This effect is known under the name of the fugacity effect of explosives.

A measure of the fugacity effect is furnished by the volume of the crater formed in the ground by the explosion of 1 kg. of explosive. The crater volume depends on the weight and properties of the explosive charge, on the properties of the medium damaged, and on the positioning of the charge relative to the medium.

A considerable influence is exerted on the fugacity effect of explosives by the extent to which the charge is sunk in the medium. Thus, for example, trotyl at the surface of normal soil gives, on explosion, a crater of about 0.15 m^3/kg, but with a charge sunk to a depth of 0.4 m, the crater volume in the same soil is 1 m^3/kg.

In order to calculate the weight c of a charge intended to blast out rock, BORESKII's well-known formula is used

$$c = k_b W^3 (0.4 + 0.6n^3), \qquad (87.5)$$

where W is the length of the line of least resistance (LLR), i.e. the distance from the centre of the charge to the rock surface, k_b is a constant depending on the properties of the rock and of the explosive, n is the ejection factor, equal to $\frac{r_c}{W}$. Here, r_c is the radius of the crater measured at the rock surface level.

The coefficient k_b for explosives of medium power can be, according to G.I.POKROVSKII, determined by the formula

$$k_b = 0,80 + 0.085N,$$

where N is the yield category of the rock. N varies from 1 to 16 (with respect to the ENV & R scale, 1944).

A typical blasting crater is shown in Fig. 225. The apparent crater depth H_c resulting from fall of part of the rock and crumbling of the crater rim proves to be less than is shown in Fig. 225, i.e. less than $W + R_k$.

It is assumed that

$$H_c = \frac{2r_c - W}{3}.$$

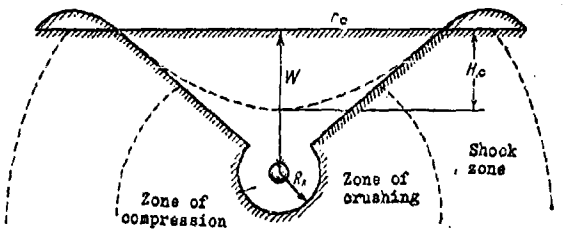
G.I. POKROVSKII, on the basis of a number of assumptions, established that it is more correct to use the following relationship in calculating the crater size:

$$c = \frac{\gamma}{28\,000} W^{\frac{\gamma}{2}} (1 + n^2)^2,$$

where γ is the volumetric weight of the earth in kg/m^3.

According to data by POKROVSKII, the relationship is true for explosions of charge weights up to 1600 tons.

Figure 225. Crater formed by ejection of rock as a result of an explosion.



The volume of material ejected by optimum sinking of charges in earth amounts to 1 - 1.5 m^3/kg of explosive.

Three zones can be clearly distinguished as a result of an explosion in the ground : these are the zones of compression, crushing and shock.

The zone of compression is formed as a result of earth being ejected by the detonation products followed by extremely intense packing. The zone

of crushing, situated behind the sphere of compression, is characterised by destruction of continuity between the earth particles, partial crushing and the formation of fissures. Within the shock sphere the ground structure is partially destroyed.

The radius of each of these zones is

$$R \sim \sqrt[3]{c}.$$

In this relationship the proportinality coefficient depends on the nature of the explosive and of the medium. Thus, for normal soils, the radius of the sphere of compression is approximately equal to

$$R_{comp} = 0.45\sqrt[3]{c}.$$

Buildings found within the zone of crushing suffer considerable damage in the majority of cases.

It is well-known from experience in the Second World War that the zones of destruction of terrestrial buildings by explosion of aerial bombs can be determined by the empirical formula

$$R_{dest} = k\sqrt{c}\ m; \qquad (87.7)$$

where $k = 0.5$ for brick structures, $k = 0.25$ for concrete walls and roofs. The weight of the charge is taken in kilograms.

In order to determine the radius of destruction as a function of the wall thickness L of the building, we use the formula

$$R = k_1\sqrt{\frac{c}{L}}, \qquad (87.8)$$

which is found to be in satisfactory agreement with experiment.

For distances at which splitting of brick walls is observed, it is assumed that $k_1 = 0.4$, for the formation of cracks in brick walls and ceilings $k_1 = 0.6$ and for the destruction of light elements of buildings (destruction of wall partitions, bracing, doors, window frames etc) $k_1 = 3$ ($L = 1$). Destruction of the latter type is observed for aerial bombs with

a calibre of 1000 kg at distances of around 60m.

According to data by M.A.SADOVSKII, the radii of the zones of destructive effect are determined, over a very wide range of charge weights, by the general relationship

$$R = kc^n,$$

where n varies from 1/3 to 2/3.

On the basis of results from experimental data processing, it can be concluded that the zone of severe destruction from the effects of large calibre aerial bombs (FAB-1000 and FAB-2000) amounts to about 50 - 55 equivalent charge radii. Hence, it follows that this destruction is chiefly dependent on the effect of the air shock wave. The zone of direct effect of the detonation products, as shown above, does not exceed 10 - 12 charge radii.

It is of interest to estimate the approximate limits for which destruction of obstacles is dependent on the impulse (dynamic effect) or the pressure (according to SADOVSKII - the "static" effect).

The dynamic effect is observed when the ratio $\frac{\tau}{\theta} \ll 1$, but the static effect, on the contrary, is observed when the ratio $\frac{\tau}{\theta} \gg 1$, ; where τ is the time of action of the shock wave on the obstacle, θ is the relaxation period of the obstacle (for elastic systems $\theta = T$, i.e. the period of natural oscillation of the system).

According to data by SADOVSKII, the periods of natural oscillation of the most common elements of building structures, and also the values of the "static" (F times) and the dynamic (I times) destructive loading, have the values given in Table 122.

According to OLISOV and SADOVSKII, the impulsive effect of a shock wave is observed for $\frac{\tau}{T} \leqslant 0.25$.

Table 122

Periods of natural oscillation of structural elements, and destructive loading stresses.

Structure	Brick walls		Ferro-concrete wall, 0.25m	Ceilings with wooden beams	Light partitions	Glass
	2 bricks	1.5 bricks				
T, sec.	0.01	0.015	0.015	0.5	0.07	0.04 - 0.02
Static loading P, kg/cm^2	0.25	0.15	5.0	0.10 - 0.16	0.05	0.05 - 0.10
Impulsive loading, i, $\frac{kg \cdot sec}{m^2}$	220	190	-	-	-	-

The "static" type of effect of a shock wave is observed for $\frac{\tau}{T} \geqslant 10$. Consequently, for those structural elements such as walls, the impulsive effect will be observed for $\tau \leqslant 0.002$ sec and the "static" effect for $\tau \geqslant 0.1$ sec, for glass structures the impulsive effect will be for $\tau \leqslant 0.005$ sec and the "static" effect for $\tau \geqslant 0.2$ sec.

Comparing, for a charge of given weight, the time of action of the shock wave, calculated for example by SADOVSKII's experimental formula

$$\tau = 1.5 \sqrt[6]{c}\, \sqrt{R}\, 10^{-3} \qquad (87.9)$$

with the period of oscillation of the structure, it can be judged that under the action of such a loading (dynamic or "static") it will be destroyed.

An analysis, carried out by SADOVSKII, shows that severe destruction is determined by the impulse of the shock wave, even for heavy "blockbusters".

The law of propagation of shock waves has been studied by many investigators. The most reliable experimental investigations in this sphere within

the Soviet Union have been carried out by SADOVSKII, TSEKHANSKII, OLISOV and VLASOV.

In order to determine experimentally such parameters of shock waves in air as pressure and impulse, as a result of which the destructive effect of an explosion is chiefly determined, extensive use has been made of various mechanical instruments.

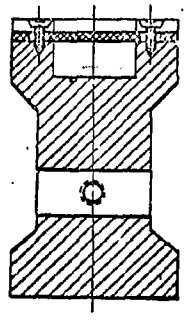
Instruments for measuring impulses should possess natural oscillation periods exceeding by an order or more the time of action of the shock wave. If the contrary is the case, the instruments will only measure an undefined portion of the impulse.

Instruments for measuring pressure, on the contrary, should have a period of oscillation considerably less than the time of action of the over-pressure.

The accuracy of measurement of impulse or pressure is determined by the design of the instrument and by its working principle. The modern equipment, devised by G.S.TSEKHANSKII , is adequate for measuring shock wave impulses over a wide range of values.

Diaphragm pressure gauges (Fig. 226) have been widely used for studying the explosion field. According to the flexure of the diaphragm of this instrument, some idea is given of the magnitude of the impulse or pressure of the shock wave. Lead diaphragms are used to measure impulses, which have a low natural frequency. The frequency can be increased by using rigid aluminium diaphragms. However, as pointed out by TSEKHANSKII, in either of these cases the periods of the diaphragms are found to be commensurate with the time of action of the explosion. Consequently, diaphragm pressure gauge instruments cannot be used for accurate quantitative measurements.

Figure 226. Diaphragm pressure gauge instrument.



Reliable quantitative data concerning the maximum pressures of a strong air shock wave are obtained on the basis of measurements made of the shock wave velocities, which are easily measured to a high degree of accuracy. The pressure of a shock wave is determined thus by the formula

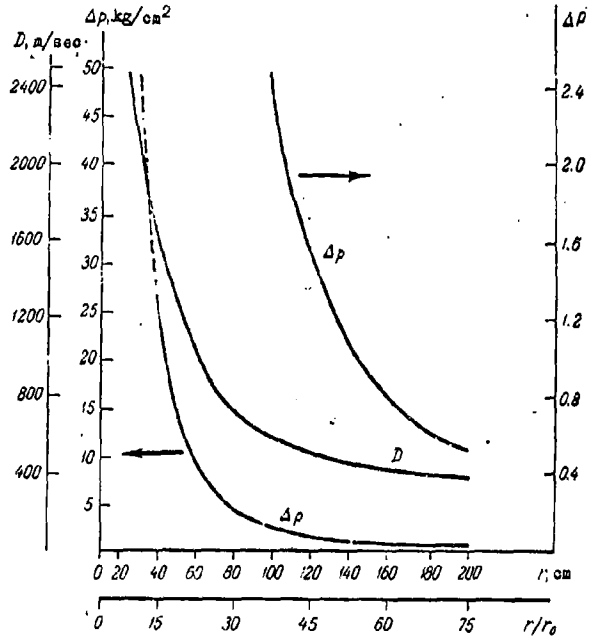
$$p_1 - p_a = \frac{2}{k+1}\rho_a D_s^2 \left(1 - \frac{c_a^2}{D_s^2}\right).$$

Numerous measurements of shock wave velocities have been carried out by A.S.ZAVRIYEV using various types of modern measuring and recording equipment. The results obtained for charges of TH(trotyl-hexogen) 50/50 weighing 135 g. are shown in Fig.227. The overpressure as a function of the distance r from the charge centre is given on two scales. The author estimates the maximum error in measurement of the overpressure to be 5 - 7%.

By using small charges of explosive, data on the propagation of a shock wave can ve obtained as a function of the distance from the site of the explosion, by using mirror scanning with an intensity gate(see para.46). For explosives which have small chemical losses when detonated, the relationships

$D = f_1(r/r_0)$ and $\Delta p = f_2(r/r_0)$ obtained will be applicable with accuracy to a charge of large weight, since for these explosive charges geometric scaling is quite justified. Photographic methods can be used to great advantage for establishing the relationship $D = f(r)$ close to the explosive charge. Calculation of the pressure at the shock front, even for a very powerful shock wave, with respect to the known velocity does not cause any special difficulties.

Figure 227. Dependence of velocity and overpressure at the shock front on distance from the centre of the explosion.



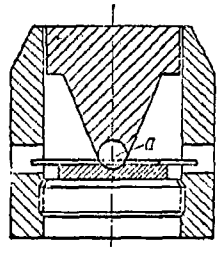
Ballistic pendulums are widely employed for measuring impulses. Numerous measurements have been carried out by SADOVSKII by means of these instruments.

The so-called ball indicators have also been used for measuring the pressures of air shock waves (Fig.228). The pressure of the shock wave is estimated by the diameter of an impression on a copper or aluminium plate. The impression is formed as a result of steel sphere a attached to a piston and freely movable in the body of the instrument, being forced into the plate. The period of the

instrument for use with copper plates and a light piston is approximately 0.2 msec, which defines the possibility of usage of the instrument for measuring pressure only at quite considerable distances from the explosion focus. This same instrument, but with the weight of the piston and the hardness of the plate selected accordingly, can be used for measuring impulses.

It should be borne in mind, however, that since the resistance of the plate material depends on the rate of deformation and upon the energy of the piston, then the calibration of the instruments should be carried out under conditions analogous with the effect of the shock wave, and this presents considerable difficulties.

Figure 228. Ball indicator.



A number of measurements of shock wave pressures have been carried out by SADOVSKII by means of a piezzoelectric manometer designed by [illegible].

The pressure-absorbing elements in this instrument are quartz plates. By means of a delay circuit it was possible to record the piezzo-current on a Schleiffer oscillograph. The accuracy of measurement guaranteed by the instrument amounts to ± 6% .

For determining very large pressures (in excess of 10,000 kg/cm^2) and also for plotting the relationship between pressure and time, M.A.Sadovskii and A.I.Korotkov used Hopkinson's measuring rod, suitably improved. This instrument, called a mechanical pressure recorder, operates in the following manner.

Suppose the shock wave encounters the end of the steel rod; if the pressure of the wave does not exceed the elastic limits of the rod, then the tension at its end, at any instant of time, will be equal to the pressure of the wave. A longitudinal compression wave will be propagated through the rod, practically undamped and having an approximately constant velocity equal to the velocity of sound c_0 in the rod material.

On reaching the opposite end of the rod, the wave is reflected and now moves back as a tension wave. If the rod is cut into two pieces such that the point of sectioning is in good contact, then, as a result of the passage of the compression wave the sections of the rod will be pressed together with a force equal to ps, where s is the cross-sectional area of the rod and p is the magnitude of the pressure in the wave. On arrival of the tensile wave at the point of sectioning, contact is broken and a piece of the bar of length l flies off, carrying a certain momentum equal to

$$mv = \int_0^{t_1} sp\,dt.$$

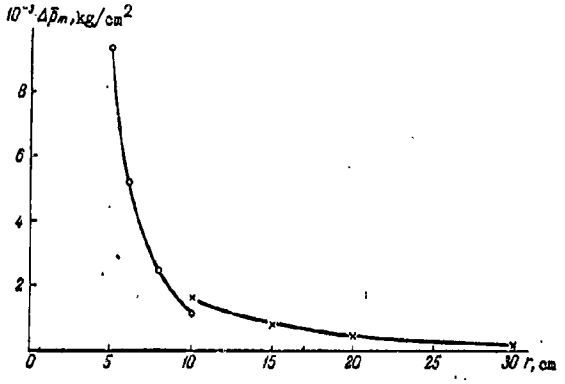
The upper mimit of integration is $t_1 = \frac{2l}{c_0}$, since the wave follows the path l twice.

By using pieces of rod of different lengths l_1, l_2, l_3 etc., the average pressure can be measured in the different sections by the curve $p = f(t)$ according to the momentum of the piece of rod measured by some method or other.

The advantages of such an instrument are obvious. Amongst its disadvantages are the necessity for carrying out a large number of experiments to construct the curve $p = f(t)$, and the low accuracy in determining small pressures ("tail" of the curve).

The results of measurements of pressure for a shock wave in air reflected from a calibrated rod, obtained by A.I. KOROTKOV, are presented in Fig.229.

Figure 229. Relationship between pressure as a result of reflection of a shock wave from the face of a steel rod and distance from the explosion centre.



The average pressures over a time $5 \cdot 10^{-6}$ sec are plotted on the graph and not the actual maximum pressures on reflection. According to data by KOROTKOV the difference between the actual and the average maximum pressures over a time of $5 \cdot 10^{-6}$ sec is about 10 - 15%. The pressure at different distances was measured by instruments differing somewhat in construction. As a consequence of this the curves in Fig.229 do not join up. Charges of a 50/50 mixture trotyl-hexogen with a weight of 155 g. were exploded. The values of the pressure close to the charge verify the validity of the calculation of the initial parameters of shock waves in air, as presented in Chapter IX . It should be taken into account, however, that as a result of the reflection of very intense shock waves the pressure on reflection exceeds the pressure at the shock front by at least a factor of 8.

For measuring the pressure at the shock front and its variation with time at a fixed point in space, the best method is to use piezzo detectors together with cathode ray oscillographic recording of the piezzo-currents.

The double-piston impulsometer by TSEKHANSKII (Fig. 230) is quite widely used as an instrument for measuring shock wave impulses. The piston of the instrument consists of two parts : a lower and an upper part. Into the recess formed by the lower portion of the piston and the upper portion of the casing a stop collar is inserted. Under the action of the shock wave the piston moves downwards. Passing through a path length x the upper piston, on encountering the stop collar is arrested, but the lower piston continues to move and deforms a conical crusher gauge. The impulse is determined by means of special calibration tables, according to the magnitude of deformation of the crusher gauge. Calibration is accomplished by dropping a piston of predetermined weight onto the crusher gauge. By simultaneous measurement of the impulse with several impulsometers, having different clearances x, the curve of $y(x)$ can be plotted and $p(t)$ can be determined by means of it, i.e. the change of pressure acting on the impulsometer with time.

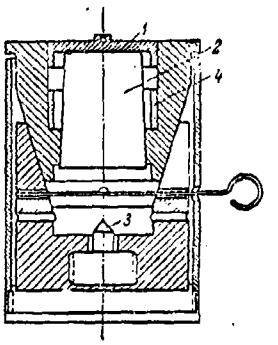


Figure 230. Double piston impulsometer : 1, 2 - Pistons ; 3- Crusher gauge; 4.- Stop collar .

Actually, the velocity of the piston is

$$v = \frac{dx}{dt},$$

whence

$$dt = \frac{dx}{v}. \tag{87.10}$$

The impulse

$$I = mv, \quad v = \frac{I}{m},$$

and

$$dI = p\,dt, \quad dt = \frac{dI}{p}.$$

Substituting the values of dt and v in expression (87.10) we obtain

$$p = \frac{dI}{dx}\frac{I}{m}. \tag{87.11}$$

At the same time,

$$t = \int_{x_1}^{x_2} \frac{m}{I}\,dx. \tag{87.12}$$

Thus, for every path length with respect to a known dependence of $I(x)$, the pressure and the corresponding time can be found, i.e, the function $p(t)$ can be determined.

By plotting graphically the function $I(x)$ (Fig. 251), the pressure can be found for any point with respect to the angle of slope of the tangent at the given point to the axis x.

Figure 251. Relationship between the impulse recorded by the impulsometer and the path of the upper piston.

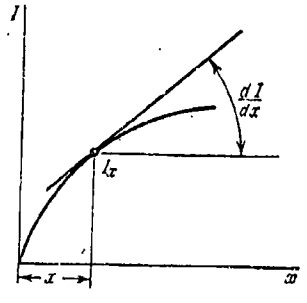
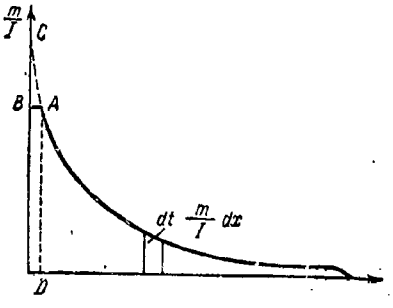


Figure 252. Subsidiary graph for establishing the dependence of pressure on time.



In order to determine the time t_i corresponding to a given pressure, a graph is plotted (Fig. 252) in which the section AC is hypothetical, since for the experiments carried out the variation of x does not commence at zero. However, the error introduced by this circumstance does not exceed 5 - 7%.

The double-piston impulsometer only measures the positive phase of the impulse. At the instant when the external pressure becomes less than the pressure inside the instrument, disengagement of the piston occurs if the clearance x is sufficiently large.

The dependence of the impulse on the path x of the upper piston has the form shown in Fig. 233, according to TSEKHANSKII for charges of trotyl with a weight of 8 kg. The dependence of the pressure and also of the time of action of the shock wave on distance is shown in Fig. 234 for the same charges.

It can be seen from Fig. 233 that the positive phase of the impulse is integrated completely at a path x of the piston equal to 5 - 6 mm. The magnitude of the impulse determined experimentally, as Sadovskii showed, corresponds to the value calculated by the theoretical formula

$$i = A\frac{c^{\frac{2}{3}}}{R}, \qquad (87.15)$$

where, for explosives of the trotyl and ammatol type, $A = 52 - 56$, and for flegmatized hexogen $A \approx 75$.

Figure 233. Dependence of impulse as recorded by the impulsometer on the path of the upper piston.

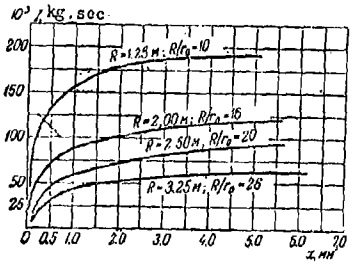
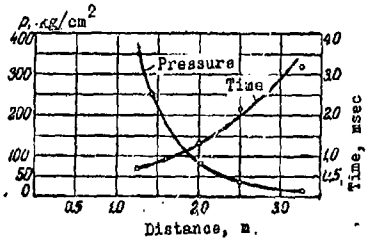


Figure 234. Dependence of maximum pressure at the shock front and its time of action on distance.



The time of action of a shock wave agrees with that calculated by SADOVSKII'S experimental formula

$$\tau = 1.5 \sqrt[6]{c}\, \sqrt{R} \cdot 10^{-3} \text{ sec.}$$

For relatively close distances from the explosion source $(R < (15-20)\ r_0)$, the formula

$$i = \frac{BC}{R^2}, \qquad (87.14)$$

gives a more satisfactory agreement with experiment for determining impulses, which is also found to be in complete agreement with theory (see para. 85).

By processing the numerous experimental data obtained by the various investigators, and the data from his own experiments, M.A. SADOVSKII established the following empirical formulae for calculating overpressures at the shock fronts :

$$\left.\begin{aligned} \Delta p &= 0.95 \frac{\sqrt[3]{q}}{r} + 3.9 \frac{\sqrt[3]{q^2}}{r^2} + 13.0 \frac{q}{r^3} \quad (\text{For Trotyl}), \\ \Delta p &= 1.09 \frac{\sqrt[3]{q}}{r} + 4.5 \frac{\sqrt[3]{q^2}}{r^2} + 15.0 \frac{q}{r^3} \end{aligned}\right\} \qquad (87.15)$$

(for a mixture of trotyl with hexogen in the proportion 50/50). The formulae are used for large-scale concentrated charges (sphere, cylinder, with height equal to the diameter, cube etc.), exploded at the earth's surface. For this $0.1 \leqslant \frac{q^{1/3}}{r} \leqslant 1.0$ (for trotyl $q \geqslant 100$ kg).

STONER and BLAKNEY plotted a similar relationship for charges of pentolite (a mixture of trotyl with T.E.N in the proportion 50/50) :

$$\Delta p = \frac{8.63}{z} + \frac{295.1}{z^2} + \frac{7823}{z^3} \text{ atm}, \qquad (87.16)$$

where

$$z = \frac{r}{\left(\frac{\rho_{\text{exp}}}{\rho_{\text{eq}}}\right)^{1/3}},$$

$\rho_{expl.}$ is the density of the explosive charge, $\rho_{aq.}$ is the specific gravity of water and ω is the volume of the charge.

By introducing the argument z, SADOVSKII'S formula for trotyl-hexogen, which resembles pentolite in its characteristics, will have the form

$$\Delta p = \frac{10.9}{z} + \frac{450}{z^2} + \frac{15000}{z^3} \quad kg/cm^2 . \qquad (87.17)$$

Sadovskii noted that the ratio of the coefficients in this formula to the coefficients of relationship (85.15) are subject to the following rule :

$$k = \frac{10.9}{8.63} = 1.26 = \sqrt[1]{2^1},$$
$$k^2 = \frac{450}{295} = 1.53 \approx \sqrt[1]{2^2},$$
$$k^3 = \frac{15000}{7823} = 1.92 \approx 2.0 = \sqrt[1]{2^3}.$$

The reason for the difference between the relationships $\Delta p = f(r)$ established by SADOVSKII and STONER, in the opinion of Sadovskii, consists in the fact that STONER exploded the charges at a relatively high altitude, which eliminated the effect of reflection from the surface of the ground on the overpressure.

Thus, an explosion on the ground, with respect to overpressure at the shock front, is equivalent to a charge of twice the mass exploded at such a distance from the surface of the earth that reflection has practically no influence on the profile of the shock wave. (In the region where measurements were carried out, it is a spherical and nota hemispherical shock wave, as occurs as a result of explosion on the ground). The formula established by M.A.SADOVSKII is in good agreement with the numerous experimental data of various authors.

The shape of the charge exerts a certain influence on the efficiency

of an explosion, mainly in the case when it takes place in the air and has attack against ground targets as its objective.

It has been established that as a result of the explosion of large-scale charges of cylindrical shape (or close to cylindrical) for a sufficiently large value of $\frac{h}{d}$ and if the charges are disposed normally to (or close to normal) the surface of the ground, then the zone of intense and average destruction is increased somewhat in the direction perpendicular to the lateral surface of the charge.

This effect may be intensified if the charge, at the instant of explosion is located at a certain distance from the ground and if a method of initiation is used which will ensure radial propagation of the detonation from the axis of symmetry of the charge.

The optimum height of explosion of a charge is selected from conditions which preclude the possibility of formation in the ground of any significant crater. In this case, the so-called "dead" space does not arise in the vicinity of the explosion focus, and spreading of the explosion products parallel to the surface of the ground is suitably ensured.

The positive effect of the factors discussed is explained by the fact that by suitable choice of the shape of the charge and of methods of its initiation, the formation of a quite sharply defined cylindrical shock wave is achieved as a result of the explosion. The breakaway of such a wave from the front of the detonation products, as is well-known, occurs at an appreciably larger distance from the explosion centre than for a spherical explosion, and as a result of this a more even fall of the shock wave parameters is ensured during the process of its propagation.

The results of comparable experiments with cylindrical and spherical charges whow that at identical distances the pressure of the air shock wave in the case of the cylindrical charge is greater than for the explosion of a spherical charge. Less difference is observed in the impulses, which should explain the lesser depth and consequently also the lesser time of action of the wave in the case of explosion of a cylindrical charge.

A supplementary factor, intensifying the directional effect of an explosion in the case considered, is the sudden confinement of the axial dispersion of the detonation products from the ends of the charge and, consequently, a corresponding increase of the effective, active part of the charge.

Significant effects , resulting from the use of all the possibilities mentioned, may be attained only in the case of exposed charges or charges enclosed in an envelope with a high filling coefficient. With a relatively small filling coefficient rapid equalisation of the energy in the explosion products occurs, as a result of which the shock wave very soon acquires a shape close to spherical.

.....

CHAPTER XIV

EXPLOSIONS IN DENSE MEDIA

§ 88. Propagation of Shock Waves in Dense Media

The study of shock waves propagating in dense media (metal, concrete, water) presents a difficult but extremely important problem in the theory of an explosion.

The solution of this problem is clearly linked with the question of the equation of state of any arbitrary body at high pressures.

If the equation of state and the isentropy equation of the body is known, it is possible to establish the fundamental laws of propagation of shock waves in that body for the one-dimensional case. In fact, the perturbations which are propagated in a body as a result of an explosion will not, of course, be one-dimensional.

The most interesting case is the study of the propagation in the body of spherical and cylindrical waves. However, the study of one-dimensional motions is the first essential step which contributes to an understanding of the processes taking place.

Let us consider some supplementary considerations relative to the equations of state of dense media at high pressures. It was shown earlier (see Chapter VII) that the equations of state of solids and liquids can be represented, in a quite general form, by the expression

$$p = \Phi(v) + f(v)\,T. \tag{88.1}$$

In solving hydrodynamic problems, we shall be interested not only in the equation of state itself, but in the isentropy equation which defines the equation of energy in a system of hydrodynamic equations. Consequently,

having been given the isentropy equation, it is of great interest to determine the corresponding equation of state, which may also be compared with the equation of state (88.1) given in statistical physics. For this, the equation of isentropy should be in a form convenient for hydrodynamic application.

We shall give the isentropy equation in the form

$$p = A(S)F(v), \tag{88.2}$$

where $A(S)$ is a function of the entropy S. We shall derive the equation of state corresponding to the isentropy (88.2) in the form

$$p = \Phi(v) + Tf(v). \tag{88.3}$$

By using the well-known thermodynamic expression

$$\left(\frac{\partial p}{\partial v}\right)_S = \left(\frac{\partial p}{\partial v}\right)_T - \frac{T}{c_v}\left(\frac{\partial p}{\partial T}\right)_v^2,$$

we find the isentropy equation

$$p = \Phi(v) + N(S) f e^{-\int \frac{f\,dv}{c_v}}. \tag{88.4}$$

Comparing this expression with (88.2), we obtain

$$1 - \alpha N(S) = A(S), \quad f e^{-\int f \frac{dv}{c_v}} = \alpha\Phi,$$

where α is a constant.

Integrating the latter equation, we have

$$f(v) = \frac{c_v\Phi}{k_0 - \int \Phi\,dv}, \quad p = \Phi(v) + \frac{c_v\Phi T}{k_0 - \int \Phi\,dv}, \tag{88.5}$$

where k_0 is the constant of integration.

We now recall that in equation (88.1), $\Phi(v)$ characterises the elastic force of repulsion acting between the molecules of the medium; $Tf(v)$ gives the "thermal" component of the pressure. We shall neglect the forces of attraction acting between the molecules of the medium, since, at pressures greater than the internal pressure of the medium, the repulsive forces considerably

exceed the attractive forces.

The internal energy of the medium can be written in the form

$$dE = c_v\,dT + T\left(\frac{\partial p}{\partial T}\right)_v dv - p\,dv = T\,dS - p\,dv. \tag{88.6}$$

Since

$$T\left(\frac{\partial p}{\partial T}\right)_v - p = -\Phi(v),$$

then

$$dE = c_v\,dT - \Phi\,dv. \tag{88.7}$$

Integrating equation (88.7) we have

$$E - E_0 = \bar{c}_v(T - T_0) - \int_{v_0}^{v} \Phi\,dv. \tag{88.8}$$

On the other hand, from (88.6) and (88.1) we obtain

$$dS = c_v\,d\ln T + f(v)\,dv, \tag{88.9}$$

which, after integration, gives

$$S - S_0 = c_v \ln\frac{T}{T_0} + \int_{v_0}^{v} f\,dv, \tag{88.10}$$

$$f = \frac{c_v\Phi}{k_0 - \int \Phi\,dv}, \tag{88.11}$$

whence

$$\Delta S = S - S_0 = c_v \ln\left[\frac{T}{T_0}\,\frac{k_0 - \int_{v_0}^{} \Phi\,dv}{k_0 - \int_{v}^{} \Phi\,dv}\right]. \tag{88.12}$$

For a slightly-compressible medium

$$\Delta E = c_v\,\Delta T - \Phi(\bar{v}), \tag{88.13}$$

where

$$\bar{v} = \frac{v_0 + v}{2},$$

and

$$\Delta S = c_v\frac{\Delta T}{T_0} - f(\bar{v})\,dv = c_v\left[\frac{\Delta T}{T_0} + \frac{F(\bar{v})\,\Delta v + k_0}{F(\bar{v})\,\bar{v} - k_0}\right], \tag{88.14}$$

since

$$f(v) = \frac{c_v F(\bar{v})}{k_0 - F(\bar{v})\,\bar{v}}.$$

It can be assumed to a high degree of accuracy that

$$F(v) = A_0(v^{-k} - v_0^{-k}) = A_0(\rho^k - \rho_0^k), \tag{88.15}$$

then

$$f(v)=\frac{c_v A_0\left(\rho^k-\rho_0^k\right)}{k_0+\frac{A_0}{\rho}\left(\frac{\rho^k}{k-1}+\rho_3^k\right)}, \tag{88.16}$$

and the isentropy equation takes the form

$$p=A(S)\left(\rho^k-\rho_0^k\right). \tag{88.17}$$

As experiments show, for example those carried out by SHEKHTER in studying the propagation of shock waves in water, and JENSEN's calculations (choosing $A(S)$ in the correct manner), at pressures exceeding 50,000 kg/cm^2 k may be assumed equal to 3 (or somewhat greater). As a result of this, the thermal component of the pressure is relatively small in magnitude compared with the magnitude of the other pressures.

In other words

$$\frac{f(v)}{F(v)}\ll 1.$$

Thus it becomes obvious that the change of entropy in solids and liquids as a result of a compressive shock wave is very insignificant.

Let us determine the parameters of a shock wave propagating in a dense medium.

The energy equation (neglecting the quantities E_0 and p_0) gives

$$E=\frac{p}{2}(v_0-v). \tag{88.18}$$

Comparing it with expressions (88.8) and (88.1), we obtain the Hugoneot adiabatic equation

$$c_v T-\int_{v_0}^{v}\Phi\,dv=\frac{p}{2}(v_0-v)=c_v\frac{p-F}{f}-\int_{v_0}^{v}E\,dv. \tag{88.19}$$

In the case when

$$F(v)=A_0\left(v^{-k}-v_0^{-k}\right)$$

relationship (88.19) can be written in the form

$$\frac{p}{2}(v_0-v)=\frac{p-A_0\left(v^{-k}-v_0^{-k}\right)}{A_0\left(v^{-k}-v_0^{-k}\right)}\left[k_0+A_0 v\left(\frac{v^{-k}}{k-1}+v_0^{-k}\right)\right]- \tag{88.20}$$

$$-A_0\frac{kv_0}{k-1}+A_0 v\left(\frac{v^{-k}}{k-1}+v_0^{-k}\right).$$

Hence, for a strong wave $(p \to \infty)$

$$\frac{v_0 - v}{2} = \frac{\frac{k_0}{A_0} + \frac{v^{1-k}}{k-1} + vv_0^{-k}}{v^{-k} - v_0^{-k}}, \qquad (88.21)$$

which defines the quantities $\frac{v_0}{v}$ or $\frac{\rho}{\rho_0}$. In the case when $k_0 = 0$, we arrive at the equation

$$\left(\frac{\rho}{\rho_0}\right)^{k+1} - \frac{\rho}{\rho_0} = \frac{k+1}{k-1}\left(\frac{\rho}{\rho_0}\right)^{k} + 1. \qquad (88.22)$$

For $k = 3$, for example, we have

$$\left(\frac{\rho}{\rho_0}\right)^{4} - 2\left(\frac{\rho}{\rho_0}\right)^{3} - \frac{\rho}{\rho_0} - 1 = 0,$$

whence

$$\frac{\rho}{\rho_0} \approx 2.3.$$

Since the energy increases slowly for a large increase of pressure, then the shock wave is replaced by a normal compression wave, assuming constant entropy, since in this case the value of the ratio of the densities $\frac{\rho}{\rho_0} = 2.3$ even for water, will correspond to a pressure of around several millions of kg/cm^2 (and greater for metals).

Only at ultra-high pressures will the medium acquire gaseous properties and the entropy commence to increase sharply, however, as a result of this the gas will not be ideal, but degenerated.

The criterion for a strong shock wave can now be established.

In the case of propagation of a shock wave in the atmosphere (in any rarefied medium), the density of the medium at the shock front approaches its limiting value for a ratio of the pressure at the shock front to the initial pressure of about 30 - 50. In the case of propagation in a dense medium, at immense pressures (around 100,000 kg/cm^2) the shock wave is identified with an acoustic wave.

It is obvious that the pressure at the shock front is not a criterion

of the fact that we have either a strong or a weak wave. The quantity $\frac{u}{c} = M_a$, may be such a criterion, where u is the flow velocity at the shock front, c is the local velocity of sound. For $M_a < 1$ the wave may be assumed weak, and for $M_a > 1$ it may be assumed strong. For a shock wave propagating in a rarefied medium

$$M_a = \sqrt{\frac{(p - p_0)(v_0 - v)}{kpv}}, \tag{88.23}$$

which, for a strong wave, gives

$$M_a = \sqrt{\frac{2}{k(k-1)}};$$

$$\text{for} \quad k = \frac{7}{5} \quad M_a = 1.9.$$

For a longitudinal wave, assuming that

$$\frac{v_0}{v} = \frac{(k+1)p + (k-1)p_a}{(k-1)p + (k+1)p_a}, \tag{88.24}$$

we find

$$M_a = \sqrt{\frac{2(p - p_a)^2}{kp[p(k-1) + p_a(k+1)]}};$$

for

$$\frac{p}{p_a} = \frac{1 + \frac{k(k+1)}{4} + \sqrt{1 + \frac{(k+1)^2}{16}}}{1 - \frac{k(k-1)}{2}}$$

$$M_a = 1.$$

For example, for $k = \frac{7}{5}$, the value $M_a = 1$ is attained for $\frac{p}{p_a} = 3$. For a detonation wave $M_a = \frac{1}{k}$, i.e. M_a is always less than unity.

We shall further use the fact that as a result of separation of the detonation wave from the solid wall, the entropy at the separated shock front increases very insignificantly, and consequently the problem is considered as an acoustic approximation. This is also obvious from what has been said above, since the quantity M (Mach number) for a detonation wave is always less than unity.

For a dense medium where the isentropy equation (88.17) holds good,

$$c^2 = \left(\frac{\partial p}{\partial \rho}\right)_S = kA_0\rho^{k-1} = k\frac{p}{\rho}\left[\frac{1}{1-\left(\frac{\rho_0}{\rho}\right)^k}\right],$$

therefore

$$M_a = \sqrt{\frac{(p-p_0)(v_0-v)}{kpv}\left[1-\left(\frac{\rho_0}{\rho}\right)^k\right]} = \sqrt{\frac{1}{k}\left(\frac{\rho}{\rho_0}-1\right)\left[1-\left(\frac{\rho_0}{\rho}\right)^k\right]}. \tag{33.25}$$

whence, even for a medium having a finite value of v, at the shock front

$$M_a \leqslant \sqrt{\frac{2}{k(k-1)}},$$

which, for $k=3$ gives $M_a \leqslant 0.52$, i.e. M_a is always considerably less than unity and the shock wave in this medium can always be considered as an acoustic approximation.

Wave Propagation in a Dense Medium. For a travelling shock wave the Riemann solution of the basic gas-dynamic equations can be used, written for one-dimensional motion:

$$\left.\begin{aligned}\frac{\partial u}{\partial t}+u\frac{\partial u}{\partial x}+\frac{1}{\rho}\frac{\partial p}{\partial x}=0,\\ \frac{\partial \rho}{\partial t}+u\frac{\partial \rho}{\partial x}+\rho\frac{\partial u}{\partial x}=0.\end{aligned}\right\} \tag{33.26}$$

This solution has the form

$$x=(u+c)t+F(u), \quad u=\frac{2}{k-1}(c-c_0). \tag{33.27}$$

In certain cases longitudinal waves may also originate in the medium. In particular, these waves (two-directional waves) originate in the dispersing detonation products as a result of their interaction with the medium.

These waves, as is well-known, may be described by the general solutions of the gas-dynamic equations (see Chapter V).

For an isentropy index of $k=3$, the general solution, as we already know, has the form

$$\left.\begin{aligned}x=(u+c)t+F_1(u+c),\\ x=(u-c)t+F_2(u-c).\end{aligned}\right\} \tag{33.28}$$

Equations (88.26) and (88.27) are based on these solutions, which we shall now consider.

Suppose that at the point $x=0$ and time $t=0$ a linear charge of explosive of length a detonates from left to right. We shall consider two important practical cases :

1) the left hand end of the charge is open and there is no tamping;

2) the entire process is symmetrically propagated to both sides, which reduces the problem to one of detonation at the walls.

The wave system originating under these conditions is shown in Figs. 255 and 256.

At the beginning of the process, the first two cases may be considered as simultaneous.

The travelling detonation wave in the case of isentropic law of expansion of the detonation products

$$p=A\rho^k=A\rho^3 \tag{88.29}$$

will be described by the equations

$$x=(u+c)\,t,\quad u-c=\frac{D}{2}. \tag{88.30}$$

At time $t=\frac{a}{D}$, the detonation wave at the point $x=a$ reaches the boundary of separation of the two media. As a result of this, the following wave system originates.

In the detonation products there arise either two rarefaction waves (for flow in air, water, etc), or a compression wave and a rarefaction wave, separated by weak discontinuities (for flow of the detonation products in a slightly compressive medium). The first wave is conjugate with the wave in equation (88.23) and is described by the equations

$$x=(u+c)\,t,\quad x=a+(u-c)\left(t-\frac{a}{D}\right). \tag{88.31}$$

Figure 235. System of waves in a dense medium and in the detonation products (left-hand end of charge open).

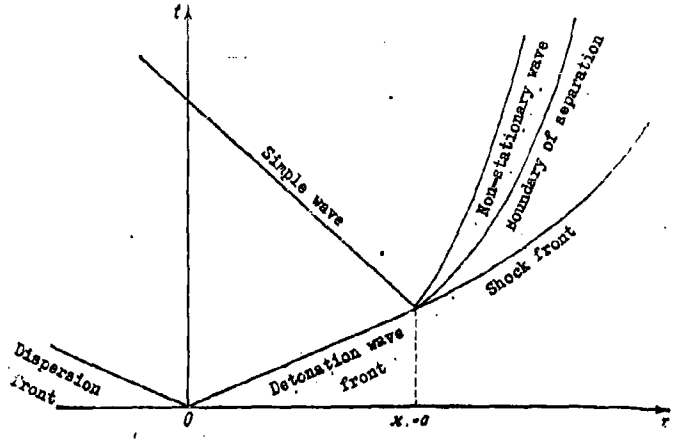
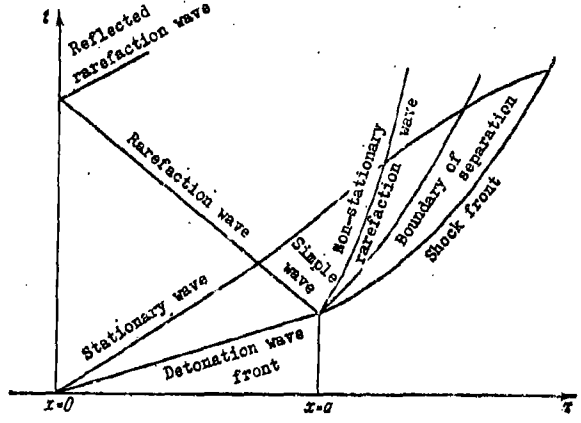


Figure 236. System of waves in a dense medium(symmetrical problem).



This ensues from the condition that for $t=\frac{a}{D}$

$$F_1(u+c)=0$$

and

$$F_2(u-c)=a-(u-c)\frac{a}{D}.$$

The second wave is located more to the right of the initial position of the boundary of separation

$$x=(u+c)t, \quad x=(u-c)t+F_2(u-c), \tag{88.32}$$

which is separated on the right by the particularly strong discontinuity from the arbitrary medium, so that $F_2(u-c)$ in equation (88.32) will be defined below from the condition of coincidence at the boundary of separation of the detonation products and the medium.

Similar, , but more complex relationships hold for an arbitrary value of $k=\frac{2n+3}{2n+1}$.

The travelling shock wave which originates in the arbitrary medium is described by the equations of (88.27)

$$\bar{u}=\frac{2}{k-1}(\bar{c}-\bar{c}_0), \quad x=(\bar{u}+\bar{c})t+F_1(\bar{u}) \tag{88.33}$$

(here the bar over $\bar{u}$ and $\bar{c}$ denotes that these quantities refer to the given arbitrary medium).

It is obvious that to the left and right of the boundary of separation

$$p=\bar{p}, \quad u=\bar{u}=\frac{dx}{dt}. \tag{88.34}$$

From these conditions we shall determine the law of motion of the boundary of separation, and also the quantities F_1 and F_2 .

For the detonation products we have

$$p=A\rho^3=Bc^2. \tag{88.35}$$

For the arbitrary medium, for which the isentropy equation (88.17) is valid, since $\rho\sim c^{\frac{2}{k-1}}$, we have

$$\bar{p} = \bar{B}\left(\bar{c}^{\frac{2k}{k-1}} - \bar{c}_0^{\frac{2k}{k-1}}\right). \qquad (88.36)$$

Hence, at the boundary of separation

$$(\eta c)^3 = \bar{c}^{\frac{2k}{k-1}} - \bar{c}_0^{\frac{2k}{k-1}},$$

where

$$\eta^3 = \frac{B}{\bar{B}}.$$

It follows from equations (88.34), (88.32) and (88.33) that

$$c = \frac{x}{t} - \dot{x}, \quad \bar{c} = \bar{c}_0 + \frac{k-1}{2}\dot{x},$$

where

$$\dot{x} = u = \frac{dx}{dt},$$

whence

$$\eta^3\left(\frac{x}{t} - \dot{x}\right)^3 = \left(\bar{c}_0 + \frac{k-1}{2}\dot{x}\right)^{\frac{2k}{k-1}} - \bar{c}_0^{\frac{2k}{k-1}}. \qquad (88.37)$$

We have obtained the differential equations defining the law of motion of the boundary of separation of the two media.

It is obvious that the initial conditions are as before,

$$t = \frac{a}{D}, \quad x = a;$$

so that

$$\frac{x}{t} = D = u_0 + c_0.$$

Thus,

$$\eta^3 (D - u_0)^3 = \left(\bar{c}_0 + \frac{k-1}{2} u_0\right)^{\frac{2k}{k-1}} - \bar{c}_0^{\frac{2k}{k-1}}, \qquad (88.38)$$

which determines the initial value of u_0, the velocity of the boundary of separation.

We determine the initial value of the pressure from the formula

$$p_0 = p_1\left(\frac{c_0}{c_1}\right)^3 = p_1\left(\frac{D - u_0}{c_1}\right)^3,$$

where

$$p_1 = \frac{\rho_0 D^2}{4} \text{ and } c_1 = \frac{3}{4}D$$

are the values of p and c at the detonation wave front, ρ_0 is the initial density of the explosive.

Solving equation (88.38) we can determine, for the boundary of separation

$$x = x(t), \quad u = u(t).$$

For the detonation products it can be calculated that

$$t = t_2(u - c), \quad x = x_2(u - c),$$

where the suffix 2 refers to the wave (rarefaction or compression) passing through the detonation products from the boundary of separation. The quantities x_2 and t_2 are variables and also F_2 is a function of $(u - c)$, which defines F_2 in equation (88.32).

The determination of $F_2(u - c)$ leads to the result

$$\frac{x - x_2}{t - t_2} = u - c. \tag{88.39}$$

For the arbitrary medium we can evaluate

$$t = t_1(\bar{u}), \quad x = x_1(\bar{u}).$$

These functions define $F_1(\bar{u})$ in the equation (88,27). As a result we have

$$\frac{x - x_1}{t - t_1} = \bar{u} + \bar{c}. \tag{88.40}$$

It now remains to determine the law of motion of the shock front originating in the arbitrary medium.

In the approximation (acoustic) considered, we have, taking into account equation (88.32),

$$D_s = \frac{d\bar{x}}{dt} = \frac{1}{2}(\bar{u} + \bar{c} + \bar{u}_0 + \bar{c}_0) = \frac{k+1}{2(k-1)}\bar{c} + \frac{k-3}{2(k-1)}\bar{c}_0, \tag{88.41}$$

where $\bar{u}_0$ is the velocity of the medium ahead of the shock front, usually equal to zero and $\bar{x}$ is a coordinate of the shock front.

From equations (88.40) and (88.41) we have

$$\bar{c} = \frac{2}{k+1}\bar{c}_0 + \frac{x - x_1}{t - t_1}\frac{k-1}{k+1}, \tag{88.42}$$

which gives

$$D_s = \frac{d\bar{x}}{dt} = \frac{\bar{c}_0}{2} + \frac{1}{2}\frac{x - x_1}{t - t_1}. \tag{88.43}$$

Solving this equation we determine

$$\Phi(\bar{x};\ t) = 0, \tag{88.44}$$

i.e. the law of motion of the shock front.

In the case of the left hand end of the charge being open(flow of the detonation products in a vacuum or in air) the solution found will be valid, in practice, for any value of t. In the case of detonation at the wall, the rarefaction wave (88.51) formed at time $t=\frac{3}{2}\frac{a}{D}$ at the point $x=\frac{3}{4}a$ (for $k=3$ for the detonation products), passes through the point of weak discontinuity in the detonation wave itself, since in this case the solution of equation (88.27) is determined only by the interval $\frac{x}{t}\geqslant\frac{D}{2}$. The value of $t=\frac{3}{2}\frac{a}{D}$ is determined from the condition that at the point of weak discontinuity $u=0$ and $c=\frac{D}{2}$.

For $\frac{x}{t}\leqslant\frac{D}{2}$ a new wave (Riemann wave) originates, proceeding towards the wall and defined by the equations (see Chapter V)

$$x-a=(u-c)\left(t-\frac{a}{D}\right);\quad u+c=\frac{D}{2}. \tag{88.45}$$

This wave overtakes the point of weak discontinuity between the waves (88.55) and (88.52), after which the wave again formed, propagating in both directions, overtakes the boundary of separation between the two media and changes the parameters of the shock wave.

Further, for $t=\frac{3a}{D}$ (resulting from equation (88.45), if one assumes that at the wall $u=0$ and $c=\frac{D}{2}$) for $x=0$), breakaway of the wave (88.45) occurs, which leads to the formation of new waves as a result of the encounters of the various points of weak and strong discontinuities.

Let us consider an actual case. We shall assume that $k=3$ for the arbitrary medium ; then the basic formula (88.57) has the form :

$$\eta^3\left(\frac{x}{t}-\dot{x}\right)^6=(\bar{c}_0+\dot{x})^3-\bar{c}_0^3, \tag{88.46}$$

whereupon $\bar{u}=\bar{c}-\bar{c}_0$.

Assuming that $\frac{x}{t}=D$, we can determine $\dot{x}_0=u_0$ at the instant of impact of the detonation wave with the second medium.

Equation (88.37) can be solved analytically. Since

$$x = \bar{u}t + \frac{t}{\eta}\left[(\bar{u}+\bar{c}_0)^3 - \bar{c}_0^3\right]^{\frac{1}{3}}, \tag{38.47}$$

then, differentiating equation (88.47) with respect to t and then integrating we obtain

$$\eta \int \frac{d\bar{u}}{\left[(\bar{u}+\bar{c}_0)^3 - \bar{c}_0^3\right]^{\frac{1}{3}}} + \ln t\left[(\bar{u}+\bar{c}_0)^3 - \bar{c}_0^3\right]^{\frac{1}{3}} = \text{const},$$

which gives

$$t = t_0\left[\frac{(\bar{u}+\bar{c})^3 - \bar{c}_0^3}{\bar{c}_0^3}\right]^{-\frac{1}{3}}\left\{\frac{\bar{u}+\bar{c}_0 - \left[(\bar{u}+\bar{c}_0)^3 - \bar{c}_0^3\right]^{\frac{1}{3}}}{\bar{c}_0}\right\}^{\frac{\eta}{2}} \times$$

$$\times\, e^{\frac{\eta}{2}\arctan\frac{\eta}{\sqrt{3}}\,\frac{\bar{c}_0}{(\bar{u}+\bar{c}_0) - \left[(\bar{u}_0+\bar{c}_0)^3 - \bar{c}_0^3\right]^{\frac{1}{3}}}}. \tag{38.48}$$

t_0 is determined from the conditions that for $x = a$, $\bar{u} = u_0$ and $t = \frac{a}{D}$. Formulae (88.42) and (88.48) give the solution of the problem in parametrical form. By eliminating $\bar{u}$, from these equations, the law of motion of the boundary of separation can be found.

If the first scheme be considered, i.e. flow to the left in vacuo, then for $t \to \infty$, $\bar{u} \to 0$. In the vicinity of the point $\frac{1}{t} = 0$, we have

$$t = t_0\left[\frac{(\bar{u}+\bar{c})^3 - \bar{c}_0^3}{\bar{c}_0^3}\right]^{-\frac{1}{3}} e^{\frac{\eta}{\sqrt{3}}\arctan\frac{\eta}{3}}, \tag{38.49}$$

and

$$x_{\lim} = x_0\left[\frac{(\bar{u}+\bar{c}_0)^3 - \bar{c}_0^3}{\bar{c}_0^3}\right]^{\frac{1}{3}}\left\{\frac{\bar{u}}{\bar{c}} + \frac{1}{\eta}\left[\frac{(\bar{u}+\bar{c}_0)^3 - \bar{c}_0^3}{\bar{c}_0^3}\right]^{\frac{1}{3}}\right\} = \frac{x_0}{\eta}, \tag{38.50}$$

where

$$x_0 = \bar{c}_0 t_0.$$

Hence, since $x_0 = \bar{c}_0 t$, we obtain

$$x_{\lim} = \frac{\bar{c}_0 t_0}{\eta} e^{\frac{\eta}{\sqrt{3}}\arctan\frac{\eta}{3}}. \tag{38.51}$$

It follows from (88.51) that for $t \to \infty$ x_{11m} tends towards a positive constant, and this indicates that the boundary of separation is moved to the ultimate distance .

We shall now solve the problem for the case when η is small. It follows from (88.46) that $\dot{x}$ is also small ; equation (88.46) thus gives

$$\frac{dx}{dt} = \dot{x} = \frac{\eta^3 \frac{x^3}{t^3}}{3\left[\bar{c}_0^2 + \eta^3 \frac{x^2}{t^2}\right]}. \qquad (88.52)$$

On integrating this expression, we find that

$$x^4\left[2\eta^3 \frac{x^2}{t^2} + 3\bar{c}_0^2\right] = a^4\left[2\eta^3 D^2 + 3\bar{c}_0^2\right]. \qquad (88.53)$$

Evaluating for $\eta^3 = 0.1$ and $\bar{c}_0 = \frac{D}{2}$ gives

$$\frac{u_0}{D} = \frac{2}{9} = 0.22, \quad \frac{p_0}{p_1} = 1.12, \quad \frac{x_{11m}}{a} = \left(\frac{19}{15}\right)^{\frac{1}{4}} = 1.06$$

(this corresponds approximately with the case of propagation of the wave in aluminium).

Similar calculations by a precise formula for the case $\eta^3 = 1.0$; $\bar{c}_0 = \frac{D}{5}$ (corrsponding approximately with the case of propagation of the shock wave in water) leads to the results

$$\frac{u_0}{D} = 0.4, \quad \frac{p_0}{p_1} = 0.51, \quad \frac{x_{11m}}{a} = 2.5.$$

The working formulae are (88.47) and (88.48) and (88.53) is for approximate solutions. By using them we can determine $\frac{u_0}{D}$ and $\frac{x_{11m}}{a}$, after which we can determine $\bar{c}_0$ and p_0 from the usual formulae.

"Cavitation" of a Dense Medium at the Free Surface. When any dense medium, the expansion of which is described by the equation

$$p = A(\rho^k - \rho_0^k), \qquad (88.54)$$

is moving in such a manner that its leading portions have a higher velocity and pressure than the tail ends, then as a result of its expansion, phenomena

resembling cavitation are possible, i.e. fissuring of the medium may occur.

Since the different parts of the medium, as a result of expansion, are moving with different velocities, then intense stretching of the medium occurs. In the case of a liquid this leads to disintegartion into a number of separate droplets. In the case of a solid (metallic) body, cavitation can develope only as a result of a quite large velocity gradient.

Let us consider first of all cavitation in any liquid. It follows from (88.27) that we can expect, with a large degree of certainty, the following distribution of velocities in the medium and of the velocity of sound in the shock wave, approaching the free surface of the liquid :

$$u+c=\frac{x-a}{t},\quad u-c=-c_a,\quad \text{for}\quad k=3, \tag{88.55}$$

where u is the velocity of the medium, c is the local velocity of sound in the medium, c_a is the velocity of sound in the undisturbed medium, a is a constant determining the stretching by the shock wave.

The qualitative solution of the problem of cavitation is of prime interest to us.

The rarafaction wave, originating as a result of the shock wave reaching the free surface of the liquid, as follows from equations (88.28) and (88.40), is characterised by the relationships

$$u+c=\frac{x-a}{t};\quad u-c=\frac{x-l}{t-\tau}, \tag{88.56}$$

where l is a coordinate of the free surface ; τ is the time of arrival of the shock wave at the free surface.

The front of the rarefaction wave, as derived from equations (88.55) and (88.56) , will move according to the law

$$x-l=-c_a(t-\tau). \tag{88.57}$$

The coordinate $x=\bar{x}$, for which $c=c_a$, is determined from relationship (88.56) :

$$c_a = \frac{1}{2}\left(\frac{x-a}{t} - \frac{x-l}{t-\tau}\right). \qquad (88.58)$$

As a result of this

$$\bar{u} = \frac{1}{2}\left(\frac{\bar{x}-a}{t} + \frac{\bar{x}-l}{t-\tau}\right) = \frac{\bar{x}-a}{t} - c_a. \qquad (88.59)$$

Solving this equation we find

$$\bar{x} = l\frac{t}{\tau} - \frac{a}{\tau}(t-\tau) + 2c_a\frac{t}{\tau}(t-\tau) \qquad (88.60)$$

the law of motion of the front beginning cavitation. The velocity of the cavitation front is equal to

$$\bar{u} = \frac{l-a}{\tau} - 3c_a + 2c_a\frac{t}{\tau}. \qquad (88.61)$$

For future calculations we shall transfer to Lagrangrian coordinates, for which we shall suppose that $u = \frac{dx}{dt}$ and we shall determine the relationship between x and x_0 (x_0 is the Langrangian coordinate).

For the initial shock wave

$$\frac{dx}{dt} = \frac{x-a}{2t} - \frac{c_a}{2}. \qquad (88.62)$$

Integrating (88.62) we find

$$x = -c_a t + A\sqrt{t}.$$

In order to determine the constant A we shall assume that $x = x_0$ for the instant of time τ, corresponding to the arrival of the shock wave at the free surface. Then

$$A = c_a\sqrt{\tau} + \frac{x_0 - a}{\sqrt{\tau}},$$

whence

$$x = a - c_a t + c_a\sqrt{t\tau} - (x_0 - a)\sqrt{\frac{t}{\tau}}. \qquad (88.63)$$

Similarly, for the rarefaction wave we have

$$\frac{dx}{dt} = \frac{1}{2}\left(\frac{x-a}{t} + \frac{x-l}{t-\tau}\right).$$

Integration gives

$$x = \frac{l}{\tau}t - \frac{a}{\tau}(t-\tau) + A_1\sqrt{t(t-\tau)}.$$

The constant A_1 is determined from the condition

$$x = l - c_a(t-\tau) = a + (x_0 - a)\sqrt{\frac{t}{\tau}} + c_a\sqrt{t\tau} - c_a t,$$

and

$$x_0 = l\sqrt{\frac{\tau}{t}} + (a - c_a t)\left(1 - \sqrt{\frac{\tau}{t}}\right),$$

which gives

$$\frac{t}{\tau} = \left(\frac{l - a + c_a\tau}{x_0 - a + c_a t}\right)^2; \quad x - l = -c_a\tau\left[\left(\frac{l - a + c_a\tau}{x_0 - a + c_a t}\right)^2 - 1\right].$$

Hence,

$$A_1 = \frac{1}{\tau}\sqrt{x_0^2 - l^2 + 2(x_0 - l)(c_a\tau - a)}$$

and

$$x = \frac{l}{\tau}t - \frac{a}{\tau}(t-\tau) + \frac{\sqrt{t(t-\tau)}}{\tau}\sqrt{(x_0 - l)[x_0 + l + 2(c_a\tau - a)]}. \tag{88.64}$$

At the line defined by equation (88.60), particles of the medium acquire the maximum possible velocity $\bar{u}$, for which $c = c_a$, $p = p_0$. Further, every particle flies apart with this velocity, independently of one-another, since cavitation of the medium occurs.

We shall determine this maximum possible velocity. From equations (88.60) and (88.64) we find that

$$4c_0^2 t(t-\tau) = (x_0 - l)[x_0 + l + 2(c_a\tau - a)]. \tag{88.65}$$

Expression (88.65) gives the relationship between x_0 and t along the line at which cavitation occurs. Form (88.61) we find

$$t = \frac{\tau\bar{u}}{2c_a} + \frac{3\tau}{2} - \frac{l - a}{2c_a}.$$

Substituting the relationship for t obtained in (88.65), we find the relationship between x_0 and $\bar{u}$:

$$(x_0 - l)[(x_0 + l) + 2(c_a\tau - a)] = 4c_a^2\left(\frac{\bar{u}\tau}{2c_a} + \frac{3}{2}\tau - \frac{l - a}{2c_a}\right)\left(\frac{\bar{u}\tau}{2c_a} + \frac{\tau}{2} - \frac{l - a}{2c_a}\right). \tag{88.66}$$

Let us carry out a few calculations. If at the instant of arrival at the free surface, $u = u_1$ and $c = c_1$ at the shock front, then $u_1 - c_1 = -c_a$ and $2c_1 - c_a = \frac{l-a}{2\tau}$, whence

$$c_1 = \frac{c_a}{2} + \frac{l-a}{2\tau}; \quad u_1 = -\frac{c_a}{2} + \frac{l-a}{2\tau}.$$

On flying apart, the first particle attains a velocity of

$$\bar{u}_{max} = \frac{l-a}{\tau} - c_a = 2u_1.$$

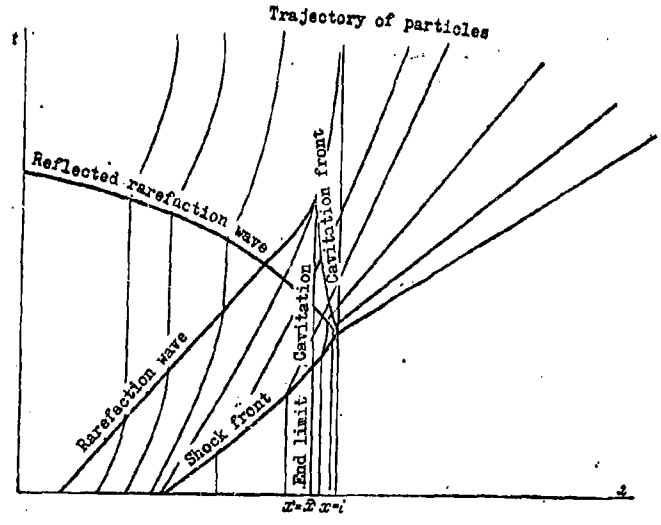
Let us establish the region of existence of the solution which we have found. It is obvious that for

$$u = 0 \quad \text{and} \quad c = c_a,$$

$$x = a + c_a t.$$

This expression gives the law of motion of the rear of the shock front.

Figure 237. Wave system at the free surface of a liquid.



The velocity of motion of the head of the shock front is

$$D_s = \frac{dx}{dt} = \frac{u + c + c_a}{2} = \frac{x - a}{2t} + \frac{c_a}{2},$$

whence

$$x = a + c_a t + A\sqrt{t},$$

whereupon the constant A is determined from the condition such that for $t = \tau$, $x = l$. Finally, we obtain the law of motion of the shock front in the form

$$x = a + c_a t + (l - a - c_a \tau)\sqrt{\frac{t}{\tau}}. \tag{88.67}$$

Fig. 237 gives a schematic picture of the motion of all the wave fronts: the shock front and the rarefaction wave following behind it, the front of the rarefaction wave after reflection from the free surface, the line of movement of the cavitation front, and also the trajectory of the liquid particles.

In a metal, cavitation can be initiated considerably later than the attainment of zero pressure, since considerable cohesive forces will act in it between the particles, thus opposing the tensile stresses.

Fissuring commences when the tensile stresses, which originate as a result of the velocity gradient, exceed the cohesive forces.

§ 89. Propagation of a Spherical Shock Wave in Water.

The problem of propagation of a shock wave in water is solved more simply if it be assumed that detonation of the charge is instantaneous. In this case one can assume approximately that for the rarefaction wave travelling through the detonation products, the relationship

$$u = \frac{2}{k-1}(c_1 - c). \tag{89.1}$$

will be valid.

It can be assumed to an even greater degree of accuracy that for water

the following relationship is valid between the velocity of the particles of the medium and the local velocity of sound $(\bar{c})$:

$$u = \frac{2}{n-1}(\bar{c} - \bar{c}_a). \qquad (89.2)$$

The accuracy of this relationship increases with respect to increase in distance from the centre of symmetry.

Substituting expressions (89.1) and (89.2) in the equations of motion and in the continuity equation we obtain

$$\left.\begin{aligned} &\frac{\partial c}{\partial t} + \left(\frac{2}{k-1}c_1 - \frac{k+1}{k-1}c\right)\frac{\partial c}{\partial r} = 0, \\ &\frac{\partial c}{\partial t} + \left(\frac{2}{k-1}c_1 - \frac{k+1}{k-1}c\right)\frac{\partial c}{\partial r} + \frac{2(c_1 - c)c}{r} = 0 \end{aligned}\right\} \qquad (89.3)$$

(for the detonation products)

and

$$\left.\begin{aligned} &\frac{\partial \bar{c}}{\partial t} + \left(\frac{n+1}{n-1}\bar{c} - \frac{2}{n-1}\bar{c}_a\right)\frac{\partial \bar{c}}{\partial r} = 0, \\ &\frac{\partial \bar{c}}{\partial t} + \left(\frac{n+1}{n-1}\bar{c} - \frac{2}{n-1}\bar{c}_a\right)\frac{\partial \bar{c}}{\partial r} + \frac{2\bar{c}(\bar{c} - \bar{c}_a)}{r} = 0 \end{aligned}\right\} \qquad (89.4)$$

(for the shock wave in water).

Integrating the continuity equation and neglecting the Euler equation, which for cylindrical and spherical waves is not compatible with the continuity equation (but which implies an insignificant error in the Law of Conservation of Momentum), we shall, by taking the isentropy equation for the detonation products of condensed explosives in the form

$$p = A_0\rho^3 \qquad (k = 3), \qquad (89.5)$$

and for water, the isentropy equation in the form

$$p = A(\bar{\rho}^3 - \bar{\rho}_a^3) \qquad (n = 3), \qquad (89.6)$$

arrive at the following solutions (waves) with respect to both sides of the boundary of separation :

$$t=-\frac{2c-c_1}{c_1^2}r+\Phi_1[r^2c(c_1-c)];\quad u+c=c_1 \tag{89.7}$$

(for the detonation products)

and

$$t=-\frac{2\bar{c}-\bar{c}_a}{\bar{c}_a^2}r+\Phi_2[r^2\bar{c}(\bar{c}-c_a)];\quad u=\bar{c}-\bar{c}_a \tag{89.8}$$

(for water).

The arbitrary function Φ_1 is determined from the condition that $t=0$ and $r=r_0$. As a result of this (89.7) is transcribed in the form

$$\frac{c}{c_1}=1-\frac{u}{c_1}=\frac{1-\left(\frac{r}{r_0}-\frac{c_1t}{r_0}\right)^2}{4\frac{r}{r_0}\frac{c_1t}{r_0}}. \tag{89.9}$$

If necessary, more accurate solutions can be used

$$t=\frac{r}{2c_1}\left[\left(\frac{\beta^2}{c_1^2}-1\right)\ln\frac{\frac{\beta}{c_1}-1}{\frac{\beta}{c_1}+1}+2\frac{\beta}{c_1}\right]+\Phi_1\left[2\left(\frac{\beta^2}{c_1^2}-1\right)\right], \tag{89.10}$$

where

$$\beta=u-c=c_1-2c$$

and

$$t=\frac{r}{2\bar{c}_a}\left[\left(\frac{a^2}{\bar{c}_a^2}-1\right)\ln\frac{\frac{a}{\bar{c}_a}-1}{\frac{a}{\bar{c}_a}+1}+2\frac{a}{\bar{c}_a}\right]+\Phi_2\left[\left(2\frac{a^2}{\bar{c}_a^2}-1\right)\right], \tag{89.11}$$

where $a=u+\bar{c}=2\bar{c}-\bar{c}_a$. In this case, equation (89.10), taking into account the condition that for $t=0$, and $r=r_0$, will have the form

$$t=\frac{r}{2c_1}\left\{\left[\left(\frac{\beta^2}{c_1^2}-1\right)\ln\frac{\frac{\beta}{c_1}-1+\sqrt{\frac{r}{r_0}\left(\frac{\beta^2}{c_1^2}-1\right)+1}+1}{\frac{\beta}{c_1}+1+\sqrt{\frac{r}{r_0}\left(\frac{\beta^2}{c_1^2}-1\right)+1}-1}\right]+\right.$$
$$\left.+2\left[\frac{\beta^2}{c_1^2}-\sqrt{\frac{r}{r_0}\left(\frac{\beta^2}{c_1^2}-1\right)+1}\right]\right\}. \tag{89.12}$$

More to the right of the rarefaction wave described by equations (89.9) or (89.12) should be found the wave reflected from the boundary of separation.

The solutions of equations (89.10) and (89.11) are found from the equations

$$\left.\begin{aligned}\frac{\partial\alpha}{\partial t}+\alpha\frac{\partial\alpha}{\partial r}+\frac{\alpha^2-\beta^2}{2r}=0,\\ \frac{\partial\beta}{\partial t}+\beta\frac{\partial\beta}{\partial r}+\frac{\beta^2-\alpha^2}{2r}=0,\end{aligned}\right\} \tag{89.13}$$

in which it is assumed that either $\beta=u-c=c_i-2c$ and $\alpha=\alpha_0=$ const, or $\alpha=u+\bar{c}=2\bar{c}-\bar{c}_a$ and $\beta=\beta_0=$ const.

In accordance with a hypothesis by A.A.BULGAKOV and N.I.POLYAKOV the wave, reflected from the boundary of separation, can be approximated to a stationary wave, i.e. it can be described by the equations

$$\frac{u^2}{2}+\frac{c^2}{k-1}=\frac{A}{2},\qquad 2uc^{\frac{2}{k-1}}=\frac{B}{r^2}. \tag{89.14}$$

In the case when $k=3$ these equations assume the form

$$u^2+c^2=A,\quad 2uc=\frac{B}{r^2}, \tag{89.15}$$

whence

$$\alpha=\sqrt{A+\frac{B}{r^2}},\quad \beta=\sqrt{A-\frac{B}{r^2}}. \tag{89.16}$$

In order to determine the arbitrary function Φ_2 in (89.8) or in (89.11), it is necessary to know the law of motion of the boundary of separation.

Calculations show that the velocity of motion of the boundary of separation of a spherical wave falls more rapidly than in the case of a plane wave, just as one would expect.

In the case of detonation of gaseous mixtures the initial pressures at the shock front will be small, and a liquid can be assumed to be incompressible. As a result of the detonation of condensed explosives , in the case of a spherical explosion, the pressure in the explosion products at the shock front falls off considerably at a distance of about $2r_0$, and as a result of further development of the process a liquid may also be assumed to be incompressible.

It is essential to note that in the approximation we are considering (acoustic) for a compressible liquid, we are justified, in the case of a spherical wave, in using the relationship

$$D_{\text{в}} = \frac{dr}{dt} = \frac{1}{2}(u_{\text{в}} + \bar{c} + \bar{c}_{\text{а}}). \tag{89.17}$$

For $n = 3$, using the relationship $c = \bar{c}_{\text{а}} + u_{\text{в}}$, we obtain

$$D_{\text{в}} = \bar{c} = u_{\text{в}} + \bar{c}_{\text{а}}. \tag{89.18}$$

For an arbitrary value of n,

$$D_{\text{в}} = \frac{1}{2}(u_{\text{в}} + \bar{c} + \bar{c}_{\text{а}}) = \frac{n+1}{2(n-1)}\bar{c} - \frac{3-n}{2(n-1)}\bar{c}_{\text{а}} = \bar{c}_{\text{а}} + \frac{n+1}{4}u_{\text{в}}. \tag{89.19}$$

In order to determine the law of motion of the shock front, it is necessary to evaluate the arbitrary function Φ. The law of motion of the shock front of a spherical shock wave will be differentiated from the law of motion of the shock front of a plane wave in that the velocity of the shock front will decrease more rapidly with distance; therefore for equal time intervals, the length of a spherical shock wave will be less than the length of a plane shock wave.

It can be assumed approximately that, beginning at small distances from the point of explosion (for $r = r_1 > 2r_0$), the law of motion of the front of a spherical shock wave is determined by the relationship

$$D_{\text{в}} = \frac{dr}{dt} = c_{\text{а}} + \frac{n+1}{4}u_{\text{в}} = \bar{c}_{\text{а}} + \frac{n+1}{4}\frac{r_1 u_1}{r} = \bar{c}_{\text{а}} + \frac{r_1 u_1}{r}, \tag{89.20}$$

where $u_{\text{в}}$ for $n = 3$ is determined by the well-known acoustic relationship

$$u_{\text{в}} = \frac{r_1 u_1}{r}, \tag{89.21}$$

and u_1 is the value of the velocity $u_{\text{в}}$ for $r = r_1$.

It is obvious from (89.20) that at a distance of around $(8 - 12)r_0$ the velocity of the shock front becomes practically equal to the initial velocity of sound, since u_1 is of the order of magnitude equal to $c_{\text{а}}$, which follows immediately from experimental data.

It follows from relationship (89.20) and from the isentropy equation that the dependence of the pressure at the shock front on distance can be expressed by the formula

$$(p_s - p_a)(v_a - v_s) = \frac{p_s - p_a}{\rho_a}\left(1 - \frac{\rho_a}{\rho_s}\right) = u_s^3 = \\ = \frac{r_1^2 u_1^2}{r^2} = \frac{p_s}{\rho_a}\left[1 - \frac{1}{\left(\frac{p}{A\rho_0^n} + 1\right)^{\frac{1}{n}}}\right]. \qquad (89.22)$$

Hence, at small distances from the explosion point, where a liquid is still compressible

$$p_s \sim \frac{1}{r^2\left(1 - \frac{\rho_a}{\rho_s}\right)}$$

or

$$p_s \sim \frac{1}{r^2\left[1 - \frac{1}{\left(\frac{p}{A\rho_0^n} + 1\right)^{\frac{1}{n}}}\right]}. \qquad (89.23)$$

At large distances, where a liquid is practically incompressible, or, more precisely its compressibility is subject to a linear law,

$$\Delta p = nA\rho_a^{n-1}\Delta\rho, \qquad (89.24)$$

the pressure will depend on the distance:

$$\Delta p = \frac{\sqrt{nA\rho_a^{n+1}}\, r_1 u_1}{r}, \qquad (89.25)$$

i. e. the acoustic formula will be valid.

Completely analagous conclusions can be drawn also for a cylindrical explosion.

The study of the process of expansion in a liquid of the products of an actual detonation is more complex. However, just as for propagation in air, the explosion field at small distances from the point of explosion (about $(3-5)r_0$) approximates to the explosion field for the case of

an instantaneous detonation.

The solution of the problem of expansion of the sphere of detonation products, assuming that the process of expansion at a certain distance $r_1 \approx 2r_0$, will be equivalent to the process of expansion of an ideal gas in an incompressible medium. Here and henceforth we note that, in accordance with VLASOV, for the detonation products

$$\frac{p}{p_1} = \left(\frac{r_1}{r}\right)^{3k} \tag{89.26}$$

approximately, where $k \approx \frac{7}{5}$, $p_1 = \bar{p}_1 \left(\frac{r_0}{r_1}\right)^6$, $\bar{p}_1 = \frac{\rho_0 D^2}{8}$.

For a spherical wave in an incompressible medium, the basic hydrodynamic equations have the form

$$\frac{\partial u}{\partial t} + u\frac{\partial u}{\partial r} + \frac{1}{\rho_a}\frac{\partial p}{\partial r} = 0; \quad \frac{\partial u}{\partial r} + \frac{2u}{r} = 0 \tag{89.27}$$

and lead to the following general solution

$$ur^2 = f(t); \quad \frac{p - \varphi(t)}{\rho_a} = \frac{df}{r\,dt} - \frac{f^2}{2r^4}, \tag{89.28}$$

where $f(t)$ and $\varphi(t)$ are arbitrary functions of time, so that it may be assumed with a high degree of accuracy that $\varphi(t) = p_a$. As a result of this, the law of motion of the boundary of separation can be written in the form

$$p_1\left(\frac{r_1}{r}\right)^{3k} = p_a + \rho_a\left[\frac{df}{r\,dt} - \frac{f^2}{2r^4}\right], \tag{89.29}$$

so that, at the boundary of separation

$$\frac{df}{dt} = \frac{du}{dt}r^2 + 2ur\frac{dr}{dt} = \frac{du}{dt}r^2 + 2u^2r = \frac{1}{2}\frac{du^2}{dr}r^2 + 2u^2r.$$

and therefore equation (89.29) assumes the form

$$\frac{du^2}{dr} + 3\frac{u^2}{r} = \frac{2p_1}{\rho_a}\frac{r_1^{3k}}{r^{3(k+1)}} - \frac{2p_a}{\rho_a r}. \tag{89.30}$$

Its solution, for the condition that $u = u_1$ for $r = r_1$, has the form

$$u^2 = \left(u_1^2 + \frac{2}{3(k-1)}\frac{p_1}{\rho_a} + \frac{2p_a}{3\rho_a}\right)\left(\frac{r_1}{r}\right)^3 - \left[\frac{2}{3(k-1)}\frac{p_1}{\rho_a}\left(\frac{r_1}{r}\right)^{3k} + \frac{2p_a}{3\rho_a}\right]. \tag{89.31}$$

The limiting distance which the detonation products attain can be determined from relationship (89.31), assuming that $u = 0$:

$$\frac{p_1}{k-1}\left(\frac{r_1}{r}\right)^{3k} + p_a = \left(\frac{3}{2}\rho_a u_1^2 + \frac{p_1}{k-1} + p_a\right)\left(\frac{r_1}{r}\right)^3. \qquad (89.32)$$

Neglecting the first term of the left hand side of the equation, which is small in comparison with p_a and $\frac{p_1}{k-1}\left(\frac{r_1}{r}\right)^3$, and in the right hand side p_a and $\rho_a u_1^2$, which are small in comparison with p_1, we arrive at the expression

$$\left(\frac{r}{r_1}\right)^3 = \frac{p_1}{(k-1)p_a} \qquad (89.33)$$

Applying relationship (89.26) and assuming that $r_1 = 2r_0$, we obtain finally

$$\left(\frac{r}{r_1}\right)^3 = \frac{\rho_0 D^2}{8(k-1)p_a}\left(\frac{r_0}{r_1}\right)^9 = \frac{\rho_0 D^2}{8(k-1)p_a}\frac{1}{16 \cdot 32}. \qquad (89.34)$$

For $\rho_0 = 1.6$ g/cm^3, $D = 7000$ m/sec, $k = 1.4$, we find, for typical condensed explosives, $\left(\frac{r}{r_1}\right)^3 = 500$, or $\left(\frac{r}{r_0}\right)^3 = 500 \cdot 8 = 4000$, which gives $\frac{r}{r_0} \approx 16$.

Thus, the limiting distance differs but slightly from the distance attained by the detonation products in air. With increase of the depth at which the explosion takes place in water, the external counterpressure increases and therefore the limiting volume of the detonation products is decreased in the ratio $\left(\frac{p_a}{p_h}\right)^{1/k}$, where p_h is the counterpressure at a depth h.

The expansion of the detonation products (gaseous bubble) takes place with gradually increasing velocity. Towards the end of the expansion, the pressure of the gas falls below the hydrostatic pressure. As a consequence of this the gas bubble begins to contract with gradually increasing velocity. Compression of the bubble will take place until the increase of pressure inside the bubble is no longer compensated by the inertia of the convergent flow of water. Towards the end of the compression, the pressure inside the bubble becomes greater than the hydrostatic pressure.

Thus, the gaseous bubble will pulsate. With favourable conditions

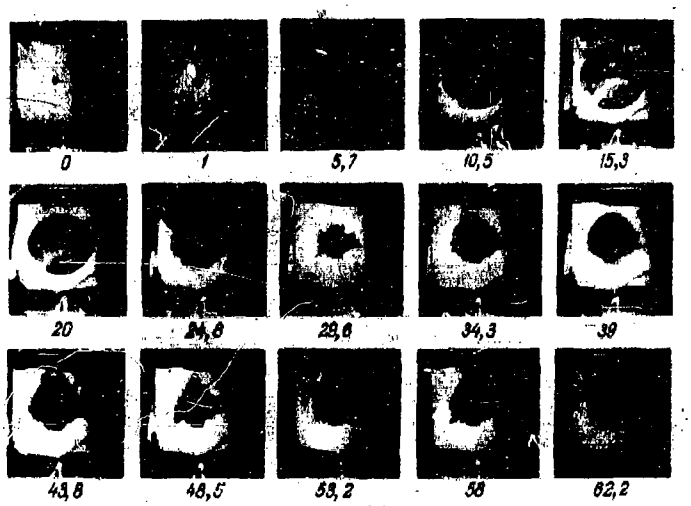
(absence of the effect of boundary surfaces) up to ten or more pulsations of the gaseous bubble will take place. The process of pulsation of the bubble will go on with its simultaneous emergence at the free surface.

Pulsation and emergence of the gaseous bubble can be clearly seen on the series of cine-frames, obtained with high-speed cine-film (Fig. 238).

The variation of the radius of the bubble, according to COLE, for the explosion of a 250 g. charge of tetryl at a depth of 91.5 m. is shown in Fig. 239 as a function of time.

It should be pointed out that use of the solutions in equation (89.28) for a shock wave propagating even in a very slightly compressible medium has no physical significance, since the velocity of propagation of sound in such a medium is always finite and not infinitely large, which follows formally from these solutions. Moreover, it follows from the solution of equation (89.28) that the velocity in the shock wave, more correctly in the compression wave, falls from the boundary of separation to the shock front, although actually the pressure at the front is higher. However, if one assumes that $\varphi(t) = p_*$, then $\varphi(t)$ can be determined from the condition for terminal velocity of the wave.

Figure 258. Pulsation of the gaseous bubble resulting from the explosion of a charge of tetryl. The figures below the frames denote time intervals after detonation in milliseconds.



We note that the equation for an incompressible liquid describes relatively satisfactorily only the law of motion of the boundary of separation. Consequently, in order to describe the acoustic stage of propagation of the wave the acoustic equations should be used, taking into account the nonlinear terms, i.e. to assume that in the travelling wave the relationship

$$u = \int \sqrt{-dp\,dv} = \int c \frac{d\rho}{\rho}. \tag{89.35}$$

is satisfied, and which can be written in the form

$$u \approx c \frac{\Delta\rho}{\rho} = \frac{2}{n-1}(c - c_a), \tag{89.36}$$

whereupon

$$u \sim \frac{1}{r}. \tag{89.37}$$

The momentum possessed by the water behind the shock front can be determined by relationships similar to those which we used in para. 85.

In conclusion, let us consider the case of a point explosion in water. The equation of state for the water can be written in the form

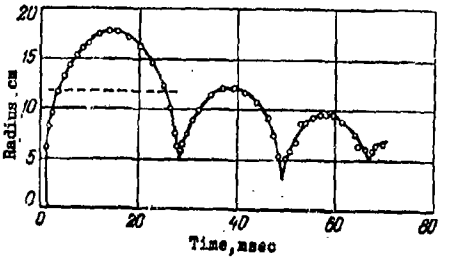
$$p = A(S)(\rho^n - \rho_0^n). \tag{89.38}$$

and the power index can be chosen quite arbitrarily corresponding to the lesser value A. If we accept the approximation that

$$p = A(S)\rho^n \tag{89.39}$$

then it is easy to find solutions for the case of a point explosion. These solutions become particularly simple for $n = 7$. Actually, by using the basic solutions for similarity-solution type motion

Figure 239. Dependence of radius of gaseous bubble on time interval after detonation.



$$\frac{d\ln z}{dx} = \frac{(a_1 - x)\frac{d\ln y}{dx} - (n-1)}{[N(n-1)+n+1]x - 2} =$$

$$= \frac{(a_1 - x)^2 - y}{y\left[\frac{2(a_1-1)}{n} + x(N+1)\right] - x(1-x)(a_1 - x)}, \tag{89.40}$$

$$d\ln\xi + d\ln(x - a_1) + \frac{(N+1)x}{x - a_1}d\ln z = 0 \tag{89.41}$$

and seeking the solution in the form

$$x = x_1 = \frac{2a_1}{n+1}, \quad y = y_1 = \frac{2n(n-1)a_1^2}{(n+1)^2}, \tag{89.42}$$

we arrive at the following result:

$$u = \frac{2a_1}{n+1}\frac{r}{t}, \qquad c = \frac{\sqrt{2n(n-1)}}{n+1}\frac{a_1 r}{t}. \tag{89.43}$$

As a result of this the following conditions should be fulfilled

$$[N(n-1)+n+1]x_i=2;$$
$$y_i\left[\frac{2(a_i-1)}{n}+x_i(N+1)\right]=x_i(1-x_i)(a_i-x_i). \qquad (89.44)$$

Hence, we see that since

$$a_i=\frac{2}{N+3} \qquad n=\frac{\gamma+1}{N-1}. \qquad (89.45)$$

For $N=2$ we obtain $n=7$. As a result of this

$$\rho\sim z\sim\frac{r}{t^{0.4}}. \qquad (89.46)$$

The law of motion of the shock front is expressed by the relationship

$$D_s=\frac{2}{5}\frac{r}{t}\sim r^{-\frac{3}{2}}. \qquad (89.47)$$

The dependence of the pressure on distance is expressed by the relationship

$$p\sim r^{-3}. \qquad (89.48)$$

The respective constants can be determined from the energy equation.

With this we conclude the short discussion of the basic laws of the most important types of non-stationary motion in liquids. We note only that after passage of the shock front through the surface of a liquid cavitation commences, which leads to the ejection of atomised liquid into the atmosphere.

§ 90. Some Problems concerned with the Theory of an Explosion in a Liquid.

In order to interpret some of the experimental data relating to the study of shock wave propagation in liquids and the interaction of a compressed liquid with various obstacles, it is of great interest to consider theoretically a number of ideas relevant to this range of problems.

First of all we shall consider the question of limiting compression of a liquid. Suppose that in a volume a there is an explosive and in a volume b there is any liquid (Fig.240). The walls of the vessel containing this liquid

and also the explosive we shall assume to be absolutely solid. Knowing the calorific value and density of the explosive, and also the density of the liquid and its equation of state, we find the limiting volume which this liquid occupies after detonation of the explosive, resulting from its compression by the detonation products.

Suppose the equation of state of the explosion products has the form

$$p = A_0 \rho^k, \tag{90.1}$$

and the equation of state of the liquid has the form

$$p = A(\rho^n - \rho_a^n) \tag{90.2}$$

(where ρ_a is the initial density of the liquid) (we shall neglect changes of entropy, which is permissible for pressures up to 200,000 kg/cm^2). Then the following relationships are obvious for the limiting state of equilibrium of the explosion products and of the liquid :

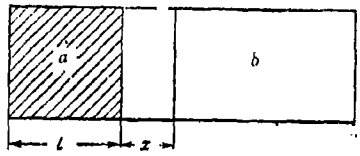
$$\bar{p} = p_i \left(\frac{\bar{\rho}}{\rho_0}\right)^k = \bar{p}_i \left(\frac{l}{l+\bar{x}}\right)^k = A\rho_a^n \left[\left(\frac{\bar{\rho}^*}{\rho_a}\right)^n - 1\right] = A\rho_a^n \left[\left(\frac{\lambda}{\lambda - \bar{x}}\right)^n - 1\right], \tag{90.3}$$

where $\bar{x}$ defines the position of the boundary of separation of the explosion products and the liquid in the equilibrium state, $\bar{\rho}$ and $\bar{\rho}^*$ are the densities of the explosion products and of the liquid in this state, $\bar{p}$ is the equilibrium pressure $\bar{p}_i$ is the initial average pressure of the explosion products,

$$\bar{p}_i = \frac{\rho_0 D^2}{2(k+1)}, \tag{90.4}$$

where ρ_0 is the initial density of the explosive, and D is the detonation velocity.

Figure 240. Compression of a liquid by the explosion products.



Since the initial effective velocity of sound in the liquid is

$$c_a^* = \sqrt{nA\rho_a^{n-1}} = ac_a, \tag{90.5}$$

where c_a is the normal initial velocity of sound in the liquid (the coefficient a is a correction which takes into account the inaccuracy of the equation of state (90.2) for small pressures), then relationship (90.5) can be written in the form

$$\frac{n}{2a^2(k+1)}\frac{\rho_0 D^2}{\rho_a c_a^2} = \left(1+\frac{\bar{x}}{l}\right)^k\left[\left(\frac{\frac{\lambda}{l}}{\frac{\lambda}{l}-\frac{\bar{x}}{l}}\right)^n - 1\right]. \tag{90.6}$$

Hence, it is possible to determine that

$$\frac{\bar{x}}{l} = f\left(\frac{\rho_0}{\rho_a};\ \frac{D}{c_a};\ \frac{\lambda}{l}\right). \tag{90.7}$$

For a specified explosive and liquid

$$\frac{\bar{x}}{l} = f\left(\frac{\lambda}{l}\right).$$

If we designate

$$\frac{n}{2a^2(k+1)}\frac{\rho_0 D^2}{\rho_a c_0^2} = A_1.$$

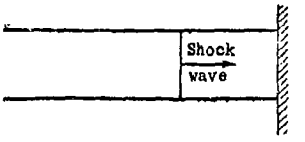
then it can be shown in the general case that

$$\frac{\bar{x}}{l} = f\left(A_1;\ \frac{\lambda}{l}\right). \tag{90.8}$$

Calculations for a typical explosive and water show that for $\lambda/l = 1$, the density of the water is increased by no more than 50%. It is well-known that the initial density at the shock front in water can be greater.

The next problem which must be solved in order to analyse the processes involved in shock wave propagation in water, is the problem concerning reflection of a shock wave from a non-deformable wall (Fig.241).

Figure 241. Reflection of a shock wave in water from a non-deformable wall,



We shall conduct the discussion for the case of reflection of a plane wave impacting at right angles to the wall. We shall also, as above, neglect the change of entropy on reflection. It is well-known that even as a result of reflection of an air shock wave the entropy does not increase very strongly; on reflection of a detonation wave it is increased but little. This is associated with the fact that for the detonation wave the Mach number

$$M = \frac{u_i}{c_i} < 1 = \frac{1}{3}.$$

For the liquid, in the impacting wave $\frac{u}{c} < 1$ (up to pressures not exceeding $1\ 0^6$ kg/cm^2), therefore the change of entropy can, in fact, be neglected.

If the reflection be considered as an acoustical approximation, as we have decided to so do, then for the wave proceeding from left to right the Riemann invariant is conserved up to and after reflection, which, in the case of the equation of state (90.2) is written in the following manner :

$$u + \frac{2}{n-1} c = u_{\text{refl}} + \frac{2}{n-1} c_{\text{refl}}. \tag{90.9}$$

At the instant of reflection at the wall

$$u_{\text{refl}} = 0 \text{ and } c_{\text{refl}} = c + \frac{n-1}{2} u. \tag{90.10}$$

Since in the impacting shock wave, which propagates as a result of expansion of the explosion products,

$$c = c_a + \frac{n-1}{2} u, \tag{90.11}$$

then

$$c_{\text{refl}} = 2c - c_a, \tag{90.12}$$

hence it follows that

$$\Delta_{\text{refl}} = c_{\text{refl}} - c = 2\Delta c = 2(c - c_a). \tag{90.13}$$

The pressure and velocity of sound are connected by the relationship

$$p - p_a = B\left(c^{\frac{2n}{n-1}} - c_a^{\frac{2n}{n-1}}\right), \tag{90.14}$$

therefore

$$p_{refl} - p_a + Bc_a^{\frac{2n}{n-1}} = \left[2\left(p - p_a + Bc^{\frac{2n}{n-1}}\right)^{\frac{n-1}{2n}} - B^{\frac{n-1}{2n}} c_a\right]^{\frac{2n}{n-1}}.$$

Let $p - p_a = \Delta p$, then

$$\Delta p_{refl} = p_{refl} - p_a = -Bc_a^{\frac{2n}{n-1}} + Bc_a^{\frac{2n}{n-1}} + 2(p - p_a),$$

whence

$$\Delta p_{refl} = 2\Delta p, \tag{90.15}$$

which is valid for a weak wave.

In the case of a strong wave, neglecting the quantities p_a and c_a, we have

$$p_{refl} = 2^{\frac{2n}{n-1}} p. \tag{90.16}$$

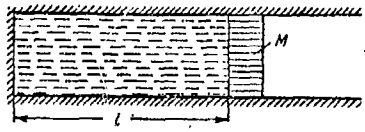
The result depends strongly on the power index n in equation (90.14), consequently it is not precise. For $n = 3$, $p_{refl} = 8p$, and for $n \to \infty$ $p_{refl} = 4p$. The true value of n for pressures in the range 1 to 10^6 kg/cm^2 lies between 5 and 8. A difference in pressures of a factor of two is obtained.

It can be assumed that by measuring the ratio between the "incident" and the "reflected" pressures, we can determine the value of n, however these same measurements are unfortunately characterized by low accuracy.

We shall consider now the problem of projection of a solid body by a compressed liquid (Lagrange's problem in internal ballistics, where the projection of a solid body by a compressed gas is considered). Suppose we have a tube, filled with a compressed liquid (Fig.242); the cross sectional area of the tube is equal to unity. In front of the liquid there is a body of mass M. The density of the liquid is ρ_l , the pressure is p_l , the mass of the liquid $m = l\rho_l$. We shall choose initially a coordinate of the liquid - projectile boundary and we shall assume that motion is initiated at time $t = 0$. The motion is determined by the equations :

$$x = (u - c)\,t + F(C),$$
$$u = \frac{2}{n-1}(c_i - c). \quad (90.17) \qquad (90.17)$$

Figure 242. Projection of a body by a compressed liquid.



In accordance with the Law of Conservation of Momentum, the following relationship will hold good at the surface of the body

$$M\frac{du}{dt} = Mu\frac{du}{dx} = p, \qquad (90.18)$$

assuming the equation of state to be in the form

$$p = A(\rho^3 - \rho_a^3) = B(c^3 - c_a^3), \qquad (90.19)$$

where

$$c = \sqrt{3A}\rho, \quad B = \frac{1}{\sqrt{27A}}, \quad (n = 3),$$

we shall transcribe equation (90.18) in the form

$$M\frac{du}{dt} = Mu\frac{du}{dx} = B(c^3 - c_a^3). \qquad (90.20)$$

Since

$$u = c_i - c, \quad du = -dc,$$

then, from (90.20) we obtain

$$M\frac{dc}{dt} = M(c_i - c)\frac{dc}{dx} = -B(c^3 - c_a^3). \qquad (90.21)$$

On integrating this equation we have

$$t = -\frac{M}{B}\int \frac{dc}{c^3 - c_a^3} = \frac{M}{3Bc_a^2}\left[\frac{1}{2}\ln\frac{(c-c_a)^2}{c^2 + cc_a + c_a^2} - \sqrt{3}\tan^{-1}\frac{\sqrt{3}c}{c + 2c_a}\right] + \text{const};$$

$$x = -\frac{M}{B}\int \frac{(c_i - c)\,dc}{c^3 - c_a^3} = \frac{Mc_i}{3Bc_a^2}\left[\frac{1}{2}\ln\frac{(c-c_a)^2}{c^2 + cc_a + c_a^2} - \sqrt{3}\tan^{-1}\frac{\sqrt{3}c}{c + 2c_a}\right] + \frac{M}{B}\int \frac{c\,dc}{c^3 - c_a^3} =$$

$$= \frac{Mc_i}{3Bc_a^2}\left[\frac{1}{2}\ln\frac{(c-c_a)^2}{c^2 + cc_a + c_a^2} - \sqrt{3}\tan^{-1}\frac{\sqrt{3}c}{c + 2c_a}\right] + \frac{M}{3Bc_a}\left[\frac{1}{2}\ln\frac{(c-c_a)^2}{c^2 + cc_a + c_a^2} + \frac{\sqrt{3}}{2}\tan^{-1}\frac{\sqrt{3}c}{c + 2c_a}\right],$$

whence

$$x=\frac{M}{3Bc_a}\left[\frac{1}{2}\left(\frac{c_a}{c_a}+1\right)\ln\frac{(c-c_a)^2}{c^2+cc_a+c_a^2}-\right.$$
$$\left.-\frac{\sqrt{3}}{2}\left(2\frac{c_i}{c_a}-1\right)\tan^{-1}\frac{\sqrt{3}c}{c+2c_a}\right]+\text{const.} \qquad (90.22)$$

Since for $t=0$ $x=0$, $u=0$, $c=c_i$, then

$$t=\bar{t}(c)=\frac{M}{6Bc_a^2}\left[\ln\left(\frac{c-c_a}{c_i-c_a}\right)^2\frac{c_i^2+c_ic_a+c_a^2}{c^2+cc_a+c_a^2}-\right.$$
$$\left.-2\sqrt{3}\left(\tan^{-1}\frac{\sqrt{3}c}{2c_a+c}-\tan^{-1}\frac{\sqrt{3}c_a}{2c_a+c_i}\right)\right], \qquad (90.23)$$

$$x=\bar{x}(c)=\frac{M}{6Bc_a}\left[\ln\left(\frac{c-c_a}{c_i-c_a}\right)^2\frac{c_i^2+c_ic_a+c_a^2}{c^2+cc_a+c_a^2}\left(\frac{c_i}{c_a}+1\right)-\right.$$
$$\left.-\sqrt{3}\left(2\frac{c_i}{c_a}-1\right)\left(\tan^{-1}\frac{\sqrt{3}c}{2c_a+c}+\tan^{-1}\frac{\sqrt{3}c_a}{2c_a+c_i}\right)\right]. \qquad (90.24)$$

Knowing that $t=\bar{t}(c)$ and $x=\bar{x}(c)$, we determine $F(c)=\bar{x}(c)-(u-c)\bar{t}(c)$.

The rarefaction wave in the liquid will be determined by the relationship

$$x-\bar{x}(c)=(u-c)(t-\bar{t}(c)),\quad u+c=c_i. \qquad (90.25)$$

The law of motion of the projectile is described by relationships (90.23) and (90.24), where c is introduced as a parameter.

At time $t=\tau=\frac{l}{c_i}$, the front of the rarefaction wave reaches the wall located at the section $x=-l$, and gives rise to a new reflected rarefaction wave.

This wave will be characterised by the equations

$$x-\bar{x}=(u-c)(t-\bar{t}),$$
$$x=(u+c)t+F(u+c). \qquad (90.26)$$

We determine the arbitrary function $F(u+c)$ in the following manner. In the section $x=-l$, $u=0$ for any value of t. Therefore

$$F(0+c)=-[l+(0+c)t];$$

since

$$-(l+\bar{x})=(0-c)(t-\bar{t}),$$

then

$$t=\bar{t}+\frac{l+\bar{x}}{0+c}\quad\text{and}\quad F(0+c)=-\left[l+(0+c)\left(\bar{t}+\frac{l+\bar{x}}{0+c}\right)\right]$$

or

$$F(0+c) = -[2l + \bar{x} + (0+c)\bar{t}].$$

Now we must bear in mind, that

$$\bar{t} = \bar{t}(c) = \bar{t}(0+c), \quad \bar{x} = \bar{x}(c) = \bar{x}(0+c).$$

Since we have the further relationship $u - c = -c_a$, in order to determine $\bar{t}(c)$ and $\bar{x}(c)$, then

$$c = \frac{u+c-c_a}{2} \quad \text{and} \quad f(c) \to f\left(\frac{u+c-a_a}{2}\right) = f(u+c).$$

Thus, for $u \neq 0$ we have

$$F(u+c) = -[2l + (u+c)\bar{t}(u+c) + \bar{x}(u+c)] \tag{90.27}$$

and

$$x = (u+c)t - 2l - \bar{x} - (u+c)\bar{t}. \tag{90.28}$$

Finally, we write equations for the reflected wave in the form

$$\left.\begin{aligned} x - \bar{x} &= (u-c)(t-\bar{t}), \\ x - \bar{x} + 2l &= (u+c)(t-\bar{t}), \end{aligned}\right\} \tag{90.29}$$

where $\bar{t} = \bar{t}(u+c)$, $\bar{x} = \bar{x}(u+c)$, whereupon $c \to \frac{u+c-c_a}{2}$.

Adding, and subtracting equation (90.29) we obtain

$$\left.\begin{aligned} x + l &= u(t-\bar{t}), \\ l &= c(t-\bar{t}). \end{aligned}\right\} \tag{90.30}$$

For $u > 0$, in fact, $x = -l$, which is proof of the validity of the determination of $F(u+c)$. The wave reflected from the wall will be propagated to the right according to the law

$$\frac{dx}{dt} = u + c. \tag{90.31}$$

From the second equation of (90.29) we obtain

$$dx = \frac{d\bar{x}}{d(u+c)} d(u+c) + d(u+c)(t-\bar{t}) + \\ + (u+c)\,dt - (u+c)\frac{d\bar{t}}{d(u+c)} d(u+c). \tag{90.32}$$

Comparing (90.31) and (90.32) we find

$$t = \bar{t} + (u+c)\bar{t}' - x', \tag{90.33}$$

where the derivatives are taken with respect to $(u+c)$.

It follows from (90.32) that

$$x = \int (u+c)[2\bar{t}' + (u+c)\bar{t}'' - \bar{x}''] d(u+c). \qquad (90.34)$$

Equations (90.33) and (90.34) determine the front of the reflected rarefaction wave in parametrical form.

Solving equations (90.23),(90.24), (90.33) and (90.34) simultaneously we determine the time $\bar{t}$ and the coordinate $\bar{\bar{x}}$ when the reflected wave reaches the projectile.

The problem can be further condidered as a normal thermodynamic approximation, assuming that thepressure is independent of the distance, but is dependent only on the time. With other conditions

$$p = A(\rho^3 - \rho_a^3),$$

where

$$\bar{\bar{\rho}}\,\bar{\bar{x}} = \rho x \qquad (90.35)$$

($\bar{\bar{\rho}}$ is the density at time $\bar{t}$ for $x = \bar{\bar{x}}$, i.e. near the projectile). Consequently,

$$p = A\left(\bar{\bar{\rho}}^3 \frac{\bar{\bar{x}}^3}{x^3} - \rho_a^3\right),$$
$$M\frac{du}{dt} = Mu\frac{du}{dx} = A\left(\bar{\bar{\rho}}^3 \frac{\bar{\bar{x}}^3}{x^3} - \rho_a\right). \qquad (90.36)$$

Hence,

$$\frac{M}{A}u^2 = \frac{M}{A}\bar{\bar{u}}^2 + \bar{\bar{\rho}}^3\bar{\bar{x}} + 2\rho_a^3\bar{\bar{x}} - \left(\bar{\bar{\rho}}^3\frac{\bar{\bar{x}}^3}{x^2} + 2\rho_a^3 x\right). \qquad (90.37)$$

This solution is significant whilst $\rho \geqslant \rho_a$. For $\rho = \rho_a$

$$\rho_a x_{\text{lim}} = \bar{\bar{\rho}}\,\bar{\bar{x}}, \qquad (90.38)$$

$$u_{\text{lim}}^2 = u^2 + \frac{A\rho_a^3}{M}[x_{\text{lim}} + 2x]\left(\frac{x_{\text{lim}}}{\bar{\bar{x}}} - 1\right)^2. \qquad (90.39)$$

Later, the motion of the body will be inertial if the external resistance is not taken into account. Since expansion of the liquid can take place only for values of $\rho \geqslant \rho_a$, then the limiting velocity which may be acquired by the liquid as a result of free expansion in vacuo cannot exceed the value

$$u_{max} = c_i - c_a,$$

or in the more general case

$$u_{max} = \frac{2}{n-1}(c_i - c_a). \qquad (90.40)$$

Thus, equation (90.39) is valid only in the case when $u_{lim} \leqslant u_{max}$, which is fulfilled. After u attains the value u_{max}, further expansion is quite impossible and motion will take place inertially.

In the wave reflected from the projectile

$$x = x_{proj} = x_{lim} \quad u = u_{proj} = u_{lim}$$

as a result of this

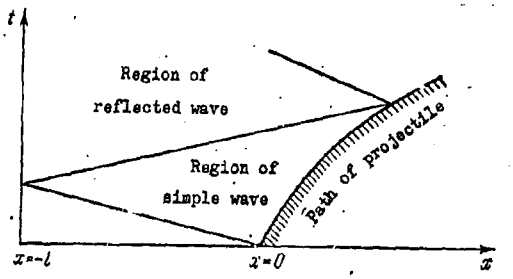
$$x_{lim} = \frac{\bar{\rho}\bar{x}}{\rho_0}. \qquad (90.41)$$

Obviously, the condition should also be fulfilled that

$$\bar{\rho}\bar{x} = m.$$

However, because of the fact that for $t = \bar{t}$ the density at different values of x is different, this condition is not precisely fulfilled. Therefore it is essential to determine $\bar{\rho}$ precisely from the condition of equation (90.41). The difference in the determinations of $\bar{\rho}$ will be a measure of the accuracy of the "thermodynamic" approximation.

Figure 245. System of waves in a liquid created by a projectile.

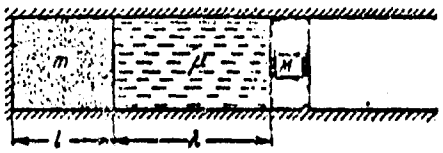


The system of waves created by the projectile is shown in Fig. 245.

§ 91. Lagrange's Problem for the system Gas - Liquid - Projectile.

Now let us consider the more general problem. Suppose that in a tube, with an area of cross section $s = 1$, an explosive charge of mass m is detonated in a volume l; to the right is a liquid of volume λ and mass μ_0. The liquid is in contact with a projectile of mass M (Fig. 244).

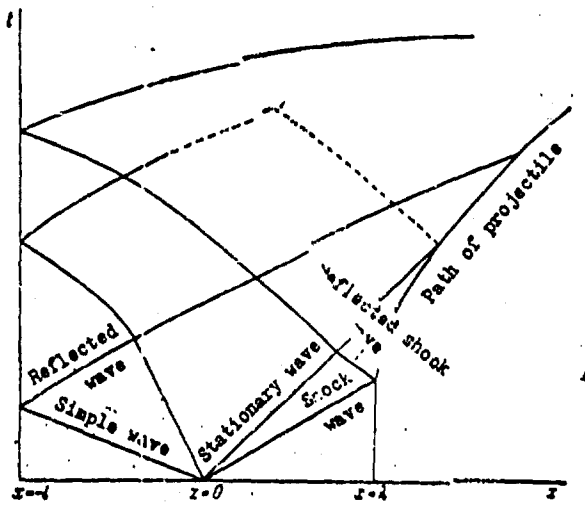
Figure 244. Projection of a solid body by a Gas - liquid system.



Initially, we shall take a coordinate at the boundary of separation of the explosive and the liquid. The detonation, which we shall assume to be instantaneous, occurs at time $t = 0$.

The system of waves originating from this is shown in Fig. 245.

Figure 245. System of waves originating in a gas and a liquid by the projection of a solid body.



Best Available Copy

The first rarefaction wave (reflected) passing through the explosion products is described by the equations

$$x=(u-c)t, \quad u=\bar{c}_1-c \tag{91.1}$$

within the interval of time $\bar{c}_1 t \leqslant x \leqslant (u_x-c_x)t$, where

$$\bar{c}_1=\frac{1}{2}\sqrt{\frac{3}{2}}D.$$

A stationary wave will be propagated to the right

$$u=u_x, \quad c=c_x, \quad p=p_x \tag{91.2}$$

within the interval of time $(u_x-c_x)t \leqslant x \leqslant u_x t$, whereupon u_x and p_x are determined from the equation

$$u_x=\bar{c}_1\left[1-\left(\frac{p_x}{p_1}\right)^{\frac{1}{3}}\right]=\bar{c}_a\left[\frac{\sqrt{3A}\,\rho_a}{\bar{c}_a}\left(1+\frac{p}{A\rho_a^3}\right)^{\frac{1}{3}}-1\right], \tag{91.3}$$

where ρ_a and $\bar{c}_a$ are the initial density and velocity of sound in the liquid, for which the equation of state is defined by (90.19). A stationary shock wave will pass through the liquid

$$\left.\begin{aligned} u&=u_x, \\ \bar{c}&=\bar{c}_s, \\ p&=p_s=p_x. \end{aligned}\right\} \tag{91.4}$$

The shock wave will reach the projectile at time $t_1=\frac{\lambda}{D_s}$. The velocity of the shock wave is

$$D_s=\frac{u_x+\bar{c}_s+\bar{c}_a}{2},$$

since

$$u_x=\bar{c}_s-\bar{c}_a,$$

then

$$D_s=\bar{c}_s=u_x+\bar{c}_a \text{ and } t_1=\frac{\lambda}{\bar{c}_s}=\frac{\lambda}{u_x+\bar{c}_a}. \tag{91.5}$$

As a result of reflection of the shock wave from the projectile, a

reflected shock wave originates which proceeds to the left. The wave is characterised by the equations:

$$\left.\begin{aligned} x &= (u-\bar{c})\,t+\Phi(u-\bar{c}),\\ u+\bar{c} &= u_s+\bar{c}_s, \end{aligned}\right\} \tag{91.6}$$

where $\Phi(u-\bar{c})$ is the same as in the previous problem (cf. § 90). Here and henceforth, for the parameters characterising the liquid, we shall put a line above, except for the velocity and the pressure p.

At time $t_2=\frac{l}{c_1}$ the rarefaction wave passing through the explosion products is reflected from the wall and a wave is originated which is described by the equation

$$u-c=\frac{x}{t},\quad u+c=\frac{x+2l}{t}. \tag{91.7}$$

At time $t_3=\frac{l}{c_m}$ in the section

$$x_3=-l+u_m t_3=l\left(\frac{u_m}{c_m}-1\right), \tag{91.8}$$

the simple wave

$$u-c=u_m-c_m,\quad u+c=\frac{x+2l}{t}. \tag{91.9}$$

originates.

The rarefaction wave (91.6) moving in the liquid, at time $t_4=\frac{2l}{c_m}$ in the section

$$x_4=2l\frac{u_m}{c_m} \tag{91.10}$$

reaches the boundary of separation, and the wave

$$x=(u-\bar{c})\,t+\Phi(u-\bar{c}),\quad x=(u+\bar{c})\,t+F(u+\bar{c}), \tag{91.11}$$

originates, whereupon $F(u+\bar{c})$ can be found from the obvious conditions that at the boundary of separation the velocity and pressure to left and right are equal, and as a result of this

$$u=\frac{dx}{dt}. \tag{91.12}$$

However, the form of this function is extremely complex (See K.P.STANYUKOVICH " Non-stabilising Motion in Continuous Media", , § 68). The final solution will also be extremely complex, since in the newly-originating waves $\Phi(u-\bar{c})$ and $F(u+\bar{c})$, should be taken into account.

It is of considerable interest to consider the limiting phase of the motion. We know that in reflected waves the pressure depends slightly on the coordinate x and falls rapidly with time. It can be assumed that this same law will be valid in the wave (91.6) and in all succeeding waves.

First of all it is necessary to elucidate the law of distribution of velocity inside the liquid. In the limiting state, for $t \to \infty$

$$\bar{c} \to \bar{c}_a \quad \text{and} \quad p \to p_a \quad ;$$

as a result of this

$$u = xf(t) + \varphi(t) \tag{91.15}$$

and

$$u = u_0 = \text{const.} \tag{91.14}$$

are possible. We shall establish which of these ywo laws is valid.

The maximum flow velocity of the products from an instantaneous detonation in vacuo is

$$u_{max} = \bar{c}_i . \tag{91.15}$$

The liquid will have this same velocity for the condition that its mass, and the mass of the projectile tend to zero. On the other hand, as a result of disintegration of the compressed liquid, its maximum velocity is

$$\bar{u}_{max} = \bar{c}_s - \bar{c}_a. \tag{91.16}$$

Obviously, if $u_{max} \geqslant \bar{u}_{max}$, i.e. if

$$\bar{c}_i > \bar{c}_s - \bar{c}_a, \tag{91.17}$$

then the liquid will move with constant velocity, since the detonation

products behind will "speed up" the liquid.

As a result of the final mass of the liquid and of the projectile, it is necessary, for constant velocity, to obtain an inequality for the velocity of motion of the boundary of separation between the explosion products and the liquid :

$$u_{x\max} > \bar{c}_s - \bar{c}_a. \tag{91.18}$$

In the contrary case when

$$u_{x\max} \leqslant \bar{c}_s - c_a, \tag{91.19}$$

the velocity in the leading portion of the liquid will be greater than at the boundary of separation and the regime of motion of the liquid (91.13) is established, for which $u \sim x$. The wave (91.9), propagating in the explosion products, is characteristic in that the pressure in it is greater to the right than to the left (this is a compression wave). The compression wave moving through the liquid will "drag away" the particles of liquid to the left, reducing their velocity, whereupon this process will be propagated from left to right, which leads to a velocity distribution defined by relationship (91.13). If $m > \mu + M$, the "ramming" process of the liquid will begin again, which leads to the law described by equation (91.14). If $m < \mu + M$, then the flow is defined by equation (91.15).

Let us explain how either the condition $\bar{c}_l \geqslant \bar{c}_s - \bar{c}_a$ or the stronger condition $\bar{c}_l > \bar{c}_s - \bar{c}_a$ (91.20) can be attained.

The equation of state of the explosion products has the form

$$p = A_0 \rho^3, \tag{91.21}$$

the equation of state of the liquid is

$$p = A(\bar{\rho}^3 - \bar{\rho}_a^3). \tag{91.22}$$

For the explosion products we write

$$p = B_0 c^8 \tag{91.23}$$

and for the liquid

$$p = B(\bar{c}^3 - \bar{c}_0^3). \tag{91.24}$$

At the boundary of separation between the explosion products and the liquid $p_x = p_0$.

In the case $\mu = M \to 0$, the pressure in an infinitely thin layer of liquid will be

$$\bar{p}_1 = \frac{\rho_0 D^2}{8}. \tag{91.25}$$

Therefore

$$B(\bar{c}_0^3 - \bar{c}_0^3) = B_0 \bar{c}_1^3.$$

whence

$$\bar{c}_0^3 = \frac{B_0}{B}\bar{c}_1^3 + \bar{c}_0^3. \tag{91.26}$$

The condition that $c_1 > \bar{c}_0 - \bar{c}_0$ gives $(c_1 + \bar{c}_0)^3 > \frac{B_0}{B}c_1^3 + c_0^3$, whence

$$3\bar{c}_0(\bar{c}_1 + \bar{c}_0) > \left(\frac{B_0}{B} - 1\right)\bar{c}_1^2 \tag{91.27}$$

or

$$3\frac{c_0}{c_1}\left(1 + \frac{c_0}{c_1}\right) > \frac{B_0}{B} - 1.$$

Since for trotyl

$$B_0 = \frac{4}{3}\sqrt{\frac{2}{3}} \cdot 10^{-6}; \quad \bar{c}_1 = 4.5 \cdot 10^5 \text{ cm/sec},$$

and for water

$$B = \frac{5\sqrt{3}}{9} \cdot 10^{-6}, \quad c_0 = 1.5 \cdot 10^5 \text{ cm/sec},$$

then we obtain

$$\frac{4}{3} > \frac{4}{3}\sqrt{\frac{2}{3}}\frac{9}{5\sqrt{3}} - 1 = \frac{4\sqrt{2}}{5} - 1 = 1.12 - 1 = 0.12. \tag{91.28}$$

Consequently, the inequality (91.20) for infinitely small masses of liquid

and projectile is attained. It can be assumed that it is also attained for final masses of liquid and projectile not exceeding certain values.

Let us pass on to finding the limiting velocities of motion of the liquid and of the projectile for the most general law of distribution of velocity in the liquid, when

$$u = xf(t) + \varphi(t)$$

and

$$\bar{\rho} = \frac{\bar{\alpha}}{t}, \tag{91.29}$$

where $\bar{\alpha}$ = const.

For the detonation products, as usual, we take

$$u = x\psi(t), \quad \rho = \frac{\alpha}{t}. \tag{91.30}$$

The Law of Conservation of Mass for the explosion products and for the liquid will respectively have the form

$$m = \int_0^{u_x t} \rho\, dx = \frac{\alpha}{t}\int_0^{u_x t} dx = \alpha u_x = \alpha x_x \psi(t); \tag{91.31}$$

$$\mu = \int_{u_x t}^{u_0 t} \bar{\rho}\, dx = \frac{\bar{\alpha}}{t}\int_{u_x t}^{u_1 t} dx = \bar{\alpha}(u_0 - u_x) = \bar{\alpha}(x_0 - x_x) f(t). \tag{91.32}$$

Here u_x and x_x are the velocity and position of the boundary of separation between the explosion products and the liquid, u_0 and x_0 are the velocity and position of the projectile.

As a result of this, the relationship

$$u_x = x_x\psi(t) = x_x f(t) + \varphi(t),$$

is fulfilled, whence

$$x_x = \frac{\varphi(t)}{\psi(t) - f(t)}, \quad u_x = \frac{\varphi(t)\psi(t)}{\psi(t) - f(t)}. \tag{91.33}$$

Since for $t \to \infty$ u_x = const and $x_x = u_x t$ within the limit, then

$$\psi(t) = \frac{1}{t}, \quad \varphi(t) = u_x(1 - tf(t)).$$

Thus, for the explosion products

$$u = \frac{x}{t}, \tag{91.34}$$

$$m = \alpha \frac{x_\infty}{t}. \tag{91.35}$$

For the liquid

$$\mu = \bar{\alpha}(x_0 - x_x) f(t), \tag{91.36}$$

$$u = xf(t) + u_x [1 - tf(t)] = u_x + f(t)[x - u_x t]. \tag{91.37}$$

We now write the Law of Conservation of Energy

$$mQ = \frac{m\bar{c}_1^2}{k(k-1)} = \frac{mD^2}{2(k^2-1)} = \frac{1}{2}\int_0^{u_\infty t} \rho u^2 dx + \frac{1}{2}\int_{u_\infty t}^{u_0 t} \bar{\rho} u^2 dx + \frac{Mu_0^2}{2} \tag{91.38}$$

The last term in the right hand portion takes into account the kinetic energy of the projectile; the left hand portion determines the initial energy of the explosive charge. We shall neglect the potential energy. Since $p \sim \rho^k$, $\alpha \int \rho\, dx \sim \frac{x}{t}$, then the integral $\int \rho^k dx \sim \frac{1}{t^k}\int dx \sim \frac{x}{t}\frac{1}{t^{k-1}} \to 0$

for $t \to \infty$;

$$\frac{1}{2}\int_0^{u_\infty t} \rho u^2 dx = \frac{a}{2t^3}\int_0^{u_\infty t} x^2 dx = \frac{ax_\infty^3}{ft^3} = \frac{au_\infty^3}{6} = \frac{mu_\infty^2}{6},$$

$$\frac{1}{2}\int_{u_\infty t}^{u_0 t} \bar{\rho} u^2 dx = \frac{\bar{\alpha}}{2t}\int_{u_\infty t}^{u_0 t} [f(t)(x - u_\infty t) + u_\infty]^2 dx =$$

$$= \mu\left[\frac{f^2t^2}{6}(u_0^2 + u_0 u_\infty + u_\infty^2) + \frac{ft(1-ft)}{2}u_x(u_0 + u_\infty) + \frac{(1-ft)^2}{2}u_\infty^2\right].$$

If we introduce $\theta = f(t)t$, , then the latter relationship assumes the form

$$\frac{1}{2}\int_{u_\infty t}^{u_0 t} \bar{\rho} u^2 dx =$$

$$= \frac{\mu}{6}\{\theta^2(u_0^2 + u_0 u_x + u_\infty^2) + 3u_x(1-\theta)[\theta(u_0 + u_\infty) + (1-\theta)u_x]\}.$$

Thus, the energy balance is

$$mQ = \frac{mD^2}{2(k^2-1)} = \frac{mu_\infty^2}{6} + \frac{\mu}{6}\{\theta^2(u_0^2 + u_0u_\infty + u_\infty^2) + \\ + 3u_\infty(1-\theta)[\theta(u_0+u_\infty) + (1-\theta)u_\infty]\} + \frac{Mu_0^2}{2}. \qquad (91.39)$$

Since it follows from (91.32) that

$$f(t) = \frac{u_0 - u_\infty}{x_0 - x_\infty},$$

then it can be assumed, within the limit, that $f(t) = \frac{1}{t}$ or that $\theta = 1$ and

$$mQ = \frac{mu_\infty^2}{6} + \frac{\mu}{6}(u_0^2 + u_0u_\infty + u_\infty^2) + \frac{Mu_0^2}{2}. \qquad (91.40)$$

As a result of this, for the liquid and also for the explosion products

$$u = \frac{x}{t}. \qquad (91.41)$$

If for all masses of liquid $u = u_\infty = u_0 = \text{const}$ (which corresponds to the case $\theta = 0$), then

$$mQ = \frac{mu_0^2}{6} + \frac{(\mu + M)u_0^2}{2}. \qquad (91.42)$$

Relationships (91.40) and (91.42) are determinate. From (91.42) we determine the limiting velocity which the projectile acquires :

$$u_0 = \sqrt{\frac{2mQ}{\frac{m}{3} + \mu + M}}. \qquad (91.43)$$

In the other limiting case (91.40), it is first necessary to find the relationship between u_∞ and u_0 and then to determine the velocity u_0 ; it is obvious that

$$\frac{x_0 - x_\infty}{x_\infty} = \frac{u_0 - u_\infty}{u_\infty} = \frac{\lambda}{l} = \frac{\rho_0\mu}{\rho_\Delta m}, \qquad (91.44)$$

where ρ_0 is the initial density of the explosive and ρ_Δ is the density of the liquid. Thus,

$$\frac{u_0}{u_\infty} = 1 + \frac{\rho_0\mu}{\rho_\Delta m} = 1 + \omega. \qquad (91.45)$$

As a result of this, relationship (91.40) assumes the form

$$mQ = \frac{m}{6}\frac{u_0^2}{(1+\omega)^2} + \frac{\mu u_0^2}{6}\left(1 + \frac{1}{1+\omega} + \frac{1}{(1+\omega)^2}\right) + \frac{Mu_0^2}{2}, \qquad (91.46)$$

whence

$$u_0 = \sqrt{\frac{2mQ}{\frac{m}{3(1+\omega)^2} + \frac{\mu}{3(1+\omega)^2}[(1+\omega)^2 + (1+\omega) + 1] + M}}$$

or

$$u_0 = (1+\omega)\sqrt{\frac{2mQ}{\frac{m}{3} + \mu\left(1 + \omega + \frac{\omega^2}{3}\right) + M(1+\omega)^2}}. \qquad (91.47)$$

For $u_0 = u_\infty$, $\omega = 0$ relationship (91.47) transforms into relationship (91.43). We note that the law $\rho = \frac{a}{t}$, where $a = \text{const}$, is fulfilled only for $k = 3$. However, if $\frac{\mu + M}{m} \gg 1$, then this law is satisfactorily fulfilled also for other values of k.

It is of interest to calculate the momentum of the explosion products, of the liquid and of the projectile. The total momentum is determined from the relationship

$$I = \int_0^{u_\infty t} \rho u\, dx + \int_{u_\infty t}^{u_1 t} \bar{\rho} u\, dx + Mu_0. \qquad (91.48)$$

Obviously,

$$I = \frac{a}{t^2}\int_0^{u_\infty t} x\, dx + \frac{\bar{a}}{t}\int_{u_\infty t}^{u_1 t} [xf(t) + u_\infty(1 - f(t)t)]\, dx + Mu_0 =$$

$$= \frac{au_\infty^2}{2} + \bar{a}\left[\frac{u_0^2 - u_\infty^2}{2} tf(t) + u_\infty(u_0 - u_\infty)(1 - f(t)t)\right] + Mu_0,$$

or

$$I = \frac{mu_\infty}{2} + \mu\left[\frac{u_0 + u_\infty}{2}\theta + u_\infty(1 - \theta)\right] + Mu_0. \qquad (91.49)$$

If $\theta = 0$, then

$$I = \frac{mu_0}{2} + (\mu + M)u_0. \qquad (91.50)$$

If $\theta = 1$, then

$$I = \frac{mu_\infty}{2} + \frac{\mu}{2}(u_\infty + u_0) + Mu_0, \qquad (91.51)$$

which gives, after substitution of $u_\infty = \frac{u_0}{1+\omega}$,

$$I = u_0\left[\frac{m}{2(1+\omega)} + \frac{\mu}{2}\left(1+\frac{1}{1+\omega}\right)+M\right]. \qquad (91.52)$$

Substituting here the value of u_0 from (91.47), we finally arrive at the relationship

$$I = \sqrt{\frac{2mQ}{\frac{m}{3}+\mu\left(1+\omega+\frac{\omega^2}{3}\right)+M(1+\omega)^2}}\left[\frac{m}{2}+\mu\left(1+\frac{\omega}{2}\right)+M(1+\omega)\right]. \qquad (91.53)$$

Similarly, for the case $\theta = 0$ (when $\omega = 0$) also), we have

$$I = \left[\frac{m}{2}+\mu+M\right]\sqrt{\frac{2mQ}{\frac{m}{3}+\mu+M}}. \qquad (91.54)$$

The relationships derived here give a quite accurate result for determining both the velocities and momentum of the system explosion products - liquid - projectile. However, for convenience of calculation it is more convenient to introduce the detonation velocity $D = 4\sqrt{Q}$ in place of Q, and $\frac{\rho_0}{\rho_a}\frac{\mu}{m} = \omega$ in place of ω; then relationship (91.47) assumes the form

$$\frac{u_0}{D} = \frac{1+\frac{\rho_0}{\rho_a}\frac{\mu}{m}}{4}\times \times\sqrt{\frac{2}{\frac{1}{3}+\frac{\mu}{m}\left[1+\frac{\rho_0}{\rho_a}\frac{\mu}{m}+\frac{1}{3}\left(\frac{\rho_0}{\rho_a}\frac{\mu}{m}\right)^2\right]+\frac{M}{m}\left(1+\frac{\rho_0}{\rho_a}\frac{M}{m}\right)^2}}. \qquad (91.55)$$

If the velocity of the total mass of liquid is uniform, then

$$\frac{u_0}{D} = \frac{1}{4}\sqrt{\frac{2}{\frac{1}{3}+\frac{\mu+M}{m}}}. \qquad (91.56)$$

Let us examine the essential difference between these two relationships. For $\mu = 0$ both expressions (91.55) and (91.56) are, of course, in agreement. For $\mu \to \infty$ (91.55) and (91.56) give respectively

$$\frac{u_0}{D} = \frac{1}{4}\sqrt{\frac{6m}{\mu}} \to 0, \quad \frac{u_0}{D} = \frac{1}{4}\sqrt{\frac{2m}{\mu}} \to 0.$$

If $\rho_a = \rho_0$ and $m = \mu = M$, we obtain respectively

$$\frac{u_0}{D} = \frac{1}{2}\sqrt{\frac{2}{\frac{1}{3}+1+1+\frac{1}{3}+4}} = \frac{1}{4}\sqrt{\frac{6}{5}}, \quad \frac{u_0}{D} = \frac{1}{4}\sqrt{\frac{6}{7}}.$$

In this case the ratio of the velocities of the projectile is equal to

$\sqrt{\frac{7}{5}} = 1.2$. If $D = 8000$ m/sec, then the difference amounts to $0.2 \frac{8000}{4}$ m/sec = 400 m/sec. It is quite significant. However, for $\mu + M > 2m$, for example for $\mu + M = 3m$, it does not exceed 100 m/sec and it can be neglected.

Since for the relationships as stated, when $n \approx 2(\mu + M)$, the velocity of ejection of the liquid and of the projectile does not exceed 2000 m/sec, and the limiting velocity of ejection of liquid compressed by a detonation pressure around 3500 - 3000 m/sec, then relationship (91.55), in which the distribution of velocity with respect to the coordinate is taken into account, is more reliable.

For $\mu + M < \frac{m}{2}$ it may be assumed that in the liquid the velocity is everywhere constant and equal to u_0; then relationship (91.56) should be used. However, the difference will not be too considerable in calculations, as we have shown.

§ 92. Propagation of Waves in Solids.

The theory of propagation of weak waves, longitudinal and transverse, in solids has been quite fully developed. Moreover the numerous experimental data concerning the behaviour of solids for relatively small dynamic and static stresses are accurate.

The study of the behavour of solids for the large stresses which arise as a result of explosions has been initiated only relatively recently, and in this sphere our data, both theoretical and practical, are still very inadequate.

We shall endeavour to develope here and investigate more deeply certain well-known results of the theory of propagation of strong (non-linear) waves in solids, originating as a result of large, rapidly fluctuating explosive or

other stresses.

In contrast from a liquid, which, after the relief of any practically attainable stress, returns to the initial state such that only the temperature of the final state may differ somewhat from the temperature of the initial state, solids possess a so-called residual deformation; in addition, the very crystalline structure of the solid may be changed or may even disappear at sufficiently high pressures. As a result of this, the residual deformation resulting from tension is usually greater than that from compression.

Even as a result of the propagation of weak waves the effect of residual deformation may be considerable. Therefore the theory of propagation of waves in solids has its difficulties compared with the theory of propagation of waves in liquids, however in many cases the low compressibility of solids facilitates solution of the problem.

It is well-known that as a result of the action of any force applied to a solid, for example a metal, a travelling deformation wave (stress wave) originates in it, depending upon the magnitude of this force calculated per unit of surface, i.e. depending on the applied pressure, the wave will have a different intensity.

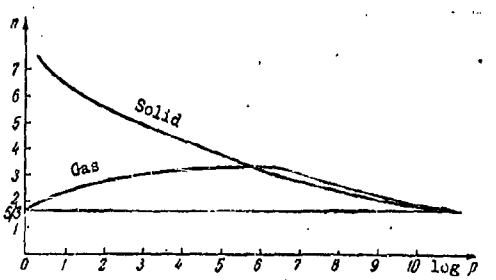
As a result of the reflection of waves from the free surface of the body or by relieving the stress, new waves originate - stress relieving waves.

Nowadays, in order to solve some of the principal theoretical and technical problems presented by the necessity of investigating the question of the action of very high pressures on metals or other solids when strong waves originate within these solids, and when the equation relating deformation and stress does not obey Hook's Law. The dependence of the density of the body on the pressure or deformation as a result of the stress only obeys Hook's Law

for pressures(deformations) which are not very large. For pressures of tens and hundreds of thousands of atmospheres Hook's Law is quite applicable. For a number of solids the slope of the curve $\sigma = \sigma(\varepsilon)$ is decreased in a certain region as a result of compression. For pressures of the order of millions of atmospheres a solid body actually becomes quasi-liquid and even gaseous, and in this region of pressure $p \sim \rho^n$, where n is the index of polytropy; within the limit this index, for still greater pressures, tends to a value of $n \approx \frac{5}{3}$ (Fig. 246). If the laws of propagation of weak deformation have been well investigated within the limits of applicability of Hook's Law, then the laws of propagation of strong waves of stress and stress relief, when the body is in a plastic state and it is necessary to take into consideration the compressibility of the material of which the body consists, have been studied in insufficient detail and reliability.

As a result of the detonation of high explosives near the surface of any solid obstacle pressures are developed which are capable of severely deforming a certain volume of the material of which the obstacle is composed. As a result of this, a powerful compression wave passes through the material of the obstacle in the initial stage (a loading stress wave). Since the pressure of the explosion products falls rapidly with time, a rarefaction wave passes through the material of the obstacle (relief wave).

Figure 246. Dependence of Index of Polytropy on pressure, for a solid and a gas (system).



We shall consider the problem of one-dimensional stress-loading and relief of material of the obstacle.

The basic equations, taking into account the change in density of the material of the obstacle, have the following well-known form in Lagrange coordinates :

$$\frac{\partial u}{\partial t}+\frac{\partial p}{\partial h}=0,\quad \frac{\partial u}{\partial h}=\frac{\partial v}{\partial t},\quad u=\frac{\partial x}{\partial t}, \tag{92.1}$$

where u is the velocity, p is the pressure and v is the specific volume,

$$h=\int_0^{x_0}\rho_0\,dx_0=\int_0^{x}\rho\,dx, \tag{92.2}$$

where h is the mass of the obstacle material (Lagrange coordinates), ρ_0 and ρ are the initial and transient density of the material, x_0 and x are the Lagrange and transient coordinates, and t is the time.

The pressure and specific volume should be connected by the relationship (equation of state)

$$p=p(v); \tag{92.3}$$

for this, it is assumed that the entropy is always constant, since in solids and liquids for pressures around 10^6 kg/cm^2 the entropy changes but little in practice, even in shock waves.

It is usual to introduce into the theory of elasticity and plasticity the tension

$$\sigma=-p \tag{92.4}$$

in place of p, and for v the deformation

$$\varepsilon=\frac{v-v_0}{v}=\frac{\rho_0}{\rho}-1. \tag{92.5}$$

Thus, equations (92.1) and (92.2) assume the form

$$\frac{\partial u}{\partial t}=\frac{\partial \sigma}{\partial h},\quad \frac{\partial u}{\partial h}=\frac{1}{\rho_0}\frac{\partial \varepsilon}{\partial t},\quad u=\frac{\partial x}{\partial t}. \tag{92.6}$$

Moreover, it is necessary to know the relationship

$$\sigma = \sigma(\varepsilon). \tag{92.7}$$

First of all we shall find the particular solutions of these equations. Assuming that $u = u(p)$ or that $u = u(\sigma)$, we arrive at the following relationships defining the particular solutions

$$h = \sqrt{-\frac{dp}{dv}}\, t + F(p), \quad du = \sqrt{-dp\, dv} = \sqrt{-\frac{dp}{dv}}\, dv, \tag{92.8}$$

or

$$h = \sqrt{\rho_0 \frac{d\sigma}{d\varepsilon}}\, t + F(\sigma), \quad du = \sqrt{\frac{d\sigma\, d\varepsilon}{\rho_0}} = \sqrt{\frac{d\sigma}{\rho_0 d\varepsilon}}\, d\varepsilon. \tag{92.9}$$

If the relationship between p and v or σ and ε be given approximately by the expression

$$p - p_0 = A(v - \alpha)^{-k}, \tag{92.10}$$

or

$$\sigma - \sigma_0 = B(\varepsilon - \varepsilon_0)^{-k}, \tag{92.11}$$

where k, A, p_0, σ_0, ε_0 and B are constants, then it is easy to find the general solutions of the basic equations. These solutions have the most simple form if $k = \frac{2n+3}{2n+1}$, where $n = -1, 0, 1, 2, \ldots, \infty$. For the purpose of obtaining a practical solution to the series of problems, it is sufficient to choose $n = -1$, then $k = -1$ (for pressures up to 10,000 kg/cm^2 in the case of metals, and

$$p - p_0 = A(v - \alpha), \quad \sigma - \sigma_0 = B(\varepsilon - \varepsilon_0), \tag{92.12}$$

which gives Hook's Law. For $n = 0$, $k = 3$ and

$$p - p_0 = A(v - \alpha)^{-3}, \quad \sigma - \sigma_0 = B(\varepsilon - \varepsilon_0)^{-3}, \tag{92.13}$$

which establishes the relationship between the tensions and the deformations at high(up to 10^6 kg/cm^2) pressures, acting on metallic or "rock" obstacles.

We shall find first of all the general solutions for an approximation of the equation of state (92.10). Since

$$\frac{\partial p}{\partial h}=\frac{\partial p}{\partial v}\frac{\partial v}{\partial h}=-\frac{Ak}{(v-\alpha)^{k+1}}, \qquad (92.14)$$

then, by reversing the dependent and independent variables in equation (92.1) we arrive at the equations

$$\frac{\partial h}{\partial v}=\frac{Ak}{(v-\alpha)^{k+1}}\frac{\partial t}{\partial u}, \quad \frac{\partial t}{\partial v}=\frac{\partial h}{\partial u}. \qquad (92.15)$$

We now introduce the "effective" velocity of sound

$$\omega=\omega_i\left(\frac{v-\alpha}{v_i-\alpha}\right)^{-\frac{k-1}{2}},$$

where

$$\omega_i=c_i\frac{v_i-\alpha}{v_i}, \quad c_i=\frac{v_i}{v_i-\alpha}\sqrt{(p_i-p_0)(v_i-\alpha)}, \qquad (92.16)$$

here v_i, p_i, c_i, and ω_i are the initial values of v, p, c, and ω. As a result, the equations in (92.15) assume the form

$$\left.\begin{aligned}\frac{\partial u}{\partial \omega}+\frac{2}{k-1}\rho_i c_i\left(\frac{\omega}{\omega_i}\right)^{\frac{k+1}{k-1}}\frac{\partial t}{\partial u}=0,\\ \frac{\partial h}{\partial u}+\frac{k-1}{2}\rho_i c_i\left(\frac{\omega}{\omega_i}\right)^{\frac{k+1}{k-1}}\frac{\partial t}{\partial \omega}=0,\end{aligned}\right\} \qquad (92.17)$$

where ρ_i is the initial density.

Hence, by eliminating h, we arrive at the equation determining t:

$$\left(\frac{k-1}{2}\right)^2\left[\frac{\partial^2 t}{\partial \omega^2}+\frac{k+1}{k-1}\frac{1}{\omega}\frac{\partial t}{\partial \omega}\right]=\frac{\partial^2 t}{\partial u^2}. \qquad (92.18)$$

The solution of this equation in the case when $k=\frac{2n+3}{2n+1}$, for $n=-1, 0, 1, 2, \ldots\ldots$, n is, as is well-known (see para. 25):

$$t=\frac{\partial^{n+1}}{\partial i^{*n+1}}\left[F_1\left(\sqrt{2(2n+1)i^*}+u\right)+F_2\left(\sqrt{2(2n+1)i^*}-u\right)\right], \qquad (92.19)$$

where $i^*=\frac{\omega^2}{k-1}$ is the effective enthalpy. F_1 and F_2 are arbitrary functions.

Knowing that $t=t(i^*;u)=t(\omega;u)$, we determine $h=h(\omega;u)$ from (92.17), which also solves the problem of finding the general solutions

Best Available Copy

of the system (92.1).

In the case when $n=-1,\ k=-1$

$$\left.\begin{aligned} t &= F_1(\omega+u)+F_2(\omega-u),\\ h &= \rho_i c_i\,[F_1(\omega+u)-F_2(\omega-u)], \end{aligned}\right\} \qquad (92.20)$$

whereupon

$$\omega=\omega_i\frac{v-a}{v_i-a},\quad c_i\frac{v-a}{v_i}=\frac{v-a}{v_i-a}\sqrt{(p_i-p_0)(v_i-a)}. \qquad (92.21)$$

Hence it is easy to find

$$\left.\begin{aligned} \omega &= \Phi_1(h+\rho_i c_i t)+\Phi_2(h-\rho_i c_i t),\\ u &= \Phi_1(h+\rho_i c_i t)-\Phi_2(h-\rho_i c_i t), \end{aligned}\right\} \qquad (92.22)$$

where Φ_1 and Φ_2 are new arbitrary functions.

In the case when $n=0,\ k=3$

$$\left.\begin{aligned} t &= \frac{F_1(\omega+u)+F_2(\omega-u)}{\omega},\\ \frac{\partial h}{\partial\omega} &= -\rho_i c_i\left(\frac{\omega}{\omega_i}\right)^2\frac{\partial t}{\partial u}=\frac{\rho_i c_i\omega}{\omega_i^2}(F_2'-F_1'), \end{aligned}\right\} \qquad (92.23)$$

whereupon

$$\omega=\omega_i\frac{v_i-a}{v-a}=c_i\frac{(v_i-a)^2}{v_i(v-a)}=\frac{v_i-a}{v-a}\sqrt{3(p_i-p_0)(v_i-a)}. \qquad (92.24)$$

Similar special and general solutions can also be found in the case when the basic equations are expressed in Euler coordinates.

We shall show first of all that the transition from one set of coordinates to another can easily be carried out, knowing that $u=\left(\frac{\partial x}{\partial t}\right)_h$, hence by the well-known expression $u=u(t,h)$, it is easy to find on integrating that $x=x(t,h)$ and to determine

$$u=u(t,x),\quad \omega=\omega(t,x). \qquad (92.25)$$

Equation (92.1), in Euler coordinates, will have the form

$$\left.\begin{aligned} &\frac{\partial u}{\partial t}+u\frac{\partial u}{\partial x}+\frac{1}{\rho}\frac{\partial p}{\partial x}=0,\\ &\frac{\partial \ln\rho}{\partial t}+u\frac{\partial \ln\rho}{\partial x}+\frac{\partial u}{\partial x}=0, \end{aligned}\right\} \qquad (92.26)$$

or

$$\left.\begin{aligned} \frac{\partial u}{\partial t}+u\frac{\partial u}{\partial x}&=\frac{\varepsilon+1}{\rho_0}\frac{\partial \sigma}{\partial x},\\ \frac{\partial \varepsilon}{\partial t}+u\frac{\partial \varepsilon}{\partial x}&=(\varepsilon+1)\frac{\partial u}{\partial x}. \end{aligned}\right\} \tag{92.27}$$

As a result of this the special solution will be

$$\left.\begin{aligned} x&=(u\pm c)\,t+F(u),\\ du&=\sqrt{-dp\,dv}. \end{aligned}\right\} \tag{92.28}$$

where $c=\sqrt{\frac{dp}{d\rho}}$ is the velocity of sound, or

$$\left.\begin{aligned} x&=\left[u\pm(\varepsilon+1)\sqrt{\frac{d\sigma}{\rho_0\,d\varepsilon}}\right]t+F(u),\\ du&=\sqrt{\frac{d\sigma\,d\varepsilon}{\rho_0}}=\sqrt{\frac{d\sigma}{\rho_0\,d\varepsilon}}\,d\varepsilon, \end{aligned}\right\} \tag{92.29}$$

whereupon

$$c=(\varepsilon+1)\sqrt{\frac{d\sigma}{\rho_0\,d\varepsilon}}.$$

The general solutions have the form of equation (92.19) ; thus,

$$x=ut-\frac{\partial\psi}{\partial u},\quad t=\frac{\partial\psi}{\partial t^n}, \tag{92.30}$$

where

$$\psi=\frac{\partial^n}{\partial t^{n-n}}\left[F_1\left(\sqrt{2(2n+1)\,t^n}+u\right)+F_2\left(\sqrt{2(2n+1)\,t^n}-u\right)\right]. \tag{92.31}$$

The relationship between x and h can again be found from the relationship $u=\left(\frac{\partial x}{\partial t}\right)_h$ by integrating it for the specified initial conditions.

Concerning Certain Motions of Material, as a result of Stress Loading and Stress Relieving. Suppose that a column of material be exposed to a stress ; as a result of this a simple wave passes through it, described by the special solution of the basic equations. First of all we shall assume that the extension of the column is unlimited, then we shall consider the end of the column and we shall study the reflection of the simple wave from its end.

If the simple wave goes from left to right, then we arrive at the solution

$$h=-\sqrt{-\frac{dp}{dv}}t+F(p),\quad du=-\sqrt{-\frac{dp}{dv}}dv. \tag{92.32}$$

Knowing for $h=0$ $(x_0=0)$ the law of applicability of the force $p=f(t)$ or $t=\varphi(p)$, , we determine $F(p)=-\varphi(p)\sqrt{-\frac{dp}{dv}}$, where $v=v(p)$.

Thus, the solution takes the form

$$h=\sqrt{-\frac{dp}{dv}}[t-\varphi(p)],\quad u=-\int\sqrt{-\frac{dp}{dv}}dv. \tag{92.33}$$

For the equation of state

$$\left.\begin{aligned} p-p_0&=A(v-\alpha)^{-k},\\ -\frac{dp}{dv}&=kA(v-\alpha)^{-(k+1)}=kA\left(\frac{p-p_0}{A}\right)^{\frac{k+1}{k}}\end{aligned}\right\} \tag{92.34}$$

and the solution of (92.33) can be written in the form

$$\left.\begin{aligned} u&=\frac{2}{k-1}\sqrt{kA^{\frac{1}{k}}}[p-p_0]^{\frac{k-1}{2k}}+\text{const},\\ h&=\sqrt{\frac{k}{A^{\frac{1}{k}}}}(p-p_0)^{\frac{k+1}{2k}}[t-\varphi(p)].\end{aligned}\right\} \tag{92.35}$$

Since for $p=p_a$, $u=0$, where p_a is the initial pressure in the material, then

$$u=\frac{2}{k-1}\sqrt{kA^{\frac{1}{k}}}\left[(p-p_0)^{\frac{k-1}{2k}}-(p_a-p_0)^{\frac{k-1}{2k}}\right]. \tag{92.36}$$

Let us consider the case of application of an explosive stress, i.e. we shall assume that a stress(pressure) is applied momentarily to the material of the obstacle and that it is gradually removed.

It is well-known from theory and from experiments that we can assume, with a high degree of accuracy, that

$$p=\frac{B}{t^r}, \tag{92.37}$$

where $B=\text{const}$, $r=\text{const}$, which gives

$$\varphi(p)=t=\frac{B^{\frac{1}{r}}}{p^{\frac{1}{r}}}. \tag{92.38}$$

Hence, the solution of the given problem for very high pressures in the medium, where $\frac{dp}{dv} < 0$, will have the form

$$\left.\begin{aligned} h &= \sqrt{\frac{k}{A^{\frac{1}{k}}}}\left[(p-p_0)^{\frac{k+1}{2k}}\left[t-\left(\frac{B}{p}\right)^{\frac{1}{r}}\right]\right], \\ u &= \frac{2}{k-1}\sqrt{kA^{\frac{1}{k}}}\left[(p-p_0)^{\frac{k-1}{2k}}-(p_s-p_0)^{\frac{k-1}{2k}}\right]. \end{aligned}\right\} \qquad (92.39)$$

Since at the boundary for $u \geqslant 0$ $p = \frac{B}{t^r}$, then

$$u = \frac{dx}{dt} = \frac{2}{k-1}\sqrt{kA^{\frac{1}{k}}}\left[\left(\frac{B}{t^r}-p_0\right)^{\frac{k-1}{2k}}-(p_s-p_0)^{\frac{k-1}{2k}}\right]. \qquad (92.40)$$

Hence,

$$x = \frac{2}{k-1}\sqrt{kA^{\frac{1}{k}}}\int\left[\left(\frac{B}{t^r}-p_0\right)^{\frac{k-1}{2k}}-(p_s-p_0)^{\frac{k-1}{2k}}\right]dt + \text{const}, \qquad (92.41)$$

and the constant is determined from the condition that for $x=0$, $t=\tau$, i.e. motion commences at $t=\tau$ when

$$p = p_1 = \frac{B}{\tau^r}. \qquad (92.42)$$

It is obvious that initially x increases, then for the condition that $u=0$, i.e. for the condition that $p = p_s$,

$$\frac{B}{t_1^r} - p_0 = p_s - p_0$$

or

$$t_1 \geqslant \left(\frac{B}{p_s}\right)^{\frac{1}{r}}, \qquad (92.43)$$

and the value of x begins to decrease. For $t = t_1$

$$x = x_{\max} = \frac{2}{k-1}\sqrt{kA^{\frac{1}{k}}}\left[\int_{\tau}^{t_1}\left(\frac{B}{t_1^r}-p_0\right)^{\frac{k-1}{2k}}dt-(p_s-p_0)^{\frac{k-1}{2k}}(t_1-\tau)\right]. \qquad (92.44)$$

We shall now calculate the impulse which is imparted to the medium ; obviously this impulse is determined by the relationship

$$I = S\int_{\tau}^{t} p\,dt = \frac{SB}{r-1}\left[\tau^{-(r-1)} - t^{-(r-1)}\right]. \qquad (92.45)$$

For $t = t_1$

$$I_{max} = \frac{SB}{r-1}\left[\tau^{1-r} - t_1^{1-r}\right] = \frac{SB}{(r-1)\tau^{r-1}}\left[1 - \left(\frac{p_a}{p_i}\right)^{r-1}\right]. \qquad (92.46)$$

A definite relationship exists between x_{max} and I_{max}.

For large initial pressures the value of p_0 is unimportant, therefore

$$x_{max} = \frac{2}{k-1}\sqrt{kA^{\frac{1}{k}}}\left\{\frac{B\tau^{1-\frac{r}{2k}(k-1)}}{\left[(k-1)\frac{r}{2k}-1\right]}\left[1-\left(\frac{p_a}{p_i}\right)^{\frac{k-1}{2k}-\frac{1}{r}}\right]-\right.$$

$$\left.-\frac{B}{t_1^{r-1}}\left[\left(\frac{p_a}{p_i}\right)^{\frac{r-1}{r}}-\frac{p_a}{p_i}\right]\right\}. \qquad (92.47)$$

Here we shall assume that the quantity $(k-1)\frac{r}{2k} - 1 \neq 0$. In the contrary case the dependence of x on t will be logarithmic.

Further, the quantity $\frac{p_a}{p_i}$, can be neglected, and so finally

$$x_{max} = \frac{2}{k-1}\sqrt{kA^{\frac{1}{k}}}\frac{B}{\left[(k-1)\frac{r}{2k}-1\right]\tau^{\frac{r}{2k}(k-1)-1}},$$

$$I_{max} = \frac{SB}{(r-1)\tau^{r-1}}.$$

Hence,

$$x_{max} \sim I_{max}, \qquad (92.48)$$

i.e. we arrive at the fundamental conclusion that the magnitude of the compression is proportional to the magnitude of the maximum impulse of the compression.

If the stress loading wave passing through the body is reflected from a more rigid obstacle, then the reflected wave proceeds to the left and, on reaching the end where the load was previously applied, it is reflected from

this end. If there is now no load, then cavitation phenomena may be observed in the material, as a consequence of the tensile stresses arising as a result of this. If the load still remains, then these phenomena will be weakened or will not be observed at all.

As a result of the action of an explosive loading, shattering of the material should be observed in the process of its compression; it can be assumed that the greater the impulse loading the stronger are these shattering effects. A partial but nevertheless strong reflection of the compression wave will also occur from the boundary of destruction.

The rarefaction wave, formed on arrival of the reflected compression wave at the open end, will contribute to the ejection of shattered particles of the medium. If the load be removed slowly, then this ejection will not be intense. On rapid removal of the load, on the contrary, the whole of the shattered region may be scoured of fragments of the medium.

Thus, as a result of an explosion in air, despite the fact that the impulse is less than for an explosion with an aqueous "ram", the overall depth of the depression in the medium may be larger than for an explosion in water.

§ 93. Elements of the Theory of an Explosion in the Ground.

The study of the propagation of the explosion products and of the shock wave in the ground is an important theoretical and practical problem. The conditions of propagation of the explosion products in the ground, despite the fact that from a density point of view earth differs but little from water or any other liquid, differs sharply from the propagation of explosion products in liquid media. This is associated with the porosity (discreteness) of

the ground.

Actually, as a result of compression of the earth adhesion of the individual particles takes place at first, which increases the bulk density, and then later at still higher pressures the mechanical [illegible] of which the ground is composed. Since the porosity of the ground is considerable, then in ground saturated with water , the compression, as a consequence of particle adhesion may be considerably greater than the normal adiabatic compression.

Also, just as for an explosion in a liquid, the zone of significant adiabatic compression of the ground is extremely small, and for an explosion in an unconfined medium it does not exceed 8 - 10 times the initial volume of the explosive as a consequence of the rapid drop in pressure of the explosion products.

Compression of the ground, occurring as a result of elimination of its porosity, takes place even at relatively small pressures, of the order of hundreds of atmospheres (for typical soils) and consequently involves a considerably larger zone, of the order of several hundreds of times the inttial volume of explosive.

Thus, at distances of two- three charge radii (taking the explosive charge as a sphere), where the adiabatic compression of the ground is negligible, up to a distance of 7 - 8 charge radii a strong change of density will be observed after the passage of the shock wave. The change of density will be irreversible whereas in a liquid medium after relieving the pressure, the density of the medium assumes its initial value . It is precisely these circumstances, associated with compression of the ground, which also make the problem of propagation of the explosion products in the ground different

Best Available Copy

from the same problem for liquids.

We note also that for an explosion in the ground a considerable part of the explosion energy is expended irreversibly on crushing the particles of soil and on heat. The greatest part of the lost energy will be expended on the creation of irreversible deformation of the soil (in a liquid medium a similar form of deformation is absent at small pressures, but at high pressures part of the energy goes into dissociation). The presence of similar, irreversible losses determines to a considerable extent the radius of the destructive effect of an explosion in the ground.

The magnitude of these irreversible energy losses, expended per unit mass or volume of earth, depends on the pressure and falls with decreasing pressure. For small residual pressures the energy losses are insignificant, which leads to the possibility of formation of weak compression waves, reminiscent in their nature of seismic waves. However, the energy of seismic waves is very insignificant in comparison with the initial explosion energy.

Let us pass on to an account of certain theoretical principles of propagation of an explosion in the ground.

The connection between the pressure and the density in the compressed products of a ground explosion is expressed by the following relationships :

$$\left.\begin{aligned} &\text{for} \quad p < p_{crit}\, \rho = \rho_0, \\ &\text{for} \quad p > p_{crit}\, \rho = \rho_0^* = \frac{\rho_0}{a}. \end{aligned}\right\} \qquad (93.1)$$

Here, ρ_0 is the initial density of the ground, ρ_0^* is the density at a pressure p, p_{crit} is the critical pressure for which the ground ceases to be porous.

The quantity a is a characteristic quantity depending on the properties of the ground and on the pressure, and it can be determined in the following

manner. Let the density of the ground in the natural state be ρ_0 and known to us ; let the density (average) of the soil particles be ρ_1 . Then the auxiliary quantity α is determined by the obvious expression

$$\alpha = \frac{\rho_0}{\rho_1},$$

for the condition that we do not assume adiabatic compression of the soil particles. In taking into account adiabatic compression and introducing the coefficient of compression $\beta = \frac{\rho_1}{\rho_0}$, we arrive at the relationship

$$\alpha_0 = \frac{\rho_0}{\rho_0} = \alpha\beta.$$

for determining the value of α_0 .

The process of shock wave propagation (compression wave) in the ground as a result of expansion of the detonation products may be represented as a process of propagation of the zone of compression of the ground; behind the shock front the change of density of the compressed soil will be of a purely adiabatic nature. The change of entropy behind the shock front can be neglected for the reason that in any dense medium the thermal component in the equation of state for that medium is small in comparison with the "elastic" component of the pressure.

The parameters of the front of the propagating shock wave are determined by the well-known relationships :

$$\left.\begin{aligned} D_s &= v_0^2 \frac{p_s - p_0}{v_0 - v_s}, \\ u_s^2 &\approx (p_s - p_0)(v_0 - v_s) \\ &\quad (\text{for } p > p_{\text{lim}}) \end{aligned}\right\} \qquad (93.2)$$

Here D_s is the velocity of the shock front, u_s is the particle velocity behind the shock front, p_s is the pressure at the wave front, v_s is the specific volume at the wave front and p_0, v_0 are the initial pressure and specific volume.

Knowing the quantity $\alpha_0 = \frac{v_s}{v_0} = \frac{\rho_0}{\rho_s}$, we can write these relationships

in the form

$$p_s - p_0 = \rho_0 D_s^2 (1-\alpha), \quad u_s = (1-\alpha) D_s. \tag{93.3}$$

whence it follows that

$$p_s - p_0 = \frac{\rho_0 u_s^2}{1-\alpha}. \tag{93.4}$$

Neglecting the adiabatic compression of the particles of earth in comparison with the compression for eliminating its porosity, a theory can be postulated concerning the propagation of shock waves in the ground. We shall consider the propagation of a shock wave in an infinite medium.

For this purpose we must integrate the basic hydrodynamic equations

$$\left.\begin{aligned} u_t + uu_r + \frac{p_r}{\rho} &= 0, \\ \rho_t + u\rho_r + \rho u_r + \frac{2\rho u}{r} &= 0, \end{aligned}\right\} \tag{93.5}$$

for both the expanding explosion products and the medium in which they are propagating.

At the boundary of separation between the explosion products and the medium, the following boundary conditions obviously apply in the first phase of propagation of the explosion products

$$\left.\begin{aligned} p_2 &= p_1, \\ u_2 &= u_1 = \frac{dr}{dt}, \end{aligned}\right\} \tag{93.6}$$

where p_2 is the pressure in the explosion products, p_1 is the pressure in the ground, u_2 is the velocity in the explosion products and u_1 is the velocity in the ground.

At the shock front, which in the vicinity of the explosion source may be assumed to be strong and therefore p_0 can be neglected in comparison with the pressure p_s, the following conditions will be attained

$$p_s = \rho_0 D_s^2 (1-\alpha), \quad u_s = (1-\alpha) D_s, \quad D_s = \frac{dR}{dt}. \tag{93.7}$$

As a result of the expansion of the detonation products and since the

process of compression of the ground association with the elimination of its porosity is practically irreversible, the position may ultimately be reached when at the boundary of separation between the detonation products and the ground, the pressure is quite small and further motion of the ground will be inertial; as a result of this, the limiting conditions of equation (93.6) will finally be formally achieved, but they will no longer be taken into consideration.

In consequence of the fact that the mass of earth set into motion behind the shock front very rapidly begins to exceed the mass of the explosion products, the following simplified concept of the expansion of the detonation products can be applied. First of all, it can be assumed that the detonation took place instantaneously and consequently we can consider the expansion of the gas, as if at rest prior to commencement of expansion and occupying a volume equal to the initial volume of the explosive, and secondly it can be assumed that at the boundary of separation between the detonation products and the ground, the condition

$$\rho_r = \rho_{expl}\left(\frac{r_0}{r}\right)^3, \tag{93.8}$$

is fulfilled for the detonation products, where ρ_{expl} is the initial density of the explosive, r_0 is the radius of the explosive charge, r is the present distance of the boundary of separation. Relationship (93.8) follows from the Law of Conservation of Mass. Since expansion of the explosion products is isentropic, we obtain from this relationship for the pressure at the boundary of separation

$$\frac{p_r}{p_i} = \left(\frac{\rho_r}{\rho_{expl}}\right)^k = \left(\frac{r_0}{r}\right)^{3k}, \tag{93.9}$$

where $p_i = \frac{\rho_{expl} D^2}{8}$ is the initial pressure of the detonation products and D is the velocity of the detonation wave.

If we suppose further that the ground, after elimination of its porosity,

is incompressible, we are able to integrate immediately the system of equations in (93.5). The solution will have the form

$$\left.\begin{aligned} ur^2 &= f(t), \\ \frac{p-\varphi(t)}{\rho_0^*} &= \frac{\dot{f}}{r} - \frac{f^2}{2r^4}. \end{aligned}\right\} \qquad (93.10)$$

The general solution of (93.10) depends on the two arbitrary functions $f(t)$ and $\varphi(t)$; these arbitrary functions can be determined from the condition at the boundary of separation (93.6) and at the shock front (93.7).

Since $u = \frac{dr}{dt} = \dot{r}$, at the boundary of separation, then by transforming the solution (93.10) and taking into consideration that $\dot{f} = r^2\dot{r}$, $\ddot{f} = r^2\ddot{r} + 2r\dot{r}^2$, we have

$$\frac{p-\varphi}{\rho_0^*} = r\ddot{r} + \frac{3}{2}\dot{r}^2 = ru\frac{du}{dr} + \frac{3}{2}u^2. \qquad (93.11)$$

Substituting the value of the pressure at the boundary of separation from (93.9), we finally arrive at the following equation determining the law of motion of the boundary of separation :

$$\frac{du^2}{dr} + 3\frac{u^2}{r} = \frac{2\bar{p}_n}{\rho_0^* r_0}\left(\frac{r_0}{r}\right)^{3k+1} - \frac{2\varphi}{\rho_0^* r_0}\frac{r_0}{r}. \qquad (93.12)$$

This equation could be integrated if we know the form of the arbitrary function $\varphi = \varphi(t)$; however, it can be confirmed in advance that since the process of compression of the ground, associated with the elimination of its porosity, is irreversible, then over a period of time or with increase of the distance traversed by the boundary of separation, this function decreases and, within the limit (for $r \to \infty$) tends to zero.

We can write the solution of equation (93.12) in the form

$$u^2 = A\frac{r_0^3}{r^3} - \frac{2}{3(k-1)}\frac{\bar{p}_i}{\rho_0^*}\left(\frac{r_0}{r}\right)^{3k} - \frac{2}{3\rho_0^*}\frac{r_0^3}{r^3}\int \varphi(t)\, r^2\, dr; \qquad (93.13)$$

the constant A is determined from the condition that $r = r_0$, $u = u_i$ (u_i is the initial velocity of motion of the ground).

Analysis of this solution shows that with a sufficiently rapid decrease of the function $\varphi(t)$, the velocity u of the boundary of separation tends to zero only for $r \to \infty$.

The more precise solution to the problem with the simultaneous application of both boundary conditions, which enables a compatible determination of the functions $\varphi(t)$ and $f(t)$ to be given, is of no insignificence, since at large distances from the explosion point, as we have shown, a considerable portion of the explosion energy is irreversibly expended on heating up and deforming particles of earth, and the basic equation - namely, the equation defining the Law of Conservation of Momentum - ceases to be valid, since we have not taken into account the appropriate dissipative forces in it.

We shall continue the solution of the problem with the assumptions made above, and we shall determine the law of motion of the shock front. For this purpose, first of all assuming simply that $\varphi(t) = 0$, we shall determine the form of the arbitrary function $f(t)$.

The assumption that $\varphi(t) = 0$, is quite valid, since this arbitrary function is small in comparison with the pressure in the vicinity of the explosion source, and it decreases sharply with increasing distance.

Since $u = \frac{dr}{dt}$, then

$$3f(t)\,dt = dr^3. \tag{93.14}$$

From equation (93.13) we have, for $\varphi(t) = 0$

$$u^2 = u_1^2 \frac{r_0^3}{r^3} + \frac{2}{3(k-1)} \frac{p_1}{\rho_0^*} \frac{r_0^3}{r^3} \left[1 - \left(\frac{r_0}{r}\right)^{3(k-1)}\right]. \tag{93.15}$$

Hence we determine

$$f^2 = u_1^2 r_0^3 r + \frac{2}{3(k-1)} \frac{p_1}{\rho_0^*} r_0^3 r \left[1 - \left(\frac{r_0}{r}\right)^{3(k-1)}\right],$$

where

$$r = \sqrt[3]{3 \int f(t)\,dt},$$

which, after eliminating r and solving the equation, gives the form of the function $f(t)$.

We now determine the pressure and velocity in the shock wave zone propagating in the ground :

$$\frac{p}{\rho_0} = \frac{f}{r} - \frac{f^2}{2r^4}, \quad u = \frac{f}{r^2}. \tag{93.16}$$

Since at the shock front

$$p_* = \rho_0 \frac{u_*^2}{1-\alpha} \tag{93.17}$$

and, in addition,

$$u_* = (1-\alpha) D_*, \quad D_* = \frac{dR}{dt},$$

then, on the basis of equation (93.16) we have, for $r = R$

$$\frac{f}{r} - \frac{f^2}{2r^4} = (1-\alpha)\left(\frac{dR}{dt}\right)^2, \tag{93.18}$$

$$(1-\alpha)\frac{dR}{dt} = \frac{f}{r^2}. \tag{93.19}$$

The non-correspondence in the form of the two equations is explained by the fact that we have neglected $\varphi(t)$.

These solutions also determine the law of motion of the shock front. The solution of either one of these equations can be carried out numerically.

Before dealing with the analysis of the results obtained, we shall consider the effect of the dissipative forces leading to the irreversible energy losses. We shall assume that the magnitude of the irreversible lost energy per unit mass of the material of which the ground is composed is proportional to the energy density at a given point of the medium, i.e. we shall assume that

$$\Delta\varepsilon = -\xi\varepsilon, \tag{93.20}$$

where ε is the energy density per unit mass of ground, and ξ is the proportionality coefficient. Here , we can write the Law of Conservation of Energy in the form

$$E = E_0 - \xi \int_{r_0}^{r} \varepsilon 4\pi r^2 \rho_0 \, dr, \tag{93.21}$$

whereupon

$$\varepsilon = \frac{E}{\frac{4}{3}\pi r^3 \rho_0^*}.$$

Thus,

$$\frac{dE}{E} = 3\xi \frac{dr}{r},$$

which gives

$$\frac{E}{E_0} = \left(\frac{r_0}{r}\right)^{3\xi}. \qquad (93.22)$$

Here E primarily determines the energy of motion of the medium, since for an adiabatic process the internal energy of the slightly-compressible ground can be neglected.

It is obvious that for a given law of energy loss, the kinetic energy of will decrease with increase of mass of the moving ground.

For the ultimate solution of the problem concerning motion of the ground we shall effect one further simplification, which however hardly affects the accuracy of the result obtained, namely, we shall write the expression for the velocity of the boundary of separation in the form

$$u^2 = \frac{r_0^3}{r^3} A_0,$$

where

$$A_0 = u_1^2 + \frac{2}{3(k-1)} \frac{\bar{p}_1}{\rho_0^*}, \qquad (93.23)$$

i.e. we shall neglect the quantity $\left(\frac{r_0}{r}\right)^{3k}$ in expression (93.15).

It is easy to convince oneself of the fact that as a result of this the arbitrary function of time $f(t)$ can be written as

$$f(t) = Bt^{\frac{1}{b}},$$

whence

$$u = B \frac{t^{\frac{1}{b}}}{r^3}, \qquad (93.24)$$

where

$$B = r_0^2 u_1 \tau^{-\frac{1}{5}}.$$

It is not difficult to see from this that the law of motion of the boundary of separation will be determined by the relationship

$$r = \sqrt{\frac{5}{2} B}\, t^{\frac{2}{5}} + \text{const}, \qquad (93.25)$$

where the constant is determined from the condition that $t = \tau$ for $r = r_0$.

The law of motion of the shock front is determined by the relationship

$$R = \sqrt{\frac{5}{2}\frac{B}{1-a}}\, t^{\frac{2}{5}} + \text{const}. \qquad (93.26)$$

Here the constant is determined from the condition that $t = \tau$ for $R = r_0$. Using equation (92.25) we find

$$R = \frac{r}{\sqrt{1-a}} + r_0\left(1 - \frac{1}{\sqrt{1-a}}\right). \qquad (93.27)$$

On the other hand,

$$\frac{dR}{dt} \approx \sqrt{\frac{t^{-\frac{4}{5}}}{R} - \frac{t^{\frac{2}{5}}}{2R^4}},$$

whence

$$R \approx \bar{B} t^{\frac{2}{5}} + \text{const}. \qquad (93.28)$$

We obtain relationship (93.27) from the formula determining the velocity of the medium and equation (92.28) from the formula determining the pressure; the lack of agreement between these two formulae, as we assumed above, is insignificant, which enables us to assume that $\varphi(t) = 0$.

We shall now calculate the circumstances such that the compression wave will be propagated with the velocity of sound(in the given medium) at considerable distances. The velocity of propagation of the compression wave can be written in the form

$$D_* = \frac{u_*}{1-a} + c_* = \frac{dR}{dt}, \qquad (93.29)$$

where

$$u_* = B\frac{t^{\frac{1}{5}}}{R^2},$$

and it is more accurate than the corresponding expression in formula (93.3), where we did not take into account the elastic properties of the medium.

Thus, the law of motion of the front of the compression wave will be expressed approximately by the relationship

$$R = \sqrt{\frac{5}{2}\frac{B}{1-\alpha}}\, t^{\frac{2}{5}} + c_a t + \text{const.} \qquad (93.30)$$

It is essential to note that the length of the shock wave or the compression wave increases considerably with distance at large distances from the site of the explosion. By length of the wave is understood the interval between the wave front and the boundary of separation between the wave and the explosion products. The wave length

$$\lambda = R - r = (r - r_0)\left[\sqrt[3]{\frac{1}{1-\alpha}} - 1\right] + c_a (t - \tau). \qquad (93.31)$$

We now note that the motion of the shock wave has a similarity solution nature, as a result of the approximation we have made; the law of motion of the wave front in the vicinity of the explosion source, corresponds in accuracy to the law of motion of the front of a strong air shock wave from a point explosion source, the theory of which was, in due course, developed by L.I. SYEDOV and K.P.STANYUKOVICH.

The relationships found by us for the velocity and pressure may be finally presented in the following manner :

$$u = \frac{B t^{\frac{1}{5}}}{r^{\frac{4}{5}}}, \quad \frac{p}{p_0} = \frac{B}{5}\frac{t^{-\frac{4}{5}}}{r} - \frac{B^2 t^{\frac{2}{5}}}{2r^4}. \qquad (93.32)$$

These relationships can easily be interpreted physically. Actually, neglecting adiabatic compression of the ground, having already lost its porosity, it can be assumed that all the energy of the explosion is expended on imparting to the ground kinetic energy and on its irreversible deformation. Neglecting for the present the energy losses on irreversible deformation,

It is easy to write the following energy balance, based on the Law of Conservation of Energy :

$$E_0 = \frac{M\bar{u}^2}{2}, \tag{93.33}$$

where $M = \frac{4}{3}\pi\rho_0 R^3$ is the mass of the ground.

Hence, it is obvious that the average velocity of motion of the ground is determined by the relationship

$$\bar{u}^2 = \frac{2E_0}{\frac{4}{3}\pi\rho_0 R^3}, \tag{93.34}$$

which corresponds to formula (93.25).

We now come to the determination of the momentum of the ground moving behind the shock front. For this purpose we find first of all the relationship between the energy, mass and momentum of the ground.

Since for any given instant of time the velocity of motion of the ground behind the shock front is determined by the expression $u = \frac{B_0}{r^2}$, and the energy can be found by means of the integral

$$E_0 = \frac{B_0^2}{2}\int_r^R \frac{4\pi\rho_0 r^2}{r^4}\,dr = \frac{B_0^2}{2}\cdot 4\pi\rho_0\left[r^{-1} - R^{-1}\right], \tag{93.35}$$

then the momentum

$$I_0 = B_0\int_r^R 4\pi\rho_0\frac{r^2}{R^2}\,dr = B_0\cdot 4\pi\rho_0(R-r) \tag{93.36}$$

can be represented in the form

$$I_0 = \sqrt{2ME_0\frac{r}{R}\left(1-\frac{r}{R}\right)}. \tag{93.37}$$

In the case of a stationary process, the momentum is determined by the relationship

$$I_{st} = \sqrt{2ME_0}. \tag{93.38}$$

We denote the ratio of the momentum for non-stationary flow to the momentum for stationary flow by θ_1 then

$$0 = \sqrt{\frac{r}{R}\left(1 - \frac{r}{R}\right)}. \qquad (93.39)$$

Since $R = a_1(r - r_0) + c_a(t - \tau) + r \approx (a_1 + 1)r \sim c_a t$,

$$r = B_0 t^{\frac{2}{5}},$$

where

$$a_1 = \sqrt[3]{\frac{1}{1 - a}} - 1,$$

then

$$0 = \sqrt{\frac{r(a_1 r + c_a t)}{[(a_1 + 1)r + c_a t]^2}} \approx \sqrt{\frac{r}{ar + c_a t}} \sim \sqrt{t^{-\frac{3}{5}}} \sim t^{-\frac{3}{10}} \approx r^{-\frac{3}{4}}. \qquad (93.40)$$

This ratio is decreased according to increase of distance from the point of explosion.

Relationship (93.37) can only be used for the condition of completely total expansion of the detonation products, when the residual energy of the explosion products is small in comparison with the initial energy, and this will correspond to distances greater than 8 - 10 initial charge radii. For smaller distances, the energy transferred to the moving ground is determined by the relationship

$$E_1 = E_0\left[1 - \left(\frac{p_0}{p_1}\right)^{\frac{k-1}{k}}\right] = E_0\left[1 - \left(\frac{r_0}{r}\right)^{3(k-1)}\right]. \qquad (93.41)$$

As a result of this, the momentum of the detonation products is

$$\bar{I} = \bar{0}\sqrt{2M_{expl}E_0\left(\frac{r_0}{r}\right)^{3(k-1)}}, \qquad (93.42)$$

where $M_{expl} = \frac{4}{3}\pi\rho_{expl}r_0^3$ is the mass of the explosive charge,

$E_0 = M_{expl}Q$ (Q is the energy per unit mass of explosive).

The total momentum of the ground and of the detonation products is equal to

$$I = \theta \sqrt{2ME_0\left[1-\left(\frac{r}{r_0}\right)^{3(k-1)}\right]} + \bar{\theta}\sqrt{2ME_0\left(\frac{r_0}{r}\right)^{3(k-1)}} \qquad (93.43)$$

The quantity $\bar{\theta}$, characterising the non-stationary nature of the motion of the detonation products, can be assumed to be equal to 0.80 - 0.85, in accordance with the results of the theory of non-stationary motion of a gas.

The total momentum arriving at 1 cm^2, at a distance r from the site of the explosion, is determined by the formula

$$i = \frac{I}{4\pi r^2} = \frac{\sqrt{2ME_0}}{4\pi r^2}\left[\theta\sqrt{1-\left(\frac{r_0}{r}\right)^{3(k-1)}} + \bar{\theta}\sqrt{\left(\frac{r_0}{r}\right)^{3(k-1)}}\right]. \qquad (93.44)$$

In order to determine the flow of momentum passing through 1 cm^2 of the surface of a sphere of radius r, the following procedure can be carried out: since the momentum for a given energy is proportional to the square root of the mass set into motion, then the quantity i^* is determined by the relationship

$$i^* = \frac{\theta^*\sqrt{2M_{expl}E\left(1+\frac{M}{M_{expl}}\right)}}{4\pi r^2}, \qquad (93.45)$$

where the coefficient θ^*, assuming non-stationary motion and depending on the velocity distribution in the medium, can be taken as equal to

$$E = E_0 - \Delta E,$$

for distances of $r > (5-8)r_0$.

In order to define formula (93.44) more accurately, which determines both the momentum of the medium for a given instant of time and also the flow of momentum through any given surface, it is necessary to take into account the irreversible energy losses. For this, it is necessary in (93.45) that by the quantity of energy one should understand the total energy of the

medium for a given instant or time or for a given distance:

$$\theta^* = \sqrt{\frac{r}{R}\left(1 - \frac{r}{R}\right)}. \qquad (93.46)$$

where ΔE is the irreversible energy losses.

Assuming in equation (93.22) that $E = E_0\left(\frac{r_0}{r}\right)^{3k}$, we arrive at the following relationships :

$$i = \frac{\sqrt{2ME_0}}{4\pi r^2}\left(\frac{r_0}{r}\right)^{\frac{3}{2}\xi}\left[\theta\sqrt{1 - \left(\frac{r_0}{r}\right)^{3(k-1)}} + \bar{\theta}\sqrt{\left(\frac{r_0}{r}\right)^{3(k-1)}}\right], \qquad (93.47)$$

$$i^* = \frac{\theta^*\sqrt{2ME_0}}{4\pi r^2}\left(\frac{r_0}{r}\right)^{\frac{3}{2}\xi}\sqrt{1 + \frac{M_{expl}}{M}}. \qquad (93.48)$$

In these relationships, the quantity ξ, which characterises the extent of the energy losses, is indeterminate. If we suppose very roughly that $\xi = \frac{1}{3}$, we arrive at the following results :

$$i = \frac{\sqrt{2ME_0}}{4\pi r^2}\left(\frac{r_0}{r}\right)^{\frac{1}{2}}\left[\theta\sqrt{1 - \left(\frac{r_0}{r}\right)^{3(k-1)}} + \bar{\theta}\sqrt{\left(\frac{r_0}{r}\right)^{3(k-1)}}\right], \qquad (93.49)$$

$$i^* = \frac{\theta^*\sqrt{2ME_0}}{4\pi r^2}\left(\frac{r_0}{r}\right)^{\frac{1}{2}}\sqrt{1 + \frac{M_{expl}}{M}}. \qquad (93.50)$$

It is known from experiments that at relatively large distances from the site of the explosion, exceeding $(8 - 10)\,r_0$, the impulse acting on any obstacle at a distance r from the site of the explosion, is determined by the relationship

$$i^*_{eksp} = \bar{A}\frac{M^{\frac{2}{3}}_{expl}}{r^2} \qquad (93.51)$$

Since at these same distances

$$\theta^* \approx \frac{r(R-r)}{R^2} \approx \bar{\theta}\left(\frac{r_0}{r}\right)^{\frac{3}{2}}. \qquad (93.52)$$

where $\bar{\theta} = \frac{\bar{c}_1}{c_a}\left(\frac{5}{2}\frac{u_{a_1}}{\bar{c}_1}\right)$, then relationship (93.48) assumes the form

$$i^* = \bar{\theta}\frac{\sqrt{2ME_0}}{4\pi r^2}\left(\frac{r_0}{r}\right)^{\frac{3}{2}\xi + \frac{3}{2}}\sqrt{1 + \frac{M_{expl}}{M}}. \qquad (93.53)$$

Conformance of the experimental and theoretical formulae in the sense of dependence of the quantity i^* on distance will occur for $\xi = \frac{1}{3}$, which is equal to the value which we have taken. However, there will be no agreement of the dependence of the quantity i^* on M_{expl} as a result of this.

This non-conformance should be related to the not entirely accurate determination of the impulses, and also to the fact that as a result of the reflection of the material from the obstacle, because of lateral spreading, complementary lateral compressions of the medium may take place, which involve the appearance of the destruction wave around the obstacle. This will reduce the magnitude of the impulse more considerably for large charges than for small charges. As a consequence of this, the experimental dependence of i^* on M_{expl}, will be more feeble than will the theoretical dependence.

Let us pass on to a few numerical determinations of the momentum of the medium behind the shock front. Neglecting the lateral compression of the ground near the obstacle, it is easy to see that the impulsive loading acting on this obstacle will be equal to double the momentum of the medium behind the shock front.

On the basis of the well-known results of the theory of an explosion, formula (93.53) can be used to determine the impulse at distances greater than 8 - 10 charge radii.

We now write this formula in the form

$$i^* = \frac{1}{3}\frac{\bar{c}_1}{c_a}\frac{5}{2}\left(\frac{u_{s1}}{\bar{c}_1}\right)^{\frac{1}{6}}\sqrt{1+\frac{M_{expl}}{M}}\sqrt{2\rho_0\rho_{expl}}\left(\frac{M_{expl}}{\frac{4}{3}\pi\rho_{expl}}\right)^{1+\frac{\xi}{2}} r^{-\left(\frac{3}{2}\xi+2\right)} \quad (93.54)$$

Substituting in it $\frac{\bar{c}_1}{c_a} = 6$, $\frac{u_{s1}}{\bar{c}_1} = \frac{1}{3}$, $\rho_0 = 2$, $\rho_{expl} = 1.6$, $Q = 1$ cal/g = $= 4.18 \cdot 10^{10}$ erg/g, we have, for $\frac{M_{expl}}{M} \ll 1$, in the CGS system of units,

$$\left.\begin{aligned} i^* &= 16 \cdot 10^4 M_{expl}^{\frac{11}{12}} r^{-\frac{5}{4}} \left(\text{for } \xi = \frac{1}{6} \right), \\ i^* &= 16 \cdot 10^4 M_{expl} r^{-2} \quad \left(\text{for } \xi = 0 \right). \end{aligned}\right\} \tag{93.55}$$

Up to now we have assumed that the whole region between the boundary of separation and the shock front is occupied by moving ground, however, as a consequence of the fact that the pressure inside the ground falls with increasing distance, retardation of the rear portions of the moving ground should be observed, down to its complete cessation, i.e. sooner or later breakaway of the shock wave from the detonation products should take place. In the ground this phenomenon should be somewhat more characteristic than in air. Indeed, the zone where the ground is retarded will apparently be transmitted with variable velocity and the wave length in the ground will not be constant. In the limiting case, just as in air, assuming that the wave length is constant and neglecting the irreversible energy losses, we arrive at the following relationship

$$i = \bar{A} \frac{M_{expl}^{\frac{2}{3}}}{r}, \tag{93.56}$$

where $\bar{A}$ = const. Taking into account the losses as before, we can write this relationship in the form

$$i = \bar{\bar{A}} \frac{M_{expl}^{\frac{2}{3}+\frac{3}{2}}}{r^{1+\frac{3}{2}\xi}}, \tag{93.57}$$

where $\bar{\bar{A}}$ = const.

The divergence between the experimental and theoretical relationships occurs mainly for the dependence of the impulse on the charge weight.

We note that in deriving the relationship determining the momentum of the ground, we do not take into account the internal pressure. Actually, at

distances greater than $10 r_0$ the internal pressure plays no further part.

In conclusion we shall attempt to determine the radius of the so-called zone of destruction, assuming that in the zone of destruction the ground itself is deformed by the passage through it of the shock front. The average energy density $\bar{\varepsilon}$ depends on distance in the following manner

$$\bar{\varepsilon} = \frac{M_{expl} Q}{\frac{4}{3}\pi \rho_0 r^3} = \frac{u_{0\,crit}^2}{2}, \tag{93.58}$$

where $u_{0_{crit}}$ is the critical velocity of motion of the ground as a result of which deformation takes place.

Knowing the limiting energy density ε_*, at which noticeable deformation of the ground ceases, we arrive at the following relationship :

$$\frac{r_{lim}}{r_0} = \sqrt[3]{\frac{\rho_{expl}}{\rho_0 \varepsilon_*} Q}, \tag{93.59}$$

where r_{lim} is the limiting radius of destruction.

Assuming for typical soils that $\varepsilon_* = 10^7$ erg/g, $\rho_{expl} = 1.6$ g/cm^3, $\rho_0 = 2$ g/cm^3, $Q = 4 \cdot 10^{10}$ erg/g, we obtain $\frac{r_{lim}}{r_0} = 15$.

An energy density of $\varepsilon_* = 10^7$ erg/g corresponds approximately to a pressure of 20 kg/cm^2.

Actually, as a result of the density variation from the value ρ_0 to the value ρ_0^* the pressure intensity p_{crit} accomplishes an amount of work

$$W = \varepsilon_* = 4\pi x_1^3 \rho_{crit} \frac{\Delta x}{x_1}, \tag{93.60}$$

where

$$\frac{\Delta x}{x_1} = \frac{x_2 - x_1}{x_1} = \sqrt[3]{\frac{\rho_0^*}{\rho_0}} - 1;$$

x_1 and x_2 are the radii of the elementary spheres containing a mass of earth equal to unity. Since $4\pi x_1^3 = \frac{3}{\rho_0}$, then

$$\varepsilon_k = 3\frac{p_{crit}}{\rho_0}\left[\sqrt{\frac{\rho_0^*}{\rho_0}} - 1\right]. \qquad (93.61)$$

Assuming that $\frac{\rho_0^*}{\rho_0} \approx 2$, we arrive at the relationship

$$\varepsilon_k \approx \frac{p_{crit}}{\rho_0},$$

which, for $\rho_0 = 2$,gives $\varepsilon_k \approx \frac{p_{crit}}{2}$ and for $p_{crit} = 20 \cdot 10^6$ bar , $\varepsilon_k = 10^7$ erg/g.

We note that the theory of explosion in the ground still requires further development.

Some experimental data obtained by the Artillery Academy verify the validity of the assumption that starting at some quite small distance from the centre of the charge (about 2 to $3r_0$) , we are justified in neglecting the compressibility of the soil particles in the case when the porosity of the ground has already been eliminated.

It has been established that the initial pressure at the shock front in the ground , resulting from detonation of a charge of hexogen attains a value of $2 \cdot 10^5$ kg/cm^2, as a result of which the rapid change of density is equal to 1.45, and the density of the ground (clay) is thus shown to be equal to 2.1 g/cm^3. The density of the ground is taken as equal to 2.8 g/cm^3.

It follows from this that for $r = r_0$, the increase in density occurs mainly on account of the elimination of porosity. The initial velocity of motion of the ground behind the wave front has been shown to be equal to 1720 m/sec.

Using relationship (93.4)

$$p_* = \frac{\rho_0 u_*^2}{1-\alpha},$$

and also the relationship for the detonation products for $k = 3$

$$\frac{u_s}{D} = 1 - \frac{3}{4}\left(\frac{p_s}{p_l}\right)^{\frac{1}{3}},$$

we arrive at the equation

$$\left(1 - \frac{u_s}{D}\right)^3 = \frac{27}{16}\frac{}{\rho_{0\,expl}}\frac{\rho_0 u_s^2}{D^2(1-a)}.$$

For

$$a = \frac{1}{1.43} = 0.7, \quad , \quad D = 8000 \text{ m/sec}, \quad \rho_0 = 2.1 \, , \quad \rho_{0\,expl} = 1.65,$$

we obtain $u_s = 1900$ m/sec, which is close to the experimental value given above.

§94. Explosion with Blowout.

Explosion in an infinite Medium. After completion of the process of detonation of an explosive charge, when the detonation wave reaches the boundary of separation between the explosive and the medium, motion of the medium commences under the action of the expanding detonation products. As a result of this a shock wave originates in the medium.

As a result of an explosion in tough metals the pressure at the shock front is greater than the pressure at the front of the detonation wave. For less rugged materials and, for example, as a result of an explosion in water, the pressure at the shock front is less than at the front of the detonation wave.

We shall not consider here the law relating to the propagation of a shock wave and we shall not take into account the multiple wave processes in the medium as a result of reflected waves, but we shall occupy ourselves with the overall picture of an explosion.

As a result of the explosion of a mass of explosive in an infinite inert medium, the volume V_∞, occupied by the expanding explosion products,

is proportional to the mass m of explosive and depends on the properties of the medium. Expansion of the detonation products proceeds from an initial pressure of

$$\bar{p}_i = (k-1)\rho_0 Q, \qquad (94.1)$$

(where k is the index of polytropy for the explosion products, ρ_0 is the density of the explosive charge and Q is the specific energy of the explosive) up to the final pressure $\bar{p}_a$, determined by the properties of the medium. In the initial stage of expansion (for $p_k \leqslant p \leqslant p_i$) it proceeds according to the law $p \sim V^{-k} \sim r^{-3k}$, then for $\bar{p}_a \leqslant p \leqslant p_k$ the expansion proceeds according to the law $p \sim V^{-k_1} \sim 2^{-3k_1}$, where $k_1 = \frac{c_p}{c_v}$ is the isentropy index.

For typical explosives

$$k = 3\ ; \quad k_1 = 1.4 - 1.25\ ; \quad \bar{p}_i \approx 10^5\ \text{kg/cm}^2\ ; \quad p_k \approx 10^3\ \text{kg/cm}^2.$$

For expansion in air or in water, where there is practically no viscous force to be overcome and practically no expenditure of energy on deformation of the medium, and its rarefaction $\bar{p}_a = p_a$, where p_a is the back-pressure of the medium. If $p_a = 1\ \text{kg/cm}^2$, then

$$V_\infty = AV_0, \qquad (94.2)$$

where V_0 is the initial volume of the explosive, $A \approx 1000$. For expansion of the detonation products in a solid medium $\bar{p}_a > p_a$. For materials with a different hardness the value of $\bar{p}_a$ can vary from 1 kg/cm^2 to 1000 kg/cm^2. As a result of this, the corresponding value of V_∞ is decreased in relation to that determined from equation (94.2) by a factor of $10^{\frac{1}{k^*}}$ or $1000^{\frac{1}{k^*}}$. In the general form, we can write that

$$V_\infty = AV_0\left(\frac{p_a}{\bar{p}_a}\right)^{\frac{1}{k^*}}, \qquad (94.3)$$

where k^* is the effective value of k, depending on the properties of the medium. For example, for typical soils

$V_\infty \approx 50\, V_0$.

The volume of the zone of destruction V_R of the ground and of any medium considerably exceeds the volume which can be occupied by the detonation products (see Fig. 247), but it is always proportional to V_∞, i.e.

$$\frac{V_R}{V_\infty} = \alpha = \text{const.} \qquad (94.4)$$

Experiment shows that for different media, including soils and rocks, $1 < \alpha < 10$, whereupon the lesser value corresponds to the toughest metal and the larger value corresponds to the toughest ground.

Thus, it can be verified that

$$V_R = \alpha V_\infty = \alpha A V_0 \left(\frac{p_a}{\bar{p}_a}\right)^{\frac{1}{k^*}}. \qquad (94.5)$$

The mass of the deformed ground $M = \rho V_R$, (ρ is the density of the ground) can be expressed via the mass of the explosive thus:

$$M = \frac{\rho}{\rho_0}\left(\frac{p_a}{\bar{p}_a}\right)^{\frac{1}{k^*}} \alpha A m_e = A_1 m_e. \qquad (94.6)$$

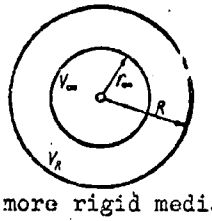


Figure 247. Zone of destruction of a medium.

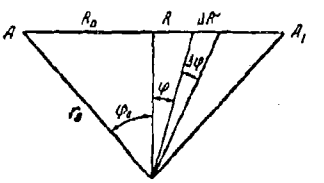
The quantities α and $\bar{p}_a$ are found from experiment. For pliable media the value of k^* is closer to k_1 than for more rigid media. For the latter the value of k^* is closer to k; for soils and slightly durable metals $p_a < \bar{p}_k$, therefore $k^* = k_1$, for hard metals $k > k^* > k_1$, and for the toughest metals $k^* \approx k$.

Explosion in a Finite Medium. The most interest is presented by the study of an explosive charge inserted to a certain depth h_0 from the earth's surface, which we shall assume to be horizontal. As a result of this the force of gravity should be taken into account.

We shall calculate the energy which is expended in overcoming the force of gravity by the explosion of a charge at a depth h_0, in the case when the

crater formed after the explosion is represented by a cone with a base radius of R_0 (see Fig. 248). We shall calculate the "gravitational" energy for the case when there is ejection of soil at the

Figure 248. For the calculation of blowout.



... since an element of mass of the earth is bounded by cones with bas radii $R+dR$; R, then

$$dM=\frac{2}{3}\pi\rho h_0 R\,dR=\frac{2}{3}\pi\rho h_0^3\frac{\sin\varphi\,d\varphi}{\cos^5\varphi}. \qquad (94.7)$$

The total mass is

$$M=\frac{\pi}{3}\rho h_0^3\tan^2\varphi_0. \qquad (94.8)$$

The element of mass bounded by the sections $(h+dh;\ h)$ is

$$dM_h=2\pi\rho h^2\,dh\,\frac{\sin\varphi\,d\varphi}{\cos^5\varphi}. \qquad (94.9)$$

Then the energy necessary for the ejection of an element of mass dM at the surface AA', is determined by the equation

$$dE_g=g(h_0-h)\,dM_h=2\pi\rho g\frac{\sin\varphi\,d\varphi}{\cos^5\varphi}(h_0-h)h^2dh, \qquad (94.10)$$

where g is the acceleration due to gravity.

Thus, integrating within the limits from h_0 to 0 and from 0 to φ_0, we find

$$E_g=\frac{\pi\rho g h_0^4}{12}\tan^2\varphi_0=\frac{Mgh_0}{4}. \qquad (94.11)$$

In the region bounded by the cones with base radii $(R+dR,\ R)$,

$$dE_g=\frac{\pi\rho g\,h_0^4\sin\varphi\,d\varphi}{6\cos^5\varphi}=\frac{gh_0}{4}dM. \qquad (94.12)$$

If it be assumed that the explosion energy is propagated isotropically (which, of course, is not altogether so), then in this region the explosion energy which acts is

$$dE_e=Q\,dm_e=m_eQ\frac{\sin\varphi\,d\varphi}{2}=\frac{E_e}{2}\sin\varphi\,d\varphi, \qquad (94.13)$$

where E_e is the total explosion energy. The explosion energy propagating inside the cone will be

$$E_{\varphi 0}=E_e\frac{1-\cos\varphi_0}{2}. \qquad (94.14)$$

Thus

$$\frac{dE_g}{dE_0} = \frac{\pi \rho g h_0^4}{3E_0 \cos \varphi}. \qquad (94.15)$$

Obviously, if the energy losses in breaking up the ground are not taken into account, ejection will occur for the condition that $dE_0 \geqslant dE_g$, whence it follows that

$$\frac{\pi \rho g h_0^4}{3 \cos^3 \varphi} \leqslant E_0.$$

Thus, for a given depth h_0

$$\cos \varphi = \cos \varphi_0 \geqslant \left(\frac{\pi \rho g h_0^4}{3E_0}\right)^{\frac{1}{3}}. \qquad (94.16)$$

The maximum possible depth is determined from this relationship for $\varphi_0 = 0$

$$h_0 = h_{0m} = \left(\frac{3E_0}{\pi \rho g}\right)^{\frac{1}{4}}. \qquad (94.17)$$

By means of equation (94.17) we write equation (94.16) in the form

$$\cos \varphi_0 \geqslant \left(\frac{h_0}{h_{0m}}\right)^{\frac{4}{3}}. \qquad (94.18)$$

Relationships (94.16) and (94.17) give the optimum values for h_0 and the angle of flare of the cone φ_0. If the irreversible losses be taken into account, then the values of h_0 and φ_0 will be less than those determined by these relationships.

We shall now calculate the residual velocity a_0, with which part of the ground will be ejected from the crater at an angle φ from the normal. We shall calculate the maximum velocity of ejection below, but for the present we shall only assume that the particles of earth acquire the velocity quite rapidly, but in the process of its ejection, part of the velocity is expended on overcoming the force of gravity.

It is obvious that, from the Law of Conservation of Energy, we can write

$$\frac{a_0^2}{2}dM + dE_g = dE_e,$$

whence

$$a_0 = \sqrt{2\left[\frac{dE_e}{dM} - \frac{dE_\eta}{dM}\right]} = \sqrt{\frac{3}{2}\frac{E_e\cos^3\varphi}{\pi\rho h_0^3} - \frac{gh_0}{2}}, \qquad (94.19)$$

or

$$a_0 = \sqrt{\frac{gh_0}{2}\left[\left(\frac{h_{0m}}{h_0}\right)^4\cos^3\varphi - 1\right]}.$$

For $\cos\varphi = \left(\frac{h_0}{h_{0m}}\right)^{\frac{4}{3}}$, $a_0 = 0$, and for $\varphi = 0$

$$a_0 = a_{0m} = \sqrt{\frac{gh_0}{2}\left[\frac{h_{0m}^4}{h_0^4} - 1\right]}.$$

If $h_0 = h_{0m}$, then for $\varphi = 0$, $a_{0m} = 0$. The relationship

$$\frac{E_\eta}{E_e} = \frac{\pi\rho g h_0^4\tan^2\varphi}{12E_e} = \left(\frac{h_0}{h_{0m}}\right)^4\left(\frac{\tan\varphi}{2}\right)^2. \qquad (94.20)$$

For $\varphi = \varphi_0$

$$\frac{E_g}{E_e} = \left(\frac{h_0}{h_{0m}}\right)^4\left(\frac{\tan\varphi_0}{2}\right)^2 = \frac{1}{4}\left[\left(\frac{h_0}{h_{0m}}\right)^{\frac{4}{3}} - \left(\frac{h_0}{h_{0m}}\right)^4\right]. \qquad (94.21)$$

The relationship

$$\frac{E_g}{E_e} = \frac{\pi\rho g h_0^4\tan^3\varphi_0}{6E_e(1-\cos\varphi_0)} = \frac{\pi\rho g h_0^4(1+\cos\varphi_0)}{6E_e\cos^3\varphi_0} \qquad (94.22)$$

For $\cos\varphi_0 = \left(\frac{\pi\rho g h_0^4}{3E_e}\right)^{\frac{1}{3}}$

$$\frac{E_g}{E_{\varphi_0}} = \frac{1}{2}\left(\frac{\pi\rho g h_0^4}{3E_e}\right)^{\frac{1}{3}}\left[1 + \left(\frac{\pi\rho g h_0^4}{3E_e}\right)^{\frac{1}{3}}\right] = \frac{1}{2}\cos\varphi_0(1+\cos\varphi_0).$$

For a finite value of $\frac{h_1}{h_{0m}} = \lambda$, the value of $\frac{E_g}{E_e}$ attains a maximum. We can easily find from (94.21), that

$$\lambda = \left(\frac{1}{2}\right)^{\frac{3}{8}} \approx \frac{2}{3}.$$

As a result of this

$$\frac{E_g}{E_e} = \frac{\sqrt{3}}{2\cdot 9} \approx 0.1; \quad \cos\varphi_0 = \left(\frac{1}{3}\right)^{\frac{1}{2}} = \frac{\sqrt{3}}{3} \approx 0.58;$$

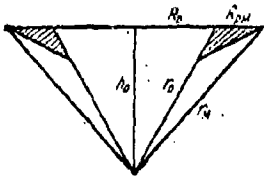
$$\frac{R_0}{h_0} = \tan\varphi_0 = \sqrt{2} \approx 1.4.$$

On the basis of the relationships introduced, the parameters can be evaluated for the crater formed by the explosion and the subsequent ejection of material.

We shall now define more precisely the ideas discussed above concerning blowout and explosion.

The initial shape of the crater should be conical, which is perfectly natural, since ejection of the medium takes place more or less along the radii R. However, near the surface of the crater a rarefaction (relaxation) wave originates, which leads to the fact that at the surface itself they may be complementarily destroyed and a certain mass of the medium may be ejected. (Fig. 249). As a result of this, the radius of the crater is somewhat increased (from R_0 to R_{cm}) and the shape of the crater is altered. It is not very simple to take this effect accurately into account, and we shall not consider this here. All the relationships introduced above are of significance if $h \leqslant h_{cm} \leqslant R_{cm}$, where R_{cm} is the maximum radius of the zone of collapse, taking into account the effect of the free surface.

Figure 249. Volume of collapsed rock.



From this condition and from equation (94.6), it follows that

$$\frac{3E_0}{\pi\rho g} \leqslant R_{cm}^4 = \left(\frac{3V_{cm}}{4\pi}\right)^{\frac{4}{3}} = \left(\frac{3M_{cm}}{4\pi\rho}\right)^{\frac{4}{3}}, \qquad (94.25)$$

where V_{cm} and M_{cm} are the volume and mass of the zone of collapse. Since

$$M_{cm} = A_1 \frac{E_0}{Q} = A_1 m_0, \qquad (94.24)$$

where $A_1 = \frac{\rho}{\rho_0}\bar{\alpha}A\left(\frac{p_0}{p_a}\right)^{\frac{1}{k^2}}$ (see equation (94.6)); $\bar{\alpha}$ is a coefficient characterising the increase in the zone of collapse, then equation (94.24) can be written in the form

$$\frac{g'_{expl}}{4Q} \geqslant \frac{\rho_0}{\rho A_1^{4/3}},$$

where $r_{expl} = \left(\frac{3}{4\pi}\frac{m_e}{\rho_0}\right)^{\frac{1}{3}}$ is the radius of the explosive charge.

Hence it follows that the greater the calorific value of the explosive Q, the moreso is the inequality (94.25) fulfilled as a result of the greater force of gravity. In the absence of a gravitational force, the inequality (94.25) is never fulfilled.

We shall now consider the various possibilities of formation of a crater as a result of an explosion :

1. If $r_0 > R_{rm}$, then for $h_0 \geqslant h_{0m}$ the crater is not formed, but a so-called camouflet is obtained.

2. If $h_0 < R_{rm}$, then for $h_0 \geqslant h_{0m}$ partial bulging of the surface will be observed in the vicinity of the epicentre (above the site of the explosion).

3. If $h_0 < R_{rm}$, for $h_0 < h_{0m}$ we shall have the case considered above, when a crater is formed.

With decrease of h the profile of the crater will be altered (the angle φ_0 will be increased).

The first two cases are of no interest at present and we shall next occupy ourselves with a more detailed analysis of the third case.

Now, let $h_0 \ll h_{0m} < R_{rm}$. . The angle of flare of the crater cone is determined from relationship (94.15)

$$\cos\varphi_0 = \left(\frac{\pi\rho g h_0^4}{3E_e}\right)^{\frac{1}{8}} = \left(\frac{h_0}{h_{0m}}\right)^{\frac{4}{3}}, \qquad (94.25)$$

as a result of which $\frac{\pi\rho g h_0^4}{3E_e} \ll 1$. . The radius of the crater

$$R_0 = h_0 \tan\varphi_0 = h_0\sqrt{\left(\frac{3E_e}{\pi\rho g h_0^4}\right)^{\frac{2}{3}} - 1}.$$

The specified relationships will be valid only for the condition that

$$R_0 = \frac{h_0}{\cos\varphi_0} \ll R_{rm}. \qquad (94.26)$$

Thus, the magnitude of the angle of flare of the cone is determined from the relationship

$$\cos\varphi_0 = \cos\varphi_{0\,\text{lim}} = \frac{h_0}{R_{rm}}. \qquad (94.26)$$

If $\varphi_{0\,\text{lim}} \leqslant \varphi_0$, then $\cos\varphi_0 \geqslant \frac{h_0}{r_{rm}}$ and the crater radius will be

$$R_{0\,\text{lim}} = h_0 \quad \varphi_{0\,\text{lim}} = \sqrt{R_{rm}^2 - h_0^2}. \qquad (94.27)$$

The limiting condition (94.26) leads to this relationship:

$$\cos\varphi_{0\,\text{lim}} = \frac{h_0}{\left(\frac{3}{4\pi}\frac{A}{\rho}\frac{E_e}{Q}\right)^{\frac{1}{3}}} = \frac{h_0}{r_{\text{expl}}}\sqrt[3]{\frac{\rho}{\rho_0 A_1}}. \qquad (94.28)$$

Thus, if $R_0 \leqslant R_{rm}$, then on integration the angle φ is changed from 0 to φ_0, and for $R_0 > R_{rm}$ from 0 to $\varphi_{0\,\text{lim}}$. The relationships presented above completely define the crater which is formed as a result of the explosion of an explosive charge of mass m at a depth h_0, if $h_0 \leqslant R_{rm}$.

If $R_0 \leqslant R_{rm}$, then $\cos\varphi_0$ is calculated from relationship (94.25); if $R_0 > R_{rm}$, then $\cos\varphi_0 = \cos\varphi_{0\,\text{lim}}$ is calculated from relationship (94.28). Then we can calculate

$$R_0 = h_0 \tan\varphi_0 \quad \text{and} \quad M = \frac{\pi}{3}\rho h_0^3 \tan^2\varphi_0.$$

A criterion of this case, as a result of formation of a crater, will be the dimensionless quantity

$$\eta_\varphi = \frac{\cos^3\varphi_0}{\cos^3\varphi_{0\,\text{lim}}} = \frac{A_1 g h_0}{4Q}. \qquad (94.29)$$

If $\eta_\varphi > 1$, then $\varphi_{0\,\text{lim}} > \varphi_0$, and we shall be concerned with the case when $R_0 < R_{rm}$, as a result of which the force of gravity plays the principal rôle; if $\eta_\varphi < 1$, then $\varphi_{0\,\text{lim}} < \varphi_0$ and we shall be concerned with the case when $R_0 > R_{rm}$, as a result of which the radius of collapse of the medium plays the principal rôle.

If there is no gravitational field, then we shall always be concerned

with the second case. The very same will be the case as a result of using very high calorific value explosives. Only in the case of a very pliable medium, when the quantity A_1 is large, shall we be concerned with the first case for higher values of Q. As a result of the presence of a strong gravitational field we may be concerned with both cases, depending on the value of g, Q and the quantity A_1, which characterises the medium.

We shall now determine the ultimate relationship between the mass of the medium ejected from the crater by the explosion, the mass of the explosive, its calorific value (or explosion energy), the initial depth of the explosion centre and we shall examine the optimum depth for which the ejected mass proves to be a maximum for the two cases $\eta_* > 1$ and $\eta_* < 1$.

For $\eta_* > 1$ we have

$$M = \frac{\pi}{3} \rho h_0^3 \tan^2 \varphi_0, \tag{94.30}$$

where

$$1 \geqslant \cos \varphi_0 \geqslant \left(\frac{\pi \rho g h_0^4}{3E_*} \right)^{\frac{1}{3}}$$

for $\cos^3 \varphi_0 = \frac{\pi \rho g h_0^4}{3E_*}$,

$$M = \frac{\pi}{3} \rho h_0^3 \left[\left(\frac{3E}{\pi \rho g h_0^4} \right)^{\frac{2}{3}} - 1 \right]. \tag{94.31}$$

It is obvious that the mass of the ejected material has a maximum for a definite depth h_0, and this maximum will occur for

$$\bar{h}_0 = \left(\frac{E_*}{9\pi\rho g} \right)^{\frac{1}{4}} = \frac{h_{0m}}{27^{1/4}} = 0.44 h_{0m}$$

(the inequality $\frac{\pi \rho g h_0^4}{3E_*} < 1$ 1 is satisfied for this).

Substituting the value we have found for $h_0 = \bar{h}_0$ in equations (94.25), (94.26) and (94.31), we arrive accordingly at the expressions:

$$\cos\bar{\varphi}_0 = \frac{1}{3};\quad \bar{\varphi}_0 \approx 70°;\quad \bar{R}_0 = 2\sqrt{2}\bar{h}_0 = 2\sqrt{2}\left(\frac{E_*}{9\pi\rho g}\right)^{\frac{1}{4}};$$

$$M = \frac{8\pi}{3}\rho\left(\frac{E_*}{9\pi\rho g}\right)^{\frac{3}{4}}. \qquad (94.32)$$

For $\eta_\varphi < 1$ we have

$$M = \frac{\pi}{3}\rho r_0^3 \sin^2\varphi_0 \cos\varphi_0 = \frac{\pi}{3}\rho h_0^3 \tan^2\varphi_0, \qquad (94.33)$$

where $1 \geqslant \cos\varphi_0 \geqslant \frac{h_0}{r_{rm}}$

For $\cos\varphi_0 = \frac{h_0}{R_{rm}}$

$$M = \frac{\pi}{3}\rho R_{rm}^2 h_0\left(1 - \frac{h_0^2}{R_{rm}^2}\right). \qquad (94.34)$$

It is obvious that just as in the previous case, the mass of ejected material for a definite depth h_0 has a maximum value. This maximum will occur for $\bar{h}_0 = \frac{\sqrt{3}}{3}R_{rm}$. For this

$$\left.\begin{aligned} &\tan\bar{\varphi}_0 = \sqrt{2};\ \cos\bar{\varphi}_0 = \sqrt{\frac{1}{3}};\quad \sin\bar{\varphi}_0 = \sqrt{\frac{2}{3}};\quad \bar{\varphi}_0 \approx 55°; \\ &\bar{M} = \frac{2\sqrt{3}}{27}\pi\rho R_{rm}^3 = \frac{2\pi}{g}\rho\bar{h}_0^3. \end{aligned}\right\} \qquad (94.35)$$

As we can see, depending on whether the criterion η_φ is greater or less than unity, different optimum angles of the cone are obtained.

For $\eta_\varphi > 1$ $\bar{\varphi}_0 \approx 70°$; for $\eta_\varphi < 1$ $\bar{\varphi}_0 \approx 55°$.

We shall now relate the purely theoretical results which we have obtained with the basic experimental data.

It is well-known that for a certain depth of insertion of the charge (which is not always optimum in the sense of obtaining the maximum ejected mass), the crater radius is

$$R_0 = \lambda m^{\frac{1}{3}}, \qquad (94.36)$$

where λ is an experimentally determined coefficient.

Assuming that $R_{0m} = R_0$, we can write equation (94.36) in the form

$$R_{0m}^3 = \lambda^3 m_*. \qquad (94.37)$$

It is further obvious that

$$M_{rm} = \frac{4}{3}\pi\rho\bar{r}_{0m}^3 = \frac{4}{3}\pi\rho\lambda^3 m_e. \qquad (94.38)$$

Comparing equations (94.24) and (94.38), we find that

$$A_1 = \frac{4}{3}\pi\rho\lambda^3. \qquad (94.39)$$

On the other hand

$$A_1 = \frac{\rho}{\rho_0}\bar{\alpha}A\left(\frac{p_a}{p_a}\right)^{\frac{1}{k^2}},$$

and therefore

$$\frac{4}{3}\pi\rho_0\lambda^3 = \bar{\alpha}A_1\left(\frac{p_a}{p_a}\right)^{\frac{1}{k^2}}. \qquad (94.40)$$

These relationships establish the relationship between the empirical parameters α, A, A_1 and λ.

Since the quantity A is quite well known, λ is determined by experiment, then we can find A_1 from equation (94.39), and from equation (94.40) we can find the extremely important coefficient $\bar{\alpha}$; We note that $\bar{\alpha} = f\left(\frac{p_a}{p_a}\right)$.

We now determine the momentum of the material ejected as a result of the explosion. First of all we determine the so-called total (scalar) momentum (J_t). It is obvious that

$$dJ_t = a\,dM = a_{lim}dM = \sqrt{\frac{2\pi\rho h_0^3 E_e}{3\cos^3\varphi}}\,d\varphi\sin\varphi, \qquad (94.41)$$

whence, integrating within the limits of variation of the angle φ from 0 to φ_0, (assuming that $\varphi_0 = \varphi_{0lim}$), we find

$$J_t = 2\sqrt{\frac{2}{3}\pi\rho h_0^3 E_e}\left[\frac{1-\sqrt{\cos\varphi_0}}{\sqrt{\cos\varphi_0}}\right] = \bar{\delta}\sqrt{2ME_e}, \qquad (94.42)$$

where

$$\bar{\delta} = \frac{2}{\sqrt{\cos\varphi_0}}\,\frac{1-\sqrt{\cos\varphi_0}}{\tan\varphi_0}. \qquad (94.43)$$

It is useful here to introduce instead of the total explosion energy E_e,

that portion of the energy E_{φ_0}, which is propagated within a specified cone with a vertex angle of $2\varphi_0$.

From equation (94.13) we find

$$E_{\varphi_0} = E_0 \frac{1-\cos\varphi_0}{2}, \tag{94.44}$$

and as a result of this equation (94.42) assumes the form

$$J_1 = \theta\sqrt{2ME_{\varphi_0}}, \tag{94.45}$$

where

$$\theta = \frac{2\sqrt{2\cos\varphi_0}}{\sqrt{1+\cos\varphi_0}\,[1+\sqrt{\cos\varphi_0}]}. \tag{94.46}$$

For example, for $\varphi_0 = 0$, $\theta = 1$; $\frac{E_{\varphi_0}}{E_0} = 0$; for $\varphi_0 = 60°$, $\theta = 0.95$; $\frac{E_{\varphi_0}}{E_0} = \frac{1}{4}$.

We now determine the projection of the momentum J_z on the z axis, perpendicular to the surface of the earth. It is obvious that

$$dJ_z = a_{\text{lim}}\cos\varphi\, dM = \sqrt{\frac{2\pi\rho h_0^3 E_0}{3\cos\varphi}}\sin\varphi\, d\varphi. \tag{94.47}$$

Hence,

$$J_z = 2\sqrt{\frac{2}{3}\pi\rho h_0^3 E_0}\,[1-\sqrt{\cos\varphi_0}] = \theta_1\sqrt{2ME_0}, \tag{94.48}$$

where

$$\theta_1 = \frac{2(1-\sqrt{\cos\varphi_0})}{\tan\varphi_0}. \tag{94.49}$$

Further, substituting E_0 by E_{φ_0}, we find that

$$J_z = \theta_1\sqrt{2ME_{\varphi_0}}, \tag{94.50}$$

where

$$\theta_1 = \frac{2\sqrt{2}\cos\varphi_0}{(1+\sqrt{\cos\varphi_0})\sqrt{1+\cos\varphi_0}}. \tag{94.51}$$

For example, for $\varphi_0 = 0$, $\theta_1 = 1$; $\varphi_0 = 60°$, $\theta_1 = \frac{2}{3}$. We can write that $\theta_1 = \theta\sqrt{\cos\varphi_0}$, whereupon the coefficient θ is a measure of the velocity distribution depending upon the quantity of the mass of ejected material through different angles. If there were not this distribution, then $\theta = 1$ and

$J_{t0} = \sqrt{2ME_{\varphi_0}}$.

Now we can finally write down that

$$J_t = \theta J_{t0}; \quad J_z = J_t \sqrt{\cos\varphi_0} = \theta \sqrt{2ME_{\varphi_0}\cos\varphi_0} = \theta J_{t0} \sqrt{\cos\varphi_0}. \qquad (94.52)$$

However, for practical calculations it is more convenient to use relationships (94.42) and (94.48).

From these relationships, for example, it follows that for $\varphi_0 = 60°$,

$$J_t = 0.48\sqrt{2ME_0}; \quad J_z = \frac{1}{3}\sqrt{2ME_0} = \frac{2}{3}\sqrt{2ME_{\varphi_0}}.$$

In the general form, without predetermining the law of distribution of velocities with respect to mass, we can write

$$J_t = \int_0^{\varphi_0} a(\varphi)\, dM(\varphi); \quad J_z = \int_0^{\varphi_0} \cos\varphi\, a(\varphi)\, dM(\varphi),$$

where $a = a[M(\varphi)] = a(\varphi)$ is the law of distribution of velocities with respect to mass.

The theoretical relationships which we have obtained above may be made more precise by additionally taking into account the energy which, as a result of propagation of the shock wave, is expended on heating up and on irreversible deformation of the medium. These energy losses at a large depth of insertion of the charge may be considerable, and should be determined experimentally.

§ 95. Impact of Meteorites against a Solid Surface.

It is well-known that as a result of the impact of solid bodies with velocities in excess of several kilometres per second, a phenomenon closely resembling the appearance of an explosion has been observed.

For an impact velocity of greater than 3 - 4 km/sec, the crystalline structure of the meteorite and a certain volume of the medium with which the meteorite collides is destroyed, and an explosion occurs in the full sense of the word.

We shall define more precisely those processes which may be observed as a result of impact at velocities greater than a few kilometres per second.

Explosion of a Meteorite in an Infinite Medium. We shall consider first of all the "explosion of a meteorite" in an infinite medium. It is obvious that the problem may be posed in the following manner. Suppose that in a certain volume, equal to the volume of the meteorite, energy $E_0 = \frac{M_0 u_0^2}{2}$. be liberated instantaneously. The mass $m_{\bar{k}}$, inside of which "vapourisation" of the medium will occur, is obviously determined by the relationship

$$M_0 \varepsilon_k + m_{\bar{k}} \varepsilon_{\bar{k}} = \eta \frac{M_0 u_0^2}{2} = \eta E_0, \tag{95.1}$$

where $\eta < 1$ is the energy efficiency factor

$$\varepsilon_k = \frac{u_k^2}{2}, \quad \varepsilon_{\bar{k}} = \frac{\bar{u}_k^2}{2}, \tag{95.2}$$

where ε_k and $\varepsilon_{\bar{k}}$ is the energy density required for "vapourisation" of the material of the medium and of the medium and u_k and $\bar{u}_k$ are the limiting velocities required to "vaporise" unit mass of material of the meteorite and of the medium.

If $u_0 > u_k \geqslant u_{\bar{k}}$, then it is possible to make a distinction between the quantities ε_k and $\varepsilon_{\bar{k}}$ for the impacting body and for the body receiving the impact.

Then equation (95.1) assumes the form

$$M_0 + m_k = \eta \frac{M_0 u_0^2}{u_k^2}. \tag{95.3}$$

Since the value of ε_k is close to the energy density Q liberated by the explosion of condensed explosives, and since experimental relationships are well-known for the effect of explosions at the surface and inside different bodies, which relate the mass of the charge of explosive (m_*), its specific energy (Q), the radius, depth and shape of the crater in different media, then it is more advantageous to write Q in place of ε_k and $\varepsilon_{\bar{k}}$ in relationships (95.1) and (95.3).

Actually, for typical explosives $Q = 1 \div 1.5$ kcal/g, and ε_k for

example, has the value of 2 ; 1 and 5 kcal/g for iron, aluminium and granite respectively. Consequently, we can write down that

$$m_* Q = \eta E_0 = \eta \frac{M_0 u_0^2}{2}. \tag{95.4}$$

Hence it follows that

$$m_* = \eta \frac{M_0 u_0^2}{2Q}. \tag{95.5}$$

After expansion of the gas up to an energy density value equal to Q, the ultimate expansion stage may be likened to the expansion of the explosion products from an explosive, but somewhat more dense than the normal explosive.

Actually, the density of rock is about 3 g/cm^3, the density of iron is about 8 g/cm^3 and the density of a standard explosive is 1.6 g/cm^3.

Thus, the volumetric energy density in the case being considered will be several times greater than in the case of explosion of normal explosives.

We shall now put the problem somewhat more precisely.

As a result of an impact and an explosion, a shock wave is formed which will be propagated through the medium. Since at the shock front part of the energy will be expended on "destruction" of the medium, then it is necessary to take into account this energy loss in writing down the Law of Conservation of Energy for this shock front.

For a strong wave these conditions will have the form :

$$E_1 = \frac{p_1}{2}(V_0 - V_1) - \varepsilon_k^*, \tag{95.6}$$

$$u_1^2 = p_1(V_0 - V_1), \tag{95.7}$$

$$D_* = \frac{V_0^2 p_1}{V_0 - V_1} = \left(\frac{V_0 u_1}{V_0 - V_1}\right)^2. \tag{95.8}$$

Thus the relationship $E_1 = f(p_1; V_1)$ depends on the equation of state of the medium and in a certain sense on the initial impact velocity, since at different pressures the equation of state may be approximated differently.

From equations (95.6) and (95.7) we have

$$E_1 = \frac{u_1^2}{2} - \varepsilon_k^*. \tag{95.9}$$

By ε_k^* in these relationships one should understand the energy going into one or other of disturbance and destruction of the crystalline lattice. Obviously, this process of destruction of the crystal lattice will continue until at the shock front

$$E_1 + \frac{u_1^2}{2} \geqslant \varepsilon_k^*. \tag{95.10}$$

Form equations (95.9) and(95.10) it follows that the process of destruction of the lattice will take place for

$$\frac{u_0^2}{2} \geqslant \varepsilon_k^*. \tag{95.11}$$

By introducing $u_k^* = \sqrt{2\varepsilon_k^*}$, we can define more precisely the condition $u_0 \geqslant u_k^*$, which is formulated above. Since from equation (95.11) it follows that $u_1 \geqslant u_k^*$, and that $u_1 \approx \frac{u_0}{2}$ then $u_0 \geqslant 2u_k^*$ or

$$\frac{u_0^2}{2} \geqslant 2u_k^{*2} = 4\varepsilon_k^*. \tag{95.12}$$

In the first instant of time after impact, when the regime of motion and " "flow" has not yet been established, "vapourisation" will take place for the condition that $u_0 \geqslant u_k^*$, then after an interval of time $\tau = \frac{2l}{u_0}$ a regime is quite rapidly established when "vapourisation" will take place for the condition that $u_0 > 2u_k$.

We shall define more precisely once more what is understood by ε_k^*. For vapourisation $\varepsilon_k^* = \varepsilon_i$, for fusion $\varepsilon_k^* = \varepsilon_k$, for simple "disintegration" (dispersion) of the medium $\varepsilon_k^* = \varepsilon_k$. In the first two cases, the expenditures of energy in the expansion process, going into latant heat of vaporisation and fusion, are restored again to the medium in the process of expansion, except for a small portion of the medium which has already expanded as a result of discharge from the dense medium(from the crater) into the atmosphere or into an empty space. However, these losses can, in general, be neglected, all the

more, since relatively the initial energy as a result of this will be greater than in the case of simple dispersion of the medium. Finally, the energy expenditure $\varepsilon_k^* = \bar{\varepsilon}_k$ will be irreversible. It can be assumed, as was done above, that $\varepsilon_k^* = Q$ approximately, for different media. Consequently, it is always possible to introduce, just as in the case of an atomic explosion, the trotyl (TNT) equivalent, which arises from the Law of Conservation of Energy, i.e. the kinetic energy (E_0) of the impacting body, taking into account losses (allowing for efficiency), can be equated to the energy of an explosive (TNT) having a mass m and a calorific value Q assuming that $mQ = \eta E_0$.

It can be assumed for simplicity that the process of detonation in a dense medium is instantaneous. The process of "destruction" we shall arbitrarily call the process of "vaporisation".

As a result of a detonation, the energy density at the front of the detonation wave is :

$$\varepsilon_{i.d.} = E_{i.d.} + \frac{u_{i.d.}^2}{2}; \tag{95.13}$$

where

$$E_{i.d.} = \frac{p_{i.d.}(V_{0d} - V_{i.d})}{2} = \frac{u_{i.d.}^2}{2}. \tag{95.14}$$

is the potential energy ; thus,

$$\varepsilon_{i.d.} = u_{i.d.}^2 = 2Q. \tag{95.15}$$

For an instantaneous detonation, the mean energy density is :

$$\bar{\varepsilon}_d = \frac{u_{i.d.}^2}{2} = Q. \tag{95.16}$$

In the second case, when $\varepsilon_d = Q$, the problem is reduced to the comparison of Q, the effect of the impact with the effect of an explosion with a charge mass of $2m$, and a calorific value of $\frac{Q}{2}$ by the hypothesis of instantaneous detonation. In the first case, the problem is reduced approximately to the case of real detonation of an explosive charge with a mass m, and calorific value Q.

we understand by a case of real detonation the case when the pressure at the front of the detonation wave is twice as big as the average pressure and the energy density at the front is $u_1^2 = 2Q$.

Both cases are sufficiently equivalent to one another, which follows from explosion theory.

The first case breaks down to a more simple analysis and we shall now discuss it further.

Now, the equivalent mass of an explosive charge m_e having a calorific value Q will be determined, for future calculations, by relationship (95.5)

Explosion of a Meteorite in a Finite Medium. First of all we shall determine the maximum depth of the depression - crater, formed by the impact of a meteorite with the surface of any medium. This depth is determined by the depth of penetration and by the radius of the vaporised mass of the medium. It is necessary to further take into account that after the process of vaporisation ceases, disintegration of the medium will simply take place at the front of the dying shock wave and part of this disintegrated medium may be ejected outwards, which further increases the depth of the crater ; however, this additional depth will be less than the depth of the vaporised zone.

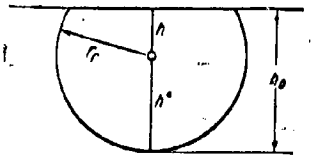


Figure 250. Calculation of crater depth.

Thus, the total crater depth (Fig. 250) is

$$h_0 = h + h^*, \tag{95.17}$$

where

$$h = \left(\frac{2M_0}{c_m S\rho} \ln \frac{u_0}{u_k^*}\right) \cos z, \quad h^* = r_* = \sqrt[3]{\frac{3m_e}{4\pi\rho}}. \tag{95.18}$$

In these relationships, M_0 is the mass of the meteorite, u_0 is its velocity,

c_x is the resistance factor, S is the surface of impact of the meteorite and ρ is its density, z is the angle between the direction of the velocity of of the meteorite and the normal to the surface of impact, and r_z is the radius of the collapsed zone - "vaporised" zone. Since

$$m_* = \eta \frac{M_0 u_0^2}{2Q}$$

(here and in future we shall understand by the quantity $Q = \frac{u_k^{*2}}{2} = \varepsilon_k^*$, the energy density required for destruction of lattice binding or of the finely divided rock), then

$$h_0 = \frac{2M_0}{c_x S \rho} \cos z \ln \frac{u_0}{u_k^*} + \sqrt[3]{\frac{3\eta M_0 u_0^2}{8\pi\rho Q}} \quad (u_\infty^* = u_\infty \approx u_k^*). \tag{95.19}$$

Since $M_0 = \delta l S$; then we can write that

$$\frac{M_0}{S\rho} = l \frac{\delta}{\rho} = \bar{\alpha}^* \frac{\delta}{\rho} \sqrt[3]{\frac{3M_0}{4\pi\delta}}, \tag{95.20}$$

where $\bar{\alpha}^*$ is the shape factor of the meteorite ; for a sphere, for example, $\bar{\alpha}^* = 1$. Now, equation (95.19) is conveniently presented in the form

$$h_0 = \sqrt[3]{\frac{3\bar{\eta}\eta M_0 u_0^2}{8\pi\rho Q}},$$

where

$$\bar{\eta}^3 = 1 + \Delta = 1 + \cos z \sqrt[3]{\frac{2Q\delta^2}{\eta\rho^2 u_0^2} \frac{2}{c_x} \bar{\alpha}^* \ln \frac{u_0}{u_k^*}}.$$

The mass of the medium ejected from the crater(assuming that the shape of the crater is conical), is determined by the relationship

$$M = \frac{\pi}{3} \rho h_0^3 \tan^2 \varphi_0 = \frac{\bar{\eta}\eta M_0 u_0^2}{8Q} \tan^2 \varphi_0. \tag{95.21}$$

Now we shall determine the normal projection of the impulse of the explosion (see equation (94.48))

$$J_z = \bar{\theta}_1 \sqrt{2ME_*}. \tag{95.22}$$

Since

$$E_* = \eta E_0, \quad M = \frac{\bar{\eta}\eta E_0}{4Q} \tan^2 \varphi_0,$$

then

$$J_z = \sqrt{\frac{2\bar{\eta}}{Q}}\,\eta E_0 (1 - \sqrt{\cos\varphi_0}). \qquad (95.23)$$

For

$$\eta_\varphi = \frac{A g h_0}{4Q} \leqslant 1, \quad \cos\varphi_0 = \frac{h_0}{r_{r.m}} = \left(\frac{\bar{\eta}}{A}\right)^{\frac{1}{3}}.$$

For $\eta_\varphi \geqslant 1$;

$$\cos\varphi_0 = \frac{h_0}{r_0} = \left(\frac{\pi\rho g h_0^4}{3E_*}\right)^{\frac{1}{3}} = \left(\frac{\bar{\eta} g h_0}{4Q}\right)^{\frac{1}{3}} = \left(\frac{\bar{\eta} g}{4Q}\right)^{\frac{1}{3}} \left(\frac{3\bar{\eta}\eta M_0 u_0^2}{8\pi\rho Q}\right)^{\frac{1}{9}}.$$

We shall evaluate the dimensionless quantities A, η, and $\bar{\eta}$, entering into these relationships. As we have shown above, the quantity η is slightly less than unity :

$$\bar{\eta}^{\frac{1}{3}} = 1 + \frac{2\bar{\alpha}}{c_\infty}\cos z \sqrt[3]{\frac{2\delta Q}{\eta\rho u_0^2}} \ln\frac{u_0}{u_\infty^*}$$

for $u_0 = u_\infty$, $\bar{\eta} = 1$; if $z = 0$, $c_\infty = 2$, $\bar{\alpha} = 1$, and $\rho = \delta$; we shall have :

$$\bar{\eta}^{\frac{1}{3}} = 1 + \left(\ln\frac{u_0}{u_\infty}\right)\sqrt[3]{\frac{2Q}{u_0^3}} = 1 + \left(\frac{u_\infty^*}{u_0}\right)^{\frac{2}{3}} \ln\frac{u_0}{u_\infty^*}.$$

Let $u_0 = e^3 u_\infty^* \approx 20 u_\infty^*$, then $\bar{\eta}^{\frac{1}{3}} = 1 + \frac{3}{7.5} = 1 + \frac{1}{2.5} = 1{,}4.$

The quantity $\bar{\eta}^{\frac{1}{3}} = \bar{\eta}^{\frac{1}{3}}_{\max} = 1 + \frac{1}{e^{1/3}} = 1.5$ for $u_0 = e u_\infty^*$. Consequently, the range of variation of $\bar{\eta}$ is not very significant. Since $\eta < 1$, $A \gg 1$ then the second term, into which $\bar{\eta}^{\frac{1}{3}}$ enters, does not play a large role; it is small in comparison with the first term ; however, this quantity $\bar{\eta}^{\frac{1}{3}}$ is always easy to find if the shape of the impacting body is known.

We shall now evaluate the essential quantity A . Since

$$A = \bar{\alpha} A_1 \frac{\rho}{\rho_0}\left(\frac{p_a}{p_a}\right)^{\frac{1}{k^2}} = \frac{4}{3}\pi\rho\lambda^3,$$

then, having experimental data for λ , it is easy to calculate q and the quantity $\bar{\alpha}\left(\frac{p_a}{p_a}\right)^{\frac{1}{k^2}}$.

The following table gives the va. of λ, A, ρ and $a\left(\frac{p_a}{p_a}\right)^{\frac{1}{k^*}}$ for different media, for $p_a = 1$ kg/cm^2, $A_1 = 1000$, $k^* = \frac{7}{5}$.

Medium	ρ	λ	A	$a\left(\frac{p_a}{p_a}\right)^{\frac{1}{k^*}}$
Sand	2 - 3	100	10^7	$7 \cdot 10^3$
Clay	3.5	50	$1.7 \cdot 10^6$	$8 \cdot 10^2$
Granite	4	10	$1.6 \cdot 10^4$	6.4
Aluminium	2.6	10	10^4	6
Iron	8	5	$4 \cdot 10^3$	0.8

The velocity of disintegration of the blasted medium is determined by the relationship (see § 94, relationship (94.19)) :

$$a_0 = \left(\frac{3E_* \cos^3\varphi}{2\pi\rho h_0^3} - \frac{gh_0}{2}\right)^{\frac{1}{2}} = \left[\frac{gh_0}{2}\left(\frac{3E_* \cos^3\varphi}{\pi\rho g h_0^4} - 1\right)\right]^{\frac{1}{2}}. \qquad (95.24)$$

Substituting the value of h_0 and E_*, we arrive at the expression

$$a_0 = \left[\frac{2Q}{\eta}\cos^3\varphi - \frac{g}{2}\left(\frac{3\eta\bar{\eta}M_0u_0^2}{8\pi\rho Q}\right)^{\frac{1}{3}}\right]^{\frac{1}{2}}. \qquad (95.25)$$

For $\varphi = 0$

$$a_0 = a_{0m} = \sqrt{2Q}\left[\frac{1}{\eta} - \frac{g}{4Q}\left(\frac{3\bar{\eta}\eta M_0u_0^2}{8\pi\rho Q}\right)^{\frac{1}{3}}\right]^{\frac{1}{2}}. \qquad (95.26)$$

The mass which is disseminated within the region bounded by the cones with base radii $(R + dR; R)$, i.e. inside a given solid angle for $d\phi = \text{const}$, is determined by the relationship (see § 94, (94.7))

$$dM = \frac{2}{3}\pi\rho h_0^3 \frac{\sin\varphi\, d\varphi}{\cos^3\varphi} = \frac{\eta\bar{\eta}M_0u_0^2}{2Q}\frac{\sin\varphi\, d\varphi}{2\cos^3\varphi}. \qquad (95.27)$$

This mass will also have a velocity a_0, determined from equation (95.25). It is easy to satisfy oneself of the fact that since

$$\eta_\gamma = \frac{Agh_0}{4Q} = \frac{Ag}{4Q}\left(\frac{3\bar{\eta}\eta E_0}{4\pi\rho Q}\right)^{\frac{1}{3}}. \qquad (95.28)$$

then for relatively small energy reductions $\eta_* < 1$ and the angle of flare of the crater, formed as a result of impact and explosion, is independent of the force of gravity. On the contrary, for a large initial energy the limiting angle is determined by the acceleration due to gravity at the given planet.

For $\eta \ll 1$ we have

$$J_z = \frac{\eta E_0}{\sqrt{Q}} \sqrt{2\bar{\eta}} \left[1 - \left(\frac{\bar{\eta}}{A}\right)^{\frac{1}{6}}\right]. \tag{95.29}$$

The minimum velocity will be for $\cos^3 \varphi_0 = \frac{\bar{\eta}}{A}$, when

$$a_0 = a_{0\min} = \left[\frac{2Q}{A} - \frac{gh_0}{2}\right]^{\frac{1}{2}} \geqslant 0. \tag{95.30}$$

The total disintegrating mass is

$$M = \frac{\bar{\eta}\eta M_0 u_0^2}{8Q}\left[\left(\frac{A}{\bar{\eta}}\right)^{\frac{2}{3}} - 1\right].$$

For $\eta_* \geqslant 1$

$$J_z = \frac{\eta E_0}{\sqrt{Q}} \sqrt{2\bar{\eta}} \left[1 - \left(\frac{\bar{\eta} g}{4Q}\right)^{\frac{1}{6}} \left(\frac{3\bar{\eta}\eta M_0 u_0^2}{8\pi\rho Q}\right)^{\frac{1}{18}}\right] =$$

$$= \eta E_0 \sqrt{\frac{2\bar{\eta}}{Q}} \left[1 - \left(\frac{\bar{\eta} g h_0}{4Q}\right)^{\frac{1}{6}}\right].$$

The mimimum velocity will be equal to zero for

$$\cos^3 \varphi_0 = \frac{\bar{\eta} g h_0}{4Q}.$$

The total disintegrating mass is

$$M = \frac{\bar{\eta}\eta M_0 u_0^2}{8Q}\left[\left(\frac{4Q}{\bar{\eta} g}\right)^{\frac{2}{3}} \left(\frac{8\pi\rho Q}{3\bar{\eta}\eta M_0 u_0^2}\right)^{\frac{2}{9}} - 1\right] =$$

$$= \frac{\bar{\eta}\eta M_0 u_0^2}{8Q}\left[\left(\frac{4Q}{\bar{\eta} g h_0}\right)^{\frac{2}{3}} - 1\right].$$

If we now compare the projection of the momentum to the normal for the falling body

$$J_{0z} = M_0 u_0 \cos z$$

and the reactive force of ejection J_z

$$\frac{J_z}{J_{0z}} = \sqrt{\frac{2\bar{\eta}}{Q}} \frac{\eta M_0 u_0^3 (1 - \sqrt{\cos\varphi_0})}{2M_0 u_0 \cos z} = \sqrt{\frac{2\bar{\eta}}{Q}} \frac{\eta u_0 (1 - \sqrt{\cos\varphi_0})}{2\cos z}.$$

Since $Q = \frac{u_k^{*2}}{2}$, then finally

$$\frac{J_z}{J_{0z}} = \sqrt{\bar{\eta}} \frac{\eta(1 - \sqrt{\cos\varphi_0})}{\cos z} \frac{u_0}{u_k^*}. \qquad (95.31)$$

Since in the medium $\sqrt{\bar{\eta}\eta} = 2$, $\varphi_0 = 60°$, then for $z = 0$

$$\frac{J_z}{J_{0z}} = 0{,}6 \frac{u_0}{u_k^*}. \qquad (95.32)$$

For example, for an achondrite (stony meteorite), impacting in aluminium with a velocity $u_0 = 40$ km/sec, for which $u_k^* = 2$ km/sec,

$$\frac{J_z}{J_{0z}} \approx 12.$$

For larger velocities of impact the reactive impulse always exceeds the momentum of the falling body, and therefore the overall momentum acquired by the medium as a result of impact is practically independent of the angle.

CHAPTER XV

SYMPATHETIC DETONATION

§ 96. Transmission of a Detonation through Air

An explosive charge can effect detonation of another charge situated at some distance from the first one. This phenomenon, discovered in the middle of the last century, has attained the name of sympathetic detonation.

We shall call the charge effecting the detonation the active charge, and the one in which detonation is effected we shall call the passive charge.

The experimental and theoretical investigation of this problem is of extremely important significance, since the results of these investigations will provide the starting data for establishing the so-called safe distances for storage and production of explosives, and may be used for the construction of detonation circuits for munitions.

It has been established that the range of sympathetic detonation depends on many factors : mass, density, detonation velocity of the active charge, the physico-chemical characteristics of the passive charge, the nature of the charge container and the properties of the transmitting medium ; in addition it depends on the direction of the detonation of the active charge, the dimensions of the receptive surface of the passive charge.

Thus, for approximately equal conditions, the excitability of the passive charge is determined mainly by its sensitivity towards detonation, and the excitation capability of the active charge is determined by the detonation velocity, which characterises the power of the explosive, and by the weight and structure of the charge.

The effect of the nature of the transmitting medium is determined by the

fact that, depending on the nature of the medium, retardation takes place of the flow of detonation products or of the shock wave. The stronger this retardation, the less will be the range of transmission of sympathetic detonation. The mechanism of the process of excitation by sympathetic detonation remains quantitatively invariable for different transmitting media and different passive charges, although detonation in certain cases is effected in the passive charge of high explosive by the stream of detonation products from the active charge, and in other cases by the shock wave propagating in the inert medium separating the charges, etc.

Let us consider in more detail the problem of transmission of a detonation through different media. We shall begin with the transmission of a detonation through air.

A considerable number of papers has been devoted to the problem of transmission of a detonation through air. In this case, part of the energy of the active charge can be transferred to the passive charge by three routes :

a) by the shock wave propagating in the air ;

b) by the stream of detonation products and

c) by solid particles impelled by the explosion.

If complete detonation of the charge takes place and if in the direction towards the passive charge, and if the active charge is not enclosed in a casing, then the transfer of energy by solid particles disintegrated as a result of rupture of the casing can be excluded. There remains transfer of energy by the air shock wave and by the stream of detonation products.

It has been established by experiments, that stimulation of detonation in charges of explosive without a clearly-defined period of burning takes place only in the zone where the parameters of the shock wave from the active charge, and the parameters of the stream of detonation products are large (the pressure at the shock front $p \geq 200 - 500$ kg/cm^2). If the shock wave approaches the passive

charge with the parameters at its front having lower values, then a period of burning always precedes detonation. However, just as in the first case, so also in the second case, stimulation of an explosive transformation is of a thermal nature. This situation well explains the effect of various factors on the range of transfer of a detonation. With increasing density (reduced porisity) of the passive charge, the range of detonation transfer is increased. This is explained by the fact with decrease in density the coefficient of thermal conductivity of the explosive is decreased (the thermal contact between particles is worsened). As a consequence of this a higher temperature of heatup is attained of the surface layer of the charge. Moreover, in a porous charge, as a consequence of break through into the pores of heated air and hot products of combustion of the surface layers of the charge, the mass velocity of combustion is sharply increased, which favours transition from combustion to detonation. And, finally, in a porous charge with a low mechanical stability, as a result of the effect on it of the shock wave, practically adiabatic compression takes place of the air inclusions, which in this case play the role of "hot spots". As shown by BOWDEN and JOFFE (See Chapter II), heating up of the air in the "hot spots" to 450 - 600°C leads to an explosion, as a result of a shock. In order to achieve this heatup, it is sufficient that the shock wave should approach the charge and be reflected from it with an over-pressure at the front $\Delta p = 8 - 15$ kg/cm^2. If reflection does not occur, then the parameters of the wave which will ensure ignition of the explosive, on account of compression of air cavities, should be considerably higher ($\Delta p = 30 - 50$ kg/cm^2) Phlegmatised explosives, theparticles of which are coated with a film of low-melting substances(paraffin, wax etc) are less sensitive to the effect of this factor, since the energy of the compressed air bubble will be expended not on heating up and ignition of the explosive, but on melting the film.

Combustion of high explosive powders is easily transformed into detonation,

especially if large quantities of the explosive burn. The transition to detonation also promotes retardation of the air stream behind the shock front on encountering the passive charge. In virtue of this, the shock waves which are capable of igniting the explosive charge must be considered dangerous from the point of view of stimulation of detonation.

If the compression and heatup of the air inclusions is of no significant magnitude, then in order to determine the range of ignition, it is necessary to solve simultaneously the equations of heat transfer from the heat transfer agent (the shock wave) and the thermal conductivity equation (for the passive charge). For this it is necessary to know how the temperature of the air stream behind the shock front will vary in the vicinity of the passive charge. It is obvious that the dimensions of the passive charge will be of important significance for this, since they determine the conditions for the shock wave bypassing it. Moreover, it is important to know the thermal constants of the explosive(its thermal conductivity, specific heat, ignition temperature), and also the heat transfer factor from the air in the shock wave to the explosive and its dependence on the various factors. The solution of this problem presents well-known difficulties and at present it cannot be accomplished sufficiently accurately, in view of the fact that we do not know a number of the quantities involved. They must be determined experimentally.

In principle, the problem of ignition of an explosive charge by a shock wave in air may be solved according to the following scheme. As a result of the action on the explosive charge by the shock wave, heating up of the charge takes place only in a thin layer. The temperature of the surface layer is determined by two processes : transfer of heat from the air heated by the shock wave, and the removal of heat to the depth of the charge . If the flow of heat from the

shock wave penetrates into the mass of the charge to a depth which is considerably less than the linear dimensions of the charge to the face opposite from the wave, then the charge may be considered as a plane wall. In this case only the thermal flow need be considered in a direction perpendicular to the surface on which the shock wave acts. Taking into account the small penetration of the obstacle (even for penetrating shock waves they are no more than a few mm), the process of heat transfer may be assumed to be one-dimensional. It is described by the following equation :

$$\rho c \frac{\partial T}{\partial t} = \frac{\partial}{\partial x}\left(\eta \frac{\partial T}{\partial x}\right). \qquad (96.1)$$

The boundary conditions are

$$\left.\begin{aligned} &\eta \frac{\partial T}{\partial x} = -\alpha (T_a - T), \\ &\text{for } t = 0 \ , \quad T = T_0 \text{ for any value of } x \ , \\ &\text{for } x \to \infty \ , \quad T = T_0 \text{ for any value of } t. \end{aligned}\right\} \qquad (96.2)$$

Here ρ, c , and η are the density, specific heat and thermal conductivity of the explosive, α is the heat transfer factor, T is the temperature of the explosive (for $x = 0$, T is the temperature at the surface of the explosive), T_a is the temperature of the heat transfer agent (the temperature of the air in the shock wave).

The mechanism of the process of ignition of the explosive by the shock wave is essentially not different from the mechanism of ignition of an explosive by a burning gas, which, according to K.K.ANDREYEV may be postulated in the following manner. When the temperature of the surface layer reaches a certain limit (the boiling point for volatile explosives or the temperature of gassification and partial decomposition of solid and non-volatile explosives), vapours or the first products of decomposition are formed. Having a small

shock wave penetrates into the mass of the charge to a depth which is considerably less than the linear dimensions of the charge to the face opposite from the wave, then the charge may be considered as a plane wall. In this case only the thermal flow need be considered in a direction perpendicular to the surface on which the shock wave acts. Taking into account the small penetration of the obstacle (even for penetrating shock waves they are no more than a few mm), the process of heat transfer may be assumed to be one-dimensional. It is described by the following equation :

$$\rho c \frac{\partial T}{\partial t} = \frac{\partial}{\partial x}\left(\eta \frac{\partial T}{\partial x}\right). \tag{96.1}$$

The boundary conditions are

$$\left.\begin{aligned} &\eta \frac{\partial T}{\partial x} = -\alpha (T_a - T), \\ &\text{for } t = 0 \ , \ T = T_0 \text{ for any value of } x \ , \\ &\text{for } x \to \infty \ , \ T = T_0 \text{ for any value of } t. \end{aligned}\right\} \tag{96.2}$$

Here ρ, c , and η are the density, specific heat and thermal conductivity of the explosive, α is the heat transfer factor, T is the temperature of the explosive (for $x = 0$, T is the temperature at the surface of the explosive), T_a is the temperature of the heat transfer agent (the temperature of the air in the shock wave).

The mechanism of the process of ignition of the explosive by the shock wave is essentially not different from the mechanism of ignition of an explosive by a burning gas, which, according to K.K.ANDREYEV may be postulated in the following manner. When the temperature of the surface layer reaches a certain limit (the boiling point for volatile explosives or the temperature of gassification and partial decomposition of solid and non-volatile explosives), vapours or the first products of decomposition are formed. Having a small

volume specific heat, they are rapidly heated up to a temperature at which exothermic reactions proceed with high velocity, i.e. ignition occurs.

The direction of flow of the hot air behind the shock front promotes acceleration of the progress of the gaseous reactions. This is explained by the presence in the hot air of ions and radicals, and, moreover, the directional flow leads to an increase in the number of collisions, i.e. it leads to an increase in the number of elementary reaction events per unit time. The effect of directional flow on acceleration of the reaction is obvious from the following example noted by RAND. An ethylene - air mixture is ignited at a temperature of T = 1464°K by adiabatic compression, but it is ignited in the range of temperature 704 - 726°K by the action of a shock wave (in a shock tube).

If, however, at the instant of ignition it is stopped by the action of the external source of heat which, in the case we are considering, implies rarefactions originating at the surface of the charge, then the process may, depending on the depth of the heated layers, either die out or it may be converted into a stationary process.

In the case when at the beginning of rarefaction, the temperature distribution in the heated layer is established by the corresponding normal combustion, then ignition transforms into normal combustion.

If on the charge there acts an intense shock wave, but of small depth, ignition may not occur, since the surface temperature after this time does not attain critical ($T_{crit.}$). If, however, the surface temperature also becomes equal to $T_{crit.}$, but the thickness of the heated layer is less than that which corresponds to stationary combustion under the given conditions, then ignition does not transform into normal combustion, since the heat received will not compensate the heat transfer in the depth of the substance. In this case the temperature gradient will be greater than the corresponding stationary

combustion, which also depends on the excess of heat transfer over heat received. On this is based, in particular, extinction of a combustible powder in a reaction chamber as a result of repulsion of the jet.

By solving equation (96.1) for the boundary conditions of equation (96.2), the ignition time may be determined, i.e. the time required to attain a definite temperature $T_{crit.}$ at the surface of the charge. We note that the temperature $T_{crit.}$ is independent of the flash point, as defined in Chapter II. Autocatalytic reactions exert a strong influence on the process for normal spark ignition. The flash point depends on the mass of explosive, the conditions of determination and a number of other factors. For ignition of explosives by a shock wave, as a consequence of the fact that its reaction time is small, one can neglect in the great majority of cases the energy liberated by chemical reactions in the solid phase in the explosive as a result of heating it up to a temperature $T_{crit.}$, which may be assumed to be close to the boiling point or to the temperature of commencement of intense decomposition.

The solution of equation (96.1) for a solid semi-space with a plane wall has the following form :

$$\Delta T(x;\ t) = (\pi\rho c\eta)^{-\frac{1}{2}} \int_0^t \alpha(\tau)\,[T_a(\tau) - T(\tau)]\,(t-\tau)^{-\frac{1}{2}}\, e^{-\frac{\omega^2\rho c}{2\eta(t-\tau)}}\, d\tau, \quad (96.3)$$

where $T(\tau)$ is the surface temperature at time τ and $T_a(\tau)$ is the temperature of the heat transfer agent. For the surface of a charge of explosive ($x = 0$) relationship (96.3) is considerably simplified :

$$\Delta T(0;\ t) = (\pi\rho c\eta)^{-\frac{1}{2}} \int_0^t \alpha(\tau)\,[T_a(\tau) - T(\tau)]\,(t-\tau)^{-\frac{1}{2}}\, d\tau. \quad (96.4)$$

If the heat transfer factor α, and the difference between the temperatures of the heat transfer agent and the surface of the charge be substituted by their average values, then we arrive at the following expression :

$$T - T_0 = \frac{2\alpha_{av}\Delta T_{av}\sqrt{t}}{\sqrt{\pi\rho c\eta}}, \qquad (96.5)$$

where T_0 is the initial temperature of the explosive.

At the instant of ignition $T = T_{crit.}$ and the ignition time in accordance with relationship (96.5) will be equal to

$$\tau = 0.785\frac{(T_{crit.}-T_0)^2}{\alpha_{av}^2(\Delta T_{av})^2}c\rho\eta. \qquad (96.6)$$

Formula (96.6) was proposed in this form by Ya. M. PAUSHKIN.

We note that in solving equation (96.1) and in the derivation of relationship (96.6), c, ρ and η have been assumed to be constants. Relationship (96.6) enables us to analyse qualitatively the effect of various factors on the sensitivity of explosives to ignition by a shock wave.

It is found that the density, specific heat, thermal conductivity and the critical temperature $T_{crit.}$ exert the primary influence on the sensitivity towards ignition of an explosive. $T_{crit.}$ depends on the external conditions, primarily on the pressure, but this relationship has not yet been established.

If ignition is accomplished by shock waves of not very high intensity, then $T_{crit.}$ for high explosives may be assumed to be equal to the boiling point, which for trotyl gives $T_{crit.} = 310^{\circ}C$ and for hexogen $T_{crit.} = 255^{\circ}C$. With increase of specific heat, the quantity of heat required to heat upthe substance to the temperature $T_{crit.}$ increases. The thermal conductivity also exerts a similar influence. For approximately the same conditions, its reduction will bring about a higher value of the temperature at the surface of the explosive charge. Increase of the thermal conductivity and of the specific heat may explain the poor ignitibility of phlegmatised explosives in comparison with the pure explosives. Thus, for hexogen

$\eta \approx 5 \cdot 10^{-4}$ cal/cm. sec. deg. , $c_v = 0.54$ cal/cm^3 deg.,

and for paraffin

$\eta = 6.4 \cdot 10^{-4}$ cal/cm. sec. deg., $c_v = 0.64$ cal/cm^3 deg.

According to this same principle, the ignitions conditions are improved with decrease of density, since as a result of this the coefficient of thermal conductivity is decreased and the heat transfer factor is increased(on account of the increase in the specific surface). According to data by A.F. BELYAYEV, $\eta = 4.8 \cdot 10^{-4}$ for trotyl with a density of 1.56 g/cm^3 , and for trotyl with a density of 0.85 g/cm^3, $\eta = 5.5$ cal/cm. sec. deg.

The thermal conductivity also depends to a considerable extent on the grain size. In powdered materials made of small-sized grains, the thermal conductivity is low, because of the poor thermal contact between the grains. The improvement of ignitibility with reduction of density, as already mentioned above, is explained by the possible infusion into the pores of the hot products of decomposition of the explosive and of hot air, which may lead to ignition of the deep layers of an explosive charge.

The easy ignitibility of initiating explosives may be explained by their low specific heat and low thermal conductivity. Thus, for mercury fulminate at

$$\rho = 3.8 \text{ g/cm}^3 , \quad c_v = 0.1 \text{ cal/g. deg}$$

and

$$\eta = 2.85 \cdot 10^{-4} \text{ cal/cm. sec. deg.}$$

The ignition time depends strongly on the intensity of the heat flow, which is determined by the temperature of the heat transfer agent and by the heat transfer factor. The very considerable difficulties in calculation are due to the difficulty in determining the heat transfer factor α, which is a function of many parameters. It depends on the shape, dimensions and temperature

of the walls (of the explosive charge), on the temperature , pressure and flow velocity etc.

Values of α are usually determined by an experimental method, and the determination of α for non-stationary flow is particularly complex. However, as O.P.MARK showed, when the remaining factors are varied within relatively narrow limits, the heat transfer factor α can be assumed to be a function of the pressure and the temperature difference between the wall (the surface of the explosive charge) and the air compressed by the shock wave, i.e.

$$\alpha_{av} = k p_{av}^{n} (\Delta T_{av})^{m}, \qquad (96.7)$$

where k, m and n are coefficients established by the experiment.

In order to solve the problem of ignition of explosive charges by a shock wave in air, it is essential to know the temperature distribution behind the shock front or the variation of temperature of the air compressed by the wave as a function of time. For plane shock waves or for spherical waves with a large radius of curvature (beginning at 10 - 12 charge radii) it can be assumed without a large error that the temperature falls linearly with time. The initial temperature of the wave is equal to the temperature of the air at its front, but the final temperature depends on the fact that up to a certain value the pressure falls. According to STANYUKOVICH , T_f = 400 - 420°K for p = 1 atm, and T_f = 330 - 350°K for p = 0.5 atm.

On arrival of the shock wave at the charge, if the surface is plane and if it is disposed normal to the direction of motion of the wave, reflection occurs, as a result of which the pressure increases sharply, i.e.

$$\Delta p_2 = 2\Delta p_1 + \frac{6\Delta p_1^2}{\Delta p_1 + 7}, \qquad (96.8)$$

and the air density in the reflected wave is

$$\rho_2 = \rho_1 \frac{6p_2 + p_1}{p_2 + 6p_1}, \qquad (96.9)$$

where Δp_1 and p_1 are the overpressure and pressure at the front of the incident wave respectively, Δp_2 and p_2 are the overpressure and pressure at the front of the reflected wave, and ρ_1 and ρ_2 are the densities of the air behind the fronts of the incident and reflected shock waves.

For the derivation of equations (96.8) and (96.9) it has been assumed that $k = c_p/c_v = 1.4$. Simultaneously with reflection, a rarefaction wave begins to move from the edge of the charge towards the centre. The time of action of the reflected pressure up to the establishment of the flow regime is

$$\tau_{\text{refl}} = \frac{l}{c_{\text{av.}}}, \qquad (96.10)$$

where l is the minimum lateral size of the surface on which the shock wave acts, and $c_{\text{av.}}$ is the average velocity of the rarefaction wave, which, for small obstacles may be assumed to be equal to the velocity of sound in air in the reflected shock wave.

Knowing p_2 and ρ_2, we can determine the initial temperature T_2 in the shock wave at the instant of its reflection. For a time $t \geqslant \tau_{\text{refl.}}$, a stream of air will act on the explosive charge, air which has been retarded near the surface of the charge. If it be assumed that the specific heat of the air is constant, then the drag temperature is

$$T_{\text{drag}} = T_1 + A\frac{u^2}{2g c_p},$$

where $A = \frac{1}{427}$ is the mechanical equivalent of heat. Assuming that for air $c_p = 0.24$ kcal/kg.deg, we obtain

$$T_{\text{drag}} = T + \frac{u^2}{2000}, \qquad (96.11)$$

where T and u are the temperature and velocity of the air in the moving shock wave after completion of reflection, i.e. for $t \geqslant \tau_{\text{refl.}}$. Since we are assuming that the air temperature in the shock wave varies linearly with time, it is sufficient to determine T and u at the instant of completion of reflection. Assuming also that u varies linearly, we can write

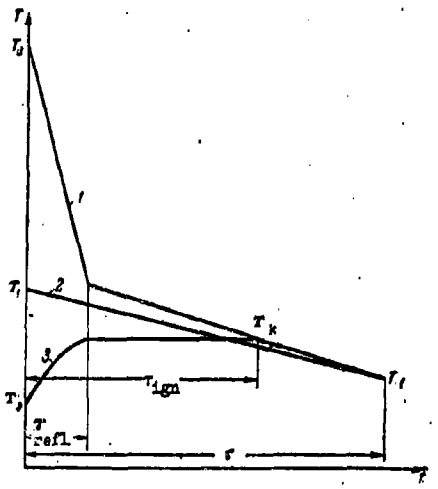
$$\frac{\Delta p}{\Delta p_1} = \frac{T}{T_1} = \left(\frac{u}{u_1}\right)^2, \qquad (96.12)$$

where Δp_1, T_1 and u are the overpressure, temperature and velocity of the air at the shock front. If it be assumed that in the shock wave

$$\Delta p = \Delta p_1 \left(1 - \frac{t}{\tau}\right), \qquad (96.13)$$

where τ is the time of action of the shock wave, which can be determined by M.A. SADOVSKII's formula, then using relationships (96.10), (96.11) and (96.12) Δp, T and u can be found at the instant of completion of reflection, i.e. for $t = \tau_{refl.}$.

Figure 251. Variation of air temperature in the shock wave and the temperature of the surface of the explosive charge as a result of an approaching shock wave.



The variation of the air temperature for the case when the shock wave is incident on a charge of explosive is shown in Fig.251(bent line 1). In the case when the shock wave skims along the surface of the charge, the variation of temperature of the air is depicted in the same figure by the straight line (straight line 2). The variation of temperature at the surface of the explosivecharge with time is shown by curve 3. It can be constructed if relationship (96.7) is used for λ_{av}, dividing the integral in (96.4) into intervals and taking out in each interval $\alpha(\tau)$ and $[T_0, \tau) - T(\tau)]$ with the mean values.

It is obvious that the transfer of heat from the air heated by a shock wave to an explosive charge will take place as long as their temperatures do not become equal. When the surface temperature attains the value $T_к$, ignition will take place. From the curves presented in Fig.251, it follows that with increase in the time of action of the shock wave with the specified parameters at the shock front, ignition of the explosive charge is more probable, the greater is the time of action (depth) of the shock wave. It is clear also that if, as a result of reflection, the temperature of the air in the shock wave does not rise above $T_к$, then even for very large times of action (several seconds) ignition of the charge will not occur. For the values of $T_к$ taken above, this means that a shock wave with an overpressure of 1.65 kg/cm^2 cannot ignite trotyl.

Since the time of reflection depends on the charge dimensions, then it is clear that if they are increased, the probability of ignition of a charge by a shock wave of given intensity should be increased. As a result of this, we must understand by charge dimensions not only its own dimensions, but also the dimensions of the obstacle near which the charge is placed, determining the time of reflection.

From the foregoing brief analysis of the process of thermal ignition of explosive charges by a shock wave, it follows that this process cannot be described by a simple empirical relationship, since the range at which ignition may be accomplished depends on a very large number of factors.

As already mentioned above, ignition may convert into normal combustion if at the instant of cessation of the action of the heat transfer agent a heated layer is formed within the explosive, corresponding to the specified conditions (pressure and temperature). K.K.ANDREYEV reckons that the supply of heat in the heated layer, necessary for normal combustion, may be a criterion of the ignitibility of a substance.

Assuming that in the condensed phase there is a temperature distribution, determined by the thermal conductivity, the temperature T can be determined at a distance x from the surface of the charge, as shown in Chapter X :

$$T = T_0 + (T_k - T_0)\, e^{-\frac{u_x}{\mu}}, \tag{96.14}$$

where u is the burning velocity and $\mu = \frac{\eta}{c_p \rho}$ is the thermal diffusivity factor.

The quantity of heat in the warmed-up layer is

$$Q = \int_0^\infty c_p \rho (T - T_0)\, dx = \frac{\eta}{u} (T_k - T_0). \tag{96.15}$$

It follows from (96.15) that for two substances with equal T_k and η but different burning velocities, the explosive which has the greater burning velocity will have the better ignitibility, since the supply of heat in the warmed-up layer necessary for ignition is inversely proportional to the burning velocity.

Relationship (96.15), as proposed by K.K. ANDREYEV, reflects the effect of the initial temperature and pressure on the ignitibility.

ANDREYEV considers that in order to determine the ignitibility, the method should, on principle, really be one in which the surface of the substance should be exposed to the action of a chemically inert heat transfer agent at a temperature equal to the combustion temperature of the substance.

We think that a shock tube can be used successfully for this purpose, in which are generated shock waves of defined intensity and depth. The parameters of the waves in the shock tube should be determined with sufficient accuracy by calculation and also established experimentally. In this way the characteristics and time of action of the heat tranefer agent are established simultaneously. In order to determine experimentally the ignition time as a result of the action of shock waves of different intensity, the thermal characteristics of the explosive (η, T_k, the storage of heat etc) may also be established by

this method.

We shall now consider the experimental material with respect to the effect of the various factors on the range of detonation transfer through air.

The density of the explosive in the active charge exerts a considerable influence on the range of transmission of a detonation. With increasing density of the charge, the range of transmission of detonation is increased. The increase of the range of transmission of detonation with increase in density of the active charge is not surprising, since the detonation velocity and the stream velocity of the detonation products associated with it, and of the shock wave increases with increase in density. It should be noted, however, that for active charges with small weights, the range of transmission depends to a very slight extent on their density, since the effect of the density is exerted on the shock wave parameters only at small distances from the charge.

Table 125

Effect of the casing of the active charge on the range of transmission of detonation.

Nature of casing of active charge	Density of active charge, g/cm^3	Density of passive charge, g/cm^3	R_{100} cm	R_{50} cm	R_0 cm
Paper	1.25	1	17	19.5	22
Steel, with a wall thickness of 4.5 mm	1.25	1	23	26	29
Paper	1	1	13	14	15
Lead, with a wall thickness of 6 mm, charge enclosed by the sides of the capsule	1	1	18	22	26

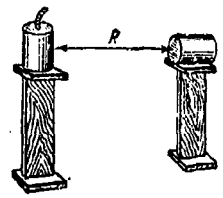
Footnotes. Here and henceforth R_{1m} is the limiting range corresponding to 100% stimulation of detonation of the passive charge.

R_{50} is the range corresponding to 50% stimulation of detonation.

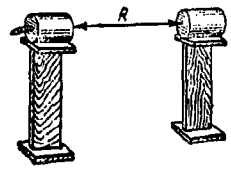
R_0 is the minimum range corresponding to 100% failure.

The range of transmission is practically independent of the initial temperature of the active charge. Thus, for a variation of the initial temperature from 0 to 100°C the range of transmission of detonation, as determined in an experiment with charges of picric acid weighing 50 g. varied, relative to a passive charge of this same explosive, from 18 to 19 cm.

Figure 252. Effect of mutual arrangement of charges on the range of transmission of detonation.



Arrangement A



Arrangement B

The casing in which the active charge is enclosed exerts a considerable influence on the range of transmission of detonation. Thus, in experiments with standard charges of picric acid, it was established that by replacing a casing of thick paper by a steel case with a thickness of 4.5 mm, closed at both ends, and of length equal to the length of the charge, the range of transmission of detonation increased. The variation of range of transmission of detonation is illustrated by the data in Table 123.

The effect of lateral covering of a charge is explained by the somewhat

directional action of the explosion created by the casing, i.e. by an increase in the active portion of the charge.

The range of transmission of detonation will be a maximum in the case when the position of the passive charge coincides with the direction of initiation of the active charge. This is explained by the fact that in the direction of propagation of the detonation wave, the initial velocity of flow of the detonation products is considerably higher than in other directions. This problem has been studied in charges of fused picric acid with a weight of 4 kg, which in some cases were arranged according to layout A, and in other cases according to layout B (Fig. 252). The results of these experiments are shown in Table 124.

Table 124

Effect of position of the passive and active charges on the range of transmission of detonation.

Effect of position of charges	$R_{1\infty}$ cm	R_{∞} cm	$R_{2\infty}$ cm	Density, g/cm^3	
				Active charge	Passive charge
According to layout A	75	85	95	1.35	1.6
According to layout B	15	20	25	1.56	1.6

By joining the active and passive charges with a tube, even of flimsy material, the range of transmission of detonation is sharply increased. The results of experiments with picric acid charges of weight 50 g. are presented in Table 125.

According to data by SHEKHTER, by joining charges with a cellulose acetate tube with a wall thickness of 0.15 mm, the range of transmission of detonation is increased by 40 - 50%. These experiments were carried out with

passive charges of trotyl, and the active charges were of phlegmatised hexogen.

Table 125

Transmission of detonation as a result of confined flight of the detonation products from the active charge.

Method of confining medium, separating charges	Density, g/cm^3		R_{50} cm
	Active charge	Passive charge	
Cylindrical steel tube with diameter 29 mm (equal to diameter of the charge), wall thickness 5 mm	1.25	1.0	125
Cardboard tube with the same dimensions ; wall thickness 1 mm	1.25	1.0	59
Non-channelled medium between charges.	1.25	1.0	19

The effect of the weight of the active charge on the range of transmission of detonation is illustrated by the data in Table 126.

Table 126

Dependence of range of transmission of detonation on weight of active charge.

Weight of active charge, g.	R_{100} cm	R_{50} cm	R_0 cm
15	5	5.5	4
29	6	7	8
50	6	8.5	11
118	11	12.5	14
231	17	20	23
400	24	25.5	27
784	28	31.5	35
1478	45	50	55
3420	65	72.5	80
6250	80	95	110

Footnotes. The density of the active charge was 1.25 g/cm^3, and of the passive charge 1.55 g/cm^3. The medium between charges was non-channelled.

These results are described satisfactorily by the formula

$$R_{50} = K q^{1/3}, \qquad (96.16)$$

where K in this case is equal to 0.38, q is the weight of the charge in kilogrammes and R_{50} is in metres. Relationship (94.16) satisfactorily expresses the relationship between R and q for charges with weights not exceeding a few hundred kilogrammes. The value of the coefficient K depends on the characteristics

of the active and passive charges and on the conditions under which stimulation occurs. The value of the coefficient K is shown in Table 127 (data by BYURLO) for a number of combinations of active and passive charges in light cases, as a result of transmission of detonation through an unconfined atmosphere. For charges with weights exceeding 1000 kg, relationship (96.16) gives several exaggerated valuesfor R. The power index n associated with q for these charges is $\frac{1}{3} \leqslant n \leqslant \frac{1}{2}$.

Table 127

Values of the coefficient K for a number of combinations of active and passive charges.

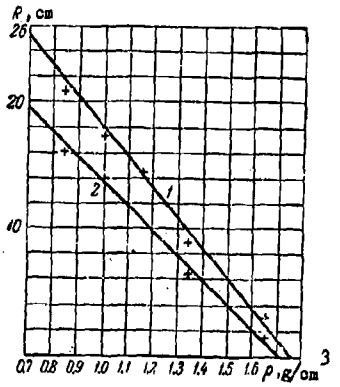
Active charge		Passive charge		K	Remarks
Explosive	Density, g/cm^3	Explosive	Density g/cm^3		
In light cases					
Tetryl	1.25	Mellinite	1.0	0.54	
Trotyl	1.25	Mellinite	1.0	0.33	
Mellinite	1.25	Trotyl	1.0	0.30	
"	1.25	Pyroxylin	1.0	0.30	
"	1.25	Diniphthallite	1.0	0.20	
"	1.25	"	1.35	0.05	
"	1.25	Mellinite	1.35	0.40	
"	1.25	Tetryl	1.35	0.50	
In wooden packages					
Nitrocellulose powder		Nitrocellulose powder	-	0.10	
Ammonium nitrate explosive		Ammonium nitrate explosive		0.25	At gravimetric density
Chlorate explosive		Chlorate explosive	-	0.40	

Relationship (96.16) has been established for strictly defined experimental conditions, which, of course, are not reproducible in all cases. Therefore

the range of transmission of detonation must be calculated in every actual case from the properties of the active and passive charges, their geometry and their mutual arrangement.

The density of the passive charge exerts a powerful influence on the range of transmission of detonation. According to BYURLO!s experiments, the range of transmission decreases linearly with increase in density of the passive charge. For active charges of mellinite with a weight of 50 g. this relationship is as shown in Fig.253.

Figure 253. Dependence of range of transmission of detonation on density of the passive charge : 1 - Density of active charge equal to 1.5 ; 2 - Density of active charge equal to 1.



Some data on the effect of density of passive charges of trotyl and phlegmatised hexogen obtained by SHEKHTER by using mirror scanning is shown in Table 128. Cylindrical passive charges were used for this, with a diameter of 25.2 mm. The active charge was phlegmatised hexogen with a density of 1.60 g/cm^3, a diameter of 25.2 mm and a weight of 55.6 g. The charges were joined by a cellulose acetate tube with a wall thickness of 0.15 mm.

These experiments indicate that the sensitivity of phlegmatised hexogen towards detonation is less than that of trotyl charges with corresponding density.

Table 128

Effect of density of passive charge on range of transmission of detonation.

Passive charge		Range of transmission of detonation, mm
Explosive	Density g/cm^3	
Trotyl, finely dispersed	1.30	150
" " "	1.40	110
" " "	1.50	100
Phlegmatised hexogen	1.40	95
" "	1.50	90
" "	1.60	75

Wetting of the passive charge considerably reduces its sensitivity towards detonation and, consequently, reduces the range of stimulation of detonation in it. This is illustrated by the data in Table 129, in which the results are presented for mellinite passive charges with a density of 1 g/cm^3 and of different moisture content, in which detonation was stimulated by mellinite charges with a density of 1.25 g/cm^3 and a weight of 50 g.

Table 129

Effect of moisture content of passive charge on range of transmission of detonation.

Moisture content of passive charge, %	R_{100} cm	R_{50} cm	R_0 cm
0.15	17	19.5	22
3.05	6	7.5	9
4.50	5	6.5	8
6.75	4	5	6
12.0	2	2.5	3
16.3	0	0.5	1

If the diameter of the passive charge is greater than limiting, then a casing with open ends has little effect on its sensitivity towards sympathetic detonation. The initial temperature of the passive charge also has little effect, if it is not so high as to cause noticeable decomposition or change the aggregate state of the charge.

The chemical nature of the explosive in the passive charge has a considerable effect on the range of stimulation

Of the various explosives(except initiators), the most sensitive are the dynamites in an inert base with a high content of nitroglycerine. Ammonites yield place according to their sensitivity just as to the dynamites, so also to trotyl and to picric acid.

Using mirror scanning, it has been possible to follow in considerable detail the nature of the development of the process of explosive transformation in a passive charge as a result of the action of a powerful shock wave on it.

It has been established by experiments that the process of explosive transformation in a passive charge sets in not immediately, but with a certain delay, the magnitude of which is measured in microseconds , and that the velocity of the process of explosive transformation along the charge is not constant, but varies, either attaining detonation velocity characteristic of the given charge, or dying out, whereupon the velocity of damping for a given charge is a quite stable value.

Fig.254 shows a typical photo-scan of the process of detonation transfer from an active charge to a passive charge through a 100 mm. layer of air. The explosive of the active charge is phlegmatised hexogen ($\rho_0 = 1.60$ g/cm^3) and the passive charge is trotyl ($\rho_0 = 1.50$ g/cm^3) . The point K identifies the end of detonation of the active charge. The band KAB is the scan of the movement of the shock wave. At point A the shock wave has encountered the passive charge.

§ 97. Transmission of Detonation through Dense Media.

In the case when the active and passive charges are separated by a dense medium (metal, water, sand etc.), the stream of detonation products do not participate in stimulation of the process of explosive transformation in the passive charge. Stimulation of detonation is accomplished by the shock wave moving through the inert medium of separation. The initial parameters of the shock wave in the inert medium at the boundary with the active charge are determined, as established in Chapter IX, by the characteristics of the charge and of the medium. Weakening of the shock wave takes place in the inert medium according to its propagation, the wave from the shock gradually becoming acoustic. If at the site of encounter with the passive charge the shock wave is still quite strong, then a shock wave originates in the passive charge, which is capable of stimulating an auto-accelerating chemical reaction. If the shock wave which originates in the passive charge has parameters which are below critical, then it will be propagated in the charge just as in the inert medium.

Experimental data on the transmission of detonation through dense media are relatively few. BYURLO, experimenting with melinite charges with a weight of 50 g, a diameter of 28 mm and a density of 1.25 g/cm^3 (active charge), established that the range of transmission of detonation relative to a passive melinite charge with a density of 1 g/cm^3 is characterised by the data presented in Table 130 for charges connected by a cardboard tube.

§ 97. Transmission of Detonation through Dense Media.

In the case when the active and passive charges are separated by a dense medium (metal, water, sand etc.), the stream of detonation products do not participate in stimulation of the process of explosive transformation in the passive charge. Stimulation of detonation is accomplished by the shock wave moving through the inert medium of separation. The initial parameters of the shock wave in the inert medium at the boundary with the active charge are determined, as established in Chapter IX, by the characteristics of the charge and of the medium. Weakening of the shock wave takes place in the inert medium according to its propagation, the wave from the shock gradually becoming acoustic. If at the site of encounter with the passive charge the shock wave is still quite strong, then a shock wave originates in the passive charge, which is capable of stimulating an auto-accelerating chemical reaction. If the shock wave which originates in the passive charge has parameters which are below critical, then it will be propagated in the charge just as in the inert medium.

Experimental data on the transmission of detonation through dense media are relatively few. BYURLO, experimenting with melinite charges with a weight of 50 g, a diameter of 28 mm and a density of 1.25 g/cm^3 (active charge), established that the range of transmission of detonation relative to a passive melinite charge with a density of 1 g/cm^3 is characterised by the data presented in Table 130 for charges connected by a cardboard tube.

AB determines the delay in the passive charge, which in this case is equal to $2 \cdot 10^{-6}$ sec. At point B the process of explosive transformation is stimulated in the passive charge, the average velocity of which over the section BC is equal to 2320 m/sec. At the section C, situated at 17.5 mm from the end of the charge (AB), the velocity of the process changes with a rapid jump from 2320 m/sec to 6600 m/sec (the normal detonation velocity of a trotyl charge with a density of 1.50 g/cm^3). DE is the shock wave formed by the flow of the detonation products from the passive charge into the atmosphere. At the site of the skip-like change of velocity of the process, a retonation wave is sometimes formed.

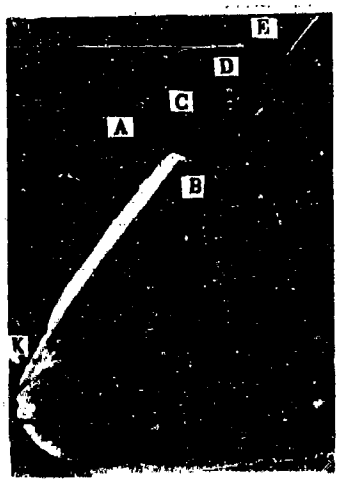


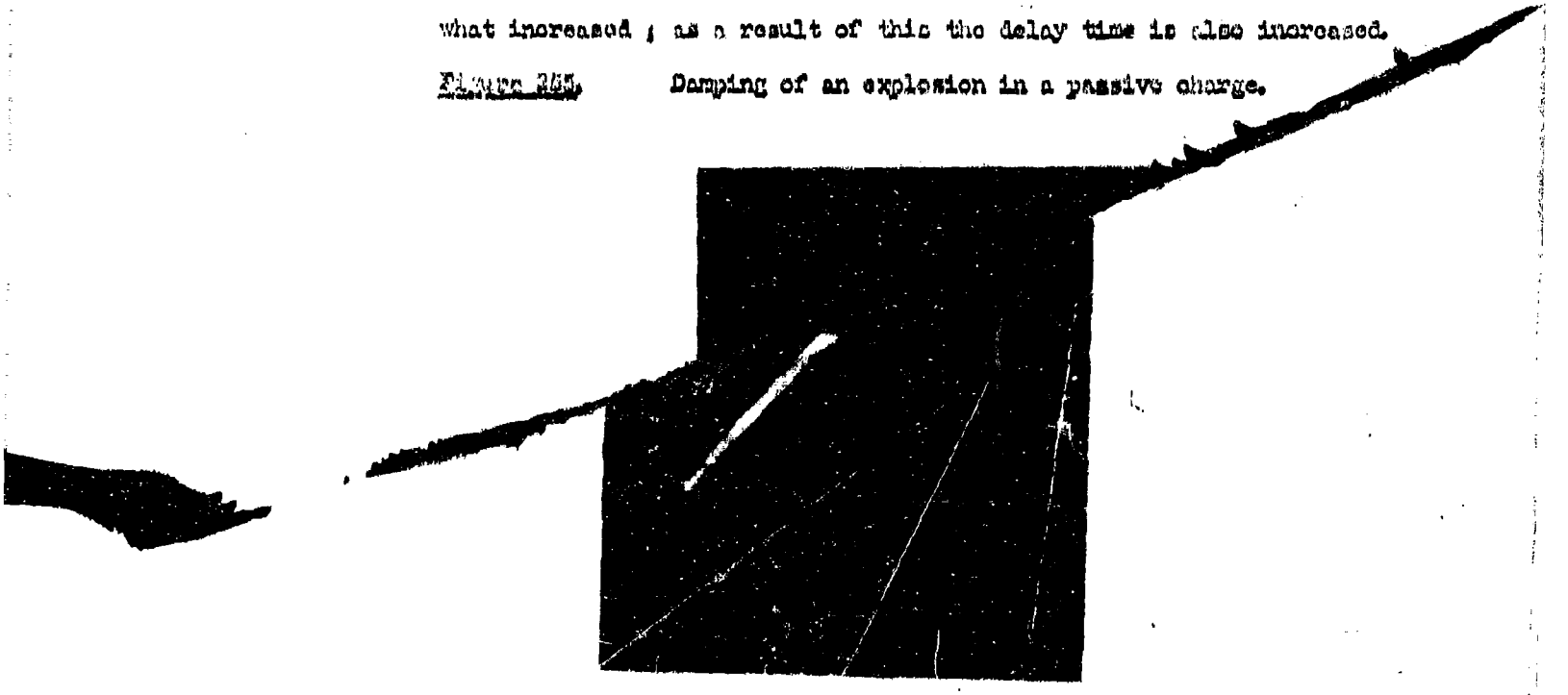
Figure 254. Photoscan of the process of detonation transmission through air.

In the case when the diameter of the charges is close to the limiting detonation transmission, a process of explosive transformation is stimulated in the passive charge, which sometimes changes into detonation and sometimes it dies out. Fig. 255 shows the dying out of an explosion in a passive charge of phlegmatised hexogen with a density of 1.50 g/cm^3. The explosion dies out at 15 mm from the end of the charge ; the velocity in this section is equal to 2470 m/sec.

The experiment shows that the velocity of the damped explosion for trotyl charges with a density of 1.30 - 1.60 g/cm^3 is equal to 2100 - 2300 m/sec.

For charges of phlegmatized hexogen within the same density range, the velocities of the damped explosions are equal to 2400 - 2700 m/sec. These velocities should be considered as critical velocities of the explosion. In all cases the velocity of this process exceeds the velocity of sound in the original explosive for normal conditions (thus, the velocity of sound in trotyl at a density $\rho_0 = 1.61$ g/cm^3 is equal to 1350 m/sec). With decrease in intensity of the action of the shock wave and of the detonation products from the active charge on the passive charge, i.e. with increase in distance between charges, the length of the section of the explosion, at the end of which the velocity increases with a jump to the normal velocity of detonation, is somewhat increased; as a result of this the delay time is also increased.

Figure 245. Damping of an explosion in a passive charge.



The delay time may be considered as the time required for ignition, combustion, and transition of combustion into an explosion.

Table 130

Transmission of detonation through dense media

Communicating medium	R_{100} cm	R_{50} cm	R_0 cm
Air	26	28	30
Water	5	4	5
Clay	2	2.5	3
Sand	1	1.5	2
Steel	1	1.5	2
Spruce (transmission parallel to the grain)	3	4	5
Spruce (transmission perpendicular to the grain)	3	3.5	4

The difference in the ranges of detonation transmission through different media was associated by BYURLO with the compressibility factor of the medium, assuming that the greater the compressibility the greater the range of detonation transmission. We note, however, that the extent of weakening of the shock waves in different media, which also determines for approximately equal conditions the range stimulation of detonation in the passive charge, is associated not only with the different compressibility of these media, but also with other characteristics, for example, with their viscosity, density etc.

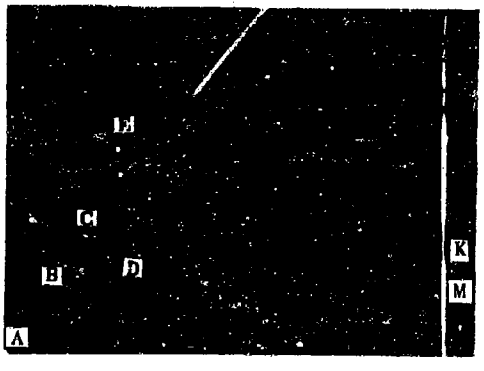
BYURLO's data, as given in the table, are inaccurate in a number of cases and also differ from the results obtained by other authors. Thus PAUK found that the range of detonation transmission through wood, for a passive charge of an explosive very sensitive to detonation - mercury fulminate - on stimulation by a charge of 75 per cent dynamite with a weight of 50 g and a detonation

velocity of 6500 m/sec, does not exceed 3.1 cm. BYURLO found that for a considerably less sensitive explosive it was equal to 3.5 - 4 cm.

We have established that the range of detonation transmission through water from a trotyl active charge with a detonation velocity of 7000 m/sec is equal to 5 cm, relative to a passive charge of PETN, which is very sensitive towards detonation. BYURLO also found that for a less sensitive melinite charge and a less powerful active charge (detonation velocity 5300 m/sec), the range is 3 - 5 cm.

The transmission of detonation through steel and water has been investigated by SHEKHTER. In the experiments on detonation transmission through steel the passive charges were prepared from trotyl with a density of 1.30 - 1.60 g/cm^3. The active charges were prepared, in all the experiments, from phlegmatised hexogen with a density of 1.60 g/cm^3 (detonation velocity 8000 m/sec). The diameters of the charges were 23.2 mm, and the weight of the active charge was 35.5 g.

Figure 256. Photo-scan of the process of detonation transmission through a metal.



A typical photo-scan of the process of detonation transmission through

a metal is shown in Fig.256. Detonation of the active charge is initiated at the point A . At B the wave arrives at the sheet of metal. The shock wave, on passing through the metal sheet equal to KM, initiates explosion of the passive charge at E, the detonation of which finishes at D. BE is the time (on some scale) taken for the shock wave to pass through the metal sheet EC, including the delay up to initiation of explosion of the passive charge.

These photographs can be used to determine approximately the delay time τ_d, according to the following considerations. If it be assumed, as was done earlier, that the velocity of the shock wave in steel is equal to the velocity of elastic collisions, then the delay time is defined as the difference between the time required for passage of the wave, plus the delay time (this total time is determined from the photo-scan) and the time required for passage of the shock wave through the layer of steel of depth h ($\tau = \frac{h}{c_0}$, where c_0 is the velocity of propagation of elastic collisions in steel). The results of the determination are shown in Table 151.

Table 151

Transmission of detonation through steel

Density of passive charge, g/cm^3	Thickness of transmitting steel plate, mm	Delay time τ_d, μ sec	Density of passive charge, g/cm^3	Thickness of transmitting steel plate, mm	Delay time τ_d, μ sec
1.30	12.0	2.1	1.50	8.0	1.0
1.30	14.0	3.3	1.50	10.0	1.2
1.30	16.0	failure	1.50	12.0	1.4
1.50	12.0	1.4	1.50	14.0	1.7
1.50	16.0	failure	1.60	12.0	1.4
1 .60	14.0	2.0	1.60	16.0	failure

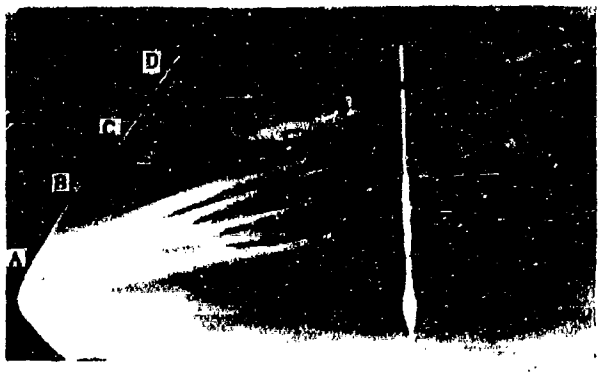
It follows from Table 131 that the delay time [illegible] passive charg[illegible] increases with increase in thickness of the transmitting plate. This is quite understandable , since with increase of the sheet of metal the wave arrives at the passive charge in a more weakened condition. The delay t [illegible]e, as a rule, does not exceed $2.5 \cdot 10^{-6}$ sec for trotyl charges pressed from fine grains. In fact, the delay time is somewhat larger than those given in Table 131, since the velocity of the shock wave in the metal exceeds the velocity of sound under normal conditions.

Over the density range investigated, there is no evidence of a decrease in range of detona tion transmission with increase in density of the passive charge. This is explained by the fa t that the parameters of the wave passing through relatively thin layersof metal,ensuring stimulation of detonation of the passive charge at the boundary, do not greatly differ for the charges used. The dependence of the range of transmission of detonation on density for a detonation transmission through air is easily established, since the corresponding variations of the shock wave parameters in air take place over a considerably greater path than the variation of the shock wave parameters as a result of its passage through a metal sheet. The same picture is characteristic not only for metals but also for the case of detonation transmission through water, where the reduction in intensity of the shock wave at distances at which sympathetic detonation of a passive charge takes place, takes place extremely sharply.

Detonation transmission for metals and alloys, the density of which is less than the density of steel (aluminium, duralumin etc.), takes place through thicker layers. Thus, relative to charges of trotyl and phlegmatised hexogen, the range of transmission exceeds 20 mm (the active charges are the same as for the case of sympathetic detonation through steel).

The higher the velocity of motion of the particles of metal at the boundary of separation between the metal and the passive charge, the greater the intensity of the shock wave in the explosive, for approximately equal conditions. In addition, retardation of the shock wave occurs more slowly in duralumin than in steel. These circumstances also predetermine the increase in range of sympathetic detonation as a result of transition from steel to duralumin as the transmitting medium.

Figure 257. Photoscan of the process of transmission of detonation through water : AB - detonation of the active charge
CD - detonation of the passive charge.



The dependence of range of transmission of detonation through water on the detonation velocity of the active charge, the density and nature of the passive charge has been studied by SHEKHTER.

All the experiments were carried out with charges having a diameter of 23.2 mm. The passive charge was inserted in a cellulose acetate or glass tube. The active charge was immersed in the test tube at a depth of 20 - 25 mm. The active charges, with a density of 1.60 g/cm^3, were prepared from trotyl and phlegmatised hexogen. In the preparation of the passive charges, besides the explosives already referred to, PETN was also used. All the experiments were

carried out using photo-recording of the process of sympathetic detonation by means of mirror scanning.

The effect of distance between the charges on the delay time was established by a method of varying the depth of the separating layer of water by 2 - 5 mm from experiment to experiment.

A typical photograph which records the process of sympathetic detonation through water is shown in Fig.257.

The results obtained from processing the photograph are shown in Table 132, in which the following symbols are used : h is the distance between the charges, τ_d is the delay time and D_h is the velocity of the shock wave in water at the point of encounter with the passive charge.

Table 132

Transmission of detonation through water

Active charge		Passive charge		h, mm	τ_d μ sec	D_h m/sec
Explosive	ρ_o g/cm^3	Explosive	ρ_c g/cm^3			
Phlegmatised hexogen	1.60	PETN	1.65	20	2.0	3620
" "	1.60	"	1.65	25	2.5	3160
" "	1.60	"	1.65	30	3.0	2380
" "	1.60	"	1.65	35	fail	2720
Trotyl	1.61	"	1.65	20	2.5	3240
"	1.61	"	1.65	25	4.5	2860
"	1.61	"	1.65	30	fail	2660
Phlegmatised hexogen	1.60	Phlegmatised hexogen	1.60	25	3.5	3300
" "	1.60	"	1.60	25	fail	3160
Trotyl	1.60	Trotyl	1.50	20	2 .5	3240
"	1.60	"	1.50	25	5.0	2960
"	1.60	"	1.50	25	fail	2860

It follows from the table that the range of transmission of detonation is determined, for a given passive charge, by the shock wave velocity D_h at the point of encounter with the passive charge.

The critical values of the parameters of the shock waves in water, i.e. waves still capable of bringing about development of the process of explosive transformation, at the limit, ... charges of explosive which have been studied, are shown in Table 135.

The pressure at the shock front in water, the flow velocity and the rise in temperature for a known shock wave velocity in water (D_h) are taken from calculations by KIRKWOOD and RICHARDSON.

The delay time in the passive charge, resulting from the data in Table 132, is increased according to the reduction in the shock wave velocity in water at the point of encounter with the passive charge. For a column of water separating the charges which is small, this time is very small (0.1 - 0.5 microsec), i.e, a normal detonation regime is established practically at once in the passive charge. For a column of water close to limiting, the detonation regime is established over a period of 5 - 5 microsec. The increase in the delay time is characteristic on approaching the limiting range of transmission.

On encountering the passive charge, reflection of the shock wave takes place, and a shock wave originates in the passive charge. If its parameters are sufficient for stimulating an intense chemical reaction, then the shock wave transforms into a detonation wave. If the parameters of the incident wave are less than critical values(these are presented in Table 133 for the explosives investigated), then the shock wave which has been created is propagated in the passive charge just as in an inert medium, gradually dying out and transforming into an acoustic wave.

Table 133

Critical parameters of shock waves in water, capable of causing sympathetic detonation of passive charges.

Shock wave parameters	Passive charge		
	Phlegmatised hexogen (ρ_0 = 1.40 - 1.60 g/cm^3)	Trotyl (ρ = 1.50 g/cm^3)	PETN (ρ = 1.65 g/cm^3)
Pressure at the shock front, kg/cm^2	29,000	22,000	18,000
Wave velocity, m/sec	5,500	2,960	2,800
Velocity of water behind shock front, m/sec	980	755	640
Rise in temperature at the wave front, °C	100	80	65

Calculation of the shock wave parameters in explosives, which will bring about sympathetic detonation of a passive charge can be carried out if the law of compressibility of the original explosive is known, and also the parameters are known of the shock wave propagated through the medium (through water in the given case) at the site of encounter with the passive charge.

If it be assumed that the connection between the pressure and density for the explosives is expressed by the relationship

$$p \sim \rho^k,$$

then the calculation presents no difficulty.

It has been shown by STANYUKOVICH that for the original explosive the value of k may be assumed equal to 6 - 7. The initial parameters of the

initiating shock waves of certain explosives have also been determined in these hypotheses. They are presented in Table 134.

The data in Table 134 shows, that just as in the case of transmission of detonation through air, the velocities of the initiating waves are equal to 2000 - 2800 m/sec, which is in good agreement with experiment.

The range of transmission of detonation through a dense separating medium may serve as a measure of the sensitivity of the explosive towards detonation. The advantage of this method, as EYRING and his colleagues noted, consists in the high reproducibility of the results. Thus, on initiating charges with a detonator cap through a layer of paper sheets with a thickness of 0.08 mm each, a change in thickness of the layer by 1 - 2 sheets of paper led, in all cases, to failure. This is verified by the data presented in Table 135.

Table 134

Initial parameters of initiating shock waves.

Parameters of shock wave in passive charge.	PETN (ρ_0 = 1.65 g/cm^3)		Phlegmatised hexogen (ρ_0 = 1.40 - 1.60 g/cm^3)		Trotyl dispersed (ρ_0 = 1.50 g/cm^3)	
	k = 6	k = 7	k = 6	k = 7	k = 6	k = 7
Wave velocity, m/sec	2010	2190	2570	2800	2220	2440
Velocity of explosive behind wave front, m/sec	574	548	730	700	655	610
Pressure at wave front, kg/cm^2	19,000	20,500	30,200	32,000	23,000	24,000
Rise in density at wave front	1.40	1.33	1.40	1.33	1.40	1.33

Table 135

Transmission of detonation through a bundle of paper sheets.

Explosive	ρ_o, g/cm^3	Minimum number of of sheets for which failures occur.	Maximum number for which detonation is still observed.
Tetryl	1.51	25	26
Tetryl	1.60	24	24
Hexogen, phlegmatised (6% wax)	1.58	17	18.5
Hexogen-trotyl mix	1.59	17	19

The reproducibility of the results, which, however, is observed also for transmission of detonation through air and other media, may be taken as the basis of recommendation of this method for determining the sensitivity of explosives towards detonation.

§ 98. Transmission of Detonation in Shot-Holes.

Resulting from the explosion of blasting charges, there are sometimes cases of failures in the transmission of the detonation or incomplete explosions with subsequent ignition and combustion of the non-detonated cartridges. Incomplete explosion and the combustion of the charges associated with it presents a great danger. Thus, in carrying out blasting operations in mines where there is a danger from gas and dust, this may lead to the explosion of methane - air and carbon - air mixtures.

Normal functioning of explosive charges, excluding incomplete explosions and firing of cartridges in shot holes, depends on the detonation capability of the explosive and the conditions of industrial application of the blasting cartridges, i.e. the nature of loading of the shot holes, the presence or absence of filling between the cartridges by coal or drill dust, clearances between the cartridges and the walls of the shot hole etc.

The detonation capability of industrial explosives depends to a large extent on their composition and technology of manufacture. It can be stated as a general rule that ammonites, not containing liquid nitroethers (nitroglycerine, nitroglycol), have an inadequate detonation capability under the conditions of their industrial application, which is sharply reduced during storage as a result of agglutination and deterioration. The introduction of small quantities of nitroglycerine and nitroglycol leads to a considerable increase of the detonation capability of ammonites.

As mentioned earlier (see Para. ..) , the range of transmission of detonation can serve as an indication of the detonation capability of an explosive. This aspect can be illustrated by the data presented in Table 156.

Table 156

Comparative data on range of transmission of detonation for cartridges with a diameter of 30 mm.

Explosive	Average distance of transmission of detonation, cm.		Coefficient of increase of range of transmission
	In open air	In a shot hole with diameter 40 mm.	
No.1	7.5	90	12
No.2	5.0	17	3.5

Composition of explosives : No.1 - Nitroglycerine - 19.5% , colloxiline (collodion) 0.5% , NH_4NO_3 - 2% , NaCl - 58%, wood meal - 2% ; No.2 - Dinitrotoluol - 9.5% , NH_4NO_3 - 90.5% .

It follows from the data presented in Table 136, that explosive No.1 has a considerably greater detonation capability under conditions of industrial application than has explosive No.2, although the latter, with respect to its efficiency, exceeds explosive No.1 by approximately a factor of two.

It is interesting to note that even such a powerful and sensitive explosive as PETN, when present as a component of ammonites exerts considerably less influence on the detonation capability of the latter explosives than nitroglycerine. This is well confirmed by the data presented in Table 137.

Table 137

Trials with nitrons on transmission of detonation in a steel mortar (diameter of mortar channel 45 mm).

Explosive	Distance between cartridges, cm.	Relative number of passive cartridges detonnated	
		without stemming	with stemming
No.3	80	3/5	3/5
	60	4/5	3/5
	40	5/5	5/5
No.4	25	0/5	1/5
	20	0/5	4/5
	15	1/5	3/5
	10	3/5	5/5

Composition of explosive No.3 : nitroglycerine - 12% , collodion - 1% , NH_4NO_3 - 33% , NaCl - 49%, peat - 5% ; Composition of explosive No.4 : PETN - 20% . dinitronaphthalene 1.5%, NH_4NO_3 - 20%, NaCl - 58.5% .

Data on the critical diameters of charges established by SHEPHERD and GRIMSHAW also confirms the powerful influence of nitroglycerine on the detonation capability of mixed explosive systems. Thus, for a system containing 5% nitroglycerine and 95% sodium chloride, the critical diameter was shown to be equal to approximately 7 mm, and the detonation velocity 870 m/sec in all.

As a result of numerous investigations (RUDAKOVSKII, SARTORIUS, PEREVERZEV et al.) it has been established, that for the presence of a radial gap between the charge and the shot hole (a tube, mortar)cases are observed of extinction of detonation for blasting cartridges of industrial explosives. This in its turn often leads to ignition and combustion of the non-detonated portion of the charge.

RUDAKOVSKII first expressed the hypothesis that this process is a consequence of the compression of the still-undetonated portion of the charge as a result of the action of the shock wave propagating along the gap with a velocity considerably in excess of the detonation velocity. By installing transverse screens at the junction of cartridges, the detonation was propagated throughout the entire charge. RUDAKOVSKII's conclusions are confirmed by experiments carried out by SHEPHERD and GRIMSHAW, in which the velocity was measured of the shock wave propagating along the gap. Thus, for one of the explosives with a detonation velocity of 5860 m/sec, the shock wave velocity was shown to be 5550 m/sec. Compression of the charge by the shock wave has also been confirmed in experiments with tetryl carried out by these same authors. They showed that the detonation velocity of tetryl with a density of 1.55 g/cm^3, on explosion in a tube with a radial gap, was increased from 7250 m/sec (open charge) to 7530 m/sec. The limiting detonation velocity of the charge without gap is equal to 7395 m/sec.

Compression of charges of ammonites usually leads to a sharp increase of their critical diameters and, as a consequence of this, to a reduction in their sensitivity towards detonation, and in certain well-known conditions

compression of charges leads to loss of detonation capability(particularly ammonites, not containing nitroglycerine).

Analysis of available data permits the conclusion to be drawn that one of the primary causes of failure in transmission of detonation in shot holes is the presence of a radial gap, which, under industrial conditions amounts to 10 - 12 mm.

.....

T - No. 1488p
E-881

SUPPLEMENT

TOWARD THE THEORY OF CUMULATION OF GASES

With the phenomenon of cumulation of a gaseous medium we encounter recesses, for example, as a result of the explosion of a cumulative charge without a metallic casing.

First of all we shall consider the following idealised scheme. Suppose that two plane surfaces are inclined at an angle ψ to a plane of symmetry, and confining a cavity containing gas (plane problem). Suppose that a force, which is applied instantaneously to these surfaces, then remains constant.

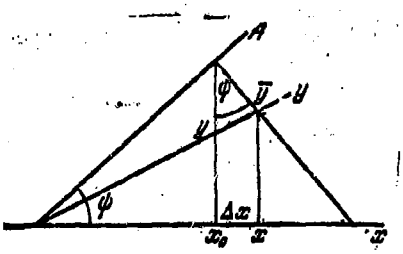


Figure 1s. Diagram of charge.

In order to explain the process which will take place after application of the force it is sufficient to consider the motion of the gas, for example in the upper semi-plane, since the motion possesses symmetry relative to the axis Ox or more accurately to the plane yOx, assuming that in this plane is disposed an absolutely solid wall (Fig. 1s).

In the case we are considering, a shock wave passes through the gas, the parameters of which are determined from the following [illegible]ous equations

$$\left.\begin{aligned} p_i - p_a &= \rho_a u_i D_a; \quad \rho_a D_a = \rho_i (D_a - u_i); \\ E_i - E_a &= \frac{p_i + p_a}{2}\left(\frac{1}{\rho_a} - \frac{1}{\rho_i}\right), \end{aligned}\right\} \tag{1}$$

where p_a is the external constant pressure.

In the case of an ideal gas, we find from these equations that

$$\left.\begin{aligned} \frac{p_i}{p_a} &= \frac{(k+1)\,p_i + (k-1)\,p_a}{(k-1)\,p_i + (k+1)\,p_a}; \quad u_i^2 = \frac{2(p_i - p_a)^2}{\rho_a\left[(k+1)\,p_i + (k-1)\,p_a\right]}; \\ D_i^2 &= \frac{(k+1)\,p_i + (k-1)\,p_a}{2\rho_a}. \end{aligned}\right\} \tag{2}$$

It is obvious that we must consider a strong wave; then, neglecting the quantity p_a, we have :

$$\frac{p_i}{p_a} = \frac{k+1}{k-1}; \quad u_i^2 = \frac{2p_i}{(k+1)\,\rho_a}; \quad D_i^2 = \frac{(k+1)\,p_i}{2\rho_a}. \tag{3}$$

The shock front, on arrival at the plane of symmetry, begins to be reflected from it. It is well-known, that if the angle through which the shock front approaches the obstacle (in this case this angle is ψ) is less then a definite value $\psi < \psi_0$, then the reflection will be regular, i.e. the front of the reflected wave originates at the obstacle itself. If $\psi > \psi_0$, then the reflection will be irregular, and as a result of this the front of the reflected wave will not be initiated at the obstacle, a supplementary shock wave will originate, moving from the obstacle to a point where the front of the incident wave and the front of the reflected wave make contact, a tangential discontinuity originates (one or several), and the picture of the phenomenon of reflection becomes somewhat complex, which will not yield to calculation. On the contrary, the regular reflection of the shock wave from the obstacle can be considered extremely simply, especially in the case of a strong incident wave.

The value of the limiting angle ψ_0 can be determined from the following relationships of the theory of oblique shock waves (see Para. 52) :

$$\operatorname{ctg}^2\psi_0 = \frac{\beta_0^2\left[\frac{k+1}{2}x_0 + 1\right] - 1}{(x_0+1)^3}, \tag{4}$$

where

$$x_0 = \frac{p_i}{p_a} - 1; \quad \beta_0 = \frac{q_i}{c_i}.$$

Here $c_i = \sqrt{\frac{kp_i}{\rho_i}}$, and q_i is the velocity of motion of the gas behind the shock front in the system of coordinates in which the point of intersection of the wave front with the obstacle is stationary ;

$$q_i = \sqrt{(D_s - u_i)^2 + D_s^2 \cot^2 \psi_0}; \tag{5}$$

thus,

$$\beta_0 = \sqrt{\left(\frac{D_s - u_i}{c_i}\right)^2 + \left(\frac{D_s}{c_i}\cot \psi_0\right)^2}. \tag{6}$$

If the wave is strong, then

$$\left.\begin{gathered}\frac{\rho_i}{\rho_0} = \frac{k+1}{k-1}, \quad x_0 = \frac{2}{k-1}, \quad \cot^2 \psi_0 = \left(\frac{k-1}{k+1}\right)^2\left[\frac{2k\beta_0}{k-1} - 1\right], \\ \beta_0 = \sqrt{\frac{k-1}{2k} + \cot^2 \psi_0 \frac{(k+1)^2}{2k(k-1)}}.\end{gathered}\right\} \tag{7}$$

Whence, for example, for $k = \frac{7}{5}$ we find $\psi_0 = 39°$. From the theory of cumulation it is known that in order to obtain higher velocities, it is essential to select a greater angle of incidence of the flow with the obstacle, i.e. small angles ψ_0. As a result of this, regular reflection of the shock wave is ensured.

We shall now calculate the parameters at the front of the reflected shock wave, assuming that the incident wave is strong and that $\psi < \psi_0$ (i.e. that the reflection is regular). For this purpose we shall use the relationships for the case of regular reflection (see Paras. 52 & 47)

$$\left.\begin{gathered}\frac{\tan(\psi - \theta)}{\tan \psi} = \frac{k-1}{k+1}; \quad \frac{\tan(\varphi - \theta)}{\tan \varphi} = \frac{\rho_i}{\rho_2}, \\ p_2 = -\frac{k-1}{k+1} p_i + \frac{2}{k+1} \rho_i D_s^2 \sin^2 \varphi \left[\cot^2 \psi + \left(\frac{k-1}{k+1}\right)^2\right], \\ \frac{\rho_2}{\rho_i} = \frac{(k+1)p_2 + (k-1)p_i}{(k-1)p_2 + (k+1)p_i}.\end{gathered}\right\} \tag{8}$$

Here p_2, θ and ρ_2 are the pressure and density at the front of the reflected

wave, θ is the angle of deflection of the velocity vector (in a system of reading where the point of intersection of the front of the incident wave with the obstacle is stationary); φ is the angle between the velocity vector behind the front of the incident wave and the reflected wave front. The angle ψ can be called the angle of incidence, and the angle $\varphi-\theta=\bar{\psi}$ the angle of reflection. From the first equation of system (8) we find the angle θ, then substituting in the last equation of this system the value of ρ_2 in the third equation, we solve simultaneously the second and third equations of the system and we determine the original values of ρ_2 and φ; after this we find the value of p_2. The velocity behind the front of the reflected shock wave is determined from the relationship

$$q_2 = q_1 \frac{\cos\varphi}{\cos(\varphi-\theta)}. \tag{9}$$

Thus, all the parameters behind the front of the reflected wave are determined. It now remains to determine the velocity in the original system of coordinates (in which the observer and object are stationary). It is obvious that this velocity is directed along the axis Ox and its magnitude is determined from the relationship

$$u_2 = \frac{D_s}{\sin\psi} - q_2 = \frac{D_s}{\sin\psi}\left[1 - \sqrt{\left(\frac{k-1}{k+1}\sin\psi\right)^2 + \cos^2\psi}\right]. \tag{10}$$

Since the quantity $\left(\frac{k-1}{k+1}\sin\psi\right)^2$ is small in comparison with $\cos^2\psi$, then

$$u_2 \approx \frac{D_s\ (1-\cos\psi)}{\sin\psi} = D_s \operatorname{tan}\frac{\psi}{2}, \tag{11}$$

i.e. for small angles ψ, the velocity of flow of the gas along the axis behind the front of the reflected shock wave is very insignificant and it can be practically neglected in further calculations.

Thus, for small angles ψ, i.e. when the original shock wave falls on

the plane of symmetry practically normally, it can be assumed that practically all the energy of the wave is potential energy, i.e. almost total retardation of the gas takes place as a result of reflection.

Let us further consider the fate of this gaseous stream. The initial parameters of this stream of gas in the case of normal reflection by a strong shock wave are determined from the following simple expressions :

$$\frac{p_2}{p_1} = \frac{(3k-1)p_1 - (k-1)p_a}{(k-1)p_1 + (k+1)p_a}, \quad \frac{\rho_2}{\rho_1} = \frac{1}{\frac{k-1}{k} + \frac{p_a}{kp_1}}. \tag{12}$$

As a result of this, the velocity of the front of the reflected shock wave is

$$D_2 = [(k-1)p_1 + p_a]\sqrt{\frac{2}{\rho_a[(k+1)p_1 + (k-1)p_a]}}, \tag{13}$$

the velocity of the gas behind the front of the reflected wave $u_2 = 0$. If the incident wave is strong, then

$$\frac{p_2}{p_1} = \frac{3k-1}{k-1}, \quad \frac{\rho_2}{\rho_1} = \frac{k}{k-1}, \quad D_2 = (k-1)\sqrt{\frac{2p_1}{(k+1)\rho_a}}. \tag{14}$$

In a stationary system of coordinates we shall have, as a result of reflection, a stationary gas which will possess the parameters

$$u = u_2 = 0, \quad c = c_2 = \sqrt{\frac{kp_2}{\rho_2}} = \sqrt{\frac{3k-1}{k}\frac{kp_1}{\rho_1}} = \sqrt{\frac{3k-1}{k}}c_1. \tag{15}$$

The dispersion of this compressed gas is described by the well-known RIEMANN (special) solution

$$u = \frac{2}{k-1}(c_2 - c), \quad u - c = \frac{x - x_0}{t}, \tag{16}$$

where the quantity $x_0 = l / \sin\psi$ determines the coordinate of the beginning of the discharge, l is the length of the generatrix. The maximum discharge velocity will be

$$u_{max} = \frac{2}{k-1}\sqrt{\frac{3k-1}{k}}c_1 = \frac{2}{k-1}c_a\sqrt{\frac{(3k-1)(k-1)}{k(k+1)}\frac{p_1}{p_a}}$$

or

$$u_{max} = 2c_a\sqrt{\frac{3k-1}{k(k^2-1)}\frac{p_1}{p_a}} \tag{17}$$

for $k=\frac{5}{3}$, $u_{max}=2c_a\sqrt{\frac{27}{20}\frac{p_i}{p_a}}$.

If the gas discharge should take place immediately with the shock front, then the relationship

$$\bar{u}=u_i+\frac{2}{k-1}(c_i-c), \tag{18}$$

should apply, where

$$u_i=\sqrt{\frac{2}{k-1}(c_0^2-c_i^2)}, \quad c_0^2=(k-1)\frac{p_i}{\rho_a}=\frac{k-1}{k}c_a^2\frac{p_i}{p_a}; \tag{19}$$

for discharge in vacuo

$$\bar{u}_{max}=\frac{2}{k-1}c_i+u_i=\frac{2}{k-1}c_i+\sqrt{\frac{2}{k-1}(c_0^2-c_i^2)}$$

or

$$\bar{u}_{max}=2c_a\sqrt{\frac{p_i}{(k+1)p_a}}\left[\sqrt{\frac{1}{k-1}}+\sqrt{\frac{1}{2k}}\right]; \tag{20}$$

for $k=\frac{5}{3}$,

$$\bar{u}_{max}=\frac{3}{2}c_a\sqrt{\frac{p_i}{p_a}}\left[1+\frac{\sqrt{5}}{5}\right]=1.08u_{max}.$$

We can see that the value of the velocity $\bar{u}_{max}$ is almost the same as u_{max} The maximum possible value for the velocity u can be found from the following expressions. Since

$$u=\frac{2}{k-1}(c_i-c)+u_i,$$

where

$$u_i=\sqrt{\frac{2}{k-1}(c_0^2-c_i^2)},$$

then

$$u=\frac{2}{k-1}(c_i-c)+\sqrt{\frac{2}{k-1}(c_0^2-c_i^2)}, \tag{21}$$

whence

$$\frac{du}{dc_i}=\frac{2}{k-1}-\sqrt{\frac{2}{k-1}}\frac{c_i}{\sqrt{c_0^2-c_i^2}}$$

and for $\frac{du}{dc_i}=0$ we have $\frac{k-1}{2}c_i^2 = c_0^2 - c_i^2$, and hence

$$c_i^2 = u_i^2 = \frac{2}{k+1}c_0^2, \tag{22}$$

i.e. there is a critical value (as in the narrowest section of a nozzle). As a result of this

$$u = \frac{2}{k-1}\left[\sqrt{\frac{k+1}{2}}c_i - c_0\right]; \tag{23}$$

for $c_0 = 0$

$$u^*_{max} = \frac{2}{k-1}c_i\sqrt{\frac{k+1}{2}} = \sqrt{\frac{k+1}{2}}u_{max}, \tag{24}$$

which is the maximum possible value of u

$$\left(\frac{d^2u}{dc_i^2} = -\frac{2}{k-1}\frac{c_0^2}{(c_0-c_i)^3} < 0\right).$$

For $k=\frac{5}{3}$, $u^*_{max} = \sqrt{\frac{4}{3}}c_i = 1.15c_i$.

This value of u^*_{max} also exceeds but little the value of u_{max}.

The minimum possible value of u will be for $c_i = 0$, when

$$u_{min} = \sqrt{\frac{2}{k-1}}c_0 \quad ; \quad \text{for} \quad c_0 = c_i$$

$$u_{max} = \frac{2}{k-1}c_0; \quad u_{min} = \sqrt{\frac{k-1}{2}}u_{max}; \tag{25}$$

for $k = 5/3$; $u_{min} = 0.6u_{max}$.

However, this value can never be attained for the shock wave process described. The variations in discharge velocity will lie within the limits between u_{max} and $\bar{u}_{max}$, i.e. the difference in velocities will not exceed 8 - 10%.

The first casem when $u = u_{max}$ will apply for normal reflection $(\psi = 0)$, the second case will apply for a glancing shock wave $\left(\psi = \frac{\pi}{2}\right)$. Therefore, through whatsoever angle the wave approaches the obstacle, it is safe to say that the discharge velocity has a value close to u_{max}. If discharge does not take place in vacuo, then it can always be said, with a high degree of accuracy

that

$$u = u_{max} - \frac{2}{k-1} c. \qquad (23)$$

The problem which we have considered here is of great theoretical interest, but under actual conditions the pressure may change with time as well as with the distance along the surface where it is applied.

In the axial-symmetrical case an additional effect - compression of the gas - originates, as a result of the convergence of conical shock waves.

We shall now consider a more complex problem. Suppose that a pressure, created by a magnetic field, is applied to the outer casing. In the axial-symmetrical case this pressure can be approximated by the following expression :

$$p = A \frac{l^2}{y^2}, \qquad (27)$$

where A = const is determined by the energy of the current flowing, required to create the magnetic field, y is the distance of any element of surface from the axis of symmetry. It is required to find the motion of the surface and of the gas inside the cavity. This problem can only be solved approximately. Assuming that every element of surface will move independently of the other elements perpendicularly to the same surface and that the shock wave is formed ahead of it almost immediately, which we shall consider as a plane wave (a given element of the shock wave can be roughly compared with a plane) in order to describe the motion of the element of surface, we arrive at the equation

$$\frac{d}{dt}(Mu) = Sp, \qquad (28)$$

where $u = \frac{dl}{dt} = \frac{1}{\cos\psi}\frac{dy}{dt}$, , S is the area of the surface element.

In writing down equation (28), we assume that the velocity of the gas in the zone of the shock wave is independent of the distance, and varies only

with time. As a result of this, for a strong wave

$$\frac{M}{S} \approx \frac{(k-1)\rho_a}{2\cos\psi}(y_0 - y). \tag{29}$$

Under the conditions we are considering, the shock wave is formed almost immediately after the commencement of motion and so becomes strong.

Comparing equations (27), (28) and (29) we arrive at this equation:

$$\frac{d}{dt}\left[(y_0 - y)\frac{dy}{dt}\right] = \frac{2A\cos^2\psi}{(k-1)\rho_a}\frac{l^2}{y^2} = b\frac{l^2}{y^2}, \tag{30}$$

where

$$b = \frac{2A\cos^2\psi}{(k-1)\rho_a}.$$

This equation must be solved for the conditions that

$$t = 0, \quad y = y_0; \quad u = \frac{dy}{dt}\frac{1}{\cos\psi} = 0. \tag{31}$$

Equation (30) has no accurate solution for the conditions of equation (31).

We now write equation (28) in the form

$$\frac{d}{dt}(Mu) = \left(\frac{dM}{dt}\frac{dy}{dt} + M\frac{d^2y}{dt^2}\right)\frac{1}{\cos\psi} = SA\frac{l^2}{y^2}; \tag{32}$$

whence

$$\frac{dM}{dt} + M\frac{\ddot{y}}{\dot{y}} = a\frac{l^2}{y^2\dot{y}}, \tag{33}$$

where $a = SA_0\cos\psi$. The solution of equation (33) can be written in the form

$$M = \frac{1}{\dot{y}}\left[-B + a\int\frac{l^2}{y^2}dt\right], \tag{34}$$

where $B = \text{const}$; $y = y(t)$ is assumed to be given.

It is obvious that for different ψ the relationship $y = y(t)$ will be different, therefore, generally speaking, equation (32) should be written in the form

$$\frac{\partial}{\partial t}(Mu) = \left(\frac{\partial M}{\partial t}\frac{\partial y}{\partial t} + M\frac{\partial^2 y}{\partial t^2}\right)\frac{1}{\cos\psi} = SA\frac{l^2}{y^2}, \tag{35}$$

here the derivatives are taken with respect to a constant y_0, and it is assumed that

$$y = y(y_0, t). \tag{35}$$

Since as a result of reduction of y_0 the pressure at the boundary increases, and consequently the velocity of motion of the boundary also increases, equal in our hypothesis to the velocity of the gas, we shall approximate the law of motion of the boundary in the form

$$y = y_0[1 - f(y_0)t^n]. \tag{37}$$

Hence,

$$\dot{y} = u = -\frac{ny_0}{\cos\psi} f(y_0)\, t^{n-1}, \tag{38}$$

and it is obvious that $f(y_0)$ should increase more strongly than $1/y_0$ for a decrease in y_0.

As a result of the approximation (37)

$$M = \frac{t^{n-1}}{ny_0 f(y_0)}\left[B - \frac{a}{y_0^2}\int \frac{t^3\,dt}{(1-f(y_0)\,t^n)^2}\right]. \tag{39}$$

If $n=3$, then

$$M = \frac{1}{3y_0 ft^2}\left[B - \frac{a}{3y_0^2 f}\int \frac{df t^3}{(1-ft^3)^2}\right] = \frac{1}{3y_0 ft^2}\left[B - \frac{a}{3y_0^2 f(1-ft^3)}\right].$$

Since for $t=0$, $M=0$, then $B = \frac{a}{3y_0^2 f}$ and

$$M = \frac{a}{9y_0^3 f^2 t^2}\left[\frac{ft^3}{1-ft^3}\right] = \frac{at}{9y_0^3 f(1-ft^3)}. \tag{40}$$

Substituting $t = \left(\frac{y_0 - y}{y_0 f}\right)^{\frac{1}{3}}$, we arrive at the expression

$$M = \frac{a}{9}\frac{(y_0 - y)^{\frac{1}{3}}}{y y_0^{10/3} f^{1/3}}. \tag{41}$$

If we assume that $f = \alpha y_0^3$, then comparing equations (29) and (41) we have

$$M = \frac{k-1}{2}\frac{\rho_0 S}{\cos\psi}(y_0 - y) = \frac{a}{9}\frac{(y_0 - y)^{\frac{1}{3}}}{y y_0^{10/3+4/3}\alpha^{4/3}};$$

whence

$$a^{-\frac{4}{3}} = \frac{9}{2a}\frac{(k-1)}{\cos\psi}\rho_0 S (y_0 - y)^{\frac{2}{3}} y y_0^{\frac{10+13}{3}}.$$

It is obvious that here we must take the average value of the quantity

$$(y_0 - y)^{\frac{2}{3}} y y_0^{\frac{10+13}{3}} = \frac{y_0^{\frac{10+13}{3}}}{y_0}\int_0^{y_0} (y_0 - y)^{\frac{2}{3}} y\, dy = \frac{9}{40} y_0^{\frac{7+13}{3}}.$$

Hence, assuming that $\beta = -\frac{15}{4}$, we find

$$a^{-\frac{4}{3}} = \frac{81}{80a}\frac{(k-1)\rho_0 S}{\cos\psi} \approx \frac{(k-1)\rho_0 S}{a\cos\psi}.$$

Thus,

$$\left.\begin{aligned} f &= a y_0^{\frac{-15}{4}}, \\ y &= y_0\left(1 - a y_0^{-\frac{15}{4}} t^2\right),\ u = -\frac{3a}{\cos\psi} y_0^{-\frac{11}{4}} t^2, \\ M &= \frac{9}{80}\frac{(k-1)\rho_0 S}{\cos\psi}\frac{(y_0 - y)^{\frac{1}{3}} y_0^{\frac{5}{3}}}{y}. \end{aligned}\right\} \qquad (42)$$

In another approximation it can be assumed that

$$f = a y_0^{-\frac{5}{2}}, \qquad (43)$$

and we do not compare the mass relationship with equation (29) ; then,

$$\left.\begin{aligned} y &= y_0\left(1 - a y_0^{-\frac{5}{2}+\frac{2}{3}} t^2\right),\ u = -\frac{a^2}{\cos\psi} y_0^{-\frac{5}{2}} t^2, \\ M &= \frac{a}{9}\frac{(y_0 - y)^{\frac{1}{2}}}{y a^{4/3}} \end{aligned}\right\} \qquad (44)$$

(comparison of the expression for mass with equation (29) leads once again to the result of (42)).

We now take into account that the angle ψ varies in the process of motion. It is obvious that

$$\tan\psi = \left(\frac{\partial y}{\partial x}\right)_t. \qquad (45)$$

Therefore equation (28) must be written in the form

$$\frac{\partial}{\partial t}\left[\frac{M}{S}\sqrt{1+\left(\frac{\partial y}{\partial x}\right)^2}\frac{\partial y}{\partial t}\right]=p=A\frac{f^2}{y^2}, \tag{46}$$

where

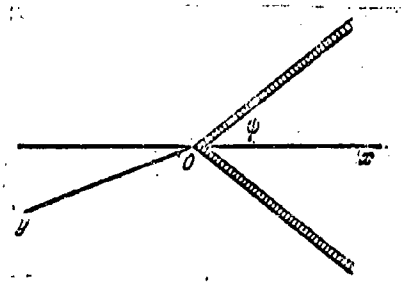
$$\frac{M}{S}=\frac{k-1}{2}\rho_0(y_0-y)\sqrt{1+\left(\frac{\partial y}{\partial x}\right)^2}. \tag{47}$$

Thus, equation (28) must be finally written in the form

$$\frac{\partial}{\partial t}\left\{(y_0-y)\left[1+\left(\frac{\partial y}{\partial x}\right)^2\right]\right\}=\frac{2A}{(k-1)\rho_0}\frac{f^2}{y^2}. \tag{48}$$

Equation (48) will be valid if each element of surface acts on the gas independently of adjacent elements. As a matter of fact, the interaction will occur. However, as a result of this we can use the equations presented above.

Figure 2s. Deformation of a cumulative surface with time.



Actually, despite the fact that the angle ψ changes during the process of motion, since the angle between the vector velocity of each element and the tangent to a given element of surface will not change, it can be assumed that the direction of motion of the gas will not change.

We shall find the shape of the surface, to which is applied the external pressure, for the hypothesis that the direction of motion of each one of its elements does not change. It is obvious as a result of this, that (Fig. 2s)

$$x=x_0+\Delta x, \tag{49}$$

where

$$x_0=y_0\cot\psi,\quad \Delta x=(y_0-y)\tan\psi; \tag{50}$$

hence it follows that

$$x = y_0(\cot\psi + \tan\psi) - y\tan\psi = \left(\frac{y_0}{\sin\psi} - y\sin\psi\right)\frac{1}{\cos\psi}. \quad (51)$$

Eliminating $y_0 = (x\cos\psi + y\sin\psi)\sin\psi$ from equation (51) and the law of motion

$$y = F(y_0; t), \quad (52)$$

we find the equation of motion of the surface in the form

$$y = F(x; t). \quad (53)$$

Further, since for the shock front the relationship

$$\bar{y} - y_0 = \frac{k+1}{2}(y - y_0), \quad (54)$$

holds good, where $\bar{y}$ is the coordinates of the shock front, we have :

$$\bar{y} = \frac{k+1}{2}y - \frac{k-1}{2}y_0 = \\ = \frac{k+1}{2}y - \frac{k-1}{2}[x\cos\psi + y\sin\psi]\sin\psi = \bar{y}(x; t). \quad (55)$$

Equation (55) is the equation of the surface of the shock front.

As a result of the convergence of similar curvo-linear shock waves, the point of their intersection will move with variable velocity, which leads to a variable jet velocity. As a result of this it is possible to obtain in certain places a velocity which is boosted in comparison with the average velocity. In order that the jet should be stable and not " dying ", it is essential that on the average the velocity fluctuation should not be large and that the velocity of the rear portions should increase relative to the frontal portions .

.....

SUBJECT INDEX

	CHAPTER
Abel's equation of state	7
Acetylides	1
Active portion of a charge	11
" " " " "	
limiting length	11
Activity	4
" partial	4
Adiabatic, for detonation wave	7
Adiabatic, Hugoniot	6
" , Poisson	6
Ammonites	1
Anmotol	1
Arrhenius' Equation	2
Arrhenius' Law	10
Autocatalytic reactions	2
Average "retarded" pressure	13
Axial cumulation	12
Azides	1
Ball indicator	13
Ballistic pendulum	11
" mechanism of a reaction	8
Ballistites	1
Belyayev - Zel'dovich Theory of combustion	10
Binding energy	2
Boiling point of explosives	10
Boltzmann districution	6
Boreskov's formula	13
Branching of a chain	10
Brisance	11
Brisance meter	11
Calorimetric bomb	3
Capsule effect	13
Cavitation of a sense medium	14
Central waves	10
Chain ignition	10
" " , theory of	10
Chain length	10
Chain reactions	10
" " , effect of adsorbtures	10
Chain reactions, induction period	10
Chain reactions, non-stationary regime	10
Characteristic temperature	3
" " surface	5
Coefficient of activity	4
" " thermal conductivity	10
Coefficient of thermal diffusivity	10
Combustion	10
Combustion, normal	10
" of condensed explosives	10
Combustion of gases	10
" " " , concentration limits	10
Combustion of gaseous explosive systems	10
Combustion of powders	10
Combustion, theory of Zel'dovich-Frank-Kamenetskii	10
Combustion, velocity of propagation	10
Composition of explosive products	4
Compression of copper crushers	11
Compression of lead cylinders	11
Conditions at a surface of discontinuity	6
Conditions for chain autoignition	10
Conditions for adiabatic medium	5
Constant, reaction velocity	4
" of chemical equilibrium	6
Contact discontinuity	9
Continuance of a chain	10
" " " " , velocity constant	10'
Control of chemical reactions	4
Cordites	1
Co-Volume	7
Criterion, of Landau	10
" " Nussel't	10
" " strong degeneration	12

	CHAPTER
Critical charge diameter	8
Critical ignition condition	10
Critical length of stationary regime	8
Critical shock energy	2
Critical stress	2
Cumulation of gases	5
Cumulative charge	12
" ", active portion	12
Cumulative charge, with lens	12
" effect	12
" focus	12
" gap	12
" jet	12
" ", process of formation	12
Cumulative surface	12
Curved drop hammer	2
D'Authriche's method	8
Degenerated electron gas	12
" " " , equation of state	12
Debye-Einstein formula	3
Depth, armour piercing	12
Destructive effect	13
Detonation	7
" , concentration limits	7
" , of condensed explosives	7
Detonation, sympathetic	15
" , wave velocity	7
" , wave, process of formation	7
Detonation wave parameters	7
" " conditions for stationary state	7
Detonation wave, limiting conditions of stability	7
Diffused ignition	10
Direct shock wave	6
Disc Photorecorder	8
Dispersion of detonation products in air	13
Dispersion of detonation prodicts in vacuo extinction of explosion	13

	CHAPTER
Efficiency of explosives	13
Electro-drop hammer, Rdultovskii's	2
Electro-optical transformer	8
Energy, binding	2
Energy of a crystal lattice	2
Energy of activation of explosives	2
Energy of interaction of molecules	8
Energy stress as a result of an explosion	11
Equation, Arrhenius's	2
" " for a degenerated electron gas	12
Equation, Bernoulli's	13
" , Euler's	5
" , of a chem isotherm	4
" , of a polarographic spiral	12
" , of a streamline	5
" , of continuity	
" of diffusion	10
" , of polytropy of state, Abel's of thermal conductivity	
Equations, basic, of gas dynamics	5
Euler's method	5
Euler's variables	5
Explosion	1
" field	13
" in a confined medium	14
" " " confined meteoric medium	14
" in an unconfined liquid	13
Dispersion of detonation products from an inclined medium	13
Double piston impulsometer	13
Dynamites	1
Effective length of jet	12
" portion of reaction zone	8
Explosion in the ground	14
" of a cumulative charge	12
" , point	13

	CHAPTER
Explosion, spherical	13
Explosive chemical compounds	1
" mixtures	1
Explosophoric atomic complexes	1
Final temperature of an explosion	3
First principles of thermodynamics	7
Flash point	2
" " , minimum	2
Fluid drift mechanism of a reaction	8
Formula, Debye-Einstein	3
Formula, Kast's	3
Diaphragm crusher gauge	13
Formula, Sadovskii's	13
Foucault-Tepler's method	8
Free energy	6
Friction pendulum	2
Fugacity effect	13
Fulminate of mercury	1
Fulminating (detonating jelly)	1
Fulminates	1
Gaseous bubble	14
Gaseous explosion mixture	1
Gas evolution	1
Gas generating reaction	4
Gelatine dynamites	1
Grisoutine	1
Heat of combustion	3
Heat of evaporation of explosives	10
Heat of unconfined medium	14
" " " metallic medium	13
" " " meteoric medium	14
Hudronite	1
Hugionot adiabatic	6
Hydrodynamic theory of detonation	7
Ideal liquid	5
Ignition (detonation) delay time	2
Impulse oscillograph	8
Impulsive action	13
" force	11
Incompressible liquid	5
Induction period	2
Initiating explosives	1
" impulse	2
Internal energy	6
Ionisation data unit	8
Isentropic motion	
Isomeric effect	3
Kast's formula	3
Lagrange's method	5
" problem	14
Laval nozzle	5
Law, Hess's	3
Law, of areas(square law)	10
Law, of cosines	10
Law, mass action	2
Leading wave	9
Lengendre transformation	5
Limiting active mass	11
Limiting charge diameter	7
Limiting initiating charge	2
Limit of autoignition	10
Liquid explosive mixtures	1
" " systems	10
Mach angle	12
Mach wave	9
Mass velocity of combustion	10
Mechanical pressure gauge	13
Method, Dautriche	8
" , Euler's	5
" , Foucault-Tepler's	8
" , Lagrange's	5
" of explosion	3
" of formation	3
Heterogeneous breakaway	10
Hess's Law of Active Masses	3
Hexogen	1
High explosives	1
"Hot spots"	2
"Hot spots", critical temperature	2
Non-gaseous compositions	10
Non-stationary motion of a medium	5
Normal chemical agent	4
Normal flame velocity	10
Nozzle theory	
Origin of chains	10
Partial activity	4
" pressure	4
Peninsula of ignition	10

	CHAPTER
Period of suto-acceleration of a reaction	2
Period of damping of a reaction	2
" " induction	2
PETN (Pentaerythritol tetranitrate)	1
Phlegmatizers	2
Photographic drum recorder	8
Picric acid	1
Piezoelectric manometer	13
Plunger instrument	2
" " , Kholevo's	2
Potential energy of an explosive	13
"Power" of explosives	11
Prandtl-Mayer problem	13
Principle of tautochronism	12
Propagation of a shock wave in a dense medium	14
Propagation of a shock wave in solid bodies	14
Propagation of a shock wave in water	14
of characteristics	5
of conjugate isentropes	9
, instantaneous X-ray	12
, soap bubble	10
Michelson's straight line	7
Mirror scanning	8
Motion of a cumulative jet	12
Mixing mechanism of a reaction	8
Nitrocellulose powder	1
Nitro-compounds	1
Nitroglycerine	1
Nitroguanidine	1
Sensitivity of explosives to friction	2
Sensitivity of explosives to shock	2
Sensitivity of explosives to shock, lower limit	2
Sensitivity of explosives to shock, upper limit	2
Sensitivity of explosives to thermal pulses	2
Sensitivity of explosives to tilt	2
Sensitizers	2
Shadow method	10
Shock adiabatic	6
Shock front	6
Shock front, width of	6
Shock mechanism of a reaction	8
Shock, polar	5
Shock wave	6
Shock wave, conditions of creation	5
Shock wave, dissipation of energy	6
Shock wave, initial parameters	6
Shock wave, initial parameters in air	9
Shock wave, initial parameters in metals	9
Shock wave, instial parameters in water	9
Propagation of detonation in condensed explosives	8
Propagation of detonation in gases	8
Pyrotechnic compositions	1
Pyroxyline powder	1
Quantum yield	10
Radial cumulation	12
Radial detonation	11
Range of transmission of detonation	15
Rdultovskii's electro-drop hammer	2
Riemann invariant	5
Sensitivity of explosives	2
" " " to the action of initiators	2
Sensitivity of explosives to concussion (vibration)	2
Ground dispersion	6
Spatial transverse shock wave	6
Specific breakaway	6
Specific heat	3
Specific heat at constant pressure	3
Specific heat at constant volume	3
Specific impulse from an explosion	11
Spectral luminosity	3
Stable motion of a medium	5
"Static" effect	13
Statistical sum	6
Statistical sum of a diatomic molecule	6
Statistical sum of an atom	6
Stimulation of detonation process	8
Stream lines	5
Super high-speed cumulation	12
Tangential shear	6

	CHAPTER
Temperature coefficient of velocity	2
Temperature of an explosion	3
Temperature, parameters of	6
" , plane, direct	6
" , polar	6
" , properties of	6
" , transition zone	6
" , transverse	6
" , width of shock front	6
Similarity solution motion	13
Simple (plane) waves	5
Smokeless powders	1
Smoke powders	1
Thermite reaction	1
Thermodynamic potential	4
Topochemical reaction	2
Transition of combustion into detonation	10
Transition of combustion into detonation for condensed explosives	10
Transition of combustion into detonation in gaseous systems	10
Transverse reflections	9
Transverse (inclined) shock waves	6
Tribochemical hypothesis	2
Trotyl	1
True stresses, diagram of	12
Velocity for armour piercing	12
" " " " , critical	12
Velocity of combustion	10
" " " , effect of density	10
Velocity of combustion, effect of temperature	10
detonation	7
, chronographic method of measuring	8
Temperature of flash (flash point)	
Temperature of flash minimum	
Tetranitromethane	1
Tetrazine	1
Tetryl	1
Theory of convergent jets	12
" " thermal flame propagation	10
Thermal corrections	3
Thermal effect	3
Thermal ignition	10
Thermal ignition, theory	10
Thermal ignition, theory of non-stationary	10
Thermal ignition, theory of stationary	10
Velocity of detonation, effect of admixtures	7
Velocity of detonation, effect of casing	8
Velocity of detonation, effect of density	7
Velocity of detonation, optical methods of measuring	8
Velocity of propagation of an explosion	1
Vertical drop hammer	2
Zone of combustion	10
" " " , width of	10
" " compression	13
" " crushing (destruction)	13
" " preheating	10
" " shock	13